

Homotopical dynamics for gradient-like flows

Guido G. E. Ledesma
Dahisy V. S. Lima
Margarida P. Mello
Ketty A. de Rezende
Mariana R. da Silveira

34º

Colóquio
Brasileiro de
Matemática



Instituto de
Matemática
Pura e Aplicada

Homotopical dynamics for gradient-like flows

Homotopical dynamics for gradient-like flows

Primeira impressão, setembro de 2023

Copyright © 2023 Guido G. E. Ledesma, Dahisy V. S. Lima, Margarida P. Mello, Ketty A. de Rezende e Mariana R. da Silveira.

Publicado no Brasil / Published in Brazil.

ISBN 978-85-244-0531-0 (print)

ISBN 978-85-244-0526-6 (ebook)

MSC (2020) Primary: 37B35, Secondary: 37B30, 37D15, 55T05, 55U15, 90C57

Coordenação Geral

Carolina Araujo

Produção Books in Bytes

Capa IMPA

Realização da Editora do IMPA

IMPA

Estrada Dona Castorina, 110
Jardim Botânico
22460-320 Rio de Janeiro RJ

www.impa.br

editora@impa.br

L473h

Ledesma, Guido

Homotopical dynamics for gradient-like flows / Guido G. E. Ledesma, Dahisy V. S. Lima, Margarida P. Mello, Ketty A. de Rezende e Mariana R. da Silveira. - 1.ed. -- Rio de Janeiro: IMPA, 2023.

34 Colóquio Brasileiro de Matemática; v. 10, 340p.: il.; 23cm

ISBN 978-85-244-0531-0 (print)

ISBN 978-85-244-0526-6 (ebook)

1. Conley Index Theory. 2. Lyapunov Graphs and Isolating Blocks. 3. Spectral Sequences and Cancellations of Critical Points. I. Lima, Dahisy V. S.; Mello, Margarida; de Rezende, Ketty A.; da Silveira, Mariana R. II. Série. III. Título

UDC: 515.1

Carolina Celano Lima/CRB-7: 2438

This book is dedicated to Professors John Franks and Charles Conley (in memoriam) whose mathematical insights and inspiring work kindled the study of most of the themes explored in this book.

Contents

Foreword	v
Preface	viii
Acknowledgements	xi
1 An Introduction to Conley Index Theory	1
1.1 Conley's Fundamental Theorem of Dynamical Systems	1
1.1.1 Basic Concepts in Topological Dynamics	1
1.1.2 Gradient flows	7
1.1.3 Existence of Lyapunov Functions	11
1.2 Conley index	15
1.2.1 Homotopy Conley Index	20
1.2.2 Sum and Product of the Conley Index	24
1.2.3 Homology Conley Index	29
1.3 Invariance under continuation	31
1.4 Morse Decomposition and Index Filtration	35
1.4.1 Attractor–repeller decomposition	35
1.4.2 Morse decomposition	37
1.5 Morse–Conley Inequalities	40
2 Poincaré–Hopf Inequalities	47
2.1 Generalized Morse–Conley Inequalities	48
2.2 Poincaré–Hopf Inequalities	51
2.2.1 Local Poincaré–Hopf Inequalities for Isolating Blocks	51
2.2.2 Global Poincaré–Hopf Inequalities for Closed Manifolds	58

2.3	Homological Refinement of Singularities into Connectivity types	60
2.3.1	Handle Theory	60
2.4	Lyapunov Graphs, Semigraphs and Obstructions to Realizations	64
2.4.1	Abstract Lyapunov Graphs and Semigraphs	65
2.4.2	Obstructions to Realizability	66
2.5	Graph Morsification and h_{κ}^{cd} -Systems	67
2.5.1	Morsification Algorithm	69
2.5.2	Morsification and the presence of cycles	78
2.5.3	h_{κ}^{cd} -Systems	82
2.5.4	Conclusion	83
3	Network Flows and Morsification	85
3.1	Brief graph theoretical background	85
3.2	h_{κ}^{cd} -system as a network flow problem	89
3.2.1	Case $n = 2i + 1$	90
3.2.2	Case $n = 2i$	100
3.2.3	On the range of κ	107
3.3	Poincaré–Hopf inequalities for closed manifolds	108
3.3.1	Poincaré–Hopf inequalities equivalent to Morse inequalities	110
3.3.2	The Morse polytope	117
3.3.3	When $\sum_{j=0}^n (-1)^j h_j$ is odd	131
3.4	Realizability of the Morse polytope	135
3.4.1	h^{cd} vectors and ntd -labellings	136
3.4.2	Betti number vectors and ntd -labellings	138
4	Building flows with Isolating Blocks	145
4.1	Two dimensional Isolating Blocks	146
4.2	Three dimensional Isolating blocks	154
4.2.1	Morse–Smale flows on $S^2 \times S^1$	162
4.3	Realizing Admissible Lyapunov graphs in higher dimensions	172
4.3.1	Constructing Isolating Blocks of Morse type	174
4.3.2	Constructing Isolating Blocks for Periodic Orbits	185
5	Dynamical Spectral Sequence	191
5.1	Introduction	191
5.2	Spectral Sequences	197
5.3	Morse Complex	204
5.4	Spectral sequences associated to filtered Morse complexes	211
5.4.1	Spectral Sequence Sweeping Algorithm	214
5.4.2	Detecting paths of flow lines	235
5.5	Ordered Cancellation via Spectral Sequences	238
5.5.1	Spectral Sequences of a Filtered Morse Chain Complex with TU differential	239
5.5.2	Global cancellation on Surfaces	242

5.5.3	Higher Dimensional Cancellation Theorem	254
5.6	Other related application	256
6	Homotopical Applications for Circle Valued Morse Functions	258
6.1	Circular Morse Graph	259
6.1.1	Circular Lyapunov digraphs for Surfaces	262
6.2	Global cancellation for circle valued Morse functions	264
6.2.1	Novikov chain complex	264
6.2.2	Spectral Sequence Sweeping Algorithm for a Novikov Complex . . .	269
6.2.3	Ordered cancellation for circle valued Morse function	286
Conclusion		302
Bibliography		307
List of Symbols		312
Index		314

Foreword

This text treats an important area in the qualitative theory of dynamical systems, so it is useful to consider the context and history of the subject and where the content of this text fits.

Dynamical systems is a subset of mathematics which deals with how various aspects of the world evolve in time. Historically one of the seminal issues addressed by dynamical systems was to describe the motion of the solar system. The genius of Newton enabled him to model the problem abstractly as a differential equation – the n -body problem. The planets were abstracted to point masses and the differential equation was derived from Newton's $F = ma$ law, assuming a force due to gravity inversely proportional to the square of the distance between bodies. Mathematicians, as they are wont to do, have focused on the abstract problem despite the fact that, after the advent of relativity, it became clear that many interesting aspects of the real world were not well modeled by Newton's equation. While the case of two bodies was relatively understandable, the situation with more bodies was intractable. But studying this model – as an end in itself – remains an active area of research.

In the late nineteenth century it became clear that there is even a question of what it means to “solve the n -body problem.” For example, even an explicit closed form solution for any initial condition would not answer the questions of can one find the periodic solutions, or can there be a non-collision singularity where some of the bodies go to infinity in finite time. As a result mathematicians like Henri Poincaré were led to study *qualitative* properties of dynamical systems such as the existence of periodic orbits, or more generally, the existence of invariant measures which would guarantee recurrent orbits. One naturally also wanted to know the topology of invariant sets and the statistical properties of invariant measures.

The flow of solutions to n -body problem is quite special in that it preserves a Lebesgue measure and hence by the Poincaré recurrence theorem every subset of positive measure will recur. In some sense the opposite extreme is exhibited by gradient flows of smooth

functions. For these the only invariant measures are the dynamically trivial ones supported on fixed points. It was Charles Conley who realized that for a very general class of flows these two types of behavior – recurrent and gradient-like – can provide a good qualitative description of the dynamics. His result (sometimes called Conley’s Fundamental Theorem of Dynamical Systems) is presented as Theorem 1.2 and Theorem 1.3 in the text.

This result has a very important consequence. Quoting Section 1.1 from the text

[T]he problem of obtaining a qualitative description of a flow is divided into two parts:

- the description of the connected components of the chain recurrent set;
- the description of how these components are connected to each other.

This dichotomy has surprising generality which is the reason Conley’s theorem is considered “Fundamental”. The so-called Smale school of dynamics was motivated by a desire to understand structurally stable systems and hence considered systems whose chain recurrent set has a hyperbolic structure since those systems have interesting stability properties. This led to a rich theory which has been an important part of the field for more than five decades and incorporates properties of invariant measures and their ergodic theory.

This text focuses on a different approach in which algebraic topology plays a central role. The *homotopy Conley index* considered in Section 1.2 is a basic ingredient in this dichotomy. It assigns a homotopy type to an isolated invariant set (e.g. a component of the chain recurrent set). The homology of this homotopy type provides a weaker but important invariant of this isolated invariant set, the *homology Conley index*, which is generally more tractable than the homotopy index.

To a large extent this text focuses on the second of these two parts of the dichotomy. One of the central concepts discussed in the text is the notion of a Lyapunov function, i.e. a function defined on the state space of the system which strictly decreases along all orbits which are not chain recurrent and which separates components of the chain recurrent set. Understanding rough properties of such functions gives a qualitative picture of how the components of the chain recurrent set are connected by orbits. For example, if there is an orbit whose forward limit set is contained in a chain recurrent component Y and whose backwards limit set is contained in a chain recurrent component X then for any Lyapunov function it follows that $f(X) > f(Y)$. Such a function f gives rise to a filtration of the state space by setting M_a to be $\{x \mid f(x) \leq a\}$ where $a \in \mathbb{R}$ is a regular value of f . If there are finitely many components of the chain recurrent set then this filtration is finite.

In this situation one can bring the tools of algebraic topology to bear on the problem of finding a qualitative understanding of how the various chain recurrent components fit together. Historically the archetype for this kind of question is the collection of Morse inequalities associated to a Morse function f on a compact manifold. In that case the chain recurrent set of the flow of the negative gradient of f consists of the finite set of critical points and the homology Conley index of each such point is non-zero only in the dimension equal to the index of the point. The algebraic content of the proof of the classical Morse inequalities answers the question, “What chain complexes over \mathbb{R} can give rise to

$H_*(M, \mathbb{R})$?" More generally gradient flows and Morse inequalities are the paradigmatic example of how one might give qualitative descriptions of the dynamics of a system.

A very useful accompaniment to this is the concept of a Lyapunov graph associated to a Lyapunov function f . To obtain it one defines an equivalence relation on the state space by $x \sim y$ if x and y lie in the same component of $f^{-1}(c)$ for some $c \in \mathbb{R}$. The quotient of the state space by this relation is then a graph with vertices corresponding to chain components. The graph is a directed graph which contains no cycles since f is strictly decreasing on non-chain recurrent orbits of the flow.

This collection of concepts, especially Lyapunov functions and the filtrations and graphs associated with them, provide the framework on which the heart of the text is based. It is worth noting that many of the results whose exposition comprises the later chapters are available only in the original research articles where they first appeared. This text provides both the needed background as well as the exposition of the state of the art in this research area.

*John Franks
Santa Barbara, California*

Preface

This book presents homotopical tools to study gradient-like flows in their local and global aspects. The phase space and consequently the flow can be continuously deformed while keeping the homotopical invariants constant. This study is called Homotopical Dynamics.

Conley's well known theorem regarding the existence of a Lyapunov function $f : M \rightarrow \mathbb{R}$ for a continuous flow $\phi_t : M \rightarrow M$ on a compact metric space M is considered by many as the fundamental theorem of Dynamical Systems. The Lyapunov function has the property that it is constant on connected components R_i of the chain recurrent set \mathcal{R} and decreases along the orbits of ϕ_t and thus, imposes a gradient-like behavior on the flow.

Therefore, the existence of a Lyapunov function is central to the themes developed in this book. It transforms our study in the Morse, Morse–Smale and Novikov settings into investigating the topological and dynamical properties of gradient-like flows. Most of our results hold for compact n -manifolds M with finite component chain recurrent set, each component being an isolated invariant set. This is the ideal setting to use Conley's homotopical index theory which is invariant under continuation. The goal is to understand the local behavior of the chain recurrent components R_i , their isolating blocks N_i and how these blocks fit together to form M . Furthermore, one aims to comprehend the global behavior of the connecting orbits to form the flow ϕ_t and study their asymptotic behaviour under continuation.

The power of Conley's homotopy index never ceases to impress by its diverse applicability. It generalizes the Morse index, in fact it can be computed for any isolated invariant set S of a continuous flow. The novelty herein lies in how this index is defined, not as a number but as the homotopy type of a space. If S is a maximal isolated invariant set of a compact neighborhood N and N^- is the exit set for the flow, then the homotopy type of the space N/N^- is the Conley index of S . This will be discussed in Chapter 1.

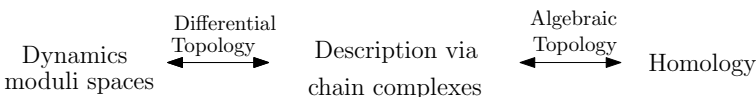
In Chapter 2 we introduce Lyapunov graphs that arise naturally from a Lyapunov function $f : M \rightarrow \mathbb{R}$ and an equivalence relation on M : $x \sim_f y$ if and only if x and y belong to the same connected component of a level set of f . This one dimensional quotient

space, M/\sim_f , is a Lyapunov graph that can be enriched with dynamical information on the vertices which represent the R_i and topological information on the edges which represent collars of codimension one closed manifolds. These graphs are a combinatorial tool which work as a book keeping device retaining many important topological and dynamical invariants. If one considers one of these graphs abstractly, it can be realized as a flow on some manifold if and only if the Poincaré–Hopf inequalities are satisfied. The Poincaré–Hopf inequalities are closely related to the Morse–Conley inequalities.

In Chapter 3 the Morsification problem for abstract graphs L is proposed, a Morsification algorithm is obtained producing a system of linear equations that are solved, obtaining the entire integral solution set, through Network Flow Theory. It is shown that the data on L satisfies the Poincaré–Hopf inequalities if and only if there exists a Betti number vector satisfying the Morse inequalities. The collection of all Betti numbers satisfying the Morse inequalities, for a given pre-assigned data in L , forms a Morse Polytope.

In Chapter 4 we turn to the realization of flows on closed manifolds by first constructing the most elementary isolating blocks. For this one uses Handle Theory to attach handles to collared codimension one closed manifolds in such a way that it realizes semigraphs of Morse type. Finally we glue the isolating blocks according to a Lyapunov graph to obtain a gradient-like flow on some closed n -manifold.

With the purpose of further exploring the global behavior of the flow on closed manifolds, it is well-known that the dynamics of moduli spaces, given by the intersections of stable and unstable manifolds, needs to be understood. An approach for this global study of the flow was elegantly proposed in Franks (1982) via the moduli spaces. This book combines this approach with the Conley index theory.



The bidirectionality of the arrows reflects the need to start from a set of information and seek understanding what are the possibilities for the corresponding information at the other end of the arrow.

Finally, in Chapters 5 and 6 the homotopical deformation of the phase space and of the flow under continuation will be investigated using the spectral sequence, which can be informally viewed as a homological iteration of chain complexes. The initial flow is associated to a Morse chain complex and, roughly speaking, the spectral sequence associated to this Morse complex and a filtration will produce a *notebook* with a registered chain complex on each page which results from the homology of the complex on the previous page.

Changing the pages of the spectral sequence, i.e., progressively considering the modules of each complex, one observes algebraic cancellations occurring. These algebraic cancellations are dynamically interpreted as the death of connecting orbits of the flow and the birth of new orbits caused by the cancellation of consecutive critical points. In the analysis of the spectral sequence, other important information is obtained, such as the ex-

istence of paths of orbits between invariant sets and bifurcations. The dynamical spectral sequence is to be computed for a filtered Morse chain complex of a Morse function, as well as for a filtered Novikov chain complex of a circle valued Morse function.

D. V. S. Lima would like to thank the São Paulo Research Foundation (FAPESP) for the support under grants 2020/11326-8 and 2016/24707-4. K. A. de Rezende would like to thank the São Paulo Research Foundation (FAPESP) for the support under grants 2016/24707-4 and 2018/13481-0 and National Council for Scientific and Technological Development (CNPq) for the support under grants 305649/2018-3. M. R. Silveira would like to thank the São Paulo Research Foundation (FAPESP) for the support under grants 2016/24707-4 and 2018/13481-0.

Acknowledgements

I would like to thank my mother, Antonia, for always believing in me and my father, Rolando, for always encouraging me to study, rest in peace dad. I want to say a huge thank you to my wife, Meylin, for the strength and encouragement she gives me to face all of the difficulties in life. I would also like to thank my son, Tiago, who makes my days challenging and full of joy, my life is more complete by having you two by my side. Finally, I would like to thank God for allowing me to meet such wonderful people as my advisor Ketty, professor Oziride and my friends and colleagues Dahisy and Mariana.

Guido G. E. Ledesma

I thank my beloved family, my wonderful mother Elizete, my father Delvan, and my incredible siblings, Delvan Jr., David and Daniela, for supporting me throughout my life, always believing in me, and giving me strength. A special thank-you goes to Ketty de Rezende for her invaluable guidance and support throughout my academic journey. I am honored to have had the privilege of working under her leadership. I want to express my deepest gratitude to Rafael Alves for all the love, unwavering support, and boundless kindness he has showered upon me. His presence in my life has been a source of strength and comfort.

Dahisy Lima

My thanks go to Ricardo. First he was my friend. Then he was husband, father, source of unconditional support, faithful appreciator of my cooking, dance partner, ideal pandemic companion. But the best is that, after 44 years together, he is still my dearest friend.

Margarida P. Mello

I wish to thank God who is my perpetual source of being and love without whom life would be meaningless. I thank my family, first and foremost, my loving husband, Pedro,

whose steadfast support and encouragement accompanied my whole career, and also our seven children, Daniel, Diana, Susanna, Joel, Beatriz, Djenane and Denise, who were my daily inspiration and always stirred up a strong sense of purpose in me. Lastly, my most profound gratitude goes to my first mathematics teacher, my mother, Maruja, and to my father, Djairo, whose enthusiasm for Mathematics led me into this unending journey in search for its hidden truths and beauty.

Ketty de Rezende

I would like to thank my parents, João Batista and Maria Hermínia, for their love, support and guidance throughout my journey. My sisters, Marina and Joana, have been pillars of strength, and I'm truly thankful for their presence in my life. I would also like to express my immense appreciation to my aunt Lúcia, whose care and love have been invaluable. Finally, my dear husband Graham deserves my deepest thanks for his constant encouragement and partnership, which have been essential in shaping who I am today.

Mariana R. da Silveira

All the authors express their gratitude to IMPA's book editorial team, who provided us with unwavering support during the preparation of this book.

1

An Introduction to Conley Index Theory

In this chapter, we will develop a powerful topological tool, called the Conley index. This index associates a topological invariant to a dynamical system so that some qualitative differences between distinct systems are expressed by different values of this invariant. Although this invariant is not always able to distinguish non-isomorphic systems, which would be ideal in an approach to classify dynamical systems, the Conley index allows us to detect very subtle differences between dynamical systems.

1.1 Conley's Fundamental Theorem of Dynamical Systems

In this section, we introduce some key concepts and ideas of Topological Dynamics with the ultimate goal of understanding Conley's Fundamental Theorem of Dynamical Systems.

1.1.1 Basic Concepts in Topological Dynamics

Let X be a Hausdorff topological space.

Definition 1.1. A *continuous flow* φ on X is a group action of the additive group of the real numbers \mathbb{R} on X , that is, a continuous map

$$\varphi : \mathbb{R} \times X \longrightarrow X$$

such that:

- (a) $\varphi(0, x) = x$, for all $x \in X$;
- (b) $\varphi(s + t, x) = \varphi(s, \varphi(t, x))$ for all $s, t \in \mathbb{R}$ and $x \in X$.

The geometric meaning of the second requirement is that starting at time zero and letting the flow run for time $t + s$ is the same as starting at the value $\varphi(t, x)$ and letting the flow run for time s (or conversely, starting at $\varphi(s, x)$ and letting the flow run for time t).

Definition 1.2. Given a continuous flow $\varphi : \mathbb{R} \times X \longrightarrow X$ and a point $x \in X$, we define the following:

- (a) the *solution* through x is the map $\varphi_x : \mathbb{R} \rightarrow X$ given by $\varphi_x(t) := \varphi(t, x)$;
- (b) the *trajectory* (or *orbit*) of $x \in X$ with respect to the flow φ is the set

$$\mathcal{O}_\varphi(x) := \{\varphi(t, x) \mid t \in \mathbb{R}\} = \varphi(\mathbb{R}, x),$$

that is, the orbit of x is the image of the solution through x , $\mathcal{O}_\varphi(x) := \varphi_x(\mathbb{R})$;

- (c) the *time t map*, for $t \in \mathbb{R}$, is the map $\varphi_t : X \rightarrow X$ given by $\varphi_t(x) := \varphi(t, x)$.

Geometrically, the trajectory of x is a curve in X parametrized by the time t that passes through the point x at the initial time $t = 0$. This curve represents all possible states of the point x as time passes.

Note that, given two points x and y in X , either their trajectories coincide or are disjoint. Hence, the space X can be decomposed into the disjoint union of such curves. This structure is called the *phase space* associated to the flow φ . Thus, the phase space represents all possible states of the points in the system.

The orbit of x can be of three different types:

- *regular orbit*: when φ_x is an injective map, the orbit of x is a bijective image of an open interval;
- *singular orbit*: when φ_x is a constant map, the orbit of x consists of the single point x (we say that x is a *rest point* or *fixed point*);
- *periodic orbit*: when φ_x is a periodic map, the orbit of x is homeomorphic to a circle. In this case, there exists $t_0 > 0$ such that $\varphi(t_0, q) = q$ and $\varphi(s, q) \neq q$, whenever $s \in (0, t_0)$.

In what follows, we consider a class of continuous flows coming from the integral curves of vector fields.

Let M be a closed smooth manifold of dimension n , and let $V : M \rightarrow TM$ be a smooth vector field on M . One of the fundamental properties of V is that it yields a continuous flow. The *flow generated by the smooth vector field V* is defined by

$$\begin{aligned} \varphi : \mathbb{R} \times M &\longrightarrow M \\ (t, x) &\mapsto \gamma_x(t) \end{aligned}$$

where $\gamma_x : \mathbb{R} \rightarrow M$ is the integral curve of V through x , that is, γ_x is a solution of the ODE

$$\begin{cases} \gamma_x(0) = x \\ \dot{\gamma}_x(t) = V(\gamma_x(t)). \end{cases}$$

This means that, for any point $x \in M$, there exists a unique curve that passes through x and follows the vector field's direction. Hence, the trajectory can be thought of as the path taken by a particle that moves along the vector field, where the particle's velocity at any given point is given by the vector assigned to that point by the vector field.

Example 1.1. Consider $M = \mathbb{R}^2$ and the vector field

$$V = x \frac{\partial}{\partial y} - y \frac{\partial}{\partial x}.$$

The flow generated by V is given by

$$\begin{aligned} \varphi_V : \mathbb{R} \times \mathbb{R}^2 &\rightarrow \mathbb{R}^2 \\ (t, x, y) &\mapsto (x \cos(t) - y \sin(t), x \sin(t) + y \cos(t)). \end{aligned}$$

The corresponding phase space is shown in Figure 1.1. The flow φ_t rotates the plane through an angle t about the origin.

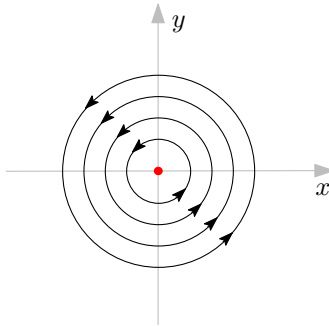


Figure 1.1: Flow on \mathbb{R}^2 .

Note that the origin $(0, 0)$ is a fixed point and any other point belongs to a periodic orbit, that is, any other trajectory is periodic.

Example 1.2. Consider $M = \mathbb{R}^2$ and the vector field

$$V = y \frac{\partial}{\partial x} + (x^2 - 1) \frac{\partial}{\partial y}.$$

The flow generated by this vector field is represented in Figure 1.2.

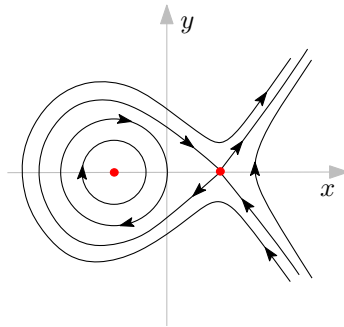


Figure 1.2: Flow on \mathbb{R}^2 .

This system contains two fixed points, namely, $(1, 0)$ and $(-1, 0)$. The tear drop is composed by a homoclinic trajectory and the hyperbolic rest point $(1, 0)$, and it bounds a set filled out with periodic trajectories.

There are some special sets that are invariant with respect to the action of the flow, that is, sets that remain unchanged under the system's evolution.

Definition 1.3. A subset $S \subset X$ is said to be an *invariant set* with respect to the flow φ if, for all $p \in S$, one has $\varphi(t, p) \in S$ for all $t \in \mathbb{R}$. In other words, $\varphi(\mathbb{R}, S) = S$.

The simplest example of an invariant set is a fixed point or equilibrium point of the system: a point $x \in X$ such that $\varphi(\mathbb{R}, x) = x$, i.e., the orbit of x is equal to x . Other examples of invariant sets are: the empty set, the entire space X , a periodic orbit and any regular orbit. However, invariant sets can also be very complicated, such as the Lorenz attractor, Cantor sets coming from Smale horseshoes or strange attractors, for example, there are invariant sets that arise in chaotic systems and exhibit intricate, fractal-like patterns.

Our main interest is to work with the Conley index which is a homotopical tool, hence, the differentiability class of the flow is not taken into account.

The following properties are easy to verify.

Proposition 1.1. Let φ be a continuous flow on a topological space X .

- (a) A set is invariant if and only if it is a union of orbits of φ .
- (b) If S is invariant under φ , then the closure \overline{S} and the complement S^c in X are also invariant sets.
- (c) The union and the intersection of any collection of invariant sets are also invariant sets.

An invariant set is said to be a maximal invariant set if it is invariant under the flow, and it is not properly contained in any other invariant subset of the system.

Definition 1.4. Let $N \subset X$ be a subset of X . The *maximal invariant set* of N is defined by

$$\text{Inv}(N, \varphi) := \{x \in X \mid \varphi(t, x) \in N, \text{ for all } t \in \mathbb{R}\}.$$

Whenever it is clear from the context which flow φ we refer to, we simply write $\text{Inv}(N)$.

Example 1.3. Let φ be a Morse–Smale flow on the 2-sphere, \mathbb{S}^2 , with two hyperbolic fixed points, namely the north pole p_N and the south pole p_S , and one attracting periodic orbit γ along the equator, as presented in Figure 1.3.

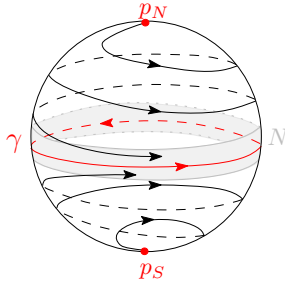


Figure 1.3: $\text{Inv}(N) = \gamma$

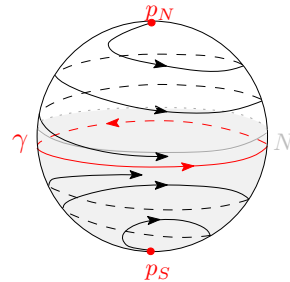


Figure 1.4: $\text{Inv}(N)$

For any compact set $N \subset \mathbb{S}^2 \setminus \{p_N, p_S\}$, the maximal invariant set of N is the periodic orbit γ . See Figure 1.3. For any compact set $N \subset \mathbb{S}^2 \setminus \{p_N\}$, the maximal invariant set of N is the bottom half of the sphere, i.e. $\gamma \cup \{p_S\} \cup W^s(p_S)$. See Figure 1.4.

The next proposition guarantees that $\text{Inv}(N)$ is indeed a maximal invariant set.

Proposition 1.2. Let $N \subseteq X$ be a subset of X .

- (a) The set $\text{Inv}(N)$ is an invariant set.
- (b) $\text{Inv}(N)$ is maximal in N with respect to this property, that is, if $P \subseteq N$ is an invariant set then $P \subseteq \text{Inv}(N)$.
- (c) If $N \subseteq X$ is compact, then $\text{Inv}(N)$ is closed in N . Hence, $\text{Inv}(N)$ is compact.

In topological dynamics, one of our goals is to study the asymptotic properties of the trajectories of the system, in particular, the behavior of the so-called limit sets.

Definition 1.5. Let φ be a continuous flow on X and $Y \subseteq X$. The ω -limit set of Y is defined as

$$\omega(Y) := \overline{\bigcap_{t>0} \varphi([t, \infty), Y)}.$$

The α -limit set of Y is defined as

$$\alpha(Y) := \overline{\bigcap_{t>0} \varphi((-\infty, t], Y)}.$$

It follows directly from the definition that ω - and α -limit sets are closed.

These sets provide information about the long-term behavior of the system. For an arbitrary set Y , the ω -limit set determines where the flow within Y is asymptotically going to and the α -limit set determines where the flow within Y is asymptotically coming from.

Example 1.4. Let φ be the Morse–Smale flow on S^2 presented in Example 1.3. One has that

$$\omega(p_N) = \omega(p_S) = \omega(\gamma) = \gamma$$

and

$$\alpha(p_N) = p_N, \quad \alpha(p_S) = p_S, \quad \alpha(\gamma) = \gamma.$$

In the particular case where Y is a single point x , one has the following: the ω -limit set of a point x is the set of all accumulation points of the trajectory of x as time goes to infinity. Intuitively, the ω -limit set $\omega(x)$ of a point x represents the set of all states that the system can approach asymptotically as time goes to infinity, starting from x . Analogously, the α -limit set $\alpha(x)$ of a point x represents the set of all states that the system can approach asymptotically as time goes to minus infinity, starting from x .

Note that two points x and y which lie on the same trajectory must have the same limit sets. Thus, we often refer to the limit set of a point as the limit set of its trajectory.

Given two subsets $Y_1, Y_2 \subseteq X$, the following equalities hold:

$$\omega(Y_1 \cup Y_2) = \omega(Y_1) \cup \omega(Y_2) \quad \text{and} \quad \alpha(Y_1 \cup Y_2) = \alpha(Y_1) \cup \alpha(Y_2).$$

Proposition 1.3. *If X is a compact Hausdorff topological space and $Y \subseteq X$ is a nonempty subset, then $\omega(Y)$ and $\alpha(Y)$ are also compact and nonempty. Moreover, if Y is connected, then $\omega(Y)$ and $\alpha(Y)$ are connected.*

The limit sets can be characterized in terms of maximal invariant sets.

Proposition 1.4. *Let φ be a continuous flow on X and $Y \subseteq X$. Then*

$$\omega(Y) = \text{Inv}\left(\overline{\varphi([0, \infty), Y)}\right) \quad \text{and} \quad \alpha(Y) = \text{Inv}\left(\overline{\varphi((-\infty, 0], Y)}\right).$$

A flow on a metric space naturally induces a flow on an invariant subset. More specifically, given an invariant set $S \subset X$, a continuous flow φ on X induces a flow on S

$$\varphi|_S : \mathbb{R} \times S \rightarrow S$$

which is continuous with respect to the subspace topology in S inherited from X . The reader can verify that if $Y \subseteq S$, then the ω -limit set of Y with respect to S is $\omega(Y) \cap S$, where $\omega(Y)$ denotes the ω -limit set of Y in X . The analogous statement also holds for the α -limit set.

The flow induced on an invariant set is an important concept in the study of dynamical systems, as it allows us to focus on the behavior of the system on specific subsets of the phase space.

For more details and proof of the propositions in this section, see Palis and de Melo (2012).

1.1.2 Gradient flows

A special case of a flow generated by a vector field is the flow associated to the gradient vector field of a real valued smooth function on a manifold. Gradient flows have important applications in optimization, in the study of partial differential equations and in the study of calculus of variations.

Let (M, g) be a closed Riemannian manifold and $f : M \rightarrow \mathbb{R}$ a smooth function. The *gradient vector field* $\nabla f : M \rightarrow TM$ is defined as the unique vector field satisfying the identity

$$g(\nabla f, \bullet) = df(\bullet).$$

The flow φ associated to the vector field $-\nabla f$ is called the *negative gradient flow* associated to f , and

$$\frac{d}{dt}\varphi(t, p) = -\nabla f(\varphi(t, p)).$$

Intuitively, the negative gradient flow moves a point in the direction of decreasing f , with the speed of motion proportional to the gradient of f at that point.

The negative gradient flow exhibits a number of key features, as we state below. First, note that given an orbit $\gamma(t) = \varphi(t, x)$, for a point $x \in M$, one has

$$\frac{d}{dt}f(\gamma(t)) = df_{\gamma(t)}(\gamma'(t)) = g(\nabla f(\gamma(t)), \gamma'(t)) = -||\nabla f(\gamma(t))||^2 \leq 0.$$

Thus:

- (a) The singularities of the vector field $-\nabla f$ are exactly the critical points of f , since

$$-\nabla f(p) = 0 \Leftrightarrow df_p = 0.$$

- (b) The function f decreases along nonsingular orbits. In fact, if $\gamma(t)$ is a nonsingular orbit, then

$$\frac{d}{dt}f(\gamma(t)) = -||\nabla f(\gamma(t))||^2 < 0.$$

- (c) The flow associated to $-\nabla f$ does not admit periodic orbits. It follows directly from the fact that f decreases along nonsingular orbits.
- (d) The limit sets of any point in M are composed by critical points of f , i.e.,

$$\alpha(p) \cup \omega(p) \subseteq \text{Crit}(f),$$

where $\text{Crit}(f)$ denotes the set of critical points of f . In fact, if $\omega(p)$ contains more than one critical point, then it necessarily contains infinitely many singularities. The proof of this fact can be found in Palis and de Melo (ibid.).

Example 1.5. Let \mathbb{S}^n be the n -dimensional sphere, i.e.

$$\mathbb{S}^n = \{(x_1, \dots, x_{n+1}) \in \mathbb{R}^{n+1} \mid x_1^2 + \dots + x_{n+1}^2 = 1\}$$

and consider the smooth function

$$f : \mathbb{S}^n \rightarrow \mathbb{R}$$

defined by $f(x_1, \dots, x_{n+1}) = x_{n+1}$, i.e. f corresponds to the height function on \mathbb{S}^n . The set of critical points of f is given by

$$\text{Crit}(f) = \{(0, \dots, 0, 1), (0, \dots, 0, -1)\},$$

which are the only singularities of the negative gradient vector field $-\nabla f$. The phase space of the corresponding negative gradient flow is represented in Figure 1.5, for the case $n = 2$.

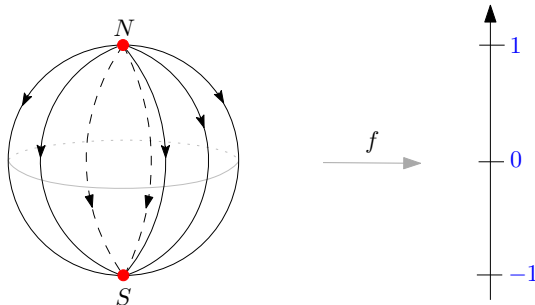


Figure 1.5: Negative gradient flow associated to the height function on \mathbb{S}^2 .

Example 1.6. Consider the function $g : \mathbb{S}^n \rightarrow \mathbb{R}$ given by the square of the height function f defined in Example 1.5, i.e. $g = f^2$. Then, the set of critical points of g is given by

$$\text{Crit}(g) = \{(0, \dots, 0, 1), (0, \dots, 0, -1)\} \cup \{(x_1, \dots, x_n, 0) \mid x_1^2 + \dots + x_n^2 = 1\},$$

which also corresponds to the singularities of the vector field $-\nabla g$. Thus, all points of the equator of \mathbb{S}^n are singularities of $-\nabla g$, hence, there are non isolated singularities. The phase space is presented in Figure 1.6.

Height functions provide a class of examples of negative gradient flows on closed manifolds. Figure 1.7 shows the negative gradient flows associated to the height functions on a deformed sphere \mathbb{S}^2 and on the torus \mathbb{T}^2 . Height functions also play an important role in Morse theory, which provides a way to study the topology of manifolds by analyzing the

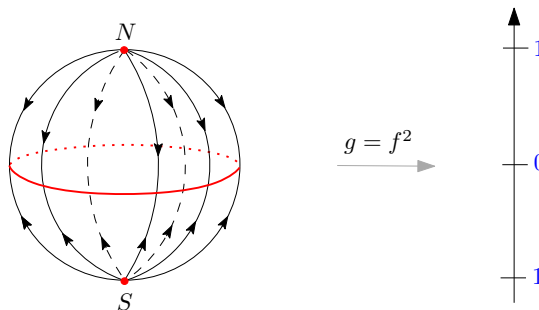


Figure 1.6: Negative gradient flow associated to the square of the height function on \mathbb{S}^2 . Non isolated singularities.

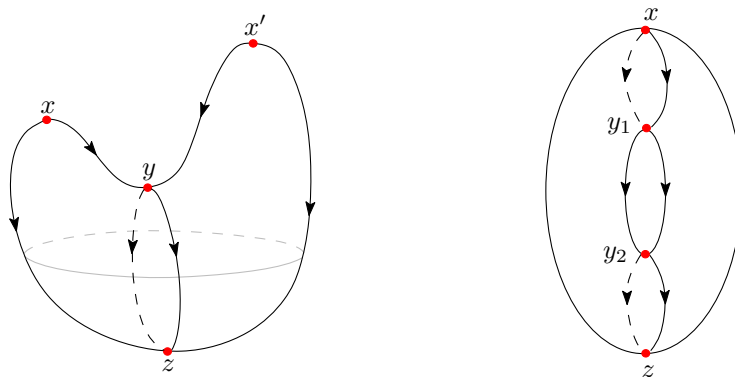


Figure 1.7: Negative gradient flows associated to height functions.

critical points of functions defined on them. We refer the reader to Banyaga and Hurtubise (2004) and Milnor (1963, 2015) for more details.

We are interested in studying further the negative gradient flow associated to a particular case of smooth function, called Morse function.

Morse functions are important in topology and differential geometry, where they play a fundamental role in the study of the topology and geometry of manifolds. In particular, the critical points of a Morse function on a manifold M can be used to construct a cell decomposition of M , yielding the so-called Morse chain complex, which encodes the homology of M (we address this chain complex in Chapter 5). Morse theory has many applications in geometry, topology, and physics.

Definition 1.6. A smooth function $f : M \rightarrow \mathbb{R}$ on a manifold M is called a *Morse function* if all its critical points are nondegenerate.

Recall that a critical point p of f is said to be nondegenerate if the Hessian matrix of f at p is nonsingular. The *Morse index* of a critical point p is defined as the number of negative eigenvalues of the Hessian matrix of f at p .

Example 1.7. The height function on \mathbb{S}^n presented in Example 1.5 is a Morse function. The square of this function, presented in Example 1.6, is not a Morse function, since the critical points on the equator are degenerate.

The Morse Lemma states that near a nondegenerate critical point of f , the function f can be approximated locally by a quadratic form whose behavior is determined by the eigenvalues of the Hessian matrix. More precisely:

Theorem 1.1 (Morse Lemma). *Let f be a smooth function on an n -manifold M , and let p be a nondegenerate critical point of f . Then, there exists a local coordinate system (x_1, x_2, \dots, x_n) around p such that f can be expressed as*

$$f(x_1, x_2, \dots, x_n) = f(p) - x_1^2 - \cdots - x_k^2 + x_{k+1}^2 + \cdots + x_n^2,$$

where k is the Morse index of k .

For the proof of the Morse Lemma, see Milnor (1963).

Note that the critical points of a Morse function are isolated. Moreover, if M is a compact manifold, then the set of critical points of f , $\text{Crit}(f)$, is finite.

A basic result of Morse theory says that almost all functions are Morse functions. More specifically, the set of Morse functions is an open and dense subset of all smooth functions $\{h : M \rightarrow \mathbb{R} \mid h \text{ is smooth}\}$ in the C^2 -topology.

Given a Morse function $f : M \rightarrow \mathbb{R}$, the negative gradient flow φ associated to the gradient vector field $-\nabla f$ presents very nice properties, as follows:

- (a) the singularities of φ are exactly the critical points of f ;
- (b) the Morse function f decreases along nonsingular orbits of φ ;
- (c) φ does not admit periodic orbits;
- (d) given any point $x \in M$, $\omega(x)$ and $\alpha(x)$ are critical points of f .

Moreover, the Morse index of a critical point p coincides with the dimension of the unstable manifold of p with respect to the negative gradient flow of a Morse function.

Definition 1.7. Let $f : M \rightarrow \mathbb{R}$ be a Morse function on M . One says that f is a *Morse–Smale function* if the flow associated to the vector field $-\nabla f$ satisfies the Morse–Smale transversality condition.

Figures 1.5 and 1.7 illustrate some negative gradient flows associated to Morse–Smale functions on surfaces.

1.1.3 Existence of Lyapunov Functions

One of the fundamental theorems in dynamical systems is the decomposition theorem proved by Conley, which states that any compact invariant set can be divided into its chain recurrent pieces and orbits that connect them. Furthermore, one can define a continuous function which is strictly decreasing outside of the chain recurrent set. In summary, the space can be decomposed into two sets such that one has recurrent dynamics and the other has a gradient-like dynamics.

In this section, we present the necessary concepts to state Conley's Fundamental Theorem of Dynamical System.

Let $\varphi : \mathbb{R} \times X \rightarrow X$ be a continuous flow on a metric space (X, d) where d is the metric on M .

Definition 1.8. A point $x \in X$ is called *chain recurrent* if for each $\epsilon > 0$ there exists a sequence of points

$$x_1 = x, x_2, \dots, x_n = x$$

in X and real numbers $t_i > 1$ such that

$$d(\varphi(t_i, x_i), x_{i+1}) < \epsilon,$$

for all $1 \leq i \leq n - 1$.

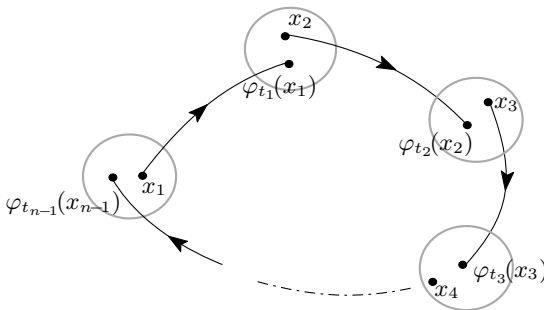


Figure 1.8: Chain recurrent point.

The set of chain recurrent points is denoted by $\mathcal{R}(\varphi)$ or simply \mathcal{R} , when the flow is clear from the context, and it is called the *chain recurrent set* of φ .

The chain recurrent set is the set of points on which complicated dynamics may take place. From the definition, it is easy to check that the chain recurrent set contains all singular orbits (rest points), all periodic orbits, homoclinic connections and maybe some other points as well. Moreover, $\mathcal{R}(\varphi)$ is invariant under φ , and if X is compact then $\mathcal{R}(\varphi)$ is closed (hence compact).

Definition 1.9. Let $\varphi : \mathbb{R} \times X \rightarrow X$ be a continuous flow on a metric space.

- (a) A flow on X is called a *chain recurrent flow* if its chain recurrent set is the whole space, i.e. $\mathcal{R}(\varphi) = X$.
- (b) A flow φ is called a *gradient-like* flow if there exists a continuous real valued function $g : X \rightarrow \mathbb{R}$ which is strictly decreasing on nonsingular orbits.
- (c) A flow is called a *strongly gradient-like* flow if its chain recurrent set is totally disconnected (consequently, it is composed only by fixed points).

Example 1.8. Any flow associated to the negative gradient vector field of a smooth function on a manifold is an example of gradient-like flow. In Section 1.1.2, we presented some examples of gradient flows.

Example 1.9. Let (r, θ) be the polar coordinates on \mathbb{R}^2 . The unit 1-sphere \mathbb{S}^1 is defined by the equation $r = 1$. Consider the vector field

$$\frac{d\theta}{dt} = \cos^2(\theta/2).$$

The phase space of the flow associated to this equation is shown in Figure 1.9. Note that there is only one fixed point, namely, the point $\theta = \pi$, which is the ω -limit set of every point in the sphere \mathbb{S}^1 . Hence, the chain recurrent set is the whole space, i.e. $\mathcal{R} = \mathbb{S}^1$, and the flow is chain recurrent.

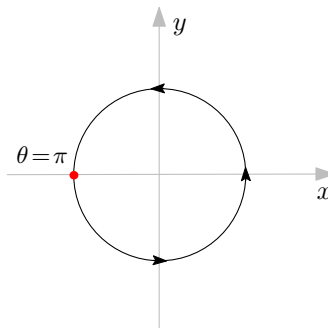


Figure 1.9: Chain recurrent flow on \mathbb{S}^1 .

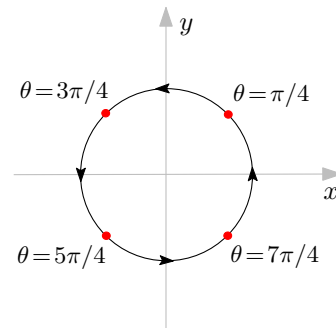


Figure 1.10: Chain recurrent flow on \mathbb{S}^1 .

Now, if we consider the vector field

$$\frac{d\theta}{dt} = \cos^2(2\theta),$$

the phase space of the flow associated to this equation is shown in Figure 1.10. The fixed points are given by the points with θ -coordinate in the set

$$\left\{ \frac{\pi}{4}, \frac{3\pi}{4}, \frac{5\pi}{4}, \frac{7\pi}{4} \right\}.$$

Once again, the chain recurrent set is the whole space, and the flow is chain recurrent.

Example 1.10. Let (r, θ) be the polar coordinates on \mathbb{R}^2 . The unit 1-sphere \mathbb{S}^1 is defined by the equation $r = 1$. Consider the vector field

$$\frac{d\theta}{dt} = \cos(\theta),$$

which is in fact the gradient vector field of the function $f(\theta) = \sin(\theta)$. The phase space of the flow φ associated to this equation is shown in Figure 1.11. The chain recurrent set is $\mathcal{R}(\varphi) = \{\pi/2, 3\pi/2\}$, hence, φ is a strongly gradient-like flow.

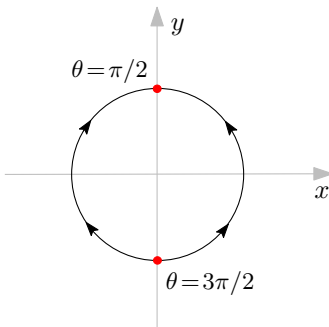


Figure 1.11: Strongly gradient-like flow on \mathbb{S}^1 .

The definition of strongly gradient-like flows is very different from the definition of gradient flow and gradient-like flow. However, they are compatible in the sense that every strongly gradient-like flow is also a gradient-like flow. This follows directly as a corollary of Conley's Fundamental Theorem of Dynamical Systems presented below.

Theorem 1.2 (Conley's Fundamental Theorem of Dynamical System). *Every flow on a compact metric space is uniquely represented as the extension of a chain recurrent flow by a strongly gradient-like flow.*

In other words, every flow φ on a compact metric space X admits a unique subflow which is chain recurrent and such that the quotient flow is strongly gradient-like. More specifically, the flow obtained by restricting the original flow φ to every component of the chain recurrent set $\mathcal{R}(\varphi)$ becomes a chain recurrent subflow. By considering the quotient

space X/\sim after collapsing the connected components of $\mathcal{R}(\varphi)$ to distinct points, the flow φ on X induces a quotient flow on the quotient space X/\sim and this flow is in fact a strongly gradient-like flow.

In summary, the unique chain recurrent subflow is given by the restriction to the chain recurrent set; and the quotient flow is the one obtained by collapsing the connected components of the chain recurrent set to distinct points.

Example 1.11. Let φ be the negative gradient flow associated to the square of the height function on S^2 , defined in Example 1.6 for the case $n = 2$. The chain recurrent set $\mathcal{R}(\varphi)$ consists of the north and south poles and all points of the equator. Hence, φ is not a strongly gradient-like flow. However, one can obtain a strongly gradient-like flow by considering the quotient flow on S^2/\sim , as presented in Figure 1.12.

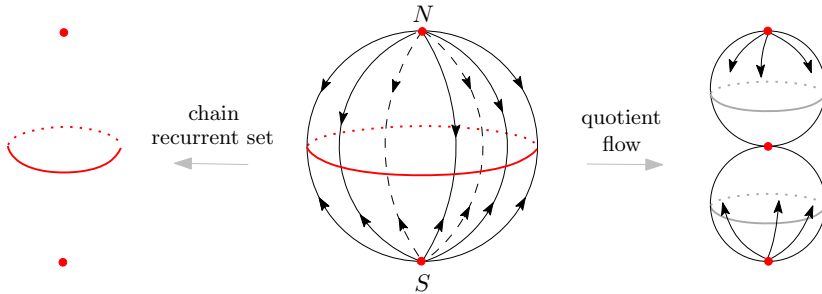


Figure 1.12: Strongly gradient-like flow induced on the quotient space S^2/\sim .

The Conley's Fundamental Theorem can also be presented in terms of the existence of special functions, known as Lyapunov functions.

Definition 1.10. Given a continuous flow φ on X , a *Lyapunov function* for φ is a continuous function $f : X \rightarrow \mathbb{R}$ such that

- (a) f strictly decreases along orbits outside $\mathcal{R}(\varphi)$, that is, if $x \notin \mathcal{R}(\varphi)$, then $f(\varphi(t, x)) < f(\varphi(s, x))$ whenever $t > s$;
- (b) f is constant on the connected components of $\mathcal{R}(\varphi)$.

Proposition 1.5. Let f be a smooth function on a smooth manifold M and let φ be the negative gradient flow associated to f , i.e., φ is generated by the vector field $-\nabla f$. Then f is a Lyapunov function for φ and φ is a gradient-like flow.

Proof. It follows directly from the properties of negative gradient flows presented in Section 1.1.2. \square

One can restate the Conley's Fundamental Theorem in terms of the existence of Lyapunov functions as follows:

Theorem 1.3. *Every continuous flow φ on a compact metric space X admits a Lyapunov function $f : X \rightarrow \mathbb{R}$ such that:*

- (a) $f(\mathcal{R}(\varphi))$ is a nowhere dense subset of \mathbb{R} ;
- (b) if $c \in f(\mathcal{R}(\varphi))$ then $f^{-1}(c) \cap \mathcal{R}(\varphi)$ is a chain recurrent component.

The main reference for the proof of the Conley's Fundamental Theorem of Dynamical Systems is Conley's monograph (see Conley 1978). Franks (1988) proved the corresponding result in the case of diffeomorphisms. Hurley extended some of Conley's results to noncompact sets (see Hurley 1991, 1992).

By Conley's Fundamental Theorem of Dynamical Systems, the problem of obtaining a qualitative description of a flow is divided into two parts:

- the description of the connected components of the chain recurrent set;
- the description of how these components are connected to each other.

In the next section, we define the Conley index, a topological invariant which provides a topological description of the local dynamics around the Morse sets associated to a Morse decomposition of a given isolated invariant set. The connection matrices introduced by Franzosa (1989) are algebraic-topological tools which enable us to study the connections between Morse sets. Roughly speaking, a connection matrix for a Morse decomposition is a matrix which has as entries homomorphisms between the homology Conley indices of Morse sets. We refer the reader to Franzosa (1989), Lima and de Rezende (2016), and Reineck (1990, 1995) for more details on connection matrix theory.

1.2 Conley index

The Conley index is a topological invariant that captures the structure of an isolated invariant set of a dynamical system. It is named after the mathematician Charles Conley, who developed this theory in the 1970's.

For simplicity, we restrict ourselves to locally compact metric spaces. In this setting, most of the essential ideas can be explained without too many technical details. From now on, let X be a locally compact metric space.

To study and understand invariant sets, one can analyze the topological features of a specific region surrounding them, known as an isolating neighborhood, which contains the invariant set. By examining the properties of this isolating neighborhood, we gain insight into the behavior and structure of its maximal invariant set, as well as the dynamics of the system as a whole.

Definition 1.11. A subset $S \subset X$ is called an *isolated invariant set* if there exists a compact neighborhood N of S in X such that $S \subset \text{int}(N)$ and $S = \text{Inv}(N)$. In this case, N is said to be an *isolating neighborhood* for S in X .

Note that isolated invariant sets are compact sets, since they are closed sets contained in a compact set.

If N is an isolating neighborhood for an invariant set S , then any smaller compact neighborhood of S is also an isolating neighborhood.

Example 1.12 (Isolated fixed point). Consider the flow φ_i on \mathbb{R}^2 generated by the vector field V_i , for $i = 0, 1, 2$, given by:

$$V_0 = \begin{cases} \dot{x}_1 = -x_1 \\ \dot{x}_2 = -x_2 \end{cases}, \quad V_1 = \begin{cases} \dot{x}_1 = x_1 \\ \dot{x}_2 = -x_2 \end{cases}, \quad V_2 = \begin{cases} \dot{x}_1 = x_1 \\ \dot{x}_2 = x_2. \end{cases}$$

In the three cases, the origin point $(0, 0)$ is a fixed point and $S = \{(0, 0)\}$ is an invariant set. The square $N = [-1, 1] \times [-1, 1]$ is an isolating neighborhood for S . Hence, S is an isolated invariant set. The phase space of these flows is shown in Figure 1.13.

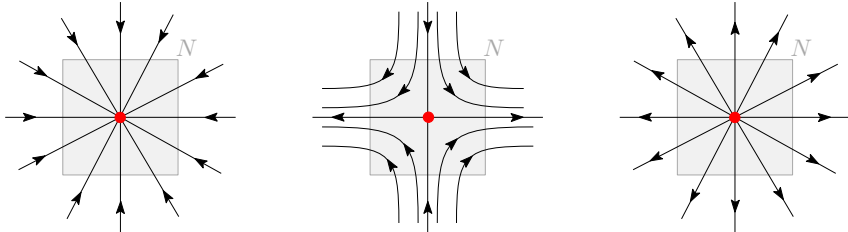


Figure 1.13: Fixed points: attracting, saddle and repelling fixed points.

There exist sets which are invariant under the flow, but they are not isolated, as the next example shows.

Example 1.13 (Center fixed point). Consider the flow on \mathbb{R}^2 associated to the vector field

$$\begin{cases} \dot{x}_1 = -x_2, \\ \dot{x}_2 = x_1. \end{cases}$$

The origin $(0, 0)$ is a rest point and $S = \{(0, 0)\}$ is an invariant set. However, S is not isolated. Indeed, there is no isolating neighborhood that has the center fixed point as its invariant set, since every neighborhood intersects some periodic orbits around $(0, 0)$.

The previous example shows that a rest point may be isolated as a rest point, but not isolated as an invariant set. On the other hand, an isolated rest point of a gradient-like system is also isolated as an invariant set.

The next result guarantees that the collection of isolated invariant sets is closed under finite intersections and finite disjoint unions.

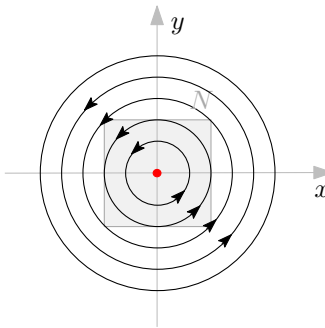


Figure 1.14: The center fixed point is not isolated.

Proposition 1.6.

- (a) *The intersection of two isolated invariant sets is isolated.*
- (b) *The union of disjoint isolated invariant sets is isolated.*

Proof. Let S_1 and S_2 be isolated invariant sets.

- (a) Clearly, $S_1 \cap S_2$ is an invariant set. Given isolating neighborhoods N_1 and N_2 for S_1 and S_2 , respectively, the intersection $N_1 \cap N_2$ is an isolating neighborhood for $S_1 \cap S_2$.
- (b) Now, suppose that $S_1 \cap S_2 = \emptyset$. Choose disjoint isolating neighborhoods N_1 and N_2 for S_1 and S_2 , respectively. Then, $N_1 \cup N_2$ is an isolating neighborhood for $S_1 \cup S_2$.

□

In general, the union of two isolated invariant sets is not isolated. For instance, consider a flow on the disk having three fixed points, as shown in Figure 1.15. Let S_1 be the invariant set composed by the fixed points a and b and the only trajectory connecting them. Analogously, denote by S_2 the invariant set composed by the fixed points b and c and the only trajectory connecting them. Hence, S_1 and S_2 are isolated invariant sets. However, $S_1 \cup S_2$ is not isolated.

Remark 1.1. *The most important property of an isolating neighborhood is that it is robust with respect to small perturbations. More specifically, if N is an isolating neighborhood for a flow, then it is still an isolating neighborhood for every sufficiently small perturbation of it. Of course, the maximal invariant set inside N can change in this process.*

The concept of an index pair plays a crucial role in the definition of the Conley index for isolated invariant sets.

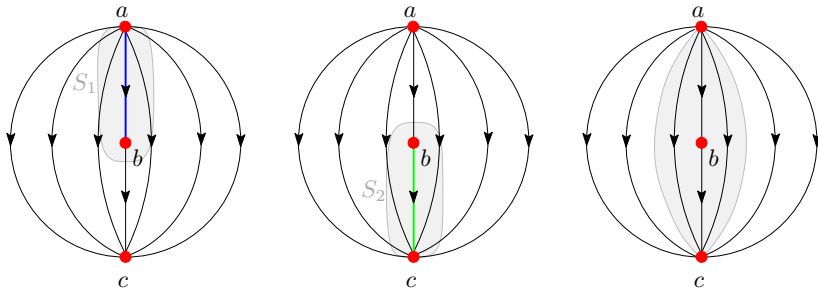


Figure 1.15: A flow on the disc. Union of isolated invariant sets may not be isolated.

Definition 1.12. Let $S \subseteq X$ be an isolated invariant set. A pair (N, L) of compact sets in X is said to be an *index pair* for S in X if $L \subset N$ and

- (a) $\overline{N \setminus L}$ is an isolating neighborhood for S in X ;
- (b) L is *positively invariant* in N , i.e., if $x \in L$ and $\varphi([0, T], x) \subset N$ then $\varphi([0, T], x) \subset L$;
- (c) L is the *exit set* of the flow in N , that is, if $x \in N$ and $\varphi([0, \infty), x) \not\subseteq N$ then there exists $T > 0$ such that $\varphi([0, T], x) \subset N$ and $\varphi(T, x) \in L$.

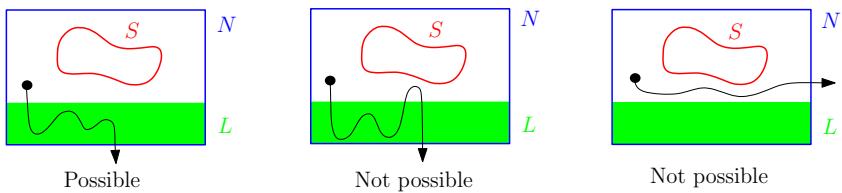
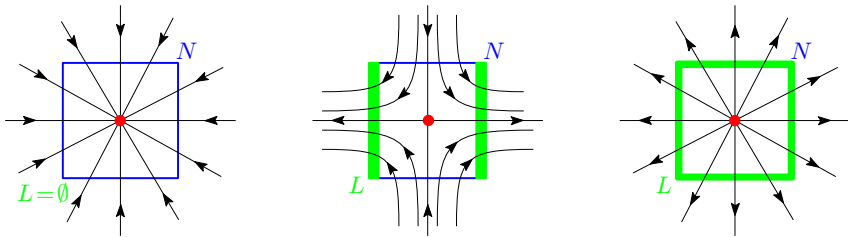
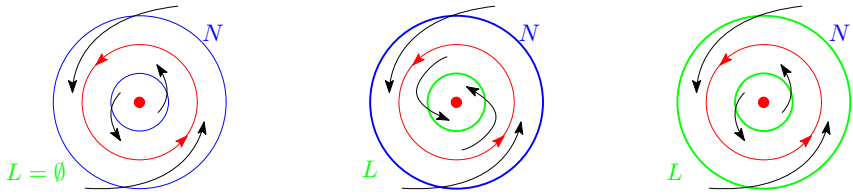


Figure 1.16: Local behavior around an index pair.

The basic idea is that the pair (N, L) of compact sets form an isolating neighborhood for the invariant set S , meaning that S is the maximal invariant set inside $\overline{N \setminus L}$. Moreover, L is the exit set for the local flow. This is the crucial property of the index pair, which states that every orbit which leaves N in forward time has to go through the exit set L before leaving N , see Figure 1.16.

Example 1.14. Consider the hyperbolic fixed points on the plane, as in Example 1.12. In Figure 1.17, we show index pairs for these isolated invariant sets.

Example 1.15. In Figure 1.18, we show some index pairs for isolated periodic orbits in the plane.

Figure 1.17: Index pair for hyperbolic fixed points in \mathbb{R}^2 .Figure 1.18: Index pair for periodic orbits in \mathbb{R}^2 .

The next result guarantees that we can always find an index pair for a given isolated invariant set.

Theorem 1.4 (Existence of index pairs - Conley and Easton (1971)). *Let $S \subseteq X$ be an isolated invariant set with respect to the flow φ . There exist compact sets N and L such that (N, L) is an index pair for S .*

The existence of index pairs (Theorem 1.4) is also proved by Salamon (1985), in the more general setting of connected simple systems.

In fact, given an isolating neighborhood of an isolated invariant set, there is always an index pair inside of it. More specifically, given any isolating neighborhood $N \subseteq X$ of S and any neighborhood U of S , there exists an index pair (N_1, N_0) for S in X such that N_1 and N_0 are positively invariant in N and $cl(N_1 \setminus N_0) \subseteq U$.

There are some special index pairs, called *isolating blocks* and denoted by (N, N^-) , which are characterized by the property that the trajectory through each point in N^- immediately leaves N in positive time.

Definition 1.13. An *isolating block* for $S \subseteq X$ is an isolating neighborhood N for S such that its entering and exiting sets, given respectively by

$$N^+ = \{x \in N \mid \phi([0, T], x) \not\subseteq N, \forall T < 0\}$$

$$N^- = \{x \in N \mid \phi([0, T], x) \not\subseteq N, \forall T > 0\},$$

are both closed.

Given an isolating block N for S , one has that (N, N^-) is an index pair for S . Therefore, isolating blocks provide special index pairs.

Example 1.16. Consider S a hyperbolic fixed point of saddle type. In Figure 1.19 we show an index pair and an isolating block for S .

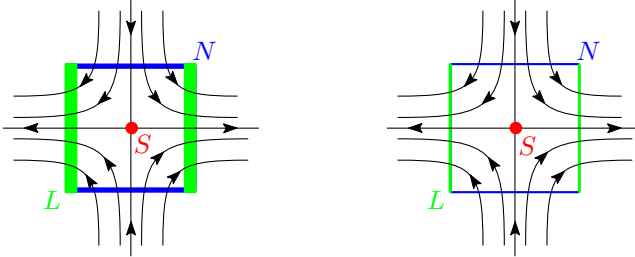


Figure 1.19: On the left, an index pair. On the right, an isolating block.

1.2.1 Homotopy Conley Index

In order to introduce the homotopy Conley index, it is necessary to review some basic concepts from homotopy theory.

A *pointed space* (Y, y_0) is a topological space Y with a distinguished point $y_0 \in Y$, which is called a *base point*.

Given a pair (N, L) of topological spaces with $L \subset N$ and $L \neq \emptyset$, consider the following equivalence relation:

$$x \sim y \Leftrightarrow \begin{cases} x = y \\ \text{or} \\ x, y \in L. \end{cases} \quad (1.1)$$

Let $N/\sim = \{[x] \mid x \in N\}$ be the quotient space with the quotient topology. More specifically, if $q : N \rightarrow N/\sim$ is the quotient map, the topology on N/\sim is defined as follows: a set $U \subseteq N/\sim$ is open iff $q^{-1}(U)$ is open in N . From a set point of view, there is a natural identification between N/\sim and $(N \setminus L) \cup [L]$.

Definition 1.14. Given a pair (N, L) of topological spaces with $L \subset N$ and $L \neq \emptyset$, denote by N/L the pointed space $(N/\sim, [L])$, where $[L]$ represents the equivalence class of the points in L under the equivalence relation defined in (1.1).

If $L = \emptyset$, it is a convention to consider $N/L = (N \cup \{\ast\}, \{\ast\})$, where $\{\ast\}$ denotes the equivalence class of the empty set.

Let (X, A) and (Y, B) be pairs of topological spaces such that $A \subseteq X$ and $B \subseteq Y$. The pairs (X, A) and (Y, B) are *homotopically equivalent* if there exist maps $f : (X, A) \rightarrow$

(Y, B) and $g : (Y, B) \rightarrow (X, A)$ such that $f(A) \subseteq B$, $g(B) \subseteq A$, $g \circ f$ is homotopic to $id_{(X, A)}$ and $f \circ g$ is homotopic to $id_{(Y, B)}$. Intuitively, two pairs of topological spaces are homotopically equivalent if they can be deformed into each other in a way which respects the distinguished subsets.

Note that homotopy equivalence of pairs is in fact an equivalence relation, and the equivalent classes of this relation are called *homotopy types*.

In this book, we use the following notation:

- the homotopy type of the pointed one-point space is denoted by $\bar{0}$;
- the homotopy type of the pointed two-point space is denoted by $\bar{1}$ or Σ^0 ;
- the homotopy type of a pointed n -sphere, for $n \geq 1$, is denoted by Σ^n .

Let S be an isolated invariant set with respect to the flow φ . The most important property of index pairs is that the homotopy type of the pointed space N/L is independent of the choice of the index pair, and therefore it depends only on the behavior of the flow near the isolated invariant set S .

Theorem 1.5 (Invariance of index pairs Conley and Easton (1971)). *Let S be an isolated invariant set with respect to the flow φ . If (N, L) and (\bar{N}, \bar{L}) are index pairs for S , then N/L and \bar{N}/\bar{L} have the same homotopy type.*

The invariance of index pairs (Theorem 1.5) is also proved by Salamon (1985), in the more general setting of connected simple systems.

Finally, we can define the Conley index as follows:

Definition 1.15. Let S be an isolated invariant set with respect to the flow φ . The *Homotopy Conley Index* of S is defined as the homotopy type of the pointed space N/L , where (N, L) is an index pair S . The homotopy Conley index of S is denoted by $h(S)$.

Example 1.17. Let S be the disjoint union of two hyperbolic saddle points with no connection between them. An index pair for S is depicted in Figure 1.20 as well as the homotopy type of the pointed space N/L , which is the homotopy Conley index of S .

We can make use of the Conley index to show the existence of a nonempty invariant subset in the phase space. The next result guarantees that if the Conley index of S is nontrivial, then S is nonempty.

Proposition 1.7 (Ważewski property). *Let S be an isolated invariant set with respect to a flow φ . If $h(S) \neq \bar{0}$ then $S \neq \emptyset$.*

Proof. Suppose that $S = \emptyset$. In this case, S is an isolating invariant set by vacuity and (\emptyset, \emptyset) is an index pair for S . Hence, $h(S) = \bar{0}$. By a contrapositive argument, it follows that if $h(S) \neq \bar{0}$ (the homotopy class of the one-point pointed space) then $S \neq \emptyset$. \square

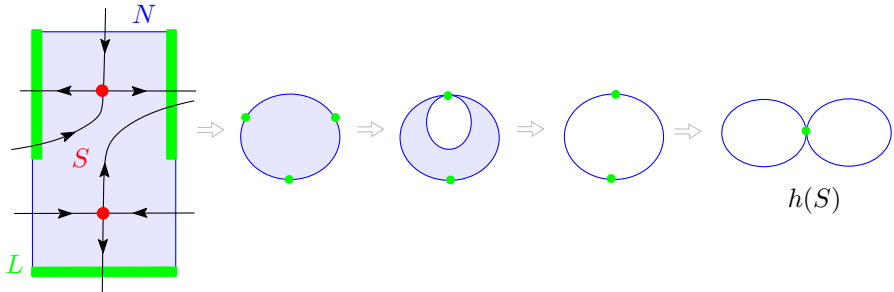


Figure 1.20: Homotopy type of the quotient space N/L .

The Ważewski property indicates that the Conley index contains information about the dynamics of an invariant set and its relation with any isolating neighborhood around it: knowledge about the dynamics on the boundary of an isolating neighborhood can be enough to determine if the dynamics within is nontrivial.

This result provides the simplest example of an existence result of an invariant set which can be obtained via the Conley index. Its converse is not true, that is, if S is not empty, it does not mean that it has nontrivial Conley index. For instance, let S be the nonhyperbolic fixed point in Figure 1.21. In this case, S is an isolated invariant set and its homotopy Conley index is trivial, i.e. $h(S) = \bar{0}$.

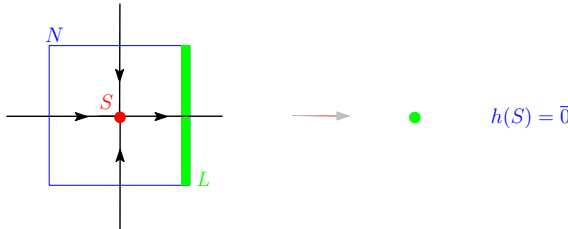


Figure 1.21: Homotopy Conley index of a nonhyperbolic fixed point.

Example 1.18 (The Conley index is “blind”). A compact pair (N, L) can be an index pair for more than one isolated invariant set. For instance, in Figure 1.22, we present different isolated invariant sets which admit the same isolating neighborhood: a nonhyperbolic saddle point, the union of two hyperbolic saddles together with a connecting orbit between them, and the union of two hyperbolic saddles with no connection.

Therefore, the Conley index loses dynamical information on the isolated invariant set itself. In other words, one can not immediately infer the dynamical structure of the isolated invariant set, given only its Conley index. Certainly, the Conley index carries information about the instability of the isolated invariant set in its surroundings.

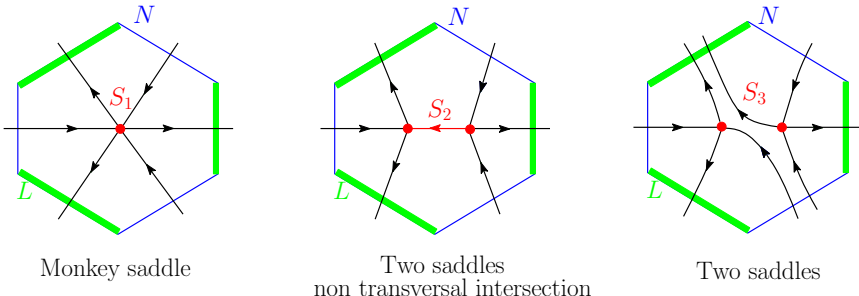


Figure 1.22: Different isolated invariant sets which admit the same isolating neighborhood.

The usefulness of the Conley index depends on how much information about the structure of the dynamics of the invariant set can be concluded from knowledge of the Conley index. Even though the Conley index captures little information on the structure of the invariant set itself, it does so in its surroundings: it captures the topology of the unstable region nearby S , and how this set fits within this local dynamics.

For example, in the case of gradient flows, the Conley index provides the dimension of the unstable manifolds of the critical points.

Example 1.19 (Homotopy Conley index of nondegenerate critical points). Consider a Morse function $f : \mathbb{R}^n \rightarrow \mathbb{R}$ and let p be a critical point of Morse index k . It follows from the Morse Theorem 1.1 that $S = \{p\}$ is an isolated invariant set. Without loss of generality, assume that p is the origin of \mathbb{R}^n and that $N = D^k \times D^{n-k}$ is an isolating neighborhood for S . Let $L = \partial D^k \times D^{n-k}$. Hence, (N, L) is an index pair for p . Note that,

$$(N, L) \simeq (D^k, \partial D^k).$$

Indeed, the flow provides a homotopy that contracts the space along the stable directions.

Thus, the Conley index of p has the homotopy type of a k -sphere, in other words, $h(p) = \Sigma^k$. Therefore, the homotopy Conley index of a nondegenerate critical point of Morse index k is the homotopy type of a k -sphere.

For the more general case of a flow on a smooth manifold with a hyperbolic rest point p , the hyperbolicity condition guarantees that near p the linear flow can be decomposed into stable and unstable linear spaces $T_x M = E^s \oplus E^u$, and due to Hartman–Grobman Theorem, the linear flow is locally topologically conjugate to the nonlinear one. Hence, the proof follows from the linear case.

On the other hand, it is interesting to note that it may be possible to compute the Conley index of an invariant set S , even if one still has not found S . In fact, it is entirely possible that we recognize a compact set as an isolating neighborhood without having any a priori

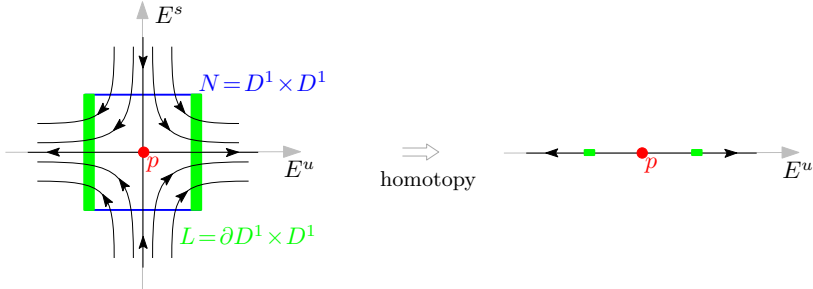


Figure 1.23: Homotopy: $(N, L) \simeq (D^k, \partial D^k)$.

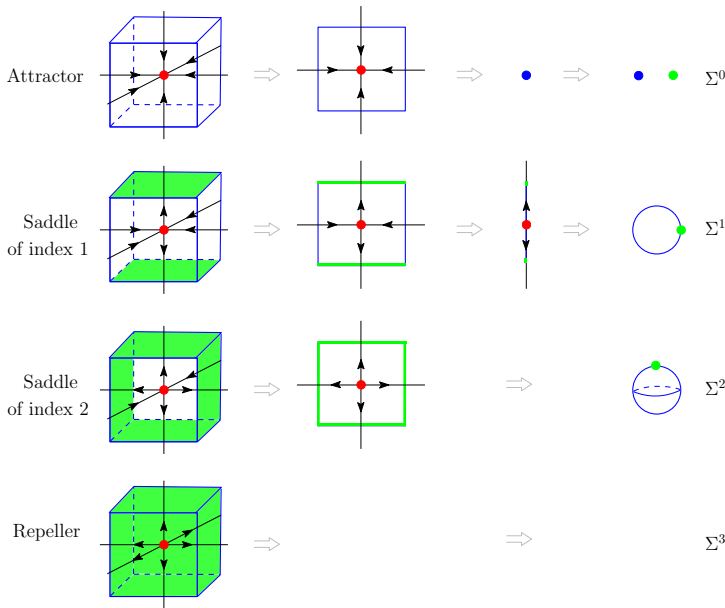


Figure 1.24: Index pair and the Conley index for hyperbolic singularities in \mathbb{R}^3 .

knowledge about the invariant set. Hence, one investigates properties of the invariant set in terms of its Conley index.

1.2.2 Sum and Product of the Conley Index

As we have shown in Proposition 1.6, the intersection and the disjoint union of isolated invariant sets are invariant sets. It is natural to ask if there is any relation between the

Conley indices of the intersection and of the disjoint union of isolated invariant sets with the Conley indices of each one of these invariant sets. This question is complicated for intersections, but for disjoint unions one can establish a simple relation.

In this section, we show how to compute the Conley indices of the disjoint union of isolated invariant sets from the Conley indices of each of these invariant sets. In order to do that, we need to recall some homotopical operations: the wedge sum and the smash product.

Definition 1.16. Given two pointed spaces (X, x_0) and (Y, y_0) , the *wedge sum* of X and Y is defined as the quotient space of their disjoint union by the identification $x_0 \sim y_0$, i.e.,

$$X \vee Y := (X \sqcup Y) / \{x_0 \sim y_0\}.$$

The wedge sum is also a pointed space with distinguished basepoint being the equivalence class of $x_0 \sim y_0$, and the binary operation \vee is associative and commutative (up to homeomorphism).

Moreover, there is a canonical basepoint respecting map $X \vee Y \rightarrow X \times Y$ which maps the wedge sum $X \vee Y$ homeomorphically onto the subspace given by $X \times y_0 \cup x_0 \times Y$, i.e.

$$X \vee Y \cong X \times y_0 \cup x_0 \times Y \subseteq X \times Y.$$

It is frequently useful to consider the identification $X \vee Y \equiv X \times y_0 \cup x_0 \times Y$.

Example 1.20. The wedge sum of two 1-spheres is homeomorphic to a figure-eight space. The wedge sum of arbitrary spheres is often called a bouquet of spheres. See Figure 1.25.

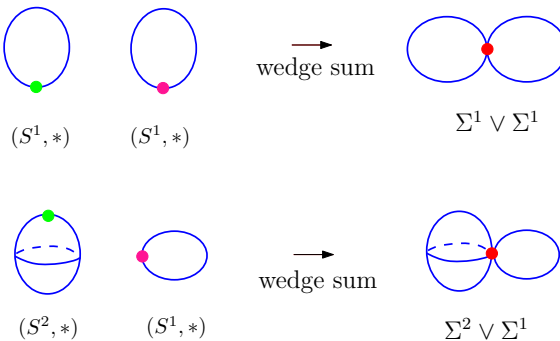


Figure 1.25: Wedge sum of spheres.

The wedge sum operation is well defined on the homotopy equivalence classes of pointed spaces:

$$[(X, x_0)] \vee [(Y, y_0)] := [(X \vee Y)].$$

For instance, the wedge sum of a pointed 1-sphere and an interval is homotopic to the wedge sum of a pointed 1-sphere and a point. Moreover, the wedge sum is an associative and commutative binary operation on the homotopy equivalence classes. The additive neutral element for this operation corresponds to the homotopy class of the one-pointed space, $\bar{0}$. There are no additive inverses. Indeed, if $[(X, x_0)] \vee [(Y, y_0)] = \bar{0}$ then $[(X, x_0)] = [(Y, y_0)] = \bar{0}$.

Definition 1.17. Given two pointed spaces (X, x_0) and (Y, y_0) , the *smash product* of X and Y is defined as the quotient space of the product space by the equivalence relation $(x, y_0) \sim (x_0, y)$, i.e.,

$$X \wedge Y := X \times Y / \{X \times y_0 \cup x_0 \times Y\}.$$

The smash product is also a pointed space with distinguished basepoint being the equivalence class of (x_0, y_0) . The following identification holds:

$$X \wedge Y = X \times Y / X \vee Y.$$

Example 1.21. The smash product of any pointed space X with a 0-sphere is homeomorphic to X , that is, $X \wedge S^0 \cong X \cong S^0 \wedge X$. See Figure 1.26.

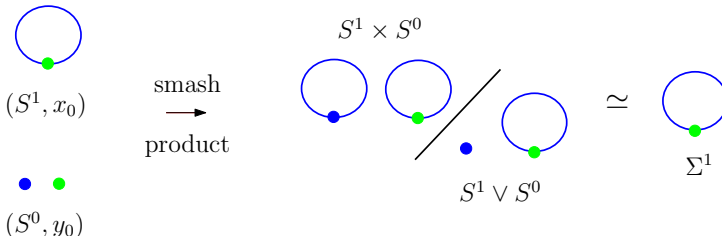


Figure 1.26: Smash product of a 2-sphere and a 0-sphere.

In general, the smash product depends on the choice of basepoints.

The smash product is not always so well-behaved as the Cartesian product, but it still enjoys the following properties.

Proposition 1.8. Let X, Y and Z be pointed spaces.

- (a) The smash product is commutative. More specifically, there is a natural homeomorphism $X \wedge Y \cong Y \wedge X$.
- (b) The product distributes over the sum. More specifically, there is a natural homeomorphism $(X \vee Y) \wedge Z \cong (X \wedge Z) \vee (Y \wedge Z)$.
- (c) If either X, Y are compact, or X, Z are locally compact, then there is a homeomorphism $(X \wedge Y) \wedge Z \cong X \wedge (Y \wedge Z)$.

(d) There are homeomorphisms $X \wedge * \cong * \cong * \wedge X$.

The next result guarantees that the collection of m -spheres are closed under the smash product.

Proposition 1.9.

- (a) The smash product of two spheres \mathbb{S}^m and \mathbb{S}^n is homeomorphic to the sphere \mathbb{S}^{m+n} , i.e. $\Sigma^m \wedge \Sigma^n = \Sigma^{m+n}$.
- (b) The smash product of a space X with a 1-sphere is homeomorphic to the reduced suspension of X , i.e. $\Sigma X \cong X \wedge \mathbb{S}^1$.

The smash product operation is well-defined on the homotopy equivalence classes:

$$[(X, x_0)] \wedge [(Y, y_0)] := [(X \wedge Y)].$$

The multiplicative identity for this operation is $\bar{1}$, the two-pointed space. However, note that $[(X, x_0)] \wedge [(Y, y_0)] = \bar{0}$ and $[(X, x_0)] \neq \bar{0} \neq [(Y, y_0)]$.

Now, given compact pairs (N, L) and (N', L') with $L \subseteq N$ and $L' \subseteq N'$, we can consider the pointed spaces N/L and N'/L' , thus the wedge sum of the corresponding homotopy classes is

$$[N/L] \vee [N'/L'] = [N \sqcup N'/L \sqcup L'],$$

and the smash product is

$$[N/L] \wedge [N'/L'] = [N \times N' / (N \times L' \cup L \times N')].$$

Now we are ready to prove that the Conley index of the disjoint union of isolated invariant sets is the wedge sum of the Conley indices of each of these invariant sets.

Proposition 1.10. *The homotopy Conley index of the disjoint union of isolated invariant sets is the wedge sum of their homotopy Conley indices.*

Proof. Let S_1 and S_2 be isolated invariant sets such that $S_1 \cap S_2 = \emptyset$. Choose index pairs (N_1, L_1) and (N_2, L_2) for S_1 and S_2 , respectively, such that N_1 and N_2 are disjoint. Note that $(N_1 \sqcup N_2, L_1 \sqcup L_2)$ is an index pair for $S_1 \sqcup S_2$. Therefore,

$$\begin{aligned} h(S_1) \vee h(S_2) &= [N_1/L_1] \vee [N_2/L_2] \\ &= [N_1 \sqcup N_2 / L_1 \sqcup L_2] \\ &= h(S_1 \sqcup S_2). \end{aligned}$$

□

Proposition 1.11. *The product of isolated invariant sets is isolated, and the homotopy Conley index is the smash product of the indices of its factors.*

Proof. Let S_1 and S_2 be isolated invariant sets with respect to the flows φ_1 and φ_2 on X_1 and X_2 , respectively. We want to prove that $S_1 \times S_2$ is an isolated invariant set with respect to the product flow $\varphi_1 \times \varphi_2$ on $X_1 \times X_2$, and $h(S_1 \times S_2) = h(S_1) \wedge h(S_2)$. Let N_i be an isolating neighborhood for S_i , for $i = 1, 2$. Then $N_1 \times N_2$ is an isolating neighborhood for $S_1 \times S_2$. If (N_i, L_i) is an index pair for S_i , for $i = 1, 2$, then

$$(N_1 \times N_2, N_1 \times L_2 \cup L_1 \times N_2)$$

is an index pair for $S_1 \times S_2$. Then,

$$h(S_1 \times S_2) = \left[\frac{N_1 \times N_2}{N_1 \times L_2 \cup L_1 \times N_2} \right] = \left[\frac{N_1}{L_1} \right] \wedge \left[\frac{N_2}{L_2} \right] = h(S_1) \wedge h(S_2).$$

□

Example 1.22 (Conley index of nondegenerate critical points). Using Proposition 1.11, we can give an alternative proof of the homotopy Conley index of a nondegenerate critical point as follows. Given a critical point x of Morse index k in \mathbb{R}^n , consider the splitting $\mathbb{R}^k \times \mathbb{R}^{n-k} = \mathbb{R}^n$. Consider a repelling singularity p_1 in \mathbb{R}^k and an attracting singularity in \mathbb{R}^{n-k} . The product of these two isolated invariant sets give rise to an index k singularity x in \mathbb{R}^n . The Conley index of $S = \{x\}$ is given by the smash product of $\Sigma^k \wedge \Sigma^0 = \Sigma^k$. See Figure 1.24.

Proposition 1.12 (Conley index of an orientable hyperbolic periodic orbit). *Given an orientable hyperbolic periodic orbit γ_k of index k , the homotopy Conley index of γ_k is $\Sigma^k \vee \Sigma^{k+1}$.*

Proof. Consider an orientable hyperbolic periodic orbit γ_k of index k . Since γ_k is hyperbolic, $S = \{\gamma_k\}$ is an isolated invariant set. Let N be a small tubular neighborhood of γ which is also an isolating neighborhood, thus

$$N = D^{n-k-1} \times \mathbb{S}^1 \times D^k.$$

Let

$$L = D^{n-k-1} \times \partial(\mathbb{S}^1 \times D^k) = D^{n-k-1} \times \mathbb{S}^1 \times \partial D^k.$$

Hence, (N, L) is an index pair for γ_k . See Figure 1.27. Note that there is a homotopy of pairs

$$(N, L) \simeq (\mathbb{S}^1 \times D^k, \mathbb{S}^1 \times \partial D^k).$$

Indeed, consider a homotopy of the pair (N, L) by flowing the stable directions of the flow. Under this homotopy, $\mathbb{S}^1 \times D^k$ corresponds to the tubular neighborhood of γ in the

center-unstable manifold E^{cu} . The exit set is $\mathbb{S}^1 \times \partial D^k$, since after the homotopy there is no more stable direction. It follows the required homotopy of pairs. Finally,

$$h(\gamma) = \left[\frac{\mathbb{S}^1 \times D^k}{\mathbb{S}^1 \times \partial D^k} \right] = \Sigma^k \vee \Sigma^{k+1},$$

which coincides with the homotopy type of an $(n + 1)$ -dimensional pinched torus. \square

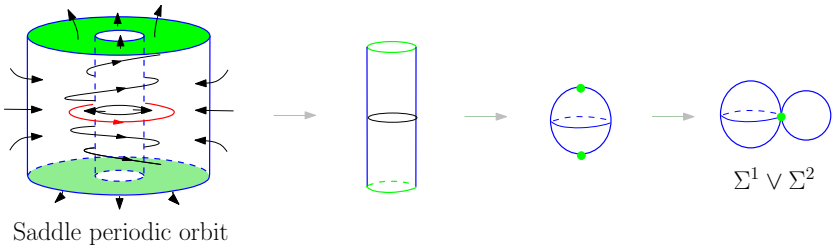


Figure 1.27: Computing the Conley index for an orientable hyperbolic saddle periodic orbit in \mathbb{R}^3 .

Proposition 1.13 (Conley index of a non orientable hyperbolic periodic orbit). *Given a non orientable hyperbolic periodic orbit γ_k of index k , the homotopy Conley index of γ_k is given by $(\mathbb{RP}^2 \sqcup \{*\}, *) \wedge (\mathbb{S}^{k-1}, *)$.*

1.2.3 Homology Conley Index

The homotopy Conley index is defined as the homotopy type of a pointed topological space. Working with homotopy classes of spaces can be extremely difficult. Hence, it is useful to consider the homological version of the Conley index, defined as follows.

Definition 1.18. Let S be an isolated invariant set with respect to the flow φ and let (N, L) be an index pair for S . The *homology Conley index* of S is defined as

$$CH_*(S, \varphi) := \widetilde{H}_*(N/L),$$

where $\widetilde{H}_n(N/L)$ denotes the n -the reduced homology group of the pointed space $(N/\sim, [L])$.

Frequently, one also uses the notations $CH(S)$ and $H_*(h(S))$ for the homology Conley index.

The reason in considering the reduced homology in the definition of the index is simple: we want the index of a one-point pointed space to be zero, i.e., trivial in all dimensions. \square

Example 1.23 (Homology Conley index of a nondegenerate critical point). Let S be a critical point of a Morse function, with Morse index k . In Example 1.19, we proved that the homotopy Conley index of S is $h(S) = \Sigma^k$. Hence, the homology Conley index of S with coefficients in \mathbb{Z} is:

$$CH_n(S) = \begin{cases} \mathbb{Z} & , \text{ if } n = k \\ 0 & , \text{ if } n \neq k. \end{cases}$$

Example 1.24 (Homology Conley Index of a hyperbolic periodic orbit). Let S be an orientable hyperbolic periodic orbit. By Example 1.24, the homotopy Conley index of S is $\Sigma^k \vee \Sigma^{k+1}$, where k is the dimension of the unstable manifold of S . Hence,

$$CH_n(S) = \begin{cases} \mathbb{Z} & , \text{ if } n = k, k+1, \\ 0 & , \text{ if } n \neq k, k+1. \end{cases}$$

It is not always true that the reduced homology of the pointed space N/L is equal to the relative homology of the pair (N, L) . However, if (N, L) is a good pair (in the sense described in Hatcher (2002)), then the isomorphism $\widetilde{H}_*(N/L) \cong H_*(N, L)$ holds.

Recall that an inclusion map $i : A \rightarrow X$ between topological spaces is a *cofibration* if it satisfies the homotopy extension property with respect to all topological spaces Y . An index pair (N, L) is called *regular* if the inclusion map $L \subset N$ is a cofibration.

The next result shows that we can always find regular index pairs.

Theorem 1.6 (Salamon (1985)). *An index pair (N, L) can always be modified in order to create an index pair (N, L') that is regular.*

We refer the reader to Section 5.1 of Salamon (ibid.) for the proof of this theorem.

Given a regular index pair (N, L) for S , the Homology Conley index of S is given by

$$CH_*(S, \varphi) := \widetilde{H}_*(N/L) \cong H_*(N, L).$$

Hence, $H_*(N, L; \mathbb{Z})$ is an invariant associated to an isolated invariant set S whenever (N, L) is a regular pair for S .

The Ważewski property, presented in Proposition 1.7 for the homotopy Conley index, also has a homological version which states that if the homology Conley index of an isolated invariant set is nontrivial, then the dynamics within is nontrivial.

Proposition 1.14 (Ważewski property). *Let S be an isolated invariant set with respect to a flow φ . If $CH_*(S) \not\cong 0$, then $S \neq \emptyset$.*

Proof. Assume that $S = \emptyset$. Hence, S is an isolated invariant set by vacuity and (\emptyset, \emptyset) is an index pair for S . Then $CH_*(S) \cong 0$. Therefore, if $CH_*(S) \not\cong 0$ then $S \neq \emptyset$. \square

Proposition 1.15 (Additivity property). *Let S be an isolated invariant set with respect to a flow φ . If $S = S_1 \cup S_2$, where S_1 and S_2 are disjoint isolated invariant sets, then*

$$CH_*(S) \cong CH_*(S_1) \oplus CH_*(S_2).$$

Proof. It follows from Proposition 1.10 that $h(S) = h(S_1) \vee h(S_2)$. Then

$$\begin{aligned} CH_*(S) &= \widetilde{H}_*(h(S)) \\ &= \widetilde{H}_*(h(S_1) \vee h(S_2)) \\ &\stackrel{(1)}{\cong} \widetilde{H}_*(h(S_1)) \oplus \widetilde{H}_*(h(S_2)) \\ &= CH_*(S_1) \oplus CH_*(S_2). \end{aligned}$$

The isomorphism in (1) holds for any regular index pair. Since regular index pairs always exist, the result follows. \square

The contrapositive of this result is often used to prove the existence of heteroclinic connections.

The next result shows that one can detect connecting orbits of a gradient-like flow using the Conley index. A flow is said to be a *gradient-like flow* on a subset $N \subset X$ if there is a real-valued function $f : X \rightarrow \mathbb{R}$ such that if $\varphi([0, t], x) \subseteq N$ and $x \neq \varphi(t, x)$ then $f(x) < f(\varphi(t, x))$. Thus, f is strictly decreasing on nonconstant segments of orbits in N .

Theorem 1.7. *Let φ be a gradient-like flow on an isolating neighborhood N and assume that N contains precisely two rest points and at least one is nondegenerate. Let $\text{Inv}(N)$ be the maximal invariant set with respect to a flow φ . If $h(\text{Inv}(N)) = \bar{0}$, then there is an orbit connecting the two rest points.*

Proof. Denote the two rest points in N by x_1 and x_2 . It is sufficient to prove that $\text{Inv}(N)$ contains an orbit γ different from the two rest points. In fact, since $\text{Inv}(N)$ is compact, the ω - and α -limit sets of any point in $\text{Inv}(N)$ are in $\text{Inv}(N)$. Hence, if $\text{Inv}(N)$ contains a regular orbit γ , it must have as α - and ω -limits the rest points, due to the gradient-like behaviour of the flow. Thus, γ is a connecting orbit between x_1 and x_2 .

Now if $S = \text{Inv}(N)$ is made up of two rest points only, i.e. there is no connecting orbit between them, then

$$\bar{0} = h(S) = h(\{x_1\}) \vee h(\{x_2\}).$$

However, $h(\{x_1\}) \vee h(\{x_2\}) \neq \bar{0}$, by the nondegeneracy condition. \square

1.3 Invariance under continuation

Continuation is one of the most important properties in Conley index theory because it allows us to study the behavior of dynamical systems under perturbations and more generally product flows.

This is a powerful result because it allows us to make predictions about the long-term behavior of a family of dynamical systems under the variation of its parameters.

Let $\varphi_\lambda : \mathbb{R} \times X \rightarrow X$ be a parameterized family of flows on X for $\lambda \in I = [-1, 1]$, i.e. the function

$$\begin{aligned}\Phi : \mathbb{R} \times M \times I &\longrightarrow M \times I \\ (t, x, \lambda) &\longmapsto \Phi(t, x, \lambda) := (\varphi_\lambda(t, x), \lambda)\end{aligned}$$

is a continuous flow on $M \times I$.

Isolating neighborhoods are robust with respect to small perturbations, i.e., if N is an isolating neighborhood for the flow φ_a , then, for sufficiently small $\delta > 0$, N is an isolating neighborhood for φ_λ such that $\lambda \in (a - \delta, a + \delta) \cap I$.

For each $\lambda \in I$, denote by $S_\lambda := \text{Inv}(N, \varphi_\lambda)$ the maximal invariant set of N with respect to the flow φ_λ . Hence, S_λ is an isolated invariant set with respect to the flow φ_λ .

Definition 1.19. The isolated invariant sets S_{λ_0} and S_{λ_1} are *related by continuation* if N is an isolating neighborhood for φ_λ , for all $\lambda \in [\lambda_0, \lambda_1]$.

The continuation relation is an equivalence relation, hence it is transitive.

The next classical example is very helpful in order to understand the relation of continuation, and it can be found in Conley's monograph (see Conley 1978) and also in Smoller (2012).

Example 1.25. Consider the following one parameter family of differential equations:

$$\dot{x} = x(1 - x^2) - \lambda,$$

where λ is the parameter. The critical points of this equation is given by the zero set of the function

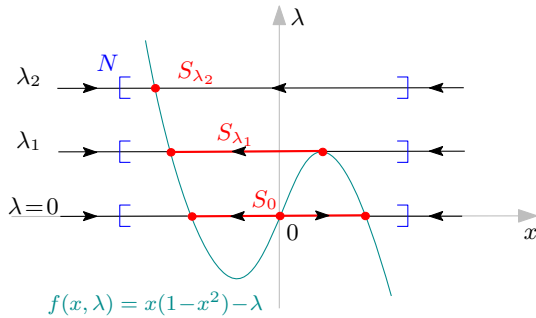
$$f(x, \lambda) = x(1 - x^2) - \lambda,$$

which is represented by the cubic curve in Figure 1.28. This curve meets each horizontal line $y = \lambda_0$ exactly in the set of critical points of the equation with parameter value λ_0 . Moreover, each horizontal line $y = \lambda_0$ in Figure 1.28 corresponds to the phase space of the equation $\dot{x} = x(1 - x^2) - \lambda_0$.

In Figure 1.28, we show three horizontal lines corresponding to three specific parameters, namely, 0, λ_1 and λ_2 .

It is easy to check that the fixed points of these equations are isolated invariant sets. More generally, any closed interval whose end points are fixed points are also isolated invariant sets. Therefore, for $\lambda = \lambda_2$, there is only one nonempty isolated invariant set; for $\lambda = \lambda_1$, one has exactly 3 nonempty isolated invariant sets; and for $\lambda = 0$, one has exactly 12 nonempty isolated invariant sets.

We also marked an interval in Figure 1.28 which is in fact an isolating neighborhood for the maximal invariant set $S_\lambda = \text{Inv}(N, \varphi_\lambda)$ contained in its interior, for each corresponding parameter λ . Therefore, S_0 , S_{λ_1} and S_{λ_2} are related by continuation. In particular, the attracting fixed point in S_{λ_2} continues to the set S_0 composed by three fixed points and the connecting orbits between them. It is interesting to note that the homotopy Conley index of S_λ is Σ^0 , for $\lambda = 0, \lambda_1, \lambda_2$.

Figure 1.28: 1-parameter family of flows on \mathbb{R} . Continuation property.

In Figure 1.29, we exhibit some other isolating neighborhoods. Note that all the three attracting points on the left are related by continuation. Since the continuation is transitive, it follows the attracting point in the flow with parameter value λ_2 continues to S_0 . Again, note that the homotopy Conley index of these isolated invariant sets are Σ^0 .

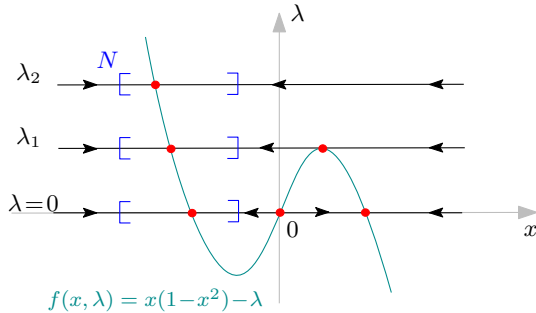


Figure 1.29: Isolated invariant sets related by continuation.

On the other hand, the rest point on the right for the parameter value λ_1 continues to the empty set, see Figure 1.30. Alternatively, one can say that the corresponding rest point bifurcates out of the empty set. Moreover, the rest point continues to the isolated invariant set consisting of the two rightmost rest points in $\lambda = 0$ and the trajectory between them. For all these cases, the isolated invariant sets present the same homotopy Conley index, which is $\bar{\Omega}$.

One could ask if the middle point in $\lambda = 0$, which is a repeller, continues to the one of the attracting fixed points. The next proposition gives a negative answer to this question.

Theorem 1.8 (Continuation Property). *Given a parameterized family of flows*

$$\varphi_\lambda : \mathbb{R} \times X \rightarrow X$$

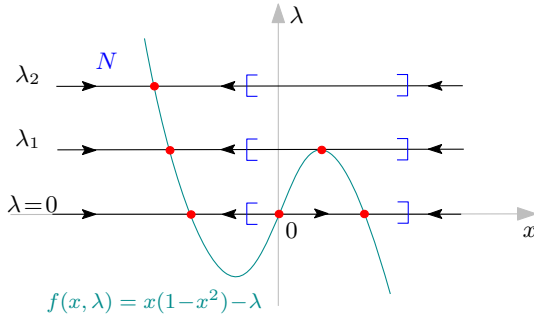


Figure 1.30: Isolated invariant sets related by continuation.

on X , let $S_\lambda := \text{Inv}(N, \varphi_\lambda)$, for a given compact set $N \subset X$. If S_{λ_0} and S_{λ_1} are related by continuation, then

$$CH_*(S_{\lambda_0}) \cong CH_*(S_{\lambda_1}).$$

The power of the Conley index comes from its property to continue to a parameter value where the understanding of the dynamics is much less complicated. By analyzing the changes in the index as a parameter is changed, one can gain insights into bifurcations and transitions that occur in the system, even in the presence of complex and nonlinear behavior.

The following example illustrates how one can use the continuation property to obtain information on the homology Conley index.

Example 1.26. Consider the family of differential equations

$$\begin{cases} \dot{x} = y, \\ \dot{y} = y + (1-\lambda)(x^2 - 1) \left(x + \frac{1}{2} \right) + \lambda(x - 1), \end{cases}$$

parametrized by $\lambda \in [0, 1]$. Denote by φ_λ the flow associated to this system, for each $\lambda \in [0, 1]$.

Note that, for $k > 0$ sufficiently large, $N = [-k, k] \times [-k, k]$ is an isolating neighborhood for $S_\lambda = \text{Inv}_{\varphi_\lambda}(N)$, for each $\lambda \in [0, 1]$.

We want to compute the homology Conley index of S_{λ_0} . Since S_0 and S_1 are related by continuation, one has that

$$CH_*(S_{\lambda_0}) \cong CH_*(S_{\lambda_1}).$$

For $\lambda = 1$, this system is reduced to

$$\begin{cases} \dot{x} = y, \\ \dot{y} = y + x - 1. \end{cases}$$

Therefore, the isolated invariant set S_1 is formed by the rest point $(1, 0)$, which is a saddle point. It follows that

$$CH_*(S_0) \cong CH_*(S_1) = \begin{cases} \mathbb{Z}, & \text{if } k = 1, \\ 0, & \text{if } k \neq 1. \end{cases}$$

Overall, the Conley index is a powerful tool for studying the dynamics of nonlinear systems, providing a topological perspective that complements traditional numerical approaches. Its ability to continue across parameter values makes it particularly useful for analyzing the long-term behavior of systems and identifying the critical points where qualitative changes in behavior occur.

In Conley's theory, there is a stronger notion of continuation, namely the continuation of a Morse decomposition associated to an isolated invariant set. For more details, we refer the reader to Franzosa (1988). Applications of the continuation property of a Morse decomposition in the context of Morse–Smale flows can be found in Reineck (1990, 1995), and for the setting of Morse–Bott flows, see Lima and de Rezende (2016).

1.4 Morse Decomposition and Index Filtration

Attractor–repeller pairs and Morse sets within a Morse decompositions are special types of invariant sets that play an important role in understanding the asymptotic behavior of a dynamical system defined on an isolated invariant set S .

1.4.1 Attractor–repeller decomposition

Let $S \subset X$ be a compact invariant set with respect to a flow φ .

Definition 1.20. A subset $A \subset S$ is an *attractor* with respect to S if there is an S -neighborhood U of A such that $\omega(U) = A$. Analogously, a subset $R \subset S$ is a *repeller* with respect to S if there is an S -neighborhood V of R such that $\alpha(V) = R$.

Example 1.27. Consider the flow φ on the unit 1-sphere \mathbb{S}^1 presented in Example 1.10, whose phase space is shown in Figure 1.11. The fixed point $\theta = \pi/2$ is an attractor and the fixed point $\theta = 3\pi/2$ is a repeller. On the other hand, the rest points of the flow presented in Figure 1.10 are neither attractor nor repellers.

It is important to keep in mind that the required neighborhood in the above definition is with respect to the isolated invariant set S .

Example 1.28. Consider the negative gradient flow associated to the height function on the topological sphere \mathbb{S}^2 as in Figure 1.31. If we consider S as the whole space \mathbb{S}^2 , then the fixed point z is an attractor, x_1 and x_2 are repellers and y is neither an attractor nor a repeller. Of course, there are more attractors and repellers in \mathbb{S}^2 , for instance, the invariant set given by the rest points x_1 , x_2 and y together with the connecting orbits between them

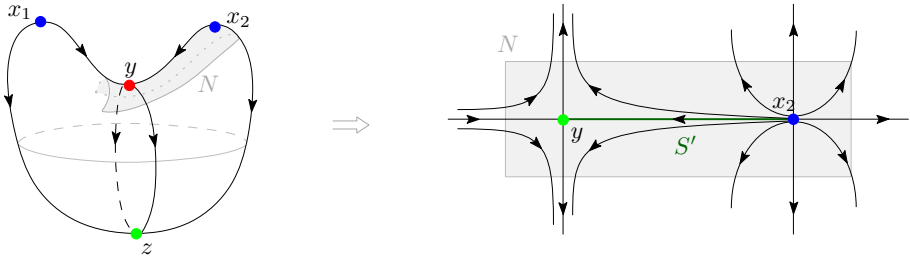


Figure 1.31: Attractors and repeller.

is a repeller set in \mathbb{S}^2 . The set composed by the rest points y, z and the connecting orbits between them, is an attractor in \mathbb{S}^2 .

However, if we consider the isolated invariant set S' given by the rest points x_2, y and the flow line connecting them, then y is an attractor w.r.t. S' and x_2 is a repeller.

Given an attractor A in S , there is a natural repeller associated to it. In fact, the set

$$A^* := \{\gamma \in S \mid \omega(\gamma) \cap A = \emptyset\}$$

is a repeller, which is called the *dual repeller* of A in S . For the proof that A^* is in fact a repeller, see Salamon (1985).

Let A be an attractor in S . Given $x \in S$, one of the following conditions is verified for $\mathcal{O}(x)$:

- $\mathcal{O}(x)$ belongs to the attractor A ;
- $\mathcal{O}(x)$ belongs to the repeller dual A^* ;
- $\mathcal{O}(x) \cap (A \cup A^*) = \emptyset$, $\omega(x) \in A$ and $\alpha(x) \in A^*$. In other words, the orbit through x is “born” in the repeller A^* and it “dies” in the attractor A . In this case, we call $\mathcal{O}(x)$ a *connecting orbit* between A and A^* .

The *set of connecting orbits* of S with respect to the pair (A, A^*) is defined as

$$C(A, A^*) := S \setminus (A \cup A^*).$$

Note that there can be no connecting orbits from the attractor A to the repeller A^* . Therefore, the pair (A, A^*) splits the isolated invariant set S in the union

$$S = A \cup C(A, A^*) \cup A^*.$$

Definition 1.21. The pair (A, A^*) is called an *attractor-repeller pair* in S and $S = A \cup C(A^*, A) \cup A^*$ an *attractor-repeller decomposition* of S .

If (A, A^*) is an attractor-repeller pair in S , then A and A^* are isolated invariant sets in X .

Example 1.29. In Figure 1.32, we present two different attractor-repeller pairs for a flow on the double torus.

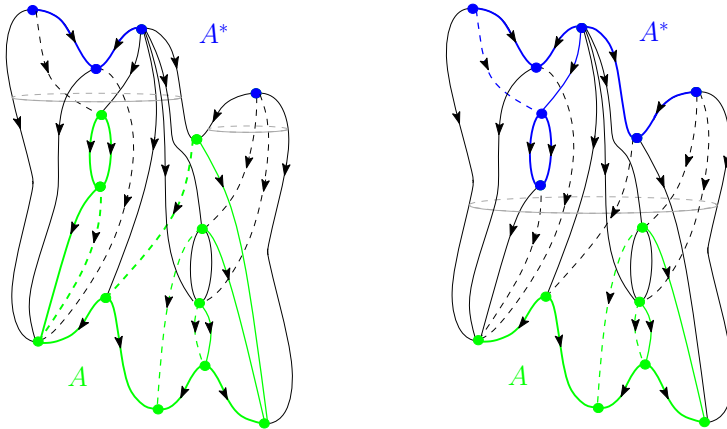


Figure 1.32: Examples of attractor-repeller decompositions on the double torus.

Remark 1.2. Given a flow φ on a compact metric space S , there is a relation between the chain recurrent set $\mathcal{R}(\varphi)$ and the set of all attractor-repeller pairs, namely,

$$\mathcal{R}(f) = \bigcap \{A \cup A^* \mid A \text{ is an attractor in } S\}.$$

This property is essential for the proof of the existence of a Lyapunov function which is strictly decreasing outside $\mathcal{R}(f)$.

1.4.2 Morse decomposition

An attractor-repeller decomposition is the simplest decomposition of an isolated invariant set into smaller invariant sets which contains all the chain recurrent behavior of the flow. A Morse decomposition is a generalization of these notions. We consider a finite collection of disjoint compact invariant sets $\{M_\pi\}_{\pi \in P}$ such that all the recurrent behavior of the flow takes place inside them. Hence, the orbits cannot cycle back and forth between two of the sets. In order to guarantee this property, we require that the trajectories must “flow downhill” with respect to some partial order on the collection $\{M_\pi\}_{\pi \in P}$.

Consider a finite indexing set P with p elements. A *partial order* on P is a relation \prec on the elements of P satisfying:

- for each $\pi \in P$, $\pi \prec \pi$ never holds;

- if $\pi \prec \pi'$ and $\pi' \prec \pi''$, with $\pi, \pi', \pi'' \in P$, then $\pi \prec \pi''$.

A subset $I \subseteq P$ is said to be an *interval* in (P, \prec) if whenever $\pi, \pi' \in I$ and $\pi \prec \pi'' \prec \pi'$, then $\pi'' \in I$. An ordered pair (I, J) of intervals is said to be an *adjacent pair of intervals* if $I \cup J$ is an interval and if $\pi \in J$ and $\pi' \in I$ implies that $\pi \not\prec \pi'$. A partial order $<$ on P is an *extension* of the partial order \prec on P if $\pi \prec \pi'$ implies $\pi < \pi'$.

Let (P, \prec) be a partially ordered set, with P finite, and let S be an isolated invariant set.

Definition 1.22. An \prec -ordered Morse decomposition of an isolated invariant set S is a collection $\mathcal{D}(S) = \{M_\pi\}_{\pi \in P}$ of mutually disjoint isolated invariant sets of S satisfying the following property: if $x \in S \setminus \cup_{\pi \in P} M_\pi$, then there exist $\pi, \pi' \in P$ such that $\pi \prec \pi'$ and $x \in C(M_{\pi'}, M_\pi)$ where

$$C(M_{\pi'}, M_\pi) := \{x \in S \mid \alpha(x) \subset M_{\pi'} \text{ and } \omega(x) \subset M_\pi\}.$$

Example 1.30. In Figure 1.33, we present two different Morse decompositions for a flow on the double torus. Of course the attractor-repeller pairs, presented in Example 1.29 are also Morse decompositions for the double torus.

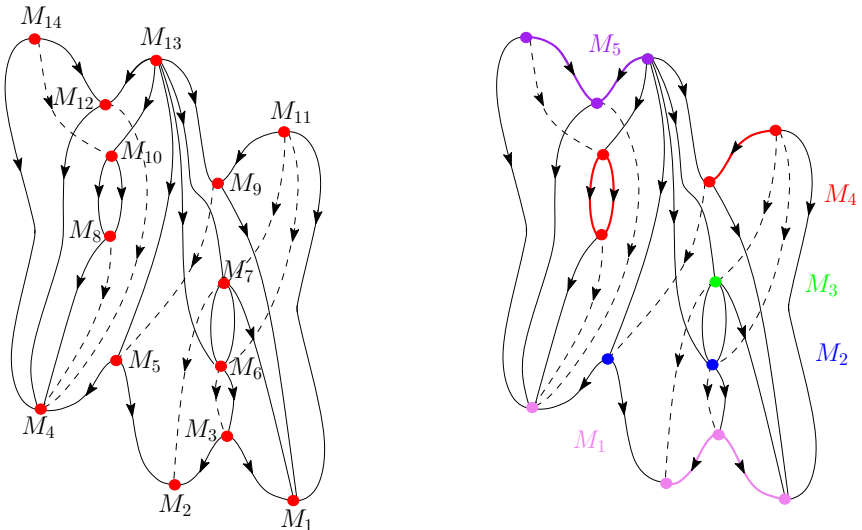


Figure 1.33: Examples of Morse decompositions for the double torus.

Let $\mathcal{D}(S) = \{M_\pi\}_{\pi \in P}$ be an \prec -ordered Morse decomposition of S . A partial order \prec on P naturally induces a partial order on $\mathcal{D}(S)$. This order is also denoted by \prec and

is called an *admissible ordering* of the Morse decomposition. The flow defines a natural order $<_f$ on $\mathcal{D}(S)$, which is called the *flow ordering*, defined by: $\pi <_f \pi'$ if and only if there exists a sequence of distinct elements of P , $\pi = \pi_1, \dots, \pi_l = \pi'$ with $C(M_{\pi_{j+1}}, M_{\pi_j}) \neq \emptyset$, for $j = 1, \dots, l - 1$.

In general, there are many admissible orders for a given Morse decomposition. However, there is a unique minimal (in the sense of the number of order relations) admissible order, which is the flow-ordering. Note that every admissible ordering of $\mathcal{D}(S)$ is an extension of the flow-ordering of $\mathcal{D}(S)$.

Associated to an admissible ordering \prec on $\mathcal{D}(S)$, there exists a collection of sets, which are referred to as *Morse sets*, and defined by

$$M_I := \left(\bigcup_{\pi \in I} M_\pi \right) \cup \left(\bigcup_{\pi, \pi' \in I} C(M_\pi, M_{\pi'}) \right),$$

where I is an interval. Franzosa (1986) proved that if (I, J) is an adjacent pair of intervals, then (M_I, M_J) is an attractor-repeller pair for M_{IJ} . Moreover, each Morse set can be viewed as the intersection of an attractor and a repeller in S . Since attractors and repellers in S are isolated invariant sets and intersections of isolated invariant sets are isolated invariant sets, then each Morse set is an isolated invariant set.

In order to simplify notation, consider a total ordering (M_1, \dots, M_n) of the Morse decomposition, where $P = \{1, 2, \dots, n\}$. Let

$$M_{ij} := \left(\bigcup_{i \leq k \leq j} M_k \right) \cup \left(\bigcup_{i \leq k_1, k_2 \leq j} C(M_{k_1}, M_{k_2}) \right),$$

for each $i, j \in P$ with $i < j$.

Theorem 1.9. *Let S be an isolated invariant set and (M_1, \dots, M_n) be an admissible ordering of a Morse decomposition of S . Then there exists an index filtration, i.e. compact sets*

$$N_0 \subseteq N_1 \subseteq N_2 \subseteq \dots \subseteq N_n$$

with the property that, whenever $i \leq j$, then (N_j, N_i) is an index pair for M_{ij} . In particular, (N_n, N_0) is an index pair for S and (N_i, N_{i-1}) is an index pair for M_i .

The proof of Theorem 1.9 can be found in Salamon (1985), Corollary 4.4.

Example 1.31. Consider the Morse–Smale flow on \mathbb{S}^2 having an attracting periodic orbit γ_1 , a repelling periodic orbit γ_2 , an attracting fixed point p_S and a repelling fixed point p_N , as in Figure 1.34.

One can consider a Morse decomposition of \mathbb{S}^2 given by

$$M_1 = \{p_S\}, \quad M_2 = \{\gamma_1\}, \quad M_3 = \{\gamma_2\}, \quad M_4 = \{p_N\}.$$

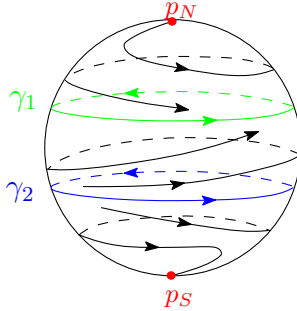


Figure 1.34: Morse–Smale flow on \mathbb{S}^2 .

For this Morse decomposition, one can find an index filtration

$$N_0 \subseteq N_1 \subseteq \cdots \subseteq N_4$$

such as the one depicted in Figure 1.35. Note that (N_i, N_{i-1}) is an index pair for M_i .

Example 1.32. Consider the flow on the double torus $\mathbb{T}^2 \# \mathbb{T}^2$ as depicted in Figure 1.36. In this picture, we exhibit an index filtration (N_0, \dots, N_5) for the Morse decomposition (M_1, M_2, \dots, M_5) of $\mathbb{T}^2 \# \mathbb{T}^2$.

1.5 Morse–Conley Inequalities

The Conley Index Theory investigates the constraints imposed on the flow by the topology of the underlying space, in particular the invariant sets. On the other hand, it also investigates which constraints the dynamics imposes on the topology of the space, i.e. one can obtain information about the topology of the space from the flow.

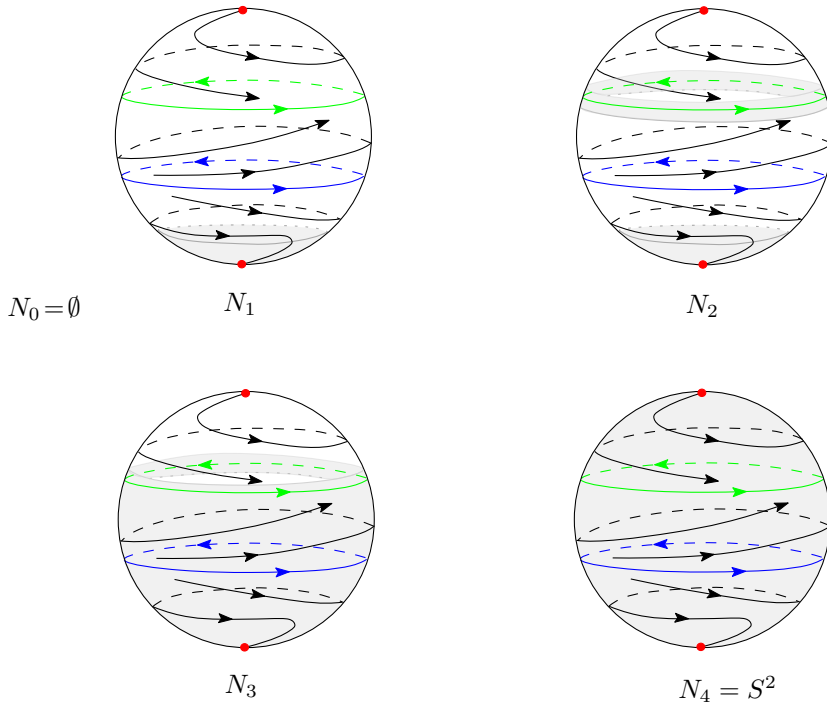
In this section, one shows that the topology of a space and the qualitative properties of a flow defined on it are intimately related, and each one of them can provide insight into the other. Essentially, the topological and dynamical information are two sides of the same coin.

Definition 1.23. Given an isolated invariant set S with respect to a flow φ , the *Conley Polynomial* of S is defined as

$$P(t, S) := \sum_{k \geq 0} b_k(h(S))t^k,$$

where $b_k(h(S))$ denotes the k -th Betti number of the space $h(S)$, i.e. the rank of $CH_k(S)$.

Example 1.33. In Figure 1.37, we present the Conley Polynomial of hyperbolic fixed points and hyperbolic periodic orbits in \mathbb{R}^2 .

Figure 1.35: Index filtration: $N_0 \subseteq N_1 \subseteq \dots \subseteq N_4$.

Theorem 1.10 (Polynomial Morse–Conley Inequality). *Let S be an isolated invariant set. Given an ordered Morse decomposition (M_1, M_2, \dots, M_n) of S , one has that*

$$\sum_{i=1}^n P(t, M_i) = P(t, S) + (1+t)Q(t), \quad (1.2)$$

where $Q(t)$ is a polynomial with nonnegative integer coefficients.

Proof. By the invariance of the index pair (Theorem 1.5), given an index filtration

$$N_0 \subseteq N_1 \subseteq N_2 \subseteq \dots \subseteq N_n$$

associated to the Morse decomposition (M_1, M_2, \dots, M_n) of S , the equality in (1.2) can be rewritten as

$$\sum_{i=1}^n \sum_v b_v(N_i, N_{i-1}) t^v = \sum_v b_v(N_n, N_0) t^v + (1+t)Q(t), \quad (1.3)$$

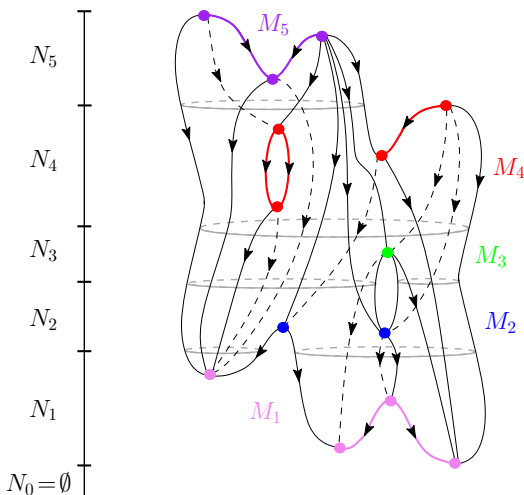


Figure 1.36: An index filtration for the Morse decomposition of $\mathbb{T}^2 \# \mathbb{T}^2$.

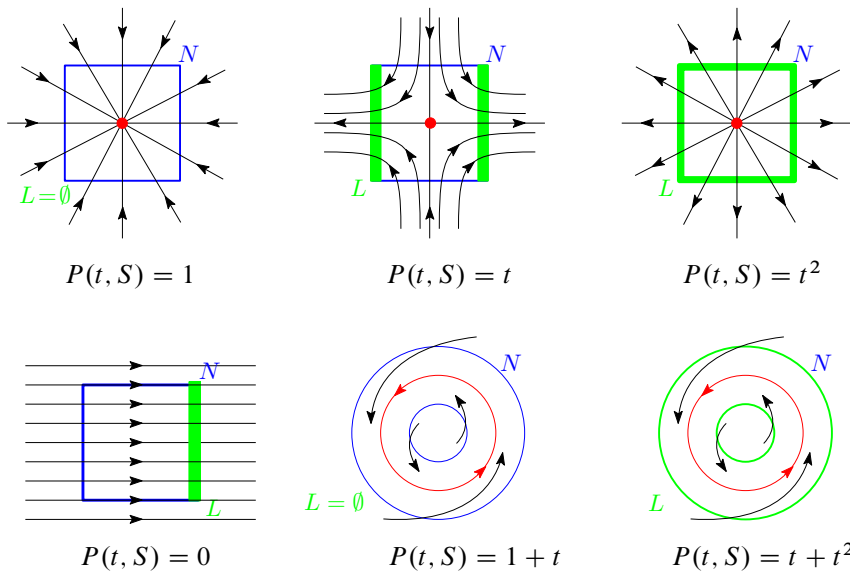


Figure 1.37: Conley Polynomial.

where $b_v(N_i, N_{i-1})$ are the relative Betti numbers.

In order to prove (1.3), we first consider a general construction for topological spaces. Given a triple of topological spaces $Z \subseteq Y \subseteq X$, each one with the subspace topology

induced from X , one has the long exact sequence in homology of the triple presented in Figure 1.38.

$$\begin{array}{ccccccc}
 & & & & & \cdots & \\
 & & & & & & \\
 & & \text{---} & \longrightarrow H_n(Y, Z) & \longrightarrow H_n(X, Z) & \longrightarrow H_n(X, Y) & \text{---} \\
 & & & & & & \curvearrowright_{\delta_n} \\
 & & & & & & \\
 & & \text{---} & \longrightarrow H_{n-1}(Y, Z) & \longrightarrow \cdots & \longrightarrow H_2(X, Y) & \text{---} \\
 & & & & & & \curvearrowright_{\delta_2} \\
 & & & & & & \\
 & & \text{---} & \longrightarrow H_1(Y, Z) & \longrightarrow H_1(Y, Z) & \longrightarrow H_1(X, Y) & \text{---} \\
 & & & & & & \curvearrowright_{\delta_1} \\
 & & & & & & \\
 & & \text{---} & \longrightarrow H_0(Y, Z) & \longrightarrow H_0(Y, Z) & \longrightarrow H_0(X, Y) & \text{---} \\
 & & & & & & \curvearrowright_{\delta_0} \\
 & & & & & & \\
 & & & & & & \text{---} \longrightarrow 0
 \end{array}$$

Figure 1.38: Long exact sequence of the triple (Z, Y, X) .

Exactness means that the composition of any two consecutive maps in this sequence must be the trivial map.

Assume that the homology groups are finitely generated. Define

$$b_j(X, Y) := \text{rank } H_j(X, Y) \quad \text{e} \quad v_j(X, Y, Z) := \text{rank im}(\delta_j).$$

By the exactness of the sequence (1.38), one has that

$$\sum_{j=0}^k (-1)^j [b_j(X, Y) - b_j(X, Z) + b_j(Y, Z)] + (-1)^{3k+3} v_k(X, Y, Z) = 0 \quad (1.4)$$

and

$$\sum_{j=0}^{k-1} (-1)^j [b_j(X, Y) - b_j(X, Z) + b_j(Y, Z)] + (-1)^{3(k-1)+3} v_{k-1}(X, Y, Z) = 0. \quad (1.5)$$

Replacing (1.5) in (1.4), one obtains

$$\begin{aligned} -(-1)^{3k}v_{k-1}(X, Y, Z) + (-1)^k[b_k(X, Y) - b_k(X, Z) + b_k(Y, Z)] \\ + (-1)^{3k+3}v_k(X, Y, Z) = 0. \end{aligned} \quad (1.6)$$

Multiplying (1.6) by $(-1)^k t^k$ and summing over $k \geq 0$, one has

$$\begin{aligned} -\sum_{k \geq 0}(-1)^{4k}v_{k-1}(X, Y, Z)t^k + \sum_{k \geq 0}(-1)^{4k+3}v_k(X, Y, Z)t^k + \\ + \sum_{k \geq 0}(-1)^{2k}\left[b_k(X, Y)t^k - b_k(X, Z)t^k + b_k(Y, Z)t^k\right] = 0. \end{aligned}$$

Hence

$$\begin{aligned} -\sum_{k \geq 0}v_{k-1}(X, Y, Z)t^{k-1}t - \sum_{k \geq 0}v_k(X, Y, Z)t^k + \\ + \sum_{k \geq 0}b_k(X, Y)t^k - \sum_{k \geq 0}b_k(X, Z)t^k + \sum_{k \geq 0}b_k(Y, Z)t^k = 0. \end{aligned} \quad (1.7)$$

In order to simplify the notation, let

$$P(t, X, Y) := \sum_{k \geq 0}b_k(X, Y)t^k,$$

$$P(t, Y, Z) := \sum_{k \geq 0}b_k(Y, Z)t^k,$$

$$P(t, X, Z) := \sum_{k \geq 0}b_k(X, Z)t^k,$$

$$Q(t, X, Y, Z) := \sum_{k \geq 0}v_k(X, Y, Z)t^k.$$

With this notation, (1.7) can be rewritten as

$$P(t, X, Y) - P(t, X, Z) + P(t, Y, Z) = (1+t)Q(t, X, Y, Z). \quad (1.8)$$

Now, returning to the dynamical setting, let (M_0, M_1, \dots, M_n) be a Morse decomposition for an isolated invariant set S . Given an index filtration

$$N_0 \subseteq N_1 \subseteq \dots \subseteq N_n$$

for (M_0, M_1, \dots, M_n) , one has that for each triple (N_0, N_{j-1}, N_j) , it holds that

$$P(t, N_j, N_{j-1}) - P(t, N_j, N_0) + P(t, N_{j-1}, N_0) = (1+t)Q(t, N_j, N_{j-1}, N_0).$$

Summing over $j = 1, \dots, n$, yields

$$\begin{aligned} \sum_{j=1}^n P(t, N_j, N_{j-1}) - \sum_{j=1}^n P(t, N_j, N_0) + \sum_{j=1}^n P(t, N_{j-1}, N_0) \\ = \sum_{j=1}^n (1+t) Q(t, N_j, N_{j-1}, N_0). \end{aligned}$$

Finally,

$$\sum_{j=1}^n P(t, N_j, N_{j-1}) = P(t, N_n, N_0) + (1+t) Q(t),$$

where $Q(t) = \sum_{j=1}^n Q(t, N_j, N_{j-1}, N_0)$. □

Theorem 1.11 (Morse–Conley Inequalities). *Let S be an isolated invariant set and (M_1, M_2, \dots, M_n) be an ordered Morse decomposition of S . Then we have the following:*

$$(a) \sum_{k=0}^m (-1)^{k+m} \sum_{j=0}^n b_k(h(M_j)) \geq \sum_{k=0}^m (-1)^{k+m} b_k(h(S));$$

$$(b) \sum_{k \geq 0} (-1)^k \sum_{j=0}^n b_k(h(M_j)) = \sum_{k \geq 0} (-1)^k b_k(h(S)).$$

Proof.

- (a) Consider the polynomial Morse–Conley inequality in (1.2), and denote the i -th coefficient of $Q(t)$ by r_i , which is a nonnegative integer. One has that

$$\sum_{i=1}^n b_0(h(M_i)) = b_0(h(S)) + r_0,$$

which implies that

$$\sum_{i=1}^n b_0(h(M_i)) \geq b_0(h(S)).$$

Again from the polynomial equality in (1.2),

$$\begin{aligned} \sum_{i=1}^n b_1(h(M_i)) &= b_1(h(S)) + r_1 + r_0 \\ &= b_1(h(S)) + r_1 + \sum_{i=1}^n b_0(h(M_i)) - b_0(h(S)), \end{aligned}$$

which implies that

$$\sum_{i=1}^n b_1(h(M_i)) - \sum_{i=1}^n b_0(h(M_i)) = b_1(h(S)) - b_0(h(S)) + r_1.$$

Since $r_1 \geq 0$, one obtains

$$\sum_{i=1}^n b_1(h(M_i)) - \sum_{i=1}^n b_0(h(M_i)) \geq b_1(h(S)) - b_0(h(S)).$$

Continuing in this fashion, we obtain the inequality in (a) for any $m \geq 0$.

- (b) Considering $t = -1$, from the polynomial Morse–Conley inequality in (1.2), one has that $\sum_{i=1}^n P(-1, M_i) = P(-1, S) + (1-1)Q(-1)$. Hence,

$$\sum_{i=1}^n \sum_{k \geq 0} b_k(h(M_i))(-1)^k = \sum_{k \geq 0} b_k(h(S))(-1)^k.$$

Equivalently,

$$\sum_{k \geq 0} (-1)^k \sum_{i=1}^n b_k(h(M_i)) = \sum_{k \geq 0} (-1)^k b_k(h(S)).$$

□

Given an isolated invariant set S , consider the particular case of the trivial Morse decomposition for S with only one Morse set, i.e. $M_1 = S$. Denoting the rank of the i -th homology Conley index by $h_i = b_i(h(S))$, and the i -Betti number of S by b_i , the Morse–Conley inequalities for S is written as:

$$\begin{aligned} b_n - b_{n-1} + - \dots \pm b_1 \pm b_0 &= h_n - h_{n-1} + - \dots \pm h_1 \pm h_0 \\ b_{n-1} - b_{n-2} + - \dots \pm b_1 \pm b_0 &\leq h_{n-1} - h_{n-2} + - \dots \pm h_1 \pm h_0 \\ &\vdots && \vdots \\ b_j - b_{j-1} + - \dots \pm b_1 \pm b_0 &\leq h_j - h_{j-1} + - \dots \pm h_1 \pm h_0 \\ b_{j-1} - b_{j-2} + - \dots \pm b_1 \pm b_0 &\leq h_{j-1} - h_{j-2} + - \dots \pm h_1 \pm h_0 \\ &\vdots && \vdots \\ b_2 - b_1 + b_0 &\leq h_2 - h_1 + h_0 \\ b_1 - b_0 &\leq h_1 - h_0 \\ b_0 &\leq h_0 \end{aligned}$$

More will be said about this inequality form in the next chapter.

2

Poincaré–Hopf Inequalities

In the last chapter, the polynomial Morse–Conley inequalities were presented for a closed smooth manifold M , showing the interdependence between the number of nondegenerate critical points, c_i , of Morse index i of a smooth real valued function $f : M \rightarrow \mathbb{R}$ and the Betti numbers of M . It was shown that these inequalities generalize to encompass the numerical homology Conley indices h_i of an isolated invariant set S of a continuous flow. In other words, the Morse–Conley inequalities can also be seen as a relation between the dynamics of an isolated invariant set S captured by the ranks of its homology Conley index and the Betti number of its phase space M .

The Morse inequalities for a closed smooth manifold M show the interdependence between the number of nondegenerate critical points of Morse index i of a smooth real valued function $f : M \rightarrow \mathbb{R}$ and the Betti numbers of M . In the last chapter, it was shown that these inequalities generalize to encompass the numerical homology Conley indices h_i of an isolated invariant set S of a continuous flow. In other words, the Morse–Conley inequalities can also be seen as a relation between the dynamics of an isolated invariant set S captured by the ranks of its homology Conley index and the Betti number of its phase space M .

Henceforth, preference will be given herein to the topological study of continuous flows on closed manifolds rather than the study of differentiable real valued maps and their critical points. In fact, with the advent of Conley index theory, differentiability is no longer a requirement for the study of continuous flows.

Conley’s fundamental theorem of Dynamical Systems, in one of its more restricted versions, provides us with the existence of a continuous Lyapunov function for any con-

tinuous flow φ on a closed manifold. With respect to this function φ is a gradient-like flow, as seen in Section 1.1.

In the last chapter, we presented the generalization of the Morse index of nondegenerate critical points to the Conley index of isolated invariant sets and the generalization of the classical Morse inequalities to the Morse–Conley inequalities for gradient-like flows with the property that the components of its chain recurrent set \mathcal{R} is a finite union of isolated invariant sets. In what follows, an alternative proof for these inequalities is shown.

In this chapter we introduce Lyapunov graphs, defined by Lyapunov functions and which are labelled with both dynamical and topological numerical invariants. The dynamical invariants are the numerical homology Conley indices and the topological invariants are the Betti numbers of the codimension one submanifolds that form the boundary of the isolating blocks. These numerical invariants are precisely the input needed to verify the Poincaré–Hopf inequalities. If the data on a Lyapunov graph does not satisfy these inequalities, there is no gradient-like flow on any compact manifold realizing it. In other words, every gradient-like flow satisfies both the local and global Poincaré–Hopf inequalities. The goal of this chapter is to present the set of Poincaré–Hopf inequalities which are closely related to the Morse–Conley inequalities.

Finally we present a Morsification algorithm for Lyapunov graphs which gives rise to a system of linear equations dubbed h_k^{cd} -Systems.

2.1 Generalized Morse–Conley Inequalities

It is beautiful to see how the role played by the number c_i of nondegenerate singularities of index i gives way to the numerical homology Conley indices h_i in the generalized version of the inequalities. Note that, in the case that all isolated invariant sets are nondegenerate singularities, each singularity of index i contributes at most one to h_i . Hence, $h_i = c_i$ for $i = 0 \dots n$ where $n = \dim M$ and one obtains the classical Morse inequalities. To obtain the generalized Morse inequalities one must sift through each of the isolated invariant sets in \mathcal{R} to determine not only those that contribute to the i -th rank of the homology Conley index, but also by how much. Then by adding the contribution of all the chain recurrent components of \mathcal{R} , one obtains h_i . Thus, one obtains the generalized Morse–Conley inequalities in Section 1.5 which describes the relationship between the topology of M and the numerical Conley indices of singularities of a gradient-like flow on M are described by the generalized Morse inequalities.

We now provide an adaptation of an elegant proof of these inequalities that are found in Milnor (2015). We first need to define some additive and subadditive functions.

Let S be a function from pairs of spaces to the integers. S is *subadditive* if whenever $X \supset Y \supset Z$ we have $S(X, Z) \leq S(X, Y) + S(Y, Z)$. S is *additive* if equality holds.

Considering $\beta_\lambda(X, Y)$ as the λ -th Betti number of (X, Y) , that is

$$\beta_\lambda(X, Y) = \text{rank } H_\lambda(X, Y)$$

and $\chi(X, Y) = \sum(-1)^\lambda \beta_\lambda(X, Y)$ as the Euler characteristic, it can be shown by analyzing the long exact sequence of (X, Y, Z) that β_λ is subadditive and χ is additive.

Moreover, if S is subadditive and $X_0 \subset \dots \subset X_n$, then $S(X_n, X_0) \leq \sum_{i=1}^n S(X_i, X_{i-1})$.

If S is additive then equality holds. If $X_0 = \emptyset$ then $S(X_n) \leq \sum_{i=1}^n S(X_i, X_{i-1})$ and equality holds if S is additive.

With the above functions one proves straightforwardly:

1. Generalized Weak Morse Inequalities

$$\beta_\lambda(M) \leq h_\lambda.$$

2. Generalized Poincaré–Hopf Equality

$$\sum(-1)^\lambda \beta_\lambda(M) = \sum(-1)^\lambda h_\lambda,$$

where h_λ denotes the λ numerical homology Conley index.

Given a compact manifold M and a continuous flow, let (M_1, \dots, M_k) be a Morse decomposition of M . Then there exists an *index filtration*, i.e. a sequence of nested compact sets

$$\emptyset = M^{a^0} \subset M^{a^1} \subset \dots \subset M^{a^k} = M$$

with the property that, whenever $i < j$, then $(M^{a^i}, M^{a^{i-1}})$ is an index pair for M_i . Also denote by $\text{rank } CH_\lambda(M_i)$ the rank of the Conley homology index of M_i which is equal to $\text{rank } CH_\lambda(M^{a^i}, M^{a^{i-1}}) = h_\lambda(M^{a^i}, M^{a^{i-1}}) = \beta_\lambda(M^{a^i}, M^{a^{i-1}})$.

It is easy to see that the *weak Morse–Conley inequalities* follow from the subadditivity of β_λ . One has:

$$\begin{aligned} \beta_\lambda(M) &= \beta_\lambda(M^{a^k}, M^{a^0}) \leq \sum_{i=1}^k \beta_\lambda(M^{a^i}, M^{a^{i-1}}) = \\ &= \sum_{i=1}^k h_\lambda(M^{a^i}, M^{a^{i-1}}) = h_\lambda(M). \end{aligned}$$

The inequality follows from subadditivity of β_λ and the last equality is the additivity property of the Conley homology index.

Also, one proves the *Generalized Poincaré–Hopf Equality* using the fact that χ_λ is additive. The proof follows easily since,

$$\begin{aligned}
\chi_\lambda(M) &= \chi_\lambda(M^{a^k}, M^{a^0}) = \sum_{i=1}^k \chi_\lambda(M^{a^i}, M^{a^{i-1}}) = \\
&\sum_{i=1}^k \sum_{\lambda=0}^n (-1)^\lambda \beta_\lambda(M^{a^i}, M^{a^{i-1}}) = \sum_{\lambda=0}^n (-1)^\lambda \sum_{i=1}^k \beta_\lambda(M^{a^i}, M^{a^{i-1}}) = \\
&\sum_{\lambda=0}^n (-1)^\lambda \sum_{i=1}^k h_\lambda(M^{a^i}, M^{a^{i-1}}) = \sum_{\lambda=0}^n (-1)^\lambda h_\lambda(M).
\end{aligned}$$

Finally one proves the Morse–Conley inequalities by defining the subadditive function $S_\lambda(X, Y) = \beta_\lambda(X, Y) - \beta_{\lambda-1}(X, Y) + \dots \pm \beta_0(X, Y)$. The inequalities are obtained by using this function on the filtration $\emptyset = M^{a^0} \subset M^{a^1} \subset \dots \subset M^{a^k} = M$.

$$S_\lambda(M) \leq \sum_{i=1}^n S_\lambda(M^{a^i}, M^{a^{i-1}}) = h_\lambda - h_{\lambda-1} + \dots \pm h_0$$

or in other words,

$$\beta_\lambda(M) - \beta_{\lambda-1}(M) + \dots \pm \beta_0(M) \leq h_\lambda - h_{\lambda-1} + \dots \pm h_0.$$

The inequalities in Section 1.5 are obtained once again. Note that in this generalization the left-hand side continues to represent the topology of the phase space M by the alternating sum of the Betti numbers $\beta_i(M)$ and the right-hand side of the inequalities are topological-dynamical invariants of the flow given by the numerical Conley indices. Henceforth, we denote the Betti numbers of M by $\gamma_i(M)$ and reserve the notation β_i for the Betti numbers of the boundaries of isolating blocks as we will see subsequently in this and following chapters.

$$\begin{aligned}
\gamma_n - \gamma_{n-1} + \dots \pm \gamma_2 \pm \gamma_1 \pm \gamma_0 &= h_n - h_{n-1} + \dots \pm h_2 \pm h_1 \pm h_0 & (n) \\
\gamma_{n-1} - \gamma_{n-2} + \dots \pm \gamma_2 \pm \gamma_1 \pm \gamma_0 &\leq h_{n-1} - h_{n-2} + \dots \pm h_2 \pm h_1 \pm h_0 & (n-1) \\
&\vdots & \vdots \\
\gamma_j - \gamma_{j-1} + \dots \pm \gamma_2 \pm \gamma_1 \pm \gamma_0 &\leq h_j - h_{j-1} + \dots \pm h_2 \pm h_1 \pm h_0 & (j) \\
\gamma_{j-1} - \gamma_{j-2} + \dots \pm \gamma_2 \pm \gamma_1 \pm \gamma_0 &\leq h_{j-1} - h_{j-2} + \dots \pm h_2 \pm h_1 \pm h_0 & (j-1) \\
&\vdots & \vdots \\
\gamma_2 - \gamma_1 + \gamma_0 &\leq h_2 - h_1 + h_0 & (2) \\
\gamma_1 - \gamma_0 &\leq h_1 - h_0 & (1) \\
\gamma_0 &\leq h_0 & (0) \\
&& (2.1)
\end{aligned}$$

2.2 Poincaré–Hopf Inequalities

In this section a set of inequalities is presented that relates the homological Conley index of the dynamics of a flow on a compact manifold with boundary to the Betti numbers of its boundary components. We have dubbed these as the Poincaré–Hopf inequalities inspired in equalities that emerge as by-products of the famous Poincaré–Hopf theorem. Subsequently these inequalities are presented for closed manifolds and referred to as global Poincaré–Hopf inequalities which provide interesting lower bounds for the number of critical points of index j in terms of alternating sums of the number of critical points of lower index and their duals.

We now present this collection of inequalities which hold for flows whose inverse flow satisfies the following duality condition on the homology Conley indices. Given a flow φ_t and an isolated invariant set $\Lambda \subset N^n$ it will be assumed that the inverse flow φ_{-t} has an isolated invariant set Λ' with the property that

$$h_i(\Lambda) = \dim CH_i(\Lambda) = \dim CH_{n-i}(\Lambda') = h_{n-i}(\Lambda').$$

In other words, it is assumed throughout our analysis that the *Conley duality condition* on the indices holds. That is, given the isolated invariant sets Λ and Λ' with index pairs (N, N^-) and (N, N^+) have the property that $\text{rank } H_j(N, N^-) = h_j$ and $\text{rank } H_j(N, N^+) = \bar{h}_j = h_{n-j}$ for $0 \leq j \leq n$. We remark that Morse–Smale flows, as well as Smale flows satisfy this duality condition. We also assume throughout this section that isolating neighborhoods are connected.

2.2.1 Local Poincaré–Hopf Inequalities for Isolating Blocks

The Poincaré–Hopf inequalities for an isolated invariant set Λ with isolating block N , where N^+ is the entering set and N^- is the exiting set for the flow, are obtained by an analysis of long exact sequences of (N, N^+) and (N, N^-) . This analysis can be found in Bertolim, Mello, and de Rezende (2003a).

Note that (N, N^-) is an index pair for Λ and (N, N^+) is an index pair for the isolated invariant set of the reverse flow, Λ' .

Consider the long exact sequences for the pairs (N, N^-) and (N, N^+) :

$$\begin{aligned} 0 &\rightarrow H_n(N^-) \xrightarrow{i_n} H_n(N) \xrightarrow{p_n} H_n(N, N^-) \xrightarrow{\partial_n} H_{n-1}(N^-) \xrightarrow{i_{n-1}} H_{n-1}(N) \xrightarrow{p_{n-1}} \\ &\rightarrow H_{n-1}(N, N^-) \xrightarrow{\partial_{n-1}} H_{n-2}(N^-) \xrightarrow{i_{n-2}} H_{n-2}(N) \xrightarrow{p_{n-2}} H_{n-2}(N, N^-) \xrightarrow{\partial_{n-2}} \dots \\ &\xrightarrow{\partial_4} H_3(N^-) \xrightarrow{i_3} H_3(N) \xrightarrow{p_3} H_3(N, N^-) \xrightarrow{\partial_3} H_2(N^-) \xrightarrow{i_2} H_2(N) \xrightarrow{p_2} H_2(N, N^-) \xrightarrow{\partial_2} \\ &\rightarrow H_1(N^-) \xrightarrow{i_1} H_1(N) \xrightarrow{p_1} H_1(N, N^-) \xrightarrow{\partial_1} H_0(N^-) \xrightarrow{i_0} H_0(N) \xrightarrow{p_0} H_0(N, N^-) \rightarrow 0 \end{aligned} \tag{2.2}$$

$$\begin{aligned}
0 &\rightarrow H_n(N^+) \xrightarrow{i'_n} H_n(N) \xrightarrow{p'_n} H_n(N, N^+) \xrightarrow{\partial'_n} H_{n-1}(N^+) \xrightarrow{i'_{n-1}} H_{n-1}(N) \xrightarrow{p'_{n-1}} \\
&\rightarrow H_{n-1}(N, N^+) \xrightarrow{\partial'_{n-1}} H_{n-2}(N^+) \xrightarrow{i'_{n-2}} H_{n-2}(N) \xrightarrow{p'_{n-2}} H_{n-2}(N, N^+) \xrightarrow{\partial'_{n-2}} \dots \\
&\xrightarrow{\partial'_4} H_3(N^+) \xrightarrow{i'_3} H_3(N) \xrightarrow{p'_3} H_3(N, N^+) \xrightarrow{\partial'_3} H_2(N^+) \xrightarrow{i'_2} H_2(N) \xrightarrow{p'_2} H_2(N, N^+) \xrightarrow{\partial'_2} \\
&H_1(N^+) \xrightarrow{i'_1} H_1(N) \xrightarrow{p'_1} H_1(N, N^+) \xrightarrow{\partial'_1} H_0(N^+) \xrightarrow{i'_0} H_0(N) \xrightarrow{p'_0} H_0(N, N^+) \rightarrow 0
\end{aligned} \tag{2.3}$$

The following elementary result will be useful in subsequent analysis of long exact sequences.

Lemma 2.1. *Consider a long exact sequences of vector spaces,*

$$\xrightarrow{h} A \xrightarrow{i} B \xrightarrow{j} C \xrightarrow{k} \dots \dots \rightarrow D \rightarrow 0,$$

then

$$\text{rank im } h = \text{rank } A - \text{rank } B + \text{rank } C - \dots \pm \text{rank } D \geq 0.$$

Proof. Note, it is easy to see that $\text{rank im } h + \text{rank im } i = \text{rank } A$. This follows from the elementary fact that $\text{rank } A = \text{rank im } i + \text{rank ker } i$ and from the exactness of the sequence, i.e., $\ker i = \text{im } h$. \square

One can read the Poincaré–Hopf inequalities as a set of constraints on the j -th numerical Conley index, h_j , of an isolated invariant set S , in terms of both the lower dimensional Betti numbers B_k of the boundaries of its isolating block, as well as the the lower dimensional numerical Conley indices of S , h_k and their duals h_{n-k} , for $0 \leq k < j$.

Theorem 2.1 (Poincaré–Hopf Inequalities). *Let φ be a gradient-like flow on an isolating block (N, N^+, N^-) and let h_i be the numerical homology Conley indices, for $i = 0, \dots, n$, and assume that the Conley duality condition is satisfied. Let $e^- = \text{rank } H_0(N^-)$, $e^+ = \text{rank } H_0(N^+)$ and $B_j^\pm = \text{rank } H_j(N^\pm)$ then the following inequalities hold:*

$$\left\{
\begin{array}{l}
-h_j \leq [(B_{j-1}^+ - B_{j-1}^-) - (B_{j-2}^+ - B_{j-2}^-) + \dots \pm (B_2^+ - B_2^-) \pm (B_1^+ - B_1^-) \\
\quad + (h_{n-(j-1)} - h_{j-1}) - (h_{n-(j-2)} - h_{j-2}) + \dots \\
\quad \pm (h_{n-1} - h_1) \pm [(h_n - h_0) \pm (e^+ - e^-)]] \leq h_{n-j} \text{ for } j = 2, \dots, i \\
(*) \left\{ \begin{array}{l} h_1 \geq h_0 - 1 + e^- \\ h_{n-1} \geq h_n - 1 + e^+ \end{array} \right.
\end{array}
\right. \tag{2.4}$$

Moreover, the Poincaré–Hopf equality holds in the odd-dimensional case $n = 2i + 1$:

$$\sum_{j=1}^{i-1} (-1)^j (B_j^+ - B_j^-) + \frac{(-1)^i (B_i^+ - B_i^-)}{2} = e^- - e^+ + \sum_{j=0}^{2i+1} (-1)^j h_j. \quad (2.5)$$

Futhermore, in the even dimensional case $n = 2 \pmod{4}$,

$$h_i + \sum_{j=1}^{i-1} (-1)^j (B_j^+ - B_j^-) - \sum_{j=0}^{i-1} (-1)^j (h_{2i-j} - h_j) + (e^+ - e^-) = 0 \pmod{2}. \quad (2.6)$$

Proof. By simultaneously analyzing the following pairs of maps

$$\{((p_i, \partial'_i), (p'_i, \partial_i)) \mid \dots, ((p_1, \partial'_1), (p'_1, \partial_1)) \}$$

of the long exact sequences (2.2) and (2.3), one obtains the Poincaré–Hopf inequalities.

We start by analyzing the long exact homology sequences, (2.2) and (2.3) for the pairs (N, N^-) and (N, N^+) in dimensions j and $n - j$, for $1 < j \leq i$ and for $n = 2i + 1$ as well as $n = 2i$. The case $j = 1$ will be analyzed separately at the end of the proof.

Analyzing the ranks of $\text{im } p_j$ in (2.2) and using Lemma 2.1, the following holds:

$$\text{rank im } p_j = h_j - B_{j-1}^- + \text{rank } H_{j-1}(N) - h_{j-1} + B_{j-2}^- - \text{rank } H_{j-2}(N) + h_{j-2} - \dots$$

$$\pm B_2^- \pm \text{rank } H_2(N) \pm h_2 \pm B_1^- \pm \text{rank } H_1(N) \pm h_1 \pm B_0^- \pm \text{rank } H_0(N) \pm h_0 \geq 0$$

$$\Rightarrow h_j \geq B_{j-1}^- - B_{j-2}^- + \dots \pm B_2^- \pm B_1^- + h_{j-1} - h_{j-2} + \dots \pm h_2 \pm h_1 \pm h_0 \pm B_0^-$$

$$- \text{rank } H_{j-1}(N) + \text{rank } H_{j-2}(N) - \dots \pm \text{rank } H_1(N) \pm \text{rank } H_0(N) \quad (2.7)$$

Similarly, by considering $\text{rank im } \partial'_j$ in (2.3), using Lemma 2.1 and the duality of the indices,

$$\begin{aligned} \text{rank im } \partial'_j &= B_{j-1}^+ - \text{rank } H_{j-1}(N) + h_{n-(j-1)} - B_{j-2}^+ + \text{rank } H_{j-2}(N) \\ &\quad - h_{n-(j-2)} + \dots \pm B_2^+ \pm \text{rank } H_2(N) \pm h_{n-2} \\ &\quad \pm B_1^+ \pm \text{rank } H_1(N) \pm h_{n-1} \pm B_0^+ \pm \text{rank } H_0(N) \pm h_n \geq 0 \end{aligned}$$

$$\Rightarrow - \text{rank } H_{j-1}(N) + \text{rank } H_{j-2}(N) - \dots \pm \text{rank } H_1(N) \pm \text{rank } H_0(N) \geq$$

$$- B_{j-1}^+ + B_{j-2}^+ \dots \pm B_2^+ \pm B_1^+ \pm B_0^+ - h_{n-(j-1)} + h_{n-(j-2)} + \dots \pm h_{n-1} \pm h_n \quad (2.8)$$

From (2.7) and (2.8) one obtains

$$h_j \geq -[B_{j-1}^+ - B_{j-1}^-] + [B_{j-2}^+ - B_{j-2}^-] + \dots \pm [B_0^+ - B_0^-] \\ - [h_{n-j+1} - h_{j-1}] + [h_{n-j+2} - h_{j-2}] + \dots \pm [h_n - h_0] \quad (2.9)$$

Analyzing the ranks of $\text{im } p'_j$ in (2.3) and using Lemma 2.1, the following holds:

$$\begin{aligned} \text{rank im } p'_j &= h_{n-j} - B_{j-1}^+ + \text{rank } H_{j-1}(N) - h_{n-j+1} + B_{j-2}^+ - \text{rank } H_{j-2}(N) + \\ &\quad + h_{n-j+2} - \dots \pm B_2^+ \pm \text{rank } H_2(N) \pm h_{n-2} \\ &\quad \pm B_1^+ \pm \text{rank } H_1(N) \pm h_{n-1} \pm B_0^+ \pm \text{rank } H_0(N) \pm h_n \geq 0 \end{aligned}$$

$$\Rightarrow h_{n-j} \geq B_{j-1}^+ - B_{j-2}^+ + \dots \pm B_2^+ \pm B_1^+ \pm B_0^+ + h_{n-j+1} - h_{n-j+2} + \dots \\ \dots \pm h_{n-2} \pm h_{n-1} \pm h_n - \text{rank } H_{j-1}(N) \\ + \text{rank } H_{j-2}(N) - \dots \pm \text{rank } H_1(N) \pm \text{rank } H_0(N) \quad (2.10)$$

Similarly, by considering $\text{rank im } \partial_j$ in (2.2), using Lemma 2.1 and the duality of the indices,

$$\begin{aligned} \text{rank im } \partial_j &= B_{j-1}^- - \text{rank } H_{j-1}(N) + h_{j-1} - B_{j-2}^- + \text{rank } H_{j-2}(N) - h_{j-2} + \dots \\ &\quad \pm B_2^- \pm \text{rank } H_2(N) \pm h_2 \pm B_1^- \pm \text{rank } H_1(N) \pm h_1 \pm B_0^- \pm \text{rank } H_0(N) \pm h_0 \geq 0 \end{aligned}$$

$$\Rightarrow -\text{rank } H_{j-1}(N) + \text{rank } H_{j-2}(N) - \dots \pm \text{rank } H_1(N) \pm \text{rank } H_0(N) \geq \\ - B_{j-1}^+ + B_{j-2}^+ \dots \pm B_2^+ \pm B_1^+ \pm B_0^+ - h_{j-1} + h_{j-2} + \dots \pm h_1 \pm h_0 \quad (2.11)$$

From (2.10) and (2.11) one obtains

$$h_{n-j} \geq [B_{j-1}^+ - B_{j-1}^-] - [B_{j-2}^+ - B_{j-2}^-] + \dots \pm [B_0^+ - B_0^-] \\ + [h_{n-j+1} - h_{j-1}] - [h_{n-j+2} - h_{j-2}] + \dots \pm [h_n - h_0] \quad (2.12)$$

Now considering (2.9) and (2.12) one can write out the Poincaré–Hopf inequality.

$$\begin{aligned} -h_j &\leq [B_{j-1}^+ - B_{j-1}^-] - [B_{j-2}^+ - B_{j-2}^-] + \dots \pm [B_0^+ - B_0^-] \\ &\quad + [h_{n-j+1} - h_{j-1}] - [h_{n-j+2} - h_{j-2}] + \dots \pm [h_n - h_0] \leq h_{n-j} \quad (2.13) \end{aligned}$$

The last inequalities are obtained by analyzing $[(p_1, \partial'_1), (p'_1, \partial_1)]$

Actually one needs only to analyze p_1 :

$$\operatorname{rank} \operatorname{im} p_1 = h_1 - B_0^- + \operatorname{rank} H_0(N) - h_0 \geq 0$$

Similarly, by analyzing p'_1 and using the index duality:

$$\operatorname{rank} \operatorname{im} p'_1 = h_{n-1} - B_0^+ + \operatorname{rank} H_0(N) - h_n \geq 0$$

Since $B_0^- = e^-$, $B_0^+ = e^+$ and $\operatorname{rank} H_0(N) = 1$ the following inequalities are obtained:

$$\begin{aligned} e^- &\leq h_1 + 1 - h_0 \\ e^+ &\leq h_{n-1} + 1 - h_n \end{aligned} \quad (2.14)$$

Poincaré–Hopf equality for $n = 2i + 1$

We now prove the Poincaré–Hopf equality for $n = 2i + 1$.

Poincaré duality on the boundary of N implies that $B_{(2i-j)}^- = B_j^-$. Also, since $\operatorname{rank} \operatorname{im} i_n = 0$, it follows from (2.2) that:

$$\begin{aligned} -h_{2i+1} + h_{2i} - \dots - h_3 + h_2 - h_1 + h_0 \\ + 2e^- - 2B_1^- + 2B_2^- \dots + (-1)^{i-1} 2B_{i-1}^- + (-1)^i B_i^- = \\ = \sum_{j=0}^{2i+1} (-1)^j \operatorname{rank} H_j(N) \end{aligned} \quad (2.15)$$

Similarly, using the long exact sequence of the pair (N, N^+) , (2.3), the fact that $\operatorname{rank} \operatorname{im} i'_n = 0$ and using the duality of the indices, $h_j(\Lambda) = h_{[(2i+1)-j]}(\Lambda')$ the following equation holds for $n = 2i + 1$:

$$\begin{aligned} h_{2i+1} - h_{2i} - \dots + h_1 - h_0 + 2e^+ - 2B_1^+ + 2B_2^+ \dots + (-1)^{i-1} 2B_{i-1}^+ + (-1)^i B_i^+ = \\ = \sum_{j=0}^{2i+1} (-1)^j \operatorname{rank} H_j(N) \end{aligned} \quad (2.16)$$

Subtracting (2.15) from (2.16) and dividing by two, the following equation holds:

$$\begin{aligned} h_{2i+1} - h_{2i} + \dots - h_2 + h_1 - h_0 + (e^+ - e^-) - (B_1^+ - B_1^-) + \dots + \\ (-1)^{i-1} (B_{i-1}^+ - B_{i-1}^-) + (-1)^i \frac{(B_i^+ - B_i^-)}{2} = 0 \end{aligned} \quad (2.17)$$

which can be represented in short by the following alternative form of the classical *Poincaré–Hopf Equality*:

$$\mathcal{B}^+ - \mathcal{B}^- = e^- - e^+ + \sum_{j=0}^{2i+1} (-1)^j h_j \quad (2.18)$$

where,

$$\begin{aligned} \mathcal{B}^+ &= \frac{(-1)^i}{2} B_i^+ + (-1)^{i-1} B_{i-1}^+ \pm \dots - B_1^+ \\ \mathcal{B}^- &= \frac{(-1)^i}{2} B_i^- + (-1)^{i-1} B_{i-1}^- \pm \dots - B_1^-. \end{aligned}$$

Poincaré–Hopf equality for $n = 2i = 2 \pmod{4}$

We now prove the Poincaré–Hopf equality for $n = 2i$ with $n = 2 \pmod{4}$.

We wish to show that

$$h_i + \sum_{j=0}^{i-1} (-1)^j (B_j^+ - B_j^-) - \sum_{j=0}^{i-1} (-1)^j (h_{2i-j} - h_j) = 0 \pmod{2}. \quad (2.19)$$

In this case it is useful to use a connectivity result found in Cruz and de Rezende (1999). A singularity of Morse index j in an isolating neighborhood (N, N^+, N^-) can increase (resp. decrease) the j -th (resp. $(j-1)$ -th) Betti number of N^+ with respect to the j -th (resp. $(j-1)$ -th) Betti number of N^- . We refer to this singularity as j -disconnecting, or in short j -d (resp. $(j-1)$ -connecting, or in short $(j-1)$ -c).

In what follows, h_j^d and h_j^c indicate the number of singularities of Morse index j of type j -d and $(j-1)$ -c respectively, so that the total number of singularities of Morse index j is

$$h_j = h_j^d + h_j^c \quad (2.20)$$

Note that the above result, (2.19), is not necessarily true if $n = 2i = 0 \pmod{4}$. The reason for this is that a singularity of index i can also be of type β -i, which implies that the Betti numbers on N^+ and N^- do not change. In this case, (2.20) does not hold for $j = i$. In fact,

$$h_i = h_i^d + h_i^c + \beta\text{-i.}$$

The idea of the proof is to rewrite the numbers given by the difference in Betti numbers $B_j^+ - B_j^-$ in terms of the number of singularities of type c and d that affect B_j^\pm .

Let (N^{2i}, N^+, N^-) with N^+ having B_0^+ connected components and N^- having B_0^- connected components be an isolating neighborhood for a collection of h_k singularities, of Morse index k . Suppose the Betti numbers on N^+ are $B_0^+, B_1^+, \dots, B_{i-1}^+$ and on N^- are $B_0^-, B_1^-, \dots, B_{i-1}^-$. Also, by Poincaré duality $B_j^\pm = B_{2i-1-j}^\pm$.

The proof will be achieved by constructing two connected isolating neighborhoods (L^-, N^-) with entering set equal to the empty set and (L^+, N^+) with exiting set equal to the empty set.

One starts with the B_0^- boundary components that constitute N^- to get a connected incoming boundary one must connect the outgoing boundary components N^- with h_1^c singularities of Morse index 1. Now one proceeds to decrease B_j^- and consequently its dual B_{2i-1-j}^- to 0 by adding h_{j+1}^c singularities of Morse index $(j+1)$ and h_{2i-j}^c singularities of Morse index $2i-j$ which after each addition has the effect of decreasing by one B_j^- and consequently its dual B_{2i-1-j}^- . This is done for $j = 2, \dots, i$. The last Betti number after all singularities are added is $(B_0, B_1, \dots, B_{i-1}) = (1, 0, \dots, 0)$ to which one adds an index $2i$ singularity, a source. Hence, one forms (L^-, N^-) with a unique source.

Similarly, to get a connected outgoing boundary one must connect the incoming boundary components N^+ with h_{2i-1}^d singularities of Morse index $(2i-1)$. Now one proceeds to decrease B_j^+ and consequently its dual B_{2i-1-j}^+ to 0 by adding h_j^d singularities of Morse index j and h_{2i-1-j}^d singularities of Morse index $2i-j+1$ which after each addition has the effect of decreasing B_j^+ by one. This is done for $j = 1, \dots, (i-1)$. The last Betti number after all singularities are added is $(B_0, B_1, \dots, B_{i-1}) = (1, 0, \dots, 0)$ to which one adds an index 0 singularity, a sink. Hence, one forms (L^+, N^+) with a unique sink.

Now, form the connected sum by removing two disks, one around the sink and the other around the source to form (L, N^+, N^-) . Thus for $j = 0, \dots, (i-1)$, one has that $h_0 = h_{2i} = 0$ and

$$B_j^+ - B_j^- = h_j^d + h_{2i-1-j}^d - h_{j+1}^c - h_{2i-j}^c \quad (2.21)$$

By substituting (2.20) and (2.21) into (2.19) one obtains:

$$\begin{aligned} [h_i^c + h_i^d] + \sum_{j=0}^{i-1} (-1)^j (h_j^d + h_{2i-1-j}^d - h_{j+1}^c - h_{2i-j}^c) + \sum_{j=0}^{i-1} (-1)^{j+1} (h_{2i-j} - h_j) = \\ [h_i^c + h_i^d] + (h_{2i-1}^d - h_1^c) - (h_1^d + h_{2i-2}^d - h_2^c - h_{2i-1}^c) + \\ + (h_2^d + h_{2i-3}^d - h_3^c - h_{2i-2}^c) + \dots - (h_{i-2}^d + h_{i+1}^d - h_{i-1}^c - h_{i+2}^c) \\ + (h_{i-1}^d + h_i^d - h_i^c - h_{i+1}^c) + \sum_{j=0}^{i-1} (-1)^{j+1} (h_{2i-j} - h_j) \end{aligned} \quad (2.22)$$

By rearranging the terms, grouping them by index and using (2.20), one obtains the

desired result.

$$\begin{aligned}
[h_i^c + h_i^d] + \{-(h_1^c + h_1^d) + (h_2^c + h_2^d) - \dots \\
+ (h_{i-1}^c + h_{i-1}^d) - (h_i^c - h_i^d) \\
- (h_{i+1}^c + h_{i+1}^d) + (h_{i+2}^c + h_{i+2}^d) - \dots \\
- (h_{2i-2}^c + h_{2i-2}^d) + (h_{2i-1}^c + h_{2i-1}^d)\} + \\
+ h_{2i-1} - h_{2i-2} + \dots + h_{i+2} - h_{i+1} + h_{i-1} - h_{i-2} + \dots - h_1 = \\
2h_{2i-1} - 2h_{2i-2} + \dots + 2h_{i+2} - 2h_{i+1} + \\
+ 2h_i^d + 2h_{i-1} - 2h_{i-2} + \dots - 2h_1 = 0 \mod 2 \quad (2.23)
\end{aligned}$$

□

The Poincaré–Hopf inequality in the orientable case $n = 2$ is

$$h_1 - h_2 - h_0 + 2 - (e^+ + e^-) \geq 0 \text{ and even.} \quad (2.24)$$

If M is non-orientable the Poincaré–Hopf inequality is the same, however the expression on the left hand side of the inequality (2.24) need not be even. Inequality (2.24) appears in Franzosa and de Rezende (1993).

2.2.2 Global Poincaré–Hopf Inequalities for Closed Manifolds

Certain global topological invariants of the manifold, can make the inequalities sharper. For instance, Cornea (1989) defines a genus of a smooth closed manifold M , $g(M)$, as the maximal number of mutually disjoint, smooth, compact, connected, two-sided codimension one submanifolds that do not disconnect M . Cornea (ibid.) also proved that $g(M) \leq \beta_1(M)$.

By the Morse–Conley inequalities one has $\beta_1(M) - \beta_0(M) \leq h_1 - h_0$. It follows that, $g(M) \leq \beta_1(M) \leq h_1 - h_0 + \beta_0(M)$. Hence, one has a weaker version of the Morse inequalities with the Cornea genus:

$$h_1 \geq h_0 - 1 + g(M) \quad (2.25)$$

The advantage of the global Poincaré–Hopf inequalities is that unlike the Morse–Conley inequalities no reference is made to M and its Betti numbers.

In that spirit, one wishes to investigate these inequalities for different manifolds and Cornea genera. To do this more freely, without reference to a specific manifold, a parameter κ will play the role of the Cornea genus and we refer to these inequalities which includes $h_1 \geq h_0 - 1 + \kappa$ as the *global κ -Poincaré–Hopf inequalities*.

This parameter κ will play an important role in determining the Morse polytope, that is all the Betti numbers $(\beta_0, \beta_1, \dots, \beta_{n-1}, \beta_n)$ that satisfy the Morse inequalities for a given dynamical-topological data that satisfies the global Poincaré–Hopf inequalities,

$$(h_0, h_1, \dots, h_{n-1}, h_n, \kappa).$$

We show in the next chapter, among other interesting geometrical properties, that as κ increases the Morse polytopes become smaller as expected, since there are fewer Betti numbers $(\beta_0, \beta_1, \dots, \beta_{n-1}, \beta_n)$ that satisfy the Morse inequalities.

We refer to κ as a 1-connectivity parameter. Note that the (*) inequalities in (2.4) can also be substituted by:

$$\begin{cases} h_1 \geq h_0 - 1 + e^- + \kappa \\ h_{n-1} \geq h_n - 1 + e^+ + \kappa \end{cases}$$

We refer to these as the *local κ -Poincaré–Hopf Inequalities*.

The *global Poincaré–Hopf inequalities* are the Poincaré–Hopf inequalities for closed manifolds (2.26), (2.27), (2.28) and are in fact, a particular case of the Poincaré–Hopf inequalities for isolating blocks (2.4), (2.5), (2.6).

$$\begin{cases} -h_j \leq (h_{n-(j-1)} - h_{j-1}) - (h_{n-(j-2)} - h_{j-2}) + \\ \dots \pm (h_{n-1} - h_1) \pm (h_n - h_0) \leq h_{n-j} \text{ for } 2 \leq j \leq i \\ \begin{cases} h_1 \geq h_0 - 1 + \kappa \\ h_{n-1} \geq h_n - 1 + \kappa \end{cases} \end{cases} \quad (2.26)$$

In the case $n = 2i + 1$, we have

$$\sum_{j=0}^{2i+1} (-1)^j h_j = 0 \quad (2.27)$$

and in the case $n = 2i \equiv 2 \pmod{4}$, we have the additional constraint that

$$h_i - \sum_{j=0}^{i-1} (-1)^j (h_{2i-j} - h_j) \text{ be even.} \quad (2.28)$$

Surprisingly, it turns out that, whenever these inequalities are satisfied for a pre-assigned dynamical data (h_0, \dots, h_n) , it can be shown that there exists a collection of Betti numbers that satisfy the Morse inequalities with this same data. Conversely, if the Morse inequalities are satisfied for (h_0, \dots, h_n) and $(\gamma_0, \dots, \gamma_n)$ then (h_0, \dots, h_n) satisfies the Poincaré–Hopf inequalities. This is stated in the next theorem.

A nonnegative list of integers $(\gamma_0, \gamma_1, \dots, \gamma_{n-1}, \gamma_n)$ satisfying $\gamma_{n-k} = \gamma_k$, for $k = 0, \dots, n$, $\gamma_0 = \gamma_n = 1$, and $\gamma_{n/2}$ be even if $n \equiv 2 \pmod{4}$, is called a Betti number vector.

Theorem 2.2. *A set of nonnegative numbers (h_0, h_1, \dots, h_n) satisfies the Poincaré–Hopf inequalities in (2.26), (2.27), (2.28) if and only if it satisfies the Morse inequalities (2.1) for some Betti number vector $(\gamma_0, \gamma_1, \dots, \gamma_{n-1}, \gamma_n)$.*

This result is not merely a change of inequalities. One should note that the Morse inequalities involve (h_0, \dots, h_n) and $(\gamma_0, \dots, \gamma_n)$ whereas the global Poincaré–Hopf inequalities only involve (h_0, \dots, h_n) .

In some sense the Poincaré–Hopf inequalities pre-process admissible data, that is, if (h_0, \dots, h_n) does not satisfy the Poincaré–Hopf inequalities, there is no closed n -manifold which admits (h_0, \dots, h_n) as its dynamical data. This is a direct consequence of Theorem 2.2 and the classical results of Morse (1925).

The Poincaré–Hopf inequalities can also be used to prove the existence of critical points of index k from a priori knowledge of the existence of critical points of lower index and their duals. That is, these inequalities can also be used to give bounds on the numbers h_j with respect to alternating sums of h_s with $s < j$ and their duals h_{n-s} . In the case of negative gradient flows of Morse functions, these inequalities provide bounds on the number of singularities c_j of Morse index j with respect to alternating sums of c_s with $s < j$ and their duals c_{n-s} .

2.3 Homological Refinement of Singularities into Connectivity types

An important role in alternative proofs of the results presented in this chapter, is played by a more elaborate classification of singularities that provides not only the information on its index but also on its connectivity type. Given a nondegenerate singularity, a classical approach is to associate to it, its Morse index j . More generally, one can associate to a nondegenerate singularity the numerical Conley homology indices, $h_j = 1$ and $h_k = 0$ for all $k \neq j$. Cruz and de Rezende (1999) classified these singularities not only by their index, but also by the effect caused on the Betti numbers of the entering and exiting boundaries, N^+ and N^- , of an isolating block N containing it. In other words, a singularity of Morse index j can increase (resp. decrease) the j -th (resp. $(j-1)$ -th) Betti number of N^+ with respect to the j -th (resp. $(j-1)$ -th) Betti number of N^- . We refer to this singularity as j -disconnecting, or in short j -d (resp. $(j-1)$ -connecting, or in short $(j-1)$ -c). In the case $n = 2i = 0 \pmod{4}$, a singularity of index i is β -i, if all Betti numbers are kept constant. In order to understand the local connectivity behaviour caused by the singularity, one makes use of Handle theory.

2.3.1 Handle Theory

We now turn our attention to a homological study of an isolated invariant set S within an isolating block (N, N^+, N^-) and investigate the constraints imposed by the numerical homology Conley indices to the Betti numbers of N^+ and N^- , the entering and exiting boundaries, respectively, for the flow.

The simplest kind of n dimensional isolating block for a singularity of index ℓ is an ℓ -handle, $D^\ell \times D^{n-\ell}$ where D^j is the closed unit j -disk. However, we are interested in isolating blocks with closed codimension one manifolds, N^+ and N^- , as boundary.

Thus, by attaching ℓ -handles to collars of closed codimension one manifolds we obtain a myriad of isolating blocks for index ℓ singularities. Denote the boundary of D^j , ∂D^j , as the $(j-1)$ -sphere S^{j-1} .

Let N be a compact n -manifold and $H = D^\ell \times D^{n-\ell}$. Let $\theta : \partial D^\ell \times D^{n-\ell} \rightarrow \partial N$ be an embedding which defines the new manifold $N' = N \cup_\theta H$, which is the result of attaching an ℓ -handle to N . Alternative notations can be: $N' = N \cup H^{(\ell)}$ or $N' = N \cup H$. The map θ is an embedding which we simply refer to as an *attaching map*. The ℓ -handle is defined as the pair (H, θ) which we denote loosely as $H^{(\ell)}$. The following terms have a dynamical counterpart. For instance, the *core* of the handle is $D^\ell \times 0$ and the *cocore* is $0 \times D^{n-\ell}$. The Morse index of a singularity is the *index of the handle* which contains it and hence the dimension of the unstable manifold of the singularity must equal the dimension of the core of the handle. Similarly, the dimension of the stable manifold of the singularity must equal the dimension of the cocore of the handle.

Also, $\partial D^\ell \times 0$ is the *attaching sphere* and $0 \times \partial D^{n-\ell}$ is the *belt sphere* also known as the a -sphere and b -sphere respectively. The *attaching region* is $\partial_- H^{(\ell)} = (\partial D^\ell) \times D^{n-\ell}$ and the *belt region* is $\partial_+ H^{(\ell)} = D^\ell \times \partial D^{n-\ell}$. If N is a smooth compact n -manifold and ∂N is the disjoint union of open and closed codimension one submanifolds N^- and N^+ , we refer to (N, N^+, N^-) as a smooth manifold triad. In this case N is said to be a cobordism from N^- to N^+ and N^- and N^+ are said to be cobordant. Note that the manifolds in a cobordism are not assumed connected. According to the above definition N^+ can be thought of as the boundary components of N which the flow enters through and N^- as the boundary components which the flow exits through. We can create a further cobordism by attaching a handle H to N^- . Hence, the composition of cobordisms is well defined. See Milnor (1963) for more details.

We now turn our attention to the homological study of an isolated invariant set S within an isolating block (N, N^+, N^-) and investigate the constraints imposed by the numerical Conley indices on the Betti numbers of N^+ and N^- where N^+ and N^- are the entering and exiting boundaries, respectively, for the flow.

A handle $H^{(\ell)}$ containing a singularity of index ℓ is called *ℓ -disconnecting*, in short ℓ -d, if this handle has the algebraic effect of increasing the ℓ -th Betti number of N^+ . A handle containing a singularity of index ℓ is called *$(\ell - 1)$ -connecting*, in short $(\ell - 1)$ -c, if this handle has the algebraic effect of decreasing the $(\ell - 1)$ -th Betti number of N^+ . A handle containing a singularity of index ℓ is called *β -invariant*, in short β -i, if all Betti numbers are kept constant. Details can be found in Cruz and de Rezende (1999).

Proposition 2.1. *1. Let $n = 2i$ and $\ell \neq i$ or $n = 2i + 1$ and $\ell \neq i, i + 1$. Then*

(a) if $H^{(\ell)}$ is ℓ -d then

$$\beta_k(N^+) = \begin{cases} \beta_k(N^-) & \text{for all } k \neq \ell, n - \ell - 1 \\ \beta_k(N^-) + 1 & \text{for } k = \ell, n - \ell - 1 \end{cases}$$

or else,

(b) if $H^{(\ell)}$ is $(\ell - 1)$ -c then

$$\beta_k(N^+) = \begin{cases} \beta_k(N^-) & \text{for all } k \neq \ell - 1, n - \ell \\ \beta_k(N^-) - 1 & \text{for } k = \ell - 1, n - \ell \end{cases}$$

2. if $n = 2i$ and $\ell = i$ even, then

(a) if $H^{(\ell)}$ is $(\beta\text{-}i)$ then

$$\beta_k(N^-) = \beta_k(N^+) \text{ for all } k$$

(b) if $H^{(\ell)}$ is $\ell\text{-}d$ then

$$\beta_k(N^+) = \begin{cases} \beta_k(N^-) \text{ for all } k \neq i, i-1 \\ \beta_k(N^-) + 1 \text{ for } k = i, i-1 \end{cases}$$

or else,

(c) if $H^{(\ell)}$ is $((\ell-1)\text{-}c)$ then

$$\beta_k(N^+) = \begin{cases} \beta_k(N^-) \text{ for all } k \neq i, i-1 \\ \beta_k(N^-) - 1 \text{ for } k = i, i-1 \end{cases}$$

3. if $n = 2i + 1$ and $\ell = i$ then

(a) if $H^{(\ell)}$ is $(\ell\text{-}d)$ then

$$\beta_k(N^+) = \begin{cases} \beta_k(N^-) \text{ for all } k \neq i \\ \beta_k(N^-) + 2 \text{ for } k = i \end{cases}$$

or else,

(b) if $H^{(\ell)}$ is $((\ell-1)\text{-}c)$ then

$$\beta_k(N^+) = \begin{cases} \beta_k(N^-) \text{ for all } k \neq i+1, i-1 \\ \beta_k(N^-) - 1 \text{ for } k = i+1, i-1 \end{cases}$$

4. if $n = 2i + 1$ and $\ell = i + 1$ then

(a) if $H^{(\ell)}$ is $((\ell-1)\text{-}c)$ then

$$\beta_k(N^+) = \begin{cases} \beta_k(N^-) \text{ for all } k \neq i \\ \beta_k(N^-) - 2 \text{ for } k = i \end{cases}$$

or else,

(b) if $H^{(\ell)}$ is $(\ell\text{-}d)$ then

$$\beta_k(N^+) = \begin{cases} \beta_k(N^-) \text{ for all } k \neq i+1, i-1 \\ \beta_k(N^-) + 1 \text{ for } k = i+1, i-1 \end{cases}$$

The possible effects for a handle containing a singularity of index ℓ in the case that the ambient n -manifold is even dimensional, say $n = 2i$, are as follows. The Betti numbers that correspond to codimension one closed manifolds of the entering components will increase or decrease by 1 as in Figure 2.1 whenever the handle is respectively, disconnecting or connecting in nature. However, a new phenomena occurs here for middle-dimensional handles, i -handles, in an ambient manifold with $n = 2i = 0(\text{mod } 4)$, which can be attached on certain manifolds so that all Betti numbers remain unaltered. These are β -invariant handles, β -i for short. More on these handles will be said in Chapter 4. Each of these cases are represented in Figure 2.1.

On the other hand, if the ambient n -manifold is odd dimensional, say $n = 2i + 1$, the β -invariant handles in Figure 2.1 do not occur. The Betti numbers correspond to codimension one closed manifolds which are even dimensional, $2i$ and precisely for the middle dimensional i -handle which is i -d and $i + 1$ -handle which is i -c, the i -th Betti number of the entering components will increase or decrease by 2 whenever the handle is respectively, disconnecting or connecting in nature. All other ℓ -handles exhibit the algebraic effect of increasing the ℓ -th Betti number of the entering boundary by one if the handle is disconnecting or decreasing the $\ell - 1$ -th Betti number of the entering boundary by one if the handle is connecting. See Figure 2.1.

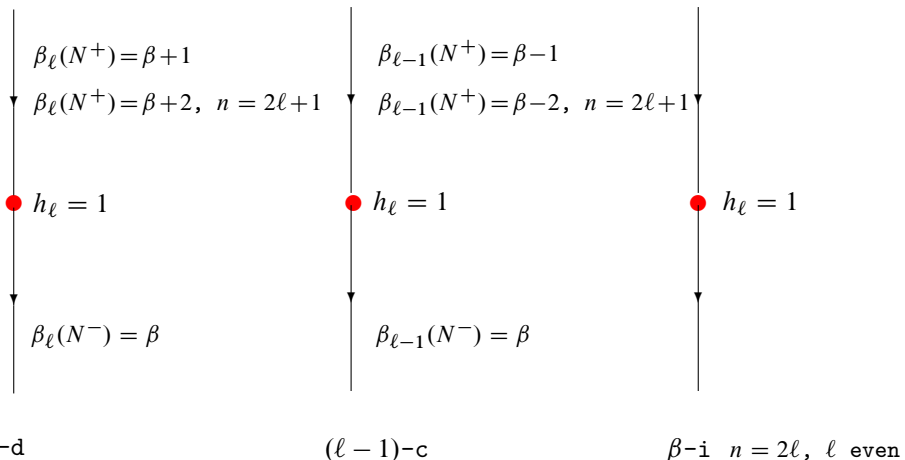


Figure 2.1: The possible algebraic effects of ℓ -handles.

2.4 Lyapunov Graphs, Semigraphs and Obstructions to Realizations

Lyapunov graphs were initially introduced by Franks (1982) and turn out to be an excellent bookkeeping device that retains simultaneously local and global dynamical-topological information of the flow and its phase space which is a closed n -manifold M .

Recall that results of Conley (1978) imply the existence of a continuous Lyapunov function $f : M \rightarrow \mathbb{R}$ associated to the flow $\varphi_t : M \rightarrow M$, on a closed n -manifold M with the property that it strictly decreases along orbits outside of the chain recurrent set \mathcal{R} , that is, if $x \notin \mathcal{R}$ then $f(\varphi_t(x)) < f(\varphi_s(x))$ for $t > s$ and is constant on the chain recurrent components of \mathcal{R} . For our purposes, we further assume that \mathcal{R} is a finite component chain recurrent set where each component R_k is an isolated invariant set.

Define the following equivalence relation on M : $x \sim_f y$ if and only if x and y belong to the same connected component of a level set of f . We call this one dimensional quotient space, M/\sim_f , a *Lyapunov graph*. We will refer to a Lyapunov graph associated to an n -manifold M simply as a *Lyapunov graph in dimension n* . Due to the fact that f decreases along orbits of the flow, this graph is directed and has no oriented cycles. We say that f has $c \in \mathbb{R}$ as a *critical value* if $f(R_k) = c$ for some k , otherwise it is said to be a *regular value*. A point v in M/\sim_f is called a *vertex* if $f(v) = c$ where c is a critical value and $f^{-1}(c)$ contains R_k for some k . Otherwise it is an *edge point*. Hence, each vertex v_k represents components R_k of the chain recurrent set \mathcal{R} and thus can be labelled with dynamical-topological invariants. For instance, we may label a vertex v_k with the numerical homology Conley indices of the associated R_k and denote it by $h(v_k) = (h_0(v_k), \dots, h_n(v_k))$. Each edge represents a level set $f^{-1}(a)$ times an interval $(0, 1)$ and hence can be labelled with topological invariants of the level set, such as, the Betti numbers. We remark that the choice of labellings on a graph will depend very much on the type of results that one seeks to prove.

Given a finite set V we define a *directed semigraph* $G' = (V', E')$ as a pair of sets $V' = V \cup \{\infty\}$, $E' \subset V' \times V'$. As usual, we call the elements of V' vertices and since we regard the elements of E' as ordered pairs, these are called directed edges. Furthermore the edges of the form (∞, v) and (v, ∞) are called *semi-edges* (or dangling edges as in de Rezende (1987)). Note that whenever G' does not contain semi edges, G' is a graph in the usual sense. The graphical representation of the graph will have the semi-edges cut short, sometimes referred herein as dangling edges.

Similarly, one may define a Lyapunov semigraph for an isolated invariant set R which is a component of \mathcal{R} of the flow φ_t . If f is a Lyapunov function associated to φ_t and $c = f(R)$ then for $\varepsilon > 0$, the component of $f^{-1}[c - \varepsilon, c + \varepsilon]$ that contains R is an isolating neighborhood for R . Take $(N, N^-) = (f^{-1}[c - \varepsilon, c + \varepsilon], f^{-1}(c - \varepsilon))$ as an index pair for R . Thus, N/\sim_f is a *Lyapunov semigraph*. The labelling of vertices and edges will be the same as for a Lyapunov graph. We will refer to a Lyapunov semigraph associated to an n -manifold N simply as a *Lyapunov semigraph in dimension n* .

2.4.1 Abstract Lyapunov Graphs and Semigraphs

We are ready to define an abstract Lyapunov graph (semigraph) in dimension n and question its realizability on a compact n -manifold.

By inferring some properties of Lyapunov graphs, we choose to define an *abstract Lyapunov graph (semigraph)* in dimension n as a finite, connected, oriented graph, that has no oriented cycles. Moreover, each vertex is labelled with a chain recurrent flow on a compact n -dimensional space or with dynamical-topological invariants. Also, each edge is labelled with some topological invariants of a closed $(n-1)$ -dimensional manifold. Let us make this definition more precise for our purposes.

First of all, the edge labelling chosen for abstract Lyapunov graphs (semigraphs) is the Betti numbers of a closed codimension one manifold which the edge represents. A *Betti number vector* is a list of nonnegative integers with $(\gamma_0, \gamma_1, \dots, \gamma_{n-1}, \gamma_n)$ where $\gamma_{n-k} = \gamma_k$, $\gamma_0 = \gamma_n = 1$ and $\gamma_{n/2}$ is even if n is even. Thus, because of duality one represents $(\gamma_0, \gamma_1, \dots, \gamma_n)$ by $(1, \gamma_1, \dots, \gamma_{\lfloor \frac{n}{2} \rfloor})$.

We also choose the vertex labelling of abstract Lyapunov graphs (semigraphs) to be the numerical homology Conley indices, $\dim CH_j(R_k) = h_j(v_k)$, with $j = 0, \dots, n$ of the chain recurrent component R_k which by hypothesis is an isolated invariant set.

Recall that a vertex v_k represents a chain recurrent flow R_k on a compact n -dimensional space X that may contribute to the Cornea genus of the phase space, and which is collapsed to a point under the equivalence relation \sim_f . For this reason it is necessary to account for the parameter $\kappa(v_k)$ related to the Cornea genus of X and thus each vertex is labelled with a list of nonnegative integers $(h_0(v_k), \dots, h_n(v_k), \kappa(v_k))$, where $\kappa(v_k)$ is the *cycle number of the vertex v_k* .

To shorten and simplify notation, the vertex is labelled $h_j(v_k) = n_j$ whenever $n_j \neq 0$. Also, $\kappa(v_j) = k_j$ whenever $k_j \neq 0$. This latter notation is convenient whenever $(h_0(v_k), \dots, h_n(v_k), \kappa(v_k))$ has many zero entries.

The *cycle rank* κ_L of a graph L is the maximum number of edges that can be removed without disconnecting the graph. We define the *cycle number* of L as $\kappa = \kappa_L + \kappa_V$.

Given an abstract Lyapunov graph L with vertex set V and cycle rank κ_L , we indicate it by $L(h_0, \dots, h_n, \kappa)$ where

$$h_j = \sum_{v_k \in V} h_j(v_k) \quad \text{and} \quad \kappa_V = \sum_{v_k \in V} \kappa(v_k).$$

These definitions are easily extended to Lyapunov semigraphs.

Definition 2.1. An *abstract Lyapunov graph (semigraph) in dimension n* is an oriented graph (semigraph) with no oriented cycles, such that:

- each vertex v is labelled with a list of nonnegative integers

$$(h_0(v) = k_0, \dots, h_n(v) = k_n, \kappa(v)),$$

where $\kappa(v)$ is the *cycle number* of the vertex;

- each edge is labelled with a Betti number vector $(\beta_1, \dots, \beta_{\lfloor \frac{n-1}{2} \rfloor})$ where we omit $\beta_0 = 1$ since this is always the case.

An abstract Lyapunov graph of Morse type is an abstract Lyapunov graph with each vertex v labelled with a nondegenerate singularity of Morse index ℓ , i.e., $h_\ell(v) = 1$, and with all cycle numbers of vertices equal to zero. This is always the case since these singularities are always realized on disks whose genus is zero. Moreover, the label on the edges will be in concordance with Proposition 2.1, i.e., for each vertex labelled with a singularity of Morse index ℓ , equivalently, with numerical homology Conley index $h_\ell(v) = 1$, the positively incident edges to v will be labelled according to the possibilities of labels of N^+ and the negatively incident edges will be labelled according to the possibilities of labels of N^- as dictated by Proposition 2.1.

It is easy to see that the cycle number of an abstract Lyapunov graph of Morse type is equal to its cycle rank.

2.4.2 Obstructions to Realizability

The question asked regarding an abstract Lyapunov graph L is that of realizability. Does there exist a continuous flow φ with Lyapunov function $f : M \rightarrow \mathbb{R}$ such that its Lyapunov graph M/\sim_f is isomorphic to L ?

Theorem 2.2 asserts that any continuous flow defined on a closed manifold M , with Lyapunov function $f : M \rightarrow \mathbb{R}$ has a Lyapunov graph M/\sim_f that satisfies the Poincaré–Hopf inequalities for closed manifolds if and only if it satisfies the generalized Morse–Conley inequalities for some Betti number vector.

It is worth noting that abstract Lyapunov graphs L carry dynamical data and local topological invariants of level sets but no information on the Betti numbers of M . Hence, one cannot verify if the data they carry satisfy the Morse inequalities. On the other hand, L carries the information needed to check whether the local Poincaré–Hopf inequalities hold at each vertex. In any case, the Poincaré–Hopf inequalities, local and global, constitute necessary conditions for the existence of a gradient-like flow in the first place.

A similar question holds for an abstract Lyapunov semigraph L_v . The realizability question presents itself once again as to the existence of an isolating block with a flow whose isolated invariant set matches the numerical homology Conley indices with which v is labelled and with the Betti numbers of the entering and exiting boundary components matching the weights of the incoming and outgoing edges of v respectively. In short, an isolating block whose Lyapunov semigraph is isomorphic to L_v . As it was in the previous case, a necessary condition is that L_v satisfies the local Poincaré–Hopf inequalities.

If we restrict our attention to abstract Lyapunov semigraphs L_v where v is labelled with numerical Conley indices of a singularity of Morse index ℓ , we have the advantage that its isolating block is understood as an attachment of an ℓ handle. This simplifies the local realization question and reduces it to finding appropriate attaching maps that produce the desired effects on the boundaries of the resulting isolating block. More on this will be explored in Chapter 4.

A direct consequence of Theorem 2.2 is that the data on $L(h_0, \dots, h_n)$ satisfies the global Poincaré–Hopf inequalities in (2.26), (2.27), (2.28) if and only if it satisfies the Morse inequalities (2.1) for some Betti number vector $(\gamma_0, \gamma_1, \dots, \gamma_{n-1}, \gamma_n)$.

Hence, the non satisfiability of the Poincaré–Hopf inequalities, (2.26), (2.27), (2.28) is an obstruction to the realization of the Lyapunov graph $L(h_0, \dots, h_n)$ on a closed manifold. Moreover, this is also true locally. If $L(h_0, \dots, h_n)$ is a Lyapunov semigraph then the the non satisfiability of the local Poincaré–Hopf inequalities (2.4), (2.5), (2.6) implies there is no compact manifold which realizes the semigraph.

There is also a global obstruction given by the cycle number κ of the graph. Cruz and de Rezende (1998) showed that the cycle rank¹ κ of a Lyapunov graph is a lower bound to the Cornea genus, $g(M)$. Hence,

$$\kappa \leq g(M) \leq \beta_1(M)$$

which generalizes a theorem of Franks (1982) which asserts that if M is simply connected then its Lyapunov graph, M/\sim_f , is a tree, i.e., $\kappa = 0$.

Hence, as mentioned previously, $\kappa > \beta_1(M)$ is an obstruction to realization. If the data on the Lyapunov semigraph satisfies the local κ -Poincaré–Hopf inequalities (2.4), (2.5), (2.6) it is said to be *admissible*. Similarly, if the data on a Lyapunov graph satisfies the global κ -Poincaré–Hopf inequalities (2.26), (2.27), (2.28) it is also said to be *admissible*.

In Chapter 3 we determine all possible Betti number vectors for realizations of an admissible Lyapunov graph $L(h_0, \dots, h_n)$ on a closed manifold.

In Chapter 4, we search for sufficient conditions that guarantee realizability of admissible Lyapunov semigraphs L_v . In other words, we construct an isolating block for a continuous flow with an isolated invariant set which has a Lyapunov graph isomorphic to L_v . In general, the realization of L_v is not unique, since, based solely on numerical Conley indices there are topologically non equivalent isolated invariant sets that realize it. In Chapter 4, one explores the sufficiency of the Poincaré–Hopf inequalities for the realizability of an abstract Lyapunov graph (semigraph) on compact manifolds.

2.5 Graph Morsification and h_κ^{cd} -Systems

One cannot help but wonder if a flow φ_t for a more intricate isolated invariant sets R with isolating block (N, N^+, N^-) could be better understood by studying a simpler isolated invariant set S with the same isolating block N and with the same entering and exiting sets, N^+ and N^- respectively. This, of course, would imply that the homotopy Conley indices are isomorphic, i.e., $h(R) = h(S)$ since it is completely determined by (N, N^+, N^-) . Consequently it would follow that the homology Conley indices are isomorphic $CH_*(R) = CH_*(S)$.

For instance, there are suspensions of subshifts of finite type R for a Smale flow whose isolating block is the same as that of a collection of periodic orbits S of a Morse–Smale

¹In this work, it was assumed that the cycle rank was equal to the cycle number

flow. See Cruz and de Rezende (1999) and Lima, Manzoli Neto, and de Rezende (2019). One can ask if the simpler dynamics of a Morse–Smale flow sheds light on the more complicated dynamics of a Smale flow or vice-versa. Is there a continuation from one flow to the other? The same question holds if one takes a more intricate isolated invariant set R for a flow φ_t with isolating block (N, N^+, N^-) and considers an isolated invariant set S made up of Morse singularities that has the same isolating block. Furthermore, one may study bifurcation behaviour or the family of flows related by continuation of φ_t .

It is well known that given a compact smooth manifold N there exists a Morse function defined on N and consequently a Morse gradient flow.

Given a continuous flow φ_t with an isolated invariant set R with isolating block (N, N^+, N^-) and numerical homology Conley indices equal to $\{h_0, h_1 \dots, h_n\}$, one would like to determine a morsified flow with precisely h_i Morse singularities of index i , for all $i = 0, \dots, n$ defined on (N, N^+, N^-) . Moreover, the set S made up of the union of these singularities and their connections must be a maximal isolated invariant set in N and thus its Conley index $h(S)$ is of the same homotopy type as $h(R)$. This Morsification process in general provides more qualitative information. Intuitively, the Morsification of a Lyapunov graph L means the removal of all vertices v of L that are not labelled with nondegenerate singularities and substitute it with a semigraph of Morse type that respects the incident edges of v .

Consider the Lyapunov semigraphs L_v , where the vertex v is labelled with the numerical homology Conley indices of an isolated invariant set R and L_S with $S = \cup_{j=1}^k v_j$, where each v_j is labelled with a nondegenerate singularity.

A *Lyapunov semigraph Morsification* of L_v to L_S preserves the same labelled incoming and outgoing edges incident to L_v and the total numerical homology Conley indices in each dimension.²

Although, our emphasis in this book is on Morsification results, it is interesting to define a broader concept of graph continuation.³ One can also define a *Lyapunov semigraph continuation*. In other words, given L_v where v is labelled with the numerical homology Conley indices of R , a semigraph continuation of L_v to a semigraph L_S where $S = \cup_{j=1}^k v_j$ will preserve the same labelled incoming and outgoing edges as L_v and the total numerical homology Conley indices in each dimension

$$h_\lambda(v) = \sum_{j=1}^k h_\lambda(v_j), \quad \forall \lambda.$$

Note that the continued Lyapunov graph need not be of Morse type. See Figure 2.2.

An abstract Lyapunov graph $L = L(h_0, \dots, h_n)$ admits a Morsification if L_v admits a Morsification for all vertices v of L .

²Bertolim, Mello, and de Rezende (2003b) introduced this concept as *vertex explosion* which we now replace, in this text, with this more suggestive term.

³The main inspiration in adopting the term continuation comes from flow continuation, although Lyapunov graph or semigraph continuation does not imply flow continuation of its realization on a closed manifold or an isolating block respectively.

One approach in attempting to find an answer to the Morsification of an abstract Lyapunov graph $L(h_0, \dots, h_n)$ which has all its edges labelled with Betti number vectors is to tackle it first locally and at a combinatorial level.

We wish to address the question of morsifiability, that is, whether a Morsification of L_v is possible. In the following example, one obtains several Morsifications L_S associated to L_v , see Figure 2.3.

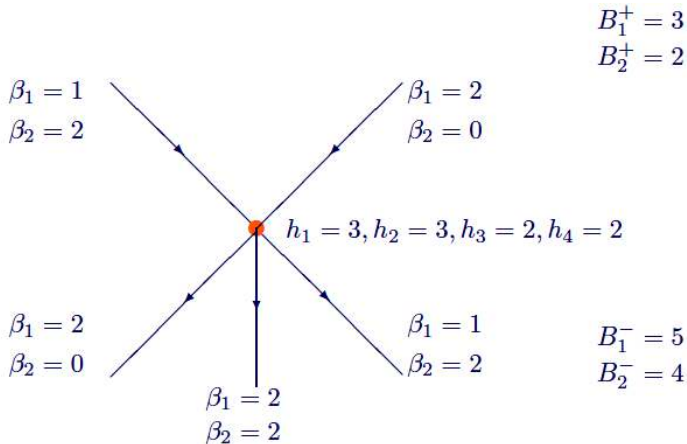


Figure 2.2: Semigraph L_v

An abstract Lyapunov graph L admits a *Morsification* if each vertex can be morsified.

Of course the data with which vertices and edges are labelled in $L(h_0, \dots, h_n)$ must satisfy the local Poincaré–Hopf inequalities at each vertex and its incident edges since this is a necessary condition for realizability. But is this enough to guarantee it can be morsified? The overarching theorem in this setting asserts that the satisfiability of the local Poincaré–Hopf inequalities are sufficient condition for the Morsification of $L(h_0, \dots, h_n)$.

Theorem 2.3. *Every abstract Lyapunov graph that satisfies the Poincaré–Hopf inequalities at each vertex can be morsified.*

In other words, admissible Lyapunov graphs are morsifiable. An example is in order. See Figure 2.4 and Figure 2.5.

2.5.1 Morsification Algorithm

The underlying idea is to locally describe under which conditions an abstract Lyapunov semigraph $L_v(h_0, \dots, h_n)$ can be morsified.

Note that it is not a question of merely choosing h_k vertices labelled with singularities of Morse index k , since one must insure that the Betti numbers on the incident edges of

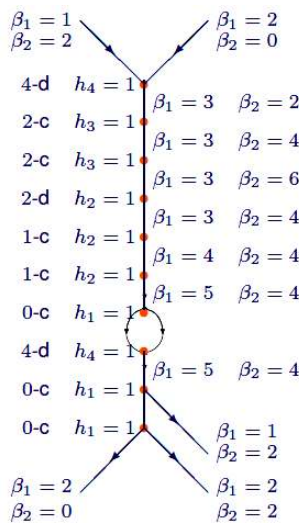
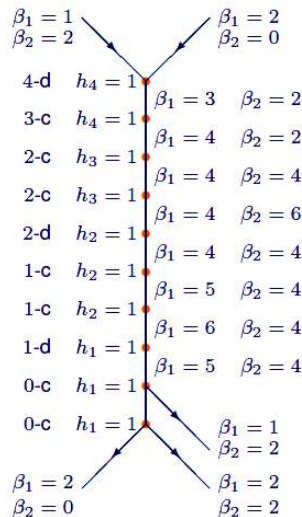


Figure 2.3: Morsifications

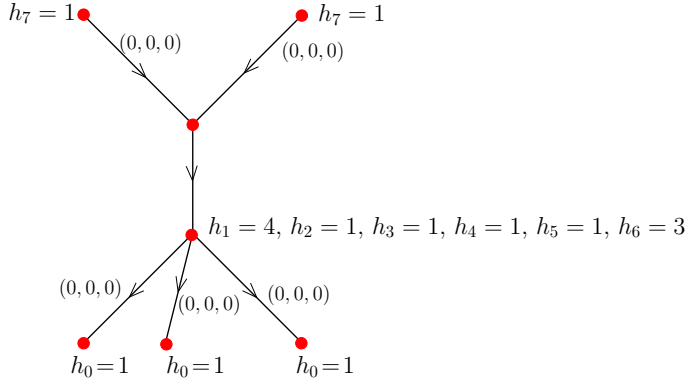


Figure 2.4: Admissible Lyapunov graph

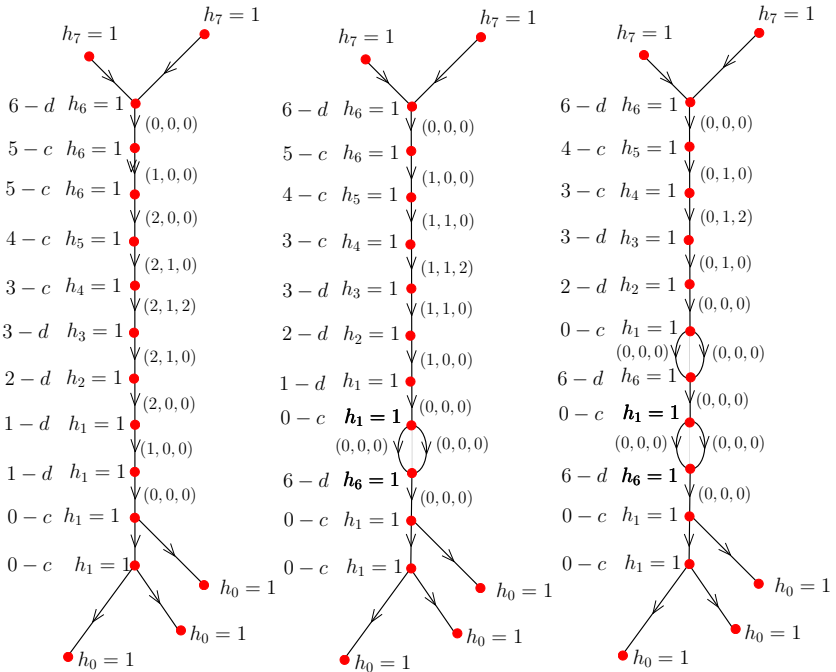


Figure 2.5: Morsifications

the Morsified graph are the same as those of $L_v(h_0, \dots, h_n)$. This does not happen by merely adding the correct number of Morse singularities. One must also gain control over the effects that each singularity has on increasing or decreasing the Betti numbers on the boundary of its isolating block as described in Proposition 2.1. The same terminology introduced for ℓ -handles in Proposition 2.1 is used for vertices labelled as a singularity of Morse index ℓ , that is, labelled with $h_\ell(v) = 1$ and all other numerical homology indices equal to zero. In other words, all vertices of an abstract Lyapunov graph labelled with $h_\ell(v) = 1$ are distinguished as being either ℓ disconnecting, ℓ -d, or $\ell - 1$ connecting, $\ell - 1$ -c. Moreover, whenever the graph represents an even dimensional manifold of dimension $2i$, a vertex labelled as a singularity of middle dimensional Morse index i may have the possibility of being β -invariant, β -i.

This is done by presenting an algorithm in terms of ℓ -d, $(\ell - 1)$ -c and β -i vertices which will in fact give more qualitative information than merely the number of singularities of each index. It also provides the type of each singularity as described in Proposition 2.1.

Semigraph Morsification Algorithm

In this section, a Lyapunov semigraph Morsification algorithm will be presented for a *saddle type* vertex v , $L_v(h_0, \dots, h_n)$ with $h_0 = h_n = 0$, $n \geq 2$, and h_i , $0 < i < n$ nonnegative integers. Recall that the semigraph corresponds to an isolated invariant set of saddle type of a gradient-like flow on an isolating block of dimension n with the topological-dynamical data given in $L_v(h_0, \dots, h_n)$. Hence, v is labelled with $\{h_1, h_2, \dots, h_{n-1}\}$ and its incoming edges labelled with $\{(\beta_0^+, \dots, \beta_{n-1}^+)\}_i^{e^+}$ and outgoing edges labelled

with $\{(\beta_0^-, \dots, \beta_{n-1}^-)\}_i^{e^-}$. Let $B_j^+ = \sum_{i=1}^{e^+} (\beta_j^+)_i$ and $B_j^- = \sum_{i=1}^{e^-} (\beta_j^-)_i$. See Figure 2.6.

Observe that $B_0^- = e^-$ and $B_0^+ = e^+$.

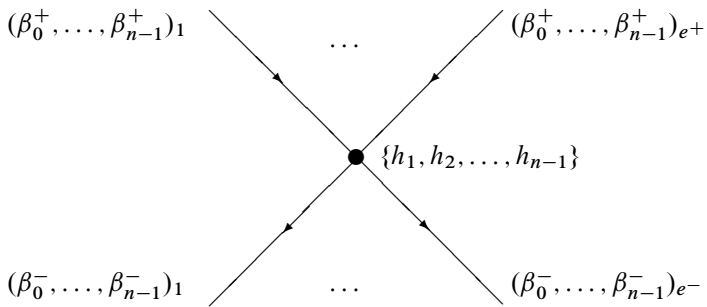


Figure 2.6: L_v Morsification

Consider an abstract Lyapunov semigraph $L_v(h_0, \dots, h_n, \kappa)$ with $e^+ \geq 0$ incoming and $e^- \geq 0$ outgoing edges. The ambient dimension is assumed to be n and is associated to a possible realization of L_v as a flow on a compact n -manifold. For a clearer picture of the Morsification algorithm that will morsify L_v in order to obtain an abstract Lyapunov semigraph of Morse type L , one should construct two semigraphs: L^- which will contain all vertices labelled with $h_k = 1$ for $k \leq i$ and L^+ which contains the remaining vertices and join them to form L where i refers to middle dimensions in both the even $n = 2i$ and odd $n = 2i + 1$ dimensional cases. The latter having two middle dimensions i and $i + 1$. The semigraph L^+ will have the property that it has e^+ incoming edges and one outgoing edge and the semigraph L^- has e^- outgoing edges and one incoming edge. We will show that the outgoing edge of L^+ and the incoming edge of L^- have the same Betti number vector and hence both semigraphs can be joined at that edge.

Schematically the Lyapunov semigraph Morsification algorithm has four basic parts:

1. adjusting the incident edges \rightarrow defines G^+ and G^- ;
2. inserting cycles according to the parameter κ ;
3. the linear morsification without middle dimensions \rightarrow defines $G^+ \cup \bigcup_{j=1}^{\ell} L_j^+$ and

$$G^- \cup \bigcup_{j=1}^{\ell} L_j^- \text{ where } \ell < \text{mid-dimension};$$
4. middle dimension morsification \rightarrow consider n odd, $n \equiv 0 \pmod{4}$, $n \equiv 2 \pmod{4}$.

For clarity, we start by assuming that the given data $(h_0, \dots, h_n, \kappa)$ on v has $\kappa = 0$ as well as $h_n = h_0 = 0$. In this case v will necessarily be a vertex of saddle type, i.e., $e^+ > 0$ and $e^- > 0$. At the end of the construction we remove these hypothesis.

The construction of L^- is done in increasing order of index, i.e., first adding h_1 vertices labelled $h_1 = 1$ up to h_i vertices labelled $h_i = 1$. The construction of L^+ is analogous, it is done in decreasing order of index, i.e., first adding h_{n-1} vertices labelled $h_{n-1} = 1$ down to h_{i+1} vertices labelled $h_{i+1} = 1$. As the vertices labelled with singularities are inserted, recall that the variation of the labels on the edges is always considered in the opposite direction of the orientation of the graph. Hence, the insertion of a vertex v and its effect on the Betti number of the edge is always accounted for on the edge positively incident to v .

The first part of the algorithm consists in adjusting the incident edges of the semigraph L^- since it must have the same number of outgoing edges as the semigraph L_v . We start by constructing a semigraph G^- which is formed using h_1 vertices labelled with $h_1 = 1$ of type 0-c. This has the effect of decreasing the 0-th Betti number by one and that is why this semigraph is an inverted Y, i.e. two outgoing edges and one incoming edge.

Choose two outgoing edges of L_v and join them with a vertex labelled with $h_1 = 1$ of type 0-c forming a semigraph G^- . The incoming edge of G^- has Betti number vector

equal to $(1, (\beta_1^-)_1 + (\beta_1^-)_2, \dots, (\beta_{n-2}^-)_1 + (\beta_{n-2}^-)_2, 1)$. Now form a semigraph G_2^- joining the incoming edge of G_1^- to a third edge of L_v using a vertex labelled with $h_1 = 1$ of type 0-c. The incoming edge of $G_1^- \cup G_2^-$ has Betti number vector $(1, (\beta_1^-)_1 + (\beta_1^-)_2 + (\beta_1^-)_3, \dots, (\beta_{n-2}^-)_1 + (\beta_{n-2}^-)_2 + (\beta_{n-2}^-)_3, 1)$. Hence, by joining all remaining edges of L_v in this fashion, one eventually obtains a semigraph G^- with e^- outgoing edges matching the labels of the outgoing edges of L_v and one incoming edge with Betti number vector equal to $(1, B_1^-, \dots, B_{n-2}^-, 1)$. Similarly, one constructs G^+ which is formed using vertices labelled with $h_{(n-1)} = 1$ of type $(n-1)$ -d.

Thus we must satisfy:

$$e^- - 1 - h_1^c = 0, \quad (2.29)$$

and

$$e^+ - 1 - h_{n-1}^d = 0. \quad (2.30)$$

Of course, each subsequent step requires that the equation

$$h_j = h_j^c + h_j^d, \quad j = 1, \dots, n \quad (2.31)$$

be satisfied so that the total numerical homology indices in L are the same as those in L_v . To be more precise and cover the rare presence of β invariant type vertices that can only occur in the mid-dimension i of an $n = 2i$ dimensional manifold where i is even, we must choose the more general form of equation (2.31)

$$h_j = h_j^c + h_j^d + \beta^i, \quad j = 1, \dots, 2i-1, \beta^i = 0 \text{ if } j \neq i \text{ or } i \text{ is even.} \quad (2.32)$$

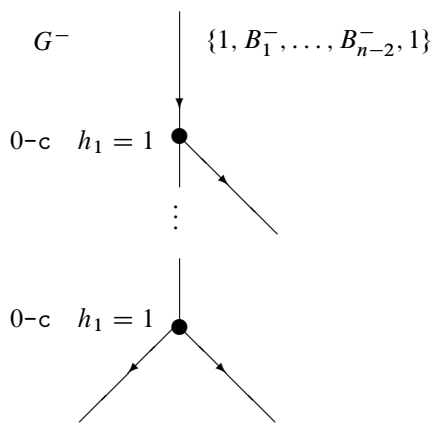


Figure 2.7: Construction of semigraph G^-

The subsequent steps of the algorithm rely on the fact that vertices labelled with $h_\ell = 1$ or $h_{\ell+1} = 1$ are the only ones responsible for the effect of increasing or decreasing the ℓ -th Betti number on any edge depending on whether it is ℓ -d or (ℓ) -c respectively. At all times, one must keep in mind that we are dealing with closed codimension one manifolds as boundary components where Poincaré duality holds. Therefore, once all singularities ℓ -d, $\ell + 1$ -c, have been used in the Morsification algorithm to construct L_ℓ^- and all singularities $(n - 1 - \ell)$ -d, $(n - \ell)$ -c have been used in the construction of L_ℓ^+ one must have $B_\ell = B_{n-1-\ell}$ on both the incoming edge of L_ℓ^- and the outgoing edge of L_ℓ^+ .

Since the insertion of any other type of vertex will not alter the ℓ -th and the $(n - \ell - 1)$ -th Betti number it is necessary that:

$$B_\ell = B_\ell^- + h_\ell^d - h_{\ell+1}^c = B_\ell^+ - h_{n-\ell-1}^d + h_{n-\ell}^c. \quad (2.33)$$

If the above equality is true then by duality the following equality holds:

$$B_{n-\ell-1} = B_{n-\ell-1}^- + h_\ell^d - h_{\ell+1}^c = B_{n-\ell-1}^+ - h_{n-\ell-1}^d + h_{n-\ell}^c.$$

The labels of B_ℓ and $B_{n-\ell-1}$ for $0 < \ell < i$ have all been adjusted.

Since these semigraphs L_k^- for $1 < k < i$ have the property that all vertices have degree 2 they can be joined. However, in the middle dimension i , if $n = 2i$ or $n = 2i + 1$, this has to be done carefully since the effect on the Betti numbers is slightly different.

The final part of the algorithm consists in inserting the middle dimensional singularities, if there are any, and joining L^+ to L^- if they have not already been joined in the previous part. Of course, all of this must be done, so that the weights on the last two edges to be joined coincide.

At this point the adjustments of the labels for the middle dimensions must be made.

Middle dimensional case for $n = 2i + 1$

Thus far two graphs $G^- \cup \bigcup_{j=1}^{i-1} L_j^-$ with incoming edge labelled with

$$\{1, B_1, B_2, \dots, B_{i-1}, B_i^-, B_{i+1}, \dots, B_{2i-1}, 1\}$$

and $G^+ \cup \bigcup_{j=1}^{i-1} L_j^+$ with outgoing edge labelled with

$$\{1, B_1, B_2, \dots, B_{i-1}, B_i^+, B_{i+1}, \dots, B_{2i-1}, 1\}$$

have been constructed.

To adjust B_i^- insert h_i^d vertices labelled with $h_i = 1$ of type i -d to the incoming edge of $G^- \cup \bigcup_{j=1}^{i-1} L_j^-$. Hence, the label on the incoming edge of the last vertex inserted of this type is $B_i^- + 2h_i^d$.

Now insert h_{i+1}^c vertices labelled with $h_{i+1} = 1$ of type i -c to the outgoing edge of $G^+ \cup \bigcup_{j=1}^{i-1} L_j^+$. Thus, the label on the outgoing edge of the last vertex inserted of this type is $B_i^+ + 2h_{i+1}^c$.

Thus, it is necessary that:

$$B_i = B_i^- + 2h_i^d = B_i^+ + 2h_{i+1}^c. \quad (2.34)$$

Since, the labels on the outgoing edge of one graph now coincides entirely with the labels on the incoming edge of the other graph, they can be joined to form a connected graph L .

Hence, at the end of this construction, we have imposed a collection of equations (2.29), (2.30), (2.31) (2.33), (2.34) forming a linear system that must be solved for $\{h_1^c, h_1^d, \dots, h_{2i}^c, h_{2i}^d\}$, in order for the algorithm to work.

$$\left\{ \begin{array}{l} h_j = h_j^c + h_j^d, \quad j = 1, \dots, 2i \\ e^- - 1 - h_1^c = 0 \\ e^+ - 1 - h_{2i}^d = 0 \\ \vdots \\ \frac{-(B_1^+ - B_1^-) + h_1^d - h_2^c - h_{2i}^c + h_{2i-1}^d}{2} = 0 \\ \frac{-(B_2^+ - B_2^-) + h_2^d - h_3^c - h_{2i-1}^c + h_{2i-2}^d}{2} = 0 \\ \vdots \\ \frac{-(B_i^+ - B_i^-)}{2} + h_i^d - h_{i+1}^c = 0 \end{array} \right. \quad (2.35)$$

Middle dimensional case for $n = 2i$

Observe that in this case the variation of the middle dimensional Betti number B_{i-1}^- and its dual B_i^- will vary by 0 if the vertex is of β -i type or by 1 otherwise. Recall that β -invariant type vertices never occur if $n = 2 \pmod 4$.

Insert h_{i-1}^d vertices labelled with $h_{i-1} = 1$ of type $(i-1)$ -d to the incoming edge of $G^- \cup \bigcup_{j=1}^{i-2} L_j^-$. Hence, the label on the incoming edge of the last vertex of this type inserted will be $B_{i-1}^- + h_{i-1}^d$. Subsequently, insert h_i^c vertices labelled with $h_i = 1$ of type $(i-1)$ -c. The label on the incoming edge of $G^- \cup \bigcup_{j=1}^{i-1} L_j^-$ will be $B_{i-1}^- + h_{i-1}^d - h_i^c$.

By duality the label B_i^- will be modified to $B_i^- + h_{i-1}^d - h_i^c$. We have constructed L^- .

Similarly, insert h_{i+1}^c vertices labelled with $h_{i+1} = 1$ of type i -c to the outgoing edge of $G^+ \cup \bigcup_{j=1}^{i-2} L_j^+$. Hence, the label on the outgoing edge of the last vertex of this type inserted will be $B_i^+ + h_{i+1}^c$. Subsequently, insert h_i^d vertices labelled with $h_i = 1$ of type i -d forming $G^+ \cup \bigcup_{j=1}^{i-1} L_j^+$ and the label on the outgoing edge of this graph will be $B_i^+ - h_i^d + h_{i+1}^c$. By duality the label B_{i-1}^+ has been modified to $B_{i-1}^+ - h_i^d + h_{i+1}^c$. We have constructed L^+ .

Moreover, it is necessary that

$$B_{i-1}^- + h_{i-1}^d - h_i^c = B_{i-1}^+ - h_i^d + h_{i+1}^c. \quad (2.36)$$

By duality if the above equation holds then the following is true

$$B_i^- + h_{i-1}^d - h_i^c = B_i^+ - h_i^d + h_{i+1}^c.$$

Since, the labels on the outgoing edge of the graph L^+ now coincides entirely with the labels on the incoming edge of the other graph L^- , they can be joined to form a connected graph L .

Hence, at the end of this construction, we have imposed a collection of equations (2.29), (2.30), (2.32), (2.33), (2.36) forming a linear system that must be solved for $\{h_1^c, h_1^d, \dots, \beta^i, \dots, h_{2i-1}^c, h_{2i-1}^d\}$ in order for the algorithm to work.

$$\left\{ \begin{array}{l} h_j = h_j^c + h_j^d + \beta^i, \quad j = 1, \dots, 2i-1, \beta^i = 0 \text{ if } j \neq i \text{ or } i \text{ is odd.} \\ e^- - 1 - h_1^c = 0 \\ e^+ - 1 - h_{2i-1}^d = 0 \\ \left\{ \begin{array}{l} -(B_1^+ - B_1^-) + h_1^d - h_2^c - h_{2i-1}^c + h_{2i-2}^d = 0 \\ -(B_2^+ - B_2^-) + h_2^d - h_3^c - h_{2i-2}^c + h_{2i-3}^d = 0 \\ \vdots \\ -(B_{i-1}^+ - B_{i-1}^-) + h_{i-1}^d - h_i^c - h_{i+1}^c + h_i^d = 0 \end{array} \right. \end{array} \right. \quad (2.37)$$

General Case

In the last section, we arrived at h^{cd} systems that must be solved to guarantee a continuation of an abstract Lyapunov graph $L_v(h_0 = 0, h_1, \dots, h_{n-1}, h_n = 0)$ where v is a saddle type vertex.

The restriction that a saddle vertex must have $h_0 = 0$ and $h_n = 0$ can easily be removed and one can consider a general saddle type vertex w and its abstract Lyapunov semigraph $L_w(h_0, h_1, \dots, h_{n-1}, h_n)$ with e^+ incoming and e^- outgoing edges.

This is done by adjusting the incident edges to the vertex w before applying algorithm described in 2.5.1. Form G_0^+ with h_n vertices labelled with $h_n = 1$ and $h_n - 1$ vertices labelled with $h_{n-1} = 1$ of the type $(n-1)$ -d which has one outgoing edge which connects to v labelled $(1, 0, \dots, 0, 1)$. We also form G_0^- with h_0 vertices labelled with $h_0 = 1$ and $h_0 - 1$ vertices labelled with $h_1 = 1$ of the type 0-c and has one incoming edge labelled $(1, 0, \dots, 0, 1)$. By joining G_0^+ to an edge positively incident to w and G_0^- to an edge negatively incident to w , we have formed a new abstract graph $L_v(\tilde{h}_0 = 0, \tilde{h}_1 = h_1 - (h_0 - 1), h_2, \dots, h_{n-2}, \tilde{h}_{n-1} = h_{n-1} - (h_n - 1), \tilde{h}_n = 0)$ which has $e^+ + 1$ positively incident edges to v and $e^- + 1$ negatively incident edges to v . Now one applies the algorithm to this abstract graph $L_v(0, \tilde{h}_1, \dots, \tilde{h}_{n-1}, 0)$. Note that the numerical homology Conley indices h_k with which v is labelled remain the same as in L_w for all dimensions $k \neq 0, 1, n-1, n$. Moreover, the incident edges to v retain the same Betti number vectors as the edges incident to w except, of course, for the two additional edges incident to v added in the construction and which are both labelled with $(1, 0, \dots, 0, 1)$. This, however, does not affect the validity of the Poincaré–Hopf inequalities, since B_k^+ and B_k^- for $k = 1, \dots, (n-1)$ remain unaltered. Furthermore, the new data on v , namely $\tilde{h}_1 = h_1 - (h_0 - 1)$, $\tilde{h}_{n-1} = h_{n-1} - (h_n - 1)$ and the number of incoming edges $e^+ + 1$ and outgoing edges $e^- + 1$ must satisfy (2.29) and (2.30), this implies that the original data $(h_0, h_1, \dots, h_{n-1}, h_n)$ must satisfy the more general formulae:

$$e^- - 1 - h_1^c + h_0 = 0 \quad (2.38)$$

and

$$e^+ - 1 - h_{2i-1}^d + h_n = 0. \quad (2.39)$$

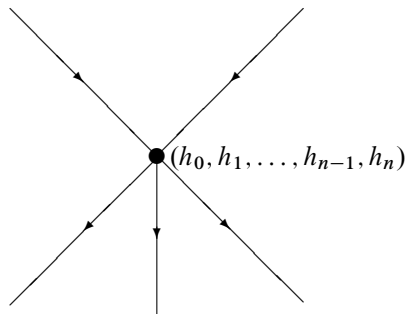
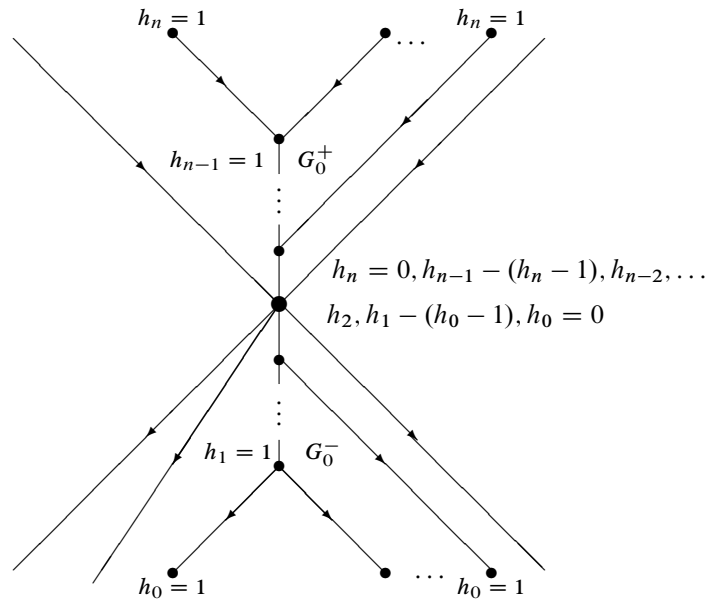
All other equations in the h^{cd} system do not change.

One has a similar situation with a repellor or attractor vertex. Without loss of generality, we assume w to be a repellor vertex since the construction is analogous for an attractor vertex. Let $L_w(h_0, h_1, \dots, h_{n-1}, h_n)$ with $e^+ = 0$ incoming and e^- outgoing edges be an abstract Lyapunov semigraph. One precedes the use of the algorithm with the construction of G_0^+ and G_0^- as described in the previous paragraph. The new vertex v has $e^+ = 1$ positively incident edge and $e^- + 1$ negatively incident edges. One can now apply the algorithm to $L_v(0, \tilde{h}_1, \dots, \tilde{h}_{n-1}, 0)$ as done previously. The data on L_v must satisfy the h^{cd} system with equations (2.29) and (2.30) substituted for (2.38) and (2.39) respectively.

2.5.2 Morsification and the presence of cycles

One last remark on the κ parameter: to include the κ parameter introduced in Section 2.4 in the Morsification algorithm for $L_v(h_0, \dots, h_n, \kappa)$ one need only substitute (2.38) and (2.39) for (2.40) and (2.41), respectively.

$$e^- - 1 - h_1^c + h_0 + \kappa = 0 \quad (2.40)$$

Figure 2.8: Generalized saddle vertex L_w .Figure 2.9: Partial morsification of L_w to create $L_v(0, \tilde{h}_1, \dots, \tilde{h}_{n-1}, 0)$

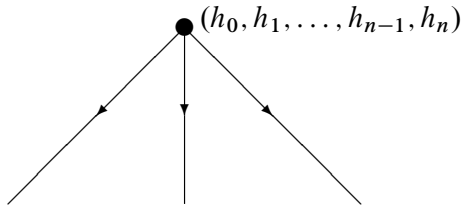


Figure 2.10: Generalized repeller vertex.

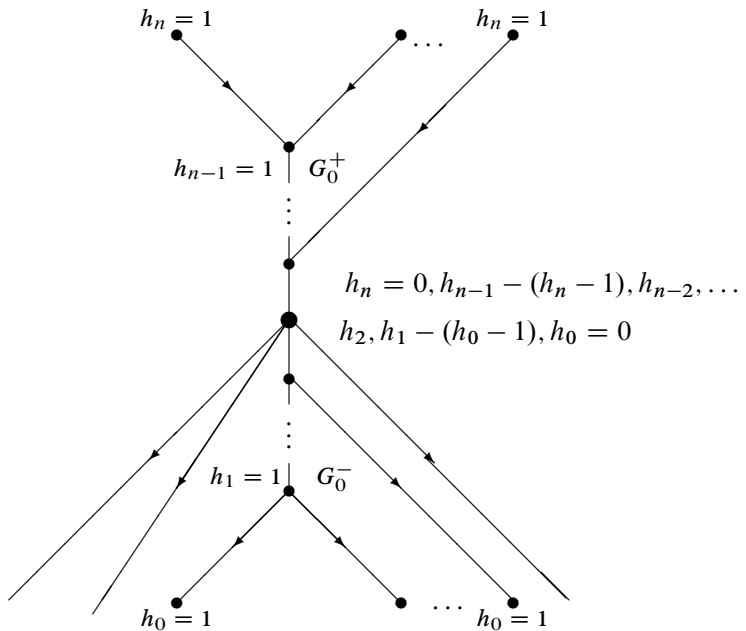


Figure 2.11: Partial morsification of a repeller vertex.

and

$$e^+ - 1 - h_{2i-1}^d + h_n + \kappa = 0. \quad (2.41)$$

Adjusting the incident edges

In this step we wish to define G^+ and G^- .

Choose $e^- - 1$ vertices labelled with $h_1 = 1$ of type 0-c. This is possible by the last inequality in (2.4). By choosing this number of vertices labelled with 1-singularities, G^- is formed with e^- outgoing edges and one incoming edge. Singularities of type 0-c do not alter the β_i with $0 < i < n - 1$. This type of singularity decreases β_0 and by duality β_{n-1} . Hence, the incoming edge of G^- has $B_0^- = B_{n-1}^- = 1$ and $B_j^- = \sum_{i=1}^e (\beta_j^-)_i$ with $j = \{1, \dots, n-2\}$. See Figure 2.13. Similarly, the graph G^+ is formed by choosing $e^+ - 1$ vertices labelled with $h_{n-1} = 1$ of type $n-1$ -d.

The insertion of cycles

An *elementary cycle* is a pair of (h_1^c, h_{n-1}^d) with one edge labelled with $(1, 0, \dots, 0, 1)$ and the other edge labelled with $(1, \beta_1, \dots, \beta_{n-2}, 1)$. See Figure 2.12.

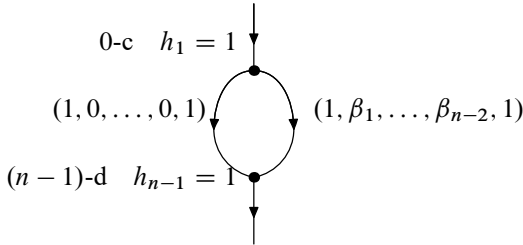


Figure 2.12: (h_1^c, h_{n-1}^d) pair

Without loss of generality, attach to G^-, κ elementary cycles where

$$(1, \beta_1, \dots, \beta_{n-2}, 1) = (1, B_1^-, \dots, B_{n-2}^-, 1).$$

Of course this attachment can also be done to G^+ . It is clear that once κ cycles are inserted the number of vertices labelled with $h_1 = 1$ of type 0-c is greater or equal to κ . Similarly, the number of vertices labelled with $h_{n-1} = 1$ of type $n-1$ -d is greater or equal to κ .

Hence all together we have inserted $h_1^c = \kappa + e^- - 1$ vertices labelled with $h_1 = 1$ of type 0-c. Similarly, we have inserted $h_{n-1}^d = \kappa + e^+ - 1$ vertices labelled with $h_{n-1} = 1$ of type $(n-1)$ -d. This is possible due to the last two inequalities in (2.4), which asserts that for this saddle vertex v ($h_0 = h_n = 0$):

$$\begin{cases} h_1 \geq -1 + e^- + \kappa \\ h_{n-1} \geq -1 + e^+ + \kappa \end{cases} \quad (2.42)$$

However, more cycles can appear in the morsification. The last cycle inserted has incoming edge labelled with

$$(1, B_1^-, B_2^-, \dots, B_{mid}^-, \dots, B_{n-2}^-, 1).$$

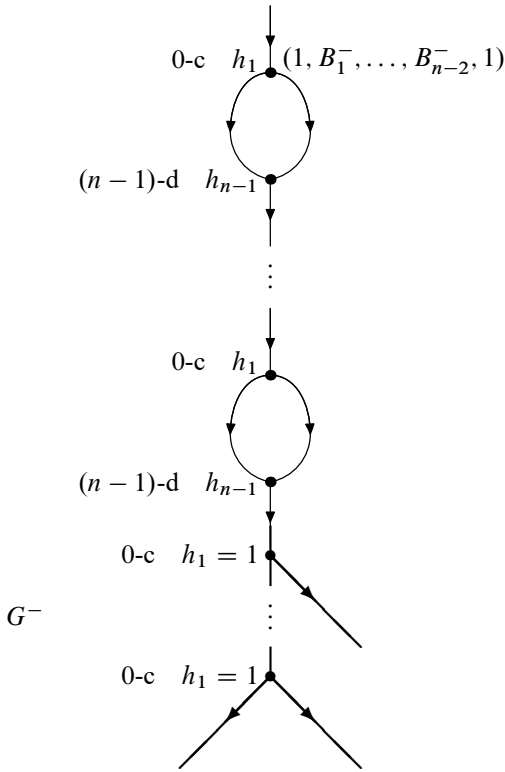


Figure 2.13: Morsification with insertion of cycles.

2.5.3 h_κ^{cd} -Systems

Hence, all these adjustments are recorded in the following h_κ^{cd} -systems which describes the morsification of a saddle vertex labelled with

$$(h_0 = 0, h_1, \dots, h_{n-1}, h_n = 0, \kappa).$$

Hence, these linear h_{κ}^{cd} -systems of equations, 2.43 in the odd dimensional case and 2.44 in the even dimensional case, must be solved for

$$(h_1^c, h_1^d, \dots, \beta_i, \dots, h_{2i}^c, h_{2i}^d, \kappa)$$

and

$$(h_1^c, h_1^d, \dots, \beta_i, \dots, h_{2i-1}^c, h_{2i-1}^d, \kappa)$$

respectively, in order for the saddle morsification algorithm to work.

$$n = 2i + 1 \left\{ \begin{array}{l} e^- - 1 - h_1^c + \kappa = 0 \\ \{ h_j = h_j^c + h_j^d, j = 1, \dots, 2i \\ e^+ - 1 - h_{2i}^d + \kappa = 0 \\ \left\{ \begin{array}{l} -(B_1^+ - B_1^-) + h_1^d - h_2^c - h_{2i}^c + h_{2i-1}^d = 0 \\ -(B_2^+ - B_2^-) + h_2^d - h_3^c - h_{2i-1}^c + h_{2i-2}^d = 0 \\ \vdots \\ \frac{-(B_i^+ - B_i^-)}{2} + h_i^d - h_{i+1}^c = 0 \end{array} \right. \end{array} \right. \quad (2.43)$$

or

$$n = 2i \left\{ \begin{array}{l} e^- - 1 - h_1^c + \kappa = 0 \\ \left\{ \begin{array}{l} h_j = h_j^c + h_j^d, j = 1, \dots, 2i-1, j \neq i \\ h_i = h_i^c + h_i^d + \beta^i, \text{ where } \beta^i = 0 \text{ if } 2i \neq 0 \pmod 4 \end{array} \right. \\ e^+ - 1 - h_{2i-1}^d + \kappa = 0 \\ \left\{ \begin{array}{l} -(B_1^+ - B_1^-) + h_1^d - h_2^c - h_{2i-1}^c + h_{2i-2}^d = 0 \\ -(B_2^+ - B_2^-) + h_2^d - h_3^c - h_{2i-2}^c + h_{2i-3}^d = 0 \\ \vdots \\ -(B_{i-1}^+ - B_{i-1}^-) + h_{i-1}^d - h_i^c - h_{i+1}^c + h_i^d = 0 \end{array} \right. \end{array} \right. \quad (2.44)$$

2.5.4 Conclusion

The Morsification occurs if the h_{κ}^{cd} -systems have a solution and this is possible if and only if the Poincaré–Hopf inequalities are satisfied. It becomes imperative to solve the h_{κ}^{cd} -systems and this will be achieved in the next chapter. The results presented therein are proved and explored at length in Bertolim, Mello, and de Rezende (2003a). The h_{κ}^{cd} -systems are modeled as network flow problems. The study of the feasibility of the particular network flow problems obtained will give rise to the Poincaré–Hopf inequalities. Furthermore, we show how to produce solutions and give the total number thereof. Our presentation will benefit from adopting the following notation

$$\left\{ \begin{array}{ll} \mathcal{B}_j = B_j^+ - B_j^-, & \text{for } j = 1, \dots, \lfloor (n-2)/2 \rfloor, \\ \mathcal{B}_j = (B_j^+ - B_j^-)/2, & \text{for } j = (n-1)/2, \text{ if } n \text{ is odd}, \\ \mathcal{B}_0^+ = -1 + e^+ + \kappa, \\ \mathcal{B}_0^- = -1 + e^- + \kappa. \end{array} \right. \quad (2.45)$$

We reproduce below the Poincaré–Hopf inequalities in a concise format, as presented in Cruz, Mello, and de Rezende (2005), to facilitate the identification of the inequalities obtained in the feasibility analysis. The inequalities are valid for integral $n \geq 3$.

$$\left\{ \begin{array}{l} h_j \geq \sum_{k=1}^{j-1} (-1)^{k+j} \mathcal{B}_k + (-1)^j (\mathcal{B}_0^+ - \mathcal{B}_0^-) + \sum_{k=1}^{j-1} (-1)^{k+j} (h_{n-k} - h_k) \geq -h_{n-j}, \\ \text{for } j = 2, \dots, \lfloor \frac{n}{2} \rfloor \end{array} \right. \quad (2.46)$$

$$h_1 \geq \mathcal{B}_0^- \quad (2.47)$$

$$h_{n-1} \geq \mathcal{B}_0^+ \quad (2.48)$$

$$n = 2i + 1 \quad \left\{ \sum_{k=1}^i (-1)^k \mathcal{B}_k + (\mathcal{B}_0^+ - \mathcal{B}_0^-) + \sum_{j=1}^i (-1)^j (h_{n-j} - h_j) = 0. \right. \quad (2.49)$$

$$n = 2i, \quad \left\{ \begin{array}{l} h_i - \sum_{k=1}^{i-1} (-1)^k \mathcal{B}_k - (\mathcal{B}_0^+ - \mathcal{B}_0^-) - \sum_{k=1}^{i-1} (-1)^k (h_{n-k} - h_k) \equiv 0 \pmod{2}. \\ i \text{ odd} \end{array} \right. \quad (2.50)$$

In the next chapter, we prove the following theorems:

Theorem 2.4. Consider an abstract Lyapunov semigraph L_B where the vertex v associated to B is labelled with $(h_0(v), \dots, h_n(v), \kappa_v)$. It admits Morsifications to Morse type Lyapunov semigraphs with cycle rank greater or equal to κ_v if and only if it satisfies the Poincaré–Hopf inequalities (2.4)–(2.6), where $\kappa_v \leq \min\{h_1 - (e^- + h_0 - 1), h_{n-1} - (e^+ + h_n - 1)\}$. Moreover, the number of possible continuations is obtained.

The local Poincaré–Hopf inequalities (2.4)–(2.6) involve the number of exiting, e^- , and entering, e^+ , boundaries of B as well as their Betti numbers. Theorem 2.4 implies the following theorem.

Theorem 2.5. Consider an abstract Lyapunov graph $L(h_0, \dots, h_n, \kappa)$. It admits Morsifications to abstract Lyapunov graphs of Morse type with cycle rank greater or equal to κ if and only if it satisfies the Poincaré–Hopf inequalities (2.4)–(2.6) at each vertex, where $\kappa \leq \min\{h_1 - (h_0 - 1), h_{n-1} - (h_n - 1)\}$. Moreover, the number of possible continuations is obtained.

3

Network Flows and Morsification

Despite its deceptively humble beginnings with Euler's solution to the Königsberg bridge problem in 1735, graph theory has enjoyed a rich and fruitful growth, both as an independent research area and in a supporting role in other interconnected areas, giving rise to busy subareas of research. Network flow theory is one such offshoot, a successful product of its modeling capabilities and theoretical results.

3.1 Brief graph theoretical background

The terminology and notation adopted in graph theory is unfortunately not uniform. The same entity may be called a *chain*, a *walk* or a *path* in Ford and Fulkerson (1962), Ahuja, Magnanti, and Orlin (1993) or Lawler (2001), respectively. Thus it behooves us to inform the choices adopted herein and help the novice in graph theory understand what will follow. The presentation will nevertheless be limited to the bare essentials, that is, the concepts, terms and facts used later on in the study of the network flow problems to be obtained.

A *directed graph* $G = (N, A)$ consists of a finite set N of distinct elements, called *nodes*, and a finite set A of distinct ordered pairs of nodes, called *arcs*. If i and j are nodes and we denote by e the ordered pair (i, j) , we say that arc e is incident to i and j , j is the *head* of e and i its *tail*. Figure 3.1 depicts a directed graph with four nodes and five arcs. It contains a path from node 0 to node 3, the sequence $0, a, 1, d, 3$, and a directed path from node 0 to node 3, the sequence $0, a, 1, c, 2, e, 3$. A *path* is a sequence of nodes and arcs $i_1, e_1, i_2, e_2, \dots, e_k, i_k$, such that each pair of successive arcs in the sequence,

say e_ℓ and $e_{\ell+1}$, are incident to the node, i_ℓ , between them in the sequence and no node is repeated. To shorten the path description we may just use the arc sequence, for instance a, d instead of $0, a, 1, d, 3$ in the first example, and a, c, e instead of $0, a, 1, c, 2, e, 3$ in the second. In fact, from the arc sequence we may infer the appropriate node sequence. In its *directed* version, the head of an arc in the sequence is the tail of the following arc. If the (omitted) sequence of nodes in path e_1, e_2, \dots, e_{k-1} is i_1, i_2, \dots, i_k , then arc e_j is a *forward* (resp., *backward*) arc in the path if its tail is node i_j and its head is node i_{j+1} (resp., its tail is node i_{j+1} and its head is node i_j). The directed graph of Figure 3.1 also contains the cycle a, c, b and the directed cycle c, e, d . A *cycle* is a closed path, where the first and last node are the same (the only repeated node). These paths and cycles are also shown in Figure 3.1. Arc d is a backward arc in path a, d . Arc b is a backward arc in cycle a, c, b . Arc a is a forward arc in path a, d .

A directed graph $\tilde{G} = (\tilde{N}, \tilde{A})$ is a *directed subgraph* of $G = (N, A)$ if $\tilde{N} \subset N$, and $\tilde{A} \subset A$. A *tree* is a directed graph with no cycles and number of arcs equal to number of nodes minus one. The paths a, d and a, c, e in Figure 3.1 (remember the paths also contains the nodes to which the arcs in the path are incident) are subgraphs of G that are trees.

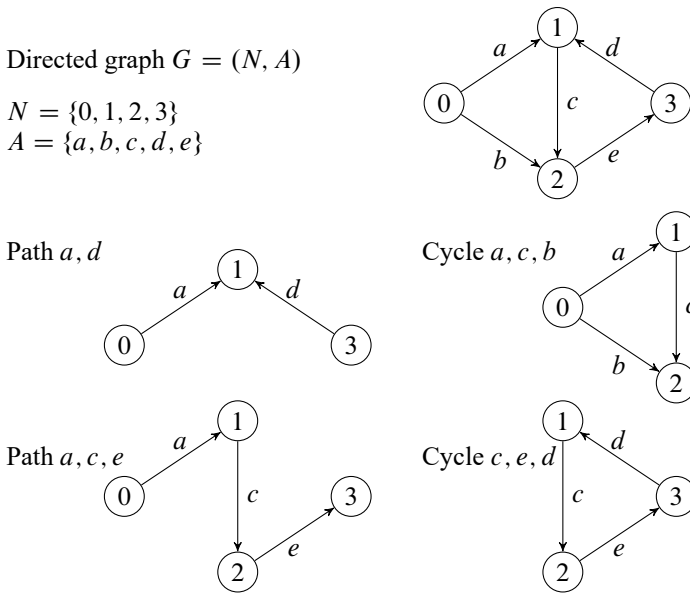


Figure 3.1: Directed graph, paths and cycles.

The *incidence matrix* representation of a directed graph opens the door to algebraic manipulations. Each row of the incidence matrix is associated with a node and each column with an arc. The column associated with arc (i, j) contains a -1 in the row associated with

node i , a 1 in the row associated with node j , and zeros in the remaining rows. Figure 3.2 shows the incidence matrix of the graph depicted in Figure 3.1.

$$\begin{array}{ccccc} & a & b & c & d & e \\ \begin{matrix} 0 \\ 1 \\ 2 \\ 3 \end{matrix} & \left[\begin{array}{ccccc} -1 & -1 & 0 & 0 & 0 \\ 1 & 0 & -1 & 1 & 0 \\ 0 & 1 & 1 & 0 & -1 \\ 0 & 0 & 0 & -1 & 1 \end{array} \right] \end{array}$$

Figure 3.2: Incidence matrix of directed graph of Figure 3.1

A *directed network* is constituted by a directed graph in which numerical values are associated with nodes and/or arcs. Suppose we associate a numerical quantity, say, a *flow*, with each arc. Let $x = (x_a, x_b, x_c, x_d, x_e)$ denote the flow associated with the arcs in the directed graph of Figure 3.1. Since the cardinality of the flow vector is equal to the number of columns of the incidence matrix of the same directed graph, we may perform the matrix vector multiplication below.

$$\left[\begin{array}{ccccc} -1 & -1 & 0 & 0 & 0 \\ 1 & 0 & -1 & 1 & 0 \\ 0 & 1 & 1 & 0 & -1 \\ 0 & 0 & 0 & -1 & 1 \end{array} \right] \left[\begin{array}{c} x_a \\ x_b \\ x_c \\ x_d \\ x_e \end{array} \right] = \left[\begin{array}{c} -x_a - x_b \\ x_a - x_c + x_d \\ x_b + x_c - x_e \\ -x_d + x_e \end{array} \right].$$

Imagine that x_{ij} is the amount of flow “moving” from i to j along arc (i, j) . Notice that the first row of the product above, the row associated with node 0, gives exactly the negative of the flow out of node 0. The row associated with node 2, the third component of the matrix vector product, is $x_b + x_c - x_e$, that is, the flow going into node 2 minus the flow going out of node 2. This is no accident, but a consequence of the sign convention that was adopted for the incidence matrix.

Now further suppose that we are given a numerical value for each node, the *node constant*. The equation

$$\text{flow into node } i - \text{flow out of node } i = \text{constant associated with node } i$$

is called a *flow conservation equation*. The simplest version of a network flow problem is to find a nonnegative flow that satisfies all flow conservation equations, or, in other words, a *feasible flow*. Most applications of network flow theory also encompass an optimization aspect. The applications considered in this chapter involve networks constituted by a directed graph and a vector of node constants, and the problem considered is an integral feasibility problem, meaning the feasible flow must also be integral. When all the node constants are zero, the flow is called a *circulation*. Circulations are not necessarily nonnegative, unless specifically required. A circulation is *elementary* when its support is minimal, that is, there is no other circulation whose support is strictly contained therein. Notice that elementary circulations are unique up to multiples. The importance of elementary circulations stems from the fact that all solutions to the flow conservation problem may

generated from a single particular nonnegative solution to the flow conservation equations plus a sum of elementary circulations. This is a consequence of the fact that the difference between two solutions is a circulation and a result from Rockafellar (1969). Translating this result to the present context, it states that any circulation may be expressed as the sum of conformal elementary circulations.¹

Here, as in many other applications, we are not only interested in nonnegative solutions to the flow conservation linear system, but chiefly in integral nonnegative solutions. Conveniently, the coefficient matrix of the flow conservation system is *totally unimodular*, i.e., every subdeterminant thereof is ± 1 or 0. This implies that, as long as the system has a nonnegative solution, it will have an nonnegative integral solution as well, see Schrijver (1986).

When the network's directed graph is a tree, the flow conservation equations have a unique solution. This follows from the fact that a tree always has at least two 'leafs' (nodes to which only one arc is incident), which means an equation with only one variable. Choose one such leaf node. By solving the associated equation and removing it and its variable from the system, we obtain another set of flow conservation equations in the subgraph (also a tree) obtained from the previous one by removing the chosen leaf node and the arc incident thereto. The system is solved by applying this procedure a finite number of times, in what algebraically would amount to solving the linear system by back substitution.

A straightforward property of network flow problems is that a necessary condition for feasibility is that the sum of the node constants must be zero. Simply notice that the sum of the elements in each column of the incidence matrix is zero and thus the sum of all equations results in the equation "zero = sum of node constants". If the network is also *connected*, that is, it contains a path linking any two distinct nodes thereof, this condition is also sufficient for the existence of a solution, albeit not necessarily a nonnegative one.

Consider a flow conservation problem with integral node constants. Its set of non-negative solutions, when nonempty, is a *polyhedron*, that is, the intersection of a finite number of half-spaces. Of special interest are the faces of dimension zero of the polyhedron, its *extreme points*. These points may not be expressed as convex combinations of two other distinct points of the polyhedron. The extreme points of the nonnegative flow conservation polyhedron correspond to feasible flows whose supports are subgraphs of trees. Figure 3.3 gives numerical examples of these definitions, for the network whose directed graph is given in Figure 3.1. The circulations y^1 , y^2 and y^3 are clearly elementary, since removing any arc from its support will destroy the cycle. Notice that flow x^2 may be obtained from flow x^1 by passing flow -2 along the cycles c, e, d , and flow -1 along the cycle a, c, e, d , or, algebraically, $x^2 = x^1 - 2y^2 - y^3$. In other words, the (non elementary) circulation $x^2 - x^1$ may be expressed as the sum $(-2y^2) + (-y^3)$ of the conformal elementary circulations $-2y^2$ and $-y^3$.

¹Two vectors $x, y \in \mathbb{R}^n$ are *conformal* if $x_i y_i \geq 0$, for $i = 1, \dots, n$.

Network: directed graph $G = (N, A)$ of Figure 3.1, set of node constants.

	Node			
Node constants	0	1	2	3
	-4	8	-3	-1

	Arc				
	a	b	c	d	e
Flow x^1	3	1	2	7	6
Flow x^2	4	0	0	4	3
Circulation y^1	1	-1	1	0	0
Circulation y^2	0	0	1	1	1
Circulation y^3	-1	1	0	1	1

Figure 3.3: Flows and circulations for network whose directed graph was given in Figure 3.1.

3.2 h_k^{cd} -system as a network flow problem

We show in this section how to model the h_k^{cd} -system as a network flow problem of the kind “find feasible integral flow satisfying flow conservation equations in network”. The structure of the directed graph that constitutes part of the network is determined by how the h^{cd} variables (the unknowns) appear in the equations of the h_k^{cd} -system. The feasibility of the corresponding network flow problem depends on this structure and the data (the quantities e^- , e^+ , κ , B_1^+ , B_2^+ , ..., $B_{\frac{n}{2}}^+$, B_1^- , B_2^- , ..., and h). The integrality of the solution, when present, will derive from the integrality of the data involved and one additional constraint when $n = 2i \equiv 2 \pmod{4}$. We show how to explore the structure of the network to obtain solutions, count them and to establish necessary and sufficient conditions on the data that guarantee the feasibility of the network flow problem. These necessary and sufficient conditions are precisely the Poincaré–Hopf inequalities.

This equivalence between the feasibility of a system of linear equations and the feasibility of a system of linear inequalities involving the set of constants of the system of equations will provide a powerful tool to establish further equivalences. The linear system of equations will act as a link between systems of inequalities involving data sets of different nature, as exemplified in Section 3.3.

First we rewrite systems (2.43) and (2.44) with the notation (2.45):

$$n = 2i + 1 \left\{ \begin{array}{l} h_1^c = B_0^-, \\ h_j^c + h_j^d = h_j, \quad \text{for } j = 1, \dots, 2i, \\ h_{n-1}^d = B_0^+, \\ h_j^d - h_{j+1}^c - h_{n-j}^c + h_{n-j-1}^d = B_j, \quad \text{for } j = 1, \dots, i-1, \\ h_i^d - h_{i+1}^c = B_i. \end{array} \right. \quad (3.1)$$

and

$$n = 2i \left\{ \begin{array}{ll} h_1^c = \mathcal{B}_0^-, \\ h_j^c + h_j^d = h_j, & \text{for } j = 1, \dots, 2i-1, j \neq i, \\ h_i^c + h_i^d = h_i - \beta^i, & \text{where } \beta^i = 0, \text{if } i \text{ is odd} \\ h_{n-1}^d = \mathcal{B}_0^+, \\ h_j^d - h_{j+1}^c - h_{n-j}^c + h_{n-j-1}^d = \mathcal{B}_j, & \text{for } j = 1, \dots, i-1. \end{array} \right. \quad (3.2)$$

We'll get acquainted with the modeling procedure by considering a few lower dimension special cases. We'll start with the easier case, $n = 2i + 1$. We'll pose and solve concrete examples for small values of n and then state the general solution. The case $n = 2i$ is similar, but has a few quirks.

3.2.1 Case $n = 2i + 1$

Let $n = 2i + 1 = 3$, and $i = 1$. The equations in (3.1) reduce to

$$\left\{ \begin{array}{rcl} h_1^c & = & \mathcal{B}_0^- \\ h_1^c + h_1^d & = & h_1 \\ h_2^c + h_2^d & = & h_2 \\ h_2^d & = & \mathcal{B}_0^+ \\ h_1^d - h_2^c & = & \mathcal{B}_1. \end{array} \right.$$

Multiplying by -1 the first, third and fifth equations, we obtain the equivalent system

$$\left\{ \begin{array}{rcl} -h_1^c & = & -\mathcal{B}_0^- \\ h_1^c + h_1^d & = & h_1 \\ -h_2^c - h_2^d & = & -h_2 \\ h_2^d & = & \mathcal{B}_0^+ \\ -h_1^d + h_2^c & = & -\mathcal{B}_1. \end{array} \right.$$

Rewriting in matrix notation, we obtain

$$\begin{bmatrix} -1 & 0 & 0 & 0 \\ 1 & 1 & 0 & 0 \\ 0 & 0 & -1 & -1 \\ 0 & 0 & 0 & 1 \\ 0 & -1 & 1 & 0 \end{bmatrix} \begin{bmatrix} h_1^c \\ h_1^d \\ h_2^c \\ h_2^d \end{bmatrix} = \begin{bmatrix} -\mathcal{B}_0^- \\ h_1 \\ -h_2 \\ \mathcal{B}_0^+ \\ -\mathcal{B}_1 \end{bmatrix}. \quad (3.3)$$

Lo and behold, we have obtained a set of flow conservation equations. The pertinent network contains a directed graph with four nodes and four arcs. The constants associated with the nodes are $-\mathcal{B}_0^-$, h_1 , $-h_2$, $-\mathcal{B}_1$ and \mathcal{B}_0^+ .

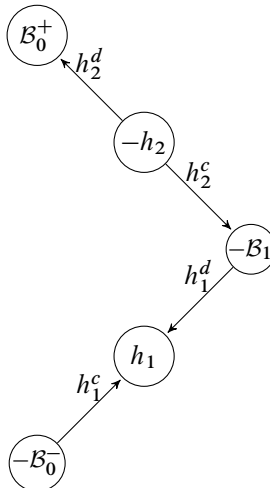
Figure 3.4: Network model for the h_{κ}^{cd} -system when $n = 3$.

Figure 3.4 depicts the resulting arrow shaped network, using the flow variables and node constants to indicate the corresponding arcs and nodes, thus avoiding the introduction of further notation. Since the directed graph in Equation (3.3) is a tree, the flow conservation equations have the unique solution

$$\begin{cases} h_1^c = \mathcal{B}_0^- \\ h_1^d = h_1 - \mathcal{B}_0^- \\ h_2^c = h_2 - \mathcal{B}_0^+ \\ h_2^d = \mathcal{B}_0^+. \end{cases}$$

Therefore the corresponding network flow problem is feasible if and only if the unique solution h^{cd} is nonnegative, that is

$$\begin{cases} \mathcal{B}_0^- = -1 + e^- + \kappa \geq 0 \\ h_1 \geq \mathcal{B}_0^- \\ h_2 \geq \mathcal{B}_0^+ \\ \mathcal{B}_0^+ = -1 + e^+ + \kappa \geq 0 \\ -\mathcal{B}_0^- + h_1 - h_2 - \mathcal{B}_1 + \mathcal{B}_0^+ = 0. \end{cases}$$

The inequalities $\mathcal{B}_0^- \geq 0$ and $\mathcal{B}_0^+ \geq 0$ are always satisfied by the data of the problem. Thus

the relevant conditions are

$$\begin{cases} h_1 \geq \mathcal{B}_0^- \\ h_2 \geq \mathcal{B}_0^+ \\ -\mathcal{B}_1 + (\mathcal{B}_0^+ - \mathcal{B}_0^-) - (h_2 - h_1) = 0, \end{cases} \quad (3.4)$$

which are precisely the set of Poincaré–Hopf inequalities (2.47)–(2.49) for the case $n = 3$.

A numerical instance of this problem is shown in Figure 3.5. Node constants and flows are shown next to the relevant graph components to ease the verification of equations using the depiction of the graph.

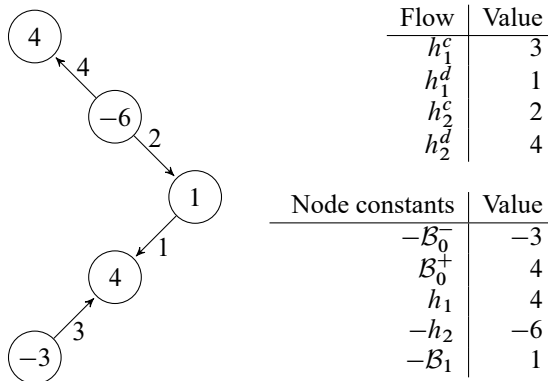


Figure 3.5: Numerical instance of network flow for the h_k^{cd} -system when $n = 3$.

Next consider $n = 2i + 1 = 5$, $i = 2$. As we manipulate the equations, the pattern of transformations effected on the system of equations (3.1) starts to take shape. These transformations have the ultimate goal of identifying a network-flow model for (3.1). For these values, the equations in (3.1) become

$$\left\{ \begin{array}{lcl} h_1^c & & = \mathcal{B}_0^- \\ h_1^c + h_1^d & & = h_1 \\ & h_2^c + h_2^d & = h_2 \\ & h_3^c + h_3^d & = h_3 \\ & h_4^c + h_4^d & = h_4 \\ & h_4^d & = \mathcal{B}_0^+ \\ h_1^d - h_2^c + & h_3^d - h_4^c & = \mathcal{B}_1 \\ h_2^d - h_3^c & & = \mathcal{B}_2. \end{array} \right.$$

Multiplying by -1 the first, third, fifth and seventh equations, we obtain the equivalent

system

$$\left\{ \begin{array}{lcl} -h_1^c & = & -\mathcal{B}_0^- \\ h_1^c + h_1^d & = & h_1 \\ -h_2^c - h_2^d & = & -h_2 \\ h_3^c + h_3^d & = & h_3 \\ -h_4^c - h_4^d & = & -h_4 \\ h_4^d & = & \mathcal{B}_0^+ \\ -h_1^d + h_2^c - h_3^d + h_4^c & = & -\mathcal{B}_1 \\ h_2^d - h_3^c & = & \mathcal{B}_2. \end{array} \right.$$

Rewriting in matrix notation, we obtain

$$\left[\begin{array}{cccccccc} -1 & 0 & 0 & 0 & 0 & 0 & 0 & 0 \\ 1 & 1 & 0 & 0 & 0 & 0 & 0 & 0 \\ 0 & 0 & -1 & -1 & 0 & 0 & 0 & 0 \\ 0 & 0 & 0 & 0 & 1 & 1 & 0 & 0 \\ 0 & 0 & 0 & 0 & 0 & 0 & -1 & -1 \\ 0 & 0 & 0 & 0 & 0 & 0 & 0 & 1 \\ 0 & -1 & 1 & 0 & 0 & -1 & 1 & 0 \\ 0 & 0 & 0 & 1 & -1 & 0 & 0 & 0 \end{array} \right] \left[\begin{array}{c} h_1^c \\ h_1^d \\ h_2^c \\ h_2^d \\ h_3^c \\ h_3^d \\ h_4^c \\ h_4^d \end{array} \right] = \left[\begin{array}{c} -\mathcal{B}_0^- \\ h_1 \\ -h_2 \\ h_3 \\ -h_4 \\ \mathcal{B}_0^+ \\ -\mathcal{B}_1 \\ \mathcal{B}_2 \end{array} \right]. \quad (3.5)$$

Again the result is a set of flow conservation equations. The directed graph whose incidence matrix is the coefficient matrix of linear system (3.5) is given in Figure 3.6. Instead of solving it directly, we decompose the network flow problem into two independent problems. Although this may be achieved as a consequence of a general result concerning biconnected components of graphs, it is easy enough to justify it directly via algebra.

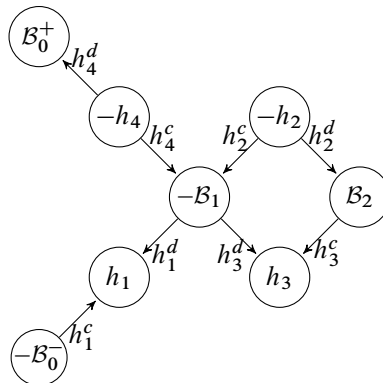


Figure 3.6: Network corresponding to the h_k^{cd} -system when $n = 5$.

To effect the decomposition, we perform several elementary row operations on the linear system (3.5). First change the order of equations, putting the second and third after

the seventh. Then add the first four equations to the fifth. These operations are shown schematically below.

$$\left[\begin{array}{cccccccc|c} -1 & 0 & 0 & 0 & 0 & 0 & 0 & 0 & -\mathcal{B}_0^- \\ 1 & 1 & 0 & 0 & 0 & 0 & 0 & 0 & h_1 \\ 0 & 0 & -1 & -1 & 0 & 0 & 0 & 0 & -h_2 \\ 0 & 0 & 0 & 0 & 1 & 1 & 0 & 0 & h_3 \\ 0 & 0 & 0 & 0 & 0 & 0 & -1 & -1 & -h_4 \\ 0 & 0 & 0 & 0 & 0 & 0 & 0 & 1 & \mathcal{B}_0^+ \\ 0 & -1 & 1 & 0 & 0 & -1 & 1 & 0 & -\mathcal{B}_1 \\ 0 & 0 & 0 & 1 & -1 & 0 & 0 & 0 & \mathcal{B}_2 \end{array} \right]$$

$$\rightsquigarrow \left[\begin{array}{cccccccc|c} -1 & 0 & 0 & 0 & 0 & 0 & 0 & 0 & -\mathcal{B}_0^- \\ 1 & 1 & 0 & 0 & 0 & 0 & 0 & 0 & h_1 \\ 0 & 0 & 0 & 0 & 0 & 0 & 0 & -1 & -h_4 \\ 0 & 0 & 0 & 0 & 0 & 0 & 0 & 0 & \mathcal{B}_0^+ \\ 0 & -1 & 1 & 0 & 0 & 0 & -1 & 1 & -\mathcal{B}_1 \\ 0 & 0 & -1 & -1 & 0 & 0 & 0 & 0 & -h_2 \\ 0 & 0 & 0 & 0 & 1 & 1 & 0 & 0 & h_3 \\ 0 & 0 & 0 & 1 & -1 & 0 & 0 & 0 & \mathcal{B}_2 \end{array} \right]$$

$$\rightsquigarrow \left[\begin{array}{cc|ccccc|cc} -1 & 0 & 0 & 0 & 0 & 0 & 0 & -\mathcal{B}_0^- \\ 1 & 1 & 0 & 0 & 0 & 0 & 0 & h_1 \\ 0 & 0 & 0 & 0 & 0 & 0 & -1 & -h_4 \\ 0 & 0 & 0 & 0 & 0 & 0 & 1 & \mathcal{B}_0^+ \\ \hline 0 & 0 & 1 & 0 & 0 & -1 & 0 & (-\mathcal{B}_1) \\ 0 & 0 & -1 & -1 & 0 & 0 & 0 & -\mathcal{B}_0^- + h_1 \\ 0 & 0 & 0 & 0 & 1 & 1 & 0 & -h_4 + \mathcal{B}_0^+ \\ 0 & 0 & 0 & 1 & -1 & 0 & 0 & -\mathcal{B}_1 \\ \hline 0 & 0 & -1 & -1 & 0 & 0 & 0 & -h_2 \\ 0 & 0 & 0 & 0 & 1 & 1 & 0 & h_3 \\ 0 & 0 & 0 & 1 & -1 & 0 & 0 & \mathcal{B}_2 \end{array} \right].$$

After these operations, the resulting system is easily decomposed into two independent linear systems, shaded in red and blue, respectively, in the last matrix above. The red system contains the first four equations and involves variables h_1^c, h_1^d, h_4^c and h_4^d . The blue system contains the remaining equations and variables. Adding a fifth redundant equation consisting of the negative of the sum of its four equations to the red system, we can identify it as a flow conservation system.

The directed graphs corresponding to these two independent systems are shown in Figure 3.7. Notice that it is as if the network in Figure 3.6 was split along the node associated with constant $-\mathcal{B}_1$. The constant of the copy of the original node that remains on the left subgraph is the negative of the sum of the other nodes in this subgraph. This ensures that

the condition “sum of node constants = zero” is automatically satisfied for the first subproblem. The node constant of the copy on the right is the constant of the original node minus the constant of its left copy.

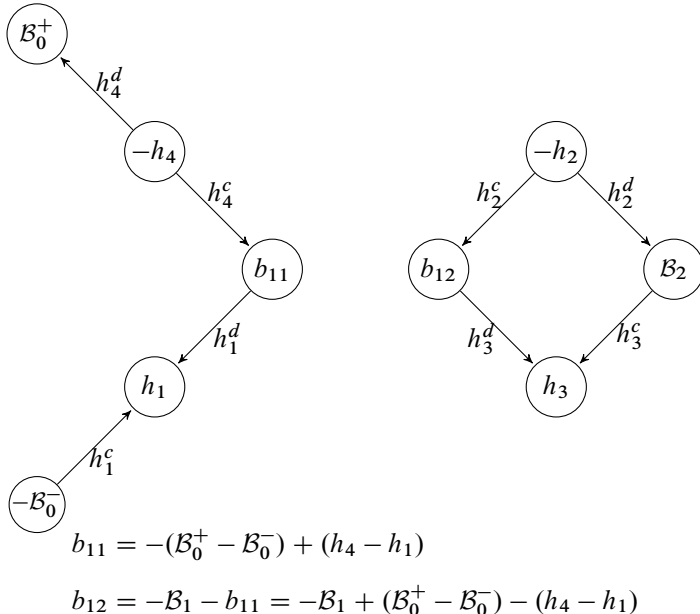
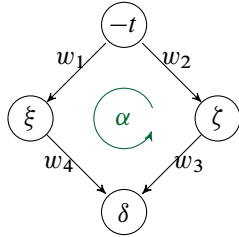


Figure 3.7: Decomposition of the network flow problem in Figure 3.6.

The network on the left of Figure 3.7 coincides in structure with the network for $n = 3$, previously considered. Thus the feasibility conditions (3.4) may be adapted and applied thereto. Next we consider the lozenge shaped network on the right of Figure 3.7. This type of network will appear repeatedly in the decomposition of networks for higher values of n . So it pays to consider a generic case, as depicted in Figure 3.8.

The rank of the lozenge subgraph incidence matrix is easily seen to be three. Therefore, the set of solutions to the flow conservation equations for the lozenge network of Figure 3.8, if nonempty, is an affine space of dimension 1 defined parametrically by the general solution given in the same figure. As mentioned, the general solution to this flow conservation system is the sum of a particular solution (a nonnegative feasible flow) and a sum of elementary circulations.

The flow shown in Figure 3.8 is straightforward to obtain, but is not necessarily feasible, i.e., nonnegative. It is obvious that this networks admits only one (up to multiples) elementary circulation: the flow of value α along the cycle w_1, w_4, w_3, w_2 , where backward arcs carry negative flow in order to satisfy the flow conservation equations. It will be convenient to fix elementary circulations to be one of two possibilities, with all ele-



General solution

$$\begin{bmatrix} w_1 \\ w_2 \\ w_3 \\ w_4 \end{bmatrix} = \begin{bmatrix} \xi \\ t - \xi \\ \delta \\ 0 \end{bmatrix} + \alpha \begin{bmatrix} 1 \\ -1 \\ -1 \\ 1 \end{bmatrix}$$

Figure 3.8: Directed lozenge network and solution.

ments equal to 1, -1 or 0. Since we are interested in integral solutions and the node constants are all integral, the number of nonnegative integral solutions is just the number of integral multiples of this elementary circulation one can add to the particular solution exhibited in Figure 3.8. The set of solutions to the flow conservation equations is the set $\{w \mid w = (\xi, t - \xi, \delta, 0) + \alpha(1, -1, -1, 1), \alpha \in \mathbb{R}\}$, the set of integral solutions is the set $\{w \mid w = (\xi, t - \xi, \delta, 0) + \alpha(1, -1, -1, 1), \alpha \in \mathbb{Z}\}$, the translation of the lattice generated by $(1, -1, -1, 1)$, and the set we are interested in is the set of nonnegative integral solutions $\{w \mid w = (\xi, t - \xi, \delta, 0) + \alpha(1, -1, -1, 1), \alpha \in \mathbb{Z}\} \cap \mathbb{Z}_+^4$.

Thus the lozenge network flow problem is feasible if and only if

$$\xi + \delta + \zeta - t = 0 \quad (3.6)$$

and

$$\begin{cases} \xi + \alpha \geq 0 \\ t - \xi - \alpha \geq 0 \\ \delta - \alpha \geq 0 \\ \alpha \geq 0. \end{cases} \quad (3.7)$$

Applying the Fourier–Motzkin method, see Korte and Vygen (2012), to (3.7) we obtain the equivalent inequality system

$$\begin{cases} t \geq 0 \\ \delta \geq 0 \\ t \geq \xi \geq -\delta. \end{cases} \quad (3.8)$$

Substituting the appropriate values in (3.4), (3.6) and (3.8), and using the fact that h_2 and h_3 are nonnegative data, we conclude that the network flow problem for the $n = 5$ case is feasible if and only if

$$\begin{cases} h_2 \geq -B_1 + (B_0^+ - B_0^-) - (h_4 - h_1) \geq -h_3 \\ h_1 \geq B_0^- \\ h_4 \geq B_0^+ \\ -B_1 + B_2 + (B_0^+ - B_0^-) - (h_4 - h_1) + (h_3 - h_2) = 0, \end{cases} \quad (3.9)$$

precisely the Poincaré–Hopf inequalities (2.46)–(2.49) for $n = 5$. As remarked before, the general solution in Figure 3.8 allows the construction of all feasible solutions of the network flow problem. The number of nonnegative integral solutions may be also computed since (3.7) gives the feasible range of variation for integral multiples of the fixed elementary circulation in Figure 3.8: $\max\{0, -\xi\} \leq \alpha \leq \min\{\delta, t - \delta\}$. A numerical example is given in Figure 3.9. The variables whose values are changed as flow is passed through the cycle are colored blue.

Furthermore, the polyhedron defined by the nonnegativity and flow conservation constraints is bounded since $0 \leq h_j^c, h_j^d \leq h_j$, for $1 \leq j \leq 4$, so it is in fact a polytope, and the convex hull of its extreme points. Notice that the supports of the first and third solutions listed in Figure 3.9 are trees, so these vectors are extreme points of the polytope defined by the h_k^{cd} -system.

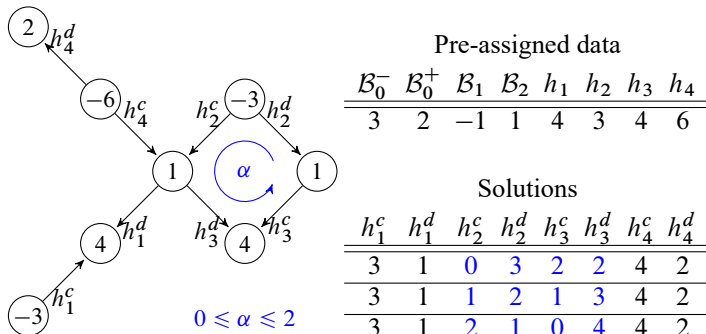


Figure 3.9: Solutions to numerical instance of a network flow problem for $n = 5$.

We briefly talk about the case $n = 2i + 1 = 7$, $i = 3$, to give a taste of the induction that leads to the final result. As before, by changing the sign of half the equations we may identify the h_k^{cd} -system as a set of flow conservation equations. The network is shown in Figure 3.10. The node constants in this figure are a giveaway of the equations that had their signs changed.

The next step in the analysis of the h_k^{cd} -system is to decompose the network into smaller independent problems as delineated in Figure 3.11. Again the definitions of b_{11} and b_{21} make sure that the sum of the node constants in the subgraph that contains the corresponding node is zero. This condition, when applied to the last subproblem, will finally involve all the elements of the pre-assigned index data and result in the Poincaré–Hopf equality (2.49).

Applying the feasibility conditions to each subproblem of the decomposition, we will

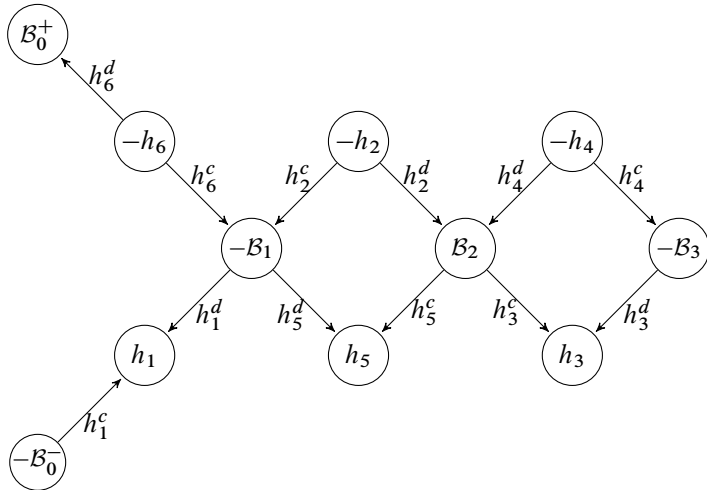
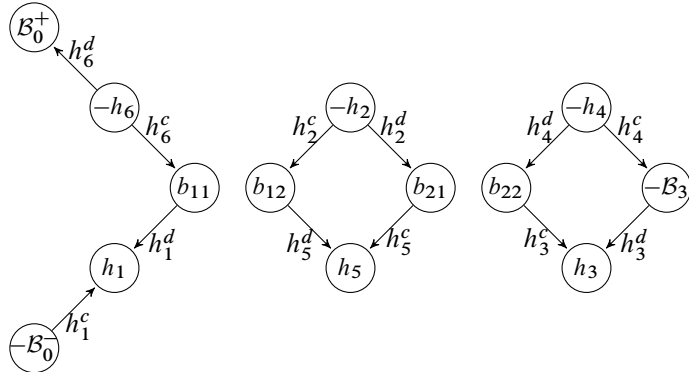


Figure 3.10: Network flow for the h_k^{cd} -system when $n = 7$.



$$b_{11} = -(\mathcal{B}_0^+ - \mathcal{B}_0^-) + (h_6 - h_1)$$

$$b_{12} = -\mathcal{B}_1 - b_{11} = -\mathcal{B}_1 + (\mathcal{B}_0^+ - \mathcal{B}_0^-) - (h_6 - h_1)$$

$$b_{21} = -b_{12} - (h_5 - h_2)$$

$$b_{22} = \mathcal{B}_2 - b_{21} = \mathcal{B}_2 + b_{12} + (h_5 - h_2)$$

$$= \mathcal{B}_2 - \mathcal{B}_1 + (\mathcal{B}_0^+ - \mathcal{B}_0^-) - (h_6 - h_1) + (h_5 - h_2)$$

Figure 3.11: Decomposition of the network flow problem in Figure 3.10.

arrive at the Poincaré–Hopf inequalities (2.46)–(2.49) for $n = 7$ below.

$$\begin{cases} h_3 \geq -\mathcal{B}_2 + \mathcal{B}_1 - (\mathcal{B}_0^+ - \mathcal{B}_0^-) + (h_6 - h_1) - (h_5 - h_2) \geq -h_4 \\ h_2 \geq -\mathcal{B}_1 + (\mathcal{B}_0^+ - \mathcal{B}_0^-) - (h_6 - h_1) \geq -h_5 \\ h_1 \geq \mathcal{B}_0^- \\ h_6 \geq \mathcal{B}_0^+ \\ -\mathcal{B}_1 + \mathcal{B}_2 - \mathcal{B}_3 + (\mathcal{B}_0^+ - \mathcal{B}_0^-) - (h_6 - h_1) + (h_5 - h_2) - (h_4 - h_3) = 0. \end{cases} \quad (3.10)$$

Now assume (3.10) is satisfied and we have a feasible integral flow. Since there are now two cycles in the network, when generating solutions, the number thereof will be the product of the range of integral values of flows one may pass through each cycle without disrupting nonnegativity of the solution. A numerical example is given in Figure 3.12. With respect to the first solution in the second table of the figure, the flow α_1 (resp., α_2) along the first cycle may vary between 0 and 1 (resp., between 0 and 2), without destroying the nonnegativity of this solution. With respect to other solutions the actual bounds may differ, but the number of integral allowable values for the first cycle (resp., second cycle) will always be 2 (resp., 3).

We may conclude that there are six feasible solutions. The variables that change as flow is passed through the first cycle are colored blue and the ones that change as flow is passed in the second cycle are colored red. Again the flows are bounded, so the polyhedron defined by the nonnegativity and flow conservation constraints is a polytope. The first, second, fifth and last solutions correspond to extreme points of this polytope. Notice that the third solution is halfway between the first and fifth one, so definitely not an extreme point.

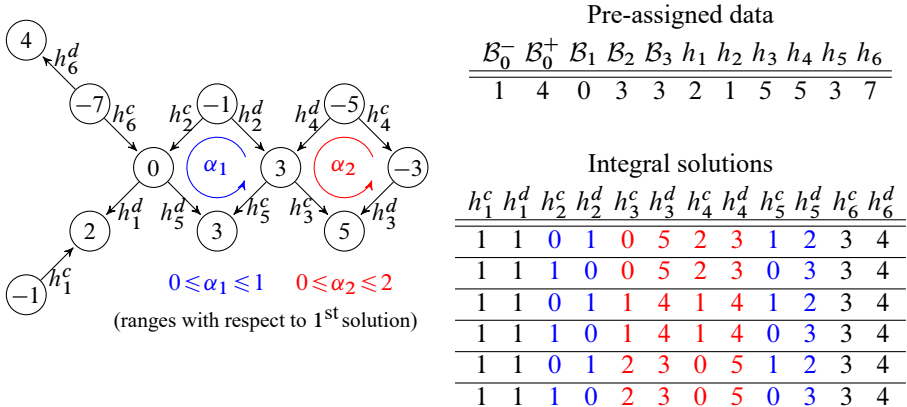


Figure 3.12: Solutions to numerical instance of a network flow problem for $n = 7$.

The procedure exemplified above and schematically summed up in Figure 3.12 was

formally developed and exploited in Bertolim, Mello, and de Rezende (2003a), where the treatment of the general case may be found.

For the fixed planar embedding adopted, the network for arbitrary odd $n = 2i + 1$ was shown to be constituted of $i - 1$ lozenge subgraphs joined at the sides, joined on the left to the middle node of an arrow shaped subgraph. Node \mathcal{B}_0^- (resp., \mathcal{B}_0^+) is at the bottom (resp., top) of the arrow shaped part on the left. Nodes $-\mathcal{B}_1, \mathcal{B}_2, -\mathcal{B}_3, \dots$ appear in this order in the middle of the network. There are two rows of nodes remaining to be labeled. To finish this task, apply the h vector in increasing index order and alternating signs to the unlabeled nodes following a zigzag path, starting at node $-\mathcal{B}_0^-$, always crossing the middle row of nodes, until the rightmost node, and then return in the same fashion. The arcs are labeled the same way, but now using the h^{cd} vector.

Bertolim, Mello, and de Rezende (*ibid.*) generalizes the feasibility analysis illustrated for the instances $n = 3, 5$ and 7 , resulting in the attainment of the general Poincaré–Hopf inequalities for $n = 2i + 1$, (2.46)–(2.49).

The decomposition of the network flow model furnishes the key to transition amongst feasible solutions. The j -th lozenge subgraph is the cycle $h_{j+1}^c, h_{n-j-1}^d, h_{n-j-1}^c, h_{j+1}^d$. Passing a flow of value $\alpha > 0$ through this cycle amounts to either increasing the flow along the first two arcs of α and decreasing the flow along the last two arcs by α , or vice-versa. So if we pass the biggest amount possible of flow, if we “saturate” this cycle, we will drive at least one of the flows in the cycle to zero. Of course, the flow may be sent in two possible opposite directions and thus lead to two potentially different saturations. For instance, the third solution in Figure 3.12 will become the first solution if we pass flow of value 1 counterclockwise along the red cycle, and will become the fifth solution if we pass flow 1 clockwise. The first action drives h_3^c to zero and the second drives h_4^c to zero. On the other hand, if we pass flow 1 counterclockwise along the first cycle, the first solution becomes the second, and both h_2^d and h_5^c are driven to zero. Since an extreme point solution is a solution whose support doesn’t contain cycles, they must all be saturated. As there are two possibilities of saturation for each cycle, there are potentially 2^{i-1} extreme point solutions to the h_κ^{cd} -system when $n = 2i + 1$.

Denote the solution set by $\mathcal{H}_\kappa^{cd} = \{h^{cd} \mid 0 \leq h^{cd} \text{ solves the } h_\kappa^{cd} \text{ system}\}$. The nonempty set \mathcal{H}_κ^{cd} is a polyhedron, since it is defined by the intersection of a finite number of linear inequalities. Furthermore, it is a polytope, since, from the second set of equalities in (3.1) plus the nonnegativity constraints, we have that $0 \leq h_j^c, h_j^d \leq h_j$, for $j = 1, \dots, n - 1$. The discussion above implies \mathcal{H}_κ^{cd} has at most 2^{i-1} extreme points. Lastly, it is an integral polytope, since all its extreme points are integral. This last property will not necessarily be true in the even n case. This idiosyncrasy shows up in another set of polytopes arising from the Morse inequalities, see Section 3.3.2.

3.2.2 Case $n = 2i$

We mimic the analysis of the odd n case, by presenting and solving the problem for small even values and then generalizing. The steps are the same as before: manipulate the system so as to model the problem as network-flow problem and then decompose the problem

into smaller problems. The smaller subproblems belong to one of three classes, and their repetitive solutions are obtained.

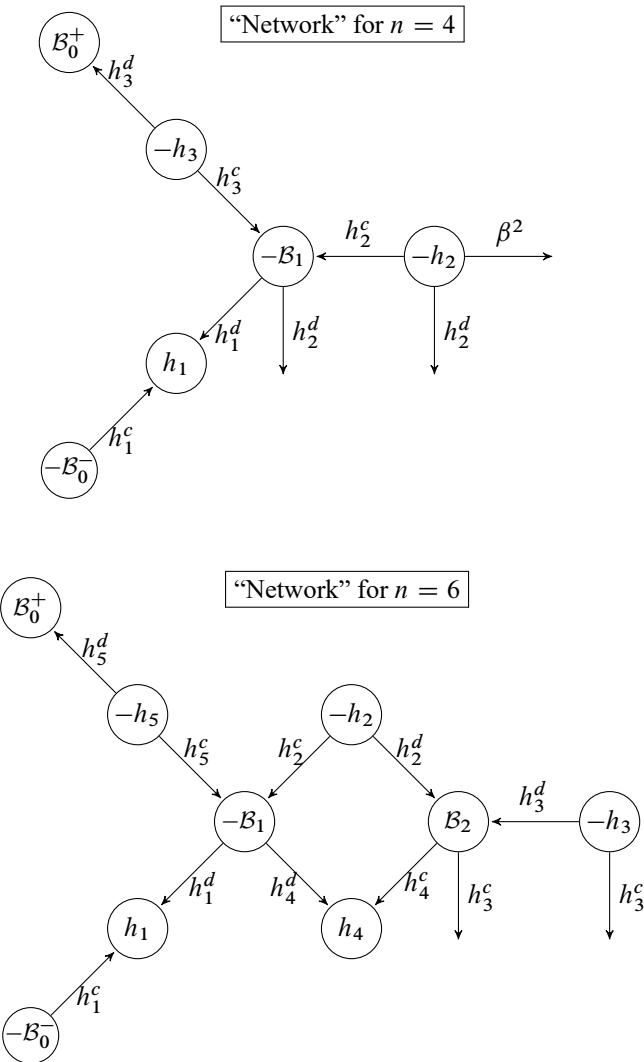
Since $n \geq 3$, we start with the h_k^{cd} -systems for $n = 4$ and $n = 6$, given below in (3.11) and (3.12), respectively.

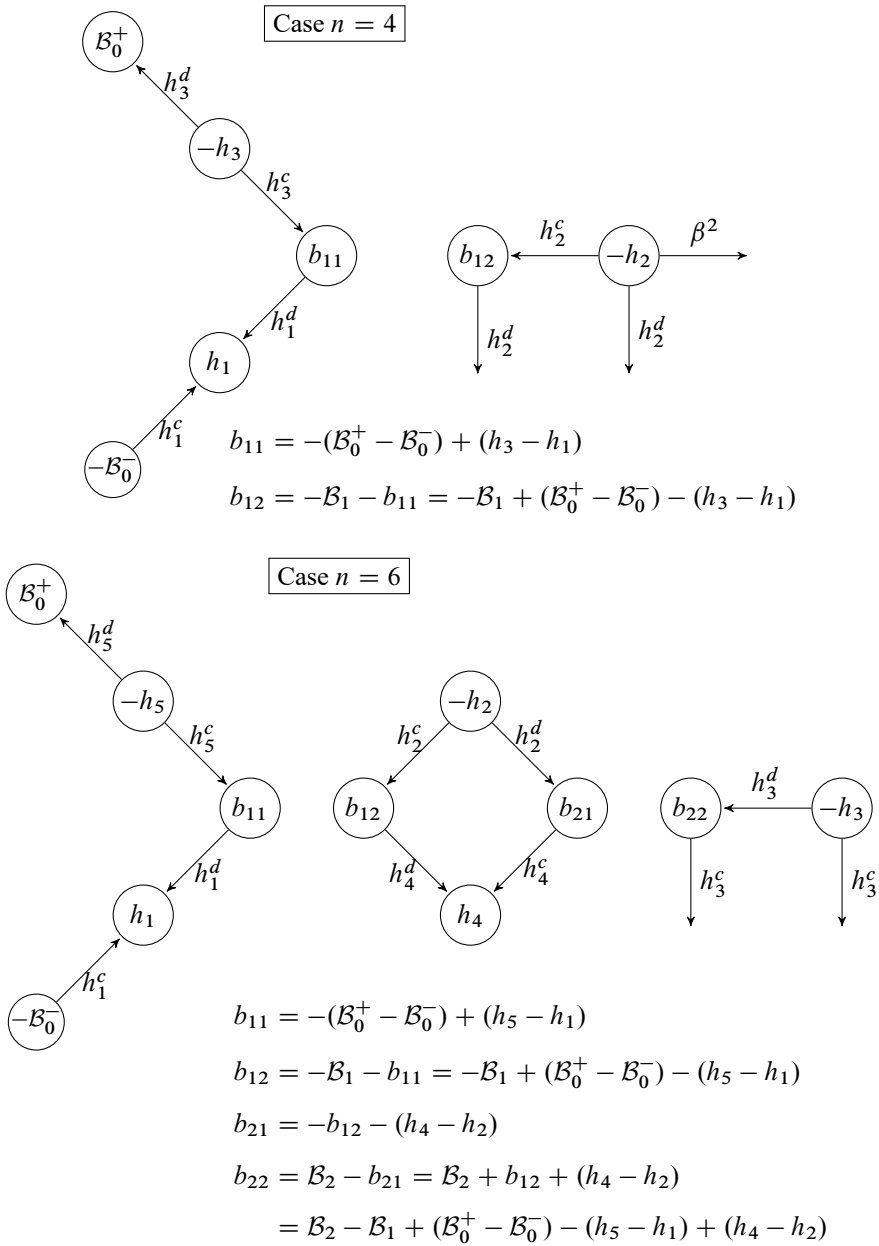
$$\left\{ \begin{array}{lll} h_1^c + & & = \mathcal{B}_0^- \\ h_1^c + h_1^d & & = h_1 \\ h_2^c + \beta^2 + h_2^d & & = h_2 \\ h_3^c + h_3^d & & = h_3 \\ h_3^d & & = \mathcal{B}_0^+ \\ h_1^d - h_2^c + & h_2^d - h_3^c & = \mathcal{B}_1, \end{array} \right. \quad (3.11)$$

$$\left\{ \begin{array}{lll} h_1^c + & & = \mathcal{B}_0^- \\ h_1^c + h_1^d & & = h_1 \\ h_2^c + h_2^d & & = h_2 \\ h_3^c + h_3^d & & = h_3 \\ + h_4^c + h_4^d & & = h_4 \\ h_5^c + h_5^d & & = h_5 \\ h_5^d & & = \mathcal{B}_0^+ \\ h_1^d - h_2^c + & h_4^d - h_5^c & = \mathcal{B}_1 \\ h_2^d - h_3^c + h_3^d - h_4^c & & = \mathcal{B}_2. \end{array} \right. \quad (3.12)$$

If we change the signs of the equations as before, the resulting system is not, alas, a set of flow conservation equations. One of the columns in the coefficient matrix will contain two entries of same sign (associated with h_2^d in the $n = 4$ system, and with h_3^c in the $n = 6$ system), and, when $n \equiv 0 \pmod{4}$, one of the columns will have only one nonzero entry (associated with β^i). Since the remaining columns of the coefficient matrix may still be interpreted as a directed graph incidence matrix, we depict the “almost directed graph” corresponding to the matrix by adding dangling arcs associated with these anomalous columns. So, for the case $n = 4$, the two arcs associated with h_2^d have their tails in the nodes associated with constants $-\mathcal{B}_1$ and $-h_2$, respectively, but no heads (totally forbidden for regular graphs), and the arc associated with β^2 has tail in the node with constant $-h_2$ and no head. When $n = 6$, h_3^c is associated with two arcs, emanating from nodes associated with constants $-\mathcal{B}_2$ and $-h_3$, respectively. These graphs are shown in Figure 3.13. The sign of the node constants indicate which of the corresponding equations were multiplied by -1 .

Nevertheless, the systems are still decomposable, using the same trick as before, of adding up equations the equations associated with the nodes in the leftmost arrow shaped subgraph, then in the first lozenge, the second, etc. The resulting decomposition and new node constants are shown in Figure 3.14. As in the odd n case, the definitions of b_{11} and b_{21} ensure the condition “sum of node constants = zero” is automatically satisfied for each of the subproblems before the last one.

Figure 3.13: “Networks” for $n = 4$ and $n = 6$.

Figure 3.14: Decomposition for the “flow” problems, cases $n = 4$ and $n = 6$.

In each decomposition we end up with $i - 1$ subproblems of the exact same type as in the odd n case, that can be analysed in the same fashion, giving rise to analogous feasibility conditions and number of solutions. It remains to show how to treat the last subproblem.

In the $n = 4$ case, the last subproblem in the decomposition sketched in Figure 3.14 consists of the system:

$$\begin{cases} -h_2^c - \beta^2 - h_2^d = -h_2 \\ h_2^c - h_2^d = b_{12} \\ h_2^c, \beta^2, h_2^d \geq 0. \end{cases} \quad (3.13)$$

The general solution to the system of equations in (3.13) is

$$\begin{bmatrix} h_2^c \\ \beta^2 \\ h_2^d \end{bmatrix} = \begin{bmatrix} b_{12} \\ h_2 - b_{12} \\ 0 \end{bmatrix} + \alpha \begin{bmatrix} 1 \\ -2 \\ 1 \end{bmatrix}. \quad (3.14)$$

In this case, however, the solution to the homogeneous system associated with the linear system in (3.13) is not, strictly speaking, a circulation, since the problem is not a network flow problem. It plays, however, the same role.

Substituting in (3.13) the general solution given in (3.14), we obtain the system of inequalities

$$\begin{aligned} \alpha &\geq -b_{12} \\ \alpha &\geq 0 \\ -2\alpha &\geq -h_2 + b_{12}, \end{aligned} \quad (3.15)$$

which is easily seen to be equivalent to

$$\max\{0, -b_{12}\} \leq \alpha \leq \frac{h_2 - b_{12}}{2}.$$

The interval $[\max\{0, -b_{12}\}, (h_2 - b_{12})/2]$, is nonempty if and only if

$$h_2 \geq b_{12} \geq -h_2.$$

Using the formula for b_{12} , we obtain

$$h_2 \geq -B_1 - b_{12} = -B_1 + (B_0^+ - B_0^-) - (h_3 - h_1) \geq -h_2. \quad (3.16)$$

Further notice that, if the aforementioned interval is nonempty, it will contain at least one integral element (the number 0 if $-b_{12} \leq 0$ and the number $-b_{12}$ if $-b_{12} > 0$), which means the inequalities give necessary and sufficient conditions for (3.13) to have integral solutions. The inequalities in (3.16) constitute precisely the unique constraint in (2.46) in the case $n = 2i = 4$. Since all the pre-assigned data are integral, the number of integral solutions of this subproblem is simply the number of integers in the interval $[\max\{0, -b_{12}\}, (h_2 - b_{12})/2]$. Since, for $n = 4$, the first subproblem (the network flow

problem with the arrow shaped directed graph) has an unique solution, the number of integers in this interval would give the overall number of solutions. For higher values of even n , one would have to multiply the number of solutions to each subproblem to obtain the total number of solutions, since they are independent.

A numerical instance of the h_k^{cd} -system for $n = 4$ is solved in Figure 3.15. In this case the characterization of extreme point solutions depends on the saturation of the unique “cycle” h_2^c, h_2^d, β^2 . Passing one unit of flow counterclockwise increases both h_2^c and h_2^d by one unit and decreases β^2 by two units. If the product $h_1^c \cdot h_2^d \cdot \beta^2$ is positive for a given feasible solution, then this solution is not an extreme point solution, since it is halfway between solutions obtained by passing a small enough positive flow in one direction and the opposite one. So, for $n = 4$, the h_k^{cd} -system will have at most 2 extreme points solutions, corresponding to the possible saturations of the “cycle” h_2^c, h_2^d, β^2 . For $n = 2i \equiv 0 \pmod{4}$, we would have $i - 1$ cycles ($i - 2$ of lozenge type, and one constituted by the arcs h_i^c, h_i^d, β^i), resulting in at most 2^{i-1} extreme points. Thus the polytope \mathcal{H}_k^{cd} constituted by the set of nonnegative solutions to the h_k^{cd} -system (which, in this case, has the additional variable β^i) has at most 2^{i-1} extreme points, when $n = 2i \equiv 0 \pmod{4}$.

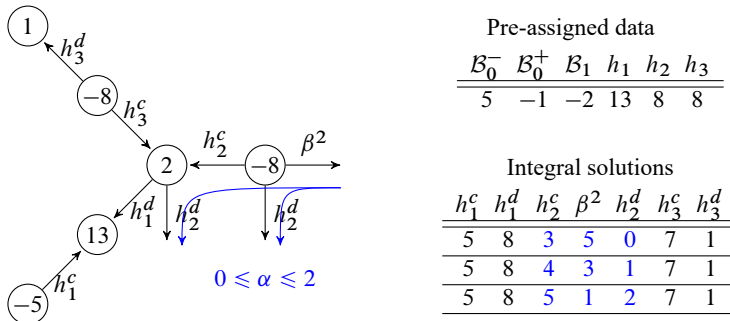


Figure 3.15: Integral solutions to numerical instance of an h_k^{cd} -system for $n = 4$.

Notice, however, that not all extreme points will be integral. In the numerical instance of Figure 3.15, saturating the cycle in one direction gives the first integral solution $(5, 8, 3, 5, 0, 7, 1)$, but if saturate the cycle in the opposite direction we obtain $(5, 8, 11/2, 0, 5/2, 7, 1)$. None of the other two integral solutions is an extreme point of \mathcal{H}_k^{cd} . The third solution in the table, for instance, is not extreme, since it is a convex combination of two other elements of \mathcal{H}_k^{cd} :

$$(5, 8, 5, 1, 2, 7, 1) = \frac{1}{5}(5, 8, 3, 5, 0, 7, 1) + \frac{4}{5}\left(5, 8, \frac{11}{2}, 0, \frac{5}{2}, 7, 1\right).$$

If we want to maintain integrality, the upper limit for α in the figure is $[5/2]$, since for each unit of flow in the cycle, the flow along β^2 is decreased by two units.

When $n = 6$, the system associated with the rightmost component of the decomposition shown in Figure 3.14 reads as follows.

$$\begin{cases} -h_3^c - h_3^d = -h_3 \\ -h_3^c + h_3^d = b_{22} \\ h_3^c, h_3^d \geq 0. \end{cases} \quad (3.17)$$

The system of linear equations in (3.17) have the unique solution

$$\begin{aligned} h_3^c &= \frac{h_3 - b_{22}}{2} \\ h_3^d &= \frac{h_3 + b_{22}}{2}, \end{aligned} \quad (3.18)$$

and this solution is feasible if and only if

$$h_3 \geq b_{22} \geq -h_3.$$

Substituting the expression for b_{22} given in Figure 3.14, we obtain

$$h_3 \geq \mathcal{B}_2 - \mathcal{B}_1 + (\mathcal{B}_0^+ - \mathcal{B}_0^-) - (h_5 - h_1) + (h_4 - h_2) \geq -h_3,$$

which is equivalent to the last of the pair of inequalities in (2.46).² The other set of inequalities in (2.46) is obtained by applying the feasibility conditions to the second subproblem in Figure 3.14, case $n = 6$.

$$h_2 \geq -\mathcal{B}_1 + (\mathcal{B}_0^+ - \mathcal{B}_0^-) - (h_5 - h_1) \geq -h_2.$$

Notice, however, that the solution (3.18) leads to another restriction when we require integrality, namely that

$$h_3 - b_{22} \equiv 0 \pmod{2},$$

which gives, substituting the the expression for b_{22} ,

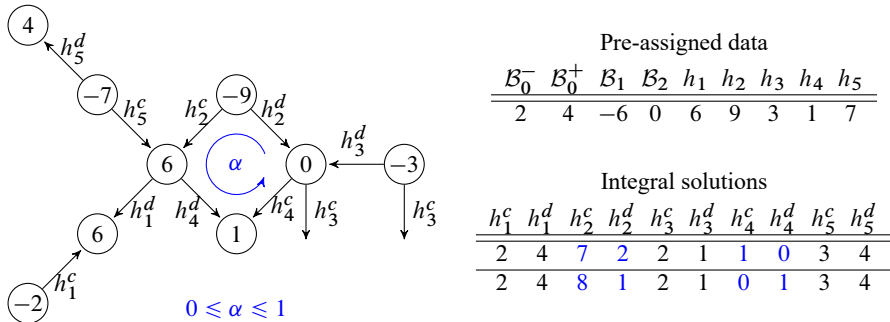
$$h_3 - \mathcal{B}_2 + \mathcal{B}_1 - (\mathcal{B}_0^+ - \mathcal{B}_0^-) + (h_5 - h_1) - (h_4 - h_2) \equiv 0 \pmod{2},$$

which coincides with (2.50) for $n = 6$.

Figure 3.16 show the integral solutions to an instance of an h_κ^{cd} -system, for the case $n = 6$.

For the general case the procedure is analogous, that is, decompose and analyse each subproblem separately. The total number of integral solutions is the product of the number of solutions for each subproblem. The Poincaré–Hopf inequalities arrive from the feasibility constraints for each subproblem. The last subproblem will give rise to the additional

²Notice that $a \geq b \geq -a$ is equivalent to $a \geq -b \geq -a$.

Figure 3.16: Solutions to numerical instance of an h_κ^{cd} -system for $n = 6$.

constraint (2.50) when $n = 2i \equiv 2 \pmod{4}$. In this case, the last subproblem has a unique solution, integral if the parity condition in (2.50) holds, so the number of extreme point solutions will be integral and depend only on the number of lozenge subgraphs, $i - 2$, of the network-flow problem associated with the h_κ^{cd} -system, resulting in at most 2^{i-2} extreme points when $n = 2i \equiv 2 \pmod{4}$.

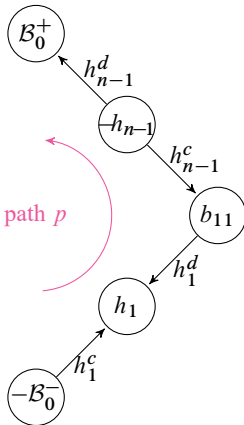
We may conclude that the polytope \mathcal{H}_κ^{cd} , if nonempty, will be an integral polytope, that is, a polytope whose extreme points are all integral, for $n = 2i + 1$ or $n = 2i \equiv 2 \pmod{4}$. However, it is interesting to note that, when $n = 2i \equiv 0 \pmod{4}$, the same polytope **will not** be integral if the parity condition in (2.50) is not satisfied, though this condition is not needed for the mere existence of integral solutions. So, when $n = 2i + 1$ or $n = 2i \equiv 2 \pmod{4}$, the polytope will coincide with the convex hull of its integral elements, but this will happen in the case $n = 2i \equiv 0 \pmod{4}$ if and only if the parity condition in (2.50) is satisfied. A similar phenomenon will occur with the Morse polytope in the case of closed manifolds.

3.2.3 On the range of κ

The value of κ has been included in \mathcal{B}_0^- and \mathcal{B}_0^+ in the several examples given. It is, however, noteworthy to consider how the value of κ affects the solutions to the h_κ^{cd} -system and how the upper bound on κ may be achieved by this analysis.

Consider the h_κ^{cd} -system given by a pre-assigned data set (h_0, h_1, \dots, h_n) , \mathcal{B}_1, \dots , where $h_0 = e^-$ and $h_n = e^+$. First we investigate the solutions to the system obtained by setting κ to zero. If this system has no nonnegative solution, there is nothing to consider. Suppose, on the other hand that the h_0^{cd} -system has a nonnegative solution h^{cd} . The network decomposition comes in handy here. The leftmost subnetwork of every decomposition is the same, the arrow-shaped subgraph depicted in Figure 3.17. Thus, when $\kappa = 0$, we must have $h_1^c = h_0 - 1$, $h_1^d = h_1 - h_1^c = h_1 - (h_0 - 1)$, $h_{n-1}^d = h_n - 1$, $h_{n-1}^c = h_{n-1} - h_{n-1}^d = h_{n-1} - (h_n - 1)$. What can we say about

the h_κ^{cd} -system? To increase the value of κ by δ means increasing the supply at the left bottom node and increase the demand at the left top node by the same amount, since $B_0^- = h_0 - 1 + \kappa$ and $B_0^+ = h_n - 1 + \kappa$. Notice that the only way to accommodate this change is to “send” flow δ along the path $h_1^c, h_1^d, h_{n-1}^c, h_{n-1}^d$. No change to the flows in the remaining arcs, belonging to the other components of the network, is either necessary or helpful. To send flow δ through a path means increasing by δ the flow in the forward arcs of the path, h_1^c and h_{n-1}^d , in this case, and decreasing by δ the flow in the backward arcs, h_1^d and h_{n-1}^c . Since flows must remain nonnegative, this limits δ to $\min\{h_1^d, h_{n-1}^c\} = \min\{h_1 - (h_0 - 1), h_{n-1} - (h_n - 1)\}$. The new solution is equal to the previous one except for these four variables. Notice that the change of κ 's value, within this range, has no impact on the number of solutions of solutions or the value of each solution, except for the cited four variables. The value of the parameter κ defines equivalence classes of solutions. Let $\kappa < \kappa'$ be two integral values in the range $[0, \min\{h_1 - (h_0 - 1), h_{n-1} - (h_n - 1)\}]$. Then the polytope $\mathcal{H}_{\kappa'}^{cd}$ is the translation of \mathcal{H}_κ^{cd} by the vector $h^{cd} = (\kappa' - \kappa)(1, -1, 0, \dots, -1, 1)$.



Where

$$\begin{aligned} B_0^+ &= h_n - 1 + \kappa \\ B_0^- &= h_0 - 1 + \kappa \\ b_{11} &= -(B_0^+ - B_0^-) + (h_{n-1} - h_1) \\ \text{path } p : & h_1^c, h_1^d, h_{n-1}^c, h_{n-1}^d \end{aligned}$$

Figure 3.17: Leftmost subnetwork in the decomposition of network corresponding to h_κ^{cd} -system.

3.3 Poincaré–Hopf inequalities for closed manifolds

In Bertolim, Mello, and de Rezende (2005b) and Bertolim, Mello, and de Rezende (2005a) we consider the Poincaré–Hopf inequalities for isolating blocks (2.46)–(2.50), and the particular case which are the Poincaré–Hopf inequalities for closed manifolds (3.19)–(3.23). This section summarizes the results in these references.

Given a Lyapunov graph $L(h_0, \dots, h_n, \kappa)$ with cycle number equal to κ , the implosion

L_C of $L(h_0, \dots, h_n, \kappa)$ is a graph with only one saddle vertex v labelled with $(0, h_1, \dots, h_{n-1}, 0, \kappa)$ and has the following properties: $e^+ = h_n$, $e^- = h_0$, $B_j^- = B_j^+ = 0$, for $j = 1, \dots, i$, if $n = 2i + 1$, and for $j = 1, \dots, i - 1$, if $n = 2i$. This implies $\mathcal{B}_j = 0$, $\mathcal{B}_0^- = h_0 - 1 + \kappa$ and $\mathcal{B}_0^+ = h_n - 1 + \kappa$. By substituting the information of the vertex v of L_C in the Poincaré–Hopf inequalities for isolating blocks (2.46)–(2.50), the Poincaré–Hopf inequalities for closed manifolds (3.19)–(3.23) below are obtained, where $0 \leq \kappa \leq \min\{h_1 - (h_0 - 1), h_{n-1} - (h_n - 1)\}$, see Bertolim, Mello, and de Rezende (2005b). Again we include, for convenience, the parity constraint (3.23) in the set, although it is not an inequality restraint.

$$\left\{ \begin{array}{l} h_j \geq \sum_{k=0}^{j-1} (-1)^{k+j} (h_{n-k} - h_k) \geq -h_{n-j}, \text{ for } j = 2, \dots, \lfloor \frac{n}{2} \rfloor \\ h_1 \geq h_0 - 1 + \kappa \\ h_{n-1} \geq h_n - 1 + \kappa \\ n = 2i + 1 \quad \left\{ \begin{array}{l} \sum_{j=0}^i (-1)^j (h_{n-j} - h_j) = 0. \end{array} \right. \\ n = 2i, \quad \left\{ \begin{array}{l} h_i - \sum_{k=0}^{i-1} (-1)^k (h_{n-k} - h_k) \equiv 0 \pmod{2}. \end{array} \right. \end{array} \right. \quad (3.19)$$

$$(3.20)$$

$$(3.21)$$

$$n = 2i + 1 \quad \left\{ \begin{array}{l} \sum_{j=0}^i (-1)^j (h_{n-j} - h_j) = 0. \end{array} \right. \quad (3.22)$$

$$n = 2i, \quad \left\{ \begin{array}{l} h_i - \sum_{k=0}^{i-1} (-1)^k (h_{n-k} - h_k) \equiv 0 \pmod{2}. \end{array} \right. \quad (3.23)$$

Below, in (3.24), we rewrite the generalized Morse inequalities (2.1) in a concise format. The main result is Theorem 3.1, that establishes the equivalence between the Poincaré–Hopf inequalities and the existence of Betti number vectors satisfying the generalized Morse inequalities and the κ -connectivity inequality $\gamma_1 \geq \kappa$. As a consequence of this fact, if the abstract Lyapunov graph $L(h_0, \dots, h_n, \kappa)$ does not satisfy the Poincaré–Hopf inequalities, it will not satisfy the Morse inequalities (3.24) for any choice of Betti number vector and hence we screen out Lyapunov graphs which cannot be realized as a continuous flow on any manifold.

$$\left\{ \begin{array}{l} \sum_{j=0}^n (-1)^{j+n} \gamma_j = \sum_{j=0}^n (-1)^{j+n} h_j \\ \left\{ \begin{array}{l} \sum_{j=0}^k (-1)^{j+k} \gamma_j \leq \sum_{j=0}^k (-1)^{j+k} h_j, \quad \text{for } k = 0, \dots, n-1. \end{array} \right. \end{array} \right. \quad (3.24)$$

Theorem 3.1. *Given an abstract Lyapunov graph $L(h_0, \dots, h_n, \kappa)$, it satisfies the Poincaré–Hopf inequalities (3.19)–(3.23), where $0 \leq \kappa \leq \min\{h_1 - (h_0 - 1), h_{n-1} - (h_n - 1)\}$, if and only if it satisfies the Morse inequalities (3.24) and the inequality $\gamma_1 \geq \kappa$ for some Betti number vector $(\gamma_0, \dots, \gamma_n)$.*

The version of Theorem 3.1 in the absence of cycles ($\kappa = 0$) was shown constructively in Bertolim, Mello, and de Rezende (2005b), by giving a recipe of how to obtain a Betti number vector satisfying (3.24) from a particular solution to the h_0^{cd} -system, and vice-versa. The theorem then follows from the equivalence between the Poincaré–Hopf inequalities and the h_0^{cd} -system. These results were generalized in Bertolim, Mello, and de Rezende (2005a). The h_κ^{cd} -system was the bridge that enabled the establishment of a link between the first set of inequalities, containing only dynamical data, and the second set, including topological data as well. This link was constructive, that is, mappings were defined to-and-fro the two sets of solutions, the h^{cd} vectors and the Betti number vectors.

The relationship between the solutions of the h_κ^{cd} -system and the Betti number vectors satisfying the Morse inequalities is rich and fruitful. It helps in establishing important properties of the *Morse polytope*, the set of nonnegative gammas that satisfy boundary and duality conditions, and the Morse and κ -connectivity inequalities. This polytope is intimately related to the polytope of solutions to the h_κ^{cd} -system, and shares some of the surprising results described in the previous section. Namely, when the data are integral and polytope not empty, it will coincide with the convex hull of its integral elements in the cases $n = 2i + 1$ and $n = 2i \equiv 2 \pmod{4}$. When $n = 2i \equiv 0 \pmod{4}$, this result requires the satisfaction of an additional hypothesis, the one corresponding to (3.23) for closed manifolds.

This relationship will be established in the sequel. First we prove the equivalence between Poincaré–Hopf and Morse inequalities and then we study the Morse polytope. Numerical examples will be given to illustrate the theoretical results.

3.3.1 Poincaré–Hopf inequalities equivalent to Morse inequalities

Consider an abstract Lyapunov graph $L(h_0, \dots, h_n, \kappa)$ with cycle number equal to κ . Since we are now dealing with closed manifolds, we obtain, from (3.1) and (3.2), the h_κ^{cd} -systems (3.25) and (3.26) below produced by the morsification algorithm.

$$n=2i+1 \left\{ \begin{array}{ll} h_1^c = h_0 - 1 + \kappa, \\ h_j^c + h_j^d = h_j, & \text{for } j = 1, \dots, 2i, \\ h_{n-1}^d = h_n - 1 + \kappa, \\ h_j^d - h_{j+1}^c - h_{n-j}^c + h_{n-j-1}^d = 0, & \text{for } j = 1, \dots, i-1, \\ h_i^d - h_{i+1}^c = 0. \end{array} \right. \quad (3.25)$$

and

$$n=2i \left\{ \begin{array}{ll} h_1^c = h_0 - 1 + \kappa, \\ h_j^c + h_j^d = h_j, & \text{for } j = 1, \dots, 2i-1, j \neq i, \\ h_i^c + h_i^d = h_i - \beta^i, & \text{where } \beta^i = 0, \text{ if } i \text{ is odd} \\ h_{n-1}^d = h_n - 1 + \kappa, \\ h_j^d - h_{j+1}^c - h_{n-j}^c + h_{n-j-1}^d = 0, & \text{for } j = 1, \dots, i-1. \end{array} \right. \quad (3.26)$$

The following equivalence result for closed manifolds follows immediately from Theorem 2.5.

Corollary 3.1. *The h_κ^{cd} -system (3.25) (resp., (3.26)), if n is odd (resp., even), has non-negative integral solutions $(h_1^c, h_1^d, \dots, h_{n-1}^c, h_{n-1}^d)$, if n is odd, and $(h_1^c, h_1^d, \dots, h_i^c, \beta^i, h_i^d, \dots, h_{n-1}^c, h_{n-1}^d)$, otherwise, if and only if the Poincaré–Hopf inequalities for closed manifolds (3.19)–(3.23) are satisfied, where $0 \leq \kappa \leq \min\{h_1 - (h_0 - 1), h_{n-1} - (h_n - 1)\}$.*

Therefore, in order to prove that if the Poincaré–Hopf inequalities (3.19)–(3.23) hold then there is a Betti number vector that satisfies the Morse inequalities (3.24) and $\gamma_1 \geq \kappa$, it suffices to show that the h_κ^{cd} -system for closed manifolds has a solution if and only if there is a Betti number vector that satisfies the Morse inequalities and $\gamma_1 \geq \kappa$.

This proof is constructive. The cases n odd, $n = 2i \equiv 0 \pmod{4}$ and $n = 2i \not\equiv 0 \pmod{4}$ are considered separately.

Case $n = 2i + 1$

Consider the map $\Gamma_\kappa : \mathbb{R}^{4i} \rightarrow \mathbb{R}^{2i+2}$, where $\Gamma_\kappa(h^{cd})$ is defined as follows:

$$\begin{aligned} [\Gamma_\kappa(h^{cd})]_0 &= [\Gamma_\kappa(h^{cd})]_{2i+1} = 1 \\ [\Gamma_\kappa(h^{cd})]_j &= \begin{cases} h_1^d - h_2^c + \kappa & \text{if } j = 1 \\ h_j^d - h_{j+1}^c, & \text{if } 2 \leq j \leq i-1 \\ h_i^d, & \text{if } j = i \\ h_{i+1}^c, & \text{if } j = i+1 \\ -h_{j-1}^d + h_j^c, & \text{if } i+2 \leq j \leq 2i-1 \\ -h_{2i-1}^d + h_{2i}^c + \kappa, & \text{if } j = 2i. \end{cases} \end{aligned} \quad (3.27)$$

The boundary conditions are satisfied by construction. Duality conditions are a consequence of the flow constraints $h_j^d - h_{j+1}^c - h_{n-j}^c + h_{n-j-1}^d = 0$, for $1 \leq j \leq i-1$ and $h_i^d = h_i^c$. By judicious manipulation of the several partial alternate sums of the components of $\Gamma_\kappa(h^{cd})$, it is possible to show that it does indeed satisfy the Morse inequalities (3.24). However, the formulas in (3.27) do not guarantee the nonnegativity of $\Gamma_\kappa(h^{cd})$ nor the satisfaction of the κ -connectivity constraint $[\Gamma_\kappa(h^{cd})]_1 \geq \kappa$. Consider the numerical instance in Figure 3.18.

With respect to the feasible solution shown in Figure 3.18, we may have $-3 \leq \alpha_1 \leq 0$ and $-4 \leq \alpha_2 \leq 1$, so there are 24 feasible integral solutions. Let h^{cd} be the solution in Figure 3.18. Calculating $\gamma = \Gamma_0(h^{cd})$ from the formulas given in (3.27), we obtain the values below, since κ is assumed to be zero.

$$\gamma = (\gamma_0, \gamma_1, \gamma_2, \gamma_3, \gamma_4, \gamma_5, \gamma_6, \gamma_7) = (1, -1, -4, 1, 1, -4, -1, 1).$$

It is straightforward to verify that this γ satisfies the boundary conditions, duality and (3.24), but fails the conditions $\gamma \geq 0$ and $\gamma_1 \geq \kappa$.

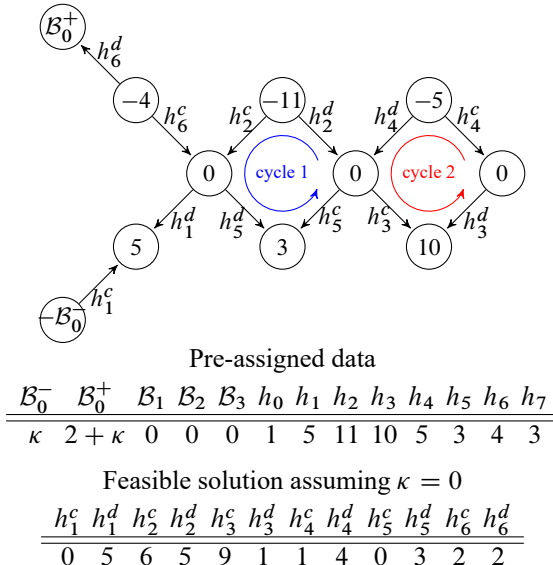


Figure 3.18: A feasible solution to a network-flow problem corresponding to a h_κ^{cd} -system for closed manifolds, for $n = 7$.

In order to guarantee the satisfaction of all constraints on γ , we need to choose a specific flow, namely the unique flow that satisfies the *complementarity condition* below.

$$h_j^c h_{n-j}^d = 0, \quad \text{for } j = 2, \dots, [n/2]. \quad (3.28)$$

Since the arcs associated with variables h_j^c and h_{n-j}^d belong to the $(j-1)$ -th cycle of the network, for $j = 2, \dots, [n/2]$, the support of a feasible solution that satisfies (3.28) has no cycles, and thus must be unique and also an extreme point.

Furthermore, if the network has nonnegative solutions, then it must have a solution satisfying (3.28). This may be achieved by sending the appropriate amount of flow in each cycle in order to drive to zero the flow in at least one of the two arcs in the product. This is the same as adding a suitable elementary circulation to the flow. For the solution in Figure 3.18, passing flow -3 through the first cycle and flow -4 through the second cycle produces the solution $h^{cd} = (0, 5, 3, 8, 5, 5, 0, 3, 0, 2, 2)$, which satisfies (3.28). Then $\Gamma_0(h^{cd}) = (1, 2, 3, 5, 5, 3, 2, 1)$ and one can easily verify that it satisfies all conditions: boundary, duality, Morse inequalities, nonnegativity and κ -connectivity. This is true for general $n = 2i + 1$.

Now let δ be an integer in the interval $[0, \min\{h_1 - (h_0 - 1), h_{n-1} - (h_n - 1)\}]$ and $h^{2,cd}$ be a solution to the h_δ^{cd} -system. Then $h^{1,cd} = h^{2,cd} - \delta(1, -1, 0, \dots, -1, 1)$ is a solution to the h_0^{cd} -system. Notice that $\Gamma_0(h^{1,cd}) = \Gamma_\delta(h^{2,cd})$. Thus there seems to exist

no gain in considering the general case of positive values for κ , except perhaps regarding the satisfaction of the κ -connectivity inequality. So the question is whether there is an $h^{cd} \in \mathcal{H}_\delta^{cd}$ that will satisfy it. Do we need to choose a special value for δ , perhaps related to κ ?

Fortunately, the same $\overset{*}{h}{}^{cd}$, the unique solution to the h_0^{cd} -system that satisfies the complementarity condition (3.28), solves this question, since the κ -connectivity constraint is always satisfied by $\Gamma_0(\overset{*}{h}{}^{cd})$. To see that, consider the two cases allowed by the complementarity condition $\overset{*}{h}{}^c{}_2 \overset{*}{h}{}^d_{n-2} = 0$. If $\overset{*}{h}{}^c{}_2 = 0$, then

$$[\Gamma_0(\overset{*}{h}{}^{cd})]_1 = \overset{*}{h}{}^d{}_1 - \overset{*}{h}{}^c{}_2 = \overset{*}{h}{}^d{}_1 = h_1 - \overset{*}{h}{}^c{}_1 = h_1 - (h_0 - 1) \geq \kappa,$$

for any $\kappa \in [0, \leq \min\{h_1 - (h_0 - 1), h_{n-1} - (h_n - 1)\}]$. If, on the other hand, $\overset{*}{h}{}^d_{n-2} = 0$, then

$$\begin{aligned} [\Gamma_0(\overset{*}{h}{}^{cd})]_1 &= [\Gamma_0(\overset{*}{h}{}^{cd})]_{n-1} = \overset{*}{h}{}^d_{n-2} + \overset{*}{h}{}^c_{n-1} = \overset{*}{h}{}^c_{n-1} \\ &= h_{n-1} - \overset{*}{h}{}^d_{n-1} = h_{n-1} - (h_n - 1) \geq \kappa, \end{aligned}$$

for any $\kappa \in [0, \leq \min\{h_1 - (h_0 - 1), h_{n-1} - (h_n - 1)\}]$.

Thus, if the h_0^{cd} -system (3.25) has a nonnegative solution, then there is a Betti number vector that solves the Morse inequalities and the κ -connectivity condition, for $0 \leq \kappa \leq \min\{h_1 - (h_0 - 1), h_{n-1} - (h_n - 1)\}$. Since the feasibility of the Poincaré–Hopf inequalities are equivalent to the existence of nonnegative integral solutions to the h_κ^{cd} -system, we conclude that the feasibility of the Poincaré–Hopf inequalities is sufficient for the existence of Betti number vectors satisfying the Morse inequalities.

From now on, for the case $n = 2i + 1$, we will use the fact that $\Gamma_0(\mathcal{H}_0^{cd}) = \Gamma_\delta(\mathcal{H}_\delta^{cd})$ to drop the subscript κ in the definition of Γ , being mindful of the convention $\Gamma = \Gamma_0$.

To show the converse result, we introduce the map $H^{cd} : \mathbb{R}^{2i+2} \rightarrow \mathbb{R}^{4i}$, comprised by the maps H^c and H^d .

$$\left\{ \begin{array}{ll} [H^d(\gamma)]_k = \sum_{j=0}^k (-1)^{j+k} (h_j - \gamma_j), & \text{for } i+1 \leq k \leq 2i \\ [H^c(\gamma)]_k = \sum_{j=0}^{k-1} (-1)^{j+k-1} (h_j - \gamma_j), & \text{for } 1 \leq k \leq i \end{array} \right. \quad (3.29)$$

$$[H^d(\gamma)]_k = \gamma_k + [H^c(\gamma)]_{k+1}, \quad \text{for } 1 \leq k \leq i-1 \quad (3.31)$$

$$[H^c(\gamma)]_k = \gamma_k + [H^d(\gamma)]_{k-1}, \quad \text{for } i+2 \leq k \leq 2i \quad (3.32)$$

$$[H^d(\gamma)]_i = \gamma_i \quad (3.33)$$

$$[H^c(\gamma)]_{i+1} = \gamma_{i+1}. \quad (3.34)$$

Now suppose there is a Betti number vector $\bar{\gamma}$ that satisfies the Morse inequalities (3.24). Now, if we closely analyse these inequalities, we realize there is some wiggle

room in the values of γ_i and γ_{i+1} . This pair of variables appears, with opposite signs, in the first equality in (3.24) and in the inequalities that follow, for $k = i + 1, \dots, 2i - 1$. The inequality corresponding to $k = i$ contains only γ_i and reads

$$\gamma_i \leq \sum_{j=0}^i (-1)^{j+i} h_j - \sum_{j=0}^{i-1} (-1)^{j+i} \gamma_j. \quad (3.35)$$

The remaining inequalities contain neither γ_i nor its dual γ_{i+1} . Thus if we change $\bar{\gamma}$ by adding the same amount δ to these two components, the new vector will continue to satisfy all conditions, except, perhaps, for (3.35). The upper bound of δ will be

$$\delta_{\max} = \sum_{j=0}^i (-1)^{j+i} h_j - \sum_{j=0}^{i-1} (-1)^{j+i} \bar{\gamma}_j - \bar{\gamma}_i,$$

the value for which (3.35) is satisfied tightly.

This amounts to establishing that, if there is a Betti number vector that satisfies the Morse inequalities (3.24), then there is one that satisfies the Morse inequalities **and** saturates the inequality for $k = i$, (3.35). The relevance of this fact is that the image $h^{cd} = H^{cd}(\gamma)$ of such a vector will be a solution to the h_0^{cd} -system, establishing the converse result. Thus Theorem 3.1 is true for $n = 2i + 1$.

Case $n = 2i$

Let $n = 2i \equiv 0 \pmod{4}$. Again we define a map Γ , but now the rules are slightly different. Notice that the domain of Γ is \mathbb{R}^{4i-1} , if $n = 2i \equiv 0 \pmod{4}$ and \mathbb{R}^{4i-2} , otherwise (when $n = 2i \equiv 0 \pmod{4}$ the vector h^{cd} contains the additional component β^i).

$$\left\{ \begin{array}{l} [\Gamma(h^{cd})]_0 = [\Gamma(h^{cd})]_{2i} = 1 \\ [\Gamma(h^{cd})]_j = \begin{cases} h_j^d - h_{j+1}^c, & \text{if } 1 \leq j \leq i-2 \\ h_{i-1}^d - (h_i^c - \delta), & \text{if } j = i-1 \\ \beta^i, & \text{if } j = i \text{ and } 2i \equiv 0 \pmod{4} \\ 2\delta, & \text{if } j = i \text{ and } 2i \equiv 2 \pmod{4} \\ -(h_j^d - \delta) + h_{j+1}^c, & \text{if } j = i+1 \\ -h_{j-1}^d + h_j^c, & \text{if } i+2 \leq j \leq 2i-1 \\ \min\{h_i^c, h_i^d\}, & \text{if } 2i \equiv 2 \pmod{4} \\ 0, & \text{ow.} \end{cases} \end{array} \right. \quad (3.36)$$

As in the case $n = 2i + 1$, we could define a more general map, to apply to solutions to the h_κ^{cd} -system, for any allowable value of κ , by altering the definition of $[\Gamma(h^{cd})]_1$ and $[\Gamma(h^{cd})]_{n-1}$ to include the summand κ , as in (3.27). Nevertheless, this is also unnecessary here, because the relationship between the solution sets of the h_κ^{cd} -systems, for different

values of the parameter κ , remains the same, they are just translations of each other and this translation cancels out when applying the map.

Let h^{cd} be a solution to the h_κ^{cd} -system that satisfies the complementarity condition (3.28), with the caveat that the last restriction in (3.28), namely $h_i^c, h_i^d = 0$, **need not** be satisfied if $n \equiv 2 \pmod{4}$. This allowance is necessary since that the last component of the “network” decomposition for the case $n = 2i \equiv 2 \pmod{4}$ has a unique solution that may not satisfy $h_i^c h_i^d = 0$ (recall the example in Figure 3.16). The map (3.36) will take this h^{cd} to a integral vector that satisfies boundary and duality conditions, Morse inequalities, nonnegativity and κ -connectivity. The numerical instance in Figure 3.19 illustrates this fact.

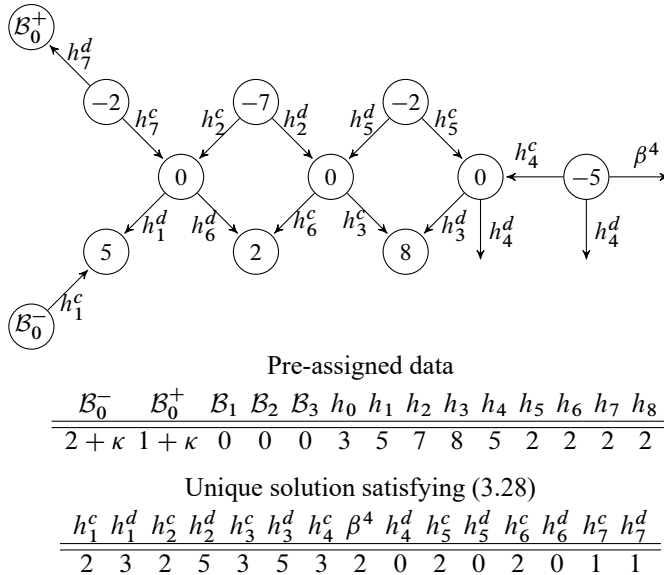


Figure 3.19: Numerical instance of network-flow corresponding to h_κ^{cd} -system for closed manifolds, for $n = 8$.

The vector $\gamma = \Gamma(h^{cd})$ resulting from the feasible solution h^{cd} given in Figure 3.19 is the following.

$$\gamma = (\gamma_0, \gamma_1, \gamma_2, \gamma_3, \gamma_4, \gamma_5, \gamma_6, \gamma_7, \gamma_8) = (1, 1, 2, 2, 2, 2, 2, 1, 1).$$

The “network” in Figure 3.19 has three “cycles”: $h_2^c, h_2^d, h_6^c, h_6^d; h_5^d, h_3^c, h_3^d, h_5^c$ and h_4^c, β^4, h_4^d . The last one is not really a cycle, but the variables constitute the support of an elementary vector of the subspace comprised of the solutions to the homogeneous version of the h_κ^{cd} -system. Without loss of generality, we choose the nonnull elements of this solution to be $(1, -2, 1)$. With respect to the solution in Figure 3.19, feasibility is maintained if

we pass flow in the interval $[0, 2]$ in the first and second cycle, and between 0 and 1 in the third “cycle”. This gives us a total of 18 integral nonnegative solutions to the h_0^{cd} -system. As before, the lack of the complementarity condition will lead to γ 's satisfying duality and boundary conditions, and Morse inequalities, but that may fail at nonnegativity and κ -connectivity.

The complementarity condition could pose an obstacle when $n = 2i \equiv 2 \pmod{4}$. This is circumvented by the introduction of δ . In practice, it is as if we were adding the variable β^i and passing flow through the last “cycle” to drive at least one of the variables h_i^c or h_i^d to zero. Notice that this necessarily assigns an even value to Γ_i , as required per the definition of a Betti number vector. In fact, when n is even, using duality and the first equation in (3.24), when have that

$$\begin{aligned}\gamma_i &= \sum_{k=0}^n (-1)^{k+n} h_k - \sum_{k=0, k \neq i}^n (-1)^{n+k} \gamma_k \\ &= \sum_{k=0}^n (-1)^k h_k - 2 \sum_{k=0}^{i-1} (-1)^k \gamma_k.\end{aligned}$$

Furthermore, since $n = 2i \equiv 2 \pmod{4}$, thus “ i ” is odd, the alternate sum of the h 's may be manipulated as follows.

$$\begin{aligned}\sum_{k=0}^n (-1)^k h_k &= (-1)^i h_i + \sum_{k=0}^{i-1} (-1)^k h_k + \sum_{k=i+1}^n (-1)^k h_k \\ &= -h_i + \sum_{k=0}^{i-1} (-1)^k h_k + \sum_{k=0}^{i-1} (-1)^k h_{n-k} \pm \sum_{k=0}^{i-1} (-1)^k h_k \\ &= -h_i + \sum_{k=0}^{i-1} (-1)^k (h_{n-k} - h_k) + 2 \sum_{k=0}^{i-1} (-1)^k h_k.\end{aligned}$$

Thus the last Poincaré–Hopf condition (3.23) is satisfied if and only if the alternate sum $\sum_{k=0}^n (-1)^k h_k$ is even, which is equivalent to asking that γ_i be even. Again using the equivalence between the Poincaré–Hopf inequalities and h_κ^{cd} -systems, we conclude that either is sufficient for the existence of a Betti number vector satisfying the Morse inequalities.

This parity condition is essential for the existence of integral solutions to h_κ^{cd} -system, as shown in Section 3.2. Consider, for instance, the following example. Let $n = 2i = 6$, $h = (3, 6, 3, 4, 1, 5, 4)$ and $\kappa = 0$. The unique solution to the corresponding h_0^{cd} -system is the nonintegral vector $h^{cd} = (2, 4, 3, 0, 3/2, 5/2, 1, 0, 1, 4)$. Nevertheless, the vector $\gamma = (1, 1, 0, 3, 0, 1, 1)$ is a nonnegative integral vector that satisfies (3.24), duality and κ -connectivity conditions. It is, in fact, the unique solution to the Morse inequalities (3.24), but notice that it fails the parity condition for the middle component $\gamma_i = \gamma_3$.

Now suppose the h_0^{cd} -system has an nonnegative integral solution h^{cd} . Thus, it has one, say \tilde{h}^{cd} , that satisfies (3.28), except possibly for $h_i^c h_i^d$ when $n = 2i \equiv 2 \pmod{4}$. Then $\Gamma(\tilde{h}^{cd})$ is clearly integral, satisfies the boundary and duality conditions and may be shown to satisfy the Morse inequalities as well. This implies that the feasibility of the h_κ^{cd} -system is sufficient for the existence of a Betti number vector satisfying Morse and κ -connectivity inequalities.

To show the converse we will need the map H^{cd} . If $n = 2i \equiv 0 \pmod{4}$, it is comprised and by the maps H^c , H^d and B , given below.

$$\left\{ \begin{array}{ll} [H^d(\gamma)]_k = \sum_{j=0}^k (-1)^{j+k} (h_j - \gamma_j), & \text{for } i \leq k \leq 2i-1 \\ [H^c(\gamma)]_k = \sum_{j=0}^{k-1} (-1)^{j+k-1} (h_j - \gamma_j), & \text{for } 1 \leq k \leq i+1 \end{array} \right. \quad (3.37)$$

$$\left\{ \begin{array}{ll} [H^d(\gamma)]_k = \gamma_k + [H^c(\gamma)]_{k+1}, & \text{for } 1 \leq k \leq i-1 \\ [H^c(\gamma)]_k = \gamma_k + [H^d(\gamma)]_{k-1}, & \text{for } i+1 \leq k \leq 2i-1 \end{array} \right. \quad (3.39) \quad (3.40)$$

$$B(\gamma) = \gamma_i. \quad (3.41)$$

When $n = 2i \equiv 2 \pmod{4}$, we use the map \tilde{H}^{cd} , which does not include a map B , only the maps \tilde{H}^c and \tilde{H}^d . It coincides with H^{cd} except in the i -th components of \tilde{H}^c and \tilde{H}^d , which are

$$\left\{ \begin{array}{l} \tilde{H}_i^c(\gamma) = H_i^c + \frac{\gamma_i}{2} \\ \tilde{H}_i^d(\gamma) = H_i^d + \frac{\gamma_i}{2}. \end{array} \right. \quad (3.42)$$

Let γ be a Betti number vector satisfying the Morse inequalities. It can be shown that $H^{cd}(\gamma)$ is a nonnegative integral vector satisfying the h_0^{cd} -system, showing the converse result needed, and concluding the proof of Theorem 3.1.

3.3.2 The Morse polytope

Consider a fixed pre-assigned index data set (h_0, h_1, \dots, h_n) and let κ be an integer in the interval $[0, \min\{h_1 - (h_0 - 1), h_{n-1} - (h_n - 1)\}]$. In this section we will suppose that the h_0^{cd} -system has a solution. In this section we study the Morse polyhedron \mathcal{P}_κ , the set of $\gamma \in \mathbb{R}_+^{n+1}$ that satisfy boundary and duality conditions, and the Morse and κ -connectivity inequalities.

We'll see that \mathcal{P}_κ bears a close relationship with the polytope \mathcal{H}_0^{cd} constituted by the nonnegative solutions to the h_0^{cd} -system, introduced on page 100, for the case $n = 2i + 1$ and on page 107, for the case $n = 2i$.

First of all we point out that \mathcal{P}_κ is a polytope, i.e., a bounded polyhedron. This follows from the nonnegativity restriction and the fact that taking all possible pairs of consecutive inequalities in (3.24) we obtain $\gamma_j \leq h_j$, for $j = 1, \dots, n$. Therefore $0 \leq \gamma_j \leq h_j$, for $0 \leq j \leq n$, for every $\gamma \in \mathcal{P}_\kappa$.

Furthermore, from its definition, we have that

$$\mathcal{P}_\kappa = \mathcal{P}_0 \cap \{\gamma \in \mathbb{R}^{n+1} \mid \gamma_1 \geq \kappa\},$$

so the analysis of \mathcal{P}_κ greatly benefits from the knowledge of \mathcal{P}_0 . In fact, \mathcal{P}_κ is simply the intersection of \mathcal{P}_0 with the half-space defined by the inequality $\gamma_1 \geq \kappa$.

It was remarked in Section 3.2, in a more general context, that, when $n = 2i + 1$ or $n \equiv 2 \pmod{4}$, all vertices of \mathcal{H}_0^{cd} are integral, a straightforward result, considering the identification of the h_κ^{cd} -system as a network-flow problem (albeit a deviant one when n is even). However, when $n \equiv 0 \pmod{4}$, the h_κ^{cd} -system may have extreme solutions that are not integral, see example on page 105. Even though condition (3.23) is not necessary for the existence of integral nonnegative solutions, it is necessary if we want to guarantee an integral polytope. This remains true for the particular case of closed manifolds.

Analogous results are true for \mathcal{P}_κ , a somewhat surprising outcome. It turns out that \mathcal{P}_κ is an integral polytope when $n = 2i + 1$ or $n = 2i \equiv 2 \pmod{4}$, or, equivalently, that \mathcal{P}_κ is the convex hull of the collection of Betti number vectors which satisfy the Morse inequalities. Nevertheless, in order for this to hold in the case $n = 2i \equiv 0 \pmod{4}$, we need one additional constraint, namely that (3.23) holds, just like for the polytope \mathcal{H}_κ^{cd} .

We have already seen that $\Gamma(\mathcal{H}_0^{cd}) \not\subset \mathcal{P}_0$. Nonetheless, we will be able to establish a 1-to-1 relationship between a subset of \mathcal{P}_0 and a subset of \mathcal{H}_0^{cd} . This result will enable an easy construction method for the Betti number vectors in this subset of \mathcal{P}_0 , from the special solution to the h_κ^{cd} -system that satisfies the complementarity condition (3.28) and the elementary circulations of the h_κ^{cd} network.

Case $n = 2i + 1$

In order to simplify the exposition, boundary and duality conditions will be used to eliminate more than half the variables, namely $\gamma_0, \gamma_{i+1}, \dots, \gamma_{2i+1}$. The duality conditions imply that

$$\sum_{j=0}^k (-1)^j \gamma_j = 1 + \sum_{j=1}^{\min\{k, 2i-k\}} (-1)^j \gamma_j,$$

for $k = 1, \dots, 2i$.

Substituting these partial sum expressions in the Morse inequalities (3.24) and using the boundary and κ -connectivity condition, we obtain the following inequalities for $\gamma^r =$

$(\gamma_1, \gamma_2, \dots, \gamma_i)$.

$$\left\{ \begin{array}{l} 0 = \sum_{j=0}^{2i+1} (-1)^j h_j, \\ 0 \leq h_0 - 1, \\ 0 \leq h_{2i+1} - 1 \end{array} \right. \quad (3.43)$$

$$0 \leq h_0 - 1, \quad (3.44)$$

$$0 \leq h_{2i+1} - 1 \quad (3.45)$$

$$\left\{ \begin{array}{l} \sum_{j=1}^{\min\{k, 2i-k\}} (-1)^{j+k} \gamma_j \leq -(-1)^k + \sum_{j=0}^k (-1)^{j+k} h_j, \text{ for } 1 \leq k \leq 2i-1 \\ \gamma_1 \geq \kappa \\ \gamma^r \geq 0. \end{array} \right. \quad (3.46)$$

$$\gamma_1 \geq \kappa \quad (3.47)$$

$$\gamma^r \geq 0. \quad (3.48)$$

Notice that (3.43)–(3.45) are actually constraints on the pre-assigned index data set, already presumed satisfied. Algebraically speaking, the *reduced Morse polytope* \mathcal{P}_κ^r defined by constraints (3.46)–(3.48) is the projection of the Morse polytope \mathcal{P}_κ onto the subspace generated by γ^r . Clearly there is a 1-to-1 relationship between $\gamma^r \in \mathcal{P}_\kappa^r$ and $\gamma \in \mathcal{P}_\kappa$. Furthermore, γ^r is an extreme point of \mathcal{P}_κ^r if and only if its corresponding $\gamma \in \mathcal{P}_\kappa$ is an extreme point of \mathcal{P}_κ .

In the following we adopt the convention of indicating the subvector (x_1, \dots, x_i) (resp., (x_1, \dots, x_{i-1})), if $n = 2i+1$ (resp., if $n = 2i$), of the vector $x = (x_0, x_1, \dots, x_n)$, by appending the superscript “ r ” to x . The biunique relationship between a vector x and its projection x^r allows us to recuperate the $(n+1)$ -component vector x from its projection, extending x^r by means of applying boundary and duality conditions to x^r .

The next proposition establishes the main properties of \mathcal{P}_κ^r and was shown in Bertolim, Mello, and de Rezende (2005a). It is a generalization of the result for $\kappa = 0$ obtained in Bertolim, Mello, and de Rezende (2005b).

Proposition 3.1. *The polytope \mathcal{P}_κ^r satisfies the following properties:*

1. *The vertices of \mathcal{P}_κ^r are integral.*
2. *Each vertex of \mathcal{P}_κ^r belongs to one of the faces:*

$$\mathcal{F}_\kappa^t = \{\gamma^r \in \mathcal{P}_\kappa^r \mid \sum_{j=1}^i (-1)^j \gamma_j = -1 + \sum_{j=0}^i (-1)^j h_j\}$$

or

$$\mathcal{F}_\kappa^0 = \{\gamma \in \mathcal{P}_\kappa^r \mid \gamma_i = 0\}.$$

3. *If $\tilde{\gamma}^r \in \mathcal{F}_\kappa^t$, then $(\tilde{\gamma}_1, \dots, \tilde{\gamma}_{i-1}, 0) \in \mathcal{F}_\kappa^0$, that is, \mathcal{F}_κ^0 is the projection of \mathcal{F}_κ^t on the plane $\gamma_i = 0$.*
4. *Each (integral) γ^r in \mathcal{F}_κ^t corresponds to an (integral) nonnegative h^{cd} satisfying the h_κ^{cd} -system for closed manifolds (3.25).*

5. If $\kappa \geq \kappa'$ then $\mathcal{P}_\kappa^r \subseteq \mathcal{P}_{\kappa'}^r$.

The proof uses the “consecutive ones” property to show that the coefficient matrix of the system of linear inequalities that defines \mathcal{P}_κ^r is totally unimodular, see Fulkerson and Gross (1965), and Hoffman and Kruskal (1956).

Proposition 3.1 implies that \mathcal{P}_κ is the convex hull of nonnegative Betti number vectors that satisfy the Morse inequalities, boundary, duality and κ -connectivity conditions. All knowledge of \mathcal{P}_κ^r may be obtained from face \mathcal{F}_κ^t in the sense that all the remaining elements of the polytope may be obtained from the ones on this face by decreasing the i -th component.

Proposition 3.2, also from Bertolim, Mello, and de Rezende (2005a), not only establishes the existence of a componentwise maximum element of \mathcal{P}_κ^r but also gives a simpler formulation for \mathcal{P}_κ^r , using this maximum.

Proposition 3.2. Suppose the h_0^{cd} -system (3.25) admits nonnegative solutions. Let \bar{h}^{cd} be the nonnegative integral solution thereto that satisfies the complementarity conditions (3.28). Let $\bar{\gamma}^* = \Gamma(\bar{h}^{cd})$ be constructed from \bar{h}^{cd} using (3.27). Then $\bar{\gamma}^r \in \mathcal{F}_0^t$ and \mathcal{P}_κ^r may be rewritten as the set of vectors that satisfy

$$\left\{ \begin{array}{l} (-1)^k \sum_{j=1}^k (-1)^j \gamma_j \leq -(-1)^k + (-1)^k \sum_{j=0}^k (-1)^j \bar{\gamma}_j^*, \quad \text{for } 1 \leq k \leq i \\ \gamma_1 \geq \kappa, \\ \gamma^r \geq 0. \end{array} \right.$$

Furthermore, $\bar{\gamma}^r$ is the maximum vector of \mathcal{P}_κ^r , componentwise.

Proposition 3.2 could have been somewhat expected since we showed that $\Gamma(\bar{h}^{cd})$ would satisfy $[\Gamma(\bar{h}^{cd})]_1 \geq \kappa$ for any admissible value of κ . This is the same as saying $\Gamma(\bar{h}^{cd}) \in \mathcal{P}_\kappa$, for any $\kappa \in [0, \min\{h_1 - (h_0 - 1), h_{n-1} - (h_n - 1)\}]$.

Although not every $h^{cd} \in \mathcal{H}_0^{cd}$ will be mapped to a vector in \mathcal{P}_0 by Γ , the following proposition gives the next best thing. It establishes a 1-to-1 relationship between a subset of \mathcal{H}_0^{cd} and \mathcal{F}_0^t . From the definition of H^{cd} , it is easy to verify that given $\bar{\gamma}^r \in \mathcal{F}_\kappa^t$, then H^{cd} maps $\bar{\gamma}$ and all the points between $\bar{\gamma}$ and its projection onto \mathcal{F}_κ^t to the same h^{cd} vector in \mathcal{H}_0^{cd} . The next proposition refines a similar one from Bertolim, Mello, and de Rezende (2005b).

Proposition 3.3. Let $\bar{h}^{cd} \in \mathcal{H}_0^{cd}$ be such that $\bar{\gamma} = \Gamma(\bar{h}^{cd}) \in \mathcal{P}_0$. Then $\bar{\gamma}^r \in \mathcal{F}_0^t$ and $H^{cd}(\bar{\gamma}) = \bar{h}^{cd}$.

Proof. First we show that $\bar{\gamma} \in \mathcal{F}_0^t$. Using the definition of Γ in (3.27), we have the

following.

$$\begin{aligned}
\sum_{j=1}^i (-1)^j \bar{\gamma}_j &= \sum_{j=1}^{i-1} (-1)^j (\bar{h}_j^d - \bar{h}_{j+1}^c) + (-1)^i \bar{h}_i^d \\
&= -\bar{h}_1^d + \sum_{j=2}^{i-1} (-1)^j \bar{h}_j^d + \sum_{j=2}^{i-1} (-1)^j \bar{h}_j^c + (-1)^i \bar{h}_i^c + (-1)^i \bar{h}_i^d \\
&= -h_1 + (h_0 - 1) + \sum_{j=2}^i (-1)^j h_j \\
&= -1 + \sum_{j=0}^i (-1)^j h_j.
\end{aligned}$$

Now we prove by induction that $H^{cd}(\bar{\gamma}) = \bar{h}^{cd}$. Let $k = i + 1$. Formulas (3.27) and (3.29) implies the following.

$$\begin{aligned}
[H^d(\bar{\gamma})]_{i+1} &= \sum_{j=0}^{i+1} (-1)^{j+i+1} (h_j - \bar{\gamma}_j) \\
&= \sum_{j=0}^i (-1)^{j+i+1} (h_j - \bar{\gamma}_j) + (-1)^{2i+2} (h_{i+1} - \bar{\gamma}_{i+1}) \\
&= h_{i+1} - \bar{h}_{i+1}^c \\
&= \bar{h}_{i+1}^d.
\end{aligned}$$

Assume, by induction, that $[H^d(\bar{\gamma}^r)]_\ell = \bar{h}_\ell^d$, for $\ell \leq k - 1$. Notice that

$$\begin{aligned}
[H^d(\bar{\gamma})]_k + [H^d(\bar{\gamma})]_{k-1} &= \sum_{j=0}^k (-1)^{j+k} (h_j - \gamma_j) + \sum_{j=0}^{k-1} (-1)^{j+k-1} (h_j - \gamma_j) \\
&= (-1)^{2k} (h_k - \bar{\gamma}_k) \\
&= h_k - (-\bar{h}_{k-1}^d + \bar{h}_k^c) \\
&= \bar{h}_k^d + \bar{h}_{k-1}^d.
\end{aligned}$$

Thus, using the induction hypothesis, we conclude that

$$[H^d(\bar{\gamma})]_k = \bar{h}_k^d,$$

which means this is true for $i + 1 \leq k \leq 2i$.

Next, let $k = i$. Then (3.30) implies

$$[H^c(\bar{\gamma})]_1 = h_0 - \bar{\gamma}_0 = h_0 - 1 = \bar{h}_1^c.$$

Suppose, by induction, that $[H^c(\bar{\gamma})]_\ell = \bar{h}_\ell^c$ for $\ell \leq k-1$. Since

$$\begin{aligned} [H^c(\bar{\gamma})]_k + [H^c(\bar{\gamma})]_{k-1} &= \sum_{j=0}^{k-1} (-1)^{j+k-1} (h_j - \gamma_j) + \sum_{j=0}^{k-2} (-1)^{j+k-2} (h_j - \gamma_j) \\ &= h_{k-1} - \bar{\gamma}_{k-1} \\ &= h_{k-1} - (\bar{h}_{k-1}^d - \bar{h}_k^c) \\ &= \bar{h}_{k-1}^c + \bar{h}_k^c, \end{aligned}$$

using the induction hypothesis, we have that

$$[H^c(\bar{\gamma})]_k = \bar{h}_k^c,$$

which must be true for $1 \leq k \leq i$.

Therefore, using the quantities already calculated, for $1 \leq k \leq i-1$,

$$\begin{aligned} [H^d(\bar{\gamma})]_k &= \bar{\gamma}_k + [H^c(\bar{\gamma})]_{k+1} \\ &= (\bar{h}_k^d - \bar{h}_{k+1}^c) + \bar{h}_{k+1}^c \\ &= \bar{h}_k^d. \end{aligned}$$

Likewise, for $i+2 \leq k \leq 2i$,

$$\begin{aligned} [H^c(\bar{\gamma})]_k &= \bar{\gamma}_k + [H^d(\bar{\gamma})]_{k-1} \\ &= -\bar{h}_{k-1}^d + \bar{h}_k^c + \bar{h}_{k-1}^d \\ &= \bar{h}_k^c. \end{aligned}$$

Finally,

$$[H^d(\bar{\gamma})]_i = \bar{\gamma}_i = \bar{h}_i^d$$

and

$$[H^c(\bar{\gamma})]_{i+1} = \bar{\gamma}_{i+1} = \bar{h}_{i+1}^c,$$

which concludes the proof. \square

It was remarked in Section 3.3.1 that if $\gamma^r \in \mathcal{P}_\kappa^r$ saturates (3.35), then $H(\gamma) \in \mathcal{H}_0^{cd}$. But saturating (3.35) is the same as belonging to \mathcal{F}_0^t . So H^{cd} maps vectors in \mathcal{F}_0^t to \mathcal{H}_0^{cd} . This fact and Proposition 3.3 imply that there is a 1-to-1 relationship between the integral elements of \mathcal{F}_0^t and the subset S of \mathcal{H}_0^{cd} that are pre-images, by H^{cd} , of $\tilde{\gamma}$ such that $\tilde{\gamma}^r \in \mathcal{F}_0^t$. Let circ^j be a 0, ± 1 elementary circulation associated with the j -th cycle of the

network for $n = 2i + 1$, for $j = 1, \dots, i - 1$. Let $\hat{h}^{cd} \in \mathcal{H}_0^{cd}$ be the nonnegative integral solution to the network flow problem that satisfies the complementarity condition (3.28). Then \mathcal{H}_0^{cd} has the parametric description

$$\mathcal{H}_0^{cd} = \{h^{cd} = \hat{h}^{cd} + \sum_{j=1}^{i-1} \alpha_j \text{ circ}^j \mid h^{cd} \geq 0, \alpha \in \mathbb{Z}^{i-1}\}.$$

Let $\gamma^* = \Gamma(\hat{h}^{cd})$. Since $[\Gamma]^r$ is a linear map,³ the face \mathcal{F}_0^r will be contained in the set

$$\left\{ \gamma^{*r} + \sum_{j=1}^{i-1} \alpha_j [\Gamma(\text{circ}^j)]^r \mid \alpha \in \mathbb{Z}^{i-1} \right\}.$$

Thus we can use the images of the $0, \pm 1$ elementary circulations to generate the elements of \mathcal{P}_0^r , as illustrated in the next example.

Recall the $n = 7$ numerical instance defined in Figure 3.18. The solution $\hat{h}^{cd} = (0, 5, 3, 8, 5, 5, 5, 0, 3, 0, 2, 2)$ to the network-flow problem, defined therein, for $\kappa = 0$, satisfies (3.28). The $0, \pm 1$ elementary circulations are chosen as

$$\text{circ}^1 = (0, 0, 1, -1, 0, 0, 0, -1, 1, 0, 0)$$

$$\text{circ}^2 = (0, 0, 0, 0, 1, -1, -1, 1, 0, 0, 0)$$

corresponding to cycles 1 and 2 depicted in Figure 3.18. The componentwise maximum element of \mathcal{P}_0 is $\gamma^* = (1, 2, 3, 5, 5, 3, 2, 1)$. Thus, Proposition 3.5 implies the polytope \mathcal{P}_κ^r is given by the inequalities

$$\begin{cases} \gamma_1 & \leqslant 2 \\ \gamma_1 - \gamma_2 & \geqslant -1 \\ \gamma_1 - \gamma_2 + \gamma_3 & \leqslant 4 \\ \gamma_1 & \geqslant \kappa \\ \gamma_1, \gamma_2, \gamma_3 & \geqslant 0. \end{cases}$$

The images of the elementary circulations by Γ produce the vectors:

$$t^1 = [\Gamma(\text{circ}^1)]^r = \begin{bmatrix} -1 \\ -1 \\ 0 \end{bmatrix} \quad \text{and} \quad [\Gamma(\text{circ}^2)]^r = \begin{bmatrix} 0 \\ -1 \\ -1 \end{bmatrix}.$$

The busy picture at the top of Figure 3.20 depicts \mathcal{P}_0^r for the pre-assigned data listed in Figure 3.18. The edges of this polytope are delineated. All of its integral points are

³Notice $\Gamma(h^{cd}) = (1, 0, \dots, 0, 1) + (0, [\Gamma(h^{cd})]_1, \dots, [\Gamma(h^{cd})]_{n-1}, 0)$, where the second term is a linear map.

indicated by gray bullets. The face \mathcal{F}_0^t is shaded in blue and the face \mathcal{F}_0^0 , the projection of \mathcal{F}_0^t onto the plane $\gamma_3 = 0$, is in red (it is a see through polytope!). A tridimensional integral frame is sketched in dashed gray to help locate the integral points. The extreme point $\vec{\gamma}^r = (2, 3, 5)$ is at the top right corner of \mathcal{F}_0^t . Several possible transitions between the integral points of \mathcal{F}_0^t are indicated. Thus, for instance $(1, 2, 5) = \vec{\gamma} + t^1$. This means that

$$(1, 1, 2, 5, 5, 2, 1, 1) = \Gamma(\vec{h}^{cd} + \text{circ}^1) = \Gamma(0, 5, 4, 7, 5, 5, 0, 2, 1, 2, 2).$$

Similarly, we have that $(2, 2, 4) = \vec{\gamma} + t^2$.

As multiples of circ^1 and circ^2 are added to \vec{h}^{cd} to generate points in \mathcal{H}_0^{cd} , the images of such points by Γ will produce points on the plane containing the blue face \mathcal{F}_0^t . Several points will belong to \mathcal{F}_0^t , but not all. As mentioned on page 111, there are 24 integral solutions in \mathcal{H}_0^{cd} , the product of the four possible values of the flow through cycle 1 and 6 possible values through cycle 2. At the bottom of Figure 3.20, we replicate the polytope, showing the images by Γ of all the integral points in \mathcal{H}_0^{cd} . Although they all belong to the plane that contains \mathcal{F}_0^t , 15 are outside the shaded blue area, and do not belong to \mathcal{F}_0^t .

As mentioned, the polytopes \mathcal{P}_κ^r , for integral κ satisfying $0 \leq \kappa \leq \min\{h_1 - (h_0 - 1), h_{n-1} - (h_n - 1)\}$, may be obtained from \mathcal{P}_0^r by finding its intersection with the set $\{\gamma^r \mid \gamma_1 \geq \kappa\}$. The polytopes \mathcal{P}_0^r , \mathcal{P}_1^r and \mathcal{P}_2^r corresponding to the pre-assigned data given in Figure 3.18 are shown in Figure 3.21. The first two have dimension 3, but the third has no volume, it is two dimensional, the faces \mathcal{F}_2^t and \mathcal{F}_2^0 are one dimensional line segments.

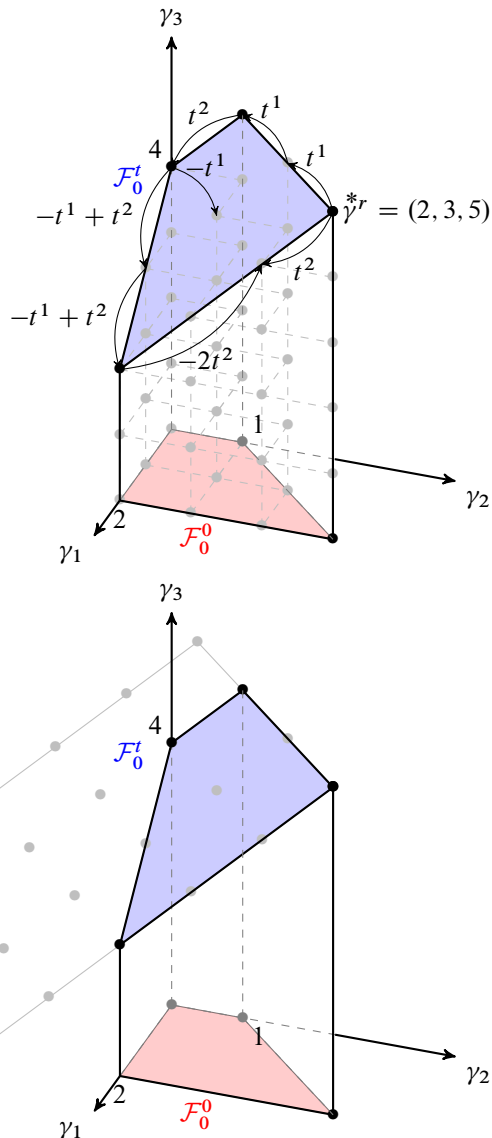
Case $n = 2i \equiv 0 \pmod{4}$

Suppose $n = 2i$, where $i \geq 2$ is even. The approach is similar to the one used in the odd case. We employ the duality conditions to eliminate $\gamma_{i+1}, \dots, \gamma_{2i-1}$, the boundary conditions to eliminate γ_0 and γ_{2i} , and the first equation in (3.24) to eliminate γ_i from the system of inequalities that defines \mathcal{P}_κ . As before, the resulting system of inequalities in $(\gamma_1, \dots, \gamma_{i-1})$ defines a polytope \mathcal{P}_κ^r whose elements are in an 1-to-1 relationship with the elements of \mathcal{P}_κ . Details of the deduction of (3.50)–(3.57) are provided in Bertolim, Mello, and de Rezende (2005b).

The middle Betti number is obtained from the first equality in (3.24) and the duality conditions:

$$\gamma_i = \sum_{j=0}^{2i} (-1)^j h_j - 2 \sum_{j=0}^{i-1} (-1)^j \gamma_j. \quad (3.49)$$

Substituting the above expression for γ_i in the Morse inequalities (3.24) and using boundary and duality conditions, they are reduced to the system below.

Figure 3.20: Morse reduced polytope \mathcal{P}_0^r for pre-assigned index data given in Figure 3.18.

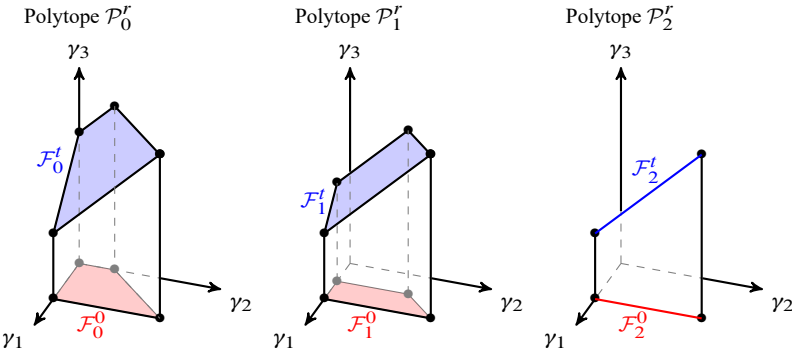


Figure 3.21: Morse reduced polytopes for pre-assigned index data given in Figure 3.18, for $\kappa = 0, 1$ and 2 .

$$\left\{ \begin{array}{l} 0 \leq h_0 - 1 \\ 0 \leq h_{2i} - 1 \end{array} \right. \quad (3.50)$$

$$0 \leq h_{2i} - 1 \quad (3.51)$$

$$\sum_{j=1}^{i-1} (-1)^j \gamma_j \leq -1 + \frac{1}{2} \sum_{j=0}^{2i} (-1)^j h_j \quad (3.52)$$

$$\left\{ \begin{array}{l} \sum_{j=1}^{i-1} (-1)^j \gamma_j \geq -1 + \max \left\{ \sum_{j=i+1}^{2i} (-1)^j h_j, \sum_{j=0}^{i-1} (-1)^j h_j \right\} \\ \sum_{j=1}^{2i-k-1} (-1)^{j+k} \gamma_j \geq -(-1)^k + \sum_{j=k+1}^{2i} (-1)^{j+k} h_j, \quad \text{for } i \leq k \leq 2i-2 \\ \sum_{j=1}^k (-1)^{j+k} \gamma_j \leq -(-1)^k + \sum_{j=0}^k (-1)^{j+k} h_j, \quad \text{for } 1 \leq k \leq i-2 \\ \gamma_1 \geq \kappa \\ \gamma^r \geq 0. \end{array} \right. \quad (3.53)$$

$$\sum_{j=1}^{2i-k-1} (-1)^{j+k} \gamma_j \geq -(-1)^k + \sum_{j=k+1}^{2i} (-1)^{j+k} h_j, \quad \text{for } i \leq k \leq 2i-2 \quad (3.54)$$

$$\sum_{j=1}^k (-1)^{j+k} \gamma_j \leq -(-1)^k + \sum_{j=0}^k (-1)^{j+k} h_j, \quad \text{for } 1 \leq k \leq i-2 \quad (3.55)$$

$$\gamma_1 \geq \kappa \quad (3.56)$$

$$\gamma^r \geq 0. \quad (3.57)$$

Restrictions (3.50)–(3.51) refer only to the pre-assigned data. The polytope \mathcal{P}_κ^r defined by (3.52)–(3.57). Notice that the right-hand-side in (3.52) will not be integral if $\sum_{j=0}^{2i} (-1)^j h_j$ is odd, or equivalently, if (3.23) doesn't hold. Indeed, one can construct examples that show this may lead to nonintegral extreme points in \mathcal{P}_κ^r . One could, in this case, replace the fraction by its floor (the biggest integer less than or equal the fraction) and the resulting set of inequalities would define the convex hull of the extreme points of the

polytope given by (3.52)–(3.52). The following results would be valid without additional hypotheses with the fraction in (3.52) replaced by its floor.

From now on, we assume (3.23) is satisfied. The case $\sum_{j=0}^{2i} (-1)^j h_j \equiv 1 \pmod{2}$ is addressed in Section 3.3.3. The following proposition is from Bertolim, Mello, and de Rezende (2005a). It plays the role Proposition 3.1 played for the odd case.

Proposition 3.4. *The polytope \mathcal{P}_κ^r defined by (3.52)–(3.57) has integral vertices and each (integral) γ^r in the polytope corresponds to an (integral) nonnegative h^{cd} satisfying (3.26). Each vertex of \mathcal{P}_κ^r belongs to one of three faces:*

$$\begin{aligned}\mathcal{F}_\kappa^t &= \left\{ \gamma^r \in \mathcal{P}_\kappa^r \mid \sum_{j=1}^{i-1} (-1)^j \gamma_j = -1 + \max \left\{ \sum_{j=i+1}^{2i} (-1)^j h_j, \sum_{j=0}^{i-1} (-1)^j h_j \right\} \right\} \\ \mathcal{F}_\kappa^b &= \left\{ \gamma^r \in \mathcal{P}_\kappa^r \mid \sum_{j=1}^{i-1} (-1)^j \gamma_j = -1 + \frac{1}{2} \sum_{j=0}^{2i} (-1)^j h_j \right\} \\ \mathcal{F}_\kappa^0 &= \{ \gamma^r \in \mathcal{P}_0^r \mid \gamma_{i-1} = 0 \}.\end{aligned}$$

Proposition 3.5. *Suppose the h_0^{cd} -system (3.26) admits nonnegative solutions. Let h^{cd} be the nonnegative integral solution thereto that satisfies the complementarity conditions (3.28). Let $\hat{\gamma}^* = \Gamma(h^{cd})$ be the vector constructed from h^{cd} using (3.36). Then $\hat{\gamma}^* \in \mathcal{F}_0^t$ and the of inequalities defining \mathcal{P}_0^r may be rewritten as*

$$(-1)^k \sum_{j=1}^k (-1)^j \gamma_j \leq -(-1)^k + (-1)^k \sum_{j=0}^k (-1)^j \hat{\gamma}_j^*, \quad \text{for } 1 \leq k \leq i-1 \quad (3.58)$$

$$\sum_{j=1}^{i-1} (-1)^j \gamma_j \leq -1 + \frac{1}{2} \sum_{j=0}^{2i} (-1)^j h_j \quad (3.59)$$

$$\gamma^r \geq 0. \quad (3.60)$$

Furthermore, $\hat{\gamma}^*$ is the maximum vector of \mathcal{P}_κ^r , componentwise.

In the odd n case, it was possible to show that the map Γ defined in (3.27) was such that $\Gamma(\mathcal{H}_0^{cd}) \supset \mathcal{P}_0 \cap \{\gamma \mid \gamma \text{ saturates (3.35)}\}$, that is, every point on the face $\{\gamma \in \mathcal{P}_0 \mid \sum_{j=0}^i (-1)^j \gamma_j = \sum_{j=0}^i (-1)^j h_j\}$ is reached by the map. When n is even, the result is different, one can show that, for Γ defined in (3.36), $\Gamma(\mathcal{H}_0^{cd}) \supset \mathcal{P}_0$. The following proposition goes further, establishing a 1-to-1 relationship between the elements of \mathcal{P}_0^r and a subset of \mathcal{H}_0^{cd} .

Proposition 3.6. *Let $\bar{h}^{cd} \in \mathcal{H}_0^{cd}$ be such that $\bar{\gamma} = \Gamma(\bar{h}^{cd}) \in \mathcal{P}_0$. Then $H^{cd}(\bar{\gamma}) = \bar{h}^{cd}$.*

Proof. It suffices to show $[H^c(\bar{\gamma})]_j = \bar{h}_j^c$ and $[H^d(\bar{\gamma})]_j = \bar{h}_j^d$ for $j = 1, \dots, 2i - 1$, since $B[\bar{\gamma}] = \bar{\gamma}_i = \bar{\beta}^i$.

Let $k = i$ in (3.37). Recall that, since $n = 2i \equiv 0 \pmod{4}$, i is even.

$$\begin{aligned}
[H^d(\bar{\gamma})]_i &= \sum_{j=0}^i (-1)^{j+i} (h_j - \bar{\gamma}) \\
&= h_0 - \bar{\gamma}_0 + \sum_{j=1}^{i-1} (-1)^j (h_j - (\bar{h}_j^d - \bar{h}_{j+1}^c)) + (h_i - \bar{\gamma}_i) \\
&= h_0 - 1 + \sum_{j=1}^{i-1} (-1)^j h_j - \sum_{j=1}^{i-1} (-1)^j \bar{h}_j^d + \sum_{j=1}^{i-1} (-1)^j \bar{h}_{j+1}^c + h_i - \bar{\beta}^i \\
&= \sum_{j=1}^{i-1} (-1)^j h_j - \sum_{j=1}^{i-1} (-1)^j \bar{h}_j^d - \sum_{j=0}^{i-1} (-1)^{j+1} \bar{h}_{j+1}^c + \bar{h}_i^c + \bar{h}_i^d \\
&= \sum_{j=1}^{i-1} (-1)^j h_j - \sum_{j=1}^{i-1} (-1)^j (\bar{h}_j^d + \bar{h}_j^c) - \bar{h}_i^c + \bar{h}_i^c + \bar{h}_i^d \\
&= \bar{h}_i^d.
\end{aligned}$$

Suppose $[H^d(\bar{\gamma})]_\ell = \bar{h}_\ell^d$ for $i \leq \ell \leq k - 1$.

$$\begin{aligned}
[H^d(\bar{\gamma})]_{k-1} + [H^d(\bar{\gamma})]_k &= (-1)^{2k} (h_k - \bar{\gamma}_k) \\
&= h_k - (-\bar{h}_{k-1}^d + \bar{h}_k^c) \\
&= \bar{h}_k^d + \bar{h}_{k-1}^d.
\end{aligned}$$

Thus $[H^d(\bar{\gamma})]_k = \bar{h}_k^d$, and using induction, this is true for $i \leq k \leq 2i - 1$.

Let $k = 1$ in (3.38).

$$[H^c(\bar{\gamma})]_1 = h_0 - \bar{\gamma}_0 = h_0 - 1 = \bar{h}_1^c.$$

Suppose $[H^c(\bar{\gamma})]_\ell = \bar{h}_\ell^c$ for $1 \leq \ell \leq k - 1$. Then

$$\begin{aligned}
[H^c(\bar{\gamma})]_{k-1} + [H^c(\bar{\gamma})]_k &= (-1)^{2k-2} (h_{k-1} - \bar{\gamma}_{k-1}) \\
&= h_{k-1} - (\bar{h}_{k-1}^d - \bar{h}_k^c) \\
&= \bar{h}_{k-1}^c + \bar{h}_k^c.
\end{aligned}$$

Therefore, $[H^c(\bar{\gamma})]_k = \bar{h}_k^c$ and this must be true for $1 \leq k \leq i + 1$.

Now let $1 \leq k \leq i - 1$. From (3.39),

$$[H^d(\bar{\gamma})]_k = \bar{\gamma}_k + [H^c(\bar{\gamma})]_{k+1} = (\bar{h}_k^d - \bar{h}_{k+1}^c) + \bar{h}_{k+1}^c = \bar{h}_k^d.$$

Finally, let $i + 1 \leq \ell \leq 2i - 1$. From (3.40),

$$[H^c(\bar{\gamma})]_k = \bar{\gamma}_k + [H^d(\bar{\gamma})]_{k-1} = (-\bar{h}_{k-1}^d + \bar{h}_k^c) + \bar{h}_{k-1}^d = \bar{h}_k^c.$$

This concludes the proof. \square

To illustrate the various properties of \mathcal{P}_κ^r we will use the numerical example introduced in Figure 3.19. It concerns an instance of dimension $n = 2i = 8$, with pre-assigned data $h = (3, 5, 7, 8, 5, 6, 2, 2, 2)$. The solution $\bar{h}^{cd} = (2, 3, 2, 5, 3, 5, 3, 3, 0, 2, 0, 2, 0, 1, 1)$, given in the same figure, satisfies the complementarity condition (3.28). The componentwise maximum of the reduced Morse polytope is $\bar{\gamma}^* = (1, 1, 2, 2, 3, 2, 2, 1, 1)$. The inequalities that define the reduced Morse polytope \mathcal{P}_0^r are

$$\begin{cases} \gamma_1 & \leq 1 \\ \gamma_1 - \gamma_2 & \geq -1 \\ \gamma_1 - \gamma_2 + \gamma_3 & \leq 1 \\ \gamma_1 - \gamma_2 + \gamma_3 & \geq 0 \\ \gamma_1, \gamma_2, \gamma_3 & \geq 0. \end{cases}$$

They may be obtained either by direct application of the formulas in (3.52)–(3.57) or using $\bar{\gamma}^*$ and Proposition 3.5.

The “network” in Figure 3.19 has three elementary circulations, given in the table below, together with the corresponding cycles (or rather, support in the third case) and their reduced images by Γ . The elementary circulation is obtained by passing flow 1 of value 1 along the cycle in the direction the arcs are listed. Backward arcs in the cycles are colored red.

elementary circulation	corresponding cycle	reduced image by Γ
circ ¹	$h_2^c, h_6^d, h_6^c, h_2^d$	$t^1 = (-1, -1, 0)$
circ ²	$h_5^d, h_3^c, h_3^d, h_5^c$	$t^2 = (0, -1, -1)$
circ ³	h_4^c, h_4^d, β^4	$t^3 = (0, 0, -1)$

The polytope \mathcal{P}_0^r and all seven of its facets are depicted in Figure 3.22. Given that $\bar{\gamma}^* \in \mathcal{F}_0^r$, the reduced images of $\bar{h}^{cd} + \alpha_1 \text{circ}^1 + \alpha_2 \text{circ}^2$ by Γ belong to \mathcal{F}_0^r , since they will be obtained from $\bar{\gamma}^*$ by adding the corresponding multiples of t^1 and t^2 . Since the flow along the first and second cycle may vary between 0 and 2, there are nine integer nonnegative $h^{cd} \in \mathcal{H}_0^{cd}$ whose images by Γ will lie on the affine plane defined that contains \mathcal{F}_0^r . Since this face contains only five integral points, four of these images will fall outside the face, as in the n odd case. These images are shown on the left, in Figure 3.23. The flow along the third “cycle” may vary between 0 and 1. Notice that $\bar{\gamma}^* + t^3 \in \mathcal{F}_0^b$. So

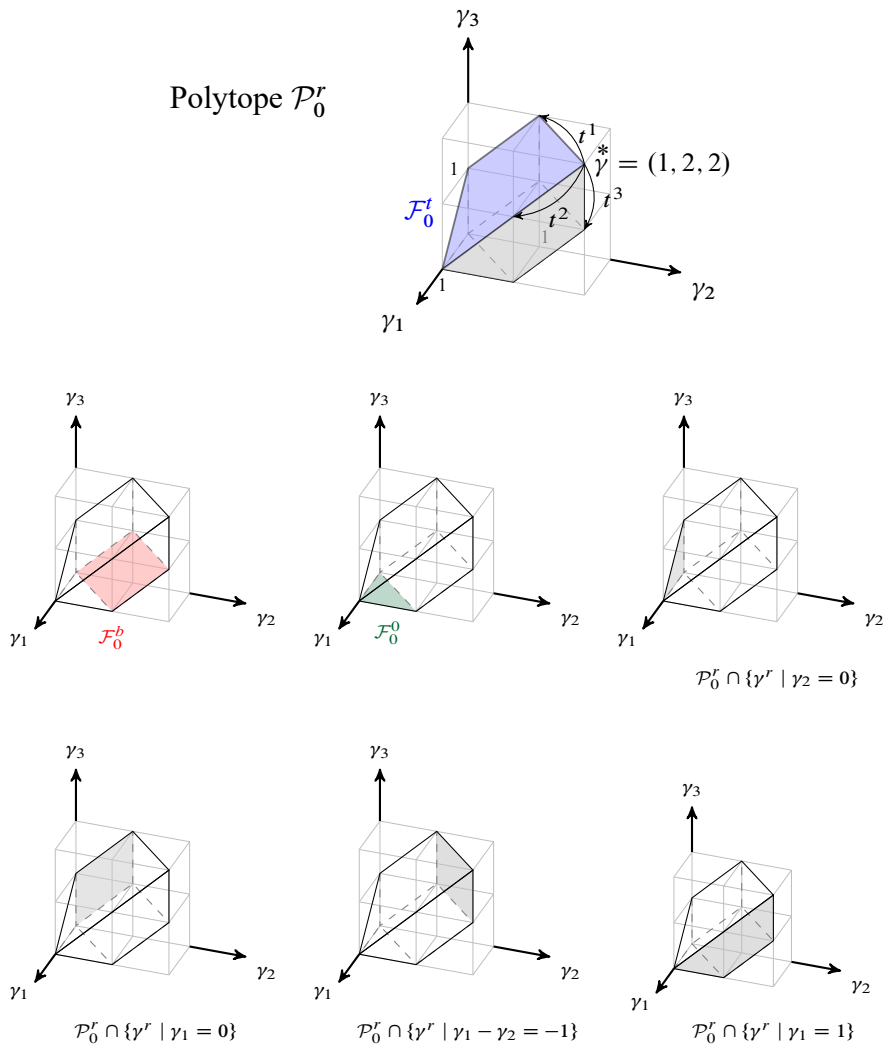


Figure 3.22: Polytope \mathcal{P}_0^r for pre-assigned data given in Figure 3.19.

the remaining 9 integral elements of \mathcal{H}_0^{cd} , namely $\overset{*}{h}^{cd} + \alpha_1 \text{circ}^1 + \alpha_2 \text{circ}^2 + \text{circ}^3$, for $\alpha_1, \alpha_2 \in \{0, 1, 2\}$, will be mapped by Γ to the affine plane containing \mathcal{F}_0^b . These are depicted on the left of Figure 3.23. Since this face contains only four integral points, five of these images will fall outside the face. Notice that the face $\mathcal{P}_0^r \cap \{\gamma^r \mid \gamma_1 = 1\}$, at the bottom right of Figure 3.22, coincides with \mathcal{P}_1^t .

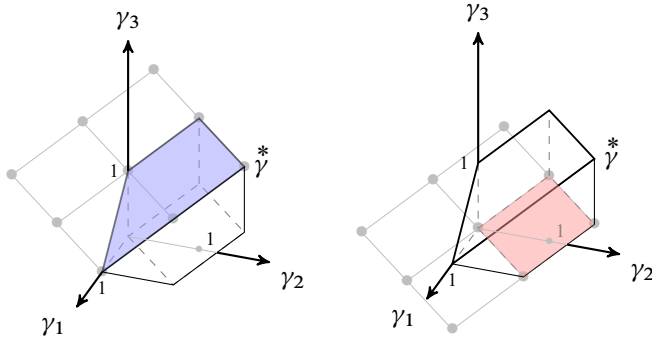


Figure 3.23: Images by Γ^r of all nonnegative integral elements of \mathcal{H}_0^{cd} , for pre-assigned data in Figure 3.19.

Only minor adjustments are needed to extend these results to the case $n = 2i \equiv 2 \pmod 4$.

3.3.3 When $\sum_{j=0}^n (-1)^j h_j$ is odd

When $n = 2i + 1$, $\sum_{j=0}^i (-1)^j (h_{n-j} - h_j) = -\sum_{j=0}^n (-1)^j h_j$, so (3.22) implies that this alternate sum be even, so there is no point in investigating the possibility of this alternate sum being odd.

When $n = 2i$, as observed on page 116, the parity of the alternate sum $\sum_{j=0}^n (-1)^j h_j$ coincides with the parity of $h_i - \sum_{k=0}^{i-1} (-1)^k (h_{n-k} - h_k)$. Therefore, if $n = 2i \equiv 2 \pmod 4$, constraint (3.23) will enforce the alternate sum to be even.

No such condition, however, is imposed when $n = 2i \equiv 0 \pmod 4$. We will see that, when this condition doesn't hold, the polytope \mathcal{H}_κ^{cd} , if nonempty, will have nonintegral extreme points, as already pointed out for the general case (B_j 's not all zero) on page 107 in the analogous situation (the parity condition of (2.50) not holding).

The existence of nonintegral extreme points of \mathcal{H}_κ^{cd} , when $n = 2i \equiv 0 \pmod 4$ and $\sum_{j=0}^n (-1)^j h_j$ is odd, follows from two facts. First, the h_κ^{cd} -system can be divided into i independent subproblems, so that a given h^{cd} is an extreme point of \mathcal{H}_κ^{cd} if and only if its restrictions to the variables of the j -th subproblem is an extreme point thereof. Second, whereas the integrality of the extreme points of the first $i-1$ subproblems is a consequence

of their nature (network flow problems) and the integrality of the data, the integrality of the extreme points of the last subproblem will hinge on the alternate sum $\sum_{j=0}^n (-1)^j h_j$ being even.

The last subproblem is small enough that we can solve it in detail. It is given by the following linear system.

$$\begin{cases} h_i^c + \beta^i + h_i^d = h_i \\ h_i^c - h_i^d = b_{i-1,2} \\ h_i^c, \beta^i, h_i^d \geq 0, \end{cases} \quad (3.61)$$

where

$$b_{i-1,2} = h_n - h_0 + \sum_{k=1}^{i-1} (-1)^k (h_{n-k} - h_k) = \sum_{k=0}^{i-1} (-1)^k (h_{n-k} - h_k). \quad (3.62)$$

This system will have nonnegative solutions if and only if $h_i \geq b_{i-1,2} \geq -h_i$, so we assume this condition is satisfied.

The variable β^i may be removed from the system using the first equation. So there is a 1-to-1 correspondence between solutions to (3.61) and the solutions to

$$\begin{cases} h_i^c + h_i^d \leq h_i \\ h_i^c - h_i^d = b_{i-1,2} \\ h_i^c, h_i^d \geq 0, \end{cases}$$

which, on the other hand, is equivalent to

$$\begin{cases} h_i^c \leq \frac{h_i + b_{i-1,2}}{2} \\ h_i^c - h_i^d = b_{i-1,2} \\ h_i^c, h_i^d \geq 0. \end{cases} \quad (3.63)$$

The extreme points (h_i^c, h_i^d) of the polytope defined by (3.63) are

If $b_{i-1,2} \geq 0$: $((h_i + b_{i-1,2})/2, (h_i - b_{i-1,2})/2)$ and $(b_{i-1,2}, 0)$.

If $b_{i-1,2} < 0$: $((h_i + b_{i-1,2})/2, (h_i - b_{i-1,2})/2)$ and $(0, -b_{i-1,2})$.

The corresponding extreme point solutions (h_i^c, β^i, h_i^d) to (3.61) are

If $b_{i-1,2} \geq 0$: $((h_i + b_{i-1,2})/2, 0, (h_i - b_{i-1,2})/2)$ and $(b_{i-1,2}, h_i - b_{i-1,2}, 0)$.

If $b_{i-1,2} < 0$: $((h_i + b_{i-1,2})/2, 0, (h_i - b_{i-1,2})/2)$ and $(0, h_i + b_{i-1,2}, -b_{i-1,2})$.

So, if $\sum_{j=0}^n (-1)^j h_j$ is odd, then $h_i - b_{i-1,2}$ will be odd and, although the existence of integral solutions is assured by the fact that one of the extreme points is integral, the polytope itself will not be integral, because one of its extreme points is not integral. Therefore, in this case, \mathcal{H}_κ^{cd} will not coincide with the convex hull of its integral points.

Clearly, the set of integral solution to (3.63) is contained in the set of solutions to

$$\begin{cases} h_i^c \leq \left\lfloor \frac{h_i + b_{i-1,2}}{2} \right\rfloor \\ h_i^c - h_i^d = b_{i-1,2} \\ h_i^c, h_i^d \geq 0. \end{cases} \quad (3.64)$$

But the polytope defined by (3.64) is integral, since its coefficient matrix is totally unimodular and its right-hand-side is integral.

Now notice that if $\sum_{j=0}^n (-1)^j h_j$ is odd, then h_i must be positive. Otherwise, if $h_i = 0$, we would forcibly have $h_i^c = h_i^d = \beta^i = 0$, and the h_κ^{cd} -system would reduce to a network-flow problem of dimension $n = 2i - 1$, with data $h' = (h_0, \dots, h_{i-1}, h_{i+1}, \dots, h_n)$. But then, constraint (3.22) requires that

$$\begin{aligned} 0 &= \sum_{j=0}^{2i-1} (-1)^j h'_j \\ &= \sum_{j=0}^{i-1} (-1)^j h_j + \sum_{j=i+1}^{2i} (-1)^{j+1} h_j \pm \sum_{j=i+1}^{2i} (-1)^{j+1} h_j \\ &= \sum_{j=0}^{i-1} (-1)^j h_j + \sum_{j=i+1}^{2i} (-1)^j h_j + 2 \sum_{j=i+1}^{2i} (-1)^{j+1} h_j \\ &= \sum_{j=0}^{2i} (-1)^j h_j + 2 \sum_{j=i+1}^{2i} (-1)^{j+1} h_j, \end{aligned}$$

which would contradict the hypothesis that $\sum_{j=0}^{2i} (-1)^j h_j$ is odd. Therefore, we must have $h_i > 0$.

So the integral solutions to the h_κ^{cd} -system for pre-assigned data $(h_0, \dots, h_i, \dots, h_{2i})$, with $\sum_{j=0}^{2i} (-1)^j h_j \equiv 1 \pmod{2}$, bear a 1-to-1 relationship with the solutions to the h_κ^{cd} -system for pre-assigned data h' , where $h'_j = h_j$, for $0 \leq j \leq 2i$, $j \neq i$, and $h'_i = h_i - 1$. Let \tilde{h}^{cd} is a solution to the h_κ^{cd} -system for the pre-assigned data h' . Let \tilde{h}^{cd} be a vector that coincides with \tilde{h}^{cd} except for the beta component, which satisfy $\tilde{\beta}^i = \beta^i + 1$. Then \tilde{h}^{cd} is a solution to the system for the pre-assigned data h . The following example illustrates this relationship.

Consider the data $h = (3, 4, 7, 8, h_4, 2, 2, 2)$. This corresponds to the example given in Figure 3.19, only now we are letting h_4 be a parameter, whereas the other components

of h are fixed. Then the Poincaré–Hopf inequality for closed manifolds

$$h_4 \geq \sum_{j=0}^3 (-1)^j (h_{8-j} - h_j) \geq -h_4$$

implies $h_4 \geq 3$. The analysis in Section 3.2 implies the solutions to the corresponding h_κ^{cd} -system are

$$\begin{aligned} h^{cd} = & (2, 3, 2, 5, 3, 5, 3, h_4 - 3, 0, 2, 0, 2, 0, 1, 1) \\ & + \alpha_1(0, 0, 1, -1, 0, 0, 0, 0, 0, 0, -1, 1, 0, 0) \\ & + \alpha_2(0, 0, 0, 0, 1, -1, 0, 0, 0, -1, 1, 0, 0, 0, 0) \\ & + \alpha_3(0, 0, 0, 0, 0, 0, 1, -2, 1, 0, 0, 0, 0, 0, 0), \end{aligned}$$

where

$$\begin{aligned} 0 \leq \alpha_1 \leq 2 \\ 0 \leq \alpha_2 \leq 2 \\ 0 \leq \alpha_3 \leq \left\lfloor \frac{h_4 - 3}{2} \right\rfloor. \end{aligned}$$

Thus the number of nonnegative integral solutions will be $3 \cdot 3 \cdot 1 = 9$ for $h_4 = 3$ and 4; $3 \cdot 3 \cdot 2 = 18$ for $h_4 = 5$ and 6; $3 \cdot 3 \cdot 3 = 27$ for $h_4 = 7$ and 8, etc. For each pair of consecutive odd-even values of h_4 , the number of nonnegative integral solutions is the same, the solutions themselves will differ only in the β^i component.

Summarizing, suppose $n = 2i \equiv 0 \pmod{4}$ and the parity condition in (3.23) is **not** satisfied by the pre-assigned data \bar{h} . Let \tilde{h} differ from \bar{h} only in the i -th component, which satisfies $\tilde{h}_i = \bar{h} - 1$. Then the polytope $\bar{\mathcal{H}}_\kappa^{cd}$ corresponding to the h_κ^{cd} -system for the pre-assigned data \bar{h} will not be integral. But the convex hull of its integral elements will bear a 1-to-1 relationship with the integral elements of $\tilde{\mathcal{H}}^{cd}$, and this last one is an integral polytope. In fact, the convex hull of the integral elements of $\bar{\mathcal{H}}_\kappa^{cd}$ is simply a translation of the vectors in the polytope $\tilde{\mathcal{H}}^{cd}$, and the translation vector is the unit vector whose support corresponds to the variable β^i .

We will see that a completely analogous phenomenon occurs with the Morse polytope, when $n = 2i \equiv 0 \pmod{4}$. Recall inequality (3.52), obtained by using boundary and duality conditions, and eliminating γ_i by means of the first equation in the Morse inequalities (3.24), reproduced below for convenience.

$$\sum_{j=1}^{i-1} (-1)^j \gamma_j \leq -1 + \frac{1}{2} \sum_{j=0}^{2i} (-1)^j h_j.$$

The reduced Morse polytope is defined by inequalities (3.52)–(3.57). The coefficient matrix of this system of inequalities is totally unimodular. Thus if the right-hand-side were

integral, all extreme points of the reduced Morse polytope \mathcal{P}_κ^r would be integral. In Section 3.3.2, the sum $\sum_{j=0}^{2i} (-1)^j h_j$ was assumed even to ensure the integrality of the right-hand-side. Suppose this is not true. Then the integral γ^r 's that satisfy (3.52)–(3.57) must also satisfy

$$\sum_{j=1}^{i-1} (-1)^j \gamma_j \leq -1 + \left\lfloor \frac{1}{2} \sum_{j=0}^{2i} (-1)^j h_j \right\rfloor,$$

since the left-hand-side of the inequality has to force an integral value. But then, if we replace (3.52) with the inequality above, we obtain a system with totally unimodular coefficient matrix and integral right-hand-side, which defines an integral polytope. Since this integral polytope contains all the integral elements of \mathcal{P}_κ^r and is also contained in \mathcal{P}_κ^r , it must be the convex hull of said elements.

Applying the floor operation has the same effect as decreasing h_i by 1. Thus the convex hull of the integral elements of \mathcal{P}_κ^r coincides with the reduced Morse polytope $\mathcal{P}_\kappa^{r'}$ corresponding to the data h' , a pre-assigned data that differs from h only in the i -th component, which satisfies $h'_i = h_i - 1$. But of course, when calculating the whole gamma vector from some reduced $\gamma^{r'}$, one would need to evaluate γ_i from the expression given in (3.49). So the same $\gamma^{r'} \in \mathcal{P}^r$ can generate a Betti number vector satisfying the Morse inequalities for h or for h' , and these two vectors will differ only in the γ_i component.

Consider again the data $h = (3, 4, 7, 8, h_4, 2, 2, 2)$. The polytope in Figure 3.22 was built for $h_4 = 5$. This polytope is also precisely the convex hull of the integral points of the polytope for $h_4 = 6$. Nevertheless, the vector $\gamma^r = (1, 2, 1)$ in this polytope expands to $\gamma = (1, 1, 2, 1, 0, 1, 2, 1, 1)$, if $h_4 = 5$, and to $\gamma = (1, 1, 2, 1, 1, 1, 2, 1, 1)$, if $h_4 = 6$.

3.4 Realizability of the Morse polytope

We refer the reader to Section 4.3 where a *null-trivial-dual-labelling*, in short, an *ntd-labelling*, which is the pairing up of all vertices (except two, one h_0 and one h_n vertex) in an admissible graph is defined. Recall that an admissible graph is one that satisfies the Poincaré–Hopf inequalities for closed manifolds. Do all admissible graphs of Morse type admit an *ntd*-labelling? Are the admissible Morse type graphs that admit an *ntd*-labelling realizable?

In this section, we will answer these questions. We shall present results obtained in Cruz, Mello, and de Rezende (2005), namely that, for fixed index data (h_0, h_1, \dots, h_n) , in general, for each integral point $(\gamma_0, \dots, \gamma_n)$ in the corresponding Morse polytope, one can associate an abstract Lyapunov graph $L(h_0, \dots, h_n, \kappa)$ with *ntd*-labelling and realize a corresponding flow on M^n , where the Betti numbers of M^n satisfy $\beta_j(M^n) = \beta_{n-j}(M^n) = \gamma_j$, for all $0 < j \leq \lfloor n/2 \rfloor$.

3.4.1 h^{cd} vectors and ntd -labellings

In this section we establish the existence of an ntd -labelling for a given abstract Lyapunov graph $L(h_0, \dots, h_n, \kappa)$ of Morse type associated with an h^{cd} vector satisfying (3.25), (resp., (3.26)) if $n = 2i + 1$ (resp., $n = 2i$). Note that all ntd -labels refer to pairs of singularities, except possibly the beta label, which may assume the specific labelling of β -i type. In the sequence we will deal with the number and types of pairings associated with the ntd -labellings.

Henceforth, we consider fixed data $(h_0, \dots, h_n, \kappa)$ that satisfy the Poincaré–Hopf inequalities (3.19)–(3.23), and fixed h^{cd} that satisfies the appropriate h^{cd} -system, (3.25) or (3.26), for this fixed data. Let

d_κ = number of κ -dual pairings,

d_j = number of dual pairings, for $j = 1, \dots, n - 2$,

η_j = number of null pairings, for $j = 1, \dots, n - 2$,

t_1 = number of trivial pairings of first type,

t_2 = number of trivial pairings of second type,

b = number of labels of type beta.

Since h^{cd} is fixed, the quantities of the various types j -c's and j -d's, are given, for instance h_j^d is the amount of $h_j = 1$ of type j -d and h_j^c is the amount of $h_j = 1$ of type $(j-1)$ -c. Since these quantities may be used in different types of pairings, we must define restrictions on the number of pairings so as not to over or underuse the available quantities. It can be shown that these restrictions form a linear system, as follows.

$$t_1 = h_0 - 1 \quad (3.65)$$

$$t_2 = h_n - 1 \quad (3.66)$$

$$d_\kappa = \kappa \quad (3.67)$$

$$\begin{cases} d_j + \eta_j = h_j^d, & \text{for } j = 1, \dots, n - 2 \\ d_{n-j-1} + \eta_j = h_{j+1}^c, & \text{for } j = 1, \dots, n - 2 \end{cases} \quad (3.68)$$

$$b = \beta^i, \quad \text{if } n = 2i \equiv 0 \pmod{4} \quad (3.69)$$

$$\eta, d \geq 0. \quad (3.70)$$

When $n = 2i + 1$, the equations (3.68) may be transformed into i independent linear systems, which can be cast into network flow problem format, as follows

$$\begin{cases} d_j + \eta_j = h_j^d, \\ -d_{n-j-1} - \eta_j = -h_{j+1}^c, \\ d_{n-j-1} + \eta_{n-j-1} = h_{n-j-1}^d, \\ -d_j - \eta_{n-j-1} = -h_{n-j}^c, \end{cases} \quad \text{for } j = 1, \dots, i - 1, \quad (3.71)$$

and,

$$\begin{cases} d_i &+ \eta_i = h_i^d, \\ -d_i &- \eta_i = -h_{i+1}^c, \end{cases} \quad \text{for } j = i. \quad (3.72)$$

If $n = 2i$, the same operation produces only the $i - 1$ linear systems (3.71).

Figure 3.24 shows the three independent network-flow problems arising from the linear system, for $n = 7$.

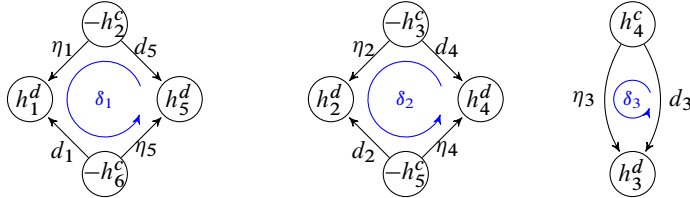


Figure 3.24: Network flow problems arising from ntd -labelling equations, for $n = 7$.

The lozenge network was already analysed and its general solution, substituting the appropriate variables in this case, is given below in (3.73)–(3.74), if $n = 2i + 1$, and in (3.73), if $n = 2i$.

$$\begin{aligned} (\eta_j, \eta_{n-j-1}, d_j, d_{n-j-1}) &= (h_{j+1}^c, h_{n-j-1}^d, h_j^d - h_{j+1}^c, 0) \\ &\quad + \delta_j(-1, -1, 1, 1), \quad \text{for } j = 1, \dots, i-1, \end{aligned} \quad (3.73)$$

$$(\eta_i, d_i) = (0, h_i^d) + \delta_i(1, -1), \quad \text{for } j = i, \quad (3.74)$$

where $[h_{j+1}^c - h_j^d]^+ \leq \delta_j \leq \min\{h_{j+1}^c, h_{n-j-1}^d\}$, for $j = 1, \dots, i-1$, and $0 \leq \delta_i \leq h_i^d$.

Therefore, the number of distinct ntd -labellings or pairings that can be assigned to a fixed abstract Lyapunov graph of Morse type described by an h^{cd} vector is simply the number of distinct integral values the various δ_j may assume, giving the totals below.

$$\prod_{j=1}^{i-1} (\min\{h_{j+1}^c, h_{n-j-1}^d\} - [h_{j+1}^c - h_j^d]^+ + 1) \cdot (h_i^d + 1), \quad \text{if } n = 2i + 1, \quad (3.75)$$

and

$$\prod_{j=1}^{i-1} (\min\{h_{j+1}^c, h_{n-j-1}^d\} - [h_{j+1}^c - h_j^d]^+ + 1), \quad \text{if } n = 2i. \quad (3.76)$$

3.4.2 Betti number vectors and ntd-labellings

The mappings between the polytope of solutions to the h_κ^{cd} -system and the Morse polytope will play an important role in the following, where we determine which *ntd*-labellings for a given nonnegative integral h^{cd} solving the h_κ^{cd} -system correspond to a topological realization of a Morse flow on a closed manifold.

Henceforth, we assume that the fixed data $(h_0, \dots, h_n, \kappa)$ satisfies the Poincaré–Hopf inequalities for closed manifolds (3.19)–(3.23).

Case $n = 2i + 1$

In this section we will employ the mapping Γ defined in (3.27) and the mapping H^{cd} defined in (3.29)–(3.34). As pointed out on page 114, given a Betti number $\bar{\gamma} \in \mathcal{P}_\kappa$, there is a host of solutions that can be constructed from $\bar{\gamma}$ by keeping all components fixed except for the two middle ones, which can vary in the range

$$0 \leq \gamma_i = \gamma_{i+1} \leq \sum_{j=0}^i (-1)^{j+i} h_j - \sum_{j=0}^{i-1} (-1)^{j+i} \gamma_j.$$

In the definitions of $\Gamma_i(h^{cd})$ and $\Gamma_{i+1}(h^{cd})$, the upper bound was adopted, resulting in the fact that Γ^r maps h^{cd} to elements in the hyperplane containing the top face of \mathcal{P}_κ^r , \mathcal{F}_κ^t . If we were to let $\Gamma_i(h^{cd}) = h_i^d - h_{i+1}^c = 0 = -h_i^d + h_{i+1}^c = \Gamma_{i+1}(h^{cd})$, the reduced vector Γ^r would belong to the hyperplane supporting \mathcal{F}_κ^0 . Of course, being \mathcal{P}_κ^r convex, if $\gamma^r \in \mathcal{F}_\kappa^t$, then the whole segment between γ^r and its projection onto \mathcal{F}_κ^0 is in \mathcal{P}_κ^r . Thus, in a way, we've associated the whole segment between one vector in \mathcal{F}_κ^t and its projection onto \mathcal{F}_κ^0 with a single h^{cd} solution to (3.25). The establishment of pairings will allow one to associate each integral γ^r on such a segment with a specific set of pairings in a natural way. This is the gist of Theorem 3.2. Later on, Theorem 3.3 tackles the issue of realization, showing that for each γ^r in this segment, exactly one of the several labellings can be realized topologically.

Given a fixed abstract Lyapunov graph of Morse type associated with a solution h^{cd} of the h_κ^{cd} -system, the vectors η , d and t give the null, dual and trivial number of pairs in a *ntd*-labelling assigned thereto. Assume $\gamma = \Gamma(h^{cd})$ belongs to \mathcal{P}_κ . We are interested in determining which *ntd*-labellings for h^{cd} correspond to a topological realization of a Morse flow on a closed $(2i + 1)$ -manifold with Betti number vector equal to γ . As mentioned, $\gamma^r \in \mathcal{F}_\kappa^t$, but the same question is posed for the Betti number vectors corresponding to integral γ^r 's below the top face of the reduced polytope.

Let h^{cd} be such that $\Gamma(h^{cd}) \in \mathcal{P}_\kappa$. Recall that all the integral vectors in the segment between $\gamma^r = \Gamma^r(h^{cd})$ and its projection on \mathcal{F}_κ^0 are associated to h^{cd} . Now the (fixed) h^{cd} vector will, in general, have several *ntd*-labellings that may be assigned thereto.

The function $G(d)$ defined below maps an *ntd*-labelling of a nonnegative integral h^{cd} , such that $\Gamma(h^{cd}) \in \mathcal{P}_\kappa$, to a Betti number vector satisfying (3.24). This mapping spreads

out evenly the ntd -labellings of h^{cd} amongst the integral vectors in the segment from $\Gamma^r(h^{cd})$ and its projection on \mathcal{F}_κ^0 .

Theorem 3.2. *Let h^{cd} be a nonnegative integral solution to the appropriate h_κ^{cd} -system, (3.25) or (3.26), such that $\gamma = \Gamma(h^{cd})$ belongs to the Morse polytope \mathcal{P}_κ . Let (η, d, t) be the null, dual and trivial pairs of an ntd -labelling of h^{cd} . Define the mapping $G(d)$ as follows*

$$G_0(d) = G_n(d) = 1, \quad (3.77)$$

$$G_1(d) = G_{n-1}(d) = d_1 - d_{n-2} + d_\kappa, \quad (3.78)$$

$$G_j(d) = G_{n-j}(d) = d_j - d_{n-j-1}, \text{ for } j = 2, \dots, i-1, \quad (3.79)$$

$$G_i(d) = G_{i+1}(d) = d_i. \quad (3.80)$$

Then $G(d)$ is a Betti number vector and its associated reduced vector lies in the segment between γ^r and its projection onto \mathcal{F}_0 .

Finally, the total number of pairings of h^{cd} is evenly split amongst the integral vectors in this segment.

Theorem 3.3. *Let h^{cd} be a nonnegative integral solution to (3.25), such that $\gamma = \Gamma(h^{cd})$ belongs to the Morse polytope \mathcal{P}_κ . Let $\tilde{\gamma}^r$ be an integral vector in the segment between γ^r and its projection onto \mathcal{F}_κ^0 . Then there is a unique ntd -labelling of h^{cd} that can be realized topologically, that is, that satisfies*

$$\tilde{\gamma}_1 = \tilde{\gamma}_{n-1} = \tilde{d}_1 + \tilde{d}_\kappa, \quad (3.81)$$

$$\tilde{\gamma}_j = \tilde{\gamma}_{n-j} = \tilde{d}_j + \tilde{d}_{n-j}, \text{ for } j = 2, \dots, i-1, \quad (3.82)$$

$$\tilde{\gamma}_i = \tilde{\gamma}_{i+1} = \tilde{d}_i, \quad (3.83)$$

where \tilde{d} is the vector of dual pairings of this unique ntd -labelling.

Furthermore, this is realizable on a generalized tori with γ_k factors of the type $S^k \times S^{n-k}$, for $k = 1, \dots, i$.

Under the correspondence defined in Theorem 3.2, the maximum element of \mathcal{P}_κ^r , $\tilde{\gamma}^r = \Gamma(h^{cd})$, corresponds to the ntd -labelling with (η^*, d^*) given by

$$d_\kappa^* = \kappa,$$

$$(\eta_j^*, \eta_{n-j-1}^*, d_j^*, d_{n-j-1}^*) = (\overset{*}{h^c}_{j+1}, \overset{*}{h^d}_{n-j-1}, \overset{*}{h^d}_j - \overset{*}{h^c}_{j+1}, 0), \text{ for } j = 1, \dots, i-1,$$

$$(\eta_i^*, d_i^*) = (0, \overset{*}{h^d}_i).$$

Thus this ntd -labelling satisfies $\eta_j^* \eta_{n-j-1}^* = 0 = d_{n-j-1}^*$, for $j = 1, \dots, i-1$.

To illustrate these findings, we return to the numerical instance described in Figure 3.18. The relevant data are $n = 2i + 1 = 7$ and $(h_0, \dots, h_7) = (1, 5, 11, 10, 5, 3, 4, 3)$. Thus

$\kappa \in \{0, 1, 2\}$. There are 24 distinct nonnegative integral h^{cd} 's that solve the h_κ^{cd} -system, for each value of κ , described parametrically below with the help of the special solution satisfying the complementarity condition and the elementary circulations.

$$\begin{aligned} h^{cd} = & (\kappa, 5 - \kappa, 3, 8, 5, 5, 5, 0, 3, 0, 2 - \kappa, 2 + \kappa) \\ & + \alpha_1(0, 0, 1, -1, 0, 0, 0, 0, -1, 1, 0, 0) \\ & + \alpha_2(0, 0, 0, 0, 1, -1, -1, 1, 0, 0, 0, 0), \end{aligned}$$

where $\alpha_1 \in \{0, 1, 2, 3\}$ and $\alpha_2 \in \{0, \dots, 5\}$. The corresponding γ^r 's belong to the affine hull of the top face of the reduced Morse polytope, shown Figure 3.20. Of these, 9 belong to \mathcal{F}_κ^t .

The numbers of dual and null pairs associated with a given h^{cd} are given by

$$\begin{aligned} (\eta_1, \eta_5, d_1, d_5) &= (h_2^c, h_5^d, h_1^d - h_2^c, 0) + \delta_1(-1, -1, 1, 1) \\ &= (3 + \alpha_1 - \delta_1, \alpha_1 - \delta_1, 2 - \kappa + \alpha_1 + \delta_1, \delta_1), \end{aligned} \quad \text{where } [\kappa - 2 - \alpha_1]^+ \leq \delta_1 \leq \alpha_1, \quad (3.84)$$

$$\begin{aligned} (\eta_2, \eta_4, d_2, d_4) &= (h_3^c, h_4^d, h_2^d - h_3^c, 0) + \delta_2(-1, -1, 1, 1) \\ &= (5 + \alpha_2 - \delta_2, \alpha_2 - \delta_2, 3 - \alpha_1 - \alpha_2 + \delta_2, \delta_2), \end{aligned} \quad \text{where } [\alpha_1 + \alpha_2 - 3]^+ \leq \delta_2 \leq \alpha_2, \quad (3.85)$$

$$\begin{aligned} (\eta_3, d_3) &= (h_4^c, 0) + \delta_3(-1, 1) \\ &= (5 - \alpha_2 - \delta_3, \delta_3) \text{ for } 0 \leq \delta_3 \leq 5 - \alpha_2. \end{aligned} \quad (3.86)$$

The reduced gamma vector associated with an *ntd*-labelling is

$$\begin{aligned} \gamma_1 &= d_1 - d_5 + \kappa = 2 + \alpha_1 \\ \gamma_2 &= d_2 - d_4 = 3 - \alpha_1 - \alpha_2 \\ \gamma_3 &= d_3 = \delta_3. \end{aligned}$$

Letting $\kappa = 1$, $c_1 = 1 = c_2$, we have $\bar{h}^{cd} = (1, 4, 4, 7, 6, 4, 4, 1, 2, 1, 1, 3)$. Then $d_\kappa = 1$ and $(\eta, d) = (4 - \delta_1, 6 - \delta_2, 4 - \delta_3, 1 - \delta_2, 1 - \delta_1, 2 + \delta_1, 1 + \delta_2, \delta_3, \delta_2, \delta_1)$, where $0 \leq \delta_1 \leq 1$, $0 \leq \delta_2 \leq 1$ and $0 \leq \delta_3 \leq 4$, so this h^{cd} admits 20 distinct *ntd*-labellings. On the other hand, the reduced Betti number vectors associated to the 20 *ntd*-labellings are not necessarily distinct. Applying the formulas in Theorem 3.2 we have that the reduced vector associated to an *ntd*-labelling from this set is given by $\tilde{\gamma} = (\tilde{\gamma}_0, \tilde{\gamma}_1, \dots, \tilde{\gamma}_7) = (1, 1, 1, \delta_3, \delta_3, 1, 1, 1)$ and $\tilde{\gamma}^r = (\tilde{\gamma}_1, \tilde{\gamma}_2, \tilde{\gamma}_2) = (1, 1, \delta_3)$. Thus, if $\delta_3 = 4$, we obtain $\tilde{\gamma}^r = (1, 1, 4) \in \mathcal{F}_1^t$ and if $\delta_3 = 0$ we obtain $\tilde{\gamma}^r = (1, 1, 0) \in \mathcal{F}_1^0$. Notice that $\tilde{\gamma}$ does not depend on δ_1 nor δ_2 . Thus there are $4 = 20/5$ pairings (the number of possible values for δ_1 and δ_2) associated with each of the five integral γ^r 's in the segment between $(1, 1, 0)$ and $(1, 1, 4)$ in \mathcal{P}_1^r . Furthermore, all five γ^r 's are associated with \bar{h}^{cd} .

The solution satisfying the complementarity condition is

$$h^{cd} = (\kappa, 5 - \kappa, 3, 8, 5, 5, 5, 0, 3, 0, 2 - \kappa, 2 + \kappa)$$

$\bar{\gamma}^r$	\bar{h}^{cd}	α_1, α_2	Range of δ_1	Range of δ_2	Range of δ_3	#ntd-labellings assoc. with $\bar{\gamma}^r$	#ntd-labellings assoc. with \bar{h}^{cd}
(2, 3, 5)	(0, 5, 3, 8, 5, 5, 5, 0, 3, 0, 2, 2)	0, 0	{0}	{0}	{0, ..., 5}	1	6
(2, 2, 4)	(0, 5, 3, 8, 6, 4, 4, 1, 3, 0, 2, 2)	0, 1	{0}	{0, 1}	{0, ..., 4}	2	10
(2, 1, 3)	(0, 5, 3, 8, 7, 3, 3, 2, 3, 0, 2, 2)	0, 2	{0}	{0, 1, 2}	{0, 1, 2, 3}	3	12
(2, 0, 2)	(0, 5, 3, 8, 8, 2, 2, 3, 3, 0, 2, 2)	0, 3	{0}	{0, 1, 2, 3}	{0, 1, 2}	4	12
(1, 2, 5)	(0, 5, 4, 7, 5, 5, 5, 0, 2, 1, 2, 2)	1, 0	{0, 1}	{0}	{0, ..., 5}	2	12
(1, 1, 4)	(0, 5, 4, 7, 6, 4, 4, 1, 2, 1, 2, 2)	1, 1	{0, 1}	{0, 1}	{0, ..., 4}	4	20
(1, 0, 3)	(0, 5, 4, 7, 7, 3, 3, 2, 2, 1, 2, 2)	1, 2	{0, 1}	{0, 1, 2}	{0, 1, 2, 3}	6	24
(0, 1, 5)	(0, 5, 5, 6, 5, 5, 5, 0, 1, 2, 2, 2)	2, 0	{0, 1, 2}	{0}	{0, ..., 5}	3	18
(0, 0, 4)	(0, 5, 5, 6, 6, 4, 4, 1, 1, 2, 2, 2)	2, 1	{0, 1, 2}	{0, 1}	{0, ..., 4}	6	30

Table 3.1: Reduced Betti number vectors on \mathcal{F}_κ^t , associated \bar{h}^{cd} and with (η, d) such that $d_i = \bar{h}_i^d$, values of α_1, α_2 , ranges of $\delta_1, \delta_2, \delta_3$, and number of distinct ntd-labellings, supposing $\kappa = 0$.

and the ntd-labelling that corresponds to the maximum Betti number vector has the following numbers of null and dual pairs:

$$\begin{aligned} d_\kappa^* &= \kappa, \\ (\eta_1^*, \eta_5^*, d_1^*, d_5^*) &= (3, 0, 2 - \kappa, 0), \\ (\eta_2^*, \eta_4^*, d_2^*, d_4^*) &= (5, 0, 3, 0), \\ (\eta_3^*, d_3^*) &= (0, 5). \end{aligned}$$

Table 3.1 illustrates the correspondence between γ^r, h^{cd} and ntd-labellings established in Theorems 3.2 and 3.3.

Case $n = 2i$

In this section we use the maps Γ defined in (3.36) and H^{Cd} defined in (3.37)–(3.41). The space where the reduced Morse polytope resides contains one representative of each dual pair, but the variable γ_i is not present. This time there is a 1-to-1 relationship between the

integral vectors in \mathcal{P}_κ and a subset of the nonnegative integral solutions

$$(h_1^c, h_1^d, \dots, h_i^c, \beta^i, h_i^d, \dots, h_{2i-1}^c, h_{2i-1}^d)$$

to the h_κ^{cd} -system.

The following theorems are the versions of Theorems 3.2 and 3.3, for the n even case.

Theorem 3.4. *Let h^{cd} be a nonnegative integral solution to (3.36), such that $\gamma = \Gamma(h^{cd})$ belongs to the Morse polytope \mathcal{P}_κ . Let (η, d, t) be the null, dual and trivial pairs and b be the number of beta labels of an ntd-labelling of h^{cd} . Define the mapping $G(d, b)$ as follows*

$$G_0(d, b) = G_n(d, b) = 1, \quad (3.87)$$

$$G_1(d, b) = G_{n-1}(d, b) = d_1 - d_{n-2} + d_\kappa, \quad (3.88)$$

$$G_j(d, b) = G_{n-j}(d, b) = d_j - d_{n-j-1}, \text{ for } j = 2, \dots, i-1, \quad (3.89)$$

$$G_i(d, b) = b. \quad (3.90)$$

Then $G(d, b) = \Gamma(h^{cd})$ is a Betti number vector.

Furthermore, the whole set of labellings associated with h^{cd} is mapped to the Betti number vector $G(d, b)$.

Theorem 3.5. *Let h^{cd} be a nonnegative integral solution to (3.36), such that $\gamma = \Gamma(h^{cd})$ belongs to the Morse polytope \mathcal{P}_κ .*

Then there is a unique ntd-labelling of h^{cd} that can be realized topologically, that is, that satisfies

$$\gamma_1 = \gamma_{n-1} = \tilde{d}_1 + \tilde{d}_\kappa, \quad (3.91)$$

$$\gamma_j = \gamma_{n-j} = \tilde{d}_j + \tilde{d}_{n-j}, \text{ for } j = 2, \dots, i-1, \quad (3.92)$$

$$\gamma_i = 2\tilde{d}_i + \tilde{b}, \quad (3.93)$$

where \tilde{d} is the vector of dual pairings and \tilde{b} is the number of beta labels of this unique ntd-labelling.

Furthermore,

1. if \tilde{b} is even, this is realizable on a generalized tori of dimension $2i$, i odd, with γ_k factors of the type $S^k \times S^{n-k}$, for $k = 1, \dots, i$.

2. if \tilde{b} is odd, this is realizable on a $n = 2i$, i even, dimensional manifold obtained as:

(a) a complex projective space \mathbf{CP}^{2k} , connected sum with a generalized tori of dimension $n = 4k$, k odd, with γ_j factors for j odd, $\gamma_j - 1$ factors for j even, of the type $S^j \times S^{n-j}$ for $j = 1, \dots, 2k$, provided $\gamma_j \geq 1$, for j even.

- (b) a generalized tori of dimension $n = 4k$, k even, connected sum with a Hamiltonian projective space \mathbf{HP}^k , with γ_j factors for $j \not\equiv 0 \pmod{4}$, $\gamma_j - 1$ factors for $j \equiv 0 \pmod{4}$, of the type $S^j \times S^{n-j}$ for $j = 1, \dots, 2k$, provided $\gamma_j \geq 1$, for $j \equiv 0 \pmod{4}$ ⁴.

To illustrate these results, consider the following example. Let $n = 2i = 8$ and $h = (2, 5, 5, 6, 5, 4, 3, 4, 2)$. The solutions to the h_k^{cd} -system are

$$\begin{aligned} h^{cd} = & (1 + \kappa, 4 - \kappa, 1, 4, 1, 5, 1, 4, 0, 4, 0, 3, 0, 3 - \kappa, 1 + \kappa) \\ & + \alpha_1(0, 0, 1, -1, 0, 0, 0, 0, 0, 0, -1, 1, 0, 0) \\ & + \alpha_2(0, 0, 0, 0, 1, -1, 0, 0, 0, -1, 1, 0, 0, 0, 0) \\ & + \alpha_3(0, 0, 0, 0, 0, 0, 1, -2, 1, 0, 0, 0, 0, 0, 0), \end{aligned} \quad (3.94)$$

where $\kappa \in \{0, 1, 2, 3\}$, $0 \leq \alpha_1 \leq 3$, $0 \leq \alpha_2 \leq 4$ and $0 \leq \alpha_3 \leq 2$. The inequalities that define the reduced Morse polytope are

$$\begin{array}{rcl} \gamma_1 & \leq & 3 \\ \gamma_1 - \gamma_2 & \geq & 0 \\ \gamma_1 - \gamma_2 + \gamma_3 & \leq & 4 \\ \gamma_1 - \gamma_2 + \gamma_3 & \geq & 2 \\ \gamma_1 & \geq & \kappa \\ \gamma_1, \gamma_2, \gamma_3 & \geq & 0. \end{array} \quad (3.95)$$

Figure 3.25 depicts the reduced polytope \mathcal{P}_0^r for this data, from three different viewpoints. The blue face is \mathcal{F}_0^r .

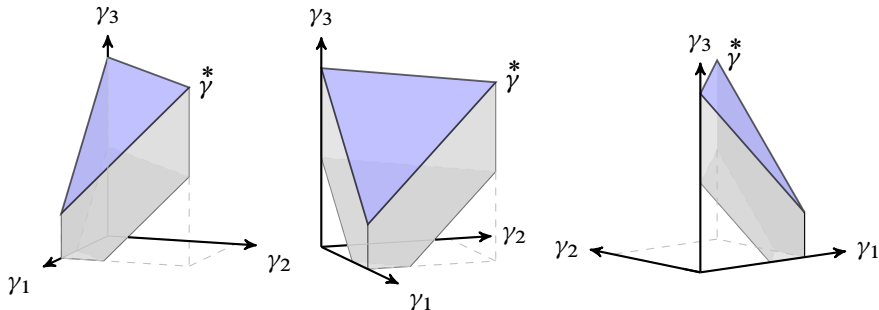


Figure 3.25: Polytope \mathcal{P}_0^r corresponding to $h = (2, 5, 5, 6, 5, 4, 3, 4, 2)$.

⁴there is one exception, when $k = 4$ it is better to use \mathbf{OP}^2 in the connected sum.

$\bar{\gamma}^r$	\bar{h}^{cd}	α_1, α_2	Range of δ_1	Range of δ_2	Range of δ_3	#ntd-labellings assoc. with $\bar{\gamma}^r, \bar{h}^{cd}$
(3, 3, 4)	(1, 4, 1, 4, 1, 5, 1, 4, 0, 4, 0, 3, 0, 3, 1)	0, 0	{0}	{0}	{0}	1
(3, 2, 3)	(1, 4, 1, 4, 2, 4, 1, 4, 0, 3, 1, 3, 0, 3, 1)	0, 1	{0}	{0, 1}	{0}	2
(3, 1, 2)	(1, 4, 1, 4, 3, 3, 1, 4, 0, 2, 2, 3, 0, 3, 1)	0, 2	{0}	{0, 1, 2}	{0}	3
(3, 0, 1)	(1, 4, 1, 4, 4, 2, 1, 4, 0, 1, 3, 3, 0, 3, 1)	0, 3	{0}	{0, 1, 2, 3}	{0}	4
(2, 2, 4)	(1, 4, 2, 3, 1, 5, 1, 4, 0, 4, 0, 2, 1, 3, 1)	1, 0	{0, 1}	{0}	{0}	2
(2, 1, 3)	(1, 4, 2, 3, 2, 4, 1, 4, 0, 3, 1, 2, 1, 3, 1)	1, 1	{0, 1}	{0, 1}	{0}	4
(2, 0, 2)	(1, 4, 2, 3, 3, 3, 1, 4, 0, 2, 2, 2, 1, 3, 1)	1, 2	{0, 1}	{0, 1, 2}	{0}	6
(1, 1, 4)	(1, 4, 3, 2, 1, 5, 1, 4, 0, 4, 0, 1, 2, 3, 1)	2, 0	{0, 1, 2}	{0}	{0}	3
(1, 0, 3)	(1, 4, 3, 2, 2, 4, 1, 4, 0, 3, 1, 1, 2, 3, 1)	2, 1	{0, 1, 2}	{0, 1}	{0}	6
(0, 0, 4)	(1, 4, 4, 1, 1, 5, 1, 4, 0, 4, 0, 0, 3, 3, 1)	3, 0	{0, 1, 2, 3}	{0}	{0}	4

Table 3.2: Reduced Betti number vectors on \mathcal{F}_t , respective \bar{h}^{cd} , values of α_1, α_2 , ranges of $\delta_1, \delta_2, \delta_3$, and number of distinct ntd-labellings, supposing $\kappa = 0$.

The 10 integral vectors belonging to the top face of \mathcal{P}_κ^r , the respective h^{cd} , values of the circulations ($c_3 = 0$ for all of them), ranges of α_j 's and number of ntd-labellings associated therewith are shown Table 3.2.

4

Building flows with Isolating Blocks

The most elementary gradient-like flows are negative gradient flows of Morse functions which have Lyapunov graphs of Morse type L which are directed graphs, have no oriented cycles, and all vertices have degree less than or equal to three. In fact, this holds for dimension $n \geq 2$, as proven in Chapter 2.

Hence, given an abstract Lyapunov graph, L , the question of Morsification is an important one. In the last chapter we determined necessary and sufficient conditions for Morsifications of L . This answers the question of morsifiability of L at the combinatorial level which naturally has topological implications as to the realizability of L as a gradient-like flow on a compact manifold.

Furthermore, non-morsifiability is an obstruction to the existence of a flow. If a graph does not admit a Morsification, it is not realizable as a gradient-like flow on any compact smooth manifold.

Initially we are interested in an elementary cobordism which is a triad (N, N^+, N^-) possessing exactly one nondegenerate singularity. These provide the simplest kinds of isolating blocks realizing a Lyapunov semigraph of Morse type possessing only one vertex. It can be realized by considering the attaching of an ℓ handle, $D^\ell \times D^{n-\ell}$, to a collar $N^- \times [0, 1]$ where N^- is a closed codimension one manifold. Let $\theta : \partial D^\ell \times D^{n-\ell} \rightarrow N^- \times \{1\}$ be an embedding which defines the new n -manifold $N' = N^- \times [0, 1] \cup_\theta H$ with N^- as exiting boundary for the flow φ . The entering boundary of the isolating block is N^+ where $\partial N' = N^+ \cup N^-$. The following alternative notations are used $N' = N^- \times [0, 1] \cup H^{(\ell)}$ or $N' = N^- \times [0, 1] \cup H$ when reference to the index of the handle is omitted.

4.1 Two dimensional Isolating Blocks

It is well known that two dimensional isolating blocks (N, N^+, N^-) for Morse singularities are D^2 -disks with zero, one, or two disjoint subdisks removed from the interior of D^2 . If p is a sink, i.e. $h_0 = 1$, then N is a disk with $N^+ = \mathbb{S}^1$; and if it is a source, $h_2 = 1$, then N is a disk with $N^- = \mathbb{S}^1$. If p is a saddle, $h_1 = 1$, then we have the following possibilities:

- in the orientable case, N is a disk with two disjoint subdisks removed from the interior of D^2 ;
- in the nonorientable case, N is a Möbius band with a subdisk removed from its interior.

This of course follows directly from the Poincaré–Hopf equalities in dimension 2 which determine uniquely the ambient manifold up to homeomorphism. In Figure 4.1, the Lyapunov semigraphs for Morse saddle and their realization as 2-dimensional isolating blocks are depicted.

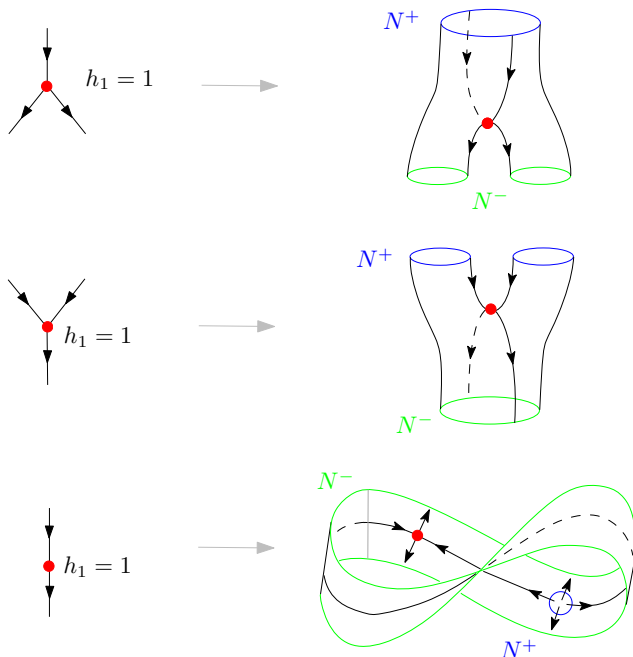


Figure 4.1: Isolating blocks and Lyapunov semigraphs for saddles on surfaces

Before we proceed, let us make use of an example which illustrates the usefulness of Lyapunov graph Morsification as a tool that aids in the realization of an abstract Lyapunov semigraph L as a gradient-like flow on an isolating block. One gains insight into the topology of the isolating block N of an isolated invariant set S by considering an associated flow corresponding to the Morsification of L .

The necessary and sufficient condition that L must satisfy at each vertex is the local Poincaré–Hopf inequalities. In dimension two these inequalities becomes an equality. See Chapter 2.

Let $\kappa = g$ be the genus of the isolating block in dimension 2 and $b = e^+ + e^-$ be the total number of boundary components, where e^+ is the number of entering and e^- the number of exiting boundary components. The data on an abstract Lyapunov semigraph can be realized if and only if one of the Poincaré–Hopf equalities below holds with $\kappa = g$, i.e., the cycle number κ equal to the genus g of the ambient manifold.

$$\text{Orientable case: } 2 - 2g - b = h_2 - h_1 + h_0 \quad (4.1)$$

$$\text{Nonorientable case: } 2 - g - b = h_2 - h_1 + h_0 \quad (4.2)$$

Example 4.1. Consider the abstract Lyapunov semigraphs L_i , with $1 \leq i \leq 5$, in Figure 4.2. Are these semigraphs realizable as gradient-like flows on a two dimensional isolating block?

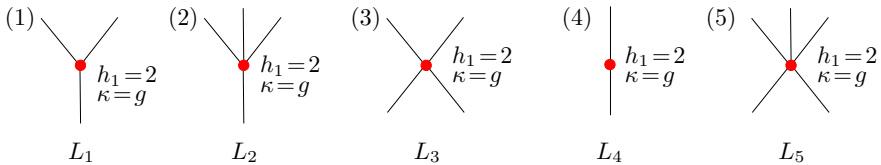


Figure 4.2: Are these graphs morsifiable?

In order to answer this question, one starts by analyzing the Poincaré–Hopf equalities (4.1) and (4.2) for the data $\{h_0 = 0, h_1 = 2, h_2 = 0\}$. One immediately concludes that any isolating block, which contains a maximal invariant set with the given data, must satisfy $b \leq 4$. Hence, L_5 can not be realized as a gradient-like flow on any smooth surface. By analyzing the possible abstract Lyapunov semigraphs L_i that satisfy the Poincaré–Hopf equalities, one obtains the morsifiable ones and consequently those which are realizable as a gradient flow on an isolating block with Lyapunov semigraph isomorphic to L_i .

The Lyapunov semigraph L_1 does not satisfy the Poincaré–Hopf equality in the orientable case (4.1) since it would imply that g is non integer, which is not possible, and hence L_1 cannot be morsified as a Morse type graph. Therefore, there is no orientable 2-dimensional isolating block that admits a realization of L_1 as a gradient-like flow. On the other hand, L_1 satisfies (4.2) in the nonorientable case, and hence it can be morsified and

admits a realization as a gradient-like flow on a nonorientable 2-manifold with $\kappa = g = 1$ and $b = 3$. Note that, this is always the case for $b = 3$ in this example. The only admissible isolating block N_3 is a Möbius band minus two disks. Since N_3 is an isolating block for an invariant set S with $h_1 = 2$, it could have as maximal isolated invariant set two saddles or a monkey saddle. See Figure 4.3.

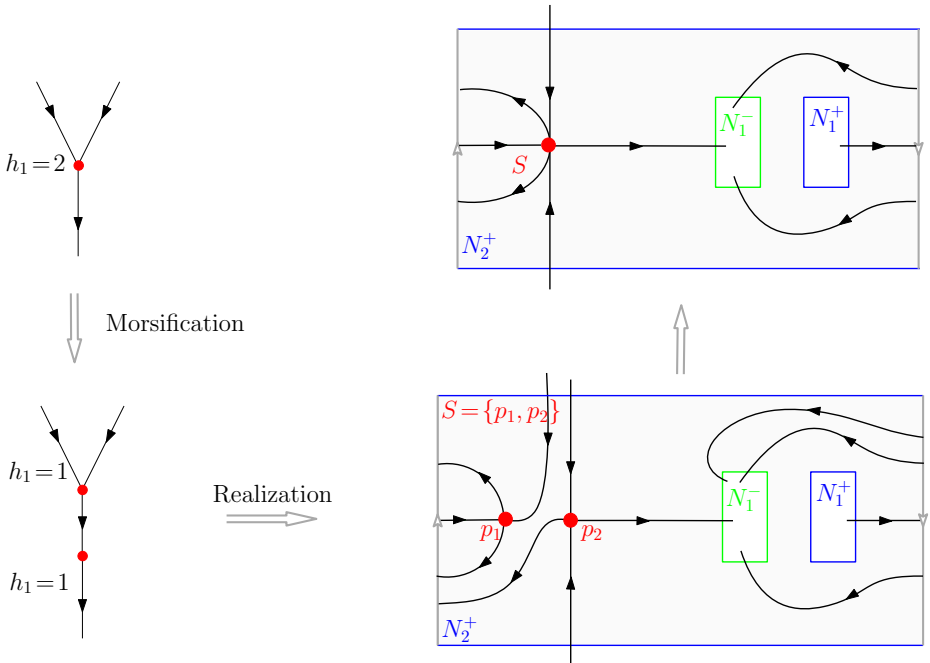
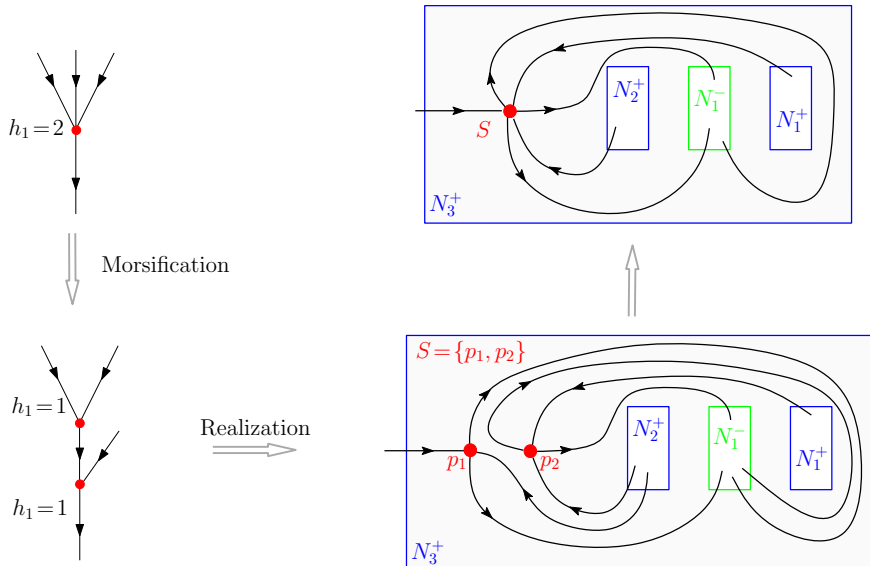
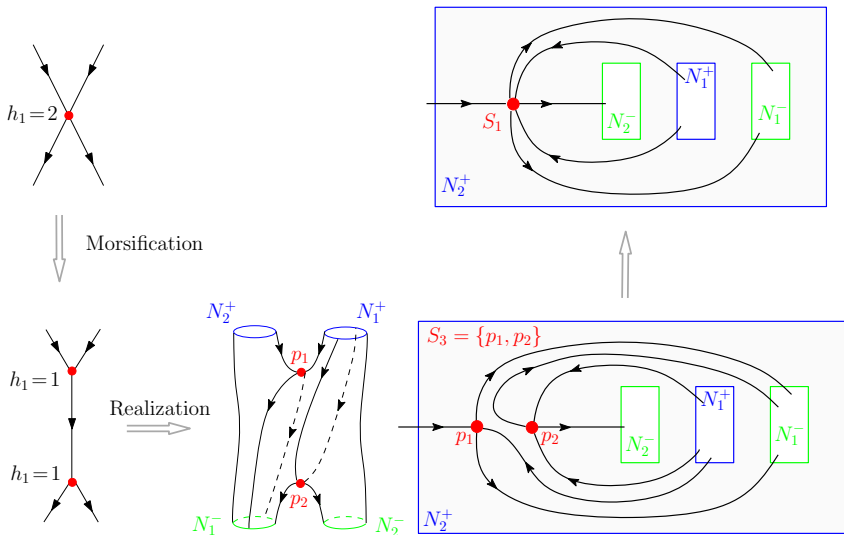


Figure 4.3: Möbius band isolating block: $b = 3$ and $\kappa = 1$

On the other hand, L_2 and L_3 satisfy the Poincaré–Hopf equality in the orientable case (4.1) and fail to do so in the nonorientable case (4.2). Hence, neither can be realized as a flow on a nonorientable 2-dimensional isolating block, since this would imply $g = 0$, which is not possible for non orientable surfaces. However, in the orientable case, L_2 and L_3 can be morsified and realized as a gradient-like flow on a 2-dimensional isolating block N_4 with $\kappa = g = 0$ and $b = 4$, i.e., a sphere minus four disks. Note that N_4 is the only admissible isolating block in the case $b = 4$, which may have as maximal isolated invariant set two saddles or a monkey saddle. See Figures 4.5 and 4.6.

Finally, consider L_4 . Since $b = 2$ and $h_1 = 2$ then (4.1) implies that $g = 1$ and one has an orientable isolating block, namely a torus minus two disks. See Figure 4.6. However, the same data for (4.2) implies $g = 2$ and one has a nonorientable isolating block, namely a Klein Bottle minus two disk, see Figure 4.7.

Figure 4.4: Disk isolating block: $b = 4$ and $\kappa = 0$ Figure 4.5: Disk isolating block: $b = 4$ and $\kappa = 0$

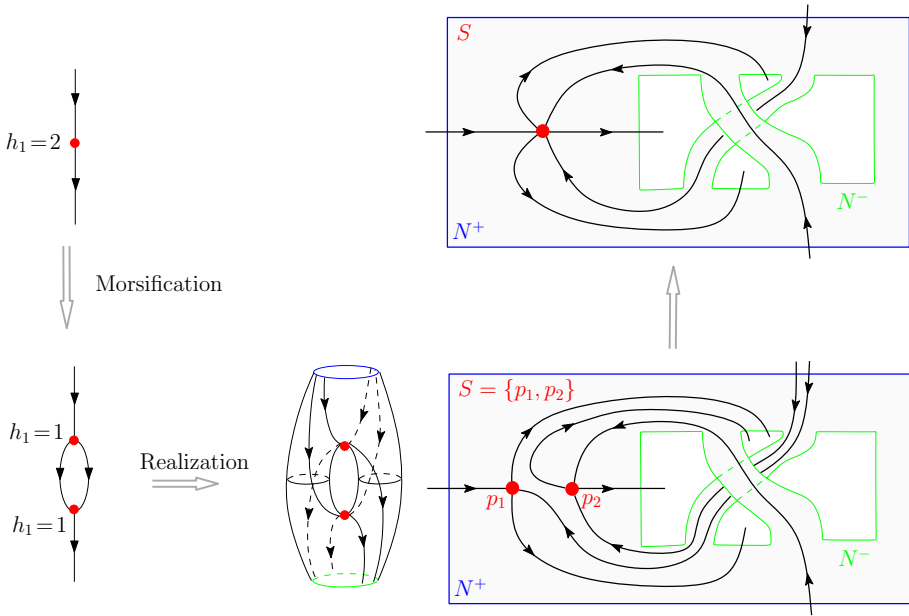


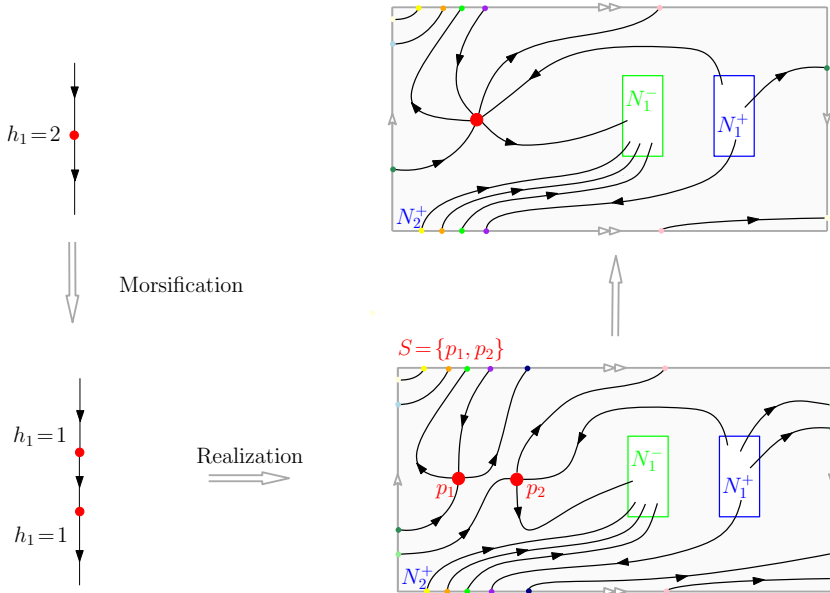
Figure 4.6: Torus isolating block: $b = 2$ and $\kappa = 1$

This example illustrates the usefulness of morsifiability in the construction of isolating blocks for degenerate singularities in dimension two. Once the most elementary building pieces have been constructed, namely isolating blocks for Morse singularities and periodic orbits, one can glue them in accordance with the abstract Lyapunov graph L in order to construct a closed orientable or nonorientable manifold of genus g with a gradient-like flow that has Lyapunov graph isomorphic to L . In this sense, one realizes an abstract Morse–Smale type graphs in dimension 2.

In higher dimensions, morsifiability does not necessarily imply realizability for some even dimensional manifolds. More will be said on this topic later in the chapter. However, in general, whenever morsifiability implies realizability, the breaking down of the isolating block into elementary Morse blocks provides greater insight into the various candidates that serve as isolating block for the more complicated dynamics.

The following theorem, see de Rezende and Franzosa (1993), gives necessary and sufficient conditions for an abstract Lyapunov graph of Morse–Smale type to be associated with a Morse–Smale flow and a Lyapunov function on a closed surface.

A nonorientable vertex on Lyapunov graphs for flows on surfaces are those whose associated Lyapunov semigraph can only be realized on a nonorientable isolating block. A nonorientable vertex on Morse–Smale Lyapunov graphs for surfaces are either a saddle vertex of degree 2 or a source (sink) vertex of degree one labelled with a periodic orbit.

Figure 4.7: Klein isolating block: $b = 2$ and $\kappa = 2$

Theorem 4.1. Let M be a closed surface. An abstract Lyapunov graph L of Morse type is associated to a Morse–Smale flow ϕ_t and a Lyapunov function f on M if and only if the following conditions are satisfied:

1. (Local conditions) If the vertex v is labelled with Λ and
 - (a) Λ is a source (sink) then the number of exiting (entering) edges e_v^- (e_v^+) is equal to one.
 - (b) Λ is a saddle then $1 \leq e_v^+ \leq 2$, $1 \leq e_v^- \leq 2$ and $e_v^+ + e_v^- \leq 3$. Moreover Λ is orientable if and only if $e_v^+ + e_v^- = 3$.
 - (c) Λ is a repelling (attracting) periodic orbit then $e_v^- \leq 2$ ($e_v^+ \leq 2$). Moreover Λ is orientable if and only if $e_v^- = 2$ ($e_v^+ = 2$).

2. (Global conditions)

- (a) If M is orientable, the cycle rank of L must be equal to the genus of M .
- (b) If M is nonorientable, twice the cycle rank of L plus the number of nonorientable vertices must be equal to the genus of M .

Proof. The necessity of the local and global conditions follow from results in the previous chapter. In order to prove that these conditions are sufficient, we construct a smooth flow

by gluing isolating blocks of Morse–Smale type in accordance to L so as to obtain a manifold of genus g with no saddle connections.

Number the vertices $j = 1, \dots, V$ of L respecting the order on the graph which is possible since the graph is directed with no oriented cycles. The desired flow is obtained by gluing these isolating blocks as follows. Consider the vertex j . Isolating blocks for sinks and sources are disks, and for saddles are as in Figure 4.1. Isolating blocks for attracting or repelling periodic orbits are either cylinders or Möbius bands. Now we glue the isolating blocks in the order in which the vertices are numbered from 1 to V . Assume each isolating block is of the form $f^{-1}(j - \frac{1}{2}, j + \frac{1}{2})$ for a function that serves as a Lyapunov function for flow on it. The desired flow is obtained by gluing these isolating blocks as follows. Assume vertices j and k , where $j + 1 \leq k$, are connected by an edge negatively incident to vertex k and positively incident to vertex j . Then the isolating block N_j for vertex j has an entering boundary component N_j^+ for the flow in $f^{-1}(j + \frac{1}{2})$ and the isolating block N_k for vertex k has an existing boundary component N_k^- for the flow in $f^{-1}(k - \frac{1}{2})$ which are both homeomorphic to circles. Then attach these boundary components by a cylinder on which there is a longitudinal flow with a Lyapunov function f which takes on the value $(j + \frac{1}{2})$ and $(k - \frac{1}{2})$ on the exiting and entering boundary components respectively.

It is necessary to take care when gluing the isolating blocks together so that the resulting manifold is homeomorphic to M_g , where g is its genus, which in the two dimensional case is determined by the Poincaré–Hopf equalities where $\kappa = g$.

Of course given a graph L with no nonorientable vertices, L can be realized on both an orientable and nonorientable surface. In order to realize it on an orientable surface of genus $\kappa = g$, all gluings must be done so as to preserve orientation. It follows from the Poincaré–Hopf equalities that since $L(h_2, h_1, h_0)$ is realized on an orientable surface, $h_2 - h_1 + h_0$ must be even. Therefore, if $L(h_2, h_1, h_0)$ is also realizable on an nonorientable surface of genus $g = \kappa$, $2 - \kappa = h_2 - h_1 + h_0$ is even, hence $g \geq 2$ and is always even. Consequently, there are at least two saddle isolating blocks with an exiting boundary C^- of one glued to the entering boundary C^+ of the other along a circle C which is not null homologous. In this case, orientation must not be preserved and this is achieved by gluing C^+ to C^- reversing orientation.

If L has nonorientable vertices then the only possible realization is on a nonorientable surface since there are isolating blocks which are either a Möbius band containing a periodic orbit or a Möbius band with a disk removed from its interior containing a saddle singularity.

Finally to guarantee that the resulting flow is Morse–Smale, the stable and unstable manifolds of the isolating sets must intersect transversally, thus in this 2-dimensional case, no saddle connections should occur. Consider a connected union of k isolating blocks $\cup_{j=1}^k N_j$ ordered from bottom to top. To insure transversality, the unstable manifolds of the saddles s_1, \dots, s_k must divide the exiting boundary of N_1 into $2k$ disjoint arcs and the stable manifolds of the saddles must divide the entering boundary of N_k into $2k$ disjoint arcs as well. This should be true for all k . There are many ways to perform this gluing and the resulting flows may not be topologically equivalent. \square

Let L be an abstract Lyapunov semigraph with vertex v with e_v incident edges and labelled with homology Conley indices (h_2, h_1, h_0) . The genus of the isolating block N_v realizing the dynamics with which v is labelled is:

$$\text{Orientable case: } g_v = \frac{(h_2 - h_1 + h_0 - e_v + 2)}{2} \quad (4.3)$$

$$\text{Nonorientable case: } g_v = (-h_2 + h_1 - h_0 - e_v + 2) \quad (4.4)$$

One actually can generalize Theorem 4.1 to consider abstract Lyapunov graphs and theirs realization as smooth gradient-like flows on surfaces. For the proof of the following theorem, see de Rezende and Franzosa (1993).

Theorem 4.2. *Let M be a closed surface. Let L be an abstract Lyapunov graph where each vertex is labelled with (h_2, h_1, h_0) . L is associated to a smooth flow ϕ_t with a finite component chain recurrent set and a Lyapunov function f on M if and only if the following conditions are satisfied:*

1. (Local conditions) For each vertex v

$$(a) \ e_v^+ \leq h_1 + 1,$$

$$(b) \ e_v^- \leq h_1 + 1 \text{ and}$$

(c) $e_v^+ + e_v^- \leq h_1 - h_2 - h_0 + 2$, where the latter inequality is strict if v is nonorientable. Furthermore, if $e^+ = 0$ then $h_2 = 1$ otherwise $h_2 = 0$; if $e^- = 0$ then $h_0 = 1$ otherwise $h_0 = 0$;

2. (Global conditions) The genus of each vertex v_i , g_{v_i} , is a nonnegative integer and if M has genus G and

$$(a) \text{ if } M \text{ is orientable, then } G = \kappa + \sum_{i=1}^V g_{v_i},$$

$$(b) \text{ if } M \text{ is nonorientable, then } G = 2\kappa + \sum_{i=1}^V g_{v_i}.$$

Note that in Theorem 4.1, $g_v = 0$ if v is orientable and $g_v = 1$ if v is nonorientable. The global conditions therein imply that if M is orientable its genus $G = \kappa$ and if M is nonorientable its genus $G = 2\kappa + \text{number of nonorientable vertices}$. Hence, Theorem 4.2 generalizes Theorem 4.1.

The global conditions in Theorem 4.2 breaks down the total genus G of the surface M into the local contribution of each isolating block N_v which realizes the semigraph L_v and the global contribution to the genus coming from the gluings of the N_v as indicated by L . The examples in Figure 4.3, Figure 4.4, Figure 4.5 and Figure 4.6 illustrate this general case where the number of incident edges e_v is equal to the number of boundary components of the isolating block b .

4.2 Three dimensional Isolating blocks

The aim in this section is to realize abstract Lyapunov graphs in dimension 3 as Morse–Smale flows on compact *orientable* smooth manifolds. In this and subsequent sections, unlike Section 4.1, we work only with compact orientable smooth manifolds.

In order to realize Morse–Smale isolating blocks, one must make use of handles, see Chapter 2. Since isolating blocks for periodic orbits are considered, we use round handles as defined below.

Definition 4.1. Let C_1 and C_2 be solid concentric cylinders of radii r_1 and r_2 , respectively, with $r_1 \geq r_2$. A *round handle* R is a 3-manifold homeomorphic to $C_1 - C_2$ containing a saddle type periodic orbit of period equal to one and with a flow defined on R as follows: the flow enters on two disjoint boundary components of R homeomorphic to annuli and exits on two other disjoint boundary components also homeomorphic to annuli. See Figure 4.8.

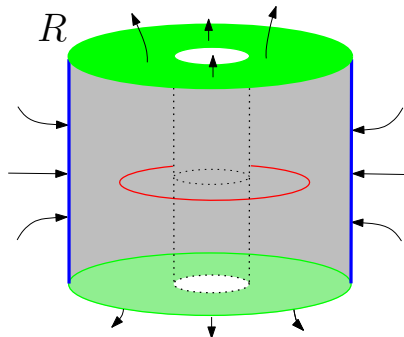


Figure 4.8: A round handle R for a saddle periodic orbit with $h_1 = h_2 = 1$.

The following proposition provides a local characterization of Lyapunov semigraphs associated to a Morse–Smale flow on a 3-manifold M where each vertex is labelled with a singularity or periodic orbit of Morse–Smale type.

Proposition 4.1. Let ϕ_t be a Morse–Smale flow on a closed orientable 3-manifold with Lyapunov function f . Let L be a Lyapunov graph with respect to f . The bounds on the degree of a vertex v of L and the weights¹ on the incident edges of v are as follows:

1. If v is a vertex labelled with a source, $h_3 = 1$ (resp., sink, $h_0 = 1$), then $e^- = 1$ and $g^- = 0$ (resp., $e^+ = 1$ and $g^+ = 0$).

¹The edges represent collars of closed surfaces, $S \times (0, 1)$ and hence the weights are merely the genera g of S .

2. If v is a vertex labelled with a repelling periodic orbit, $h_2 = h_3 = 1$, (resp., attracting periodic orbit, $h_0 = h_1 = 1$) then $e^- = 1$ and $g^- = 1$ (resp., $e^+ = 1$ and $g^+ = 1$).
3. If v is a vertex labelled with a saddle of index 2, $h_2 = 1$ (resp., saddle of index 1, $h_1 = 1$) then $e^- = 1$ and $e^+ \leq 2$ (resp. $e^+ = 1$ and $e^- \leq 2$). Furthermore, the weights on the incoming and outgoing edges of v must satisfy the condition shown in Figure 4.9.

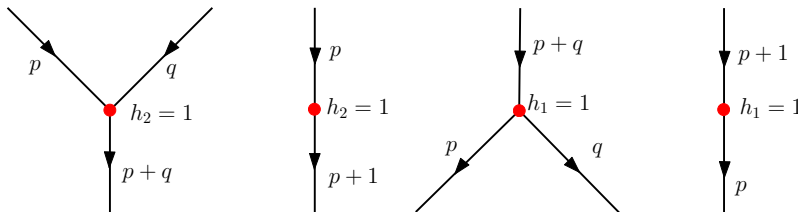


Figure 4.9: Lyapunov semigraphs labelled with saddle singularities.

4. If v is a vertex labelled with a saddle type periodic orbit, $h_1 = h_2 = 1$, then $e^+ \leq 2$ and $e^- \leq 2$ and the weights on the incoming and outgoing edges of v must satisfy the condition shown in Figure 4.10.

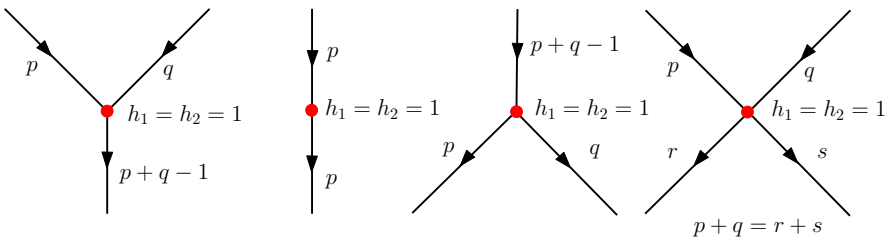


Figure 4.10: Lyapunov semigraphs labelled with saddle periodic orbits.

Conversely, given any of the Lyapunov semigraphs L_v satisfying (1)-(4) it can be realized as a smooth flow on a 3-manifold M_v with boundary surfaces of genera $g_i^+ (g_j^-)$ corresponding to the weights on the edges. Furthermore, the flow defined on M_v contains as isolated invariant set either a singularity or a periodic orbit with index equal to the labels on the vertex v .

We sketch a proof of this proposition but refer the reader to de Rezende (1993) for more details.

Proof. The proof of the necessity of the conditions follow directly from the Poincaré–Hopf inequalities in Chapter 2.

We now proceed to construct the isolating blocks for singularities and periodic orbits.

Constructing isolating blocks for singularities: Given an abstract Lyapunov semigraph L with a vertex v labelled with a singularity with $h_0 = 1$, a sink, $e^+ = 1$ and weight $g^- = 0$, there is one obvious choice for an isolating block M_v which is the 3-ball, D^3 . The sink is located at the center of D^3 and the flow is pointing transversely inward on the boundary which is homeomorphic to \mathbb{S}^2 , see Figure 4.12 (a). The construction of an isolating block for a singularity with $h_3 = 1$, a source, is obtained by reversing the flow on the isolating block for a sink.

If the vertex v is labelled with a saddle singularity with $h_1 = 1$, there are two possibilities for the indegree and outdegree of v :

$$(i) \ e^+ = 1 \text{ and } e^- = 2 \text{ or}$$

$$(ii) \ e^+ = e^- = 1.$$

The Poincaré–Hopf equality implies in the first case, if the outgoing edges have weights p and q , then the incoming edge must have weight $p + q$. In the second case, if the outgoing edge has weight p , the incoming edge must have weight $p + 1$.

In order to construct the two possible types of isolating blocks for a singularity of index $h_1 = 1$, one studies different attaching maps of an index 1 handle H_1 . Consider a flow on a solid cylinder $D^3 = D^2 \times [0, 1]$ as follows: the singularity is in the center of $D^2 \times \{\frac{1}{2}\}$ and the flow exits H_1 through the two boundary components $D^2 \times \{0\}$ and $D^2 \times \{1\}$ and enters elsewhere, as in Figure 4.11.

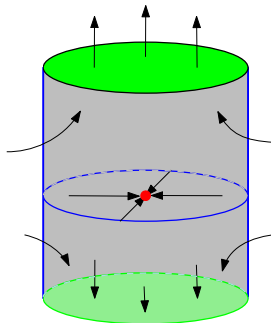


Figure 4.11: Saddle singularity in H_1 .

For the construction of an isolating block satisfying the requirements in case (i), consider two surfaces M_1 and M_2 of genus p and q , respectively. Let \mathbf{M}_1 and \mathbf{M}_2 denote the respective collarings of M_1 and M_2 , that is $\mathbf{M}_i = M_i \times [0, 1]$ for $i = 1, 2$. Now consider the transversal flow on the collars \mathbf{M}_i , $i = 1, 2$, entering for $M_i^+ = M_i \times \{1\}$ and exiting

for $M_i^- = M_i \times \{0\}$. Since \mathbf{M}_1 and \mathbf{M}_2 are disjoint, glue the handle H_1 by the attaching sphere so that $\{0\} \times D^2$ is glued on M_1^+ and $\{1\} \times D^2$ is glued on M_2^+ . The isolating block is $M_v = \mathbf{M}_2 \cup H_1 \cup \mathbf{M}_1$. Hence, the two boundary components of M_v where the flow exits are two disjoint closed 2-manifolds of genus p and q (M_1^- and M_2^- respectively). The boundary component of M_v where the flow enters is a closed 2-manifold of genus $p+q$, namely $\partial(\mathbf{M}_1 \cup H_2 \cup \mathbf{M}_2)$. One should round off the corners of $\mathbf{M}_1 \cup H_2 \cup \mathbf{M}_2$ to obtain a smooth manifold. See Figure 4.12 (b).

For the construction of an isolating block satisfying (ii), consider a surface M of genus p and its collar \mathbf{M} and consider a transversal flow on the collar \mathbf{M} entering for $M^+ = M \times \{1\}$ and exiting for $M^- = M \times \{0\}$. Attach a handle of index 1, H_1 by the attaching sphere, so that the two exiting boundaries are attached to $M^+ = M \times \{1\}$. $M_v = \mathbf{M} \cup H_2$. See Figure 4.12(c).

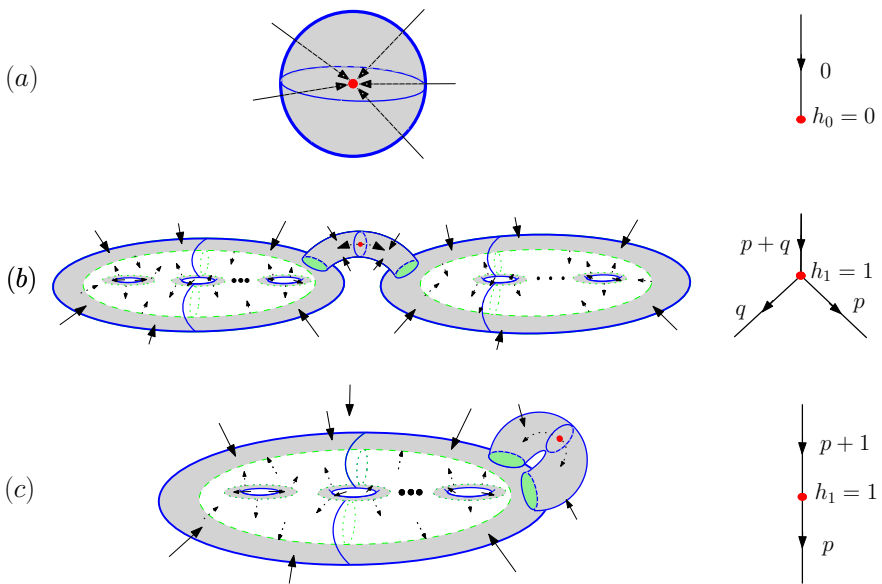


Figure 4.12: Isolating block for singularities.

Constructing isolating blocks for periodic orbits: If v is a vertex of an abstract Lyapunov graph L labelled with a repelling periodic orbit (i.e., $h_2 = h_3 = 1$) then condition 2 asserts that there is exactly one outgoing edge on v and that the weight on this edge is equal to one. Our choice of isolating block M_v must have one boundary component of genus equal to one. The obvious choice for M_v is a solid torus $D^2 \times S^1$ containing a repelling periodic orbit with the flow pointing outwardly transverse to ∂M_v . An isolating block for an attracting periodic orbit (i.e., $h_0 = h_1 = 1$) can be obtained by reversing the flow on the isolating block defined previously.

Let the vertex v of the Lyapunov semigraph be labelled with a saddle periodic orbit (i.e. $h_1 = h_2 = 1$). By condition 4, there are four possibilities for the degrees of v as depicted in Figure 4.10:

- (i) $e^+ = 2, e^- = 1$;
- (ii) $e^+ = e^- = 1$;
- (iii) $e^+ = 1, e^- = 2$, and
- (iv) $e^+ = e^- = 2$.

The Poincaré–Hopf equality implies that the weights on incoming and outgoing edges are as in Figure 4.10.

The round handle must be attached by the two annulli where the flow exits onto the collar of M , where the flow enters.

For (i) the isolating block must have two entering boundary components of genus p and q . Also it must have two exiting boundary components of genus r and s , such that $r + s = p + q$. In this case, we use a connecting invariant round handle R on two collared handlebodies \mathbf{M}_2 and \mathbf{M}_1 of genus r and s respectively. Attach the round handle R so that the flow enters on two handlebodies of genus p and q . The isolating block is defined as $M_v = \mathbf{M}_2 \cup R \cup \mathbf{M}_1$, see the Figure 4.13-(c).

For (ii) the isolating block must have one entering and one exiting boundary component. By the Poincaré–Hopf formula, both should have the same genus p . In this case it suffices to attach an invariant round handle R to a collared handlebody \mathbf{M} of genus p . The isolating block is defined as $M_v = \mathbf{M} \cup R$, as shown in Figure 4.13-(b).

For (iii) the isolating block must have one entering and two exiting boundary components. The two exiting boundary components have genus p and q . By the Poincaré–Hopf formula the entering boundary component should have genus $p + q - 1$. To realize this isolating block, attach a decreasing round handle R to two collared handlebodies \mathbf{M}_1 and \mathbf{M}_2 of genus p and q . The isolating block is defined as $M_v = \mathbf{M}_2 \cup R \cup \mathbf{M}_1$, as shown in Figure 4.13-(a). □

The following theorem provides a characterization of a Lyapunov graph associated to a Morse–Smale flow on \mathbb{S}^3 . A proof of a more general version of this theorem for Smale flows can be found in de Rezende (1987).

Theorem 4.3. *Given an abstract Lyapunov graph L whose sink (source) vertices are each labelled with an attracting (repelling) singularity or periodic orbit and saddle vertices are labelled with saddle singularities $h_1 = 1$ or $h_2 = 1$ or with a saddle periodic orbit $h_1 = h_2 = 1$, then L is associated with a Morse–Smale flow ϕ_t and a Lyapunov function f on \mathbb{S}^3 if and only if the following conditions hold:*

1. *The underlying graph L is a tree, i.e. $\kappa = 0$, with exactly one edge attached to each sink or source vertex. Moreover, the sink (source) vertex is labelled with an*

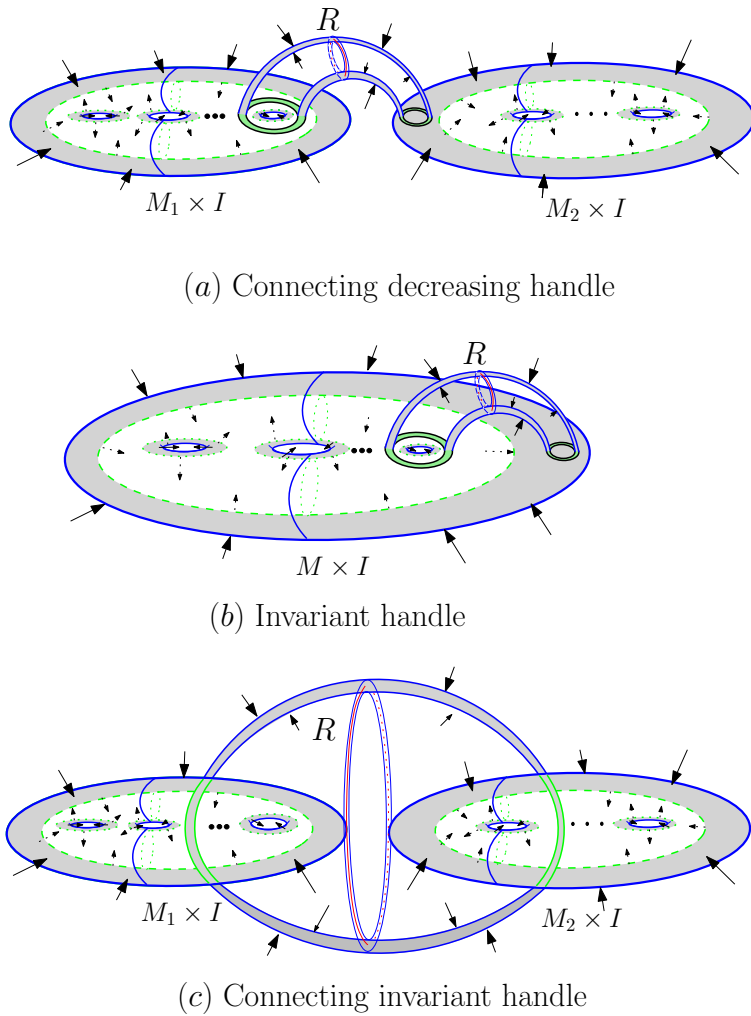


Figure 4.13: Gluing maps for round handles.

attracting $h_0 = 1$ (repelling $h_3 = 1$) singularity or an attracting $h_0 = h_1 = 1$ (repelling $h_2 = h_3 = 1$) periodic orbit.

2. If a vertex v is labelled with a singularity with $h_2 = 1$ (resp. $h_1 = 1$) then $1 \leq e^+ \leq 2$ and $e^- = 1$ (resp. $e^+ = 1$ and $1 \leq e^- \leq 2$), where e^+ (e^-) is the number of incoming (outgoing) edges of v .
3. If v is labelled with a saddle periodic orbit, $h_1 = h_1 = 1$, then $0 \leq e^+ \leq 2$ and $0 \leq e^- \leq 2$.
4. All vertices must satisfy the Poincaré–Hopf condition, i.e., for a vertex labelled with a singularity of index $h_r = 1$, the condition is

$$(-1)^r = e^+ - e^- - \sum g_j^+ + \sum g_i^-$$

and for a vertex labelled with a periodic orbit, the condition is

$$0 = e^+ - e^- - \sum g_j^+ + \sum g_i^-,$$

where $\{g_j^+\}_{j=1}^{e^+}$ ($\{g_i^-\}_{i=1}^{e^-}$) are the weights on the incoming (outgoing) edges of v .

We sketch a proof.

Proof. The necessity of these local conditions follow directly from the Poincaré–Hopf inequalities in Chapter 2. In order to prove the sufficiency of the conditions in Theorem 4.3 one must glue the isolating blocks accordingly, i.e. in such a way that the result is a Morse–Smale flow on \mathbb{S}^3 . As shown above we can locally realize singularities and periodic orbits in isolating blocks embedded in \mathbb{S}^3 , hence compact submanifolds of \mathbb{S}^3 with boundary.

The final step is to select a set of gluing maps for all the isolating blocks we have constructed and attach them according to the prescription on the abstract Lyapunov graph L so as to obtain a Morse–Smale flow on \mathbb{S}^3 .

Let M_v and M_w be isolating blocks corresponding to the vertices v and w on the Lyapunov graph L , respectively. If there is an edge going from vertex v to the vertex w with weight g , we want to glue a component C^- of ∂M_v^- of genus g to a component C^+ of ∂M_w^+ with genus g . Since C^- and C^+ are unknotted surfaces of genus g , they bound in \mathbb{S}^3 unknotted handlebodies on both sides. Let M_v (resp. M_w) be the component of the complement of C^- (resp. C^+) in \mathbb{S}^3 which contains M_v (resp. M_w). It is helpful to think of these isolating blocks as being in different three-spheres. We glue M_v to M_w attaching C^- to C^+ in order to obtain \mathbb{S}^3 . If h' denotes the attaching map, by Theorem 3.10 in Franks (1985), it can be isotoped to h so that the flow on $M = M_v \cup_h M_w$ satisfies the strong transversality condition.

By gluing M_v to M_w we have formed \mathbb{S}^3 and each boundary component of M is an unknotted surface in \mathbb{S}^3 . Choose an edge emanating from the vertex v or w to a new vertex z . Repeat the procedure for M and M_z producing a new submanifold of \mathbb{S}^3 with its boundary components being unknotted surfaces.

When a source (or sink) vertex y is reached there are two possibilities for M_y :

1. $M_y = D^3$ the three ball with a singularity $h_3 = 1$ (or a singularity $h_0 = 1$).
2. $M_y = \mathbb{S}^1 \times D^2$, solid torus if y is labelled with a repelling (or an attracting periodic orbit $h_1 = h_0 = 1$) periodic orbit $h_3 = h_2 = 1$.

We can continue this procedure adding a vertex each time and at each step obtaining a new $M \subset \mathbb{S}^3$. When all isolating blocks M_i have been attached for all vertices i then one obtains the three-sphere.

From the Lyapunov function on each M_i , one can construct a smooth Lyapunov function on \mathbb{S}^3 whose corresponding Lyapunov graph L' is topologically equivalent to the abstract Lyapunov graph L with which we started our construction. \square

Example 4.2. Let us illustrate this theorem of realizing a Lyapunov graph on \mathbb{S}^3 . Start with a graph which is a tree and that satisfies the local conditions in the Theorem 4.3, as shown in the Figure 4.14.

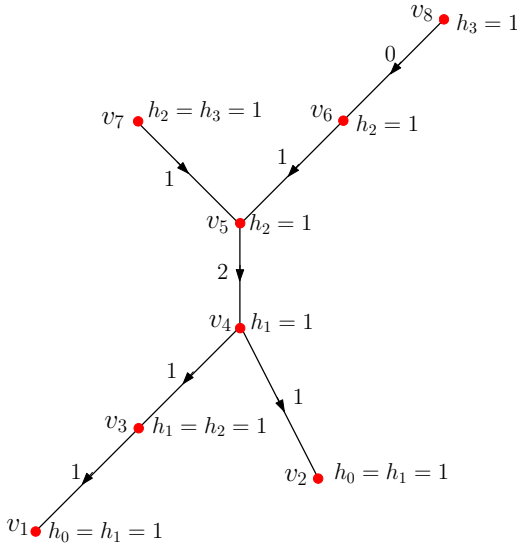


Figure 4.14: Lyapunov graph L realizable in \mathbb{S}^3 .

Now we build an isolating block for each vertex in the graph as shown in Figure 4.15.

Now, we can glue M_{v_3} to the isolating block M_{v_1} along the boundary and the resulting manifold is homeomorphic to a solid torus. Likewise, we can glue M_{v_4} to $M_{v_3} \cup M_{v_1}$ and M_{v_2} such that the resulting manifold is homeomorphic to a solid bitorus. In this fashion, we can glue M_{v_6} with M_{v_8} and obtain a solid torus. Now, we glue along the boundary $M_{v_6} \cup M_{v_8}$ and M_{v_7} to M_{v_5} to obtain a solid bitorus. Finally, we glue both solid bitorus

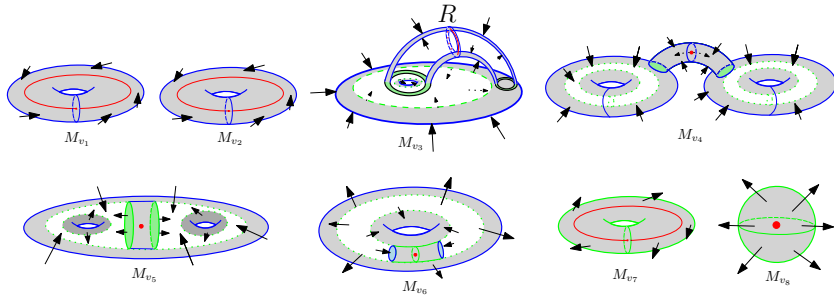


Figure 4.15: Isolating blocks realizing vertices of L .

along the boundary in such way to obtain \mathbb{S}^3 , i.e. identifying meridians of one to the longitudes of the other.

4.2.1 Morse–Smale flows on $\mathbb{S}^2 \times \mathbb{S}^1$

Due to the topology of $\mathbb{S}^2 \times \mathbb{S}^1$ there is another type of gluing of a handle to be considered which can not occur in \mathbb{S}^3 . In order to describe it, we build a round handle R_1 in $\mathbb{S}^2 \times \mathbb{S}^1$. Start with a non-separable sphere \mathbb{S}^2 and remove two disjoint disk D_1 and D_2 . Now consider a product of $\mathbb{S}^2 - (D_1 \sqcup D_2)$ with an interval I . This manifold is a 3-manifold, R_1 , such that the boundary ∂R_1 is composed by four annuli. One can put a saddle periodic orbit inside of R_1 , as shown in Figure 4.16.

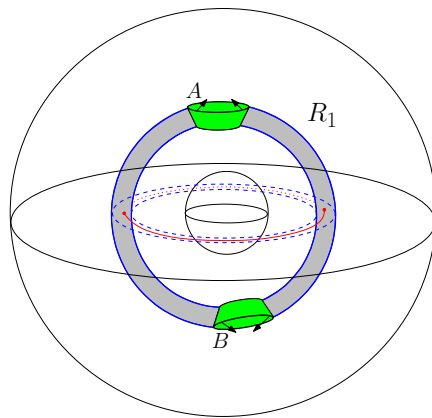


Figure 4.16: Special round handle in $\mathbb{S}^1 \times \mathbb{S}^2$.

Let N be a compact, connected 3-manifold with nonempty and connected boundary

which is inside a 3-ball in $\mathbb{S}^2 \times \mathbb{S}^1$. In the boundary of N , ∂N consider two disjoint disks D_1 and D_2 and inside each one of them other smaller disks $\bar{D}_1 \subset D_1$ and $\bar{D}_2 \subset D_2$ such that the annuli $A_1 = D_1 - \bar{D}_1$ and $B_1 = D_2 - \bar{D}_2$ have boundaries $\alpha'_1 = \partial D_1$, $\alpha'_2 = \partial \bar{D}_1$, $\beta'_1 = \partial D_2$ and $\beta'_2 = \partial \bar{D}_2$. A round handle R is homeomorphic to $\mathbb{S}^1 \times [a, b] \times [c, d]$. Consider the following circles $\beta_1 = \mathbb{S}^1 \times \{a\} \times \{c\}$, $\beta_2 = \mathbb{S}^1 \times \{b\} \times \{c\}$, $\alpha_1 = \mathbb{S}^1 \times \{a\} \times \{d\}$ and $\alpha_2 = \mathbb{S}^1 \times \{b\} \times \{d\}$. Also, consider the annuli $A = \mathbb{S}^1 \times [a, b] \times \{d\}$, $B = \mathbb{S}^1 \times [a, b] \times \{c\}$, $E = \mathbb{S}^1 \times \{a\} \times [c, d]$ and $F = \mathbb{S}^1 \times \{b\} \times [c, d]$. With this decomposition we now describe the special gluing of R_1 to the 3-manifold N . The annulus A is glued to A_1 and B to B_1 in such a way that α_1 is identified to α'_2 and α_2 is identified to α'_1 . Also, β_1 is identified to β'_1 and β_2 is identified to β'_2 . See Figure 4.17.

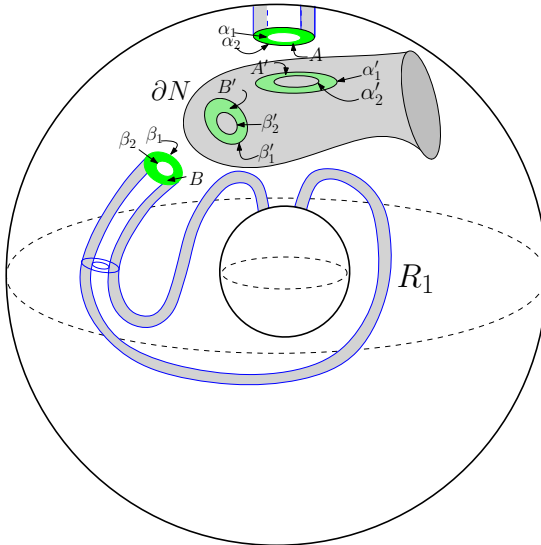


Figure 4.17: Gluing of the special round handle.

The following proposition was proved in Ledesma, Manzoli Neto, and de Rezende (2015).

Proposition 4.2. *With the previous notation, it follows that:*

1. $\partial(N \cup R_1)$ is homeomorphic to ∂N .
2. If N is a handlebody of genus g embedded in a 3-ball in $\mathbb{S}^2 \times \mathbb{S}^1$ and

$$X = N \cup R_1$$

as described above, then $\mathbb{S}^2 \times \mathbb{S}^1 - X$ is homeomorphic to a handlebody of genus g .

Before we enunciate a theorem that characterizes Lyapunov graphs on $\mathbb{S}^2 \times \mathbb{S}^1$, the following proposition characterizes a very special type of isolating block which can not be realized in \mathbb{S}^3 .

Proposition 4.3. *Let v be a vertex of L labelled with a periodic orbit and suppose that*

$$e^- = e^+ = 1 \quad \text{and} \quad g^- = g^+ = 0.$$

Then, there exists an isolating block M_v in $\mathbb{S}^2 \times \mathbb{S}^1$ for a periodic orbit with one entering and one exiting boundary component which are 2-spheres. Furthermore, $\mathbb{S}^2 \times \mathbb{S}^1 - M_v$ is homeomorphic to $D_1^3 \sqcup D_2^3$, a disjoint union of two 3-balls.

Proof. By the construction of R_1 , we have that

$$R_1 = \overline{\mathbb{S}_a^2 - (D_1^2 \cup D_2^2)} \times I$$

where \mathbb{S}_a^2 is a non-separating sphere on $\mathbb{S}^2 \times \mathbb{S}^1$. The annuli $\partial D_1^2 \times I$ and $\partial D_2^2 \times I$ are the gluing regions. For the case of a genus zero handlebody, a 3-ball should be glued to the above annuli using two 2-disks on the boundary of the 3-ball, as shown in the Figure 4.18-(a).

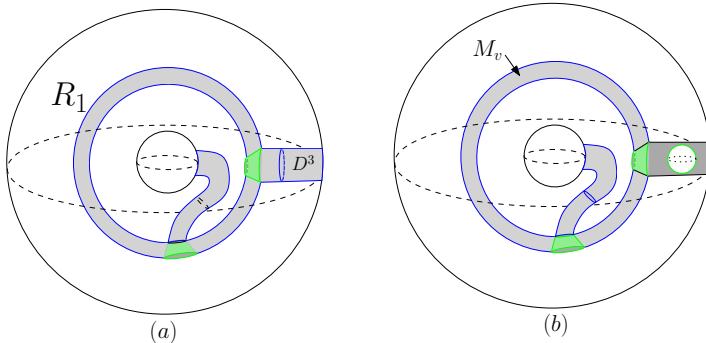


Figure 4.18: Especial round handle glues to 3-ball.

Note that the final manifold is isotopic to a tubular neighborhood of $\mathbb{S}_a^2 \vee \mathbb{S}_b^1$, where \mathbb{S}_a^2 is a fiber of $\mathbb{S}^2 \times \mathbb{S}^1 \rightarrow \mathbb{S}^1$ and \mathbb{S}_b^1 is a fiber of $\mathbb{S}^2 \times \mathbb{S}^1 \rightarrow \mathbb{S}^2$. Thus, the complement in $\mathbb{S}^2 \times \mathbb{S}^1$ is homeomorphic to a 3-ball. Therefore, the isolating block M_v is shown in Figure 4.18-(b). \square

The next theorem is a characterization of Morse–Smale flows on $\mathbb{S}^2 \times \mathbb{S}^1$. A more general theorem characterizing Smale flows on $\mathbb{S}^2 \times \mathbb{S}^1$ can be found in Ledesma, Manzoli Neto, and de Rezende (2015).

Theorem 4.4. Let L be an abstract Lyapunov graph. L is associated to a Lyapunov function and a Morse–Smale flow ϕ_t on $\mathbb{S}^2 \times \mathbb{S}^1$ if and only if the following statements hold.

1. The underlying graph L has $\kappa \leq 1$ with exactly one edge attached to each sink or source vertex. Moreover, the sink (source) vertex is labeled with an attracting $h_0 = 1$ (repelling $h_3 = 1$) singularity or an attracting $h_0 = h_1 = 1$ (repelling $h_2 = h_3 = 1$) periodic orbit.
2. If a vertex v is labelled with a saddle singularity, $h_2 = 1$ (resp. $h_1 = 1$), then $1 \leq e^+ \leq 2$ and $e^- = 1$ (resp. $e^+ = 1$ and $1 \leq e^- \leq 2$), where e^+ (e^-) is the number of incoming (outgoing) edges of v .
3. If a vertex v is labeled with a saddle periodic orbit, $h + 1 = h_2 = 1$, and $g_i^+ (g_j^-)$ are the weights on the incoming (outgoing) edges incident to v , where $G^- = \sum_{i=1}^{e^-} g_i^-$ and $G^+ = \sum_{i=1}^{e^+} g_i^+$, then there are two cases to consider: $\kappa = 0$ and $\kappa = 1$.

- (a) If $\kappa = 1$ then

$$e^- \leq 2 \quad \text{and} \quad e^+ \leq 2. \quad (4.5)$$

- (b) If $\kappa = 0$

- i. there exists at most one vertex labeled with a saddle periodic orbit with

$$e^+ = e^- = 1 \text{ and } G^- = G^+ = 0. \quad (4.6)$$

Any other vertex labeled with a periodic orbit satisfies the inequalities in (4.5).

- ii. and if no vertex on L satisfies the equality in (4.6) then there must be an edge in L with nonzero weight.

4. All vertices must satisfy the Poincaré–Hopf condition, i.e., for a vertex labelled with a singularity of index $h_r = 1$, the condition is

$$(-1)^r = e^+ - e^- - G^+ + G^-$$

and for a vertex labelled with a periodic orbit, the condition is

$$0 = e^+ - e^- - G^+ + G^-.$$

Proof. The sufficiency of the conditions of Theorem 4.4 are presented in two parts, $\kappa = 1$ and $\kappa = 0$.

Case $\kappa = 1$: Let L be an abstract Lyapunov graph with a non oriented cycle that satisfies conditions (1), (2), (3a) and (4). Suppose that a is an edge in the cycle of L

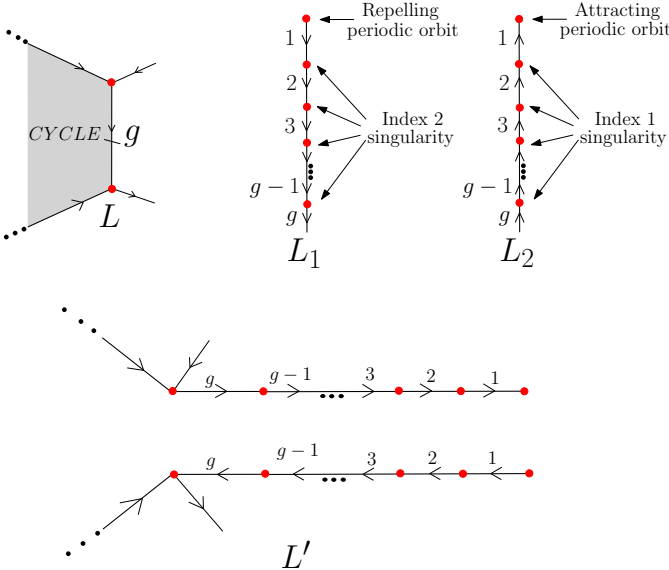


Figure 4.19: The graphs L_1 and L_2 have a dangling edge.

with weight g . Consider the graphs L_1 and L_2 each with a dangling edge as shown in Figure 4.19.

Now cut L along a and glue the graphs L_1 and L_2 by the dangling edges, as shown in Figure 4.19. Then a new abstract Lyapunov graph L' is obtained such that L' is a tree and each vertex satisfies the conditions in Theorem 4.3. Therefore, there exists a Morse–Smale flow ψ_t on S^3 with Lyapunov graph L' and such that L_1 and L_2 are associated to two handlebodies \mathcal{H}_1^g and \mathcal{H}_2^g , whose boundaries are unlinked in S^3 , as shown in Figure 4.20.

Now we cut the two neighborhoods $N(\mathcal{H}_1^g)$ and $N(\mathcal{H}_2^g)$ of \mathcal{H}_1^g and \mathcal{H}_2^g , respectively. Then, gluing $S^3 - (N(\mathcal{H}_1^g) \sqcup N(\mathcal{H}_2^g))$ along $\partial N(\mathcal{H}_1^g)$ and $\partial N(\mathcal{H}_2^g)$ in an appropriate manner, we obtain a Morse–Smale flow φ_t on $S^2 \times S^1$ with Lyapunov graph L .

Case $\kappa = 0$: In this case one considers two possibilities: (3b)(i) and (3b)(ii).

Let L be an abstract Lyapunov tree which satisfies (1), (2), (3b)(ii) and (4). By condition (3b)(ii), there is an edge a of L such that the weight of a is $g > 0$. Now cut L along a and glue the graphs L_1 and L_2 by the dangling edges as shown in Figure 4.21.

The new graphs L'_1 and L'_2 are obtained. Since L'_1 and L'_2 satisfy the conditions of Theorem 4.3, there exist Smale flows ψ_t and ϕ_t on S^3 such that L_1 corresponds to a flow on the unknotted handlebody \mathcal{H}_1^g and L_2 corresponds to a flow on the unknotted handlebody \mathcal{H}_2^g , as shown in Figure 4.22.

Then glue $((\mathcal{H}_1^g)^c, \psi_t|_{(\mathcal{H}_1^g)^c})$ and $((\mathcal{H}_2^g)^c, \psi_t|_{(\mathcal{H}_2^g)^c})$ in an appropriate manner along

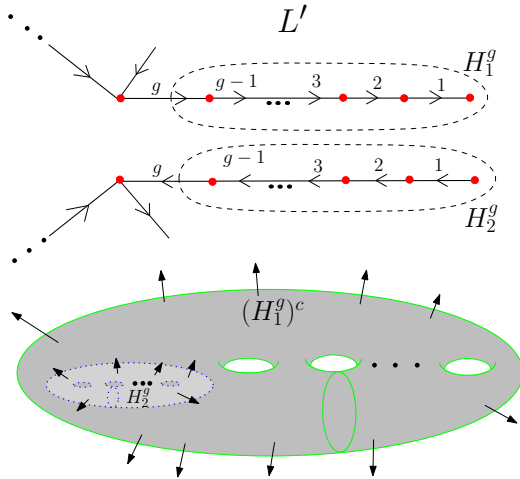


Figure 4.20: The complement of an unknotted handlebody in \mathbb{S}^3 is another unknotted handlebody of the same genus.

their boundaries. One obtains a Morse–Smale flow ξ_t on $\mathbb{S}^2 \times \mathbb{S}^1$ with Lyapunov graph L .

Let L be an abstract Lyapunov tree which satisfies (1), (2), (3b)(i) and (4). Let v be the unique vertex that satisfies (4.6). By Proposition 4.3, there exists a Morse–Smale flow ϕ_t on $\mathbb{S}^2 \times \mathbb{S}^1$ and an isolating block M_v embedded in $\mathbb{S}^2 \times \mathbb{S}^1$, associated to the vertex v . Also, $\mathbb{S}^2 \times \mathbb{S}^1 - M_v$ is homeomorphic to $D_1^3 \sqcup D_2^3$. Now, by cutting L along the incoming and outgoing edge incident to v , one obtains two semigraphs with dangling edges which can be denoted by L_1 and L_2 , as shown in Figure 4.23

We use the semigraphs L'_1 and L'_2 with dangling edges to create the new graphs \hat{L} and \tilde{L} , as shown in Figure 4.23. Then by Theorem 4.3, there exists Morse–Smale flows ϕ_t^i and φ_t^j on \mathbb{S}^3 such that L_1 and L_2 correspond to two 3-ball D_1^+ and D_2^- respectively.

One has constructed Morse–Smale flows on $(M_v, \phi_t|_{M_v})$, $(D_1^+, \phi_t|_{D_1^+})$ and on $(D_2^-, \varphi_t|_{D_2^-})$. Finally, by gluing these manifolds in an appropriate manner one obtains a Morse–Smale flow on $\mathbb{S}^2 \times \mathbb{S}^1$ with Lyapunov graph L . \square

Example 4.3. Let us illustrate a realization of a Lyapunov graph L on $\mathbb{S}^2 \times \mathbb{S}^1$. Start with a graph L that satisfies the conditions in Theorem 4.4 and assume that $\kappa = 1$ as shown in the Figure 4.24

Construct an isolating block for each vertex in L as shown in Figure 4.25.

One can proceed as in Example 4.2 since L' satisfies the conditions of Theorem 4.3. Since $M_{v'_2}$ and $M_{v'_3}$ are 3-balls, we have that $\mathbb{S}^3 \setminus M_{v'_2}$ is a 3-ball, then $(\mathbb{S}^3 \setminus M_{v'_2}) \setminus M_{v'_3}$

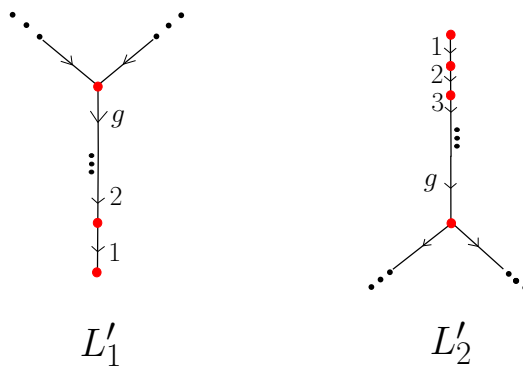
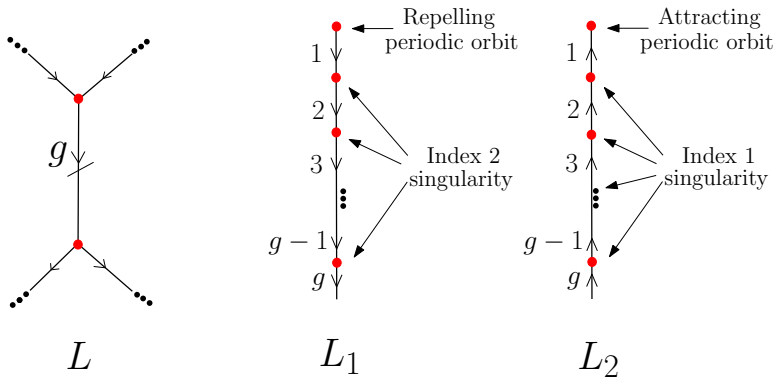


Figure 4.21: The semigraphs L_1 and L_2 have dangling edges.

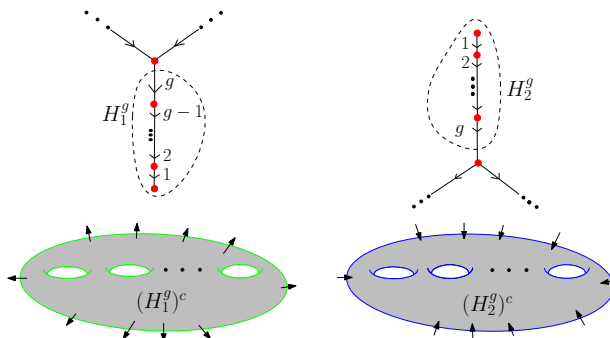
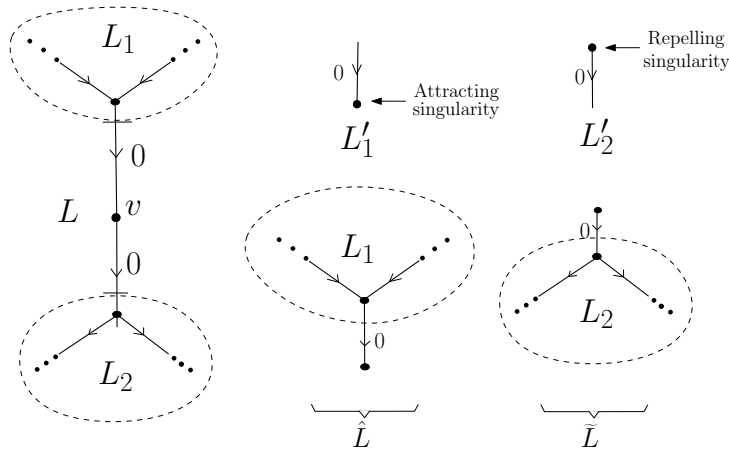
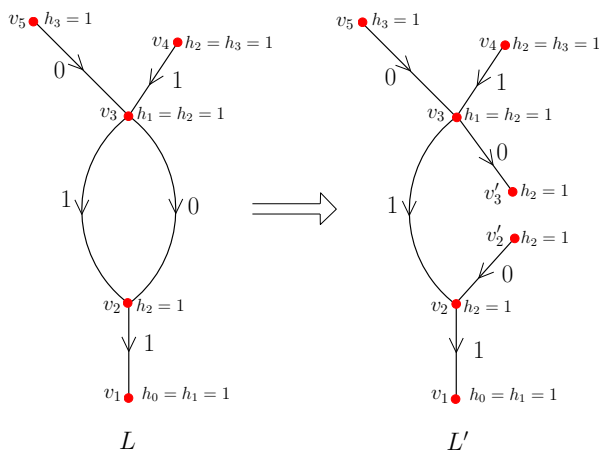


Figure 4.22: L'_1 and L'_2 correspond to Morse–Smale flows on two handlebodies in \mathbb{S}^3

Figure 4.23: v is a special vertex in $\mathbb{S}^2 \times \mathbb{S}^1$.Figure 4.24: Realizable Lyapunov graph in $\mathbb{S}^2 \times \mathbb{S}^1$ with cycle.

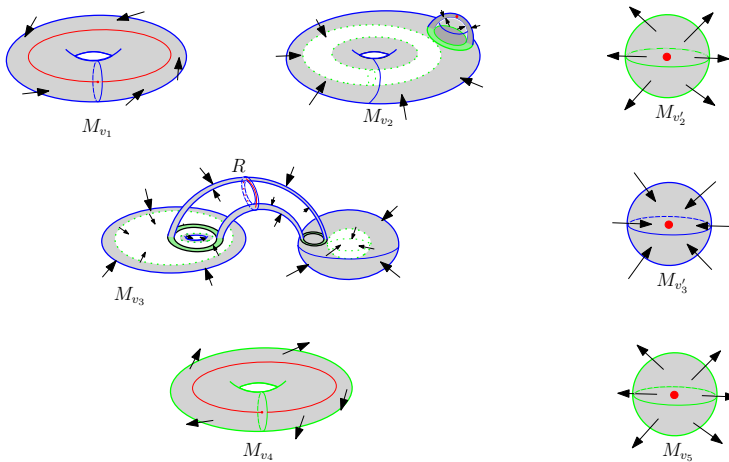


Figure 4.25: Isolating blocks associated to L' .

is a manifold as shown in Figure 4.26.

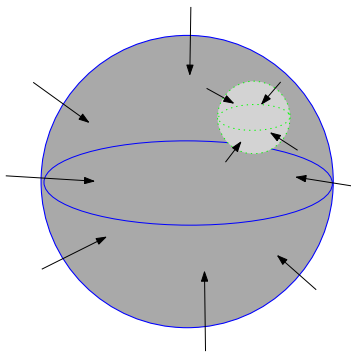


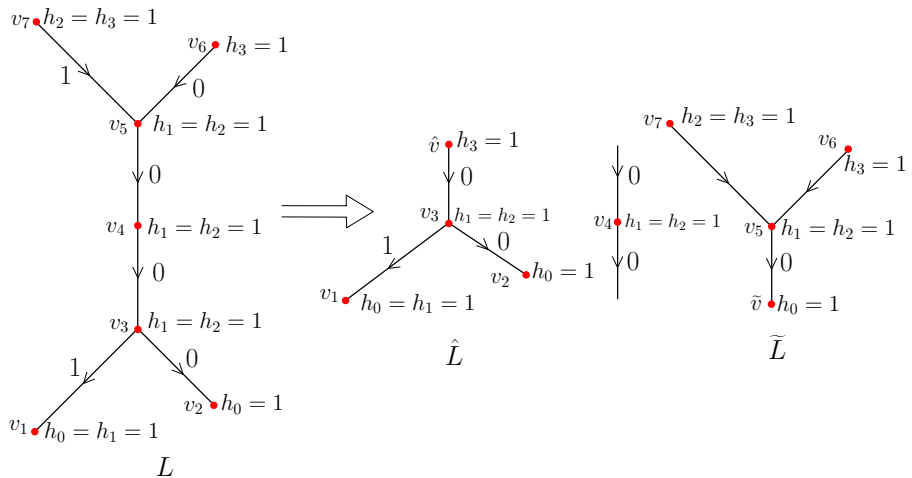
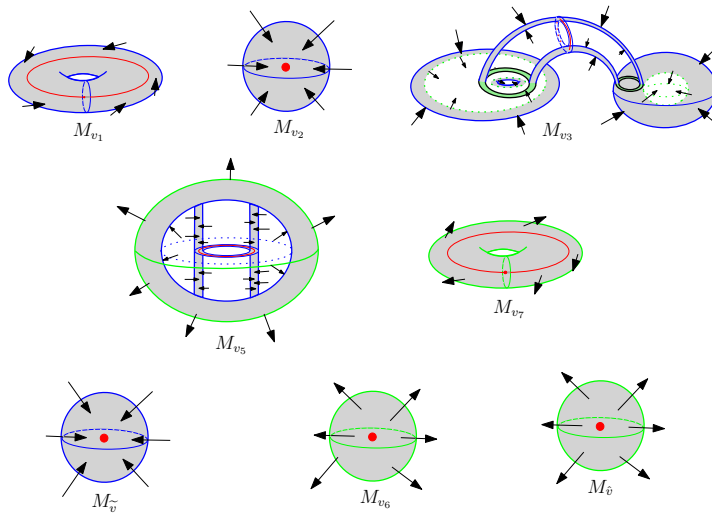
Figure 4.26: The flow enters through the external boundary component and exits through the internal boundary component.

Now we glue both components of the boundary in such way as to obtain $\mathbb{S}^2 \times \mathbb{S}^1$.

Example 4.4. In this example assume that L satisfies the conditions in Theorem 4.4, $\kappa = 0$ and also with a vertex satisfying 4.6, as shown in Figure 4.27.

Since \hat{L} and \widetilde{L} satisfy the conditions of Theorem 4.3, one can build an isolating block for each vertex of the graph as shown in Figure 4.28.

Furthermore, one can use this isolating block to define a Morse–Smale flow on \mathbb{S}^3 in the such way that $\mathbb{S}^3 \setminus M_{\hat{v}}$ and $\mathbb{S}^3 \setminus M_{\hat{v}}$ are homeomorphic to a 3-ball. Finally, by gluing

Figure 4.27: Graph without oriented cycles and with a special vertex realizable in $\mathbb{S}^2 \times \mathbb{S}^1$ Figure 4.28: Isolating block realizing \hat{L} and \tilde{L} .

both 3-balls with the isolating block shown in Figure 4.18, one obtains a Morse–Smale flow on $\mathbb{S}^2 \times \mathbb{S}^1$.

4.3 Realizing Admissible Lyapunov graphs in higher dimensions

The realizability problem for an abstract Lyapunov graph L , in dimension n , is far too general. Thus, we address questions on Morsification. Does L admit a Morsification? This was answered in the previous two chapters. Is the Morsification of L realizable? To answer this question is our goal in this section.

Recall that in Chapter 2 we defined *admissible graphs* as abstract Lyapunov graphs $L(h_0, \dots, h_n, \kappa)$ that satisfy the Poincaré–Hopf inequalities (2.4)–(2.6) at each vertex. These graphs have the property that they are morsifiable as was proved in Chapter 3.

Recall also, that by definition, Betti number vectors whose components $\{B_j^+\}_{j=0}^{n-1}$ and $\{B_j^-\}_{j=0}^{n-1}$ are integers satisfy the duality condition, that is, $B_j^+ = B_{n-1-j}^+$ and $B_j^- = B_{n-1-j}^-$ for all $j = 0 \dots n - 1$. If $n = 2i + 1$, let $B_i^+ = B_i^- = 0 \bmod 2$. Moreover admissibility implies that the integers $\{h_j\}_{j=1}^{n-1}$ satisfy the Poincaré–Hopf inequalities.

In order to simplify the amount of information with which an admissible Lyapunov graph is labelled, the following convention is adopted:

- each vertex v is labelled with a list of nonnegative integers

$$(h_0(v) = k_0, \dots, h_n(v) = k_n, \kappa(v)),$$

where $\kappa(v)$ is the *cycle number* of the vertex and any zero entry in this list is omitted;

- because of duality each edge is labelled with a Betti number vector that can be represented up to mid-dimension: $(\beta_1, \dots, \beta_{\lfloor \frac{n-1}{2} \rfloor})$ where we omit $\beta_0 = 1$ since this is always the case.

See Figure 4.29.

We now state a realizability theorem for $n = 2i + 1$.

Theorem 4.5. *Let L be an admissible Lyapunov semigraph in dimension $n = 2i + 1$ with e^+ and e^- incoming and outgoing edges. Then there exists an n -dimensional connected manifold M with boundary $\partial M = N^+ \cup N^-$, $N^+ \cap N^- = \emptyset$, and a Morse–Smale flow without periodic orbit on M such that*

1. *e^+ is the number of connected components of N^+ , the entering boundary of the flow, and e^- is the number of connected components of N^- , the exiting boundary of the flow;*
2. *if β_j^+ (respectively β_j^-) denotes the j -th Betti number of N^+ (respectively N^-), then*

$$\beta_j^+ = B_j^+, \quad \beta_j^- = B_j^-, \quad \text{for all } j = 0 \dots (n-1);$$

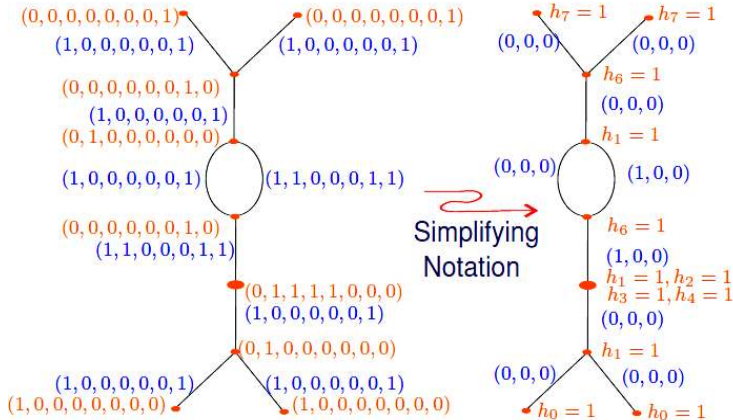


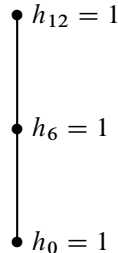
Figure 4.29: Example: Abstract Lyapunov Graph in dimension 7

3. for all $j = 1 \dots (n - 1)$, the rank of the homology Conley index is preserved, that is,

$$\text{rank } H_j(M, N^-) = h_j.$$

In this section, we layout the main steps of the proof of Theorem 4.5 and refer the reader to Bertolim, de Rezende, and Manzoli Neto (2007), Bertolim, de Rezende, Manzoli Neto, and Vago (2006), Bertolim, de Rezende, and Vago (2006), and Cruz and de Rezende (1999) for greater details as well as more general theorems.

The first natural question is to consider whether admissible Lyapunov graphs are realizable as gradient-like flows on compact manifolds with or without boundary. The answer to this question depends on the dynamical data and the ambient dimension of the manifold. For instance, for abstract Lyapunov graphs in dimension $n \equiv 0 \pmod{4}$ where β_i -vertices are present, there are examples that are non-realizable, see Figure 4.30.

Figure 4.30: Admissible non-realizable abstract Lyapunov graph in dimension $n = 12$.

Secondly, if the graph is realizable, we would like to know in how many different ways can this realizability be achieved, since an admissible Lyapunov graph can be morsified in many ways, see Bertolim, Mello, and de Rezende (2003a) and Bertolim, Mello, and de Rezende (2005a). It is natural to start our study of realizability with admissible Lyapunov graphs of Morse type, since these constitute the most elementary class.

As in Cruz and de Rezende (1999), we need to enrich the labelling of an admissible Lyapunov graph of Morse type $L(h_0, \dots, h_n, \kappa)$ by a *null-trivial-dual-labelling*, in short, an *ntd*-labelling. An *ntd*-labelling is the pairing up of all vertices (except two, one h_0 and one h_n vertex) in an admissible graph by using the types:

1. κ -dual: $\{h_{n-1} = 1 \text{ of type } (n-1)\text{-d}, h_1 = 1 \text{ of type } 0\text{-c}\}$.
2. dual: $\{h_j = 1 \text{ of type } j\text{-d}, h_{n-j} = 1 \text{ of type } (n-j-1)\text{-c}\}$, for $j = 1, \dots, n-2$.
3. null: $\{h_j = 1 \text{ of type } j\text{-d}, h_{j+1} = 1 \text{ of type } j\text{-c}\}$, for $j = 1, \dots, n-2$.
4. trivial: $\{h_1 = 1 \text{ of type } 0\text{-c}, h_0\}$ (first type) and $\{h_{n-1} = 1 \text{ of type } (n-1)\text{-d}, h_n\}$ (second type).
5. β -invariant: $\{h_i = 1 \text{ for } n = 2i \text{ and } 2i = 0 \pmod 4\}$

This labelling is related to the types of gluing maps used in the attachment of handles to construct the isolating block as shall be seen subsequently. All h_j vertices can be paired up in this way when n is odd. Whenever n is even, say $n = 2i$, recall that h_i may be of type $(i-1)\text{-c}$, $i\text{-d}$ or $\beta\text{-i}$. The vertex h_i can only be labelled with $\beta\text{-i}$ if $2i = 0 \pmod 4$. It may occur that two h_i 's labelled with $\beta\text{-i}$ singularities may form a dual pair. In order to simplify nomenclature, we still refer to this as *ntd*-labellings although in the case $n = 2i$ with $2i = 0 \pmod 4$, there may be $\beta\text{-i}$ vertices.

Our objective in this section is to layout a synopsis of a scheme devised in Bertolim, de Rezende, and Manzoli Neto (2007) and Bertolim, de Rezende, Manzoli Neto, and Vago (2006) for the construction of compact n -manifolds that realize admissible Lyapunov semigraphs of Morse–Smale type. Since the dynamics of Morse–Smale singularities and periodic orbits in dimension n is basal, one starts by considering admissible Lyapunov semigraphs with a single vertex of Morse–Smale type and investigate its realizability as a gradient-like flow on an isolating block. We refer the reader to the original papers for more detailed proofs.

This is done in the following sections, first for Morse singularities and secondly for hyperbolic periodic orbits.

4.3.1 Constructing Isolating Blocks of Morse type

One begins with the elemental question: the realization of semigraphs L_v where v is labelled as a Morse singularity of index k , i.e., $h_k = 1$. By constructing n dimensional isolating blocks for Morse singularities, which comprise the most elementary building

blocks, we are ready to tackle the global realization of admissible Lyapunov graphs as gradient-like flows on closed manifolds.

An *admissible Lyapunov graph of Morse type* is an abstract Lyapunov graph that satisfies the following:

1. every vertex v is labelled with $h_k = 1$ for some $k = 0, \dots, n$.
2. the number of incoming edges, e^+ , and outgoing edges, e^- , incident to v must satisfy:
 - (a) $e^- = 0$ and $e^+ = 1$ if $h_0 = 1$; $e^+ = 0$ and $e^- = 1$ if $h_n = 1$.
 - (b) $e^+ = e^- = 1$ if $h_k = 1$ and $1 < k < n - 1$;
 - (c) $e^+ = 1$ and $0 < e^- \leq 2$ if $h_1 = 1$; $e^- = 1$ and $0 < e^+ \leq 2$ if $h_{n-1} = 1$;
3. every vertex labelled with $h_\ell = 1$ must be of type ℓ -d or $(\ell - 1)$ -c. Furthermore, if $n = 2k$, ($2k = 0 \pmod{4}$) and $h_k = 1$, then v may be labelled with β -i.

Therefore, an abstract Lyapunov graph of Morse type in dimension n must satisfy the following local conditions depicted in Figure 4.31.

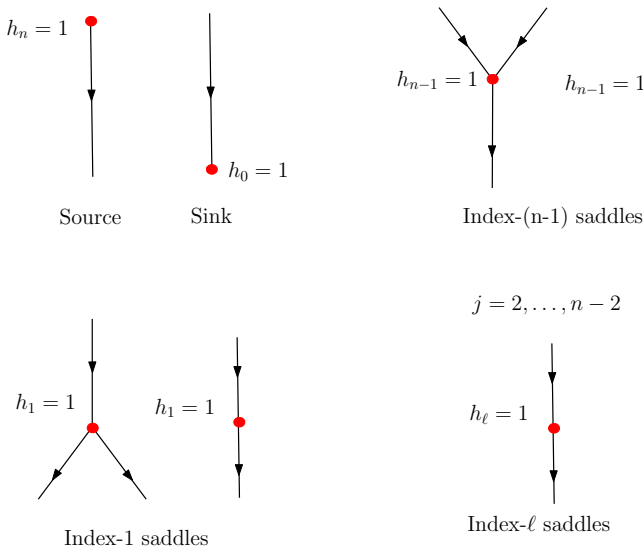
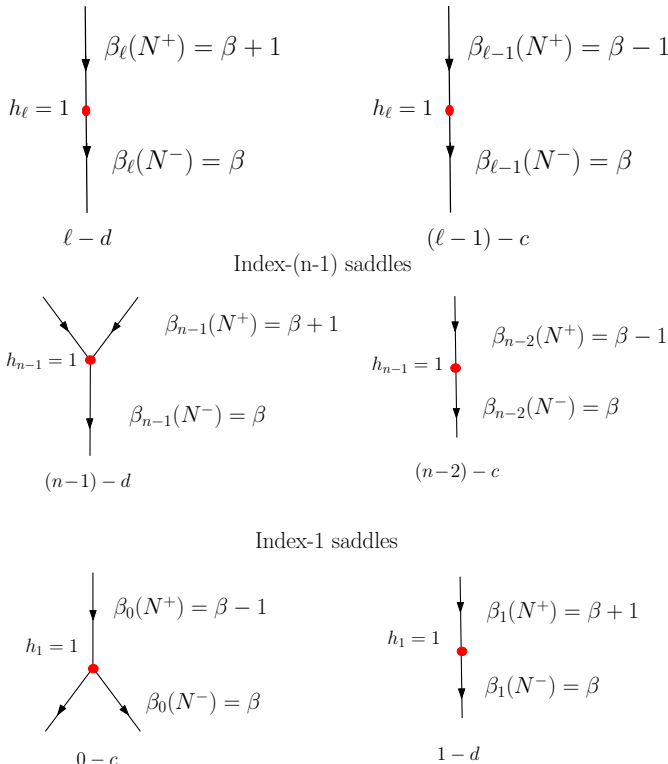
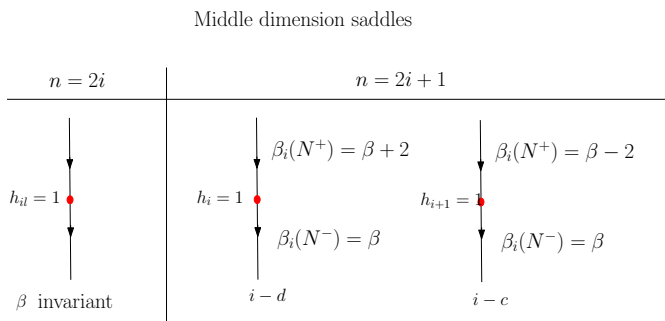


Figure 4.31: Morse type semigraphs have vertices with degree ≤ 3

We have a finer control on the effect that Morse singularities of index ℓ have on the Betti numbers of the boundary of its isolating block by taking into account the additional information whether it is $\ell - d$ or $(\ell - 1) - c$. See Figure 4.32.

Figure 4.32: Effect on the Betti numbers of N^+ and N^- for saddles of index $1 \leq \ell \leq n-1$.Figure 4.33: Morse type semigraphs in dimensions $n = 2i = 0 \pmod{4}$ and $n = 2i + 1$ for saddles of index i .

We now turn our attention to the construction of an isolating block (N, N^+, N^-) for a flow whose maximal invariant set in N is a Morse singularity of index equal to the one indicated on the vertex v of L_v as in Figure 4.32 and Figure 4.33. Moreover, the Betti numbers of the incoming and outgoing boundary components, N^+ and N^- respectively, of the flow on N , match the Betti number vectors on the incoming and outgoing edges incident to v . One says that the flow on N is a realization of an admissible Lyapunov graph of Morse type, L_v .

In order to realize the effects on the Betti numbers on the edges of the Morse type semigraphs in Figure 4.32 and Figure 4.33, it suffices to describe four types of standard gluings of handles. Namely, the trivial gluing, the null gluing the dual gluing and the invariant gluing. We describe them briefly and refer the reader to Bertolim, de Rezende, Manzoli Neto, and Vago (2006) for details.

The following notation is adopted: an n -dimensional handle of index q is denoted by H_q . See Chapter 2. The n -dimensional manifold obtained after the gluing of a handle in step i is denoted by M_i and its modified boundary by N_i . The changes produced by the gluings are described in terms of the connected sum along the boundary, denoted by \natural whereas \sharp denotes the usual connected sum.

Let M_0 be an n -dimensional manifold and N_0 its boundary.

1. A *trivial gluing* of a handle of index q , H_q , to a disc $D^n = D^q \times D^{n-q} = B_0$ creates a q -handlebody \mathcal{H}_q .

Glue the q -handle H_q to the upper hemisphere of the boundary of B_0 to obtain the q -handlebody \mathcal{H}_q defined by

$$\mathcal{H}_q = \underbrace{(D^q \times D^{n-q})}_{B_0} \cup_{\mathbb{S}^{q-1} \times D^{n-q}} \underbrace{(D^q \times D^{n-q})}_{H_q} = \mathbb{S}^q \times D^{n-q}$$

The attachment of the handle modifies M_0 to M_1 :

$$\begin{aligned} M_1 &\stackrel{\text{def}}{=} M_0 \cup_{\mathbb{S}^{q-1} \times D^{n-q}} H_q \\ &= M_0 \natural \mathcal{H}_q \end{aligned}$$

The boundary N_0 is modified to N_1 :

$$\begin{aligned} N_1 &\stackrel{\text{def}}{=} N_0 \setminus \underbrace{(\mathbb{S}^{q-1} \times \text{int}(D^{n-q}))}_{\text{interior of the attaching region of } H_q} \cup_{\mathbb{S}^{q-1} \times \mathbb{S}^{n-q-1}} \underbrace{(D^q \times \mathbb{S}^{n-q-1})}_{\text{belt region of } H_q} \\ &= N_0 \natural \partial \mathcal{H}_q = N_0 \natural (\mathbb{S}^q \times \mathbb{S}^{n-q-1}) \end{aligned}$$

The effect of the trivial gluing on the Betti numbers of the boundary is that only the q -th Betti number β_q and its dual β_{n-q-1} have changed by being increased by 1. For this reason, the trivial gluing of H_q is of type q -d.

2. A *null gluing* of two handles of consecutive indices, H_q and H_{q+1} consists of two steps. One glues H_q trivially on a disk D^{n-1} of the boundary N_0 .

$$\begin{cases} M_1 = M_0 \# \mathcal{H}_q \\ N_1 = N_0 \# \partial \mathcal{H}_q = N_0 \# (\mathbb{S}^q \times \mathbb{S}^{n-q-1}) \end{cases}$$

Now, glue H_{q+1} to \mathcal{H}_q in order to obtain an n -dimensional disk. Note that during this process the lower hemisphere of B_0 of the previous step is never modified. Hence, M_2 is obtained:

$$\begin{aligned} M_2 &\stackrel{\text{def}}{=} M_1 \cup_{\mathbb{S}^q \times D^{n-q-1}}^{(\text{null})} H_{q+1} = \\ &= M_0 \# \underbrace{(\mathcal{H}_q \cup_{\mathbb{S}^q \times D^{n-q-1}}^{(\text{null})} H_{q+1})}_{D^n} = \\ &= M_0 \# D^n = M_0. \end{aligned}$$

On the other hand,

$$N_2 = N_0 \# \partial D^n = N_0.$$

The effect of a null gluing on the Betti numbers of the boundary is globally null. After the trivial gluing of H_q of type q -d, only the q -th Betti number β_q and its dual β_{n-q-1} have changed by being increased by 1. After the gluing of H_{q+1} of type q -c the same Betti numbers β_q and β_{n-q-1} decreases by 1.

3. A *dual gluing* of two handles of complementary indices H_q and $H_{(n-q)}$ is obtained in two steps. First glue H_q to M_0 via a trivial gluing so as to obtain a q -handlebody \mathcal{H}_q . One obtains:

$$\begin{cases} M_1 = M_0 \# \mathcal{H}_q \\ N_1 = N_0 \# \partial \mathcal{H}_q = N_0 \# (\mathbb{S}^q \times \mathbb{S}^{n-q-1}) \end{cases}$$

Next, attach the $(n-q)$ -handle H_{n-q} by identifying its attaching region $\mathbb{S}^{n-q-1} \times D^q$ to the belt region of H_q :

$$\partial H_q \cap N_1 = \partial H_q \setminus (\mathbb{S}^{q-1} \times \text{int}(D^{n-q})) = D^q \times \mathbb{S}^{n-q-1} = \mathbb{S}^{n-q-1} \times D^q$$

The resulting manifold is

$$M_2 = M_0 \# \mathbb{S}^q \times \mathbb{S}^{n-q}$$

and its boundary is

$$N_2 = N_0.$$

the effect of the dual gluing on the Betti numbers of the boundary is globally null. After the first step, only the q -th Betti numbers β_q and its dual β_{n-q-1} have changed

by being increased by 1 (trivial gluing of H_q of type q-d). After the second step, the gluing of H_{n-q} decreases by 1 the same Betti numbers β_q and β_{n-q-1} (gluing of H_{n-q} of type $(n-q-1)$ -c).

4. An *invariant gluing* occurs only for the attaching of a $2k$ handle, H_{2k} , on a $4k$ -manifold where there is a possibility of gluing the corresponding handle in an invariant way, that is, in such a way that the Betti numbers of the boundary after such a gluing are the same as those of the boundary before the gluing. We say these handles H_{2k} are of type β -i. Invariant gluings occur in the construction of projective spaces \mathbb{CP}^{2k} , \mathbb{HP}^{2k} and \mathbb{OP}^{2k} and in all these cases the middle dimensional handle is necessarily of type β -i. The following orientable projective spaces are the only ones that admit a minimal 3 handle decomposition: \mathbb{CP}^2 , \mathbb{HP}^2 or \mathbb{OP}^2 .

Let \mathbb{P}^{2k} be a projective space. Let M_0 be a $2k$ submanifold with boundary N_0 . Take the interior of a $2k$ -dimensional ball B_0 out of M_0 so that the upper hemisphere of ∂B_0 is a D^{2k-1} in N_0 . Glue to B_0 a k -handle in order to obtain the complement of a ball in \mathbb{P}^{2k} , that is, $\mathbb{P}^{2k} \setminus B_n$. By identifying the boundary of this manifold to that of B_0 in M_0 , we have made the following connected sum:

$$M_1 = M_0 \# \mathbb{P}^{2k}$$

whose boundary is $N_1 = N_0$.²

In order to obtain the isolating block which realizes the admissible Lyapunov semi-graph L , there are many choices in the numbers of h_j^c 's and h_j^d 's obtained by the circulation in the network flows. See Chapter 2.

In Bertolim, de Rezende, and Vago (2006) a useful decomposition theorem which reflects the combinatorics of a vertex of L is obtained. Its first step is to determine the singularities needed to make the homological gaps recorded on the e^+ incoming and e^- outgoing edges of v , vanish. Of course, these gaps are measured by the differences $\{(B_j^+ - B_j^-)\}_{j=0}^{n-1}$ such that $(B_j^+ - B_j^-) = (B_{n-1-j}^+ - B_{n-1-j}^-)$ for all $j = 0 \dots n-1$, and $(B_i^+ - B_i^- = 0) \bmod 2$ if $n = 2i + 1$.

Moreover, the goal is to achieve the construction of an n -dimensional manifold M with the minimal number of singularities, with boundary $\partial M = N^+ \cup N^-$ such that $N^+ \cap N^- = \emptyset$ and e^+ is the number of connected components of N^+ , e^- is the number of connected components of N^- and $(B_j^+ - B_j^-)$ is the difference of the j -th Betti numbers of the boundary components.

One has the following theorem whose proof can be found in Bertolim, de Rezende, and Vago (ibid.).

Theorem 4.6. *Let e^+ and e^- be positive integers. Let $\{(B_j^+ - B_j^-)\}_{j=0}^{n-1}$ be integers such that $(B_j^+ - B_j^-) = (B_{n-1-j}^+ - B_{n-1-j}^-)$ for all $j = 0 \dots n-1$. If $n = 2i + 1$, let*

²For $n = 12$ or $n = 4k$ with $k \geq 5$ no invariant gluing with the decomposition of the form (h_0, h_{2k}, h_n) is possible. Although invariant handles may still exist for middle dimensional handles whenever $n = 4k$ but in larger decompositions. See Eells and Kuiper (1962).

$(B_i^+ - B_i^- = 0) \bmod 2$. Then any flow on any n -dimensional manifold M satisfying the given homological boundary conditions must have at least h_{\min} singularities, where

$$h_{\min} = \begin{cases} e^+ + e^- - 2 + \sum_{j=1}^{i-1} |B_j^+ - B_j^-|, | + \left| \frac{B_i^+ - B_i^-}{2} \right| & \text{if } n = 2i + 1; \\ e^+ + e^- - 2 + \sum_{j=1}^i |B_j^+ - B_j^-| & \text{if } n = 2i. \end{cases}$$

Moreover, such h_{\min} singularities are of the following indices and types. Let h_j^d denote the number of singularities of index j and type j -d, and let h_j^c denote the number of singularities of index j and type $(j-1)$ -c.

- * We have $h_1^c = (e^- - 1)$ and $h_{n-1}^d = (e^+ - 1)$.
- * For $j = 1 \dots \lfloor \frac{n}{2} \rfloor - (n \bmod 2)$, let k_j be any integer in $0 \dots |B_j^+ - B_j^-|$: if $B_j^+ \geq B_j^-$ then we have $h_j^d = k_j$ and $h_{n-j-1}^d = (|B_j^+ - B_j^-| - k_j)$, else we have $h_{j+1}^c = k_j$ and $h_{n-j}^c = (|B_j^+ - B_j^-| - k_j)$.
- * If $n = 2i + 1$, then either $B_i^+ \geq B_i^-$ and we have $h_i^d = \frac{|B_i^+ - B_i^-|}{2}$, or $B_i^+ < B_i^-$ and we have $h_{i+1}^c = \frac{|B_i^+ - B_i^-|}{2}$.

In other words, this theorem proves that the loose information on the boundary suffices to determine a minimal number of singularities that must be present in any realization, as well as their indices and types (connecting and disconnecting). This of course, is not unique as the following example in Bertolim, de Rezende, Manzoli Neto, and Vago (2006) shows.

Example 4.5. Consider an abstract Lyapunov semigraph with the vertex labelling unspecified as in Figure 4.34. One can ask what are the minimal number of singularities and their types present in a Morsification. Theorem 4.6 provides this lower bound in terms of the boundary data with which the edges are labelled.

For the boundary data given in Figure 4.34, Theorem 4.6 implies that $h_{\min} = 6$ and three vectors realizing it are:

$$\begin{cases} h_{\min}^{(0)} = (2, 1, 2, 1) \text{ corresponding to } \{h_1^c = 2, h_2^d = 1, h_3^d = 2, h_4^d = 1\} \\ h_{\min}^{(1)} = (3, 1, 1, 1) \text{ corresponding to } \{h_1^c = 2, h_1^d = 1, h_2^d = 1, h_3^d = 1, h_4^d = 1\} \\ h_{\min}^{(2)} = (4, 1, 0, 1) \text{ corresponding to } \{h_1^c = 2, h_1^d = 2, h_2^d = 1, h_4^d = 1\}. \end{cases}$$

Of course, once the numerical homology Conley indices are given, as in Figure 4.35, there are less choices for h_{\min} . Namely, $h_{\min}^{(0)} = (2, 1, 2, 1)$ and $h_{\min}^{(1)} = (3, 1, 1, 1)$.

The following theorem, which can be found in Bertolim, de Rezende, Manzoli Neto, and Vago (ibid.), provides a decomposition of the handles that build up an isolating block in terms of their gluings. By no means is this decomposition unique but it guarantees a realization of an abstract Lyapunov semigraph.

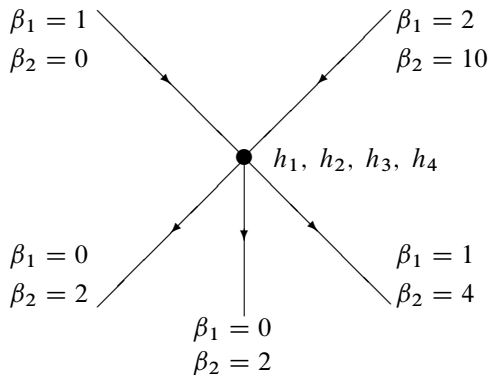
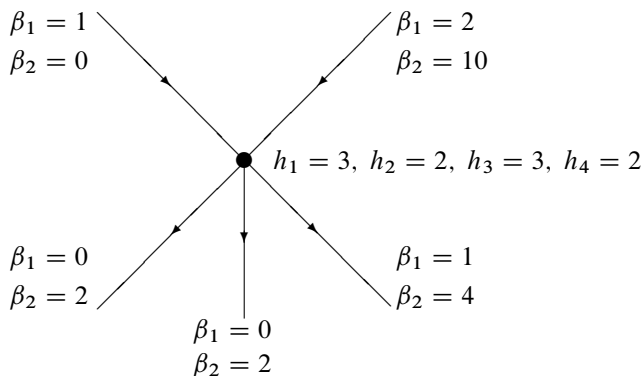


Figure 4.34: A vertex with unspecified numerical homology Conley indices

Figure 4.35: An abstract Lyapunov semigraph $n = 5$.

Theorem 4.7. Let v be a vertex of an abstract Lyapunov semigraph L . Let $\underline{h} = (h_1, \dots, h_{n-1})$ denote the label on the vertex. Then \underline{h} satisfies the Poincaré–Hopf inequalities if and only if it can be decomposed as

$$\underline{h} = \underline{h}_{\min} + \underline{h}_{\text{consecutive}} + \underline{h}_{\text{dual}} + \underline{h}_{\text{invariant}}$$

where

\underline{h}_{\min} is one of the labels associated with h_{\min} and the boundary conditions (Theorem 4.6);

$\underline{h}_{\text{consecutive}}$ is a vector corresponding to a collection of couples (H_j, H_{j+1}) with adjacent indices (necessarily of types $(j-d, j-c)$);

$\underline{h}_{\text{dual}}$ is a vector corresponding to a collection of couples (H_j, H_{n-j}) with dual indices, either of types $((j-1)-c, (n-j)-d)$ or of types $(j-d, (n-j-1)-c)$;

$\underline{h}_{\text{invariant}}$ is a vector which may be nonzero only in dimension $n = 4k$, corresponding to a collection of middle dimension H_{2k} 's of type $\beta-i$.

Proof. By Theorem 4.6, among the vertices of any Morsification, there are h_{\min} of them which are labelled in such a way that their total effect on the Betti numbers is to make the difference of the Betti numbers on the incoming and outgoing edges, vanish. Furthermore, all the other vertices together have no total effect on the difference of the Betti numbers. Either they are β -invariant (and this is possible only for the middle index $j = 2k$ in dimension $n = 4k$). Or they pair up according to the rule (H_j^d, H_{j+1}^c) , which are taken into account in $\underline{h}_{\text{consecutive}}$, or according to the rules (H_j^c, H_{n-j}^d) and (H_j^d, H_{n-j}^c) , which are taken into account in $\underline{h}_{\text{dual}}$. \square

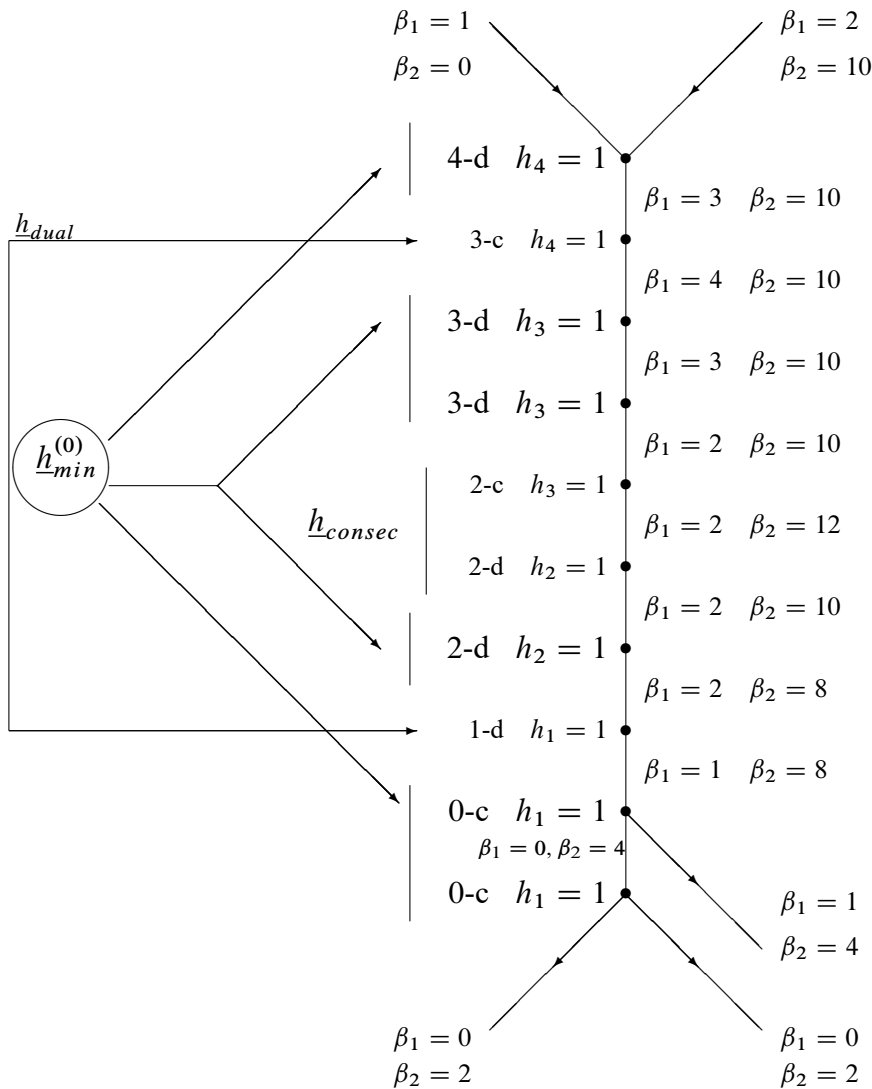
Consider the following Morsification from Bertolim, de Rezende, Manzoli Neto, and Vago (2006) in dimension $n = 5$ of the semigraph in Figure 4.35, where it is understood that for every edge we have $\beta_0 = \beta_4 = 1$ and $\beta_3 = \beta_1$. In this case $e^+ = 2$, $e^- = 3$, $(B_1^+ - B_1^-) = (1+2) - (0+0+1) = 2$, $(B_2^+ - B_2^-) = (0+10) - (2+2+4) = 2$ and $\underline{h} = (3, 2, 3, 2)$. Figure 4.36 shows the $h_{\min}^{(0)} = (2, 1, 2, 1)$ decomposition of L .

Main Steps in the Construction of an Isolating Block

By using Theorem 4.7 one can start the construction of an isolating block that realizes L by first realizing \underline{h}_{\min} . The reader is referred to Bertolim, de Rezende, Manzoli Neto, and Vago (*ibid.*) for a detailed proof.

One starts off by constructing an auxiliary manifold X possessing only incoming boundary components $\partial^+ X$ which can be described in terms of connected sums of $(n-1)$ -dimensional generalized tori and whose Betti numbers are the ones we need to define $\partial^- Y$ by $\partial^- Y := \partial^+ X$.

Next, one glues the handles of \underline{h}_{\min} to a collar of $\partial^- Y$. Start by gluing $e^- - 1$ handles of index 1 and type 0-c which connects the components of $\partial^- Y$. Then, for each one of

Figure 4.36: The $\underline{h}_{\min}^{(0)} = (2, 1, 2, 1)$ Morsification of L .

the remaining handles, if it is of type j -d and $j < n - 1$, glue it in a trivial way, with the effect of performing a connected sum with a j -handlebody. If it is of index $(j + 1)$ and type j -c, by construction it can be paired up with a ghost handle H_j of type j -d and will be attached in such a way that the two of them are glued in a null way. Ghost handles appears only in the auxiliary manifold and not in the isolating block Y itself. We are left with $e^+ - 1$ handles of index $(n - 1)$ of type $(n - 1)$ -d, which disconnects the connected sum of generalized tori. One obtains a manifold Y whose entry and exit boundaries have the needed Betti numbers.

$$\begin{cases} \#_{j=1}^i \#^{B_j^+} \mathbb{S}^j \times \mathbb{S}^{n-j-1}, & \text{if } n = 2i; \\ (\#_{j=1}^{i-1} \#^{B_j^+} \mathbb{S}^j \times \mathbb{S}^{n-j-1}) \# (\#^{\frac{B_j^+}{2}} \mathbb{S}^i \times \mathbb{S}^{n-i-1}), & \text{if } n = 2i + 1; \end{cases}$$

Two remarks are in order. Our choice of realization of \underline{h}_{\min} is done using a block which can be embedded in the sphere. However, this is arbitrary and one could have chosen, using an analogous construction, blocks which can be embedded in connected sums of generalized tori, for example.

We draw attention to the fact that since the attaching regions can all be chosen disjoint, the rank of the homology Conley index is preserved at this stage, see Conley (1978), that is,

$$\text{rank } CH_j(Y, \partial^- Y) = \text{number of handles of index } j \text{ appearing in } \underline{h}_{\min}.$$

If one wishes to control the homology Conley index of the isolating block itself then the realization of $\underline{h}_{\text{consecutive}}$, $\underline{h}_{\text{dual}}$ and $\underline{h}_{\text{invariant}}$ whenever the case, must be done carefully.

For instance, the attachment of consecutive handles as null pairs does not contribute to the homology Conley index of the isolating block since they can be removed without altering the topology.

However, gluings of consecutive handle (H_j, H_{j+1}) described subsequently has the effect of increasing the ranks of the homology Conley indices in dimensions j and $(j + 1)$ by 1, without any modification to the boundary components.

Let $\partial^- Y$ be the exit boundary of the block realizing \underline{h}_{\min} as in the previous paragraph. Let c_j be the number of consecutive couples of the form (H_j, H_{j+1}) appearing in $\underline{h}_{\text{consecutive}}$ for $j = 1 \dots n - 2$. Define N_0 as the connected sum:

$$N_0 = \partial^- Y \# (\#^{c_j} \mathbb{S}^j \times \mathbb{S}^{n-j-1})$$

and think of it as the boundary of an auxiliary manifold $X \# (\#^{c_j} \mathcal{H}_j)$ and \mathcal{H}_j denotes the j -handlebody $\mathbb{S}^j \times D^{n-j}$ obtained by gluing a *ghost handle* of index j and type j -d in a trivial way to a ball. Take a collar of N_0 and glue the handles of the class \underline{h}_{\min} to $\partial^- Y$ as described previously. Now, for all handles (H_j, H_{j+1}) of the class $\underline{h}_{\text{consecutive}}$, pair up the one of index $(j + 1)$ and type j -c with a ghost handle \hat{H}_j of one of the \mathcal{H}_j 's and attach it in such a way that the total gluing of (\hat{H}_j, H_{j+1}) is null. Glue the remaining handle H_j in a trivial way. The result of these gluings applied $\sum_j c_j$ times is that the new boundary

N_1 is homeomorphic to N_0 and hence no changes on the Betti numbers of the boundary have occurred.

Moreover, the ranks of the homology Conley indices have been increased by 1 in dimensions j and $(j + 1)$, which can again be proved by considering disjoint attaching regions or by studying long exact sequences. See Bertolim, de Rezende, Manzoli Neto, and Vago (2006) for details.

The realization of the class $\underline{h}_{\text{dual}}$ is straightforward and no extra condition on the Betti numbers of the boundary is needed. Just consider for (H_q, H_{n-q}) in $\underline{h}_{\text{dual}}$ the dual gluing so that the total effect on the Betti numbers of the boundary is globally null. Moreover, each dual gluing (H_q, H_{n-q}) applied to a block M_0 corresponds to taking the connected sum of it with a generalized torus $\mathbb{S}^q \times \mathbb{S}^{n-q}$. Therefore, the effect of each dual gluing (H_q, H_{n-q}) on the Conley index of the isolating block is nontrivial only at ranks q and $(n - q)$, that is,

$$\begin{cases} \text{rank } H_q(M_2, N_0) = \text{rank } H_q(M_0 \# \mathbb{S}^q \times \mathbb{S}^{n-q}, N_0) = \text{rank } H_q(M_0, N_0) + 1 \\ \text{rank } H_{n-q}(M_2, N_0) = \text{rank } H_{n-q}(M_0 \# \mathbb{S}^q \times \mathbb{S}^{n-q}, N_0) = \text{rank } H_{n-q}(M_0, N_0) + 1 \end{cases}$$

The realization we exhibit can be embedded in connected sums of generalized tori of dimension $n \#_j (\#^{s_j} \mathbb{S}^j \times \mathbb{S}^{n-j})$ and have boundaries which are themselves connected sums of generalized tori of dimension $(n - 1)$. This choice is motivated by the fact that it is the simplest one in terms of the description of the needed gluings, but it is arbitrary. We remark that this proof is easily adaptable to the case $n = 2i \neq 0 \pmod{4}$ since there are no β -i vertices to deal with.

4.3.2 Constructing Isolating Blocks for Periodic Orbits

There is much interest in Morse–Smale flows, as well as nonsingular Morse–Smale flows on closed n dimensional manifolds. Thus, semigraphs L_v , where v is labelled with the numerical Conley index of a hyperbolic periodic orbit $h_k = h_{k+1} = 1$ is also investigated in regard to realizability as a gradient-like flow on an isolating block for a periodic orbit with corresponding index.

The following theorem due to Franks (1982) illustrates the Morsification of a periodic orbit of a Morse–Smale flow. See Figure 4.37

Theorem 4.8. *Suppose φ is a Morse–Smale flow on an orientable manifold M with a periodic orbit γ of index k in standard form. Then given a neighborhood U of γ there exists a Morse–Smale flow $\widetilde{\varphi}$ whose vector field agrees with that of φ outside U and which has rest points p, q of indices $k + 1$ and k in U but no other chain recurrent points in U . For $\widetilde{\varphi}$, $W^u(p) \cap W^s(q)$ consists of two trajectories with the same sign if γ is twisted and opposite signs if γ is untwisted. Moreover, the unstable manifold for γ is equal to $W^u(p) \cup W^u(q)$.*

Inspired by this, it is shown in Cruz and de Rezende (1999) that a Lyapunov semigraph with a vertex labelled with a periodic orbit of index k can be morsified³ and that by

³The terminology used in Cruz and de Rezende (1999) is that of derivation from a Lyapunov semigraph

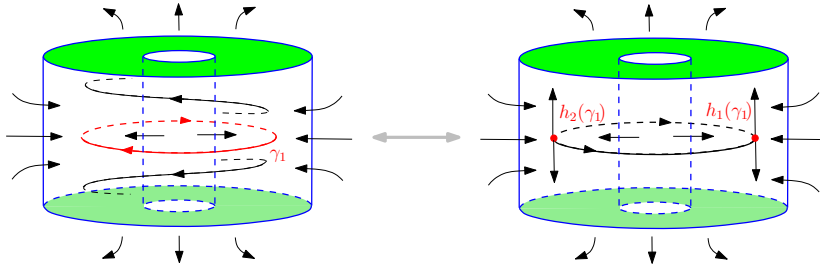


Figure 4.37: Interchanging a periodic orbit with a pair of rest points.

combining the possible connectivity types of two consecutive singularities, a singularity of index k with connectivity type $(k-1)\text{-c}$ or $k\text{-d}$ and a singularity of index $k+1$ with connectivity type $k\text{-c}$ or $k+1\text{-d}$, avoiding the β -invariant case, one produces the following table:

		singularity q of index k	
singularity p of index $k+1$	type $k\text{-d}$	type $(k-1)\text{-c}$	
type $(k+1)\text{-d}$	$(k+1)\text{-d}; k\text{-d}$	$(k+1)\text{-d}; (k-1)\text{-c}$	
type $k\text{-c}$	$k\text{-c}; k\text{-d}$	$k\text{-c}; (k-1)\text{-c}$	

Periodic orbits are classified by their connectivity types and denoted as indicated in the following table:

periodic orbit	connectivity type
R_k -disconnecting	$(k+1)\text{-d}; k\text{-d}$
R_k -disconnecting/connecting	$(k+1)\text{-d}; (k-1)\text{-c}$
R_k -invariant	$k\text{-c}; k\text{-d}$
R_k -connecting	$k\text{-c}; (k-1)\text{-c}$

In order to realize a semigraph of Morse–Smale type with a vertex labelled with a periodic orbit as a gradient flow on an isolating block we analyze the possible effects on the Betti numbers of N^+ once a round handle R of index k is attached to N^- .

The realization procedure follows along the same line as the Morse case in the previous section. One describes a set of basic gluing maps which induce maps in homology and proceed with a long exact sequence analysis.

A brief scheme of the proof is as follows:

1. Determine the non trivial homology groups of the various regions of the round handle R which is used in the analysis:

consisting of two vertices labelled with singularities of consecutive indices and in later work, the same notion is expressed as *graph continuation* and was introduced in Bertolim, de Rezende, and Manzoli Neto (2007).

*	k	$k - 1$	1	0
$H_*(\partial_A R)$	\mathbb{Z}	\mathbb{Z}	\mathbb{Z}	\mathbb{Z}
$H_*(\partial_B R)$	0	0	\mathbb{Z}	\mathbb{Z}
$H_*(\partial_{A \cap B} R)$	\mathbb{Z}	\mathbb{Z}	\mathbb{Z}	\mathbb{Z}

2. Use the Mayer–Vietoris sequence to compute the homology of $H_*(N)$:

$$\cdots \rightarrow H_{i+1}(N^-) \rightarrow H_i(\partial_{A \cap B} R) \xrightarrow{\iota_i} H_i(N) \oplus H_i(\partial_A R) \\ \xrightarrow{\sigma_i} H_i(N^-) \xrightarrow{\delta_i} H_{i-1}(\partial_{A \cap B} R) \rightarrow \cdots \quad (4.7)$$

3. With the knowledge of $H_*(N)$ at hand, use the Mayer–Vietoris once again to compute the homology of N^+ and prove the desired effect on the Betti numbers described by the semigraph.

$$\cdots \rightarrow H_{i+1}(N^+) \rightarrow H_i(\partial_{A \cap B} R) \xrightarrow{\eta_i} H_i(N^*) \oplus H_i(\partial_B R) \\ \xrightarrow{\xi_i} H_i(N^+) \xrightarrow{\Delta_i} H_{i-1}(\partial_{A \cap B} R) \rightarrow \cdots \quad (4.8)$$

We refer the reader to Cruz and de Rezende (1999) and Bertolim, de Rezende, and Manzoli Neto (2007) for more details. In Bertolim, de Rezende, and Manzoli Neto (ibid.) the construction of isolating blocks obtained by the attachments of n dimensional round handles to collars of closed $(n - 1)$ -manifolds are analyzed.

In what follows, several realizations of Lyapunov semigraphs for periodic orbits are exhibited and illustrated in the 3 dimensional case whenever possible.

Disconnecting Case

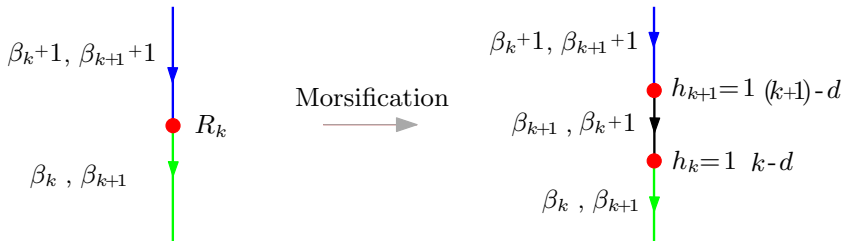


Figure 4.38: k -d and $(k + 1)$ -d, or k and $(k + 1)$ -disconnecting.

By long exact sequence analysis of (4.7) and (4.8) one obtains

$$H_{k+1}(N^+) \cong H_{k+1}(N^-) \oplus \mathbb{Z}$$

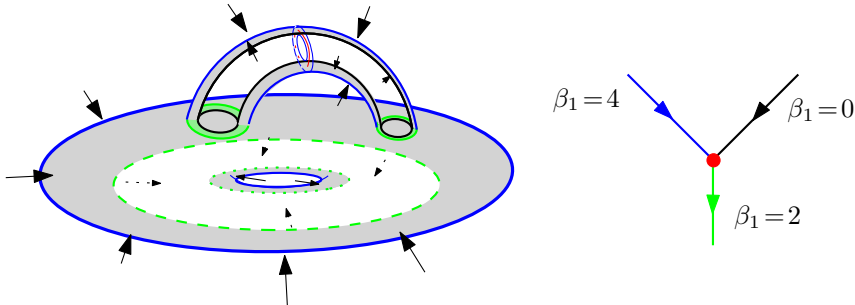


Figure 4.39: Disconnecting isolating block $N^- = \mathbb{T}_1^2$ and $N^+ = \mathbb{T}_1^2 \# \mathbb{T}_2^2 \sqcup \mathbb{S}^2$.

$$H_k(N^+) \cong H_k(N^-) \oplus \mathbb{Z}$$

$$H_i(N^+) \cong H_i(N^-), \quad i \neq k, k+1, \quad i < \lfloor \frac{n-1}{2} \rfloor.$$

Thus the manifold $N^+ = N^- \sharp [(\mathbb{S}^k \times \mathbb{S}^{n-k-1}) \sharp (\mathbb{S}^{k+1} \times \mathbb{S}^{n-k-2})]$. See Figure 4.38 and Figure 4.39.

Connecting–Disconnecting case - $N^- = \mathbb{S}^{n-k} \times \mathbb{S}^{k-1}$

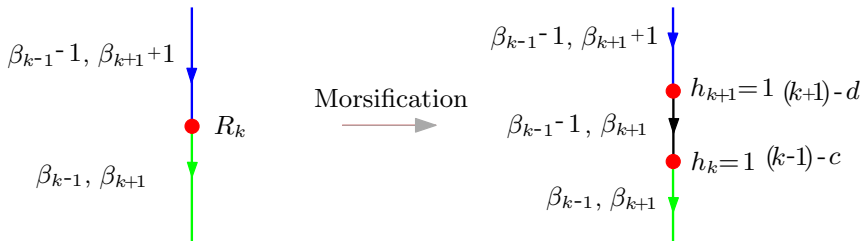


Figure 4.40: $(k-1)$ -c and $(k+1)$ -d, or $(k-1)$ -connecting and $(k+1)$ -disconnecting.

This case cannot occur in dimension 3. However, note that $\mathbb{S}^{n-k} = (\mathbb{S}^1 \times D^{n-k-1}) \cup (D^2 \times \mathbb{S}^{n-k-2})$. For any $x \in \mathbb{S}^{k-1}$ we have, $S_x^{n-k} = (S_x^1 \times D_x^{n-k-1}) \cup (D_x^2 \times S_x^{n-k-2})$. So, $\mathbb{S}^{k-1} \times \mathbb{S}^{n-k} = \mathbb{S}^{k-1} \times [(\mathbb{S}^1 \times D^{n-k-1}) \cup (D^2 \times \mathbb{S}^{n-k-2})]$. Since $\partial R = \mathbb{S}^1 \times \mathbb{S}^{k-1} \times D^{n-k-1} \cup \mathbb{S}^1 \times D^k \times \mathbb{S}^{n-k-2}$ by attaching ∂R to $\mathbb{S}^{k-1} \times \mathbb{S}^{n-k}$ we obtain N with $N^+ = (\mathbb{S}^1 \times D^k) \times \mathbb{S}^{n-k-2} \cup (D^2 \times \mathbb{S}^{k-1}) \times \mathbb{S}^{n-k-2} = \mathbb{S}^{k+1} \times \mathbb{S}^{n-k-2}$. See Figure 4.40.

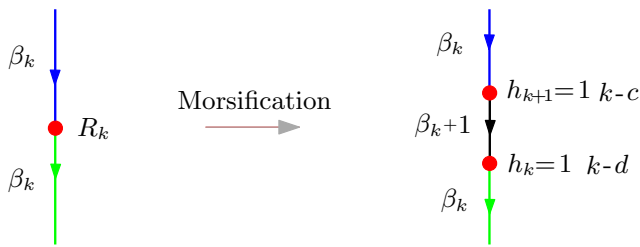
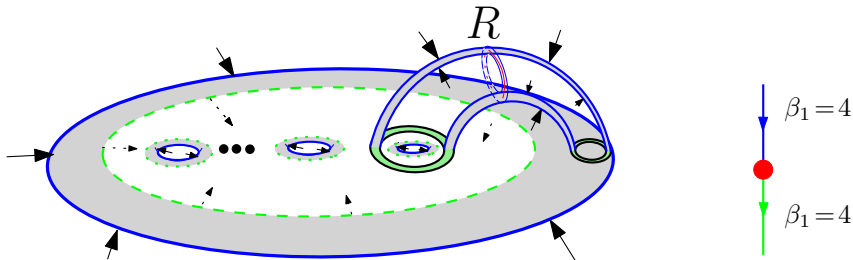


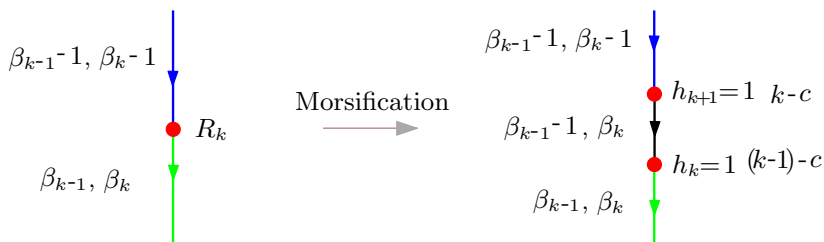
Figure 4.41: Invariant effect.

Figure 4.42: Invariant isolating block $N^- = N^+ = \sharp^2 \mathbb{T}^2 = \mathbb{T}_1^2 \sharp \mathbb{T}^2$.

Invariant Case

The manifold N^+ in this case is diffeomorphic to $\mathbb{S}^k \times \mathbb{S}^{n-k-1}$ and the isolating block N is diffeomorphic to $\mathbb{S}^k \times \mathbb{S}^{n-k-1} \times [0, 1]$. See Figure 4.41 and Figure 4.42.

Connecting case

Figure 4.43: $(k-1)$ -c and k -c, or $(k-1)$ -connecting and k -connecting.

This case can be realized by considering the reverse flow on the isolating block for the disconnecting case. See Figure 4.43 and Figure 4.44.

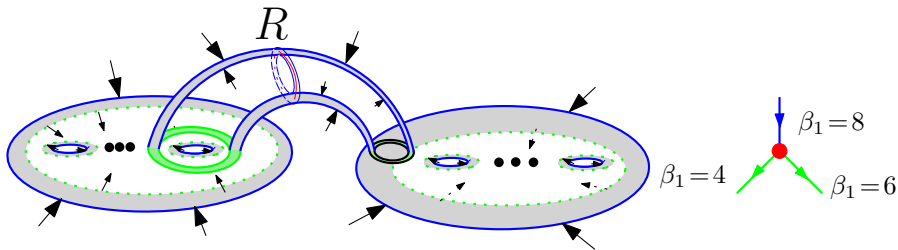


Figure 4.44: Connecting isolating block $N^- = \#^2 \mathbb{T}^2 \sqcup \#^3 \mathbb{T}^2$ and $N^+ = \#^4 \mathbb{T}^2$.

In this chapter, we have constructed n -dimensional isolating blocks for hyperbolic singularities and periodic orbits. We refer the reader to Bertolim, de Rezende, and Manzoli Neto (2007), Bertolim, de Rezende, Manzoli Neto, and Vago (2006), Bertolim, de Rezende, and Vago (2006), and Cruz and de Rezende (1999) for further results on gluing isolating blocks in accordance to a Lyapunov graph so as to obtain gradient-like flows on closed n -dimensional manifolds.

5

Dynamical Spectral Sequence

In the last chapter, we dealt with realizations of Lyapunov graphs on compact n -manifolds, $n \geq 2$. However, Lyapunov graphs are not complete topological invariants, that is, there are flows associated to the same graph which are not topologically equivalent. The reason for this is that the graph does not retain global information on the gradient-like part of the flow, i.e. the connecting orbits between the connected components of the chain recurrent set. Searching for information that enriches this theory, a dynamical investigation was initiated using the connecting manifolds and the moduli spaces, which provide global information about the flow, see Franks (1982), Salamon (1990), Weber (2006) and, in more general settings, Franzosa (1989). In the case of a gradient flow of a Morse–Smale function defined on a closed manifold, we can define an associated Morse chain complex, which provides a homological description of the flow.

5.1 Introduction

This section aims to be a guide through the key ideas to be developed in this chapter, namely the dynamical information to be retrieved from the algebra provided by a spectral sequence associated to a filtered Morse chain complex. We show how dynamics and algebra are connected walking the reader through the beauty of the main results without an exposition to the technicalities that are unavoidable when dealing with spectral sequences. In subsequent sections in this chapter we meet this challenge head on by confronting these technicalities and the somewhat cumbersome notation needed to keep track of all the mod-

ules and differentials in the spectral sequence and their dynamical counterpart represented by the set of critical points and their connecting manifolds.

Given a gradient flow of a Morse–Smale function defined on a closed manifold, it is well known that one can define an associated Morse chain complex generated by the critical points and whose differential is determined by counting the number of flow lines between pairs of critical points. Put in more rigorous terms, consider a negative gradient flow φ of a Morse–Smale function $f : M \rightarrow \mathbb{R}$ on a closed Riemannian manifold M and (C, ∂) the Morse complex associated to f and M . C is the free module generated over \mathbb{Z} by the critical points of f graded by the Morse index, $C_k = \mathbb{Z}[\text{Crit}_k(f)]$, and the boundary operator ∂ is defined on a generator p by

$$\begin{aligned}\partial_k : C_k &\longrightarrow C_{k-1} \\ p &\longmapsto \sum_{q \in \text{Crit}_{k-1}(f)} n(p, q; f)q\end{aligned}$$

where $n(p, q; f)$ is the intersection number between p and q . Moreover, the homology of the Morse chain complex coincides with the singular homology of M .

Spectral sequences were first introduced by Leray in 1946 in the context of sheaves cohomology. However, more general phenomena were discovered from those original results, one of which is discussed in this chapter. Spectral sequences break down a complicated Morse chain complex into smaller and more manageable complexes, allowing us to compute the homology of the space in an iterative process which approximates the homology of M . The filtration of the chain complex plays an essential role in this simplification procedure as we show in later sections.

Spectral sequences are thus a powerful mathematical tool and have been used to understand complicated algebraic or geometric structures. Our goal is to understand how they can be used to understand the dynamics of gradient-like flows and more specifically detect special orbits that trigger, through homotopy, the death and birth of connections due to cancellation of critical points. The deformation of a phase space can be caused by external forces acting on it and a goal in dynamical systems is to measure the long term effects in terms of the asymptotic behavior of the orbits in the flow.

A spectral sequence is a sequence of chain complexes (E^r, d^r) , where E^r is a bi-graded module, the differential d^r has bidegree $(-r, r - 1)$ and each chain complex is the homology module of the preceding one. One way to visualize a spectral sequence is as a book, where each page numbered by r has a grid of integer points with coordinates (p, q) . The index p increases in the horizontal direction and q increases in the vertical direction on the grid. Moreover, each point is labelled with a module $E^r_{p,q}$. The differential is represented as an arrow on the grid which points in the direction $(-r, r - 1)$. The total degree $k := p + q$ runs diagonally and the differential d^r decreases the total degree by one. Finally, in order to turn a page one computes the homology of the grid.

The first page of the spectral sequence is (E^0, d^0) , where d^0 has bidegree $(0, -1)$.

$$\bullet E_{0,3}^0 \quad \bullet E_{1,3}^0 \quad \bullet E_{2,3}^0 \quad \bullet E_{3,3}^0$$

$$\bullet E_{0,2}^0 \quad \bullet E_{1,2}^0 \quad \bullet E_{2,2}^0 \quad \bullet E_{3,2}^0$$

$$\begin{array}{cccc} \bullet E_{0,1}^0 & \bullet E_{1,1}^0 & \bullet E_{2,1}^0 & \bullet E_{3,1}^0 \\ & & \downarrow d^0 & \\ \bullet E_{0,0}^0 & \bullet E_{1,0}^0 & \bullet E_{2,0}^0 & \bullet E_{3,0}^0 \end{array}$$

The second page of the spectral sequence is (E^1, d^1) , where d^1 has bidegree $(-1, 0)$.

$$E^1$$

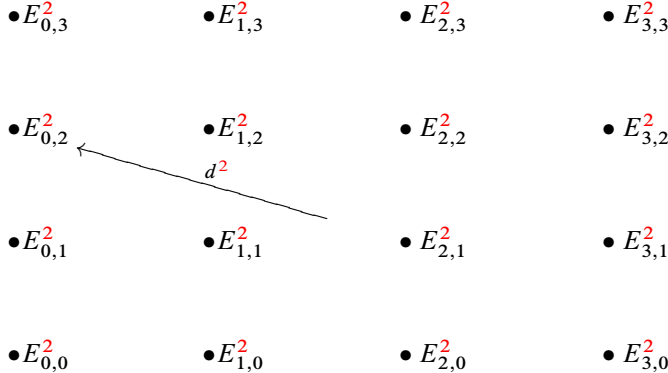
$$\bullet E_{0,3}^1 \quad \bullet E_{1,3}^1 \quad \bullet E_{2,3}^1 \quad \bullet E_{3,3}^1$$

$$\bullet E_{0,2}^1 \quad \bullet E_{1,2}^1 \quad \bullet E_{2,2}^1 \quad \bullet E_{3,2}^1$$

$$\bullet E_{0,1}^1 \quad \bullet E_{1,1}^1 \xleftarrow{d^1} \bullet E_{2,1}^1 \quad \bullet E_{3,1}^1$$

$$\bullet E_{0,0}^1 \quad \bullet E_{1,0}^1 \quad \bullet E_{2,0}^1 \quad \bullet E_{3,0}^1$$

The third page of the spectral sequence is (E^2, d^2) , where d^2 has bidegree $(-2, 1)$.



Many questions arise at this point. Does this process of turning pages converge? If so, to what does it converge? These questions are answered in this chapter.

Let us turn our attention to the computation of the spectral sequence of a filtered Morse chain complex. For didactical purposes, let us explore this through an example of a negative gradient flow of a Morse–Smale function on a torus, as in Figures 5.1 to 5.4. The filtration F considered in the Morse chain complex is induced by the filtration illustrated in Figure 5.1, where $F_p \setminus F_{p-1}$ contains a unique singularity h_k^{p+1} .

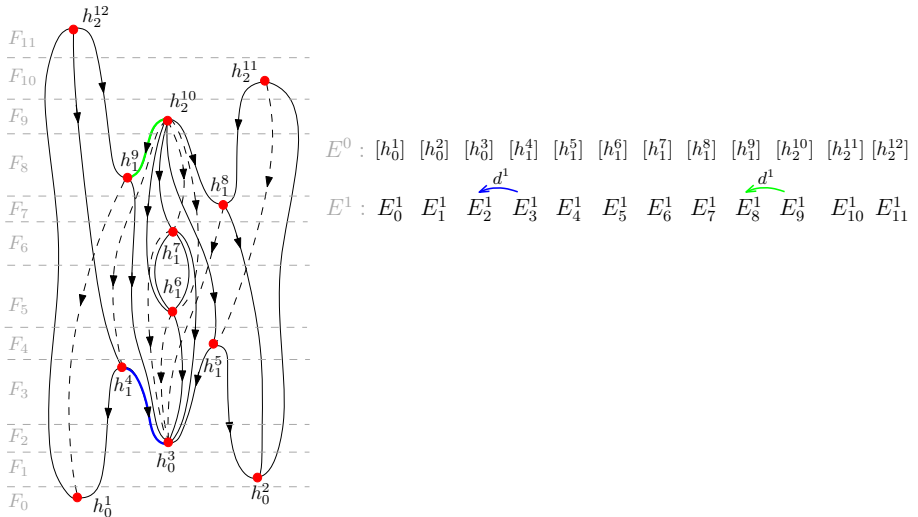
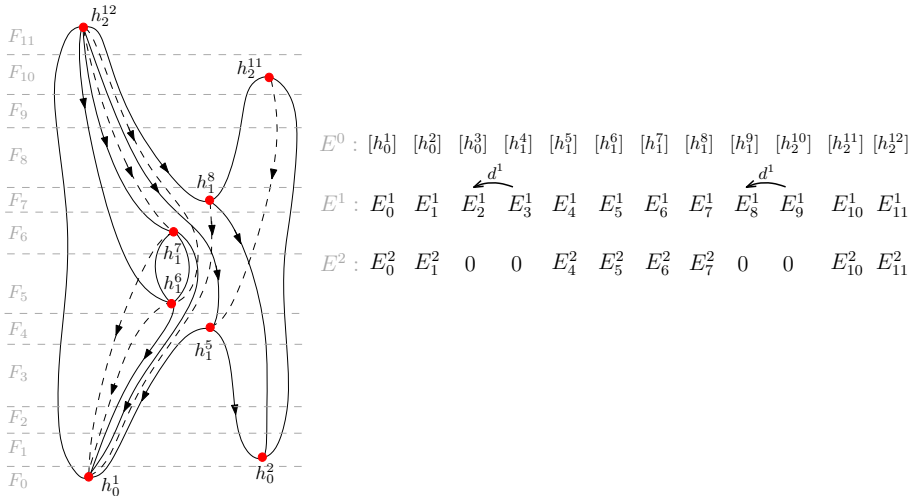
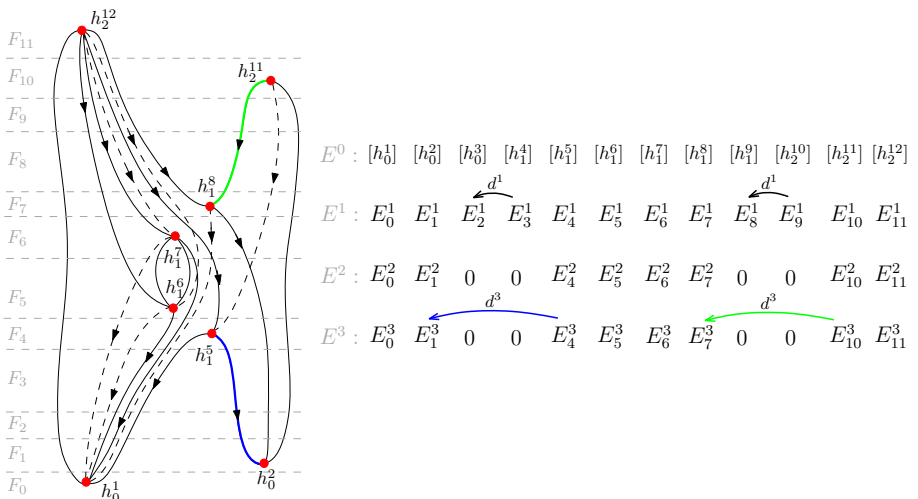
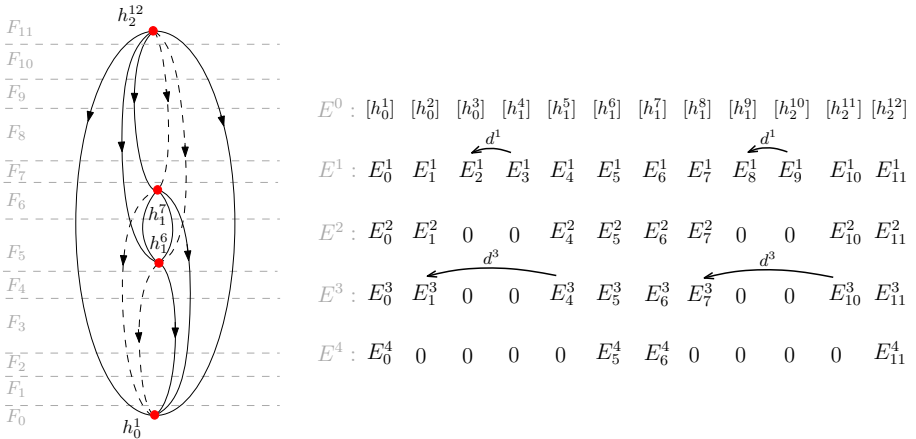


Figure 5.1: Algebraic-dynamical correspondence seen on E^1

Figure 5.2: Algebraic-dynamical correspondence seen on E^2 Figure 5.3: Algebraic-dynamical correspondence seen on E^3

Since $F_p \setminus F_{p-1}$ contains a unique singularity of Morse index k , each page of the spectral sequence may be reduced to a one dimensional grid. The reason for this is that each vertical line on a grid E^1 contains only one nonzero module, namely $E_{p,q}^1$, where

Figure 5.4: Algebraic-dynamical correspondence seen on E^4

$q = k - p$. Moreover, there is no need for the q coordinate, i.e. $E_{p,q}^1 = E_{p,k-p}^1 = E_p^1$.

This example gives us a taste of the rich dynamical information that can be retrieved from a spectral sequence analysis in the context of Morse–Smale functions on orientable surfaces, and in fact in higher dimensions. On the left note that certain connecting orbits between consecutive index singularities are highlighted in the flow. They correspond to differentials of the spectral sequence which are isomorphisms. The algebraic cancellation that occurs in E^{r+1} caused by a isomorphism d^r affects the dynamical cancellations of the consecutive index singularities.

Hence, for this family $\{f^r\}$ of Morse–Smale functions and their associated family $\{\varphi^r\}$ of negative gradient flows, the computation of the spectral sequence associated to the Morse chain complex provides concrete dynamical information. More specifically, as we "turn the pages" of the spectral sequence, i.e., progressively consider the modules E^r , we observe that each algebraic cancellation that occurs between two modules E^r , corresponds to a dynamic cancellation of a pair of critical points of f^r . Moreover, as r increases, the spectral sequence (E^r, d^r) stabilizes and converges to the homology of the Morse complex, which dynamically means that the final flow in this family is the gradient of a perfect function on the surface M . The unfolding of the spectral sequence and the algebraic cancellations provide a history of the birth and death of orbits in φ^r due to consecutive cancellations of critical points of f .

The investigation henceforth is focused on the spectral sequence $(E^r, d^r), r \geq 0$, which is associated to a chain complex (C, ∂) enriched with a filtration, with the aim of studying the deformation of the flow in a continuation, see Bertolim, Lima, et al. (2016, 2017), Cornea, de Rezende, and da Silveira (2010), Franzosa, de Rezende, and da Silveira (2014), Lima, Manzoli Neto, de Rezende, and da Silveira (2017), and de Rezende, Mello, and da Silveira (2010). We present the Spectral Sequence Sweeping Algorithm,

which computes, from the differential ∂ , the generators of the modules E^r and the differentials d^r of the spectral sequence (E^r, d^r) associated to (C, ∂) . Although this result has considerable algebraic value in itself, the main interest in this algebraic tool lies in the exploration of its dynamical implications, as cancellation, bifurcation, and existence of orbit paths results.

5.2 Spectral Sequences

In this section, we introduce spectral sequences, which are the main algebraic tool used hereafter with the objective of proving the dynamical applications in this chapter and the next. The references used herein are Davis and Kirk (2001) and Spanier (1989). A spectral sequence is a sequence of chain complexes, where each chain complex is the homology module of the preceding one. This sequence of modules approximates to an associated limit module. Spectral sequences are powerful computational tools in topology, since they extract more information from a chain complex than simply calculating its homology. They also give more elegant proofs of important theoretical results such as the Hurewicz theorem, for example.

Let R be a principal ideal domain.

Definition 5.1. A *spectral sequence* is a sequence of chain complexes (E^r, d^r) , $r \geq 0$ such that:

- E^r is an *R -bigraded module*, i.e. it is an indexed collection of R -modules $E_{p,q}^r$ for all pairs of integers p and q .
- d^r is a *differential* of bidegree $(-r, r - 1)$, i.e. it is a collection of homomorphisms $d^r : E_{p,q}^r \rightarrow E_{p-r,q+r-1}^r$ for all p and q such that $d^r \circ d^r = 0$.
- For all $r \geq 0$, there exists an isomorphism $H(E^r) \cong E^{r+1}$ where

$$H_{p,q}(E^r) = \frac{\ker d^r : E_{p,q}^r \rightarrow E_{p-r,q+r-1}^r}{\text{im } d^r : E_{p+r,q-r+1}^r \rightarrow E_{p,q}^r}$$

is the homology module of E^r .

An important point to keep in mind is that a bigrading decomposes the module E^r into pieces $E_{p,q}^r$ and then information about $E_{p,q}^r$, for some pairs of p 's and q 's, gives us information about $E_{p,q}^{r+s}$ for some other p 's and q 's, which are possibly not exactly the same pairs of indices. For example, if $E_{p,q}^r = 0$ for fixed p, q and r , then $E_{p,q}^{r+s} = 0$ for all $s \geq 0$.

For a fixed r , note that if one defines $E_k^r = \bigoplus_{p+q=k} E_{p,q}^r$, the differential d^r induces a homomorphism $\partial^r : E_k^r \rightarrow E_{k-1}^r$ such that (E_k^r, ∂_k^r) is a chain complex with the k -th homology module equal to $\bigoplus_{p+q=k} H_{p,q}(E^r)$. In Figure 5.5, we can see that each E_k^r

corresponds to a diagonal on the r -th page and all the differentials d^r are represented by arrows that start at a given diagonal and end at the diagonal immediately to its left.

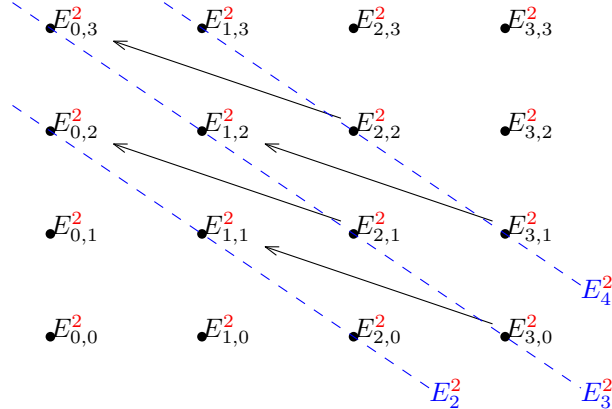


Figure 5.5: E_k^r corresponds to diagonals in the r -th page.

The most usual way to work with a spectral sequence is using theorems which state that there exists a spectral sequence where the modules E^1 or E^2 can be identified with something known and the limit term $E^\infty = \lim_{r \rightarrow \infty} E^r$ is related to something one wishes to compute. In order to define the limit term of a spectral sequence, we define

$$Z_{p,q}^0 = \ker(d_{p,q}^0 : E_{p,q}^0 \rightarrow E_{p,q-1}^0),$$

$$B_{p,q}^0 = \text{im}(d_{p,q+1}^0 : E_{p,q+1}^0 \rightarrow E_{p,q}^0).$$

Note that $B^0 \subseteq Z^0$ and $E^1 = Z^0/B^0$. Now let

$$Z(E^1)_{p,q} = \ker(d_{p,q}^1 : E_{p,q}^1 \rightarrow E_{p-1,q}^1),$$

$$B(E^1)_{p,q} = \text{im}(d_{p+1,q}^1 : E_{p+1,q}^1 \rightarrow E_{p,q}^1).$$

By the Noether isomorphism theorem, there exist bigraded submodules Z^1 e B^1 of Z^0 containing B^0 such that $Z(E^1)_{p,q} = Z_{p,q}^1/B_{p,q}^0$ and $B(E^1)_{p,q} = B_{p,q}^1/B_{p,q}^0$ for all p and q . It follows that

$$B^0 \subseteq B^1 \subseteq Z^1 \subseteq Z^0.$$

By an induction argument, we obtain the submodules:

$$B^0 \subseteq B^1 \subseteq \dots \subseteq B^r \subseteq \dots \subseteq Z^r \subseteq \dots \subseteq Z^1 \subseteq Z^0$$

for all $r \geq 0$, such that $E^{r+1} = Z^r/B^r$. Defining

$$Z^\infty = \cap_r Z^r, \quad B^\infty = \cup_r B^r,$$

the *limit of the spectral sequence* (E^r, d^r) is the bigraded module

$$E^\infty = Z^\infty / B^\infty.$$

Note that the terms E^r are successive approximations of the limit term.

Definition 5.2. A spectral sequence (E^r, d^r) is *convergent* if, given p and q , there exists $r(p, q) \geq 0$ such that, for all $r \geq r(p, q)$, $d_{p,q}^r : E_{p,q}^r \rightarrow E_{p-r, q+r-1}^r$ is trivial. If there exists $r(p, q) \geq 0$ such that $E_{p,q}^r \cong E_{p,q}^\infty$, for all $r \geq r(p, q)$, the spectral sequence is said to be *strongly convergent*.

An interesting class of examples of strongly convergent spectral sequences are the *first-quadrant spectral sequences*, i.e. the spectral sequences with the property that there exists an index r such that $E_{p,q}^r = 0$ for $p < 0$ and $q < 0$. The r -th page of a first-quadrant spectral sequence can be represented in the first quadrant of the plane, as in Figure 5.6.

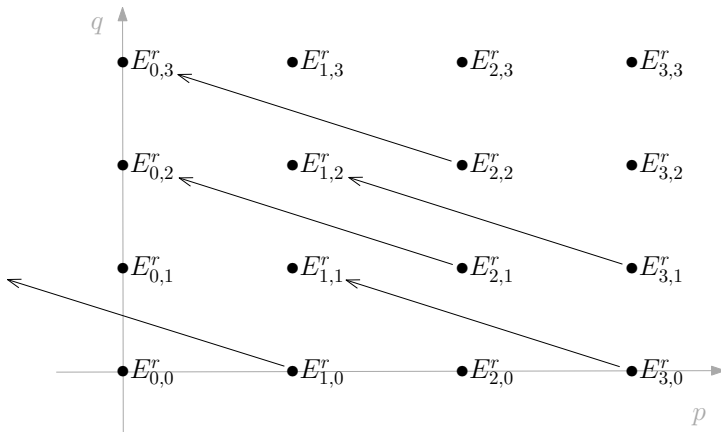


Figure 5.6: First-quadrant spectral sequence.

Note that for each k there exist a finite number of pairs p, q such that $E_{p,q}^\infty$ is nontrivial and $k = p + q$.

Definition 5.3. An *increasing filtration* or a filtration on an R -module C is a sequence of submodules $F_p C$, for all integers p , such that $F_p C \subset F_{p+1} C$. If C is a graded module, that is, $C = \{C_q\}$ is a collection of R -modules indexed by integers, a filtration must be compatible with the grading, that is, $F_p C = \{F_p C_q\}$ is a graded submodule of C for all p .

We work with filtrations which have some additional useful properties. A filtration F on a R -module C is a *convergent filtration* if $\cap_p(F_p C) = 0$ and $\cup_p(F_p C) = C$. If there exist integers p and p' such that $F_p C = 0$ and $F_{p'} C = C$, we say that F is a *finite filtration*. A filtration F on a graded R -module C is *bounded below* if, given q , there exists $p(q)$ such that $F_{p(q)} C_q = 0$.

It is obvious that every finite filtration on a graded R -module is convergent and also bounded below.

Definition 5.4. 1. Given a filtration F on a R -module C , the *associated graded module* $G(C)$ is

$$G(C)_p = F_p C / F_{p-1} C.$$

2. If C is a graded module, the associated module $G(C)$ is the bigraded module

$$G(C)_{p,q} = \frac{F_p C_{p+q}}{F_{p-1} C_{p+q}}.$$

If C is a graded module, the index p is called the *filtered degree*, q is the *complementary degree* and $k := p + q$ is the *total degree*.

We are usually more interested in the algebraic properties of C than in $G(C)$ and $G(C)$ contains some, but not necessarily all, information about C . Even when the filtration is finite, $G(C)$ may not determine C . However, for convergent filtrations, $G(C)$ is more closely tied to C than for arbitrary filtrations. For example, if $G(C) = 0$, then $C = 0$. Moreover, if R is a field and C is a finite dimensional vector space, then each $F_i C$ is a vector subspace and $G(C)$ and C have the same dimension. Hence $G(C)$ determines C up to isomorphism in this case. Whenever the filtration is finite, this fact holds for more general R if each $G(C)_n$ is free. Finally, if $R = \mathbb{Z}$ and $G(C)_p$ has no t -torsion for all p and a given prime number t , then C has no t -torsion for all p .

Let F be a filtration on a chain complex C . Recall that F is compatible with the grading and with the differential of C , that is, each $F_p C$ is a subcomplex $\{F_p C_q\}$ of C . See Figure 5.7.

In this case, F induces a filtration F on $H_*(C)$ defined by

$$F_p H_*(C) = \text{im}[H_*(F_p C) \rightarrow H_*(C)].$$

It is not difficult to prove that if a filtration F on C is convergent and bounded below, then the induced filtration on $H_*(C)$ inherits these same properties, see Spanier (1989) for more details. The next theorem gives sufficient conditions for the existence of a spectral sequence associated to a filtered chain complex. In order to provide a more complete and comprehensive text, we include here the proof given in Spanier (ibid.).

Theorem 5.1 (Existence of Spectral Sequences, Spanier). *Let (C_*, ∂_*) be a chain complex and F be a filtration on C . If F is a convergent filtration bounded below on C , then there exists a convergent spectral sequence (E^r, d^r) associated to (C_*, ∂_*) such that*

$$E^0_{p,q} = \frac{F_p C_{p+q}}{F_{p-1} C_{p+q}} = G(C)_{p,q},$$

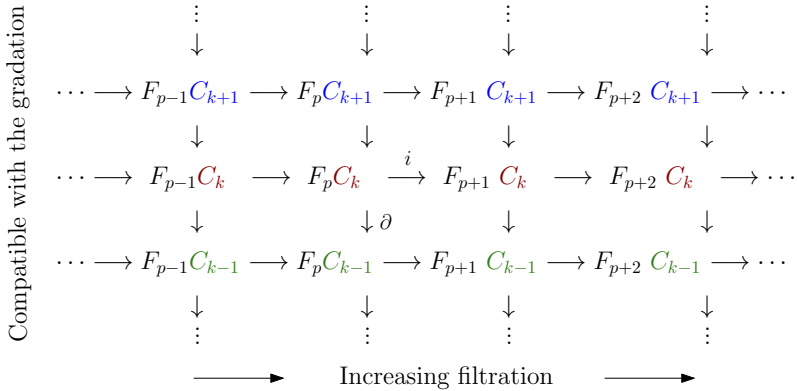


Figure 5.7: Filtration compatible with the grading and with the differential of the chain complex.

$$E^1_{p,q} \cong H_{p+q} \left(\frac{F_p C_{p+q}}{F_{p-1} C_{p+q}} \right),$$

d^1 corresponds to the boundary operator of the triple $(F_p C, F_{p-1} C, F_{p-2} C)$ and E^∞ is isomorphic to the associated bigraded module $GH_*(C)$.

Proof. The proof is divided in 4 steps:

Step 1: Defining $E = \{(E^r, d^r)\}_{r \geq 0}$.

Step 2: Calculating E_p^r for $r < 0$, $r = 0$ and $r = 1$.

Step 3: Proving that E is a spectral sequence.

Step 4: Proving the convergence of E .

We now provide a sketch of the proof of each step.

Step 1: For each arbitrary r , define

$$\begin{aligned} Z_p^r &= \{c \in F_p C \mid \partial c \in F_{p-r} C\}, \\ Z_{p,q}^r &= \{c \in F_p C_{p+q} \mid \partial c \in F_{p-r} C_{p+q-1}\}, \\ Z_p^\infty &= \{c \in F_p C \mid \partial c = 0\}, \\ Z_{p,q}^\infty &= \{c \in F_p C_{p+q} \mid \partial c = 0\}. \end{aligned}$$

Hence, we have the following sequence of graded modules ordered by inclusion

$$\dots \subseteq \partial Z_{p-1}^{-1} \subseteq \partial Z_p^0 \subseteq \partial Z_{p+1}^1 \subseteq \dots \subseteq \partial C \cap F_p C \subseteq Z_p^\infty \subseteq \dots$$

$$\dots \subseteq Z_p^1 \subseteq Z_p^0 = F_p C.$$

Then, we can define for each $r \geq 0$

$$E_{p,q}^r = \frac{Z_{p,q}^r}{Z_{p-1,q+1}^{r-1} + \partial Z_{p+r-1,q-r+2}^{r-1}}$$

and

$$E_{p,q}^\infty = \frac{Z_{p,q}^\infty}{Z_{p-1,q+1}^\infty + \partial C \cap F_p C_{p+q}}.$$

Note that the map ∂ sends an element in Z_p^r to an element in Z_{p-r}^r and an element in $Z_{p-1}^{r-1} + \partial Z_{p+r-1}^{r-1}$ to one in ∂Z_{p-1}^{r-1} . Thus, ∂ induces a homomorphism $d^r : E_p^r \rightarrow E_{p-r}^r$.

It follows that E^r is a bigraded module and d^r is a differential of bidegree $(-r, r - 1)$ in E^r .

Step 2: By definition,

$$E_{p,q}^0 = \frac{F_p C_{p+q}}{F_{p-1} C_{p+q}} = G(C)_{p,q}$$

and $d^0 : F_p C_{p+q} / F_{p-1} C_{p+q} \rightarrow F_p C_{p+q-1} / F_{p-1} C_{p+q-1}$ is the boundary operator of the quotient complex $F_p C / F_{p-1} C$.

Moreover,

$$E_{p,q}^1 = \frac{Z_{p,q}^1}{Z_{p-1,q+1}^0 + \partial Z_{p,q+1}^0}.$$

Since $\frac{Z_{p,q}^1}{Z_{p-1,q+1}^0}$ is the module of the $(p+q)$ -cycles of $F_p C / F_{p-1} C$ and $\frac{Z_{p-1,q+1}^0 + \partial Z_{p,q+1}^0}{Z_{p-1,q+1}^0}$ is the module of the $(p+q)$ -boundaries of $F_p C / F_{p-1} C$, then

$$E_{p,q}^1 \cong H_{p+q}(F_p C / F_{p-1} C).$$

Step 3: In this step, we prove that (E^r, d^r) is a spectral sequence. Note that

$$\begin{aligned} \{c \in Z_p^r \mid \partial c \in Z_{p-r-1}^{r-1} + \partial Z_{p-1}^{r-1}\} \\ = \{c \in Z_p^r \mid \partial c \in F_{p-r-1} C\} + \{c \in Z_p^r \mid \partial c \in \partial Z_{p-1}^{r-1}\} \\ = Z_p^{r+1} + (Z_{p-1}^{r-1} + Z_p^\infty) = Z_p^{r+1} + Z_{p-1}^{r-1}. \end{aligned}$$

It follows that

$$\ker(d^r : E_p^r \rightarrow E_{p-r}^r) = (Z_p^{r+1} + Z_{p-1}^{r-1}) / (Z_{p-1}^{r-1} + \partial Z_{p+r-1}^{r-1}),$$

$$\text{im}(d^r : E_{p+r}^r \rightarrow E_p^r) = (Z_{p-1}^{r-1} + \partial Z_{p+r}^r) / (Z_{p-1}^{r-1} + \partial Z_{p+r-1}^{r-1}).$$

By the Noether isomorphism theorem,

$$\begin{aligned} \frac{\ker d^r}{\text{im } d^r} &= \frac{(Z_p^{r+1} + Z_{p-1}^{r-1})}{(Z_{p-1}^{r-1} + \partial Z_{p+r}^r)} \\ &\cong \frac{Z_p^{r+1}}{Z_p^{r+1} \cap (Z_{p-1}^{r-1} + \partial Z_{p+r}^r)} \\ &= \frac{Z_p^{r+1}}{(Z_{p-1}^{r-1} + \partial Z_{p+r}^r)} = E_p^{r+1}. \end{aligned}$$

Consequently, $H_*(E^r) \cong E^{r+1}$.

Step 4: In this last step, we calculate the limit of the spectral sequence. By the Noether isomorphism theorem,

$$E_p^r = \frac{Z_p^{r+1}}{(Z_{p-1}^{r-1} + \partial Z_{p+r-1}^{r-1})} \cong \frac{(Z_p^{r+1} + F_{p-1}C)}{(F_{p-1}C + \partial Z_{p+r-1}^{r-1})}.$$

Note that in the previous expression, while the numerator decreases, the denominator increases whenever r increases. By definition, the limit is

$$\frac{\cap_r (Z_p^{r+1} + F_{p-1}C)}{\cup_r (F_{p-1}C + \partial Z_{p+r-1}^{r-1})} = \frac{(\cap_r Z_p^{r+1} + F_{p-1}C)}{(F_{p-1}C + \cup_r \partial Z_{p+r-1}^{r-1})}. \quad (5.1)$$

Since $\cup_p F_p C = C$, then $\cup_r \partial Z_{p+r-1}^{r-1} = \partial C \cap F_p C$.

Fixing q , we have that $\cap_r Z_{p,q}^r = Z_{p,q}^\infty$, since the filtration is bounded below. Hence

$$(5.1) = \frac{(Z_p^\infty + F_{p-1}C)}{(F_{p-1}C + \partial C \cap F_p C)} = \frac{Z_p^\infty}{(Z_{p-1}^\infty + \partial C \cap F_p C)} = E_p^\infty.$$

In order to prove that the sequence converges, note that for each fixed $p+q$, $E_{p,q}^r = 0$ when p is small enough, once the filtration is bounded below. Hence, for fixed p and q , there exists r such that for all $r' \geq r$, $d_{p,q}^{r'} : E_{p,q}^{r'} \rightarrow E_{p-r',q+r'-1}^{r'}$ is trivial, i.e. the spectral sequence converges.

We complete the proof interpreting the limit E^∞ as $GH_*(C)$. By definition,

$$GH_{p,q}(C) = \frac{F_p H_{p+q}(C)}{F_{p-1} H_{p+q}(C)}$$

where

$$F_p H_{p+q}(C) = \text{im}[H_{p+q}(F_p C) \rightarrow H_{p+q}(C)].$$

Hence $F_* H_{p+q}(C) = \frac{Z_p^\infty}{\partial C \cap F_p C}$ and

$$\begin{aligned} F_p H_*(C) / F_{p-1} H_*(C) &= \frac{(Z_p^\infty / \partial C \cap F_p C)}{(Z_{p-1}^\infty / \partial C \cap F_{p-1} C)} \\ &\cong \frac{Z_p^\infty}{(Z_{p-1}^\infty + \partial C \cap F_p C)} \\ &= E_p^\infty \end{aligned} .$$

□

Example 5.1. Let (C, ∂) be a finite chain complex. Consider in (C, ∂) the increasing filtration $F = \{F_p\}$ such that $F_p C \setminus F_{p-1} C$ contains all p -chains of C , that is, $F_p C \setminus F_{p-1} C = C_p$. Since F is a finite filtration, it follows from Theorem 5.1 that there exists a spectral sequence associated to this filtered chain complex. Moreover, we have that

$$E_{p,0}^0 = F_p C_p \setminus F_{p-1} C_p = \bigoplus_{x \in C_p} R\langle x \rangle$$

and $E_{p,q}^0 = 0$, for any $q \neq 0$. See Figure 5.8.

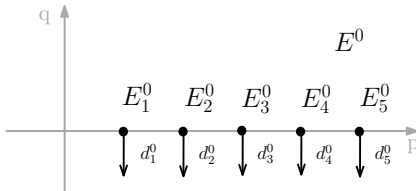


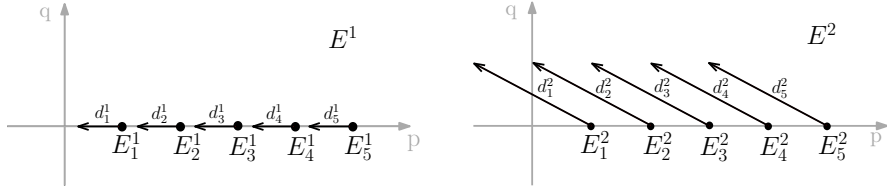
Figure 5.8: E^0 .

Note that, since $E_{p,q}^r$ is nontrivial only when $q = 0$, then the only possibly nonzero differential is d_1 . Consequently, $E_p^1 \cong E_p^0$ and $H(E^1) \cong E^2 \cong E^3 \cong E^4 \cong \dots$, see Figure 5.9.

Whenever the chain complex is the Morse chain complex associated to a Morse–Smale function on a closed manifold, which is introduced in the next section, the filtration considered in Example 5.1 is induced by a self-indexing filtration.

5.3 Morse Complex

Let M be a smooth closed n -dimensional manifold, g be a Riemannian metric and $f : M \rightarrow \mathbb{R}$ be a Morse function on M . Let φ_f be the gradient flow associated to

Figure 5.9: E^1 and E^2 .

$-\nabla^g f$.¹ In this section we introduce the Morse chain complex associated to (f, g) , which is a chain complex freely generated by the critical points of f , graded by the Morse index, and whose homology is isomorphic to the singular homology of M . For more details, we refer to Banyaga and Hurtubise (2004), Bertolim, Lima, et al. (2016), Pajitnov (2008), Salamon (1990) and Weber (2006).

Denote by $\text{Crit}(f)$ the set of critical points of f and by $\text{Crit}_k(f)$ the subset of critical points of f of Morse index k . Recall that, since M is a closed manifold, then $\#\text{Crit}(f) < \infty$ and, for every point $z \in M$, the α -limit $\alpha(z)$ and ω -limit $\omega(z)$ consist each of a single critical point of f . Moreover, given $x \in \text{Crit}(f)$, the stable and the unstable manifolds of x , defined by

$$W^s(x) := \{z \in M \mid \omega(z) = x\},$$

$$W^u(x) := \{z \in M \mid \alpha(z) = x\},$$

are submanifolds of M without boundary. More specifically, $W^s(x)$ is an embedded open disk with dimension $n - \text{ind}_f(x)$ and $W^u(x)$ is an embedded open disk with dimension equal to $\text{ind}_f(x)$. Their tangent spaces at x are respectively the stable and unstable spaces of the linearization of f at x and $T_x M = T_x W^s(x) \oplus T_x W^u(x)$.

We require that f is a Morse–Smale function, that is, $-\nabla^g f$ satisfy the **Morse–Smale transversality condition**, i.e. for every pair of critical points x and y , the unstable manifold $W^u(x)$ of x and the stable manifold $W^s(y)$ of y intersect transversally. It is proved in Smale (1961) that the transversality requirement holds for generic gradient vector fields and Riemannian metrics on M . More specifically, $-\nabla^g f$ can be C^1 approximated by a smooth gradient vector field $-\nabla^{g'} f'$ satisfying the Morse–Smale condition, where f' is a Morse function and the critical points of f and f' are C^0 -close to each other.

Given $x, y \in \text{Crit}(f)$, the *connecting manifold* of x and y is

$$\mathcal{M}_{xy} := W^u(x) \cap W^s(y)$$

and the *moduli space* between x and y is $\mathcal{M}_y^x := \mathcal{M}_{xy} \cap f^{-1}(a)$, where a is a regular value between $f(x)$ and $f(y)$. Figure 5.10 shows examples of connecting manifolds and moduli spaces for some critical points of a Morse–Smale function on a 2-manifold.

¹In order to simplify notation, we write φ for φ_f and $-\nabla f$ for $-\nabla^g f$ whenever emphasis of f and g need not be given.

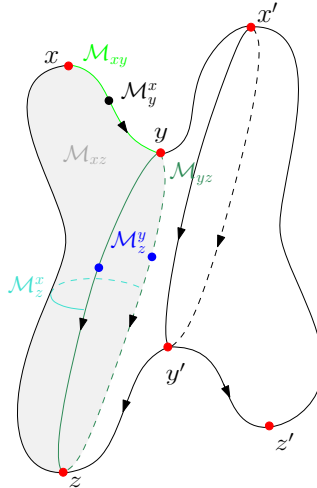


Figure 5.10: Connecting manifolds and moduli spaces.

The sets \mathcal{M}_{xy} and \mathcal{M}_y^x are closed submanifolds of M . Moreover,

$$\dim(\mathcal{M}_{xy}) = \text{ind}_f(x) - \text{ind}_f(y) \text{ and } \dim(\mathcal{M}_y^x) = \text{ind}_f(x) - \text{ind}_f(y) - 1.$$

In particular, if $\text{ind}_f(x) - \text{ind}_f(y) = 1$ then \mathcal{M}_y^x is a 0-dimensional submanifold of M . Moreover, it follows from Theorem 3.8 of Weber (2006) that \mathcal{M}_{xy} is also a compact set. Thus, $\#\mathcal{M}_y^x \leq \infty$.

Now we establish a technique to count flow lines between critical points of f with consecutive indices. The first step in this direction is to choose orientations on the connecting manifolds and moduli spaces. Recall that the unstable and stable manifolds of critical points of f are contractible and, hence, orientable. Thus, fix an orientation on $W^u(x)$ for every critical point x such that $\text{ind}_f(x) > 0$. Given a pair $x, y \in \text{Crit}(f)$, the orientations of $W^u(x)$ and $W^u(y)$ induce orientations on the connecting manifold \mathcal{M}_{xy} and the moduli space \mathcal{M}_y^x . In fact, we present below a sketch of how to obtain the induced orientation on \mathcal{M}_{xy} . Let $\mathcal{V}_{\mathcal{M}_{xy}} W^s(y)$ be the normal bundle of $W^s(y)$ restricted to \mathcal{M}_{xy} and $\mathcal{V}_y W^s(y)$ be the fiber with the orientation given by the isomorphism

$$T_y W^u(y) \oplus T_y W^s(y) \simeq T_y M \simeq \mathcal{V}_y W^s(y) \oplus T_y W^s(y).$$

The orientation on $\mathcal{V}_y W^s(y)$ determines an orientation on the normal bundle $\mathcal{V}_{\mathcal{M}_{xy}} W^s(y)$ restricted to the submanifold \mathcal{M}_{xy} . Then the orientation on \mathcal{M}_{xy} is determined by the isomorphism

$$T_{\mathcal{M}_{xy}} W^u(x) \simeq T \mathcal{M}_{xy} \oplus \mathcal{V}_{\mathcal{M}_{xy}} W^s(y). \quad (5.2)$$

If $\text{ind}_f(y) = 0$ then $\mathcal{V}_y W^s(y) = 0$ and, hence, $T_{\mathcal{M}_{xy}} W^u(x) \simeq T \mathcal{M}_{xy}$. The induced orientation on the connecting manifold \mathcal{M}_{xy} is denoted by $[\mathcal{M}_{xy}]_{\text{ind}}$. More details can

be found in Weber (ibid.), Proposition 3.1. Note that there are no restrictions on the orientability of the manifold M .

The next step is to use the orientation on the connecting manifolds to assign a number $+1$ or -1 to every connecting orbit between critical points of consecutive Morse indices. Choose orientations for the unstable manifolds of all critical points with Morse index greater than zero and denote this set of choices by O_r . Given a pair x, y of critical points such that $\text{ind}_f(x) - \text{ind}_f(y) = 1$, consider $u \in \mathcal{M}_y^x$. Denote by $[\mathcal{O}(u)]_{\text{ind}}$ the orientation induced by the orientation of \mathcal{M}_{xy} on the orbit $\mathcal{O}(u)$ of u . The *characteristic sign* n_u of the orbit $\mathcal{O}(u)$ is given by

$$[\mathcal{O}(u)]_{\text{ind}} = n_u[\dot{u}],$$

where $[\dot{u}]$ is the orientation on $\mathcal{O}(u)$ induced by the negative gradient flow.

The *intersection number* of x and y is defined by

$$n(x, y) = \sum_{u \in \mathcal{M}_y^x} n_u.$$

Example 5.2. Consider the 2-manifold M , the Morse–Smale function $f : M \rightarrow \mathbb{R}$, and fixed orientations for the unstable manifolds as in Figure 5.11. The function f has 4 critical points: one source x , a saddle y , and two sinks z and z' .

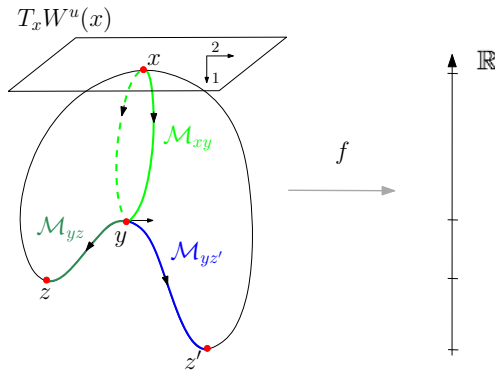


Figure 5.11: Negative gradient flow of the height function in M .

In Figure 5.12 (left), we illustrate the induced orientations on the connecting manifolds. Since z and z' have Morse index zero, the orientations of \mathcal{M}_{yz} and $\mathcal{M}_{yz'}$ are induced by the orientation of $T_y W^u(y)$. Comparing with the orientation induced by the flow, we have that $n(y, z) = n_{u_2} = -1$ and $n(y, z') = n_{u_1} = 1$. The orientation $[\mathcal{M}_{xy}]_{\text{ind}}$ is obtained through the isomorphism (5.2). Figure 5.12 (right) is a planar representation of the flow, where the union at infinity of the rectangle with the point z' represents M . In this figure,

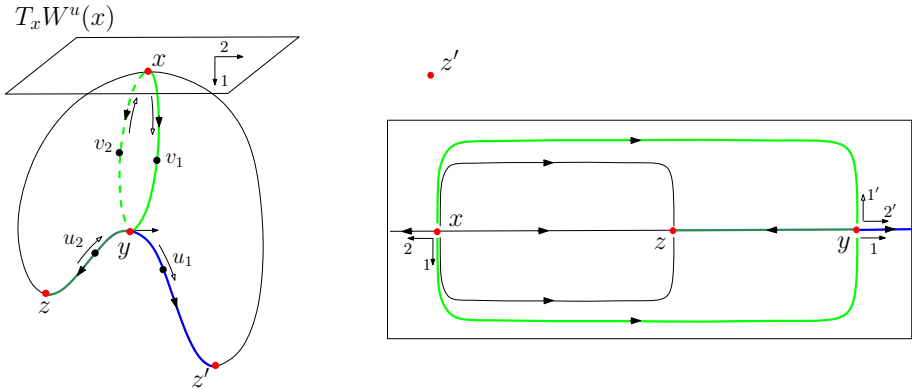


Figure 5.12: Planar representation of the flow and induced orientation.

the vector $2'$ is obtained from the orientation of $W^u(y)$ (which is compatible with the orientation of $\mathcal{V}_y W^s(y)$).

The vector $1'$ is chosen so that the orientation given by the basis $\{1', 2'\}$ is compatible with the orientation of $W^u(x)$, that is, the orientation given by the basis $\{1, 2\}$. The vector $1'$ determines the orientation $[\mathcal{M}_{xy}]_{ind}$. Hence, the orientation $[\mathcal{M}_{xy}]_{ind}$ coincides with the orientation given by the flow in $\mathcal{O}(v_1)$ and it is opposite to the orientation given by the flow in $\mathcal{O}(v_2)$, as shown in Figure 5.12. It follows that $n_{v_1} = +1$, $n_{v_2} = -1$ and, hence,

$$n(x, y) = n_{v_1} + n_{v_2} = 0.$$

Given M a smooth closed Riemannian manifold with a metric g and $f : M \rightarrow \mathbb{R}$ a Morse–Smale function on M , choose a set of orientations O_r for all unstable manifolds. Let $C = \{C_k(f)\}$ be the \mathbb{Z} -module generated by the critical points of f and graded by their Morse index, i.e.

$$C_k(f) := \bigoplus_{x \in \text{Crit}_k(f)} \mathbb{Z}\langle x \rangle,$$

if $k \geq 0$ and $C_k(f) = 0$, if $k < 0$. Let $\partial_k(x) : C_k(f) \rightarrow C_{k-1}(f)$ the map defined on a generator x of $C_k(f)$ by

$$\partial_k \langle x \rangle := \sum_{y \in \text{Crit}_{k-1}(f)} n(x, y) \langle y \rangle, \quad (5.3)$$

and extended to general chains by linearity.

The next theorem guarantees that $(C_*(f), \partial_*)$ is a chain complex and its homology coincides with the singular homology of M . An elegant proof of this result can be found in Salamon (1990), Theorem 3.1.

Theorem 5.2. 1. $\partial_{k-1} \circ \partial_k = 0$,

$$2. H_k(M) = \frac{\ker \partial_k}{\text{im } \partial_{k+1}}.$$

The pair $(C_*(f), \partial_*)$ is called a *Morse chain complex* associated to f , the metric g and the set of orientations O_r . $C_k(f)$ is called the k -th *Morse group* and the operator ∂_* is called the *Morse boundary operator* or *Morse differential*. It is proved in Salamon (ibid.) that the differential of a Morse complex is a particular case of a connection matrix for the finest Morse decomposition with the flow defined order, where each Morse set is a critical point of f . For more details on connection matrices, see Franzosa (1989) and Reineck (1990, 1995).

Example 5.3. Returning to Example 5.2, we now present the Morse chain complex associated to f . The Morse groups are $C_2(f) = \mathbb{Z}\langle x \rangle$, $C_1(f) = \mathbb{Z}\langle y \rangle$, $C_0(f) = \mathbb{Z}\langle z \rangle \oplus \mathbb{Z}\langle z' \rangle$, and $C_k(f) = 0$ for $k \in \mathbb{Z} \setminus \{0, 1, 2\}$. Moreover, $n_{u_1} = 1$, $n_{u_2} = -1$, $n_{v_1} = +1$, and $n_{v_2} = -1$, thus,

$$n(x, y) = n_{v_1} + n_{v_2} = 0, \quad n(y, z) = n_{u_2} = -1, \quad n(y, z') = n_{u_1} = 1.$$

The boundary operators $\partial_2 : C_2(f) \rightarrow C_1(f)$, $\partial_1 : C_1(f) \rightarrow C_0(f)$, and $\partial_0 : C_0(f) \rightarrow \{0\}$ are defined on the generators of $C_2(f)$, $C_1(f)$ and $C_0(f)$, respectively, by:

$$\partial_2\langle x \rangle = 0, \quad \partial_1\langle y \rangle = -\langle z \rangle + \langle z' \rangle, \quad \partial_0\langle z \rangle = 0, \quad \partial_0\langle z' \rangle = 0.$$

For all $k \in \mathbb{Z}$ with $k \neq 0, 1, 2$, ∂_k is the null operator.

Denote by $\Delta = \Delta(M, f, O_r)$ the matrix of the Morse boundary operator obtained considering an ordered basis of critical points of the Morse–Smale function f and the set O_r of orientations chosen on the unstable manifolds of all singularities with Morse index greater than zero. The columns of the matrix Δ need not be ordered with respect to the index. Figure 5.13 illustrates a possible structure for Δ with columns ordered with respect to the index.

In the remainder of this section we present some interesting properties of $\Delta(M, f, O_r)$ in the setting where M is a smooth closed surface. In this case, the nonzero entries of Δ are in blocks Δ_1 (or first block), which corresponds to connections from saddles to sinks, and Δ_2 (or second block), which corresponds to connections from sources to saddles.

The next proposition, which is proved in Bertolim, Lima, et al. (2016), asserts that changes on the orientations of the unstable manifolds produce similar matrices where one matrix can be obtained from the other through a change of basis by changing signs of some rows and columns.

Proposition 5.1. Let M be a smooth closed surface, $f : M \rightarrow \mathbb{R}$ be a Morse–Smale function on M and O_r , O'_r be two sets of orientations for all $W^u(x)$, $x \in \text{Crit}(f)$ with $\text{ind}_f(x) > 0$. If O_r and O'_r differ only by the orientations of the unstable manifolds of the critical points h^1, \dots, h^ℓ , then $\Delta(M, f, O'_r)$ is obtained from $\Delta(M, f, O_r)$ by multiplying by -1 the rows and columns corresponding to h^1, \dots, h^ℓ .

$$\begin{array}{ccccccc} & & \cdots & C_{k-1} & C_k & C_{k+1} & \cdots \\ \vdots & & 0 & & & & \\ C_{k-2} & 0 & & \boxed{\Delta_{k-1}} & & 0 & \\ & 0 & & 0 & & & \\ C_{k-1} & & 0 & & \boxed{\Delta_k} & & \\ & & 0 & & 0 & & \\ C_k & & & 0 & & \boxed{\Delta_{k+1}} & \\ & 0 & & & 0 & & \\ \vdots & & & & & & \\ & & & & & & 0 \end{array}$$

Figure 5.13: Morse differential.

Moreover, an entry in the matrix $\Delta(M, f, O_r)$ is nonzero if and only if it is nonzero in $\Delta(M, f, O'_r)$, i.e., given a smooth closed surface M and a Morse–Smale function on M , all the matrices for the Morse boundary operator are equal modulo 2.

The following theorem proves that, when working on orientable surfaces, the Morse differential takes on a very particular form.

Theorem 5.3. (Characterization of the Morse boundary operator on Orientable Surfaces) Let M be a smooth closed orientable surface and $f : M \rightarrow \mathbb{R}$ be a Morse–Smale function on M . Then the entries of a Morse differential on M belong to the set $\{-1, 0, 1\}$.

Proof. Let x, y be a pair of critical points such that $\text{ind}_f(x) - \text{ind}_f(y) = 1$. Since M is a surface, the dimension of the unstable and stable manifolds of every saddle is equal to 1, thus there are at most two connecting orbits joining a source to a saddle or a saddle to a sink. It follows that $\#\mathcal{M}_y^x \leq 2$. If $\#\mathcal{M}_y^x$ is equal to zero or 1, then clearly $n(x, y) \in \{-1, 0, 1\}$.

Assume that $\#\mathcal{M}_y^x = 2$, say $\mathcal{M}_y^x = \{u, v\}$. If x is a saddle and y is a sink, the gradient flow induces the same orientation on the orbits $\mathcal{O}(u)$ and $\mathcal{O}(v)$. However, $[\mathcal{M}_{xy}]_{\text{ind}}$ induces opposite orientations on $\mathcal{O}(u)$ and $\mathcal{O}(v)$. Hence, either $n_u = 1$ and $n_v = -1$ or $n_u = -1$ and $n_v = 1$. It follows that $n(x, y) = 0$. Finally, assume that x is a source and y is a saddle and let $\{\xi_1, \xi_2\}$ be an orientation for $W^u(x)$. Since M is an orientable surface, the ordered basis $\{\xi_1(u), \xi_2(u)\}$ and $\{\xi_1(v), \xi_2(v)\}$ are consistently oriented and the basis of $\mathcal{V}_u W^s(y)$ and $\mathcal{V}_v W^s(y)$ are consistently oriented. By the isomorphism in (5.2), the induced orientations $[\mathcal{O}(u)]_{\text{ind}}$ and $[\mathcal{O}(v)]_{\text{ind}}$ are opposite. Since the gradient flow induces the same orientations $[\dot{u}]$ and $[\dot{v}]$ then, once again $n(x, y) = 0$. See Figure 5.14. \square

The hypothesis of orientability in Theorem 5.3 is necessary. In fact, if M is the projective plane and f a perfect Morse–Smale function on M , the real intersection number between the source and the saddle is ± 2 .

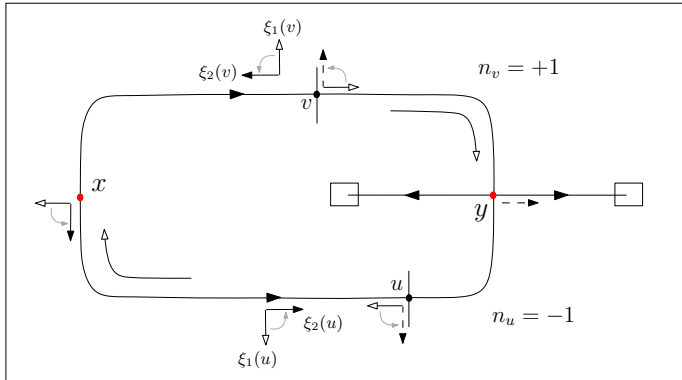


Figure 5.14: Determining characteristic sign for the source and saddle moduli spaces.

Corollary 5.1. *Let M be a smooth orientable closed surface, $f : M \rightarrow \mathbb{R}$ be a Morse–Smale function on M and Δ a matrix of the Morse boundary operator. If the orientations for the unstable manifolds are chosen consistently of all sources, then we have the following possibilities for the columns and rows of Δ corresponding to 1-chains:*

- (i) *If column j is a column in Δ_1 , then either column j contains two nonzero elements, namely 1 and -1 , or all entries in column j are zero.*
- (ii) *If row j is a row in Δ_2 , then either row j contains two nonzero elements, namely 1 and -1 , or all entries in row j are zero.*

Proof. Each saddle either connects to two sinks or it connects to one sink. By Theorem 5.3, each column of Δ corresponding to a 1-chain has either two nonzero entries, namely $+1$ and -1 , or it is a column of zeros. Moreover, each row of Δ corresponding to a 1-chain has either two nonzero entries, or it is a column of zeros. In the first case, the signs of the nonzero entries are determined by O_r . Since we are choosing the orientation of all unstable manifolds to be consistent, the nonzero entries in each row or column have opposite signs. \square

By Proposition 5.1, for any other choice of orientation, the Morse differential matrix is similar to Δ and obtained from Δ by multiplying a subset of rows and/or columns by -1 .

5.4 Spectral sequences associated to filtered Morse complexes

In this section, we introduce the Spectral Sequence Sweeping Algorithm and prove that it determines the generators of the modules E_p^r and the differentials d^r of the spectral

sequence associated to a filtered Morse chain complex. The main reference for this section is Cornea, de Rezende, and da Silveira (2010).

Let M be a smooth closed n -dimensional manifold, $f : M \rightarrow \mathbb{R}$ be a Morse–Smale function on M and $(C_*(f), \partial_*)$ be a Morse chain complex associated to f . We are interested in a specific filtration on $(C_*(f), \partial_*)$ induced by the negative gradient flow φ_f of f . Given a finest Morse decomposition $\{M_p\}_{p \in P}$, $P = \{1, \dots, m\}$, $m = \# \text{Crit}(f)$ such that there are distinct critical values c_p with $f^{-1}(c_p) \supset M(p)$, we can define a filtration on M by

$$\{F_{p-1}\}_{p=1}^m = \{f^{-1}(-\infty, c_p + \epsilon)\}_{p=1}^m.$$

Let $F = \{F_p C\}$ the induced filtration on $(C_*(f), \partial_*)$. Since for each $p \in P$ there is only one singularity in $F_p \setminus F_{p-1}$, the filtration F is called a *finest filtration*. We denote the only singularity in $F_p \setminus F_{p-1}$ by h_k^{p+1} , where k is the Morse index of the singularity. See Figure 5.15.

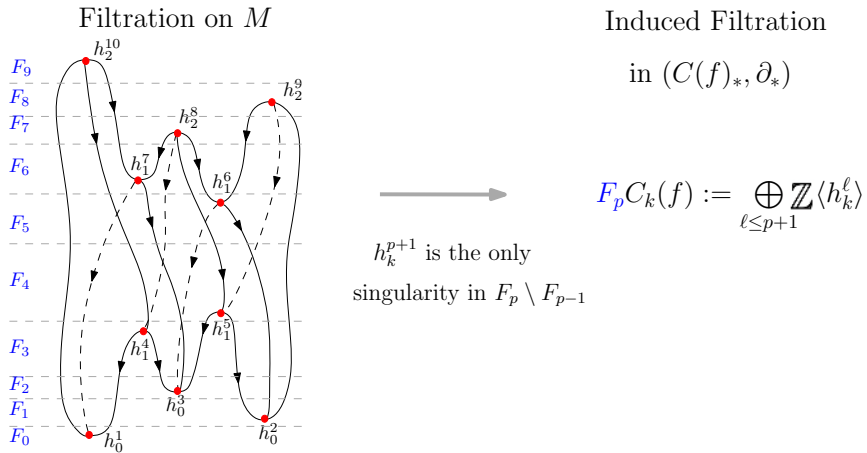


Figure 5.15: Finest filtration.

Let Δ be the matrix of the Morse boundary operator ∂ related to the ordered basis of elementary chains $\{h_{k_1}^1, h_{k_2}^2, \dots, h_{k_m}^m\}$ and let Δ_k be the submatrix of Δ whose columns correspond to k -chains and the rows correspond to $(k-1)$ -chains. The singularity h_k^{p+1} in $F_p \setminus F_{p-1}$ corresponds to column $(p+1)$ of Δ . Note that the numbering on the columns are shifted by one with respect to the subindex p of the filtration F_p .

The r -th diagonal² of Δ has entries $\Delta_{p+1-r, p+1}$ which represent the intersection numbers between the singularities M_{p+1} and M_{p+1-r} for $p \in \{r, \dots, m-1\}$. Clearly, if column $(p+1)$ intersects the submatrix Δ_k , then M_{p+1} is a singularity h_k^{p+1} of Morse

²By r -th diagonal one means the collection of entries $\Delta_{i,j}$ of Δ such that $j - i = r$.

index k and M_{p+1-r} is a singularity h_{k-1}^{p-r+1} of Morse index $k-1$. These singularities are in filtration $F_p \setminus F_{p-1}$ and $F_{p-r} \setminus F_{p-r-1}$, respectively. In this case, we say that the pair $(h_k^{p+1}, h_{k-1}^{p-r+1})$ has *gap* r .

We use the notation of the Morse boundary operator ∂ and its matrix Δ interchangeably.

It is easy to see that F is a convergent and bounded below filtration in the chain complex (C_*, ∂_*) . In fact, F is finite, that is, $F_{-1}C = 0$ and $F_p C = C$ for some p . Hence, the induced filtration on $H_*(C)$ is also convergent and bounded below. Moreover, by Theorem 5.1, there exists a convergent spectral sequence with

$$E_{p,q}^0 = F_p C_{p+q} / F_{p-1} C_{p+q} = G(C)_{p,q}$$

$$E_{p,q}^1 \cong H_{(p+q)}(F_p C_{p+q} / F_{p-1} C_{p+q})$$

and E^∞ is isomorphic to the module $GH_*(C)$.

The algebraic formulas for the modules are

$$E_{p,q}^r = Z_{p,q}^r / (Z_{p-1,q+1}^{r-1} + \partial Z_{p+r-1,q-r+2}^{r-1})$$

where,

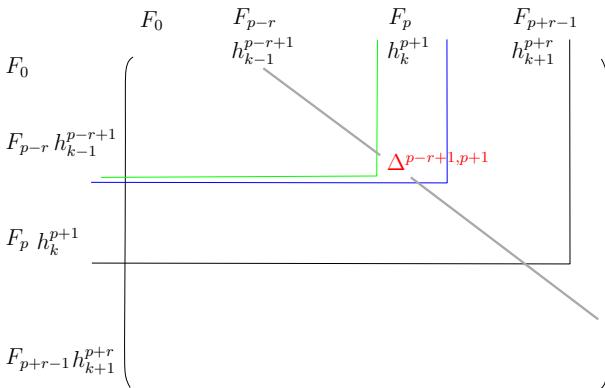
$$Z_{p,q}^r = \{c \in F_p C_{p+q} \mid \partial c \in F_{p-r} C_{p+q-1}\}.$$

Since the filtration considered is a finest filtration, where each Morse set is a singularity of index k , the only q such that $E_{p,q}^r$ is nonzero is $q = k - p$. Hence, we omit reference to q , i.e. E_p^r is in fact $E_{p,k-p}^r$.

Note that the module Z_p^r consists of all chains in $F_p C$ whose boundaries are in $F_{p-r} C$. The chains in $F_p C$ are the chains associated to the columns of Δ on and to the left of column $(p+1)$ and any linear combination of these columns. Moreover, since the boundary of the chains must be in $F_{p-r} C$, they correspond to columns or linear combinations of them with the property that the entries in rows $i > (p-r+1)$ are zeroes. An entry in matrix Δ which plays a fundamental role in encoding information of the spectral sequence in Δ is the element $\Delta_{p-r+1,p+1}$ on the r -th diagonal, row $(p-r+1)$ and column $(p+1)$. See Figure 5.16.

As r increases, there are changes in the generators of the \mathbb{Z} -modules E_p^r of the spectral sequence. One of the main results in this chapter connects these algebraic changes of the generators of the \mathbb{Z} -modules of the spectral sequence to a particular family of changes of basis over \mathbb{Q} of the differential matrix Δ , creating a collection of similar matrices $\{\Delta^r\}$. In order to do that, we introduce an algorithm called **Spectral Sequence Sweeping Algorithm (SSSA)**.

The SSSA singles out some nonzero entries of the matrix, which we refer to as primary pivots and change-of-basis pivots, of the r -th diagonal of Δ^r in order to define a matrix Δ^{r+1} . At each step, Δ^{r+1} is a change of basis of Δ^r . Hence, all Δ^r represent the boundary operator ∂ . We show that this family of matrices codify all the information on the generators of the modules E_p^r and the differentials d^r of the spectral sequence associated to a filtered Morse chain complex.

Figure 5.16: Z_p^r seen in the matrix Δ .

5.4.1 Spectral Sequence Sweeping Algorithm

In this section we present the SSSA and prove that it determines the generators of the modules E_p^r and induces the differentials d^r of the spectral sequence associated to a Morse chain complex (C_*, ∂_*) and a finest filtration F . This algorithm was first introduced in Cornea, de Rezende, and da Silveira (2010).

The SSSA gives as output a collection of similar matrices $\{\Delta^r\}$ for $r \geq 0$, where $\Delta^0 = \Delta$, and Δ^{r+1} is obtained from Δ^r performing a change of basis determined by the pivots on the r -th diagonal.

These changes of basis will later be proved to correspond to the changes in generators that happen in the spectral sequence at step r . Hence, this family of matrices will be used to determine the spectral sequence (E^r, d^r) .

Note that the SSSA as well as all other theorems in this chapter do not require the chosen basis of simple chains h_k^p be ordered with respect to k . Without loss of generality we assume the singularities to be ordered with respect to the filtration so as to simplify the notation. More generally, one can introduce a subsequence notation for the columns in order to consider only the index k columns.

For a fixed r -th diagonal the algorithm below must be applied for all k simultaneously.

A - Initial step

1. Consider the entries $\Delta_{k_i,j}$ in Δ_k where the i -th row is an h_{k-1} row (i.e. it corresponds to a $k-1$ -chain) and the j -th column is an h_k column (i.e. it corresponds to a k -chain).

Without loss of generality, we assume that the first diagonal of Δ contains nonzero entries $\Delta_{k_i,j}$, otherwise we define $\Delta^1 = \Delta$ and we repeat this step until we reach a diagonal of Δ which contains nonzero entries.

These nonzero entries will be marked as index k **primary pivots**. Note that for each nonzero $\Delta_{k_i,j}$ on Δ , the entries $\Delta_{k_s,j}$ for $s > i$ are all equal to zero.

We end this process by defining Δ^1 as Δ with the index k primary pivots on the first diagonal marked.

2. Consider the matrix Δ^1 and let $\Delta_{k_i,j}^1$ be the entries in Δ^1 where the i -th row is an h_{k-1} row and the j -th column is an h_k column. Analogously to 1, we assume that the second diagonal contains nonzero entries $\Delta_{k_i,j}^1$. We now construct a matrix Δ^2 following the procedure:

Given a nonzero entry $\Delta_{k_i,j}^1$ on the second diagonal of Δ^1 ,

- (a) if there are no primary pivots in row i and column j , mark it as an index k primary pivot,
- (b) otherwise, consider the entries in column j and row s with $s > i$ in Δ^1 .
 - (b1) If there is an index k primary pivot in an entry in column j and row s , with $s > i$, then the entry is left unmarked.
 - (b2) If there are no primary pivots in column j below $\Delta_{k_i,j}^1$, then there is an index k primary pivot in row i , say in a column t of Δ^1 , with $t < j$. In this case, the entry $\Delta_{k_i,j}^1$ is marked as a **change-of-basis pivot**.

At the end of this step we have defined a matrix Δ^2 which has the same numerical entries of Δ^1 except that some entries of the second diagonal are marked as primary and change-of-basis pivots. In Figure 5.17, primary pivots are encircled and change-of-basis pivots are encased in boxes.

B - Intermediary step

Consider a matrix Δ^r with primary and change-of-basis pivots marked on the ξ -th diagonal for all $\xi \leq r$. In this step we describe how Δ^{r+1} is defined. If there are no change-of-basis pivots in the r -th diagonal, go to step B.2 and define $\Delta^{r+1} = \Delta^r$ with diagonal $(r+1)$ marked with primary and change-of-basis pivots.

B.1 - Change of basis

Suppose $\Delta_{k_i,j}^r$ is a change-of-basis pivot. Then perform a change of basis on Δ^r by adding a linear combination over \mathbb{Q} of all the h_k columns ℓ of Δ^r with $\kappa \leq \ell < j$, where κ is the first column of Δ^r associated to a k -chain, to a positive integer multiple $u \neq 0$ of the j -th column of Δ^r , in order to zero out the entry $\Delta_{k_i,j}^r$ without introducing nonzero entries in $\Delta_{k_s,j}^r$ for $s > i$. Moreover, the resulting linear combination should be of the form $\beta^\kappa h_k^\kappa + \dots + \beta^{j-1} h_k^{j-1} + \beta^j h_k^j$ where β^ℓ are integers for $\ell = \kappa, \dots, j$.

The integer u is called a **leading coefficient** of the change of basis. If more than one linear combination is possible, we choose one which minimizes u . Let u be

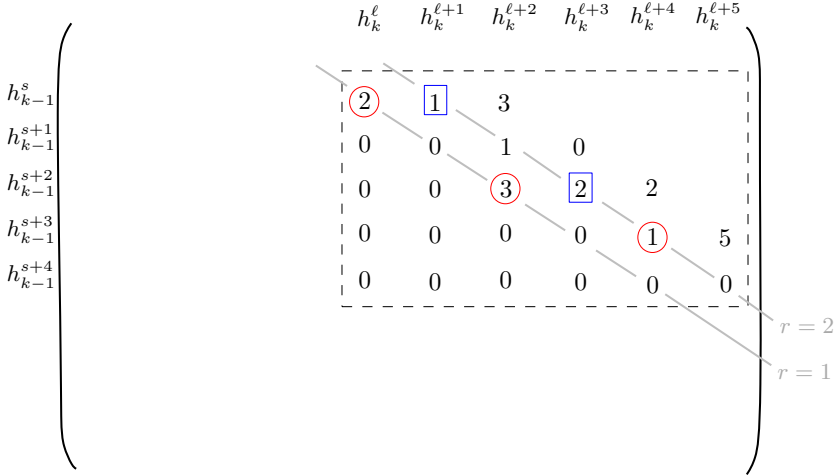


Figure 5.17: SSSA - Initial Step.

the minimal leading coefficient of a change of basis. Once this is done, we obtain a k -chain associated to the j -th column of Δ^{r+1} . It is a linear combination over \mathbb{Q} of the h_k^ℓ columns, $\kappa \leq \ell < j$, of Δ^r plus an integer multiple u of the j -th column of Δ^r such that $\Delta_{k_{j,j}}^{r+1} = 0$. It is also an integer linear combination of h_k columns of Δ on and to the left of the j -th column.

Observe that if the $\bar{\ell}$ -th column of Δ^r is an h_k column, it corresponds to an integer linear combination $\sigma_k^{\bar{\ell},r} = \sum_{\ell=\kappa}^{\bar{\ell}} c_{\ell}^{\bar{\ell},r} h_k^\ell$ of h_k columns of Δ where the κ -th column

is the first column in Δ associated to a k -chain. The notation of $\sigma_k^{\bar{\ell},r}$ indicates the Morse index k and the $\bar{\ell}$ -th column of Δ^r . Hence if the j -th column of Δ^{r+1} is an h_k column, then

$$\begin{aligned} \sigma_k^{j,r+1} = u \underbrace{\sum_{\ell=\kappa}^j c_\ell^{j,r} h_k^\ell}_{\sigma_k^{j,r}} + q_{j-1} \underbrace{\sum_{\ell=\kappa}^{j-1} c_\ell^{j-1,r} h_k^\ell}_{\sigma_k^{j-1,r}} + \dots \\ \dots + q_{\kappa+1} \underbrace{(c_\kappa^{\kappa+1,r} h_k^\kappa + c_{\kappa+1}^{\kappa+1,r} h_k^{\kappa+1})}_{\sigma_k^{\kappa+1,r}} + q_\kappa \underbrace{c_\kappa^{\kappa,r} h_k^\kappa}_{\sigma_k^{\kappa,r}} \end{aligned} \quad (5.4)$$

or, equivalently,

$$\begin{aligned}\sigma_k^{j,r+1} &= (\mathbf{u}c_k^{j,r} + q_{j-1}c_k^{j-1,r} + \cdots + q_\kappa c_\kappa^{\kappa,r})h_k^\kappa + \\ &\quad + (\mathbf{u}c_{\kappa+1}^{j,r} + q_{j-1}c_{\kappa+1}^{j-1,r} + \cdots + q_{\kappa+1}c_{\kappa+1}^{\kappa+1,r})h_k^{\kappa+1} + \\ &\quad \cdots + (\mathbf{u}c_{j-1}^{j,r} + q_{j-1}c_{j-1}^{j-1,r})h_k^{j-1} + \mathbf{u}c_j^{j,r}h_k^j\end{aligned}\quad (5.5)$$

with $c_\kappa^{\kappa,r} = 1$ and

$$\begin{aligned}c_k^{j,r+1} &= \mathbf{u}c_k^{j,r} + q_{j-1}c_k^{j-1,r} + \cdots + q_\kappa c_\kappa^{\kappa,r} \in \mathbb{Z} \\ c_{\kappa+1}^{j,r+1} &= \mathbf{u}c_{\kappa+1}^{j,r} + q_{j-1}c_{\kappa+1}^{j-1,r} + \cdots + q_{\kappa+1}c_{\kappa+1}^{\kappa+1,r} \in \mathbb{Z} \\ &\vdots \\ c_{j-1}^{j,r+1} &= \mathbf{u}c_{j-1}^{j,r} + q_{j-1}c_{j-1}^{j-1,r} \in \mathbb{Z} \\ c_j^{j,r+1} &= \mathbf{u}c_j^{j,r} \in \mathbb{Z}.\end{aligned}\quad (5.6)$$

Clearly, the first column of any Δ_k can not undergo any change of basis since there is no column to its left and this explains why $c_\kappa^{\kappa,r} = 1$.

Note that $q_{\bar{\ell}} = 0$ in $q_{\bar{\ell}} \sum_{\ell=1}^{\bar{\ell}} c_\ell^{\bar{\ell},r} h_k^\ell$ whenever the $\bar{\ell}$ -th column has a primary pivot in an row s for $s > i$.

If the primary pivot of the i -th row is on the t -th column, then the rational number q_t is nonzero in $q_t \sum_{\ell=1}^t c_\ell^{t,r} h_k^\ell$ and

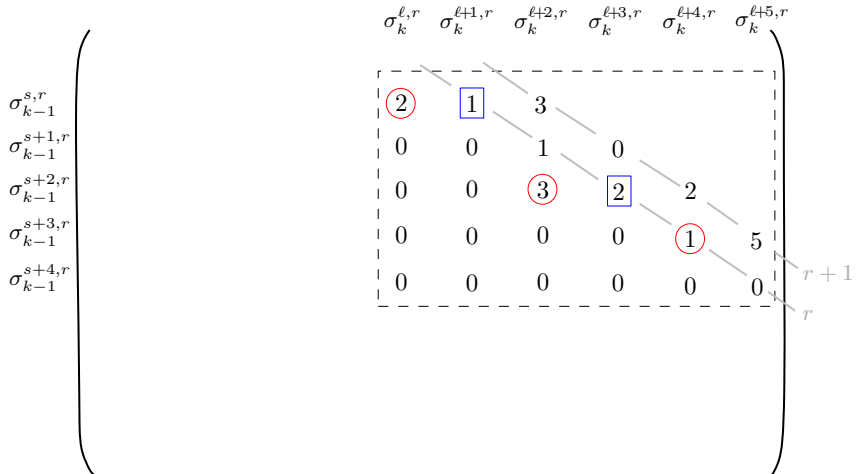
$$\Delta_{k_{i,j}}^{r+1} = \mathbf{u}\Delta_{k_{i,j}}^r + q_t \Delta_{k_{i,t}}^r = 0.$$

Since $\mathbf{u} \geq 1$ is unique, then q_t is uniquely defined.

Once the above procedure is done for all change-of-basis pivots of the r -th diagonal of Δ^r , we can define a change-of-basis matrix.

Therefore the matrix Δ^{r+1} has numerical values determined by the change of basis over \mathbb{Q} of Δ^r . In particular, all the change-of-basis pivots on the r -th diagonal Δ^r are zero in Δ^{r+1} . See Figures 5.18 and 5.19.

B.2 - Marking the diagonal $(r + 1)$ of Δ^{r+1}

Figure 5.18: SSSA - Intermeriary Step - Δ^r .

Consider the matrix Δ^{r+1} defined in the previous step. In this step we mark the $(r+1)$ -st diagonal with primary and change-of-basis pivots as follows:

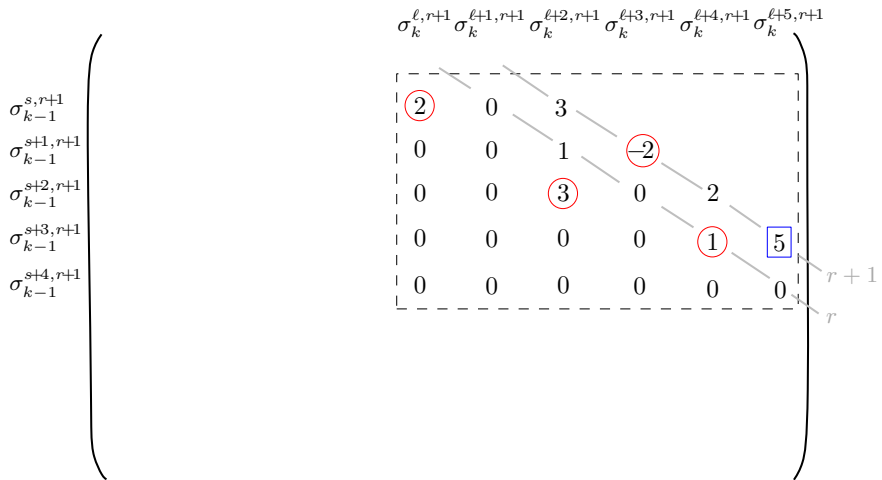
Given a nonzero entry $\Delta_{k_{i,j}}^{r+1}$,

- if there are no primary pivots in row i and column j , mark it as an index k primary pivot,
- otherwise, consider the entries in column j and row s with $s > i$ in Δ^{r+1} .
 - If there is an index k primary pivot in column j below $\Delta_{k_{i,j}}^{r+1}$, then leave this entry unmarked.
 - If there are no primary pivots in column j below $\Delta_{k_{i,j}}^{r+1}$, then there is an index k primary pivot in row i , say in a column t of Δ^{r+1} , with $t < j$. In this case mark it as a change of basis pivot. See Figure 5.19 where, as in the Initial Step, primary pivots are encircled and change-of-basis pivots are enclosed in boxes.

C - Final step

We repeat the above procedure until all diagonals have been considered.

Example 5.4. Suppose Δ given in Figure 5.20 is a Morse differential. Figures 5.21 to 5.28 are obtained when we apply the SSSA to Δ . In all figures the markup process of the SSSA iterations is done as follows: primary pivots are encircled and change-of-basis pivots are enclosed in boxes. Note that we keep track of the changes of basis at each step of the SSSA presenting the basis vertically on the left of each matrix Δ^r .

Figure 5.19: SSSA - Intermeriary Step - Δ^{r+1} .

The next proposition is a list of important properties of the collection of matrices Δ^r produced by the SSSA. The proof is a direct consequence of the SSSA rules and can be found in Cornea, de Rezende, and da Silveira (2010).

- Proposition 5.2.**
1. For each r , Δ^r is strictly upper triangular and $\Delta^r \circ \Delta^r = 0$.
 2. If $\Delta_{i,j}^r$ is a primary pivot there can be no linear combination of columns to the left of the j -th column that added to the j -th column would zero that entry as well as maintaining all entries $\Delta_{s,j}^r$ equal to zero for $s > i$.
 3. If the entry $\Delta_{p-r+1,p+1}^r$ is a primary pivot or a change-of-basis pivot, then $\Delta_{s,p+1}^r = 0$ for all $s > p - r + 1$.
 4. There can be no more than one primary pivot in a given row or column. Moreover, if there is a primary pivot in row i then there is no primary pivot in column i and vice-versa.

Let Δ be the matrix in Example 5.4 represented in Figure 5.20. Recall that the SSSA produces the sequence of matrices $\Delta^1, \dots, \Delta^8$ presented in Figures 5.21 to 5.28, respectively. Note that the entry $\Delta_{4,10}^3$ is a fractionary entry, i.e. Example 5.4 shows that during the application of the SSSA, some fractionary numbers can appear as entries of an intermediary matrix which are not pivots. However, the next result guarantees that the entries of the last matrix produced by the SSSA are all integers. The proof of this theorem can be found in de Rezende, Mello, and da Silveira (2010), Theorem 12.

Theorem 5.4. Let Δ^L be the last matrix produced by the SSSA. Then all entries in Δ^L are integer numbers.

	F_0	F_1	F_2	F_3	F_4	F_5	F_6	F_7	F_8	F_9	F_{10}	F_{11}	F_{12}	F_{13}
	h_0^1	h_{k-1}^2	h_{k-1}^3	h_k^4	h_k^5	h_k^6	h_k^7	h_k^8	h_k^9	h_{k+1}^{10}	h_{k+1}^{11}	h_{k+1}^{12}	h_{k+1}^{13}	h_n^{14}
$F_0 h_0^1$	0	0	0	0	0	0	0	0	0	0	0	0	0	0
$F_1 h_{k-1}^2$	0	0	0	2	3	2	1	0	0	0	0	0	0	0
$F_2 h_{k-1}^3$	0	0	0	2	3	1	0	2	1	0	0	0	0	0
$F_3 h_k^4$	0	0	0	0	0	0	0	0	0	0	1	-3	1	0
$F_4 2h_k^5$	0	0	0	0	0	0	0	0	0	1	0	2	0	0
$F_5 h_k^6$	0	0	0	0	0	0	0	0	0	-3	-2	1	-3	0
$F_6 h_k^7$	0	0	0	0	0	0	0	0	0	3	2	-2	4	0
$F_7 h_k^8$	0	0	0	0	0	0	0	0	0	-1	1	-2	1	0
$F_8 h_k^9$	0	0	0	0	0	0	0	0	0	2	-2	3	-1	0
$F_9 h_{k+1}^{10}$	0	0	0	0	0	0	0	0	0	0	0	0	0	0
$F_{10} h_{k+1}^{11}$	0	0	0	0	0	0	0	0	0	0	0	0	0	0
$F_{11} h_{k+1}^{12}$	0	0	0	0	0	0	0	0	0	0	0	0	0	0
$F_{12} h_{k+1}^{13}$	0	0	0	0	0	0	0	0	0	0	0	0	0	0
$F_{13} h_n$	0	0	0	0	0	0	0	0	0	0	0	0	0	0

Figure 5.20: SSSA: Δ .

The next step is to prove that the collection of matrices produced by the SSSA in fact determines the modules and the differentials of the associated spectral sequence. Recall that

$$E_p^r = Z_p^r / (Z_{p-1}^{r-1} + \partial Z_{p+r-1}^{r-1})$$

where,

$$Z_p^r = \{c \in F_p C \mid \partial c \in F_{p-r} C\}.$$

The \mathbb{Z} -module $Z_{p,k-p}^r = \{c \in F_p C_k; \partial c \in F_{p-r} C_{k-1}\}$ is generated by k -chains contained in F_p with boundaries in F_{p-r} . This corresponds in Δ to all the h_k columns on and to the left of column $(p+1)$ or linear combinations of these columns, whose boundaries (nonzero entries) are on and above row $(p-r+1)$. Similarly $Z_{p-1,k-(p-1)}^{r-1} = \{c \in F_{p-1} C_k; \partial c \in F_{p-r} C_{k-1}\}$ corresponds in Δ to the h_k columns on and to the left of column p , or linear combinations of these columns, whose boundaries are on and above row $(p-r+1)$. Finally,

$$\partial Z_{p+r-1,(k+1)-(p+r-1)}^{r-1} = \partial \{c \in F_{p+r-1} C_{k+1}; \partial c \in F_p C_k\}$$

consists of all the boundaries of elements in $Z_{p+r-1,(k+1)-(p+r-1)}^{r-1}$. This corresponds in Δ to all the h_k columns on and to the left of column $(p+1)$ and linear combinations of these columns or, equivalently, all h_k rows on and above row $(p+1)$ and linear combinations

	$\sigma_0^{1,1}$	$\sigma_{k-1}^{2,1}$	$\sigma_{k-1}^{3,1}$	$\sigma_k^{4,1}$	$\sigma_k^{5,1}$	$\sigma_k^{6,1}$	$\sigma_k^{7,1}$	$\sigma_k^{8,1}$	$\sigma_k^{9,1}$	$\sigma_{k+1}^{10,1}$	$\sigma_{k+1}^{11,1}$	$\sigma_{k+1}^{12,1}$	$\sigma_{k+1}^{13,1}$	$\sigma_n^{14,1}$
$\sigma_0^{1,1} = h_0$	0	0	0	0	0	0	0	0	0	0	0	0	0	0
$\sigma_{k-1}^{2,1} = h_{k-1}^2$	0	0	0	2	3	2	1	0	0	0	0	0	0	0
$\sigma_{k-1}^{3,1} = h_{k-1}^3$	0	0	0	2	1	0	2	1	0	0	0	0	0	0
$\sigma_k^{4,1} = h_k^4$	0	0	0	0	0	0	0	0	0	0	1	-3	1	0
$\sigma_k^{5,1} = 2h_k^5$	0	0	0	0	0	0	0	0	0	1	0	2	0	0
$\sigma_k^{6,1} = h_k^6$	0	0	0	0	0	0	0	0	0	-3	-2	1	-3	0
$\sigma_k^{7,1} = h_k^7$	0	0	0	0	0	0	0	0	0	3	2	-2	4	0
$\sigma_k^{8,1} = h_k^8$	0	0	0	0	0	0	0	0	0	-1	1	-2	1	0
$\sigma_k^{9,1} = h_k^9$	0	0	0	0	0	0	0	0	0	2	-2	3	-1	0
$\sigma_{k+1}^{10,1} = h_{k+1}^{10}$	0	0	0	0	0	0	0	0	0	0	0	0	0	0
$\sigma_{k+1}^{11,1} = h_{k+1}^{11}$	0	0	0	0	0	0	0	0	0	0	0	0	0	0
$\sigma_{k+1}^{12,1} = h_{k+1}^{12}$	0	0	0	0	0	0	0	0	0	0	0	0	0	0
$\sigma_{k+1}^{13,1} = h_{k+1}^{13}$	0	0	0	0	0	0	0	0	0	0	0	0	0	0
$\sigma_n^{14,1} = h_n$	0	0	0	0	0	0	0	0	0	0	0	0	0	0

Figure 5.21: SSSA: Δ^1 .

of these rows, which are boundaries of h_{k+1} columns that are on and to the left of column $(p+r)$. See Figure 5.16.

Theorem 5.5. Let M be a smooth closed n -dimensional manifold, $f : M \rightarrow \mathbb{R}$ be a Morse–Smale function, $(C_*(f), \partial_*)$ be a Morse chain complex associated to f , F a finest filtration on $(C_*(f), \partial_*)$ and (E_p^r, d^r) be a spectral sequence associated to this filtered chain complex. For each r , the matrix Δ^r , obtained from the SSSA applied to a matrix Δ of the Morse differential, determines the generators of E_p^r for all p . More specifically, $E_{p,k-p}^r$ is either zero or a finitely generated module whose generator corresponds to a k -chain associated to column $(p+1)$ of Δ^r .

The proof of Theorem 5.5 is based on two main ideas, which are stated in the next two propositions. The first and most important one involves deriving a formula for Z_p^r using the σ 's produced by the SSSA. In fact, since

$$E_p^r = Z_p^r / (Z_{p-1}^{r-1} + \partial Z_{p+r-1}^{r-1}),$$

knowing the generators of Z_p^r will provide us with the generator of E_p^r .

We present this formula in the next proposition. The proof of this relevant result, which we reproduce here, is based on the proof of Proposition 4.1 of Cornea, de Rezende, and da Silveira (2010).

	$\sigma_0^{1,2}$	$\sigma_{k-1}^{2,2}$	$\sigma_{k-1}^{3,2}$	$\sigma_k^{4,2}$	$\sigma_k^{5,2}$	$\sigma_k^{6,2}$	$\sigma_k^{7,2}$	$\sigma_k^{8,2}$	$\sigma_k^{9,2}$	$\sigma_{k+1}^{10,2}$	$\sigma_{k+1}^{11,2}$	$\sigma_{k+1}^{12,2}$	$\sigma_{k+1}^{13,2}$	$\sigma_n^{14,2}$
$\sigma_0^{1,2} = h_0$	0	0	0	0	0	0	0	0	0	0	0	0	0	0
$\sigma_{k-1}^{2,2} = h_{k-1}^2$	0	0	0	1	2	3	2	1	0	0	0	0	0	0
$\sigma_{k-1}^{3,2} = h_{k-1}^3$	0	0	0	2	3	1	0	2	1	0	0	0	0	0
$\sigma_k^{4,2} = h_k^4$	0	0	0	0	0	0	0	0	0	0	1	-3	1	0
$\sigma_k^{5,2} = 2h_k^5$	0	0	0	0	0	0	0	0	0	1	0	2	0	0
$\sigma_k^{6,2} = h_k^6$	0	0	0	0	0	0	0	0	0	-3	-2	1	-3	0
$\sigma_k^{7,2} = h_k^7$	0	0	0	0	0	0	0	0	0	3	2	-2	4	0
$\sigma_k^{8,2} = h_k^8$	0	0	0	0	0	0	0	0	0	-1	1	-2	1	0
$\sigma_k^{9,2} = h_k^9$	0	0	0	0	0	0	0	0	0	2	3	-1	0	0
$\sigma_{k+1}^{10,2} = h_{k+1}^{10}$	0	0	0	0	0	0	0	0	0	0	0	0	0	0
$\sigma_{k+1}^{11,2} = h_{k+1}^{11}$	0	0	0	0	0	0	0	0	0	0	0	0	0	0
$\sigma_{k+1}^{12,2} = h_{k+1}^{12}$	0	0	0	0	0	0	0	0	0	0	0	0	0	0
$\sigma_{k+1}^{13,2} = h_{k+1}^{13}$	0	0	0	0	0	0	0	0	0	0	0	0	0	0
$\sigma_n^{14,2} = h_n$	0	0	0	0	0	0	0	0	0	0	0	0	0	0

Figure 5.22: SSSA: Δ^2 .

Proposition 5.3. If κ is the first column of Δ associated to a k -chain then

$$Z_{p,k-p}^r = \mathbb{Z}[\mu^{p+1,r} \sigma_k^{p+1,r}, \mu^{p,r-1} \sigma_k^{p,r-1}, \dots, \mu^{\kappa, r-p-1+\kappa} \sigma_k^{\kappa, r-p-1+\kappa}],$$

where $\mu^{j,\xi} = 0$ whenever the primary pivot of column j is below row $(p-r+1)$ and $\mu^{j,\xi} = 1$ otherwise.

Proof. Let $\sigma_k^{p+1-\xi, r-\xi}$ be the chain associated to column $(p+1-\xi)$ of the matrix $\Delta^{r-\xi}$, for $\xi \in \{0, \dots, p+1-\kappa\}$. By definition, $\mu^{p+1-\xi, r-\xi} = 1$ if and only if the primary pivot in column $(p+1-\xi)$ is on or above row $(p+1-\xi) - (r-\xi) = p-r+1$. See Figure 5.29.

Clearly the chains corresponding to columns with primary pivots below row $(p-r+1)$ do not correspond to generators of $Z_{p,k-p}^r$. Then consider a k -chain $\sigma_k^{p+1-\xi, r-\xi}$, where $\xi \in \{0, \dots, p+1-\kappa\}$, associated to column $(p+1-\xi)$ of $\Delta^{r-\xi}$ such that the primary pivot of column $(p+1-\xi)$ is on or above row $(p-r+1)$.

Firstly we prove that $\sigma_k^{p+1-\xi, r-\xi}$ is a generator of Z_p^r . Clearly $\sigma_k^{p+1-\xi, r-\xi}$ is in $F_p C_k$ for $\xi \geq 0$. Moreover, since the $(r-\xi)$ -th step of the SSSA zeroes out all change-of-basis pivots below the $(r-\xi)$ -th diagonal, then all nonzero entries of column $(p+1-\xi)$ of $\Delta^{r-\xi}$ are on and above row $(p+1-\xi) - (r-\xi) = (p-r+1)$. Hence the boundary of $\sigma_k^{p+1-\xi, r-\xi}$ is in $F_{p-r} C_{k-1}$.

	$\sigma_0^{1,3}$	$\sigma_{k-1}^{2,3}$	$\sigma_{k-1}^{3,3}$	$\sigma_k^{4,3}$	$\sigma_k^{5,3}$	$\sigma_k^{6,3}$	$\sigma_k^{7,3}$	$\sigma_k^{8,3}$	$\sigma_k^{9,3}$	$\sigma_{k+1}^{10,3}$	$\sigma_{k+1}^{11,3}$	$\sigma_{k+1}^{12,3}$	$\sigma_{k+1}^{13,3}$	$\sigma_n^{14,3}$
$\sigma_0^{1,3} = h_0$	0	0	0	0	0	0	0	0	0	0	0	0	0	0
$\sigma_{k-1}^{2,3} = h_{k-1}^2$	0	0	0	2	0	2	1	0	0	0	0	0	0	0
$\sigma_{k-1}^{3,3} = h_{k-1}^3$	0	0	0	1	2	0	1	2	1	0	0	0	0	0
$\sigma_k^{4,3} = h_k^4$	0	0	0	0	0	0	0	0	0	3/2	5/2	0	1	0
$\sigma_k^{5,3} = 2h_k^5 - 3h_k^4$	0	0	0	0	0	0	0	0	0	1/2	1/2	1	0	0
$\sigma_k^{6,3} = h_k^6$	0	0	0	0	0	0	0	0	0	-3	-5	1	-3	0
$\sigma_k^{7,3} = h_k^7$	0	0	0	0	0	0	0	0	0	3	5	-2	4	0
$\sigma_k^{8,3} = h_k^8$	0	0	0	0	0	0	0	0	0	-1	0	-2	1	0
$\sigma_k^{9,3} = h_k^9$	0	0	0	0	0	0	0	0	0	2	0	3	-1	0
$\sigma_{k+1}^{10,3} = h_{k+1}^{10}$	0	0	0	0	0	0	0	0	0	0	0	0	0	0
$\sigma_{k+1}^{11,3} = h_{k+1}^{11} + h_{k+1}^{10}$	0	0	0	0	0	0	0	0	0	0	0	0	0	0
$\sigma_{k+1}^{12,3} = h_{k+1}^{12}$	0	0	0	0	0	0	0	0	0	0	0	0	0	0
$\sigma_{k+1}^{13,3} = h_{k+1}^{13}$	0	0	0	0	0	0	0	0	0	0	0	0	0	0
$\sigma_n^{14,3} = h_n$	0	0	0	0	0	0	0	0	0	0	0	0	0	0

Figure 5.23: SSSA: Δ^3 .

We shall now prove that any element in Z_p^r is an integer linear combination of $\mu^{p+1-\xi, r-\xi} \sigma_k^{p+1-\xi, r-\xi}$ for $\xi = 0, \dots, p+1-\kappa$ by multiple induction in p and r . We denote by ξ_1 the first diagonal in Δ that intersects Δ_k .

(A1) $p = \kappa - 1$: Let ξ be such that the boundary of h_k^κ is in $F_{\kappa-1-\xi} C_k \setminus F_{\kappa-1-\xi-1} C_k$.

- Since $Z_{\kappa-1}^r$ is generated by k -chains in $F_{\kappa-1} C_k$ with boundaries in $F_{\kappa-1-r} C_{k-1}$ and h_k^κ is the only chain in $F_{\kappa-1} C_k$, then there are two possibilities:
 1. If $\xi < r$ then $\partial h_k^\kappa \notin F_{\kappa-1-r} C_{k-1}$, hence $Z_{\kappa-1}^r = 0$.
 2. If $\xi > r$ then $\partial h_k^\kappa \in F_{\kappa-1-r} C_{k-1}$, hence $Z_{\kappa-1}^r = \mathbb{Z}[h_k^\kappa]$.
- The k -chain $\sigma_k^{\kappa,r}$ corresponds to column κ in Δ^r . Since there is no change of basis caused by the SSSA that affects the first column of Δ_k , $\sigma_k^{\kappa,r} = h_k^\kappa$. Thus, $\mu^{\kappa,r} = 1$ if and only if the boundary of h_k^κ is on or above the r -th diagonal. Hence
 1. If $\xi < r$ then $\mu^{\kappa,r} = 0$. Thus $\mathbb{Z}[\mu^{\kappa,r} \sigma_k^{\kappa,r}] = 0$
 2. If $\xi > r$ then $\mu^{\kappa,r} = 1$. Thus $\mathbb{Z}[\mu^{\kappa,r} \sigma_k^{\kappa,r}] = \mathbb{Z}[h_k^\kappa] = \mathbb{Z}[\sigma_k^{\kappa,r}]$.

Hence $Z_{\kappa-1}^r = \mathbb{Z}[\mu^{\kappa,r} \sigma_k^{\kappa,r}]$.

	$\sigma_0^{1,4}$	$\sigma_{k-1}^{2,4}$	$\sigma_{k-1}^{3,4}$	$\sigma_k^{4,4}$	$\sigma_k^{5,4}$	$\sigma_k^{6,4}$	$\sigma_k^{7,4}$	$\sigma_k^{8,4}$	$\sigma_k^{9,4}$	$\sigma_{k+1}^{10,4}$	$\sigma_{k+1}^{11,4}$	$\sigma_{k+1}^{12,4}$	$\sigma_{k+1}^{13,4}$	$\sigma_n^{14,4}$
$\sigma_0^{1,4} = h_0$	0	0	0	0	0	0	0	0	0	0	0	0	0	0
$\sigma_{k-1}^{2,4} = h_{k-1}^2$	0	0	0	2	0	1	1	0	0	0	0	0	0	0
$\sigma_{k-1}^{3,4} = h_{k-1}^3$	0	0	0	2	0	0	0	2	1	0	0	0	0	0
$\sigma_k^{4,4} = h_k^4$	0	0	0	0	0	0	0	0	0	0	0	1	-1/2	0
$\sigma_k^{5,4} = 2h_k^5 - 3h_k^4$	0	0	0	0	0	0	0	0	0	-1	-2	6	-3/2	0
$\sigma_k^{6,4} = h_k^6 - h_k^5 + h_k^4$	0	0	0	0	0	0	0	0	0	-3	-5	11	-3	0
$\sigma_k^{7,4} = h_k^7$	0	0	0	0	0	0	0	0	0	3	5	-13	4	0
$\sigma_k^{8,4} = h_k^8$	0	0	0	0	0	0	0	0	0	-1	0	-1	1	0
$\sigma_k^{9,4} = h_k^9$	0	0	0	0	0	0	0	0	0	2	0	0	1	0
$\sigma_{k+1}^{10,4} = h_{k+1}^{10}$	0	0	0	0	0	0	0	0	0	0	0	0	0	0
$\sigma_{k+1}^{11,4} = h_{k+1}^{11} + h_{k+1}^{10}$	0	0	0	0	0	0	0	0	0	0	0	0	0	0
$\sigma_{k+1}^{12,4} = 2h_{k+1}^{12} - 3h_{k+1}^{10}$	0	0	0	0	0	0	0	0	0	0	0	0	0	0
$\sigma_{k+1}^{13,4} = h_{k+1}^{13}$	0	0	0	0	0	0	0	0	0	0	0	0	0	0
$\sigma_n^{14,4} = h_n$	0	0	0	0	0	0	0	0	0	0	0	0	0	0

Figure 5.24: SSSA: Δ^4 .

(A₂) $r = \xi_1$: The columns $h_k^{p+1}, \dots, h_k^\kappa$ of Δ have nonzero entries above the ξ_1 -th diagonal, thus, on or above row $(p - \xi_1 + 1)$.

- Since $Z_p^{\xi_1}$ is composed by the k -chains in $F_p C_k$ with boundary in $F_{p-\xi_1} C_{k-1}$ and the columns of Δ associated to the chains $h_k^{p+1}, \dots, h_k^\kappa$ have nonzero entries on and above row $(p - \xi_1 + 1)$, then their boundaries are in $F_{p-\xi_1} C_{k-1}$, i.e.

$$Z_p^{\xi_1} = \mathbb{Z}[h_k^{p+1}, \dots, h_k^\kappa].$$

- The nonzero entries in the columns of Δ corresponding to the chains $h_k^{p+1}, \dots, h_k^\kappa$ are all on or above the ξ_1 -th diagonal, then $\sigma_k^{j,\xi_1} = h_k^j$, $j = \kappa, \dots, p+1$ and $\mu^{j,\xi_1} = 1$, $j = \kappa, \dots, p+1$. Hence,

$$\mathbb{Z}[\mu^{p+1,\xi_1} \sigma_k^{p+1,r}, \dots, \mu^{\kappa,\kappa-p+1+\xi_1} \sigma_k^{\kappa,\kappa-p+1+\xi_1}] = \mathbb{Z}[h_k^{p+1}, \dots, h_k^\kappa].$$

Therefore, $Z_p^{\xi_1} = \mathbb{Z}[\mu^{p+1,\xi_1} \sigma_k^{p+1,r}, \dots, \mu^{\kappa,\kappa-p+1+\xi_1} \sigma_k^{\kappa,\kappa-p+1+\xi_1}]$.

(B) Assume that

$$Z_{p-1}^{r-1} = \mathbb{Z}[\mu^{p,r-1} \sigma_k^{p,r-1}, \dots, \mu^{\kappa,r-p-1+\kappa} \sigma_k^{\kappa,r-p-1+\kappa}],$$

	$\sigma_0^{1,5}$	$\sigma_{k-1}^{2,5}$	$\sigma_{k-1}^{3,5}$	$\sigma_k^{4,5}$	$\sigma_k^{5,5}$	$\sigma_k^{6,5}$	$\sigma_k^{7,5}$	$\sigma_k^{8,5}$	$\sigma_k^{9,5}$	$\sigma_{k+1}^{10,5}$	$\sigma_{k+1}^{11,5}$	$\sigma_{k+1}^{12,5}$	$\sigma_{k+1}^{13,5}$	$\sigma_n^{14,5}$
$\sigma_0^{1,5} = h_0$	0	0	0	0	0	0	0	0	0	0	0	0	0	0
$\sigma_{k-1}^{2,5} = h_{k-1}^2$	0	0	0	1	2	0	1	1	0	0	0	0	0	0
$\sigma_{k-1}^{3,5} = h_{k-1}^3$	0	0	0	2	0	0	0	0	1	0	0	0	0	0
$\sigma_k^{4,5} = h_k^4$	0	0	0	0	0	0	0	0	0	0	0	1	0	0
$\sigma_k^{5,5} = 2h_k^5 - 3h_k^4$	0	0	0	0	0	0	0	0	0	-1	-2	6	1	0
$\sigma_k^{6,5} = h_k^6 - h_k^5 + h_k^4$	0	0	0	0	0	0	0	0	0	-3	-5	11	1	0
$\sigma_k^{7,5} = h_k^7$	0	0	0	0	0	0	0	0	0	3	5	-13	-1	0
$\sigma_k^{8,5} = h_k^8$	0	0	0	0	0	0	0	0	0	-1	0	-1	0	0
$\sigma_k^{9,5} = h_k^9$	0	0	0	0	0	0	0	0	0	2	0	0	0	0
$\sigma_{k+1}^{10,5} = h_{k+1}^{10}$	0	0	0	0	0	0	0	0	0	0	0	0	0	0
$\sigma_{k+1}^{11,5} = h_{k+1}^{11} + h_{k+1}^{10}$	0	0	0	0	0	0	0	0	0	0	0	0	0	0
$\sigma_{k+1}^{12,5} = 2h_{k+1}^{12} - 3h_{k+1}^{10}$	0	0	0	0	0	0	0	0	0	0	0	0	0	0
$\sigma_{k+1}^{13,5} = h_{k+1}^{13} + h_{k+1}^{12} - h_{k+1}^{10}$	0	0	0	0	0	0	0	0	0	0	0	0	0	0
$\sigma_n^{14,5} = h_n$	0	0	0	0	0	0	0	0	0	0	0	0	0	0

Figure 5.25: SSSA: Δ^5 .

i.e. the generators of Z_{p-1}^{r-1} are the k -chains $\sigma_k^{p+1-\xi, r-\xi}$, $\xi = 1, \dots, p+1-\kappa$ whenever the primary pivot of column $(p+1-\xi)$ is on or above row $(p-r+1)$. If the primary pivot of column $(p+1)$ is below row $(p-r+1)$, then $Z_p^r = Z_{p-1}^{r-1}$ and the result follows by the induction hypothesis. This is the case when $\mu^{p+1,r} = 0$.

Now assume that the primary pivot of column $(p+1)$ is on or above row $(p-r+1)$. Consider a k -chain $\mathfrak{h}_k = b^{p+1}h_k^{p+1} + \dots + b^\kappa h_k^\kappa$ in $Z_{p,k-p}^r$.

If $b^{p+1} = 0$ then

$$\mathfrak{h}_k \in Z_{p-1}^{r-1} = \mathbb{Z}[\mu^{p,r-1}\sigma_k^{p,r-1}, \dots, \mu^{\kappa,r-p-1+\kappa}\sigma_k^{\kappa,r-p-1+\kappa}].$$

Suppose $b^{p+1} \neq 0$. By the SSSA, the leading coefficient $c_{p+1}^{p+1,r}$ of $\sigma_k^{p+1,r}$ is minimal. It follows that $b^{p+1} = \alpha_1 c_{p+1}^{p+1,r}$, $\alpha_1 \in \mathbb{Z}$. In fact, if b^{p+1} is not an integer multiple of $c_{p+1}^{p+1,r}$, consider the integer $v > 0$ such that $vc_{p+1}^{p+1,r}$ is the largest multiple of $c_{p+1}^{p+1,r}$ with $vc_{p+1}^{p+1,r} < b^{p+1}$. Hence, $vc_{p+1}^{p+1,r} < b^{p+1} < (v+1)c_{p+1}^{p+1,r}$, and thus $0 < b^{p+1} - vc_{p+1}^{p+1,r} < c_{p+1}^{p+1,r}$. It follows that the k -chain $\mathfrak{h}_k - v\sigma_k^{p+1,r}$ has leading coefficient $b^{p+1} - vc_{p+1}^{p+1,r} < c_{p+1}^{p+1,r}$, which contradicts the fact that $c_{p+1}^{p+1,r}$ is minimal. Hence $b^{p+1} = \alpha_1 c_{p+1}^{p+1,r}$, $\alpha_1 \in \mathbb{Z}$.

$\sigma_0^{1,6} = h_0$	$\sigma_{k-1}^{2,6}$	$\sigma_{k-1}^{3,6}$	$\sigma_k^{4,6}$	$\sigma_k^{5,6}$	$\sigma_k^{6,6}$	$\sigma_k^{7,6}$	$\sigma_k^{8,6}$	$\sigma_k^{9,6}$	$\sigma_{k+1}^{10,6}$	$\sigma_{k+1}^{11,6}$	$\sigma_{k+1}^{12,6}$	$\sigma_{k+1}^{13,6}$	$\sigma_n^{14,6}$
0	0	0	0	0	0	0	0	0	0	0	0	0	0
$\sigma_{k-1}^{2,6} = h_{k-1}^2$	0	0	0	2	0	1	0	-2	0	0	0	0	0
$\sigma_{k-1}^{3,6} = h_{k-1}^3$	0	0	0	2	0	0	0	0	1	0	0	0	0
$\sigma_k^{4,6} = h_k^4$	0	0	0	0	0	0	0	0	-1	0	-3	0	0
$\sigma_k^{5,6} = 2h_k^5 - 3h_k^4$	0	0	0	0	0	0	0	0	-1	-2	5	1	0
$\sigma_k^{6,6} = h_k^6 - h_k^5 + h_k^4$	0	0	0	0	0	0	0	0	0	0	-2	0	0
$\sigma_k^{7,6} = h_k^7 - h_k^6 + h_k^5 - h_k^4$	0	0	0	0	0	0	0	0	3	5	-13	-1	0
$\sigma_k^{8,6} = h_k^8 - h_k^4$	0	0	0	0	0	0	0	0	-1	0	-1	0	0
$\sigma_k^{9,6} = h_k^9$	0	0	0	0	0	0	0	0	2	0	0	0	0
$\sigma_{k+1}^{10,6} = h_{k+1}^{10}$	0	0	0	0	0	0	0	0	0	0	0	0	0
$\sigma_{k+1}^{11,6} = h_{k+1}^{11} + h_{k+1}^{10}$	0	0	0	0	0	0	0	0	0	0	0	0	0
$\sigma_{k+1}^{12,6} = 2h_{k+1}^{12} - 3h_{k+1}^{10}$	0	0	0	0	0	0	0	0	0	0	0	0	0
$\sigma_{k+1}^{13,6} = h_{k+1}^{13} + h_{k+1}^{12} - h_{k+1}^{10}$	0	0	0	0	0	0	0	0	0	0	0	0	0
$\sigma_n^{14,6} = h_n$	0	0	0	0	0	0	0	0	0	0	0	0	0

Figure 5.26: SSSA: Δ^6 .

As a consequence, \mathfrak{h}_k can also be written as

$$\mathfrak{h}_k = \alpha_1 \sigma_k^{p+1,r} + (b^p - \alpha_1 c_p^{p+1,r}) h_k^p + \cdots + (b^\kappa - \alpha_1 c_k^{p+1,r}) h_k^\kappa.$$

Note that $\mathfrak{h}_k - \alpha_1 \sigma_k^{p+1,r} = (b^p - \alpha_1 c_p^{p+1,r}) h_k^p + \cdots + (b^\kappa - \alpha_1 c_k^{p+1,r}) h_k^\kappa \in F_{p-1}C$. Furthermore, since the boundaries of \mathfrak{h}_k and $\sigma_k^{(p+1),r}$ are on and above row $(p-r+1)$, so is the boundary of $\mathfrak{h}_k - \alpha_1 \sigma_k^{p+1,r}$. Thus, $\mathfrak{h}_k - \alpha_1 \sigma_k^{p+1,r} \in Z_{p-1}^{r-1}$. It follows from the induction hypotheses that $\mathfrak{h}_k - \alpha_1 \sigma_k^{p+1,r} = \alpha_2 \mu^{p,r-1} \sigma_k^{p,r-1} + \cdots + \alpha_\kappa \mu^{\kappa,r-p-1+\kappa} \sigma_k^{\kappa,r-p-1+\kappa}$ and, hence,

$$\mathfrak{h}_k = \alpha_1 \sigma_k^{p+1,r} + \alpha_2 \mu^{p,r-1} \sigma_k^{p,r-1} + \cdots + \alpha_\kappa \mu^{\kappa,r-p-1+\kappa} \sigma_k^{\kappa,r-p-1+\kappa}.$$

□

The second main result for the proof of Theorem 5.5 is demonstrating that all pivots generated by the SSSA are integer numbers. More specifically, even though the matrices Δ^r can have some entries which are not integer numbers, the primary pivots and change-of-basis pivots are always integers.

$\sigma_0^{1,7} = h_0$	$\sigma_{k-1}^{2,7}$	$\sigma_{k-1}^{3,7}$	$\sigma_k^{4,7}$	$\sigma_k^{5,7}$	$\sigma_k^{6,7}$	$\sigma_k^{7,7}$	$\sigma_k^{8,7}$	$\sigma_k^{9,7}$	$\sigma_{k+1}^{10,7}$	$\sigma_{k+1}^{11,7}$	$\sigma_{k+1}^{12,7}$	$\sigma_{k+1}^{13,7}$	$\sigma_n^{14,7}$
0	0	0	0	0	0	0	0	0	0	0	0	0	0
$\sigma_{k-1}^{2,7} = h_{k-1}^2$	0	0	0	2	0	1	0	0	-1	0	0	0	0
$\sigma_{k-1}^{3,7} = h_{k-1}^3$	0	0	0	2	0	0	0	0	0	0	0	0	0
$\sigma_k^{4,7} = h_k^4$	0	0	0	0	0	0	0	0	0	0	-5	0	0
$\sigma_k^{5,7} = 2h_k^5 - 3h_k^4$	0	0	0	0	0	0	0	0	0	-2	5	3	0
$\sigma_k^{6,7} = h_k^6 - h_k^5 + h_k^4$	0	0	0	0	0	0	0	0	2	0	0	0	0
$\sigma_k^{7,7} = h_k^7 - h_k^6 + h_k^5 - h_k^4$	0	0	0	0	0	0	0	0	3	5	-13	0	0
$\sigma_k^{8,7} = h_k^8 + 2h_k^6 - 2h_k^5 + h_k^4$	0	0	0	0	0	0	0	0	-1	0	-1	0	0
$\sigma_k^{9,7} = h_k^9 - h_k^5 + h_k^4$	0	0	0	0	0	0	0	0	2	0	0	0	0
$\sigma_{k+1}^{10,7} = h_{k+1}^{10}$	0	0	0	0	0	0	0	0	0	0	0	0	0
$\sigma_{k+1}^{11,7} = h_{k+1}^{11} + h_{k+1}^{10}$	0	0	0	0	0	0	0	0	0	0	0	0	0
$\sigma_{k+1}^{12,7} = 2h_{k+1}^{12} - 3h_{k+1}^{10}$	0	0	0	0	0	0	0	0	0	0	0	0	0
$\sigma_{k+1}^{13,7} = 5h_{k+1}^{13} + 5h_{k+1}^{12} + h_{k+1}^{11} - 4h_{k+1}^{10}$	0	0	0	0	0	0	0	0	0	0	0	0	0
$\sigma_n^{14,7} = h_n$	0	0	0	0	0	0	0	0	0	0	0	0	0

Figure 5.27: SSSA: Δ^7 .

Proposition 5.4. Suppose that $\Delta_{p-r+1,p+1}^r$ is either a primary pivot or a change-of-basis pivot. Then $\Delta_{p-r+1,p+1}^r$ is an integer number.

Proof. By Proposition 5.2, $\Delta_{s,p+1}^r = 0$ for all $s > p - r + 1$. Hence

$$\partial\sigma_k^{p+1,r} = \Delta_{p-r+1,p+1}^r \sigma_{k-1}^{p-r+1,r} + \cdots + \Delta_{\kappa^*,p+1}^r \sigma_{k-1}^{\kappa^*,r},$$

where κ^* is the first column associated to a $(k-1)$ -chain.

On the other hand, since $\sigma_k^{p+1,r} \in Z_p^r$, it follows from Proposition 5.3 that

$$\partial\sigma_k^{p+1,r} \in \partial Z_p^r \subset Z_{p-r}^{r+1} = \mathbb{Z}[\mu^{p-r+1,r+1}\sigma_k^{p-r+1,r+1}, \mu^{p-r,r}\sigma_k^{p-r,r}, \dots, \mu^{\kappa,2r-p+\kappa}\sigma_k^{\kappa,2r-p+\kappa}].$$

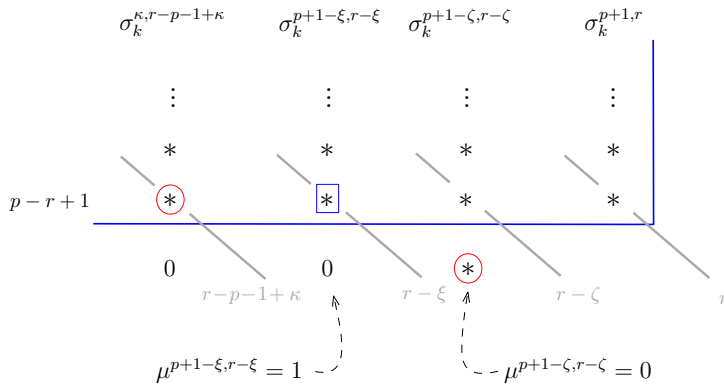
Thus, the coefficient $\Delta_{p-r+1,p+1}^r c_{p-r+1}^{p-r+1,r}$ of $h_{k-1}^{(p-r+1)}$ in $\partial\sigma^{(p+1),r}$ has to be a multiple α of the coefficient $c_{p-r+1}^{p-r+1,r+1}$ of $h_{k-1}^{(p-r+1)} \in Z_{p-r}^{r+1}$, i.e,

$$\Delta_{p-r+1,p+1}^r c_{p-r+1}^{p-r+1,r} = \alpha c_{p-r+1}^{p-r+1,r+1},$$

where $\alpha \in \mathbb{Z} \setminus \{0\}$. Hence, one has

$$\Delta_{p-r+1,p+1}^r = \frac{\alpha c_{p-r+1}^{p-r+1,r+1}}{c_{p-r+1}^{p-r+1,r}}.$$

$\sigma_0^{1,8} = h_0$	$\sigma_{k-1}^{2,8}$	$\sigma_{k-1}^{3,8}$	$\sigma_k^{4,8}$	$\sigma_k^{5,8}$	$\sigma_k^{6,8}$	$\sigma_k^{7,8}$	$\sigma_k^{8,8}$	$\sigma_k^{9,8}$	$\sigma_{k+1}^{10,8}$	$\sigma_{k+1}^{11,8}$	$\sigma_{k+1}^{12,8}$	$\sigma_{k+1}^{13,8}$	$\sigma_n^{14,8}$
0	0	0	0	0	0	0	0	0	0	0	0	0	0
$\sigma_{k-1}^{2,8} = h_{k-1}^2$	0	0	0	2	0	1	0	0	0	0	0	0	0
$\sigma_{k-1}^{3,8} = h_{k-1}^3$	0	0	0	2	0	0	0	0	0	0	0	0	0
$\sigma_k^{4,8} = h_k^4$	0	0	0	0	0	0	0	0	0	0	-5	0	0
$\sigma_k^{5,8} = 2h_k^5 - 3h_k^4$	0	0	0	0	0	0	0	0	0	-2	5	3	0
$\sigma_k^{6,8} = h_k^6 - h_k^5 + h_k^4$	0	0	0	0	0	0	0	0	0	0	0	0	0
$\sigma_k^{7,8} = h_k^7 - h_k^6 + h_k^5 - h_k^4$	0	0	0	0	0	0	0	0	3	5	-13	0	0
$\sigma_k^{8,8} = h_k^8 + 2h_k^6 - 2h_k^5 + h_k^4$	0	0	0	0	0	0	0	0	-1	0	-1	0	0
$\sigma_k^{9,8} = h_k^9 + h_k^6 - 2h_k^5 + 2h_k^4$	0	0	0	0	0	0	0	0	2	0	0	0	0
$\sigma_{k+1}^{10,8} = h_{k+1}^{10}$	0	0	0	0	0	0	0	0	0	0	0	0	0
$\sigma_{k+1}^{11,8} = h_{k+1}^{11} + h_{k+1}^{10}$	0	0	0	0	0	0	0	0	0	0	0	0	0
$\sigma_{k+1}^{12,8} = 2h_{k+1}^{12} - 3h_{k+1}^{10}$	0	0	0	0	0	0	0	0	0	0	0	0	0
$\sigma_{k+1}^{13,8} = 5h_{k+1}^{13} + 5h_{k+1}^{12} + h_{k+1}^{11} - 4h_{k+1}^{10}$	0	0	0	0	0	0	0	0	0	0	0	0	0
$\sigma_n^{14,8} = h_n$	0	0	0	0	0	0	0	0	0	0	0	0	0

Figure 5.28: SSSA: Δ^8 .Figure 5.29: Constant $\mu^{j,\xi}$.

It follows from (5.6) that $\Delta_{p-r+1, p+1}^r$ is an integer. □

In what follows we outline the proof of Theorem 5.5. For more details on each case of

the proof, see Cornea, de Rezende, and da Silveira (2010).

Proof. (of Theorem 5.5)

The entry $\Delta_{p-r+1,p+1}^r$ on the r -th diagonal of Δ^r plays a crucial role in determining $E_{p,k-p}^r$. It can either be a primary pivot, a change-of-basis pivot, an entry above a primary pivot or a zero entry with a column of zeros below it. For each one of the above possibilities, we analyze the entry $\Delta_{p-r+1,p+1}^r$ and also the row $(p+1)$, which determines the behavior of the denominator

$$Z_{p-1,k-(p-1)}^{r-1} + \partial Z_{p+r-1,(k+1)-(p+r-1)}^{r-1}.$$

Finally, we use Proposition 5.3 in order to calculate $E_{p,k-p}^r$.

- Case 1: $\Delta_{p-r+1,p+1}^r$ is a primary pivot. In this case

$$\partial Z_{p+r-1,(k+1)-(p+r-1)}^{r-1} \subseteq Z_{p-1,k-(p-1)}^{r-1}.$$

By Proposition 5.3 one has that $E_{p,k-p}^r = \mathbb{Z}[\sigma_k^{p+1,r}]$.

- Case 2: $\Delta_{p-r+1,p+1}^r$ is a change-of-basis pivot. In this case, there are two possibilities for row $(p+1)$.
 1. $\partial Z_{p+r-1,(k+1)-(p+r-1)}^{r-1} \subseteq Z_{p-1,k-(p-1)}^{r-1}$. In this case, as before, by Proposition 5.3 $E_{p,k-p}^r = \mathbb{Z}[\sigma_k^{p+1,r}]$.
 2. $\partial Z_{p+r-1,(k+1)-(p+r-1)}^{r-1} \not\subseteq Z_{p-1,k-(p-1)}^{r-1}$, i.e there exists an element in $Z_{p+r-1,(k+1)-(p+r-1)}^{r-1}$ whose boundary has a nonzero entry in row $(p+1)$, which is necessarily a primary pivot.

Claim 1: If $\partial Z_{p+r-1,(k+1)-(p+r-1)}^{r-1} \not\subseteq Z_{p-1,k-(p-1)}^{r-1}$ then

$$\begin{aligned} Z_{p-1,k-(p-1)}^{r-1} + \partial Z_{p+r-1,(k+1)-(p+r-1)}^{r-1} &= \\ &= \mathbb{Z}[\ell \sigma_k^{p+1,r}, \mu^{p,r-1} \sigma_k^{p,r-1}, \dots, \mu^{\kappa,r-p-1+\kappa} \sigma_k^{\kappa,r-p-1+\kappa}], \end{aligned}$$

where

$$\ell = \frac{\gcd\{\mu^{r+p,r-1} c_{p+1}^{p+1,r-1} \Delta_{p+1,r+p}^{r-1}, \dots, \mu^{\bar{\kappa},\bar{\kappa}-p-1} c_{p+1}^{p+1,\bar{\kappa}-p-1} \Delta_{p+1,\bar{\kappa}}^{\bar{\kappa}-p-1}\}}{c_{p+1}^{p+1,r}},$$

κ is the first column associated to a k -chain and $\bar{\kappa}$ is the first column associated to a $(k+1)$ -chain.

Proof. (of Claim 1) By the hypothesis, the denominator $Z_{p-1}^{r-1} + \partial Z_{p+r-1}^{r-1}$ is a submodule of Z_p^r which is not a submodule of Z_{p-1}^{r-1} , hence ∂Z_{p+r-1}^{r-1} must contain an integer multiple ℓ of $\sigma_k^{p+1,r}$. It remains to prove the formula for ℓ . It follows from Proposition 5.3 that a formula for ∂Z_{p+r-1}^{r-1} is

$$\mathbb{Z}[\mu^{p+r,r-1} \partial \sigma_{k+1}^{p+r,r-1}, \mu^{p+r-1,r-2} \partial \sigma_{k+1}^{p+r-1,r-2}, \dots, \mu^{\bar{k},\bar{k}-p-1} \partial \sigma_{k+1}^{\bar{k},\bar{k}-p-1}].$$

Recall that the boundaries $\partial \sigma_{k+1}^{p+r-\xi,r-1-\xi}$ with $\Delta_{i,p+r-\xi}^{r-1-\xi} \neq 0$ for some $i > p+1$ correspond to the columns which have the primary pivots below row $(p+1)$ and hence $\mu^{p+r-\xi,r-1-\xi} = 0$. Thus, for $\xi = 0, \dots, p+r-\bar{k}$, if $\mu^{p+r-\xi,r-1-\xi} = 1$ then $\Delta_{i,p+r-\xi}^{r-1-\xi} = 0$ for all $i > p+1$ and then

$$\partial \sigma_{k+1}^{p+r-\xi,r-1-\xi} = \Delta_{p+1,p+r-\xi}^{r-1-\xi} \sigma_k^{p+1,r-1-\xi} + \dots + \Delta_{\kappa,p+r-\xi}^{r-1-\xi} \sigma_k^{\kappa,r-1-\xi}.$$

Consequently, for $\xi = 0, \dots, p+r-\bar{k}$ such that $\mu^{p+r-\xi,r-1-\xi} = 1$ we have that $Z_{p-1}^{r-1} + [\partial \sigma_{k+1}^{p+r-\xi,r-1-\xi}]$ is equal to

$$Z_{p-1}^{r-1} + [\Delta_{p+1,p+r-\xi}^{r-1-\xi} \sigma_k^{p+1,r-1-\xi} + \dots + \Delta_{\kappa,p+r-\xi}^{r-1-\xi} \sigma_k^{\kappa,r-1-\xi}]. \quad (5.7)$$

Also, $Z_{p-1}^{r-1} + [\partial \sigma_{k+1}^{p+r-\xi,r-1-\xi}] \subset Z_{p-1}^{r-1} + \partial Z_{p+r-1}^{r-1}$ and hence $Z_{p-1}^{r-1} + [\partial \sigma_{k+1}^{p+r-\xi,r-1-\xi}]$ is

$$[\ell_\xi \sigma_k^{p+1,r}, \mu^{p,r-1} \sigma_k^{p,r-1}, \dots, \mu^{\kappa,r-p-1+\kappa} \sigma_k^{\kappa,r-p-1+\kappa}]. \quad (5.8)$$

Comparing the coefficients of h_k^{p+1} in (5.7) and in (5.8) we obtain

$$\Delta_{p+1,p+r-\xi}^{r-1-\xi} c_{p+1}^{p+1,r-1-\xi} = \ell_\xi c_{p+1}^{p+1,r}$$

and hence

$$\ell_\xi = \Delta_{p+1,p+r-\xi}^{r-1-\xi} c_{p+1}^{p+1,r-1-\xi} / c_{p+1}^{p+1,r}.$$

Consequently, $\ell = \gcd\{\mu^{(p+r-\xi),r-1-\xi} \ell_\xi, \xi = 0, \dots, p+r-\bar{k}\}$.

□

-Claim 1

By Proposition 5.3 and Claim 1 above, $E_{p,k-p}^r = \frac{\mathbb{Z}}{\ell \mathbb{Z}}[\sigma_k^{p+1,r}]$.

- Case 3: $\Delta_{p-r+1,p+1}^r$ is an entry above a primary pivot. It follows that $\sigma_k^{p+1,r}$ is not in $Z_{p,k-p}^r$. Thus, $Z_{p-1,k-(p-1)}^{r-1} = Z_{p,k-p}^r$ and hence $E_{p,k-p}^r = 0$.

- Case 4: $\Delta_{p-r+1,p+1}^r$ is a zero entry with a column of zeros below it. As in Case 2, there are two possibilities for row $(p+1)$.
 1. If $\partial Z_{p+r-1,(k+1)-(p+r-1)}^{r-1} \subseteq Z_{p-1,k-(p-1)}^{r-1}$ then $E_{p,k-p}^r = \mathbb{Z}[\sigma_k^{p+1,r}]$.
 2. If $\partial Z_{p+r-1,(k+1)-(p+r-1)}^{r-1} \not\subseteq Z_{p-1,k-(p-1)}^{r-1}$, by Proposition 5.3 and Claim 1
 $E_{p,k-p}^r = \frac{\mathbb{Z}}{\ell\mathbb{Z}}[\sigma_k^{(p+1),r}], \ell \in \mathbb{Z}$.
- Case 5: $\Delta_{p-r+1,p+1}^r$ is not in Δ_k^r (for example, when $p-r+1 < 0$, i.e., $\Delta_{p-r+1,p+1}^r$ is not on the matrix Δ^r). In this case we have two possibilities:
 1. If there is a primary pivot in column $(p+1)$ in a diagonal $\bar{r} < r$, then $E_{p,k-p}^r = 0$.
 2. If all the entries in column $(p+1)$ of Δ^r in diagonals lower than r are zero, then the analysis of row $(p+1)$ is analogous to Cases 2 and 4.

□

The next theorem shows how the collection of matrices Δ^r produced by the SSSA applied to Δ induces the differentials $d_p^r : E_p^r \rightarrow E_{p-r}^r$ of the spectral sequence.

Theorem 5.6. *Let M be a smooth closed n -dimensional manifold, $f : M \rightarrow \mathbb{R}$ be a Morse–Smale function, $(C_*(f), \partial_*)$ be a Morse chain complex associated to f , F be a finest filtration on $(C_*(f), \partial_*)$ and (E_p^r, d^r) be a spectral sequence associated to this filtered chain complex. If E_p^r and E_{p-r}^r are both nonzero, then the map $d_p^r : E_p^r \rightarrow E_{p-r}^r$ is induced by Δ^r , i.e., it is multiplication by the entry $\Delta_{p-r+1,p+1}^r$ which is either a primary pivot, a change-of-basis pivot or a zero entry with a column of zeros below it.*

In the remainder of this section we provide a sketch for the proof of Theorem 5.6, skipping some of the heavier calculation.

Recall that

$$E_p^{r+1} = \frac{\ker d_p^r}{\text{im } d_{p+r}^r}.$$

The idea is to prove that when E_p^r and E_{p-r}^r are both nonzero

$$\frac{\ker \delta_p^r}{\text{im } \delta_{p+r}^r} = E_p^{r+1},$$

where δ_p^r is the multiplication by the entry $\Delta_{p-r+1,p+1}^r$. Both expressions on this equality strongly depend on the entries $\Delta_{p-r+1,p+1}^r$ and $\Delta_{p+1,p+r+1}^r$. These entries are on the r -th diagonal of Δ^r and, by Theorem 5.5, the entry $\Delta_{p-r+1,p+1}^r$ can either be a primary pivot, a change-of-basis pivot, or a zero entry with a column of zeros below it. For each one of these cases, the entry $\Delta_{p+1,p+r+1}^r$ can either be a primary pivot, a change-of-basis pivot,

an entry above a primary pivot or a zero entry with a column of zeros below it. Hence, the proof is divided in several cases, and for each one of them we must calculate both E_p^{r+1} and $\frac{\ker \delta_p^r}{\text{im } \delta_{p+r}^r}$. We present the detailed proof for one of these cases.

The next lemma finds a new formulation for the leading coefficient u , whenever the entry $\Delta_{p-r+1, p+1}^r$ is a change-of-basis pivot. It consists in a technical part of the proof of Theorem 5.6 and for its detailed proof we refer to Cornea, de Rezende, and da Silveira (2010, Proposition 5.2.).

Lemma 5.1. *If $\Delta_{p-r+1, p+1}^r$ is a change-of-basis pivot and $u = \frac{c_{p+1}^{p+1, r+1}}{c_{p+1}^{p+1, r}}$ is the integer defined on the SSSA, then*

$$u = \frac{v}{\gcd\{\Delta_{p-r+1, p+1}^r, v\}}, \quad (5.9)$$

where

$$v = \frac{\gcd\{\mu^{p, r-1} c_{p-r+1}^{p-r+1, r-1} \Delta_{p-r+1, p}^{r-1}, \dots, \mu^{\kappa, \kappa-p+r-1} c_{p-r+1}^{p-r+1, \kappa-p+r-1} \Delta_{p-r+1, \kappa}^{\kappa-p+r-1}\}}{c_{p-r+1}^{p-r+1, r}}.$$

Clearly, for all other cases of the entry $\Delta_{p-r+1, p+1}^r$ we have that $u = 1$.

We also use the next result, which follows from elementary algebra.

Lemma 5.2. *Assume that m is multiplication by a nonzero integer m and let $\lambda = \frac{v}{\gcd\{m, v\}}$.*

1. *If $\mathbb{Z} \xrightarrow{m} \mathbb{Z}_v$, then $\ker m = \lambda\mathbb{Z}$ and $\text{im } m = \frac{\mathbb{Z}}{\lambda\mathbb{Z}} = \frac{\gcd\{m, v\}\mathbb{Z}}{v\mathbb{Z}}$.*
2. *If $\mathbb{Z}_t \xrightarrow{m} \mathbb{Z}_v$ and $t \geq \lambda$, then $\ker m = \frac{\lambda\mathbb{Z}}{t\mathbb{Z}}$ and $\text{im } m = \frac{\mathbb{Z}}{\lambda\mathbb{Z}} = \frac{\gcd\{m, v\}\mathbb{Z}}{v\mathbb{Z}}$.*

Proof. (of Theorem 5.6)

We present the detailed proof for the case where $\Delta_{p-r+1, p+1}^r$ is a change-of-basis pivot and $\Delta_{p+1, p+r+1}^r \neq 0$ is a primary pivot. See Figure 5.30.

Let us first determine $\frac{\ker \delta_p^r}{\text{im } \delta_{p+r}^r}$ in this case. Since $\Delta_{p-r+1, p+1}^r$ is a change-of-basis pivot, there exists a primary pivot in row $(p-r+1)$ on a diagonal below the r -th diagonal. It follows by Theorem 5.5 that $E_{p-r}^r = \mathbb{Z}_v[\sigma_{k-1}^{p-r+1, r}]$, where

$$v = \frac{\gcd\{\mu^p c_{p-r+1}^{p-r+1, r-1} \Delta_{p-r+1, p}^{r-1}, \dots, \mu^\kappa c_{p-r+1}^{p-r+1, \kappa-p+r-1} \Delta_{p-r+1, \kappa}^{\kappa-p+r-1}\}}{c_{p-r+1}^{p-r+1, r}}$$

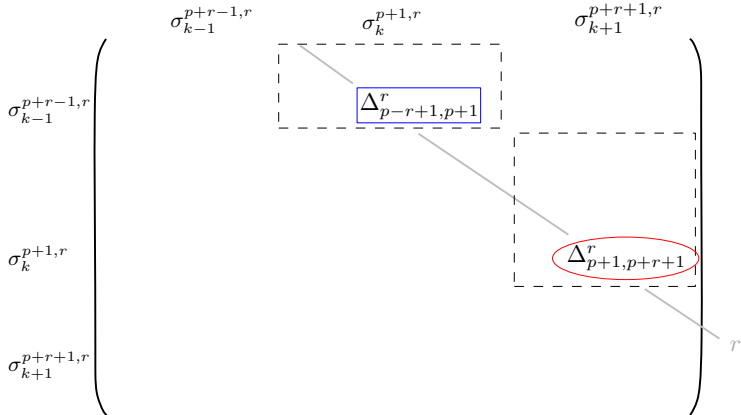


Figure 5.30: $\Delta_{p-r+1,p+1}^r$ change-of-basis pivot and $\Delta_{p+1,p+r+1}^r$ primary pivot.

and, by Lemma 5.1, we have that $u = \frac{v}{\gcd\{\Delta_{p-r+1,p+1}^r, v\}}$.

Since $\Delta_{p+1,p+r+1}^r \neq 0$ is a primary pivot, Proposition 5.2(4) guarantees that there are no primary pivots in row and column $(p+1)$ nor in row and column $(p+r+1)$ in a diagonal below the r -th diagonal. By Theorem 5.5, $E_p^r = \mathbb{Z}[\sigma_k^{p+1,r}]$ and $E_{p+r}^r = \mathbb{Z}[\sigma_{k+1}^{p+r,r}]$.

Hence we have

$$\dots \longleftarrow \mathbb{Z}_v[\sigma_{k-1}^{(p-r+1),r}] \xleftarrow{\delta_p^r} \mathbb{Z}[\sigma_k^{(p+1),r}] \xleftarrow{\delta_{p+r}^r} \mathbb{Z}[\sigma_{k+1}^{(p+r),r}] \longleftarrow \dots$$

It follows that $\text{im } \delta_{p+r}^r = \Delta_{p+1,p+r+1}^r \mathbb{Z}[\sigma_k^{(p+1),r}]$ and, by Lemma 5.2, we have $\ker \delta_p^r = \mathbb{Z}[\sigma_k^{(p+1),r}]$. Thus

$$\frac{\ker \delta_p^r}{\text{im } \delta_{p+r}^r} = \frac{\mathbb{Z}[\sigma_k^{(p+1),r}]}{\Delta_{p+1,p+r+1}^r \mathbb{Z}[\sigma_k^{(p+1),r}]} = \frac{u \mathbb{Z}[\sigma_k^{(p+1),r}]}{\Delta_{p+1,p+r+1}^r \mathbb{Z}[\sigma_k^{(p+1),r}]}.$$

Now, we calculate E_p^{r+1} for the case where $\Delta_{p-r+1,p+1}^r$ is a change-of-basis pivot and $\Delta_{p+1,p+r+1}^r$ is a primary pivot. Since $\Delta_{p-r+1,p+1}^r$ is a change-of-basis pivot, then $\Delta_{p-r+1,p+1}^{r+1} = 0$ and thus $\sigma_k^{p+1,r+1} \in Z_{p,k-p}^{r+1}$. It follows that $Z_{p-1,k-(p-1)}^{r-1} \not\subseteq Z_{p,k-p}^{r+1}$. Moreover, since $E_p^r = \mathbb{Z}[\sigma_k^{p+1,r}]$, then $\partial Z_{p+r-1,(k+1)-(p+r-1)}^{r-1} \subseteq Z_{p-1,k-(p-1)}^{r-1}$, i.e., for all $\sigma_{k+1}^{p+r-\xi,r-1-\xi}$, $\xi = 0, \dots, p+r-\bar{k}$, we can either have $\partial \sigma_{k+1}^{p+r-\xi,r-1-\xi} \in Z_{p-1,k-(p-1)}^{r-1}$ and hence $\Delta_{p+1,p+r-\xi}^{r-1-\xi} = 0$ or $\sigma_{k+1}^{p+r-\xi,r-1-\xi}$ has a primary pivot below

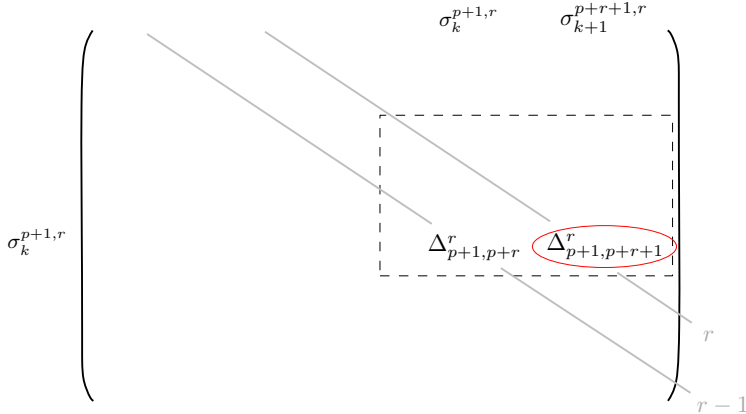


Figure 5.31: Difference between $\partial Z_{p+r-1,(k+1)-(p+r-1)}^{r-1}$ and $\partial Z_{p+r,(k+1)-(p+r)}^r$.

row $(p+1)$ and hence $\mu^{p+r-\xi, r-1-\xi} = 0$. Note that the difference between the generators of $\partial Z_{p+r-1,(k+1)-(p+r-1)}^{r-1}$ and $\partial Z_{p+r,(k+1)-(p+r)}^r$ is that the latter includes the boundary of the chain corresponding to column $(p+r+1)$, see Figure 5.31. By hypothesis, the element in column $(p+r+1)$ and row $(p+1)$ is $\Delta_{p+1,p+r+1}^r$. Since $\Delta_{p+1,p+r+1}^r$ is a primary pivot, then $E_{p,k-p}^{r+1} = \frac{\mathbb{Z}[\sigma_k^{p+1,r+1}]}{s\mathbb{Z}[\sigma_k^{p+1,r+1}]}$, where

$$\begin{aligned} s &= \frac{\gcd\{\mu^{p+r-\xi, r-1-\xi} c_{p+1}^{p+1, r-1-\xi} \Delta_{p+1, p+r-\xi}^{r-1-\xi}, \xi = -1, \dots, p+r-\bar{k}\}}{c_{p+1}^{p+1, r+1}} \\ &= \frac{\mu^{p+r+1, r} c_{p+1}^{p+1, r} \Delta_{p+1, p+r+1}^r}{c_{p+1}^{p+1, r+1}} \\ &= \frac{\Delta_{p+1, p+r+1}^r}{u}. \end{aligned}$$

The calculations for the various other cases in which the proof is divided can be found in Cornea, de Rezende, and da Silveira (2010). □

The SSSA was implemented using the software Mathematica. The implementation can be found in <http://www.ime.unicamp.br/~margarid/software/>.

5.4.2 Detecting paths of flow lines

Let M be a smooth closed n -dimensional manifold, $f : M \rightarrow \mathbb{R}$ be a Morse–Smale function, φ be the negative gradient flow of f and $(C_*(f), \partial_*)$ be a Morse chain complex associated to f . Let F be a finest filtration on $(C_*(f), \partial_*)$ and (E_p^r, d_p^r) be an associated spectral sequence. In this section, we describe how each nonzero differential d_p^r is associated to a path of connecting orbits in φ .

Consider $\{\Delta^r\}$ the collection of matrices obtained when the SSSA is applied to Δ .

An r -path of connecting orbits is a juxtaposition of connecting orbits where the orbits represented in the matrices by primary pivots or change-of-basis pivots $\Delta_{i,j}^\xi$ for $\xi < r$ may be considered with reverse orientation.

More precisely, let $\gamma_{i,j}$ be a path between the singularities h_k^j and h_{k-1}^i . If $\gamma_{i,j}$ corresponds to a connecting orbit in the flow, we say that $\gamma_{i,j}$ is an *elementary path*. However, when $\gamma_{i,j}$ does not correspond to a connecting orbit in the flow, $\gamma_{i,j}$ can be written as a sequence of elementary paths. This construction is done recursively by defining

$$\gamma_{i,j} = [\gamma_{\bar{i},j}, -\gamma_{\bar{i},\bar{j}}, \gamma_{i,\bar{j}}],$$

where $\bar{j} < j$ and $\bar{i} > i$, i.e., $h_k^{\bar{j}}$ is associated to a column of Δ to the left of h_k^j and $h_{k-1}^{\bar{i}}$ is associated to a row of Δ below h_{k-1}^i .

The negative sign indicates that $\gamma_{\bar{i},\bar{j}}$ is considered with the reverse orientation. If $\gamma_{\bar{i},\bar{j}}$ is an elementary path the corresponding connecting orbit is considered in the reverse orientation. If $\gamma_{\bar{i},\bar{j}}$ does not correspond to a connecting orbit then it is a path

$$\gamma_{\bar{i},\bar{j}} = [\gamma_{\bar{i},\bar{j}}, -\gamma_{\bar{i},\bar{\bar{j}}}, \gamma_{\bar{i},\bar{\bar{j}}}],$$

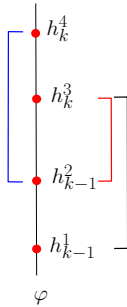
where $\bar{\bar{j}} < \bar{j}$ and $\bar{\bar{i}} > \bar{i}$, and we define

$$-\gamma_{\bar{i},\bar{j}} = -[\gamma_{\bar{\bar{i}},\bar{j}}, -\gamma_{\bar{\bar{i}},\bar{\bar{j}}}, \gamma_{\bar{i},\bar{\bar{j}}}] = [-\gamma_{\bar{i},\bar{\bar{j}}}, \gamma_{\bar{i},\bar{\bar{j}}}, -\gamma_{\bar{\bar{i}},\bar{j}}].$$

Example 5.5. Let φ be a gradient flow of a Morse–Smale function represented by the scheme in Figure 5.32 and let Δ be the associated Morse differential. The matrix Δ and the collection of matrices produced by the SSSA applied to Δ are presented in Figure 5.33.

Figure 5.34 shows the path created between h_k^4 and h_{k-1}^1 .

We know that if an entry $\Delta_{p-r+1,p+1}$ of the Morse differential Δ is nonzero, then there exists a connecting orbit joining the singularities $h_k^{p+1} \in F_p$ and $h_{k-1}^{p-r+1} \in F_{p-r}$ in the flow φ . On the other hand, if $\Delta_{p-r+1,p+1} = 0$ nothing is known about the existence of connecting orbits. By Theorem 5.6, we know that whenever E_p^r and E_{p-r}^r are both nonzero, then the entry $\Delta_{p-r+1,p+1}^r$ of Δ^r induces the map $d_p^r : E_p^r \rightarrow E_{p-r}^r$. The next theorem proves that if $\Delta_{p-r+1,p+1}^r \neq 0$ then there exists an r -path of connecting orbits joining h_k^{p+1} and h_{k-1}^{p-r+1} .

Figure 5.32: Representation of φ .

$$\begin{array}{c}
 \begin{array}{cccc}
 h_{k-1}^1 & h_{k-1}^2 & h_k^3 & h_k^4 \\
 \left(\begin{array}{cccc} 0 & 0 & 1 & 0 \end{array} \right) & & & \\
 h_{k-1}^2 & \left(\begin{array}{cccc} 0 & 0 & 1 & 1 \end{array} \right) & & \\
 h_k^3 & \left(\begin{array}{cccc} 0 & 0 & 0 & 0 \end{array} \right) & & \\
 h_k^4 & \left(\begin{array}{cccc} 0 & 0 & 0 & 0 \end{array} \right) & &
 \end{array} \\
 \Delta
 \end{array}
 \quad
 \begin{array}{c}
 \begin{array}{cccc}
 \sigma_{k-1}^{1,1} = h_{k-1}^1 & \left(\begin{array}{cccc} \sigma_{k-1}^{1,1} & \sigma_{k-1}^{2,1} & \sigma_k^{3,1} & \sigma_k^{4,1} \\ \left(\begin{array}{cccc} 0 & 0 & 1 & 0 \end{array} \right) & \left(\begin{array}{cccc} 0 & 0 & 1 & 0 \end{array} \right) & \left(\begin{array}{cccc} 0 & 0 & 1 & 0 \end{array} \right) & \left(\begin{array}{cccc} 0 & 0 & 1 & 0 \end{array} \right) \end{array} \\
 \sigma_{k-1}^{2,1} = h_{k-1}^2 & \left(\begin{array}{cccc} 0 & 0 & 0 & 1 \end{array} \right) \\
 \sigma_k^{3,1} = h_k^3 & \left(\begin{array}{cccc} 0 & 0 & 0 & 0 \end{array} \right) \\
 \sigma_k^{4,1} = h_k^4 & \left(\begin{array}{cccc} 0 & 0 & 0 & 0 \end{array} \right)
 \end{array} \\
 \Delta^1
 \end{array}$$

$$\begin{array}{c}
 \begin{array}{cccc}
 \sigma_{k-1}^{1,2} = h_{k-1}^1 & \left(\begin{array}{cccc} \sigma_{k-1}^{1,2} & \sigma_{k-1}^{2,2} & \sigma_k^{3,2} & \sigma_k^{4,2} \\ \left(\begin{array}{cccc} 0 & 0 & 1 & 0 \end{array} \right) & \left(\begin{array}{cccc} 0 & 0 & 1 & 0 \end{array} \right) & \left(\begin{array}{cccc} 0 & 0 & 1 & 0 \end{array} \right) & \left(\begin{array}{cccc} 0 & 0 & 1 & 0 \end{array} \right) \end{array} \\
 \sigma_{k-1}^{2,2} = h_{k-1}^2 & \left(\begin{array}{cccc} 0 & 0 & 1 & 1 \end{array} \right) \\
 \sigma_k^{3,2} = h_k^3 & \left(\begin{array}{cccc} 0 & 0 & 0 & 0 \end{array} \right) \\
 \sigma_k^{4,2} = h_k^4 & \left(\begin{array}{cccc} 0 & 0 & 0 & 0 \end{array} \right)
 \end{array} \\
 \Delta^2
 \end{array}
 \quad
 \begin{array}{c}
 \begin{array}{cccc}
 \sigma_{k-1}^{1,3} = h_{k-1}^1 & \left(\begin{array}{cccc} \sigma_{k-1}^{1,3} & \sigma_{k-1}^{2,3} & \sigma_k^{3,3} & \sigma_k^{4,3} \\ \left(\begin{array}{cccc} 0 & 0 & 1 & 0 \end{array} \right) & \left(\begin{array}{cccc} 0 & 0 & 1 & 0 \end{array} \right) & \left(\begin{array}{cccc} 0 & 0 & 1 & 0 \end{array} \right) & \left(\begin{array}{cccc} 0 & 0 & 1 & 0 \end{array} \right) \end{array} \\
 \sigma_{k-1}^{2,3} = h_{k-1}^2 & \left(\begin{array}{cccc} 0 & 0 & 0 & 1 \end{array} \right) \\
 \sigma_k^{3,3} = h_k^3 & \left(\begin{array}{cccc} 0 & 0 & 0 & 0 \end{array} \right) \\
 \sigma_k^{4,3} = h_k^4 - h_k^3 & \left(\begin{array}{cccc} 0 & 0 & 0 & 0 \end{array} \right)
 \end{array} \\
 \Delta^3
 \end{array}$$

Figure 5.33: Collection of matrices produced by the SSSA.

Theorem 5.7. Let (E^r, d^r) be a spectral sequence associated to a filtered Morse chain complex $(C_*(f), \Delta_*)$ of a negative gradient flow φ of a Morse–Smale function f . If the map $d^r : E_{p,q}^r \rightarrow E_{p-r,q+r-1}^r$ is nonzero, then there exists a path of connecting orbits of φ joining the singularity h_k^{p+1} which generates $E_{p,q}^1$ to the singularity h_{k-1}^{p-r+1} which generates $E_{p-r,q+r-1}^1$.

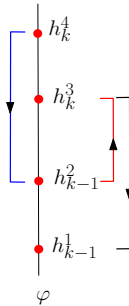


Figure 5.34: 3-path between h_k^4 and h_{k-1}^1 .

Proof. It follows by induction over r and ξ that if $\Delta_{j-\xi,j}^r \neq 0$, then there exists a r -path $\gamma_{j-\xi,j} = [\gamma_{j-\bar{r},j}, -\gamma_{j-\bar{r},j-\xi}, \gamma_{j-\xi,j-\xi}]$ for some \bar{r} and ζ less than r in the flow φ formed by connecting orbits joining the singularity h_k^j to the singularity $h_{k-1}^{j-\xi}$. The details of the proof of this statement can be found in Cornea, de Rezende, and da Silveira (2010).

Now let $d_p^r \neq 0$. By Theorem 5.6, every $d^r \neq 0$ is induced by multiplication by $\Delta_{p-r+1,p+1}^r$, which is either a primary pivot or a change-of-basis pivot. It follows by the previous statement that there is a path in the flow formed by connecting orbits joining the singularity h_k^{p+1} to the singularity h_{k-1}^{p-r+1} . □

Example 5.6. Consider a Morse differential Δ as in Example 5.5. Recall that the entry $\Delta_{1,4}^3 = 1$ is a primary pivot in Δ^3 which has its corresponding entry in Δ equal to zero, i.e., $\Delta_{1,4} = 0$. Hence, it is not known if there is a connecting orbit between h_k^4 and h_{k-1}^1 . However, there is a 3-path of connecting orbits between these two singularities.

Note that $\partial\sigma_k^{4,2} = \partial h_k^4 = h_{k-1}^2$, $\partial\sigma_k^{4,3} = \partial(h_k^4 - h_k^3) = -h_{k-1}^1$, and hence $\Delta_{1,4}^2 = 0$ and $\Delta_{1,4}^3 = -1 \neq 0$.

The entries corresponding to connecting orbits which compose the path are

- $\Delta_{j-\bar{r},j}^{\bar{r}} = \Delta_{4-2,4}^2 = \Delta_{2,4}^2 = 1 \neq 0$,
- $\Delta_{j-\bar{r},j-\xi}^{\bar{r}-\xi} = \Delta_{4-2,4-1}^{2-1} = \Delta_{2,3}^1 \neq 0$,
- $\Delta_{j-\xi,j-\xi}^{\bar{r}-\xi} = \Delta_{4-3,4-1}^{2-1} = \Delta_{1,3}^1 \neq 0$.

Hence, the path between h_k^4 and h_{k-1}^1 is $\gamma_{1,4} = [\gamma_{2,4}, -\gamma_{2,3}, \gamma_{1,3}]$. See Figure 5.34.

Theorem 5.7 is a parallel between “long flow lines” connecting consecutive singularities $h_k \in F_p$ and $h_{k-1} \in F_{p-r}$ that are far apart and higher order nonzero differentials d^r in the spectral sequence. These long flow lines are paths made up of connecting orbits where some orbits are considered in the time-reversal flow.

The motivation for allowing an orbit to be considered in the time-reversal flow comes from the special cases when M is an orientable surface and, by Theorem 5.3, this orbit corresponds in the differential matrix to an intersection number ± 1 between two singularities. In this case, by Smale's First Cancellation Theorem these two singularities may be canceled. We would be in fact considering in time-reversal, connecting orbits that could be canceled. In Figure 5.35 we go back to Example 5.5 and compare the flow $\bar{\varphi}$ obtained canceling the two singularities using Smale's First Cancellation Theorem with the flow $\widetilde{\varphi}$ associated to the last matrix obtained by the SSSA.

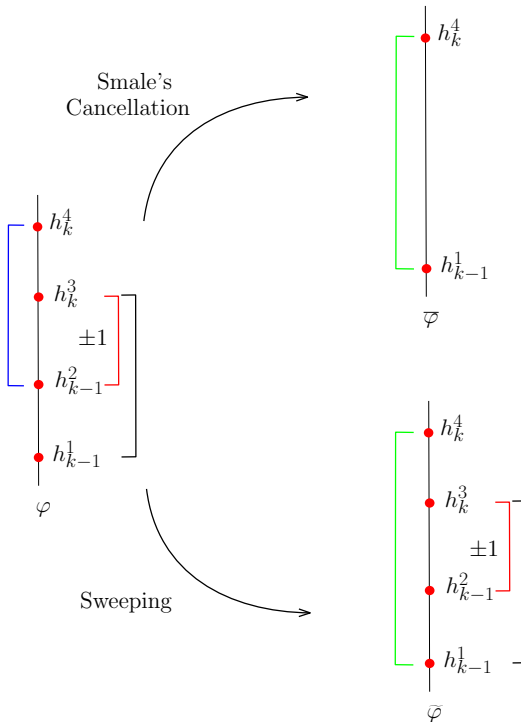


Figure 5.35: Comparing dynamical cancellation and the SSSA.

5.5 Ordered Cancellation via Spectral Sequences

Let M be a smooth orientable closed 2-dimensional manifold and $f : M \rightarrow \mathbb{R}$ be a Morse–Smale function on M . In this setting we provide a study of global continuation results for flows on M . In order to do that, we make use of a Morse chain complex (C, ∂) associated to f enriched with a finest filtration F and the associated spectral sequence

(E^r, d^r) . The main theorems in this section relate nonzero differentials d^r to cancellation of critical points using Smale's First Cancellation Theorem in order to obtain a global ordered dynamical cancellation algorithm reaching a minimal flow on M . The main references for this section are Bertolim, Lima, et al. (2016) and Bertolim, Lima, et al. (2017).

5.5.1 Spectral Sequences of a Filtered Morse Chain Complex with TU differential

In Section 5.4 we introduced a SSSA, which constructs recursively a family of matrices $\{\Delta^r\}_{r \geq 0}$, where $\Delta^0 = \Delta$ and Δ^{r+1} is obtained from Δ^r through a change of basis determined by some entries on the r -th diagonal of Δ^r called primary pivots and change-of-basis pivots. We proved that this family of matrices determines the associated spectral sequence (E^r, d^r) . In this section we show that whenever M is a closed orientable surface, we can always adopt a simplified version of the SSSA. More specifically, the changes of basis are simpler and the leading coefficient of every change of basis is always equal to 1.

Recall that whenever $\Delta_{i,j}^r$ is a change-of-basis pivot on the r -th diagonal of Δ^r , there exists a column, namely the t -th column ($t < j$), such that $\Delta_{t,i}^r$ is a primary pivot. By Step B.1 of the SSSA, we must perform a change of basis on Δ^r by adding a linear combination of all the h_k columns to the left of column j to a positive integer $u \neq 0$ (leading coefficient) multiple of the j -th column of Δ^r in order to zero out the entry $\Delta_{i,j}^r$ without introducing nonzero entries below row i , i.e., $\Delta_{s,j}^{r+1} = 0$ for all $s > i$. However, in this special case where M is an orientable closed surface, then the differential of a Morse chain complex has some important additional properties. In fact, Theorem 5.3 proves that the nonzero entries of Δ are either +1 or -1. The matrix Δ is in fact a **totally unimodular (TU) matrix**, i.e., all submatrices of Δ have determinant 0, 1, or -1 (see Lemma 5.1 of Bertolim, Lima, et al. (ibid.)). The following theorem, which is a consequence of Theorem 2.1, Propositions 3.9, 3.11, and Corollary 3.12 of Bertolim, Lima, et al. (ibid.), is a characterization of the primary pivots and change-of-basis pivots when considering the input of the SSSA restricted to TU matrices.

Theorem 5.8. *(Pivots for TU connection matrices) Suppose that the differential Δ of the Morse chain complex is a TU matrix. Then the primary pivots and change-of-basis pivots obtained when applying the SSSA over \mathbb{Z} are all equal to ± 1 .*

Consequently, it is always possible to choose the particular change of basis which uses only the t -th and the j -th column of Δ^r . More specifically, we zero out the entry $\Delta_{i,j}^r$ by adding or subtracting the t -th column to the j -th column of Δ^r . Clearly the minimal leading coefficient is always equal to 1. Hence, when M is an orientable closed surface, Step B.1 can be simplified as presented below.

B.1 - Change of basis – Surfaces

Suppose $\Delta_{k_i,j}^r$ is a change-of-basis pivot. Let $\Delta_{i,t}^r$ ($t < j$) be the primary pivot in row i . Then perform a change of basis on Δ^r by adding or subtracting the t -th column to the j -th column of Δ^r .

Let k_1, k_2, \dots be the columns of Δ associated to k -chains. The k_j -th column of Δ^{r+1} is associated to the chain

$$\begin{aligned}\sigma_k^{k_j,r+1} &= \underbrace{\sum_{\ell=1}^j c_\ell^{k_j,r} h_k^{k_\ell}}_{\sigma_k^{k_j,r}} \pm \underbrace{\sum_{\ell=1}^t c_\ell^{k_t,r} h_k^{k_\ell}}_{\sigma_k^{k_t,r}} \\ &= c_1^{k_j,r+1} h_k^{k_1} + c_2^{k_j,r+1} h_k^{k_2} + \cdots + c_{j-1}^{k_j,r+1} h_k^{k_{j-1}} + c_j^{k_j,r+1} h_k^{k_j},\end{aligned}$$

where $c^{k_\ell,r} \in \mathbb{Z}$.

Note that we are not assuming that the columns of the matrix Δ are ordered with respect to k .

Example 5.7. Consider a flow on an orientable 2-manifold M and its associated filtered Morse complex as illustrated in Figure 5.15. Let Δ be the matrix of the Morse differential ∂ with respect to the basis $\{h_0^1, h_0^2, h_0^3, h_1^4, h_1^5, h_1^6, h_1^7, h_2^8, h_2^9, h_2^{10}\}$ as in Figure 5.36. Applying the SSSA to Δ we obtain the matrices $\Delta^1, \Delta^2, \Delta^3, \Delta^4, \Delta^5$, presented in Figures 5.37 to 5.41, respectively.

By Theorem 5.5, the \mathbb{Z} -modules $E_{p,q}^r$ are determined by the SSSA applied to Δ . Recall that the most important idea in order to prove this fact was obtaining a formula for the module $Z_{p,k-p}^r$ in terms of the chains $\sigma_k^{j,r}$ determined by the SSSA. In fact, if k_{ℓ_p} is the rightmost h_k column such that $k_{\ell_p} \leq p+1$, i.e. the rightmost h_k column associated to a chain in $F_p C$, then

$$\begin{aligned}Z_{p,k-p}^r &= \mathbb{Z}[\mu^{k_{\ell_p}, r-p-1+k_{\ell_p}} \sigma_k^{k_{\ell_p}, r-p-1+k_{\ell_p}}, \\ &\quad \mu^{k_{\ell_{p-1}}, r-p-1+k_{\ell_{p-1}}} \sigma_k^{k_{\ell_{p-1}}, r-p-1+k_{\ell_{p-1}}}, \\ &\quad \dots, \\ &\quad \mu^{k_1, r-p-1+k_1} \sigma_k^{k_1, r-p-1+k_1}]\end{aligned}$$

where $\mu^{j,\xi} = 0$ whenever the primary pivot of column j is below row $(p-r+1)$ and $\mu^{j,\xi} = 1$ otherwise. Moreover, by Theorem 5.6, the SSSA induces the differentials d_p^r in the spectral sequence. More specifically, whenever E_p^r and E_{p-r}^r are both nonzero, the map $d_p^r : E_p^r \rightarrow E_{p-r}^r$ is induced by multiplication by the entry $\Delta_{p-r+1,p+1}^r$ which is either a primary pivot or a zero with a column of zero entries below it. Otherwise d_p^r is zero. By Theorem 5.8, the primary pivots in this case are always equal to ± 1 , hence the nonzero d^r 's are always isomorphisms induced by primary pivots. Since the differentials

$$\begin{array}{ccccccccc}
 & F_0 & F_1 & F_2 & F_3 & F_4 & F_5 & F_6 & F_7 & F_8 & F_9 \\
 & h_0^1 & h_0^2 & h_0^3 & h_1^4 & h_1^5 & h_1^6 & h_1^7 & h_2^8 & h_2^9 & h_2^{10} \\
 \begin{matrix} F_0 \\ F_1 \\ F_2 \\ F_3 \\ F_4 \\ F_5 \\ F_6 \\ F_7 \\ F_8 \\ F_9 \end{matrix} \begin{matrix} h_0^1 \\ h_0^2 \\ h_0^3 \\ h_1^4 \\ h_1^5 \\ h_1^6 \\ h_1^7 \\ h_2^8 \\ h_2^9 \\ h_2^{10} \end{matrix} & \left(\begin{array}{cccccc|ccc}
 0 & 0 & 0 & 1 & 0 & 0 & -1 & 0 & 0 & 0 \\
 0 & 0 & 0 & 0 & -1 & 1 & 0 & 0 & 0 & 0 \\
 0 & 0 & 0 & -1 & 1 & -1 & 1 & 0 & 0 & 0 \\
 \hline
 0 & 0 & 0 & 0 & 0 & 0 & 0 & 1 & 0 & -1 \\
 0 & 0 & 0 & 0 & 0 & 0 & 0 & -1 & 1 & 0 \\
 0 & 0 & 0 & 0 & 0 & 0 & 0 & -1 & 1 & 0 \\
 0 & 0 & 0 & 0 & 0 & 0 & 0 & 1 & 0 & -1 \\
 0 & 0 & 0 & 0 & 0 & 0 & 0 & 0 & 0 & 0 \\
 0 & 0 & 0 & 0 & 0 & 0 & 0 & 0 & 0 & 0
 \end{array} \right)
 \end{array}$$

Figure 5.36: Δ

corresponding to primary pivots are isomorphisms, then at the next stage of the spectral sequence $E_p^{r+1} = E_{p-r}^{r+1} = 0$. Note that the differentials associated to change-of-basis pivots always correspond to zero maps. In fact, if a differential $d'_p : E_p^r \rightarrow E_{p-r}^r$ corresponds to a change-of-basis pivot, then there is a primary pivot in row $p-r$ in a diagonal $\tilde{r} < r$ and thus $E_{p-r}^r = 0$.

In the remainder of this section we prove that the limit of the spectral sequence is more closely tied to the homology of the manifold when working on orientable closed surfaces.

Recall that, in the more general setting treated in Section 5.4, where one was interested in spectral sequences computed over \mathbb{Z} of a Morse chain complex associated to a gradient flow on an n -dimensional manifold, E^∞ does not determine $H_*(C)$ completely. In fact, it follows from Theorem 5.1 that

$$E_{p,q}^\infty \cong GH_*(C)_{p,q} = \frac{F_p H_{p+q}(C)}{F_{p-1} H_{p+q}(C)}.$$

However, by Theorems 5.6 and 5.8 we have that whenever M is an orientable closed surface, the differentials of the spectral sequence are induced by primary pivots, which are all equal to ± 1 . It follows that all the differentials are isomorphisms and, hence, the modules $E_{p,q}^r$ are free of torsion for all p, q and $r \geq 0$. Since the convergence of the spectral (E^r, d^r) is a strong convergence then the modules $E_{p,q}^\infty$ are free for all p and q .

$$\begin{array}{c}
 \sigma_0^{1,1} = h_0^1 & \sigma_0^{2,1} & \sigma_0^{3,1} & \sigma_1^{4,1} & \sigma_1^{5,1} & \sigma_1^{6,1} & \sigma_1^{7,1} & \sigma_2^{8,1} & \sigma_2^{9,1} & \sigma_2^{10,1} \\
 \left(\begin{array}{ccccccccc}
 0 & 0 & 0 & 1 & 0 & 0 & -1 & 0 & 0 & 0 \\
 0 & 0 & 0 & 0 & -1 & 1 & 0 & 0 & 0 & 0 \\
 0 & 0 & 0 & -1 & 1 & -1 & 1 & 0 & 0 & 0 \\
 0 & 0 & 0 & 0 & 0 & 0 & 0 & 1 & 0 & -1 \\
 0 & 0 & 0 & 0 & 0 & 0 & 0 & -1 & 1 & 0 \\
 0 & 0 & 0 & 0 & 0 & 0 & 0 & -1 & 1 & 0 \\
 0 & 0 & 0 & 0 & 0 & 0 & 0 & 1 & 0 & -1 \\
 0 & 0 & 0 & 0 & 0 & 0 & 0 & 0 & 0 & 0 \\
 0 & 0 & 0 & 0 & 0 & 0 & 0 & 0 & 0 & 0 \\
 0 & 0 & 0 & 0 & 0 & 0 & 0 & 0 & 0 & 0
 \end{array} \right)
 \end{array}$$

Figure 5.37: Δ^1

Consequently, $GH_*(C)_{p,q}$ is free for all p and q . Since the filtration is finite,

$$E_{p,q}^\infty \cong \bigoplus_{p+q=k} GH_*(C)_{p,q} \cong H_{p+q}(C).$$

We have proved the following theorem.

Theorem 5.9. *If M is a smooth orientable closed 2-dimensional manifold, $f : M \rightarrow \mathbb{R}$ is a Morse–Smale function, (C, ∂) is a filtered Morse chain complex with the finest filtration, then for all p and q the modules $E_{p,q}^\infty$ of the associated spectral sequence are free and*

$$E_{p,q}^\infty \cong H_{p+q}(C). \quad (5.10)$$

Clearly, the same result holds for smooth closed n -manifolds, $n > 2$, whose Morse differential is a TU matrix.

5.5.2 Global cancellation on Surfaces

Let M be a smooth closed oriented 2-dimensional manifold, $f : M \rightarrow \mathbb{R}$ be a Morse–Smale function on M and φ be the negative gradient flow of f . In this section we present

$$\begin{array}{c}
 \sigma_0^{1,2} = h_0^1 & \sigma_0^{2,2} & \sigma_0^{3,2} & \sigma_1^{4,2} & \sigma_1^{5,2} & \sigma_1^{6,2} & \sigma_1^{7,2} & \sigma_2^{8,2} & \sigma_2^{9,2} & \sigma_2^{10,2} \\
 \sigma_0^{2,2} = h_0^2 & & & & & & & & & \\
 \sigma_0^{3,2} = h_0^3 & & & & & & & & & \\
 \sigma_1^{4,2} = h_1^4 & & & & & & & & & \\
 \sigma_1^{5,2} = h_1^5 & & & & & & & & & \\
 \sigma_1^{6,2} = h_1^6 & & & & & & & & & \\
 \sigma_1^{7,2} = h_1^7 & & & & & & & & & \\
 \sigma_2^{8,2} = h_2^8 & & & & & & & & & \\
 \sigma_2^{9,2} = h_2^9 & & & & & & & & & \\
 \sigma_2^{10,2} = h_2^{10} & & & & & & & & &
 \end{array}
 \left(\begin{array}{ccccccccc}
 0 & 0 & 0 & 1 & 0 & 0 & -1 & 0 & 0 & 0 \\
 0 & 0 & 0 & 0 & -1 & 1 & 0 & 0 & 0 & 0 \\
 0 & 0 & 0 & -1 & 1 & -1 & 1 & 0 & 0 & 0 \\
 0 & 0 & 0 & 0 & 0 & 0 & 0 & 1 & 0 & -1 \\
 0 & 0 & 0 & 0 & 0 & 0 & 0 & -1 & 1 & 0 \\
 0 & 0 & 0 & 0 & 0 & 0 & 0 & -1 & 1 & 0 \\
 0 & 0 & 0 & 0 & 0 & 0 & 0 & 1 & 0 & -1 \\
 0 & 0 & 0 & 0 & 0 & 0 & 0 & 0 & 0 & 0 \\
 0 & 0 & 0 & 0 & 0 & 0 & 0 & 0 & 0 & 0 \\
 0 & 0 & 0 & 0 & 0 & 0 & 0 & 0 & 0 & 0
 \end{array} \right)$$

Figure 5.38: Δ^2

interesting dynamical results obtained from the analysis of the spectral sequence associated to a filtered Morse complex $(C_*(f), \partial_*)$. We construct a family of Morse–Smale flows $\{\varphi^1 = \varphi, \varphi^2, \dots, \varphi^\omega\}$ where φ^{r+1} is obtained from φ^r by canceling the pairs of critical points corresponding to the algebraic cancellations on the r -th step of the spectral sequence. This family is a continuation of φ to a minimal flow in M .

As proven in Theorem 5.6, the nonzero differentials of the spectral sequence are induced by pivots produced by the SSSA. Recall that, when working on surfaces, the Morse differentials are under more limiting conditions than in the general case. More specifically, by Theorem 5.8 the primary pivots are always equal to ± 1 , hence the differentials $d_p^r : E_p^r \rightarrow E_{p-r}^r$ associated to primary pivots are isomorphisms and the other ones are zero maps. Note that whenever we mark a primary pivot $\Delta_{j-r,j}^r = \pm 1$ on the r -th diagonal of Δ^r , the next step of the spectral sequence produces what we call an *algebraic cancellation*, i.e. $E_p^{r+1} = E_{p-r}^{r+1} = 0$. In this section we construct a sequence of dynamical cancellations of critical points using Smale’s First Cancellation Theorem which are in one-to-one correspondence with the sequence of algebraic cancellations of the modules of the spectral sequence. In order to do that, we use the SSSA.

Theorem 5.10. (Ordered Smale’s Cancellation Theorem via Spectral Sequence) Let M be a smooth closed oriented 2-dimensional manifold, $f : M \rightarrow \mathbb{R}$ be a Morse–Smale function on M , φ be the negative gradient flow of f , (C, Δ) be a Morse chain complex

	$\sigma_0^{1,3}$	$\sigma_0^{2,3}$	$\sigma_0^{3,3}$	$\sigma_1^{4,3}$	$\sigma_1^{5,3}$	$\sigma_1^{6,3}$	$\sigma_1^{7,3}$	$\sigma_2^{8,3}$	$\sigma_2^{9,3}$	$\sigma_2^{10,3}$
$\sigma_0^{1,3} = h_0^1$	0	0	0	-1	1	0	-1	0	0	0
$\sigma_0^{2,3} = h_0^2$	0	0	0	0	-1	1	0	0	0	0
$\sigma_0^{3,3} = h_0^3$	0	0	0	-1	0	-1	1	0	0	0
$\sigma_1^{4,3} = h_1^4$	0	0	0	0	0	0	0	2	-1	-1
$\sigma_1^{5,3} = h_1^5 + h_1^4$	0	0	0	0	0	0	0	-1	1	0
$\sigma_1^{6,3} = h_1^6$	0	0	0	0	0	0	0	-1	1	0
$\sigma_1^{7,3} = h_1^7$	0	0	0	0	0	0	0	1	0	-1
$\sigma_2^{8,3} = h_2^8$	0	0	0	0	0	0	0	0	0	0
$\sigma_2^{9,3} = h_2^9$	0	0	0	0	0	0	0	0	0	0
$\sigma_2^{10,3} = h_2^{10}$	0	0	0	0	0	0	0	0	0	0

Figure 5.39: Δ^3

and $F = \{F_p C\}$ be a finest filtration. If (E^r, d^r) is the associated spectral sequence, then:

1. The sequence of algebraic cancellations of the modules E^r are in one-to-one correspondence with a sequence of dynamical cancellations of critical points of f . More specifically, there exists a sequence of dynamical cancellations of singularities in φ such that, each algebraic cancellation of the modules E_p^r , E_{p-r}^r corresponds to a dynamical cancellation of singularities $h_k \in F_p$ and $h_{k-1} \in F_{p-r}$ of φ .
2. There exists a family of Morse–Smale flows $\Phi = \{\varphi^1 = \varphi, \varphi^2, \dots, \varphi^\omega\}$ where φ^{r+1} is obtained from φ^r by canceling the pairs of critical points corresponding to the algebraic cancellations in the r -th step of the spectral sequence. Moreover, Φ is a continuation and the flow φ^ω is a minimal flow on M .

The **gap** between two singularities h_k to h_{k-1} of a Morse flow with respect to a filtration F is positive integer number r such that the corresponding chains of the Morse complex satisfy $h_k \in F_p C \setminus F_{p-1} C$ and $h_{k-1} \in F_{p-r} C \setminus F_{p-r-1} C$. Note that the order of cancellation in Theorem 5.10 occurs in increasing order of the gap r . Therefore, as we traverse the diagonals of the differential matrix via the SSSA, in the dynamics longer and longer connecting orbits are produced (birth of orbits) while shorter connecting orbits corresponding to the change-of-basis pivots are eliminated (death of orbits). In summary,

	$\sigma_0^{1,4}$	$\sigma_0^{2,4}$	$\sigma_0^{3,4}$	$\sigma_1^{4,4}$	$\sigma_1^{5,4}$	$\sigma_1^{6,4}$	$\sigma_1^{7,4}$	$\sigma_2^{8,4}$	$\sigma_2^{9,4}$	$\sigma_2^{10,4}$
$\sigma_0^{1,4} = h_0^1$	0	0	0	1	1	-1	-1	0	0	0
$\sigma_0^{2,4} = h_0^2$	0	0	0	0	-1	1	0	0	0	0
$\sigma_0^{3,4} = h_0^3$	0	0	0	-1	0	0	1	0	0	0
$\sigma_1^{4,4} = h_1^4$	0	0	0	0	0	0	0	1	0	0
$\sigma_1^{5,4} = h_1^5 + h_1^4$	0	0	0	0	0	0	0	-1	1	-1
$\sigma_1^{6,4} = h_1^6 - h_1^4$	0	0	0	0	0	0	0	-1	1	-1
$\sigma_1^{7,4} = h_1^7$	0	0	0	0	0	0	0	1	0	0
$\sigma_2^{8,4} = h_2^8$	0	0	0	0	0	0	0	0	0	0
$\sigma_2^{9,4} = h_2^9$	0	0	0	0	0	0	0	0	0	0
$\sigma_2^{10,4} = h_2^{10} + h_2^8$	0	0	0	0	0	0	0	0	0	0

Figure 5.40: Δ^4

longer orbits are born due to the death of shorter ones caused by the cancellation of critical points determined by the spectral sequence. At the end of this process, we reach a minimal flow in M .

Example 5.8. Consider the flow on an orientable 2-manifold M and its associated filtered Morse complex as illustrated in Figure 5.15, Δ be the matrix of the Morse differential as in Figure 5.36 and let $\Delta^1, \Delta^2, \Delta^3, \Delta^4, \Delta^5$ be the matrices produced by the SSSA as presented in Figures 5.37 to 5.41, respectively. By Theorem 5.6, the primary pivots produced by the SSSA induce the differentials of the spectral sequence. It follows from Theorem 5.8 that these pivots are all equal to ± 1 and hence the differentials are all isomorphisms responsible for algebraic cancellations of the modules of the spectral sequence. By Theorem 5.10, each algebraic cancellation performed by the spectral sequence, corresponds to a dynamical cancellation of critical points. Figures 5.42 to 5.45 show the family of flows in a continuation of the flow φ to the minimal flow determined by the spectral sequence.

More specifically:

- The primary pivot $\Delta_{3,4}^1$ induces the differential $d_3^1 : E_3^1 \rightarrow E_2^1$, which causes the algebraic cancellation $E_3^2 = E_2^2 = 0$. Moreover, the primary pivot $\Delta_{7,8}^1$ induces the differential $d_7^1 : E_7^1 \rightarrow E_6^1$, which causes the algebraic cancellation $E_7^2 = E_6^2 = 0$. Corresponding to these algebraic cancellations, we have the dynamical cancellations of the pairs (h_0^3, h_1^4) and (h_1^7, h_2^8) , which determine the flow φ^2 as

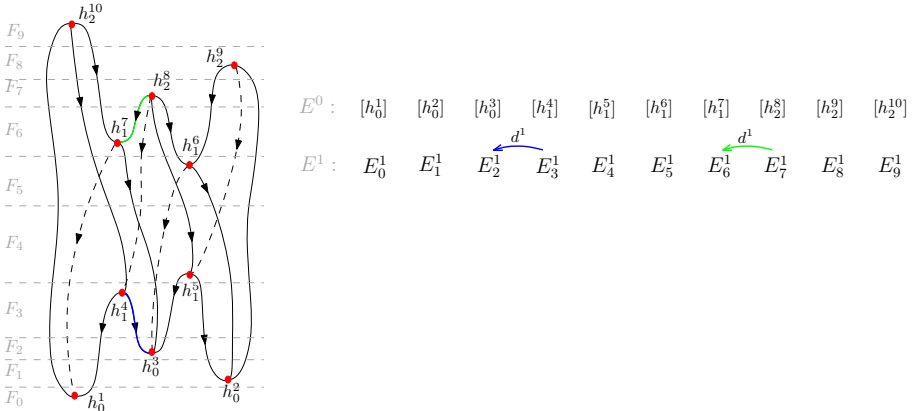
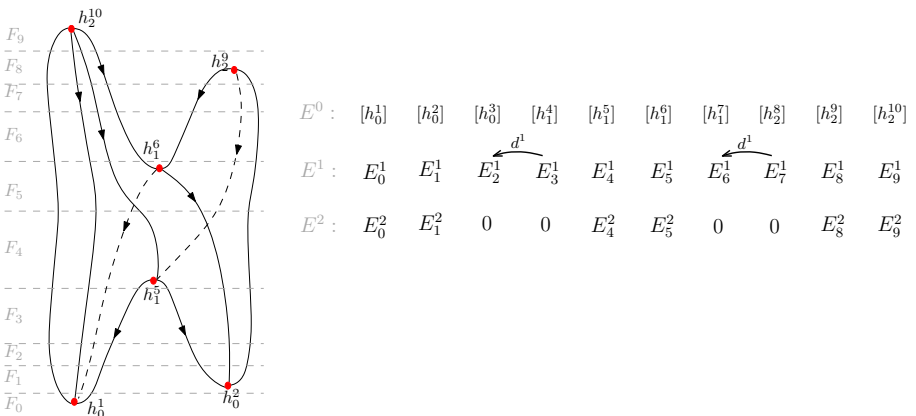
$$\begin{array}{c}
 \sigma_0^{1,5} \quad \sigma_0^{2,5} \quad \sigma_0^{3,5} \quad \sigma_1^{4,5} \quad \sigma_1^{5,5} \quad \sigma_1^{6,5} \quad \sigma_1^{7,5} \quad \sigma_2^{8,5} \quad \sigma_2^{9,5} \quad \sigma_2^{10,5} \\
 \sigma_0^{1,5} = h_0^1 \\
 \sigma_0^{2,5} = h_0^2 \\
 \sigma_0^{3,5} = h_0^3 \\
 \sigma_1^{4,5} = h_1^4 \\
 \sigma_1^{5,5} = h_1^5 + h_1^4 \\
 \sigma_1^{6,5} = h_1^6 + h_1^5 \\
 \sigma_1^{7,5} = h_1^7 + h_1^4 \\
 \sigma_2^{8,5} = h_2^8 \\
 \sigma_2^{9,5} = h_2^9 \\
 \sigma_2^{10,5} = h_2^{10} + h_2^8 + h_2^9
 \end{array}
 \left(\begin{array}{cccccc|ccc}
 0 & 0 & 0 & 1 & 1 & 0 & 0 & 0 & 0 & 0 \\
 0 & 0 & 0 & 0 & -1 & 0 & 0 & 0 & 0 & 0 \\
 0 & 0 & 0 & -1 & 0 & 0 & 0 & 0 & 0 & 0 \\
 0 & 0 & 0 & 0 & 0 & 0 & 0 & 0 & 0 & 0 \\
 0 & 0 & 0 & 0 & 0 & 0 & 0 & 0 & 0 & 0 \\
 0 & 0 & 0 & 0 & 0 & 0 & 0 & -1 & 1 & 0 \\
 0 & 0 & 0 & 0 & 0 & 0 & 0 & 1 & 0 & 0 \\
 0 & 0 & 0 & 0 & 0 & 0 & 0 & 0 & 0 & 0 \\
 0 & 0 & 0 & 0 & 0 & 0 & 0 & 0 & 0 & 0 \\
 0 & 0 & 0 & 0 & 0 & 0 & 0 & 0 & 0 & 0
 \end{array} \right)$$

Figure 5.41: Δ^5

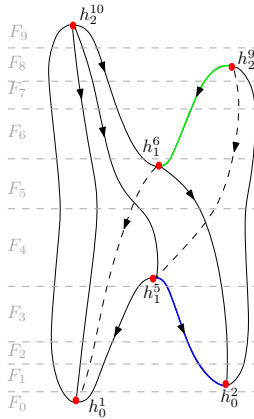
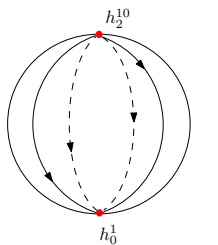
in Figure 5.43. The flow φ^2 is equal to φ outside a neighborhood of the canceled critical points and the connections between them. In φ^2 we note birth of a flow line from h_2^{10} to h_1^6 .

- Since there are no primary pivots on the second diagonal, $\varphi^2 = \varphi^3$. See Figure 5.44.
- The primary pivot $\Delta_{2,5}^3$ induces the differential $d_4^3 : E_4^3 \rightarrow E_1^3$, which causes the algebraic cancellation $E_4^4 = E_1^4 = 0$. Moreover, the primary pivot $\Delta_{6,9}^3$ induces the differential $d_8^3 : E_8^3 \rightarrow E_5^3$, which causes the algebraic cancellation $E_8^4 = E_5^4 = 0$. The corresponding canceled pairs of critical points are (h_0^2, h_1^5) and (h_1^6, h_2^9) , respectively. See Figure 5.45.

In order to prove Theorem 5.10, we construct a family of flows associated to the sequence of matrices $\{\Delta^r\}$ produced by the SSSA where the changes of basis caused by pivots reflect the changes in connecting orbits caused by the cancellation of critical points. More specifically, the aim is to construct an algebraic-dynamical correspondence where each change of basis caused by a primary pivot in row $p - r + 1$ correspond to a change in connecting orbits caused by the cancellation of h_k^{p+1} and h_{k-1}^{p-r+1} . However, when we cancel the pair of critical points h_k^{p+1} and h_{k-1}^{p-r+1} , all the connecting orbits between them, all the ones between h_k^{p+1} and index $k - 1$ critical points and also the ones between index k

Figure 5.42: Algebraic-dynamical correspondence detected by Δ^1 Figure 5.43: Algebraic-dynamical correspondence detected by Δ^2

critical points and h_{k-1}^{p+r+1} disappear while new connecting orbits between the remaining critical points arise. Hence, in order to construct this algebraic-dynamical correspondence we consider an auxiliary algorithm, which has the same rules for marking pivots and performs the same changes of basis as the SSSA, but in a different order to reflect the death and birth of connections. More specifically, if $\Delta_{p-r+1,p+1}^r = \pm 1$ is a primary pivot marked in step r of the SSSA, all changes of basis caused by $\Delta_{p-r+1,p+1}^r$ are performed in step $r + 1$. This algorithm, which is a slight change of the SSSA, is called Smale's Cancellation Sweeping Algorithm. Smale's Cancellation Sweeping Algorithm produces a family of matrices $\{\tilde{\Delta}^r\}$ where $\tilde{\Delta}^0 = \Delta$, the definitions of primary pivot and the change

Figure 5.44: Algebraic-dynamical correspondence detected by Δ^3 Figure 5.45: Algebraic-dynamical correspondence detected by Δ^4

of basis are the same as in the SSSA. The only difference is that whenever we mark a primary pivot, all the changes of basis caused by this pivot are performed in the next step.

Smale's Cancellation Sweeping Algorithm

Smale's Cancellation Sweeping Algorithm constructs a family of matrices $\{\tilde{\Delta}^r, r \geq 0\}$

recursively, where $\tilde{\Delta}^0 = \Delta$, by performing the same operations as the SSSA but in a different order. For a fixed r -th diagonal, the method described below must be applied for all Δ_k simultaneously.

A - Initial step

Without loss of generality, we assume that the first diagonal of Δ contains nonzero entries. Whenever the first diagonal contains only zero entries, we define $\tilde{\Delta}^1 = \Delta$ and we repeat this step until we reach a diagonal of Δ which contains nonzero entries.

We construct the matrix $\tilde{\Delta}^1$ performing the following procedure.

- (a) The nonzero entries $\Delta_{i,u}$ of the first diagonal are marked and called **primary pivots**.
- (b) Without loss of generality, assume that there are nonzero entries in a row i , which contains a primary pivot $\Delta_{i,u}$ on the first diagonal. For each nonzero entry $\Delta_{i,j}$ in row i , consider the entries in column j and in a row s with $s > i$ in Δ .
 - (b1) If there is a primary pivot in an entry in column j and in a row s , with $s > i$, then the entry is left unmarked.
 - (b2) If there are no primary pivots in column j below $\Delta_{i,j}$ then this entry is marked as a **change-of-basis pivot**.

At the end of the first step we define a matrix $\tilde{\Delta}^1$ as Δ with the primary pivots on the first diagonal marked and change-of-basis pivots in all the rows that contain primary pivots on the first diagonal marked.

B - Intermediate step

In this step we consider a matrix $\tilde{\Delta}^r$ with the primary pivots marked on the ξ -th diagonal for all $\xi \leq r$ and the change-of-basis pivots in the rows that have primary pivots on the r -diagonal marked. We describe how $\tilde{\Delta}^{r+1}$ is defined. If there is no change-of-basis pivot in a row that contains a primary pivot on the r -th diagonal we go directly to step B.2, that is, we define $\tilde{\Delta}^{r+1} = \tilde{\Delta}^r$ with primary and change of basis pivots marked as in step B.2.

B.1 - Change of basis

Suppose $\tilde{\Delta}_{i,j}^r$ is a change-of-basis pivot in a row i that contains a primary pivot $\tilde{\Delta}_{i,u}^r$ on the r -th diagonal. Then, perform a change of basis on $\tilde{\Delta}^r$ in order to zero out the entry $\tilde{\Delta}_{i,j}^r$ without introducing nonzero entries in $\tilde{\Delta}_{s,j}^r$ for $s > i$. Once this is done, we obtain the j -th column of $\tilde{\Delta}^{r+1}$. It is a linear combination of columns u and j of $\tilde{\Delta}^r$ such that $\tilde{\Delta}_{i,j}^{r+1} = 0$. More specifically, for each $s = 0, \dots, i$, the entry $\tilde{\Delta}_{s,j}^{r+1}$

is added to a multiple ± 1 of the entry $\tilde{\Delta}_{s,u}^r$, where u is the column of the primary pivot in row i , i.e.

$$\tilde{\Delta}_{s,j}^{r+1} = \tilde{\Delta}_{s,j}^r - \tilde{\Delta}_{i,j}^r (\tilde{\Delta}_{i,u}^r)^{-1} \tilde{\Delta}_{s,u}^r$$

Once the above procedure is done for all change-of-basis pivots in rows which have primary pivots on the r -th diagonal of $\tilde{\Delta}^r$, the matrix $\tilde{\Delta}^{r+1}$ has entries determined. In particular, all the change-of-basis pivots in $\tilde{\Delta}^r$ are zero in $\tilde{\Delta}^{r+1}$.

B.2 - Marking $\tilde{\Delta}^{r+1}$

Consider the matrix defined in the previous step. Without loss of generality, assume that the diagonal $r + 1$ contains nonzero entries. We mark the primary pivots and the change-of-basis pivots in $\tilde{\Delta}^{r+1}$ as follows:

Let $\tilde{\Delta}_{i,u}^{r+1}$ be a nonzero entry on the diagonal $r + 1$.

- (a) If there is a primary pivot in an entry in column u in a row s with $s > i$ in $\tilde{\Delta}^{r+1}$, i.e. below $\tilde{\Delta}_{i,u}^{r+1}$, then leave the entry unmarked.
- (b) Suppose there are no primary pivots in column u . Hence, there are no primary pivots in row i , otherwise this entry would have been marked as a change-of-basis pivot in a previous step and $\tilde{\Delta}_{i,u}^{r+1}$ would be zero. In this case, $\tilde{\Delta}_{i,u}^{r+1}$ is marked as a primary pivot.
- (c) Without loss of generality, assume that the there are nonzero entries in the rows i , which are the rows with primary pivots in diagonal $r + 1$. For each nonzero entry $\tilde{\Delta}_{i,j}^{r+1}$ on row i , consider the entries in column j and in a row s with $s > i$ in $\tilde{\Delta}^{r+1}$.
 - (c1) If there is a primary pivot in column j and in a row s , with $s > i$, then the entry $\tilde{\Delta}_{i,j}^{r+1}$ is left unmarked.
 - (c2) If there are no primary pivots in column j below $\tilde{\Delta}_{i,j}^{r+1}$ then this entry is marked as a change-of-basis pivot.

Once this step is done we have marked all primary pivots on diagonal $r + 1$ and all change-of-basis pivots in rows with primary pivots on the diagonal $r + 1$ of $\tilde{\Delta}^{r+1}$. The matrix $\tilde{\Delta}^{r+1}$ is completely determined.

C - Final step

We repeat the above procedure until all diagonals have been considered.

More details on this algorithm can be found in Bertolim, Lima, et al. (2016, 2017). In Bertolim, Lima, et al. (2016) (Theorem 2.2 and Corollary 5.3), the following result is proved.

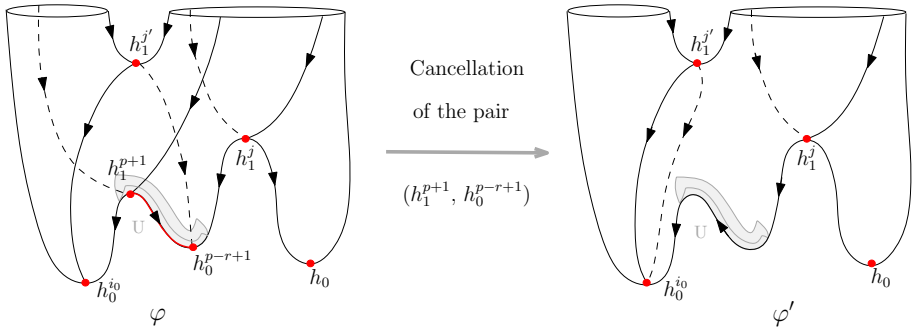


Figure 5.46: Birth and death of connections.

Proposition 5.5 (Primary Pivots Equality Property). *Let M be a smooth closed oriented n -dimensional manifold, $f : M \rightarrow \mathbb{R}$ be a Morse–Smale function on M and (C, Δ) be a Morse chain complex such that Δ is a TU matrix. Let (E^r, d^r) be the spectral sequence associated to (C, Δ) enriched with a finest filtration. The primary pivots marked when performing the SSSA over \mathbb{Z} coincide in value and position with the primary pivots marked performing Smale’s Cancellation Sweeping Algorithm.*

In order to construct the sequence of dynamical cancellations corresponding to the algebraic cancellations of the SSSA we recursively construct a family of flows $\{\varphi^r, r = 0, \dots, \omega\}$, where $\varphi^0 = \varphi$ and φ^{r+1} is obtained from φ^r removing the pairs of critical points h_k^{p+1} and h_{k-1}^{p-r+1} of the flow φ^r corresponding to the canceled modules $E_p^r = \mathbb{Z}[\sigma_k^{p+1,r}]$ and $E_{p-r}^r = \mathbb{Z}[\sigma_k^{p-r+1,r}]$ on the r -th page of the spectral sequence, such that $\Delta_{p-r+1,p+1}^r$ is a primary pivot on the r -th diagonal of Δ^r . The main idea is to prove that each algebraic cancellation of the spectral sequence can, in fact, be associated to a dynamical cancellation. More specifically, we prove that whenever a primary pivot $\Delta_{p-r+1,p+1}^r$ on the r -th diagonal of Δ^r is marked, it is actually an intersection number between two consecutive singularities h_k^{p+1} and h_{k-1}^{p-r+1} of a flow φ^r and hence we can use Smale’s First Cancellation Theorem.

Recall that if h_k^{p+1} and h_{k-1}^{p-r+1} are two consecutive critical points of f such that $n(h_k^{p+1}, h_{k-1}^{p-r+1}) = \pm 1$, then by Smale’s First Cancellation Theorem these critical points can be canceled, i.e. there exists a gradient flow φ' which coincides with the flow φ outside a neighborhood U of $\{h_k^{p+1}, h_{k-1}^{p-r+1}\} \cup \mathcal{O}(u)$, where $\mathcal{M}_{h_{k-1}^{p-r+1}}^{h_k^{p+1}} = \{u\}$. See Figure 5.46.

Since φ' coincides with φ outside U , then connections between $h_q^{\ell_2}$ and $h_{q-1}^{\ell_1}$, where $\ell_1, \ell_2 \notin \{p+1, p-r+1\}$, which do not intersect U are not changed. Also, their characteristic signs remain the same after the cancellation in U occurs.

The next proof is inspired in the proof of Theorems 6.1 and 6.2 of Bertolim, Lima, et al. (ibid.).

Proof. (of Theorem 5.10)

Without loss of generality, we assume that all orientations of $W^u(h_2)$ are chosen to be the same and, hence, the orbits in $W^s(h_1) \setminus \{h_1\}$ have opposite characteristic signs. By definition, the orbits in $W^u(h_1) \setminus \{h_1\}$ also have opposite characteristic signs. We use the notation $n(h_k, h_{k-1}, \varphi)$ when we refer to the intersection number of h_k and h_{k-1} with respect to the flow φ and $\Delta(\varphi)$ when referring to the Morse differential $\Delta(M, f, Or)$, where φ is the negative gradient flow associated to the Morse–Smale function f .

Case 1: cancellation of a saddle and a sink.

Let h_1^{p+1} be a saddle which connects with the sinks h_0^{p-r+1} and $h_0^{i_0}$. Suppose that h_1^{p+1} cancels with h_0^{p-r+1} , and let φ' be the gradient flow which coincides with the flow φ outside a neighborhood U of $\{h_1^{p+1}, h_0^{p-r+1}\} \cup \mathcal{O}(u)$, where $\mathcal{M}_{h_0^{p-r+1}}^{h_1^{p+1}} = \{u\}$.

For each saddle h_1^j which connects with h_0^{p-r+1} , the connecting orbit between h_1^j and $h_0^{i_0}$ in φ will give place to a connection between h_1^j and $h_0^{i_0}$ in φ' . Since the old and new connections have the same characteristic signs, then

$$n(h_1^j, h_0^{i_0}, \varphi') = n(h_1^j, h_0^{i_0}, \varphi) + n(h_1^{p+1}, h_0^{i_0}, \varphi)$$

Moreover, since φ' coincides with φ outside U , the only intersection numbers that are altered after cancellation are those $n(h_1^j, h_0^{i_0})$, where h_1^j is such that $\mathcal{M}_{h_0^{p-r+1}}^{h_1^j} \neq \emptyset$. Each connection between a source and h_1^{p+1} in φ will give place to a connection between this source and the sink $h_0^{i_0}$ in φ' .

In order to obtain $\Delta(\varphi')$ from $\Delta(\varphi)$ we must convert the effect of a cancellation of critical points in φ to $\Delta(\varphi)$. Define the matrix $\tilde{\Delta}$ as the matrix obtained from $\Delta(\varphi)$ by replacing all each column j by the sum of columns $p \pm 1$ and j . Replace the entries at row $p+1$ by zeros. Then $\Delta(\varphi')$ is the submatrix of $\tilde{\Delta}$ which does not contain rows $p-r+1$ and $p+1$, neither columns $p-r+1$ and $p+1$. Note that the operations to obtain $\tilde{\Delta}$ are exactly the operations performed in the Smale's Cancellation Sweeping Algorithm.

Case 2: cancellation of a source and a saddle.

Analogously to Case 1, consider the case where h_1^{p-r+1} is a saddle connecting with sources h_2^{p+1} and $h_2^{j_0}$ and suppose that h_2^{p+1} cancels with h_1^{p-r+1} . The resulting gradient flow φ' coincides with φ outside a neighborhood V of $\{h_2^{p+1}, h_1^{p-r+1}\} \cup \mathcal{O}(v)$, where $\mathcal{M}_{h_1^{p-r+1}}^{h_2^{p+1}} = \{v\}$.

For each saddle h_1^i connecting with h_2^{p+1} in φ , the connecting orbit between h_2^{p+1} and h_1^i in φ will give place to a connections between $h_2^{j_0}$ and h_1^i in φ' . Then

$$n(h_2^{j_0}, h_1^i, \varphi') = n(h_2^{j_0}, h_1^i, \varphi) + n(h_2^{p+1}, h_1^i, \varphi)$$

Moreover, the only intersection numbers altered after the cancellation are the $n(h_2^{j_0}, h_1^i)$,

where h_1^i is such that $\mathcal{M}_{h_1^i}^{h_2^{p+1}} \neq \emptyset$. Each connection between h_1^{p-r+1} and a sink in φ will give place to a connection between $h_2^{j_0}$ and this sink in φ' .

Once again, we must convert the effect of the cancellation in φ to $\Delta(\varphi)$ in order to obtain $\Delta(\varphi')$. Let $\tilde{\Delta}$ be the matrix obtained from $\Delta(\varphi)$ by replacing each column j by the sum of columns $p+1$ and j . Then $\Delta(\varphi')$ is the submatrix of $\tilde{\Delta}$ which does not contain rows $p-r+1$ and $p+1$, neither columns $p-r+1$ and $p+1$. Once more, the operations to obtain $\tilde{\Delta}$ are exactly the operations performed in the Smale's Cancellation Sweeping Algorithm.

Construction of the family $\Phi = \{\varphi^1 = \varphi, \varphi^2, \dots, \varphi^\omega\}$.

Let $\{\tilde{\Delta}^r\}$ be the matrices produced by the Smale's Cancellation Sweeping Algorithm. Define $\varphi^1 = \varphi$ and φ^{r+1} as the flow obtained from φ^r by canceling all pairs of critical points corresponding to pairs of modules $E_p^r = \mathbb{Z}[\sigma_k^{p+1,r}]$ and $E_{p-r}^r = \mathbb{Z}[\sigma_k^{p-r+1,r}]$ such that d_p^r is an isomorphism corresponding to the primary pivots $\Delta_{p-r+1,p+1}^r$ on the r -th diagonal of $\tilde{\Delta}^r$. In order to show that these flows are well defined, we must prove that whenever a primary pivot $\Delta_{p-r+1,p+1}^r$ on the r -th diagonal of $\tilde{\Delta}^r$ is marked, it is actually an intersection number between two consecutive singularities h_k^{p+1} and h_{k-1}^{p-r+1} of the flow φ^r and hence they can be canceled by Smale's cancellation Theorem. The proof is done by induction on r .

Since $\varphi^1 = \varphi$, then the entries of $\Delta(\varphi^1)$ and $\tilde{\Delta}^1$ are equal. Without loss of generality, suppose there is at least one primary pivot on the first diagonal of $\tilde{\Delta}^1$ and let $\Delta_{1,j}^1 = \pm 1$ be a primary pivot. By definition, this primary pivot corresponds to the intersection number between two singularities h_k^{p+1} and h_{k-1}^p of the flow φ^1 , which are consecutive with respect to the filtration F since the gap between them is one. By Smale's First Cancellation Theorem, we can define a flow φ^2 by canceling all pairs of critical points as cases 1 and 2 described previously. The matrix $\Delta(\varphi^2)$ is the submatrix obtained from $\tilde{\Delta}^2$ removing the columns and rows corresponding to the canceled singularities. Each entry of $\Delta(\varphi^2)$ is an intersection number between two singularities of φ^2 and, consequently, each entry of $\tilde{\Delta}^2$ which is not in rows and columns $p-r+1$ and $p+1$ is an intersection number between two singularities of φ^2 . Note that two singularities h_k^ℓ and $h_{k-1}^{\ell-2}$ of φ^2 with gap two in the filtration F are consecutive in the flow φ^2 since all the gap 1 singularities have been canceled in the previous stage.

Now suppose that in the flow φ^r each entry of $\Delta(\varphi^r)$ is an intersection number of consecutive singularities and $\Delta(\varphi^r)$ is a submatrix of $\tilde{\Delta}^r$ obtained removing rows and columns corresponding to the canceled singularities in steps $1, \dots, r-1$. Hence, each entry of the $\tilde{\Delta}^r$ which is not in rows and columns corresponding to the canceled singularities in steps $1, \dots, r-1$ is an intersection number of consecutive singularities. In particular, each primary pivot $\Delta_{p-r+1,p+1}^r$ on the diagonal r of $\tilde{\Delta}^r$ corresponds to the intersection number of consecutive singularities h_k^{p+1} and h_{k-1}^{p-r+1} of φ^r and the differential matrix $\Delta(\varphi^r)$ does not contain columns and rows of $\tilde{\Delta}^r$ corresponding to all primary

pivots marked until the diagonal $r - 1$. These singularities correspond to all pairs of singularities of φ with gap less than or equal to $r - 1$. Hence, singularities h_k^i and h_{k-1}^{i-r} of φ^r with gap r with respect to the filtration F are consecutive in the flow φ^r . It follows that a pair of singularities h_k^{p+1} and h_{k-1}^{p-r+1} such that $\Delta_{p-r+1,p+1}^r$ is a primary pivot on diagonal r of $\tilde{\Delta}^r$ can be canceled by Smale's First Cancellation Theorem. Let φ^{r+1} be the flow obtained from φ^r by canceling all pairs h_k^{p+1} and h_{k-1}^{p-r+1} such that $\Delta_{p-r+1,p+1}^r$ is a primary pivot on diagonal r of $\tilde{\Delta}^r$. It follows from Cases 1 and 2 that the differential matrix $\Delta(\varphi^{r+1})$ is a submatrix of $\tilde{\Delta}^{r+1}$ which does not contain columns and rows of $\tilde{\Delta}^{r+1}$ corresponding to all primary pivots marked in steps $1, \dots, r$.

Algebraic-dynamical correspondence.

Consider an algebraic cancellation $E_p^{r+1} = E_{p-r}^{r+1} = 0$ associated to a primary pivot $\Delta_{p-r+1,p+1}^r = \pm 1$ on the r -th diagonal of the matrix Δ^r produced by the SSSA. More specifically, row $p - r + 1$ is associated to the chain $h_{k-1}^{p-r+1} \in F_{p-r}C_{k-1} \setminus F_{p-r-1}C_{k-1}$ and the column $p + 1$ is associated to the chain $h_k^{p+1} \in F_pC_k \setminus F_{p-1}C_k$ in the filtered Morse chain complex associated to f . Let h_k^{p+1} and h_{k-1}^{p-r+1} be the two corresponding singularities in flow φ^r from the family Φ . By the Primary Pivots Equality Property 5.5, if $\Delta_{p-r+1,p+1}^r = \pm 1$ is a primary pivot then $\Delta_{p-r+1,p+1}^{r+1} = \pm 1$ is also a primary pivot in Smale's Cancellation Sweeping Algorithm. By the previous construction, $\Delta_{p-r+1,p+1}^{r+1}$ is an intersection number of the two consecutive singularities h_k^{p+1} and h_{k-1}^{p-r+1} of φ^r . By Smale's Cancellation Theorem, there is a dynamical cancellation of this pair of critical points.

Continuation to a minimal flow

The flow φ^r clearly continues to φ^{r+1} for all r .

The spectral sequence converges when the last algebraic cancellation occurs. By Theorems 5.5 and 5.6, this happens when the last primary pivot is swept on the SSSA and, by Theorem 5.9, the last chain complex coincides with the homology of M . By the Primary Pivots Equality Property 5.5, this corresponds to the last primary pivot in Smale's Cancellation Sweeping Algorithm, which happens after the last dynamical cancellation and the differential matrix associated to φ^ω is a null matrix. By the algebraic-dynamical correspondence, the singularities in φ^ω are in one-to-one correspondence with the nonzero modules of the spectral sequence. Consequently, φ^ω has exactly one index k singularity for each generator of the k -th homology of the last chain complex and, hence, φ^ω is the minimal flow. Thus, we constructed, via the spectral sequence, a continuation from φ_f to the minimal flow φ^ω . □

5.5.3 Higher Dimensional Cancellation Theorem

Let M be a smooth closed oriented n -dimensional manifold, $f : M \rightarrow \mathbb{R}$ be a Morse-Smale function on M and (C, Δ) be a Morse chain complex such that Δ is a TU matrix. Let (E^r, d^r) be the spectral sequence associated to (C, Δ) enriched with a finest filtration.

It was proved in Section 5.4 that the SSSA applied to Δ of an n -dimensional complex C , generates a sequence of matrices $\{\Delta^r\}$ that determines the generators of the modules E^r and the differentials d^r of the associated spectral sequence. We emphasize that these algebraic results hold without dimensional restrictions for M . Moreover, the simplified SSSA presented in Section 5.5.1 as well as Theorem 5.8, Proposition 5.5 and Theorem 5.9 also apply to n -dimensional manifolds as long as the differential Δ is a TU matrix.

This raises the question under which hypothesis dynamical results as the ones obtained in Theorem 5.10 also hold for n -dimensional manifolds. More specifically, up to what point a sequence of algebraic cancellations in (E^r, d^r) determines a sequence of dynamical cancellations in a parameterized family of flows. This question is answered for n -manifolds with $n \geq 6$ in Theorem 5.11, which was proved in Bertolim, Lima, et al. (2017).

Theorem 5.11. *Let M be a simply connected n -manifold with $n \geq 6$, $f : M \rightarrow \mathbb{R}$ be a Morse–Smale function on M and φ be the flow associated to the vector field $-\nabla f$. Consider (C, Δ) the Morse chain complex associated to f and assume that Δ is a totally unimodular matrix,*

$$\#\text{Crit}_j(f) = \begin{cases} 1, & j = 0, n \\ 0, & j = 1, n-1 \end{cases},$$

$\text{Crit}_2(f)$ contains only disconnecting critical points and $\text{Crit}_{n-2}(f)$ contains only connecting critical points. If (E^r, d^r) is the associated spectral sequence for the finest filtration $F = \{F_p C\}$ defined by f , then:

- (a) *There exists a sequence of Morse–Smale flows $\{\varphi^1 = \varphi, \varphi^2, \dots, \varphi^\omega\}$ where φ^r continues to φ^{r+1} .*
- (b) *The algebraic cancellations of the modules E^r of the spectral sequence are in one-to-one correspondence with dynamical cancellations of critical points of f .*
- (c) *The flow φ^ω is the minimal flow on M associated to a perfect Morse–Smale function.*

The proof of Theorem 5.11 requires that the regular level sets of each flow in the family is simply connected. One way to guarantee this condition is making use of Theorem 3.2 of Cruz and de Rezende (1999), which shows the effect of the attachment of a handle corresponding to a critical point of index k on the Betti numbers β_i of the boundaries on n -manifolds. Recall that an index k critical point is of type disconnecting if it increases β_k and it is of type connecting if it decreases β_{k-1} . More specifically, a connecting critical point of index 2 decreases β_1 by one and a disconnecting critical point of index $n - 2$ increases $\beta_1 = \beta_{n-2}$ by one.

The dimensional restriction, $n \geq 6$ is required to make use of the Smale’s Second Cancellation Theorem, see Theorem 6.4 of Milnor (2015). In fact, even when the intersection number between two singularities on a n -dimensional manifold, $n > 2$, is equal to ± 1 , there may be several connecting orbits between them. The Smale’s Second Cancellation Theorem guarantees that whenever the intersection number between two critical points x

and y is ± 1 , the flow can be modified locally so that the connection between x and y is a unique flow line.

For more details on the proof of this theorem, see Bertolim, Lima, et al. (2017), Theorems 1.1 and 1.2.

5.6 Other related application

The discovery of the SSSA marks the beginning of a systematic study of the dynamical implications detected by the algebraic behavior of a spectral sequence.

In proving the Paths Theorem we draw a parallel between "long flow lines" connecting consecutive singularities $h_k \in F_p$ and $h_{k-1} \in F_{p-r}$ that are far apart and higher order nonzero differentials d' in the spectral sequence. These long flow lines are paths made up of connecting orbits where some orbits are considered in the time-reversal flow.

One of the main results herein is a dynamical interpretation of the unfolding of a spectral sequence, proving the existence of a continuation of the flow where the dynamical cancellations of critical points are in one-to-one correspondence to the algebraic cancellations within the spectral sequence. This algebraic technique provides all the history of cancellations, birth and death of orbits in a continuation from the initial flow to a minimal flow on the manifold.

A natural extension of this work is a generalization of the SSSA, Theorems 5.5 and 5.6 for connection matrices associated to more general Morse decompositions, which would allow an exploration of the dynamical implications derived from the study of spectral sequences in settings with richer invariant sets such as periodic orbits and degenerate singularities. The first step in this direction was given in Section 7 of Bertolim, Lima, et al. (2016), where the authors consider a filtered Morse chain complex with an arbitrary coarser filtration. In Lima, de Rezende, and da Silveira (2023) these results were used in the exploration of dynamical implications of a spectral sequence analysis of a filtered chain complex associated to a nonsingular Morse–Smale flow on a closed orientable 3-manifold M^3 .

An interesting result that also arises from the analysis of a filtered Morse complex and the associated spectral sequence, but now considering \mathbb{Z}_2 coefficients, is presented in Franzosa, de Rezende, and da Silveira (2014). It relates the changes in generators of the modules of the spectral sequence to bifurcation behavior in the flow. As the SSSA sweeps the Morse differential, which is a special case of connection matrix (for more details see Franzosa (1986), Franzosa (1989), Salamon (1990)), it creates a family of connection matrices $\{\Delta'\}$ and transition matrices $\{T'\}$, see Franzosa and Mischaikow (1998), corresponding to the changes in generators of the modules E' of the spectral sequence. This algebraic procedure is interpreted as a continuation of the flow where the transition matrices produce information on the bifurcation behavior, see Figure 5.47.

In Franzosa, de Rezende, and da Silveira (2014), the authors introduce directed graphs called flow schematics and bifurcation schematics reflecting the bifurcations that could occur if the sequence of connection matrices and transition matrices is realized in a continua-

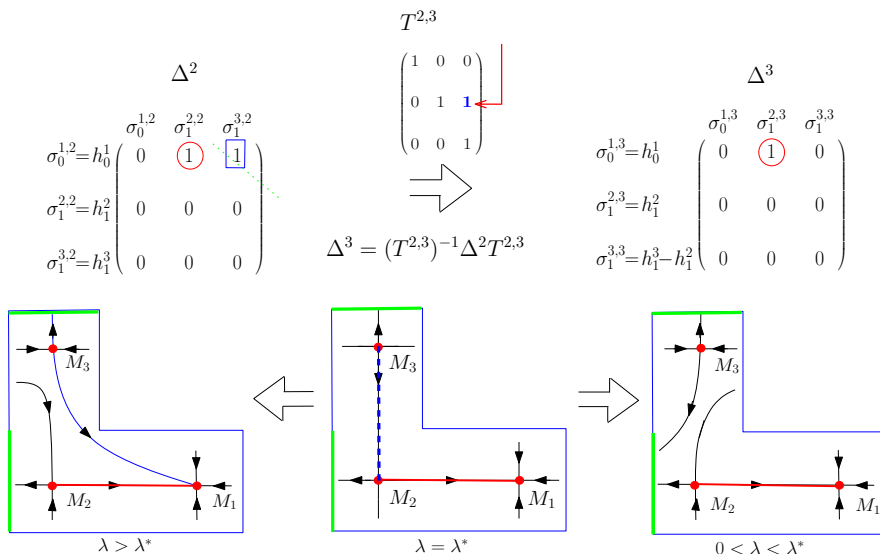


Figure 5.47: Bifurcation corresponding to changes in generators of the modules of the spectral sequence associated to the Morse complex of the initial flow.

tion of a Morse decomposition. Finally, a theorem of dynamical interpretation establishes conditions on a family of flows under which a continuation could occur.

6

Homotopical Applications for Circle Valued Morse Functions

The goal of this chapter is to demonstrate the extensive applicability of the homotopical and homological tools that have been developed in the preceding chapters. In the context of circle valued Morse functions, circular Lyapunov functions and describing the associated negative gradient flow through a chain complex, many results presented in the earlier chapters carry over. By doing so, we aim to illustrate the power and versatility of these mathematical tools and inspire their further exploration and development.

Let M be a closed smooth connected n -manifold and $f : M \rightarrow \mathbb{S}^1$ be a smooth map from M to the one-dimensional sphere¹. Since \mathbb{S}^1 is locally diffeomorphic to \mathbb{R} , then for each point x of M there exists a neighborhood V of $f(x)$ in \mathbb{S}^1 which is diffeomorphic to an open interval of \mathbb{R} . Hence, the map $f|_{f^{-1}(V)}$ is identified to a smooth map from $f^{-1}(V)$ to \mathbb{R} and, consequently, we are able to define the concepts of nondegenerate critical points, Morse index, gradient-like vector fields as in the classical case of smooth real valued function. A smooth map $f : M \rightarrow \mathbb{S}^1$ is a *circle valued Morse function* if all its critical points are nondegenerate. The set of critical points of f is denoted by $\text{Crit}(f)$ and $\text{Crit}_k(f)$ is the set of critical points of f of index k .

Consider the exponential function $\text{Exp} : \mathbb{R} \rightarrow \mathbb{S}^1$ given by $t \mapsto e^{2\pi i t}$ and the infinite cyclic covering $E : \bar{M} \rightarrow M$ induced by $f : M \rightarrow \mathbb{S}^1$ from the universal covering

¹ \mathbb{S}^1 is viewed as the submanifold $\{(x, y) \in \mathbb{R}^2 \mid x^2 + y^2 = 1\}$ and endowed with the corresponding smooth structure.

Exp . Let t be the generator of the structure group of (\overline{M}, E) . We have the following commutative diagram:

$$\begin{array}{ccc} \overline{M} & \xrightarrow{F} & \mathbb{R} \\ E \downarrow & & \downarrow \text{Exp} \\ M & \xrightarrow{f} & \mathbb{S}^1 \end{array}$$

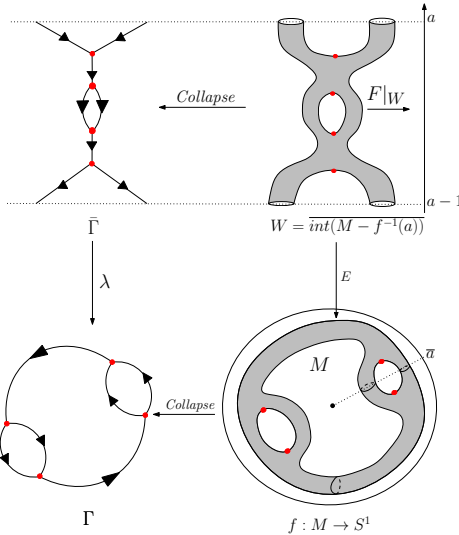
where the map $F : \overline{M} \rightarrow \mathbb{R}$ is such that $F(tx) = F(x) - 1$ for all $x \in \overline{M}$. Moreover, f is a circle valued Morse function if and only if F is a real valued Morse function. Note that if $\text{Crit}(F)$ is non empty then it has infinite cardinality. If \overline{M} is non compact, we can not make use of classical Morse theory to study F , however, if we restrict F to a fundamental cobordism W of \overline{M} , which is compact, then techniques of Morse theory can be applied. Given a regular value a of F , the *fundamental cobordism* W is defined as $W = F^{-1}([a-1, a])$. Hence, W is a cobordism with both boundary components diffeomorphic to V . The cobordism W can be viewed as the manifold M obtained by cutting along the submanifold $V = f^{-1}(\alpha)$, where $\alpha = \text{Exp}(a)$.

In Section 6.1, similar results to those in Chapter 4 on Lyapunov functions for flows on compact manifolds are presented for circle valued Lyapunov functions.

In Section 6.2, we present dynamical results obtained from the exploration of the homological description given by a chain complex associated to a circle valued Morse function using algebraic techniques similar to the ones developed in Chapter 5. We consider the case of a circular Morse function $f : M \rightarrow \mathbb{S}^1$ on a closed orientable surface M , $(\mathcal{N}_*(f), \Delta)$ and the Novikov complex associated to f , whose modules are freely generated by the critical points of f , over the ring $\mathbb{Z}((t))$ of Laurent series in one variable with integer coefficients and finite negative part. In this context we introduce an associated spectral sequence (E^r, d^r) , with the aim of exploring the changes in the generators of the modules E^r and in the differentials d^r in order to understand possible continuations of the flow given by cancellations of critical points within a family $\{f^r\}$ of circle valued Morse functions. Specifically, as we “flip through the pages” of the spectral sequence, i.e., progressively consider the modules E^r , we prove that each algebraic cancellation that occurs between two modules E^r , traced by the SSSA, corresponds to a dynamic cancellation of a pair of critical points of f^r . The unfolding of the spectral sequence and the algebraic cancellations provide a history of the birth and death of orbits in φ^r due to consecutive cancellations of critical points of f^r . Furthermore, it is possible to detect all periodic orbits that arise within the family $\{f^r\}$.

6.1 Circular Morse Graph

Our goal is to extend to the Novikov theory context, the notion of Lyapunov functions. Let ϕ be a flow on a closed manifold M and \mathcal{R} be the chain recurrent set associated to ϕ . Let $f : M \rightarrow \mathbb{S}^1$ be a C^∞ circle valued function, $a \in \mathbb{S}^1$ be a regular value of f and $W = F^{-1}([a-1, a])$ the fundamental cobordism associated to f , as shown in Figure 6.1.

Figure 6.1: W is a fundamental cobordism

In this setting, W is a compact manifold with boundary endowed with the semiflow $\Phi|_W$ which is the restriction to W of the lifting Φ of the flow ϕ . And since a is a regular value, $\Phi|_W$ is transverse to the boundary. See Ledesma, Manzoli Neto, de Rezende, and Vago (2018) for more details.

Definition 6.1. The circle valued function $f : M \rightarrow \mathbb{S}^1$ is said to be a *circular Lyapunov function* on M associated to ϕ , if

1. the image by f of each connected component of the chain recurrent set $R(\phi)$ is a constant;
2. on each fundamental cobordism W , $F|_W$ decreases along the semiorbits, that is, if $x \notin R(\Phi)$ and $\bar{x} \in E^{-1}(x)$, then $F|_W(\Phi(\bar{x}, t)) < F|_W(\Phi(\bar{x}, s))$ whenever $t > s$ and $\Phi(\{\bar{x}\} \times [s, t]) \in W$.

Definition 6.2. A circular Lyapunov function f on M is called a *finite circular Lyapunov function* if the chain recurrent set $R(\phi)$ of the flow ϕ associated to f consists of finitely many chain transitive pieces.

Let $g : M \rightarrow \mathbb{P}$, where $\mathbb{P} = \mathbb{R}$ or \mathbb{S}^1 be a continuous function. Let \sim denote the equivalence relation for points of M given by: $x \sim y$ if x and y belong to the same connected component of a level-set of f and let Γ denote the set of the associated equivalence classes. Finally, let *collapse* denote the map $M \rightarrow \Gamma$ projecting each point of M onto its equivalence class. If Γ is endowed with the quotient topology with respect to

the quotient map *collapse*, then there exists a well defined map $\hat{g} : \Gamma \rightarrow \mathbb{P}$ making the following diagram commute, in which all the appearing functions are continuous.

$$\begin{array}{ccc} M & \xrightarrow{g} & \mathbb{P} \\ \text{collapse} \downarrow & \nearrow \hat{g} & \\ \Gamma & & \end{array}$$

Let M be a compact manifold. Let $f : M \rightarrow \mathbb{S}^1$ be a finite circular Lyapunov function. Let E be a cyclic connected cover of M , Exp denote the exponential function and F be a lift of f . Denote by ϕ (resp. by Φ) the flow defined on M (resp. \overline{M}) associated to f (resp. F). Then, the following diagram is commutative

$$\begin{array}{ccccccc} F : & \overline{M} & \xrightarrow{\text{collapse}_1} & \overline{\Gamma} & \xrightarrow{\hat{F}} & \mathbb{R} & \\ & \downarrow E & & \downarrow \lambda & & \downarrow \text{Exp} & \\ f : & M & \xrightarrow{\text{collapse}_2} & \Gamma & \xrightarrow{\hat{f}} & \mathbb{S}^1 & \end{array}$$

in which Γ is a finite connected one dimensional CW complex and all the vertical maps are local homeomorphisms.

By assumption there are finitely many critical values $\{c_i\}_{i=1}^n$ where $n \geq 1$. Then again $\hat{f}^{-1}(\mathbb{S}^1 \setminus (\cup_{i=1}^n \{c_i\}))$ consists of finitely many open intervals. These intervals are contained in the future edges of Γ .

Let $A = \hat{f}^{-1}([c_i - \epsilon, c_i + \epsilon])$. Note that A is made of finitely many components and only one component A_r of A contains a critical component (of f -level c_i) containing points of $R(\phi)$. Combining this fact with the previous observations, we have that A_r is homeomorphic to a compact small neighbourhood of a vertex with finite degree $d \geq 1$, while all the other components of A consist of compact intervals (not containing any vertex). Therefore, Γ is a standard finite graph and by construction $\overline{\Gamma}$ is an infinite graph with infinitely many vertices with finite degree. In particular, for any regular F -level \bar{a} such that $\text{Exp}(\bar{a}) = a$, we have that $\hat{F}^{-1}([\bar{a} - 1, \bar{a}])$ is a graph with dangling edges, homeomorphic to $\Gamma \setminus \hat{f}^{-1}(a)$.

Definition 6.3. Using the above notation, let us provide Γ with the orientation induced by the orientation of the flow ϕ defined on M . Since f is finite circular Lyapunov function, we call Γ a *circular Lyapunov digraph* associated to the function f on M .

Finally, one enriches the information carried by a circular digraph by labelling

- each edge of the graph by the list $\{\beta_0 = 1, \beta_1, \dots, \beta_{n-2}, \beta_{n-1} = 1\}$ of the Betti numbers of the corresponding level (note that if M is orientable, then for all $j = 0, \dots, n-1$, one has, by the Poincaré duality, $\beta_j = \beta_{n-1-j}$);
- each vertex of the graph by the list $\{h_0(v), \dots, h_n(v)\}$, corresponding to numerical Conley indices of an isolated invariant set corresponding to the vertex.

The following theorem provides local and global properties of circular Lyapunov digraphs.

Theorem 6.1. *Let M be a connected, closed, smooth n -manifold. Let ϕ be a smooth flow on M with finite circular Lyapunov function $f : M \rightarrow \mathbb{S}^1$ such that f is non homotopically trivial. Let Γ be a circular Lyapunov digraph associated to f and v be a vertex in Γ . Then:*

1. (Local conditions) The number of exiting and entering edges of v , respectively denoted by $e^-(v)$ and $e^+(v)$, satisfy:
 - (a) $e^-(v) \leq h_1(v) + 1$;
 - (b) $e^+(v) \leq (h_1(v))^* + 1$ (where $*$ indicates the index of the time-reversed flow).
2. (Global conditions) $1 \leq \beta(\Gamma) \leq g(M)$,

For the complete proof of Theorem 6.1, see Ledesma, Manzoli Neto, de Rezende, and Vago (2018).

6.1.1 Circular Lyapunov digraphs for Surfaces

Let us now turn our attention to surfaces, both orientable and nonorientable, with circular Lyapunov functions. We adopt the notation $M = n\mathbb{T}^2$ to mean an orientable surface of genus n i.e., a connected sum of n tori for $n > 0$. If the surface is nonorientable of genus n we denote by $M = n\mathbb{RP}^2$, the connected sum of n projective planes. Since $\kappa \geq 1$, these are the surfaces that admit circular flows. Let v be labelled with the numerical Conley indices (h_0, h_1, h_2) and define its genus by:

$$g_v = \begin{cases} \frac{(-h_2 + h_1 - h_0 - e_v + 2)}{2} & \text{if } M \text{ is orientable} \\ -h_2 + h_1 - h_0 - e_v + 2 & \text{if } M \text{ is nonorientable} \end{cases}$$

The following theorem is a complete characterization of circular Lyapunov digraphs for surfaces. See Ledesma, Manzoli Neto, de Rezende, and Vago (ibid.) for more details and the proof.

Theorem 6.2. *Let M be a compact connected surface and Λ be a connected digraph whose vertices are labelled with $(h_0, h_1, h_2) \in \mathbb{N}^3$. Then Λ is the circular Lyapunov digraph associated with a smooth flow on M with a finite-component chain recurrent set and a circular Lyapunov function f if and only if the following conditions are satisfied.*

1. (Local conditions) The labels of all vertices v satisfy the Poincaré–Hopf inequalities:

$$e_v^+ \leq h_1 + 1, \quad e_v^- \leq h_1 + 1, \quad e_v^+ + e_v^- \leq h_1 - h_2 - h_0 + 2$$

where the latter inequality is strict if v corresponds to a chain recurrent component inside a non-orientable surface with boundary. Furthermore, if $e_v^+ = 0$ ($e_v^- = 0$), then $h_2 = 1$ ($h_0 = 1$), otherwise $h_2 = 0$ ($h_0 = 0$).

2. (Global condition) The genus of M is given by

$$\begin{cases} \beta(\Lambda) + \sum_{i=1}^V g_{v_i} & \text{if } M \text{ is orientable} \\ 2\beta(\Lambda) + \sum_{i=1}^V g_{v_i} & \text{if } M \text{ is nonorientable} \end{cases}$$

where the sums are taken over all of the V vertices of Λ .

The following is an example of a circular Lyapunov digraph and the associated smooth circular flow on a bitorus.

Example 6.1. In Figure 6.2, we have a smooth flow defined on $M = 2\mathbb{T}^2$. It has four singularities, a repelling singularity, for which $(h_0, h_1, h_2) = (0, 0, 1)$, a saddle singularity, for which $(h_0, h_1, h_2) = (0, 1, 0)$, a monkey saddle singularity, for which $(h_0, h_1, h_2) = (0, 2, 0)$, and a periodic orbit, for which $(h_0, h_1, h_2) = (0, 0, 0)$. Therefore the circular Lyapunov digraph Λ associated with the given circular Lyapunov function has four vertices v_1 , v_2 , v_3 and v_4 , corresponding to repelling singularity, saddle singularity, monkey saddle singularity and the periodic orbit, respectively, and labelled by the corresponding triple (h_0, h_1, h_2) . Each v_1 , v_2 , v_3 and v_4 have genus 0. The digraph Λ has cycle rank $\beta(\Lambda) = 2 \geq (M)$.

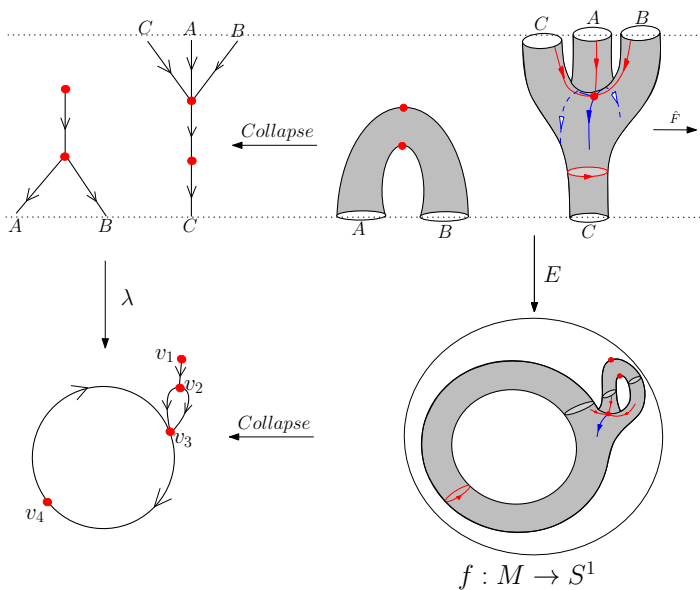


Figure 6.2: Smooth flow, circular Lyapunov function, fundamental cobordism and associated digraphs.

6.2 Global cancellation for circle valued Morse functions

Inspired by the SSSA introduced in Chapter 5 and the interesting dynamical results that arise from the application of this new homological technique, in this section we introduce the SSSA for a Novikov complex $(\mathcal{N}_*(f), \Delta)$ associated to a circle valued Morse function $f : M \rightarrow \mathbb{S}^1$.

6.2.1 Novikov chain complex

In this section, we introduce the Novikov complex for a circle valued Morse function $f : M \rightarrow \mathbb{S}^1$ on a closed connected manifold M . Further details on Novikov Theory can be found in Pajitnov (2008). Also, we prove a characterization of the Novikov differential in the case where M is an orientable surface, which is essential for both dynamical and algebraic results. The main reference herein is Lima, Manzoli Neto, de Rezende, and da Silveira (2017).

Recall that the concepts of nondegenerate critical points, Morse index, gradient-like vector fields are defined as in the classical case of smooth real valued Morse functions. Also analogously to the classical case, we assume that the circle valued Morse functions f are such that the vector field $v = -\nabla f$ satisfies the *transversality condition*, i.e., the lift of v to \overline{M} satisfies the classical transversality condition of unstable and stable manifolds. We denote by \bar{v} the lift of v to \overline{M} and arbitrarily choose orientations for all unstable manifolds $W^u(p)$ of critical points of f .

However, if $\text{Crit}(F)$ is non empty then it has infinite cardinality. Hence, if \overline{M} is not compact it is not possible to construct a Morse complex and apply the usual Morse theory to F . The way to overcome this difficulty, which we present here, is the Novikov theory, constructed by S.P. Novikov in the early 1980's. This theory associates to each circle valued Morse function $f : M \rightarrow \mathbb{S}^1$ such that the gradient v satisfies the transversality condition, the Novikov chain complex $(\mathcal{N}_*(f), \partial)$.

We start describing the ring of the coefficients of the Novikov modules. Denote by $\mathbb{Z}[t, t^{-1}]$ the Laurent polynomial ring. Let $\mathbb{Z}((t))$ be the set of all Laurent series

$$\lambda = \sum_{i \in \mathbb{Z}} a_i t^i$$

in one variable with coefficients $a_i \in \mathbb{Z}$, such that the part of λ with negative exponents is finite, i.e., there exists $n(\lambda)$ such that $a_k = 0$ if $k < n(\lambda)$. The set $\mathbb{Z}((t))$ has a natural structure of a commutative ring such that the inclusion $\mathbb{Z}[t, t^{-1}] \subset \mathbb{Z}((t))$ is a homomorphism. Moreover, by Theorem 2.4 of Pajitnov (2008), $\mathbb{Z}((t))$ is a Euclidean ring.

For each pair of critical points $p \in \text{Crit}_k(f)$ and $q \in \text{Crit}_{k-1}(f)$, the *Novikov incidence coefficient* between p and q is defined as

$$N(p, q; f) = \sum_{\ell \in \mathbb{Z}} n(p, t^\ell q; \bar{v}) t^\ell,$$

where $n(p, t^\ell q; \bar{v})$ is the intersection number between the critical points p and $t^\ell q$ of F , i.e., it is the number of the flow lines of \bar{v} from p to $t^\ell q$, counted with signs, considering the orientations on the unstable manifolds $W^u(p)$ and $W^u(t^\ell q)$, as defined in Section 5.3.

Let \mathcal{N}_k be the $\mathbb{Z}((t))$ -module freely generated by the set $\text{Crit}_k(f)$ of index k critical points of f . The k -th *Novikov boundary operator* or *Novikov differential* is the map $\partial_k : \mathcal{N}_k \rightarrow \mathcal{N}_{k-1}$, defined on a generator $p \in \text{Crit}_k(f)$ by

$$\partial_k(p) = \sum_{q \in \text{Crit}_{k-1}(f)} N(p, q; f)q$$

and extended to all chains by linearity. By Proposition 1.3 of Pajitnov (ibid.) we have that $\partial_k \circ \partial_{k+1} = 0$ and hence $(\mathcal{N}_*(f), \partial)$ is a chain complex, which is called the *Novikov complex* associated to the pair (f, v) .

The following proposition is proved in Pajitnov (ibid.), Theorem 1.8.

Proposition 6.1. *Let M be a closed manifold, $f : M \rightarrow \mathbb{S}^1$ be a circle valued Morse function and $v = -\nabla f$ satisfying the transversality condition. Then for every k we have*

$$H_k(\mathcal{N}_*(f), \partial) = H_k(\overline{M}) \bigotimes_{\mathbb{Z}[t, t^{-1}]} \mathbb{Z}((t)).$$

Fixing a set of orientations for the unstable manifolds and an ordered basis of chains corresponding to critical points of f we can associate the Novikov differential ∂ to a matrix Δ where the columns correspond to generators $p, q \in \text{Crit}(f)$ of the chains and the entries are the coefficients $N(p, q; f)$ of the Novikov differential ∂ . Without loss of generality, one assumes the chains corresponding to critical points of the basis are chosen in increasing order of their Morse indices, hence the columns of Δ are also ordered with respect to the Morse indices of the critical points and Δ is as in Figure 6.3.

$$\begin{matrix} & \mathcal{N}_0 & \cdots & \mathcal{N}_{k-1} & \mathcal{N}_k & \mathcal{N}_{k+1} & \mathcal{N}_{k+2} & \cdots & \mathcal{N}_n \\ \mathcal{N}_0 & & & & & & & & \\ \vdots & & \ddots & & & & & & \\ \mathcal{N}_{k-2} & & & & & & & & \\ & & & & \boxed{\Delta_{k-1}} & & & & \\ \mathcal{N}_{k-1} & & & 0 & & \boxed{\Delta_k} & & & 0 \\ & & & & & & & & \\ \mathcal{N}_k & & & & 0 & & \boxed{\Delta_{k+1}} & & \\ & & & & & & & & \\ \mathcal{N}_{k+1} & & & & & & 0 & & \boxed{\Delta_{k+2}} \\ & & & & & & & & \\ \vdots & & & 0 & & & & & \ddots \\ \mathcal{N}_n & & & & & & & & \end{matrix}$$

Figure 6.3: Novikov differential matrix - matricial representation of ∂ .

Example 6.2. Consider a negative gradient flow of a circle valued Morse function f defined on the torus \mathbb{T}^2 , a regular value of f , a , and the chosen orientations for the unstable manifolds of the critical points of f , as in Figure 6.4.

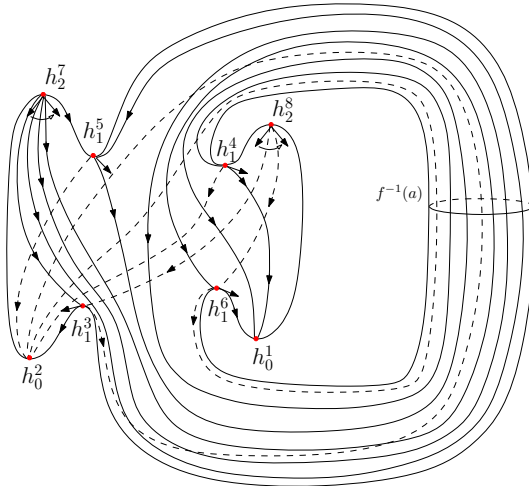


Figure 6.4: circle valued Morse function on the torus - Figure from Lima, Manzoli Neto, de Rezende, and da Silveira (2017).

The generators of \mathcal{N}_0 are $\{h_0^1, h_0^2\}$, the generators of \mathcal{N}_1 are $\{h_1^3, h_1^4, h_1^5, h_1^6\}$ and the generators of \mathcal{N}_2 are $\{h_2^7, h_2^8\}$. The Novikov differential associated to ∂ is presented in Figure 6.5.

We are interested in the case where M is an orientable surface. In this case, the nonzero entries of the matrix Δ are in block Δ_1 , which corresponds to connections from saddles to sinks, and block Δ_2 , which corresponds to connections from sources to saddles. The block Δ_1 (respectively, Δ_2) is referred to as the first block (respectively, second block) of Δ . From this point on, we use the notation Δ to denote interchangeably the Novikov differential ∂ and its matrix representation.

The following two results provide a characterization of the Novikov differential Δ when M is an orientable surface. In order prove these results, we must introduce a fundamental domain for M and f . Recall that, if \overline{M} is non compact, one can not apply classical Morse theory to study F , however, we can restrict F to a fundamental cobordism W of \overline{M} . A cobordism $W = F^{-1}([a-1; a+\lambda])$, where a is a regular value of F and $\lambda \in \mathbb{N}$, is said to be a *fundamental domain* for (M, f) if W contains a lift of each orbit of v from p to q for every pair of critical points $p \in \text{Crit}_k(f)$ and $q \in \text{Crit}_{k-1}(f)$.

Theorem 6.3. Let M be a smooth orientable closed surface, $f : M \rightarrow \mathbb{S}^1$ be a circle valued Morse function on M and $(\mathcal{N}_*(f), \Delta)$ be a Novikov complex associated to f . The

$$\begin{array}{ccccccccc}
 & h_0^1 & h_0^2 & h_1^3 & h_1^4 & h_1^5 & h_1^6 & h_2^7 & h_2^8 \\
 \begin{matrix} h_0^1 \\ h_0^2 \\ h_1^3 \\ h_1^4 \\ h_1^5 \\ h_1^6 \\ h_2^7 \\ h_2^8 \end{matrix} & \left(\begin{array}{cccccc|cc}
 0 & 0 & | & 0 & 1 & t & 1 & 0 & 0 \\
 0 & 0 & | & t-1 & -1 & -1 & -t & 0 & 0 \\
 0 & 0 & | & 0 & 0 & 0 & 0 & 1 & -1 \\
 0 & 0 & | & 0 & 0 & 0 & 0 & -t^2 & 1 \\
 0 & 0 & | & 0 & 0 & 0 & 0 & t-1 & 0 \\
 0 & 0 & | & 0 & 0 & 0 & 0 & t & -1 \\
 0 & 0 & | & 0 & 0 & 0 & 0 & 0 & 0 \\
 0 & 0 & | & 0 & 0 & 0 & 0 & 0 & 0
 \end{array} \right)
 \end{array}$$

Figure 6.5: Novikov differential.

Novikov incidence coefficient $N(p, q; f)$ is either zero, a monomial $\pm t^\ell$ or a binomial $t^{\ell_1} - t^{\ell_2}$.

Proof. The proof makes use of Theorem 5.3, however it holds only in the setting of a Morse function on a closed surface. In order to construct the necessary setting, consider a fundamental domain $W_\lambda = F^{-1}([a-1, a+\lambda])$, which is an orientable compact surface with boundary ∂W_λ . If $\partial W_\lambda = \emptyset$, we define $\tilde{W}_\lambda = W_\lambda$. Otherwise, since $\partial W_\lambda^- = F^{-1}(a-1)$ and $\partial W_\lambda^+ = F^{-1}(a+\lambda)$, we define \tilde{W}_λ as the surface obtained from W_λ by gluing a 2-dimensional disk D^2 to each connected component of ∂W_λ through the boundary of D^2 . Moreover, one can assume that each of the disks contains a unique nondegenerate singularity: a source if the disk is glued to ∂W_λ^+ and a sink if the disk is glued to ∂W_λ^- . The extension of Morse function $F : W_\lambda \rightarrow \mathbb{R}$ to the Morse function $\tilde{F} : \tilde{W}_\lambda \rightarrow \mathbb{R}$ on the closed surface \tilde{W}_λ gives us the necessary setting.

Now let p and q be critical points of f of Morse indices k and $k-1$ respectively. Since, each flow line from p to q lifts to W_λ , then $N(p, q; f)$ can be obtained by analyzing \tilde{W}_λ . By Theorem 5.3, $n(p, t^\ell q; \bar{v})$ is zero when there are two flow lines from p to $t^\ell q$ and it is -1 or $+1$, when there is one flow line from p to $t^\ell q$. Hence the Novikov incidence coefficient $N(p, q; f)$ is either 0, if there are two flow lines between p and q in v intersecting $f^{-1}(a)$ the same number of times, it is $\pm t^\ell$, if there is only one flow line between p and q intersecting ℓ times $f^{-1}(a)$ or $t^{\ell_1} - t^{\ell_2}$, if there are two flow lines between p and q in v , one intersecting ℓ_1 times and the other intersecting ℓ_2 times $f^{-1}(a)$. \square

Corollary 6.1. (Characterization of the Novikov differential) Let M be a smooth orientable closed surface, $f : M \rightarrow \mathbb{S}^1$ be a circle valued Morse function and $(\mathcal{N}_*(f), \Delta)$ be the associated Novikov complex. Suppose that the orientation on the unstable manifold of all critical points of index 2 are chosen consistently. Then there are three possibilities

for either a column or a row of Δ corresponding to a 1-chain:

- (1) all entries are zero.
- (2) there is exactly one nonzero entry, which is a binomial $t^{\ell_1} - t^{\ell_2}$, $\ell_1, \ell_2 \in \mathbb{Z}$.
- (3) there are exactly two nonzero entries, which are monomials t^{ℓ_1} and $-t^{\ell_2}$, $\ell_1, \ell_2 \in \mathbb{Z}$.
- (4) there is exactly one nonzero entry, which is a monomial t^ℓ , $\ell \in \mathbb{Z}$.

Proof. Suppose f has at least one critical point h_1^j of index 1 and suppose its corresponding chain is the j -th element in the chosen ordered basis. Hence, there are exactly two flow lines whose ω -limit (respectively, α -limit) sets are this saddle. Since orientations on the unstable manifolds of all critical points of index 2 are chosen consistently, the flow lines associated to this stable manifold (respectively, unstable manifold) of a saddle have opposite characteristic signs. Consequently, there are at most two nonzero entries in row j (respectively, column j). It follows that:

1. If there are two flow lines between the saddle h_1^j and a sink h_0^i intersecting a regular level set $f^{-1}(a)$ ℓ times, then $N(h_1^j, h_0^i; f) = t^\ell - t^\ell = 0$. Analogously, if there are two flow lines between a source $h_2^{i'}$ and the saddle h_1^j intersecting a regular level set $f^{-1}(a)$ ℓ times, then $N(h_2^{i'}, h_1^j; f) = 0$.
2. If there is one flow line between the saddle h_1^j and a sink h_0^i intersecting $f^{-1}(a)$ ℓ_1 times, and one flow line between h_1^j and a sink $h_0^{i'}$ intersecting $f^{-1}(a)$ ℓ_2 times then:
 - $N(h_1^j, h_0^i; f) = \pm t^{\ell_1}$ and $N(h_1^j, h_0^{i'}; f) = \mp t^{\ell_2}$ if $i \neq i'$;
 - $N(h_1^j, h_0^i; f) = \pm t^{\ell_1} \mp t^{\ell_2}$ if $i = i'$.

Analogously, if there is one flow line between a source $h_2^{i'}$ and the saddle h_1^j intersecting $f^{-1}(a)$ ℓ_1 times, and one flow line between a source $h_2^{i'}$ and the saddle h_1^j intersecting $f^{-1}(a)$ ℓ_2 times then:

- $N(h_2^{i'}, h_1^j; f) = \pm t^{\ell_1}$ and $N(h_2^{i'}, h_1^j; f) = \mp t^{\ell_2}$ if $i \neq i'$;
- $N(h_2^{i'}, h_1^j; f) = \pm t^{\ell_1} \mp t^{\ell_2}$ if $i = i'$.

3. Finally,

- if there is one flow line between the saddle h_1^j and a sink h_0^i intersecting $f^{-1}(a)$ ℓ times, and one flow line between h_1^j and an attractor periodic orbit, then $N(h_1^j, h_0^i; f) = \pm t^\ell$;

- if there is one flow line between a source h_2^i and the saddle h_1^j intersecting $f^{-1}(a)$ ℓ times, and one flow line between h_1^j and a repeller periodic orbit, then $N(h_2^i, h_1^j; f) = \pm t^\ell$.

□

6.2.2 Spectral Sequence Sweeping Algorithm for a Novikov Complex

Let M be a closed orientable surface, f be a circle valued Morse function on M , $(\mathcal{N}_*(f), \Delta)$ be a Novikov complex and $\mathcal{F} = \{\mathcal{F}_p \mathcal{N}\}$ be a filtration on this complex defined by

$$\mathcal{F}_p \mathcal{N} = \mathbb{Z}((t)) \left[h_{k_1}^1, h_{k_2}^2, \dots, h_{k_{p+1}}^{p+1} \right]. \quad (6.1)$$

The filtration F is clearly a finest filtration. Since F is bounded below and convergent, by Theorem 5.1 there exists a convergent spectral sequence with

$$E_{p,q}^0 = \mathcal{F}_p \mathcal{N}_{p+q} / \mathcal{F}_{p-1} \mathcal{N}_{p+q} = G(\mathcal{N})_{p,q},$$

$$E_{p,q}^1 \cong H_{(p+q)}(\mathcal{F}_p \mathcal{N}_{p+q} / \mathcal{F}_{p-1} \mathcal{N}_{p+q}),$$

$$E_{p,q}^\infty \cong GH_*(\mathcal{N})_{p,q} = \frac{F_p H_{p+q}(\mathcal{N})}{F_{p-1} H_{p+q}(\mathcal{N})}$$

and, for all $r \geq 0$,

$$E_{p,q}^r = Z_{p,q}^r / (Z_{p-1,q+1}^{r-1} + \partial Z_{p+r-1,q-r+2}^{r-1}),$$

where

$$Z_{p,q}^r = \{c \in \mathcal{F}_p \mathcal{N}_{p+q} \mid \partial c \in \mathcal{F}_{p-r} \mathcal{N}_{p+q-1}\}.$$

A square matrix is called a *Novikov matrix* if it is a strictly upper triangular matrix with square zero and entries in the ring $\mathbb{Z}((t))$. In particular, a Novikov differential is a Novikov matrix.

Inspired by the SSSA defined in Section 5.4, in this section, we introduce the SSSA for a Novikov differential associated to a Novikov complex $(\mathcal{N}_*(f), \Delta)$ on an orientable surface. The SSSA has as its output a family of Novikov matrices $\{\Delta^r, r \geq 0\}$ recursively constructed, where $\Delta^0 = \Delta$ and Δ^{r+1} is obtained from Δ^r through a change of basis determined by the pivots on the r -th diagonal of Δ^r .

Spectral Sequence Sweeping Algorithm for a Novikov matrix

As in Section 5.4, for each r -th diagonal, the method described below must be applied for all Δ_k , $k = 0, 1, 2$ simultaneously. Steps A and B.2, which are responsible for marking pivots are identical to the SSSA for a Morse differential. Step C is also performed

identically. However, since the entries on a Novikov matrix are in $\mathbb{Z}((t))$, Step B.1, which is when the algorithm performs the changes of basis, must be different.

B.1 - Change of basis - SSSA for Novikov Matrices

In this step we consider a matrix Δ^r with the primary and change-of-basis pivots marked on the ξ -th diagonal for all $\xi \leq r$. This step describes how the entries of Δ^{r+1} are determined.

Suppose $\Delta_{i,j}^r$ is a change-of-basis pivot on the r -th diagonal. Since there is a change-of-basis pivot in row i , then there must be a column, namely u -th column, associated to a k -chain such that $u < j$ and $\Delta_{i,u}^r$ is a primary pivot. Then, perform a change of basis in Δ^r in order to zero out the entry $\Delta_{i,j}^r$ without introducing nonzero entries in $\Delta_{s,j}^r$ for $s > i$. We prove in Theorem 6.4 that all the entries in Δ^r which are marked as primary pivots are equal to $\pm t^{l_1} \pm t^{l_2}$ which are invertible in $\mathbb{Z}((t))$.

Denote by k_1 the first column of Δ^r associated to a k -chain and by $\sigma_k^{j,r}$ the k -chain corresponding to column j of Δ^r . Then

$$\sigma_k^{j,r} = \sum_{\ell=k_1}^j c_\ell^{j,r} h_k^\ell,$$

and column j of Δ^{r+1} corresponds to

$$\sigma_k^{j,r+1} = \sigma_k^{j,r} - \Delta_{i,j}^r (\Delta_{i,u}^r)^{-1} \sigma_k^{u,r} = c_{k_1}^{j,r+1} h_k^{k_1} + \cdots + c_{j-1}^{j,r+1} h_k^{j-1} + c_j^{j,r+1} h_k^j \quad (6.2)$$

where $c_\ell^{j,r+1} \in \mathbb{Z}((t))$ and $c_j^{j,r+1} = 1$.

After the change of basis is performed, the k -chain associated to column j of Δ^{r+1} is a linear combination over $\mathbb{Z}((t))$ of columns u and j of Δ^r such that $\Delta_{i,j}^{r+1} = 0$ and $\Delta_{s,j}^{r+1} = 0$ for $s > i$.

Note that, in the SSSA, the columns of the matrix Δ are not necessarily ordered with respect to k . In this section, without loss of generality, we consider the singularities to be ordered with respect to the Morse index for the sole reason of simplifying notation.

In order to perform the change of basis (6.2) in step B.1 of the SSSA, recall that the primary pivots must be invertible polynomials in the ring $\mathbb{Z}((t))$. Otherwise, the change of basis in (6.2) would not be well defined.

The next lemma is an important property of the matrices produced by the SSSA. It asserts that there cannot be more than one primary pivot in a fixed row or column. Moreover, if there is a primary pivot in row i , then there is no primary pivot in column i and vice versa. Its proof is consequence of the SSSA rules and very similar in nature to proof of Proposition 5.2(1), which can be found in Cornea, de Rezende, and da Silveira (2010).

$$\sigma_0^{1,1} = h_0^1 \left(\begin{array}{ccccccccc} \sigma_0^{1,1} & \sigma_0^{2,1} & \sigma_1^{3,1} & \sigma_1^{4,1} & \sigma_1^{5,1} & \sigma_1^{6,1} & \sigma_2^{7,1} & \sigma_2^{8,1} \\ 0 & 0 & 0 & 1 & t & 1 & 0 & 0 \\ 0 & 0 & t-1 & -1 & -1 & -t & 0 & 0 \\ 0 & 0 & 0 & 0 & 0 & 0 & 1 & -1 \\ 0 & 0 & 0 & 0 & 0 & 0 & -t^2 & 1 \\ 0 & 0 & 0 & 0 & 0 & 0 & t-1 & 0 \\ 0 & 0 & 0 & 0 & 0 & 0 & 0 & -1 \\ 0 & 0 & 0 & 0 & 0 & 0 & 0 & 0 \end{array} \right)$$

Figure 6.6: Δ^1 .

$$\sigma_0^{1,2} = h_0^1 \left(\begin{array}{ccccccccc} \sigma_0^{1,2} & \sigma_0^{2,2} & \sigma_1^{3,2} & \sigma_1^{4,2} & \sigma_1^{5,2} & \sigma_1^{6,2} & \sigma_2^{7,2} & \sigma_2^{8,2} \\ 0 & 0 & 0 & 1 & t & 1 & 0 & 0 \\ 0 & 0 & t-1 & -1 & -1 & -t & 0 & 0 \\ 0 & 0 & 0 & 0 & 0 & 0 & 1 & -1 \\ 0 & 0 & 0 & 0 & 0 & 0 & -t^2 & 1 \\ 0 & 0 & 0 & 0 & 0 & 0 & t-1 & 0 \\ 0 & 0 & 0 & 0 & 0 & 0 & 0 & -1 \\ 0 & 0 & 0 & 0 & 0 & 0 & 0 & 0 \end{array} \right)$$

Figure 6.7: Δ^2 .

Lemma 6.1. Let Δ be a Novikov differential for which the SSSA is proved correct up to step R . Let $\Delta^1, \dots, \Delta^R$ be the family of Novikov matrices produced by the SSSA until step R . If $\Delta_{i,j}^r$ and $\Delta_{m,l}^r$ are two primary pivots, then $\{i, j\} \cap \{m, l\} = \emptyset$.

Example 6.3. Consider a flow on the torus \mathbb{T}^2 given in Example 6.2. The Novikov differential Δ is presented in Figure 6.5. The SSSA applied to Δ determines the sequence of Novikov matrices $\Delta^1, \dots, \Delta^6$ illustrated in Figures 6.6 to 6.11

Characterization of the Novikov Matrices

The main goal of this section is to prove that the SSSA applied to a Novikov differential of a 2-dimensional orientable smooth manifold is correct, i.e. the changes of basis can always be chosen as in Step B.1 of the SSSA for Novikov matrices. This is done by

$$\left(\begin{array}{ccccccccc} \sigma_0^{1,3} & \sigma_0^{2,3} & \sigma_1^{3,3} & \sigma_1^{4,3} & \sigma_1^{5,3} & \sigma_1^{6,3} & \sigma_2^{7,3} & \sigma_2^{8,3} \\ \sigma_0^{1,3} = h_0^1 & 0 & 0 & 1 & t & 1 & 0 & 0 \\ \sigma_0^{2,3} = h_0^2 & 0 & 0 & t-1 & 0 & -1 & 0 & 0 \\ \sigma_1^{3,3} = h_0^3 & 0 & 0 & 0 & 0 & 0 & 0 & t^{-1} \\ \sigma_1^{4,3} = h_1^4 + (t-1)^{-1}h_1^3 & 0 & 0 & 0 & 0 & 0 & 0 & t^2 - 1 + 1-t \\ \sigma_1^{5,3} = h_1^5 & 0 & 0 & 0 & 0 & 0 & t-1 & (t-1)t^{-1} \\ \sigma_1^{6,3} = h_1^6 & 0 & 0 & 0 & 0 & 0 & 0 & t \\ \sigma_2^{7,3} = h_1^7 & 0 & 0 & 0 & 0 & 0 & 0 & 0 \\ \sigma_2^{8,3} = h_2^8 + t^{-1}h_2^7 & 0 & 0 & 0 & 0 & 0 & 0 & 0 \end{array} \right)$$

Figure 6.8: Δ^3 .

$$\left(\begin{array}{ccccccccc} \sigma_0^{1,4} & \sigma_0^{2,4} & \sigma_1^{3,4} & \sigma_1^{4,4} & \sigma_1^{5,4} & \sigma_1^{6,4} & \sigma_2^{7,4} & \sigma_2^{8,4} \\ \sigma_0^{1,4} = h_0^1 & 0 & 0 & 1 & t & 1 & 0 & 0 \\ \sigma_0^{2,4} = h_0^2 & 0 & 0 & t-1 & 0 & 0 & 0 & 0 \\ \sigma_1^{3,4} = h_1^3 & 0 & 0 & 0 & 0 & 0 & 0 & t^2 - 1 \\ \sigma_1^{4,4} = h_1^4 + (t-1)^{-1}h_1^3 & 0 & 0 & 0 & 0 & 0 & -t^2 & 1-t \\ \sigma_1^{5,4} = h_1^5 + (t-1)^{-1}h_1^3 & 0 & 0 & 0 & 0 & 0 & t-1 & (t-1)t^{-1} \\ \sigma_1^{6,4} = h_1^6 & 0 & 0 & 0 & 0 & 0 & 0 & t \\ \sigma_2^{7,4} = h_2^7 & 0 & 0 & 0 & 0 & 0 & 0 & 0 \\ \sigma_2^{8,4} = h_2^8 + t^{-1}h_2^7 & 0 & 0 & 0 & 0 & 0 & 0 & 0 \end{array} \right)$$

Figure 6.9: Δ^4 .

$$\left(\begin{array}{ccccccccc} \sigma_0^{1,5} & \sigma_0^{2,5} & \sigma_1^{3,5} & \sigma_1^{4,5} & \sigma_1^{5,5} & \sigma_1^{6,5} & \sigma_2^{7,5} & \sigma_2^{8,5} \\ \sigma_0^{1,5} = h_0^1 & 0 & 0 & 1 & 0 & 0 & 0 & 0 \\ \sigma_0^{2,5} = h_0^2 & 0 & 0 & t-1 & 0 & 0 & 0 & 0 \\ \sigma_1^{3,5} = h_0^1 & 0 & 0 & 0 & 0 & 0 & 0 & 0 \\ \sigma_1^{4,5} = h_1^4 + (t-1)^{-1}h_1^3 & 0 & 0 & 0 & 0 & 0 & 0 & 0 \\ \sigma_1^{5,5} = h_1^5 - t h_1^4 & 0 & 0 & 0 & 0 & 0 & t-1 & (t-1)t^{-1} \\ \sigma_1^{6,5} = h_1^6 + t(t-1)^{-1}h_1^3 & 0 & 0 & 0 & 0 & 0 & 0 & t \\ \sigma_2^{7,5} = h_2^7 & 0 & 0 & 0 & 0 & 0 & 0 & 0 \\ \sigma_2^{8,5} = h_2^8 + t^{-1}h_2^7 & 0 & 0 & 0 & 0 & 0 & 0 & 0 \end{array} \right)$$

Figure 6.10: Δ^5 .

$$\begin{array}{ccccccccc}
 & \sigma_0^{1,6} & \sigma_0^{2,6} & \sigma_1^{3,6} & \sigma_1^{4,6} & \sigma_1^{5,6} & \sigma_1^{6,6} & \sigma_2^{7,6} & \sigma_2^{8,6} \\
 \sigma_0^{1,6} = h_0^1 & 0 & 0 & | & 0 & | & 0 & 0 & 0 \\
 \sigma_0^{2,6} = h_0^2 & 0 & 0 & | & t-1 & 0 & 0 & 0 & 0 \\
 \sigma_1^{3,6} = h_1^3 & 0 & 0 & | & 0 & 0 & 0 & 0 & 0 \\
 \sigma_1^{4,6} = h_1^4 + (t-1)^{-1} h_1^3 & 0 & 0 & | & 0 & 0 & 0 & 0 & 0 \\
 \sigma_1^{5,6} = h_1^5 - t h_1^4 & 0 & 0 & | & 0 & 0 & 0 & t-1 & (t-1)t^{-1} \\
 \sigma_1^{6,6} = h_1^6 - h_1^4 & 0 & 0 & | & 0 & 0 & 0 & t & 0 \\
 \sigma_2^{7,6} = h_2^7 & 0 & 0 & | & 0 & 0 & 0 & 0 & 0 \\
 \sigma_2^{8,6} = h_2^8 + t^{-1} h_2^7 & 0 & 0 & | & 0 & 0 & 0 & 0 & 0
 \end{array}$$

Figure 6.11: Δ^6 .

proving Theorem 6.4, which asserts that given a Novikov differential Δ , all primary pivots determined by the SSSA are invertible polynomials in the ring $\mathbb{Z}((t))$. In fact, they are monomials with coefficient ± 1 or binomials with coefficients ± 1 . The terms monomial and binomial are be used when we refer to polynomials in $\mathbb{Z}((t))$ of the form $\pm t^\ell$ and $t^{\ell_1} - t^{\ell_2}$, respectively, where $\ell, \ell_1, \ell_2 \in \mathbb{Z}$.

Theorem 6.4. *Let M be a smooth closed orientable 2-dimensional manifold, $f : M \rightarrow \mathbb{S}^1$ be a circle valued Morse function and $(N_*(f), \Delta)$ a Novikov chain complex with a finest filtration. Then the primary pivots and the change-of-basis pivots marked by the SSSA are either monomials t^ℓ or binomials of the form $t^{\ell_1} - t^{\ell_2}$, where $\ell, \ell_1, \ell_2 \in \mathbb{Z}$.*

The proof of Theorem 6.4 is established combining the characterization of the columns of the first block of the matrices Δ^r , obtained in Theorem 6.5, and the characterization of the rows of the second block, obtained in Theorem 6.6.

Theorem 6.5 (First Block Characterization). *Let Δ be a Novikov differential for which the SSSA is proved correct up to step R. Then we have the following possibilities for an h_1 -column j of the matrix Δ^r and $r \leq R$:*

1. *all the entries in column j are equal to zero;*
2. *there is only one nonzero entry in column j and it is a binomial $t^\ell - t^{\tilde{\ell}}$, where $\ell, \tilde{\ell} \in \mathbb{Z}$;*
3. *there are exactly two nonzero entries in column j and they are monomials t^ℓ and $-t^{\tilde{\ell}}$, where $\ell, \tilde{\ell} \in \mathbb{Z}$;*
4. *there is only one nonzero entry in column j and it is a monomial t^ℓ , where $\ell \in \mathbb{Z}$.*

Proof. The proof is done by induction in r . It follows from the characterization of the columns of Δ proved in Corollary 6.1 that columns of Δ^1 are of types 1, 2, 3 or 4. Assuming that the conclusion of the theorem holds for $r < R$, we prove that it also holds for $r + 1$.

Without loss of generality, suppose there is a change-of-basis pivot $\Delta_{i,j}^r$ in the r -th diagonal. Then there must be a primary pivot $\Delta_{i,u}^r$ in a column $u < j$. By the induction hypothesis, column u of Δ^r can be of types 2, 3 or 4 and for each one of these cases column j can be of types 2, 3 or 4. We must analyze column j of Δ^{r+1} for each one of these cases.

Suppose column u is of type 2 (resp., type 4). The only nonzero entry in column u is the primary pivot $\Delta_{i,u}^r$ which is a binomial (resp., monomial). In this case, $\Delta_{i,j}^{r+1} = 0$ and all the other entries in column $r + 1$ remain the same. Consequently, if column j of Δ^r is of type 2 or 4 then column j of Δ^{r+1} is of type 1. Moreover if column j of Δ^r is of type 3 then column j of Δ^{r+1} is of type 4.

Now suppose column u is of type 3. Then $\Delta_{i,u}^r$ is a monomial and there is $s < i$ such that $\Delta_{s,u}^r$ is also a monomial.

- If column j is of type 2 or 4, then $\Delta_{i,j}^{r+1} = 0$ and $\Delta_{s,j}^{r+1} = -\Delta_{s,u}^r(\Delta_{i,u}^r)^{-1}\Delta_{i,j}^r$. Hence, column j remains of the same type. In Figure 6.12 we show part of the block (rows i and s , for the case where column j is of type 4) as the r -th diagonal is swept.

$$\begin{array}{ccc} \begin{matrix} u & & j \\ \vdots & & \vdots \\ \cdots & t^l & \cdots & 0 & \cdots \\ \vdots & \ddots & \vdots & & \\ \cdots & \textcolor{red}{t^\ell} & \cdots & \boxed{-t^{\tilde{\ell}}} & \cdots \\ \vdots & & \vdots & & \end{matrix} & \xrightarrow{\text{SSSA}} & \begin{matrix} u & & j \\ \vdots & & \vdots \\ \cdots & t^l & \cdots & t^{\tilde{\ell}-\ell+l} & \cdots \\ \vdots & \ddots & \vdots & & \\ \cdots & \textcolor{red}{t^\ell} & \cdots & 0 & \cdots \\ \vdots & & \vdots & & \end{matrix} \end{array}$$

Figure 6.12: Δ_k^r and Δ_k^{r+1} , respectively.

- If the column j is of type 3, then the change-of-basis pivot $\Delta_{i,j}^r$ is a monomial and there exists $\bar{s} < i$ such that $\Delta_{s,j}^r$ is also a monomial. If $s = \bar{s}$, then $\Delta_{i,j}^{r+1} = 0$ and $\Delta_{s,j}^{r+1} = \Delta_{s,j}^r - \Delta_{s,u}^r(\Delta_{i,u}^r)^{-1}\Delta_{i,j}^r$, which is either a binomial or zero. See Figure 6.13, where we represent part of the block, as the r -th diagonal is swept.

Hence, column j turns into a column of type 2 or 1, respectively. On the other hand, if $s \neq \bar{s}$, then $\Delta_{i,j}^{r+1} = 0$, $\Delta_{s,j}^{r+1} = -\Delta_{s,u}^r(\Delta_{i,u}^r)^{-1}\Delta_{i,j}^r$, which is a monomial, and the other entries of column j remain the same. Hence, column j remains of type 3.

□

The first step to prove Theorem 6.6 is established in the next lemma, which asserts that

$$\begin{array}{ccc}
 & u & j \\
 & \vdots & \vdots \\
 s & \cdots & -t^l & \cdots & t^{\tilde{l}} & \cdots \\
 & \vdots & \ddots & \vdots & & \\
 i & \cdots & \textcolor{red}{t^\ell} & \cdots & \boxed{-t^\ell} & \cdots \\
 & \vdots & & \vdots & &
 \end{array} \xrightarrow{\text{SSSA}} \begin{array}{ccc}
 & u & j \\
 & \vdots & \vdots \\
 s & \cdots & -t^l & \cdots & t^{\tilde{l}} - t^{\tilde{l}-\ell+1} & \cdots \\
 & \vdots & \ddots & \vdots & & \\
 i & \cdots & \textcolor{red}{t^\ell} & \cdots & 0 & \cdots \\
 & \vdots & & \vdots & &
 \end{array}$$

Figure 6.13: Δ^r and Δ^{r+1} , respectively.

the changes of basis caused by change-of-basis pivots in block Δ_1 do not affect the pivots in block Δ_2 .

Lemma 6.2. *Let Δ be a Novikov differential and suppose the SSSA is proved correct up to step R . For all $r \leq R$, let T^r be the change-of-basis matrix such that $\Delta^{r+1} = (T^r)^{-1} \Delta^r T^r$. Then the multiplication by $(T^r)^{-1}$ does not change the primary and change-of-basis pivots in block Δ_2 .*

Proof. We prove the result for the particular case where we have a unique change-of-basis pivot on the r -th diagonal in the first block of Δ^r , namely $\Delta_{i,j}^r$. The general case is an easy consequence of this, repeating the same argument for all change-of-basis pivots in the first block of Δ^r .

Let $\Delta_{i,u}^r$ be the primary pivot in row i . The entries on the principal diagonal of T^r are all 1's and the only nonzero entry off the principal diagonal is $T_{u,j}^r = -\Delta_{i,j}^r (\Delta_{i,u}^r)^{-1}$. Consequently, the principal diagonal of $(T^r)^{-1}$ has its entries all equal to 1's and the only nonzero entry off the principal diagonal is $(T^r)_{u,j}^{-1} = -T_{u,j}^r = \Delta_{i,j}^r (\Delta_{i,u}^r)^{-1}$. Therefore, multiplying Δ^r by $(T^r)^{-1}$ only affects row u of Δ^r . By Lemma 6.1, there are no primary pivots in row u and, consequently, there are no change-of-basis pivot in row u . \square

As a consequence of Lemma 6.2, the SSSA can be applied separately in blocks Δ_1 and Δ_2 . Moreover, except mentioned otherwise, we consider the changes of basis on the SSSA without performing the pre-multiplication by $(T^r)^{-1}$.

In what follows we introduce some notation and terminology which is used from now on. Let $\Delta_{i,j}^r$ be a change-of-basis pivot in row i caused by a primary pivot $\Delta_{i,u}^r$, i.e. in step $(r+1)$, one has

$$\sigma_k^{j,r+1} = \sigma_k^{j,r} - \Delta_{i,j}^r (\Delta_{i,u}^r)^{-1} \sigma_k^{u,r}.$$

Note that the only modified column of the matrix Δ^r is column j , where for each $s = 0, \dots, i$, the entry $\Delta_{s,j}^r$ is added to a multiple of the entry $\Delta_{s,u}^r$. In other words, $\Delta_{s,j}^{r+1} = \Delta_{s,j}^r - \Delta_{i,j}^r (\Delta_{i,u}^r)^{-1} \Delta_{s,u}^r$. Figure 6.14 shows columns u and j of the block Δ_k as the r -th diagonal is swept.

$$s \begin{pmatrix} u & & j \\ \vdots & & \vdots \\ \cdots & \Delta_{s,u}^r & \cdots & \Delta_{s,j}^r & \cdots \\ & \ddots & \ddots & \ddots & \vdots \\ i & \cdots & \boxed{\Delta_{i,u}^r} & \cdots & \boxed{\Delta_{i,j}^r} & \cdots \\ \vdots & & & & \vdots & \end{pmatrix}$$

Figure 6.14: Δ_k^r with marked change-of-basis pivot.

In the situation described above, we say that the entry $\Delta_{s,u}^r$ in column u generates² the entry $\Delta_{s,j}^{r+1}$ in column j in Δ^{r+1} , whenever $\Delta_{s,u}^r \neq 0$. Note that if an entry in column u generates an entry in column j then we must have $j > u$, i.e. $\Delta_{s,u}^r$ generates entries in columns on the right of column u .

In order to clarify this new terminology we give some examples of configurations where an entry $\Delta_{s,u}^r \neq 0$ generates an entry $\Delta_{s,j}^{r+1}$. Suppose that $\Delta_{i,u}^r = t^\ell$ and $\Delta_{i,j}^r = -t^{\tilde{\ell}}$. Then some of the possibilities for the entries in positions (s, u) and (s, j) of Δ^r are:

- (i) $\Delta_{s,u}^r = -t^\ell$ and $\Delta_{s,j}^r = t^{\tilde{\ell}}$. In this case, $\Delta_{s,j}^{r+1} = \Delta_{s,j}^r - \Delta_{i,j}^r (\Delta_{i,u}^r)^{-1} \Delta_{s,u}^r = t^{\tilde{\ell}} - t^{\tilde{\ell}} t^{-\ell} t^\ell$, see Figure 6.13.
- (ii) $\Delta_{s,u}^r = t^\ell$ and $\Delta_{s,j}^r = 0$. In this case, $\Delta_{s,j}^{r+1} = \Delta_{s,j}^r - \Delta_{i,j}^r (\Delta_{i,u}^r)^{-1} \Delta_{s,u}^r = t^{\tilde{\ell}} t^{-\ell} (t^\ell - t^{\tilde{\ell}})$, see Figure 6.12.
- (iii) $\Delta_{s,u}^r = t^\ell - t^{\tilde{\ell}}$ and $\Delta_{s,j}^r = 0$. In this case, $\Delta_{s,j}^{r+1} = \Delta_{s,j}^r - \Delta_{i,j}^r (\Delta_{i,u}^r)^{-1} \Delta_{s,u}^r = t^{\tilde{\ell}} t^{-\ell} (t^\ell - t^{\tilde{\ell}})$, see Figure 6.15.

$$s \begin{pmatrix} u & & j \\ \vdots & & \vdots \\ \cdots & t^\ell - t^{\tilde{\ell}} & \cdots & 0 & \cdots \\ & \ddots & \ddots & \vdots & \vdots \\ i & \cdots & \boxed{t^\ell} & \cdots & \boxed{-t^{\tilde{\ell}}} & \cdots \\ \vdots & & & & & \end{pmatrix} \xrightarrow{\text{SSSA}} s \begin{pmatrix} u & & j \\ \vdots & & \vdots \\ \cdots & t^\ell - t^{\tilde{\ell}} & \cdots & t^{\tilde{\ell}-\ell+l} - t^{\tilde{\ell}-\ell+\tilde{\ell}} & \cdots \\ & \ddots & \ddots & \vdots & \vdots \\ i & \cdots & \boxed{t^\ell} & \cdots & 0 & \cdots \\ \vdots & & & & & \vdots \end{pmatrix}$$

Figure 6.15: Δ^r and Δ^{r+1} , respectively.

We prove later on that, as a consequence of Theorem 6.6, cases (i), (ii), (iii) above are the only possibilities up to sign of generating entries by a change of basis in block Δ_2 . In block Δ_1 , as we have seen, there are more possibilities.

²If an entry $\Delta_{s,u}^\xi$ with $\xi < r$ does not change until step r , i.e. $\Delta_{s,u}^\xi = \Delta_{s,u}^{\xi+1} = \dots = \Delta_{s,u}^r$, and $\Delta_{s,u}^r$ generates $\Delta_{s,j}^{r+1}$, we say that $\Delta_{s,u}^\xi$ generates $\Delta_{s,j}^{r+1}$.

Note that if an entry $\Delta_{s,u}^r$ generates an entry in Δ^{r+1} , then there must be a primary pivot in column u and row $i > s$, which was marked in step $\xi < r$. Hence, $\Delta_{s,u}^r$ can not be marked as a pivot in any given step r . We have proved the following result.

Lemma 6.3. *An entry which is or will be marked as a primary or a change-of-basis pivot never generates entries.*

Let Δ be a Novikov differential.

- (a) When an entry $\Delta_{s,u}^r$ generates another one $\Delta_{s,j}^{r+1}$, we say that $\Delta_{s,j}^{r+1}$ is an *immediate successor* of $\Delta_{s,u}^r$.
- (b) A sequence of entries $\{\Delta_{s,j_0}^{\xi_0}, \Delta_{s,j_2}^{\xi_2}, \dots, \Delta_{s,j_f}^{\xi_f}\}$ such that each entry is an immediate successor of the previous one is called a *generation sequence*.
- (c) Given an entry $\Delta_{s,u}^\xi$ of Δ^ξ , the $\Delta_{s,u}^\xi$ -lineage is defined to be the set of all generation sequences whose first element is $\Delta_{s,u}^\xi$.

We say that all the elements in these sequences are in the same lineage or that they are in $\Delta_{s,u}^\xi$ -lineage. Also, an element of a generation sequence is said to be successor of every element of this sequence which is to its left.

Lemma 6.4. *Let Δ be a Novikov differential for which the SSSA is proved correct up to step R . Suppose that the second block of Δ has the property that at most one change-of-basis pivot is marked in each row from the beginning until the end of the SSSA. Therefore, each lineage of an entry in Δ_2 is formed by a unique generation sequence.*

Proof. Since the SSSA applied to the first block of Δ does not interfere in the number of change-of-basis pivots identified in the second block, we assume that the only nonzero entries in Δ are in Δ_2 . By Lemma 6.1 and since each row has at most one change-of-basis pivot, then an entry $\Delta_{s,u}^\xi$ generates at most one immediate successor and this successor generates at most one immediate successor. Thus, $\Delta_{s,u}^\xi$ -lineage is represented in one finite sequence: $\{\Delta_{s,u_0}^{\xi_0}, \Delta_{s,u_1}^{\xi_1}, \Delta_{s,u_2}^{\xi_2}, \dots\}$, where $2 \leq \xi_0 < \xi_1 < \xi_2 < \dots \leq m-1$, and $u_0 < u_1 < u_2 < \dots \leq m$ and m is the order of Δ . □

Suppose that $\Delta_{s,u}^\xi$ -lineage is formed by a unique generation sequence. If this generation sequence contains only monomials (binomials, resp.), we say that $\Delta_{s,u}^\xi$ -lineage is a *monomial* (*binomial*, resp.) lineage. However, in some cases the generation sequence could contain both monomials and binomials. In fact, when row s is of type 3, $\Delta_{s,u}^\xi$ and $\Delta_{s,j}^\xi$ are monomials, then the lineages of these two entries merge giving rise to a binomial, see Figure 6.13.

Consider a row s which contains both monomials and binomials and suppose the first binomial in row s appears in $\Delta^{\xi+1}$. Looking back at the lineage history, we must have two monomial lineages $\{\Delta_{s,u}^\xi, \Delta_{s,u_1}^{\xi_1}, \Delta_{s,u_2}^{\xi_2}, \dots, \Delta_{s,u_f}^{\xi_f}\}$ and $\{\Delta_{s,j}^\zeta, \Delta_{s,j_1}^{\zeta_1}, \Delta_{s,j_2}^{\zeta_2}, \dots, \Delta_{s,j_f}^{\zeta_f}\}$, where $\xi_f, \zeta_f \leq \xi$, $\Delta_{s,u_f}^\xi = \Delta_{s,u_f}^\zeta$ and $\Delta_{s,j_f}^{\zeta_f} = \Delta_{s,j_f}^\xi$. The binomial appears in $\Delta^{\xi+1}$ as a consequence of a change of basis caused by a change-of-basis pivot Δ_{i,j_f}^ζ and a primary pivot Δ_{i,u_f}^ζ in a row $i > s$, as we can see in Figure 6.16.

$$\Delta_k^\zeta = \begin{pmatrix} & u_f & j_f \\ & \vdots & \vdots \\ s & \cdots & \Delta_{s,u_f}^\zeta & \cdots & \Delta_{s,j_f}^\zeta & \cdots \\ & \vdots & \ddots & \vdots & \vdots & \cdots \\ i & \cdots & \textcircled{\Delta_{i,u_f}^\zeta} & \cdots & \boxed{\Delta_{i,j_f}^\zeta} & \cdots \\ & \vdots & & \vdots & & \end{pmatrix}$$

Figure 6.16: Merging two monomial lineages and generating a binomial.

The entry Δ_{s,u_f}^ζ generates the binomial $\Delta_{s,j_f}^{\xi+1}$ and, in this case, we say that the $\Delta_{s,j}^\zeta$ -lineage ceases and the $\Delta_{s,u}^\zeta$ -lineage is an *eventual binomial lineage*. Note that, from this point on, $\Delta_{s,u}^\zeta$ -lineage contains only binomials.

Recall that, by Lemma 6.3, we have that pivots do not generate entries. Hence, if an element of a lineage is marked as a pivot, we also say that this lineage ceases.

Theorem 6.6 (Second Block Characterization). *Let Δ be a Novikov differential for which the SSSA is proved correct up to step R . Then we have the following possibilities for a nonzero row s on the second block of the matrix Δ^r produced by the SSSA in step $r \leq R$ without performing the pre-multiplication by $(T^r)^{-1}$:*

- (A) all nonzero entries are binomials of the form $t^\ell - t^{\tilde{\ell}}$, where $\ell, \tilde{\ell} \in \mathbb{Z}$;
- (B) all nonzero entries are monomials of the form t^ℓ , where $\ell \in \mathbb{Z}$;
- (C) all nonzero entries are either monomials t^ℓ or binomials $t^\ell - t^{\tilde{\ell}}$. Moreover, if a column j in Δ_2 contains a binomial, then there are no monomials in columns j' in Δ_2 with $j' > j$.

Proof. In order to prove (A), (B) and (C), we must simultaneously prove the following statements:

- (i) If an entry t^ℓ is a primary pivot in row i then at most one entry will be marked as a change-of-basis pivot in row i .
- (ii) An entry $t^\ell - t^{\tilde{\ell}}$ is never marked as a change-of-basis pivot, i.e. all change-of-basis pivots are monomials t^ℓ , for some $\ell \in \mathbb{Z}$.

- (iii) If $\Delta_{s,j}^r = t^l - t^{\tilde{l}}$, $\Delta_{i,j}^r$ is a change-of-basis pivot in row $i > s$ and $\Delta_{i,u}^r$ is the primary pivot in row i with $u < j$, then $\Delta_{s,u}^r$ is zero.
- (iv) A primary pivot $\Delta_{i,u}^r$ and a change-of-basis pivot $\Delta_{i,j}^r$ in row i are always monomials with opposite signs, i.e., $\Delta_{i,j}^r = \pm t^\ell$ and $\Delta_{i,u}^r = \mp t^{\tilde{\ell}}$, for $\ell, \tilde{\ell} \in \mathbb{Z}$.
- (v) A monomial $\Delta_{s,u}^r$ above a primary pivot $\Delta_{i,u}^r$ and a monomial $\Delta_{s,j}^r$ above a change-of-basis pivot $\Delta_{i,j}^r$ always have opposite signs, i.e., $\Delta_{s,j}^r = \pm t^l$ and $\Delta_{s,u}^r = \mp t^{\tilde{l}}$, for $l, \tilde{l} \in \mathbb{Z}$.

The proof of (A), (B), (C), (i), (ii), (iii), (iv) and (v) is done by induction on $r \leq R$.

For the base case, we suppose, without loss of generality, that there is a change-of-basis pivot $\Delta_{i,i+2}^2$ on the second diagonal, see Figure 6.14. Recall that the rows in Δ^2 are characterized by Corollary 6.1 and row i must be of type 3. The proof of this case is done analyzing the effect of this change of basis on a row s with $s < i$ for all possible row types. It follows easily by observing Figures 6.12, 6.13 and 6.15.

Now, suppose that Theorem 6.6 and items (i) through (v) hold for $r < R$. We show that they also hold for $r + 1$. By the induction hypothesis, at most one entry in a fixed row in Δ_2 is marked as change-of-basis pivot up to step r . It follows from Lemma 6.4 that, for an entry $\Delta_{s,u}$, the $\Delta_{s,u}$ -lineage is formed by a unique generation sequence until Δ^{r+1} , which is either a binomial lineage, if $\Delta_{s,u}$ is a binomial; or a monomial lineage or an eventual binomial lineage, if $\Delta_{s,u}$ is a monomial³.

By the induction hypothesis, it follows that if $\Delta_{i,j}^r$ is a change-of-basis pivot on the r -th diagonal and $\Delta_{i,u}^r$ is the primary pivot of row i , then these entries must be monomials. More specifically, $\Delta_{i,j}^r = \pm t^\ell$ and $\Delta_{i,u}^r = \mp t^{\tilde{\ell}}$, for $\ell, \tilde{\ell} \in \mathbb{Z}$.

In order to prove that the nonzero rows in Δ^{r+1} are of type A , B or C , we must perform all the possible changes of basis. Clearly, after the change of basis, row i remains of the same type. Each row $s < i$ in Δ^r is of type A , B or C , and thus one has the following cases to analyze the effect of the change of basis in row s . Again keep in mind the configurations on Figures 6.12 to 6.15.

- If $\Delta_{s,u}^r = 0$, then row s remains unaltered.
- If $\Delta_{s,u}^r \neq 0$ and $\Delta_{s,j}^r = 0$, then row s remains of the same type. In fact, $\Delta_{s,j}^{r+1} = -\Delta_{i,j}^r (\Delta_{i,u}^r)^{-1} \Delta_{s,u}^r$, which is a monomial if $\Delta_{s,u}^r$ is a monomial, or a binomial if $\Delta_{s,u}^r$ is a binomial.
- If $\Delta_{s,u}^r \neq 0$ and $\Delta_{s,j}^r \neq 0$, then row s turns into a row of type B or C . In fact, by the induction hypothesis, $\Delta_{s,u}^r = \pm t^l$ and $\Delta_{s,j}^r = \mp t^{\tilde{l}}$. Then $\Delta_{s,j}^{r+1} = \Delta_{s,j}^r -$

³Note that in this proof, whenever we assume the induction hypothesis for r , the index r is shifted by one, i.e. $r + 1$, when referring to the lineages.

$\Delta_{i,j}^r (\Delta_{i,u}^r)^{-1} \Delta_{s,j}^r$, and hence $\Delta_{s,j}^{r+1}$ is a zero entry or a binomial with coefficients equal to ± 1 .

Hence, every row $s \in \Delta_2$ of Δ^{r+1} is of type A, B or C.

The detailed proof that items (i), (ii), (iii), (iv) and (v) hold for Δ^{r+1} can be found in Lima, Manzoli Neto, de Rezende, and da Silveira (2017). \square

Proof. (of Theorem 6.4) The proof follows by induction in r . Let Δ be a Novikov differential. By the characterization of Δ proved in Corollary 6.1, the entries of Δ are invertible in $\mathbb{Z}((t))$ and thus the SSSA can be applied to Δ . Since there are no change-of-basis pivots in Δ^1 and Δ^2 , the first time where a change of basis might occur is from Δ^2 to Δ^3 . Hence the entries of the matrices Δ , Δ^1 and Δ^2 are the same and the differences between these matrices are only the marked pivots. Consequently, the SSSA is correct until step 2. It follows from Lemma 6.2, that the SSSA can be applied to each block of Δ separately. Also, by Theorems 6.5 and 6.6 the pivots in Δ^3 are invertible. Therefore, the SSSA is correct for Δ^3 . Now suppose the SSSA is proved correct until step r . It follows from Theorems 6.5 and 6.6 that the SSSA is correct for Δ^{r+1} . \square

The next example shows that, during the application of the SSSA, infinite series can appear as entries of an intermediate matrix whichs are not pivots due to multiplication by $(T^r)^{-1}$. However, note that the last matrix produced by the SSSA does not contain entries which are infinite series.

Example 6.4. Recall that the SSSA is applied to the Novikov matrix Δ of Example 6.3 presented in Figure 6.5 produces the sequence of Novikov matrices $\Delta^1, \dots, \Delta^6$ as in Figures 6.6 to 6.11, respectively. Note that the entry $\Delta_{3,7}^3$ is an infinite Laurent series.

The next result proves that the entries of the last matrix Δ^L produced by the SSSA are never infinite series. More specifically, they are all Laurent polynomials in $\mathbb{Z}((t))$.

Theorem 6.7. *Let $(\mathcal{N}_*(f), \Delta)$ be a Novikov complex on a surface, and Δ^L the last matrix produced by the SSSA over $\mathbb{Z}((t))$. Then, the nonzero entries of Δ^L are either monomials t^ℓ or binomials $t^\ell - t^{\tilde{\ell}}$.*

The first step in order to prove Theorem 6.7 is to prove Lemma 6.5, which guarantees that if a column j of Δ^L has at least a nonzero entry, then row j must be null. The proof of this result follows the same steps of the proof of its analogous version in de Rezende, Mello, and da Silveira (2010), where the coefficients of the differential which is the input for the SSSA are either in \mathbb{Z} or in a field \mathbb{F} .

Lemma 6.5. *Given a Novikov complex $(\mathcal{N}_*(f), \Delta)$ on surfaces, let Δ^L be the last matrix produced by the SSSA over $\mathbb{Z}((t))$. Then $\Delta_{j\bullet}^L \Delta_{\bullet j}^L = 0$ for all j .*

Proof. If $\Delta_{\bullet j}^L = 0$ then it is clear that $\Delta_{j \bullet}^L \Delta_{\bullet j}^L = 0$. Assume that $\Delta_{\bullet j}^L \neq 0$ and that column j is an h_k -column for an integer k . Denote by $\Delta_{i_1, j_1}^L, \dots, \Delta_{i_s, j_s}^L$ the primary pivots in block Δ_k^L such that $i_1 < i_2 < \dots < i_s$. It follows from the SSSA rules that j_1, \dots, j_s are the non null columns of Δ_k . Moreover, Δ_{i_s, j_s}^L is the unique nonzero entry in row i_s . Row i_{s-1} has nonzero primary pivot in column j_{s-1} and may have another one nonzero entry in column j_s , which is an entry above a primary pivot, and so on. Since $\Delta^L \circ \Delta^L = 0$, then

$$0 = \Delta_{i_s \bullet}^L \Delta_{\bullet j'}^L = \Delta_{i_s j_s}^L \Delta_{j_s j'}^L,$$

for all j' . The entry $\Delta_{i_s j_s}^L$ is nonzero because it is a primary pivot, hence $\Delta_{j_s j'}^L = 0$ for all j' , i.e., $\Delta_{j_s \bullet}^L = 0$. Analogously,

$$0 = \Delta_{i_{s-1} \bullet}^L \Delta_{\bullet j'}^L = \Delta_{i_{s-1} j_{s-1}}^L \Delta_{j_{s-1} j'}^L + \Delta_{i_{s-1} j_a}^L \Delta_{j_s j'}^L,$$

for all j' . Since $\Delta_{i_{s-1} j_{s-1}}^L \neq 0$ and $\Delta_{j_s j'}^L = 0$, it follows that $\Delta_{j_{s-1} j'}^L = 0$ for all j' , i.e., $\Delta_{j_{s-1} \bullet}^L = 0$. Using the same arguments, we prove that the entries on the rows j_{s-2}, \dots, j_1 are all equal to zero. \square

Proof. (of Theorem 6.7) It follows from Theorems 6.5 and 6.6 that if we do not perform the pre-multiplication by $(T^s)^{-1}$ for any $s = 1, \dots, r-1$, the entries of Δ^r are monomials t^ℓ or binomials $t^{\ell_1} - t^{\ell_2}$. Moreover, the pre-multiplication only affects row j if column j contains a primary pivot. However, by Lemma 6.5, these rows will be zeroed out by the time SSSA reaches the last matrix Δ^L .

\square

Recovering the associated spectral sequence

Let M be a smooth closed orientable 2-dimensional manifold, $f : M \rightarrow \mathbb{S}^1$ be a circle valued Morse function, $(\mathcal{N}_*(f), \Delta)$ be a Novikov chain complex with the finest filtration F and (E^r, d^r) be the associated spectral sequence. In this section, we prove that the SSSA recovers the generators of the modules E^r and induces the differentials d^r .

The first and most important step in the direction of detecting the generators of the modules of the spectral sequence is the next proposition, which establishes a formula for the modules $Z_{p,k-p}^r$ in terms of the chains $\sigma_k^{i,j}$'s determined by the SSSA applied to Δ . Its proof is an adaptation of the proof of Proposition 5.3 for the context of the Novikov differentials, which now have entries in the ring $\mathbb{Z}((t))$.

Proposition 6.2. *Let κ be the first column in Δ associated to a k -chain and consider $\mu^{j,\kappa} = 0$ whenever the primary pivot of column j is below row $(p-r+1)$ and $\mu^{j,\kappa} = 1$ otherwise. Then*

$$Z_p^r = \mathbb{Z}((t))[\mu^{p+1,r} \sigma_k^{p+1,r}, \mu^{p,r-1} \sigma_k^{p,r-1}, \dots, \mu^{\kappa, r-p-1+\kappa} \sigma_k^{\kappa, r-p-1+\kappa}].$$

The next theorem proves that the matrix Δ^r obtained from the SSSA applied to Δ determines the modules and differentials of the associated spectral sequence. Its proof is inspired in the proof of Theorems 5.5 and 5.6. It can also be found in Lima, Manzoli Neto, de Rezende, and da Silveira (2017).

Theorem 6.8. *Let M be a smooth closed orientable 2-dimensional manifold, $f : M \rightarrow \mathbb{S}^1$ be a circle valued Morse function, $(N_*(f), \Delta)$ be a Novikov chain complex with the finest filtration F and (E^r, d^r) be the associated spectral sequence.*

1. *Each module E_p^r is either zero or a finitely generated $\mathbb{Z}((t))$ -module whose generator corresponds to a k -chain associated to column $(p+1)$ of Δ^r .*
2. *If E_p^r and E_{p-r}^r are both nonzero, then the map $d_p^r : E_p^r \rightarrow E_{p-r}^r$ is induced by multiplication by the entry $\Delta_{p-r+1, p+1}^r$.*

Proof. As in Theorems 5.5 and 5.6, the entry $\Delta_{p-r+1, p+1}^r$ on the r -th diagonal of Δ^r plays a crucial role in determining the generators of E_p^r and the differentials d_p^r . The proof analyzes all the possibilities for $\Delta_{p-r+1, p+1}^r$ and shows how the modules and differentials are determined in each case.

1. We prove that E_p^r is either zero or a finitely generated $\mathbb{Z}((t))$ -module generated by $\sigma_k^{p+1, r}$.

- (a) First, let us suppose that the entry $\Delta_{p-r+1, p+1}^r$ is identified by the SSSA as a primary pivot, a change-of-basis pivot or a zero entry with a column of zeros below it. Since $\Delta_{s, p+1}^r = 0$ for all $s > p - r + 1$ then $\sigma_k^{p+1, r}$ is a generator of Z_p^r . Thus, we have the following possibilities for row $(p+1)$.

- If $\partial Z_{p+r-1}^{r-1} \subseteq Z_{p-1}^{r-1}$, then by Proposition 6.2, $E_p^r = \mathbb{Z}((t))[\sigma_k^{p+1, r}]$. In the case where $\Delta_{p-r+1, p+1}^r$ is a primary pivot then $\sigma_k^{p+1, r}$ is a generator of Z_p^r , but it is not in Z_{p-1}^{r-1} . Since there are no primary pivots in row $(p+1)$, then $\partial Z_{p+r-1}^{r-1} \subseteq Z_{p-1}^{r-1}$.
- If $\partial Z_{p+r-1}^{r-1} \not\subseteq Z_{p-1}^{r-1}$, i.e., there exist elements in Z_{p+r-1}^{r-1} whose boundary has a nonzero entry in row $(p+1)$.

Claim 2: If $\partial Z_{p+r-1}^{r-1} \not\subseteq Z_{p-1}^{r-1}$, then $Z_{p-1}^{r-1} + \partial Z_{p+r-1}^{r-1} = Z_p^r$.

Proof. (of Claim 2) We must prove that $\sigma_k^{p+1, r} \in Z_{p-1}^{r-1} + \partial Z_{p+r-1}^{r-1}$. The beginning of the proof is analogous to the proof of Claim 1 on Theorem 5.5. Recall that it was proven comparing the coefficients of h_k^{p+1} in (5.7) and in (5.8). In the Novikov setting, the coefficients of h_k^{p+1} in the set of generators of the $\mathbb{Z}((t))$ -module in (5.7) is $\Delta_{p+1, p+r-\xi}^{r-1-\xi}$ and the coefficient of h_k^{p+1} in the set of the generators of the $\mathbb{Z}((t))$ -module in (5.8) is ℓ_ξ . Note that

$\Delta_{p+1,p+r-\xi}^{r-1-\xi}$ is either a pivot or a zero entry for each $\xi = 0, \dots, p + r - \bar{\kappa}$ since $\Delta_{i,p+r-\xi}^{r-1-\xi} = 0$ for all $i > p + 1$. Moreover, since $\partial Z_{p+r-1}^{r-1} \not\subseteq Z_{p-1}^{r-1}$, then the entries $\Delta_{p+1,p+r-\xi}^{r-1-\xi}$ can not all be zeros. It follows from Theorem 6.4 that if $\Delta_{p+1,p+r-\xi}^{r-1-\xi}$ is nonzero then it is invertible in $\mathbb{Z}((t))$. Then $\sigma_k^{p+1,r} \in Z_{p-1}^{r-1} + \partial Z_{p+r-1}^{r-1}$ and hence $Z_{p-1}^{r-1} + \partial Z_{p+r-1}^{r-1} = Z_p^r$.

□

Claim 2

By Proposition 6.2 and Claim 2, $E_p^r = 0$.

- (b) If the entry $\Delta_{p-r+1,p+1}^r$ is an entry above a primary pivot, then $\sigma_k^{p+1,r}$ is not a generator of Z_p^r and hence $E_p^r = 0$.
- (c) Finally, we consider the case where $\Delta_{p-r+1,p+1}^r$ is not in Δ_k^r . If there is a primary pivot in column $(p + 1)$ in a diagonal $\bar{r} < r$, then $\sigma_k^{p+1,r}$ is not a generator of Z_p^r and hence $E_p^r = 0$. Otherwise, if the nonzero entries in column $(p + 1)$ of Δ^r are on and above the r -the diagonal, then $\sigma_k^{p+1,r}$ is a generator of Z_p^r . In this case, once again we have to analyze row $(p + 1)$.
 - If $\partial Z_{p+r-1}^{r-1} \subseteq Z_{p-1}^{r-1}$ then, by Proposition 6.2, $E_p^r = \mathbb{Z}((t))[\sigma_k^{p+1,r}]$.
 - Otherwise, by Proposition 6.2 and Claim 2, $E_p^r = 0$.

2. Given $\delta_p^r : \mathbb{Z}((t))[\sigma_k^{p+1,r}] \rightarrow \mathbb{Z}((t))[\sigma_{k-1}^{p-r+1,r}]$ the multiplication by the entry $\Delta_{p-r+1,p+1}^r$ and $\tilde{\delta}_p^r$ the map induced in E_p^r , we prove that

$$\frac{\ker \tilde{\delta}_p^r}{\text{im } \tilde{\delta}_{p+r}^r} \cong \frac{\ker \delta_p^r}{\text{im } \delta_{p+r}^r} \cong E_p^{r+1}.$$

Recall that, by Theorem 6.8 (1), the modules E^r are determined by the SSSA. Hence we can use the SSSA to calculate E^r and E^{r+1} whenever necessary. Since E_p^r and E_{p-r}^r are both nonzero, the entry $\Delta_{p-r+1,p+1}^r$ in Δ^r is either a primary pivot or a zero with a column of zero entries below it. Moreover, $E_p^r = \mathbb{Z}((t))[\sigma_k^{p+1,r}]$ and $E_{p-r}^r = \mathbb{Z}((t))[\sigma_{k-1}^{p-r+1,r}]$.

- (a) Let us first consider the case where $\Delta_{p-r+1,p+1}^r$ is a primary pivot. By Theorem 6.4, $\Delta_{p-r+1,p+1}^r$ is invertible in $\mathbb{Z}((t))$ and hence $\ker \delta_p^r = 0$. It follows that $\frac{\ker \tilde{\delta}_p^r}{\text{im } \tilde{\delta}_{p+r}^r} = 0$. On the other hand, $\Delta_{p-r+1,p+1}^r$ is a primary pivot then no changes

of basis are performed on column $(p+1)$ after step r . Hence $\sigma_k^{p+1,r+1} = \sigma_k^{p+1,r} \notin Z_p^{r+1}$ and, consequently, $Z_p^{r+1} = Z_{p-1}^r$. It follows that $E_p^{r+1} = 0$.

- (b) Now suppose $\Delta_{p-r+1,p+1}^r = 0$ with a column of zeroes below it. In this case $\tilde{\delta}_p^r = \delta_p^r = 0$ and hence $\ker \delta_p^r \cong E_p^r = \ker \tilde{\delta}_p^r$. We must analyse all the possibilities for the entry $\Delta_{p+1,p+r+1}^r$ in row $(p+1)$.

- (i) If $\Delta_{p+1,p+r+1}^r$ is an entry above a primary pivot then $E_{p+r}^r = 0$. Hence $\tilde{\delta}_p^r = \delta_{p+r}^r = 0$ and, consequently, $\frac{\ker \tilde{\delta}_p^r}{\text{im } \tilde{\delta}_{p+r}^r} = E_p^r$. On the other hand, since $\Delta_{p+1,p+r+1}^r$ is an entry above a primary pivot, then $\mu^{p+r+1,r} = 0$ and hence $E_p^{r+1} = E_p^r$.
- (ii) If $\Delta_{p+1,p+r+1}^r$ is a primary pivot then $E_{p+r}^r = \mathbb{Z}((t))[\sigma_k^{p+r+1,r}]$. Moreover, by Theorem 6.4, $\Delta_{p+1,p+r+1}^r$ is invertible in $\mathbb{Z}((t))$ and hence $\text{im } \delta_{p+r}^r = \mathbb{Z}((t))[\sigma_k^{p+1,r}]$. It follows that

$$\frac{\ker \tilde{\delta}_p^r}{\text{im } \tilde{\delta}_{p+r}^r} \cong \frac{\ker \delta_p^r}{\text{im } \delta_{p+r}^r} \cong \frac{\mathbb{Z}((t))[\sigma_k^{p+1,r}]}{\mathbb{Z}((t))[\sigma_k^{p+1,r}]} = 0.$$

On the other hand, since the element in column $(p+r+1)$ and row $(p+1)$ is $\Delta_{p+1,p+r+1}^r$, which is a primary pivot, then $\partial Z_{p+r}^r \not\subseteq Z_{p-1}^r$. By Claim 2, we have that $E_p^{r+1} = 0$.

- (iii) If $\Delta_{p+1,p+r+1}^r = 0$ with a column of zero entries below it then $\tilde{\delta}_{p+r}^r = \delta_{p+r}^r = 0$ and hence

$$\frac{\ker \tilde{\delta}_p^r}{\text{im } \tilde{\delta}_{p+r}^r} = E_p^r \cong \mathbb{Z}((t))[\sigma_k^{p+1,r}].$$

On the other hand, $\partial Z_{p+r-1}^{r-1} \subseteq Z_{p-1}^{r-1}$ and the difference between the generators of ∂Z_{p+r-1}^{r-1} and ∂Z_{p+r}^r is that the latter includes the boundary of the chain corresponding to column $(p+r+1)$. Since the element in row $(p+1)$ and column $(p+r+1)$ is $\Delta_{p+1,p+r+1}^r = 0$ then $\partial Z_{p+r}^r \subseteq Z_{p-1}^r$. Thus $E_p^{r+1} = \mathbb{Z}((t))[\sigma_k^{p+1,r}]$.

If $\Delta_{p+1,p+r+1}^r$ is a change-of-basis pivot then $E_p^r = 0$, which contradicts the hypothesis. Hence we have analysed all the possibilities for $\Delta_{p+1,p+r+1}^r$.

Therefore, whenever E_p^r and E_{p+r}^r are both nonzero $\mathbb{Z}((t))$ -modules,

$$\frac{\ker d_p^r}{\text{im } d_{p+r}^r} = E_p^{r+1} = \frac{\ker \tilde{\delta}_p^r}{\text{im } \tilde{\delta}_{p+r}^r}.$$

□

Corollary 6.2. *Each nonzero differential d_p^r of the spectral sequence (E^r, d^r) is an isomorphism.*

Proof. In fact, by the proof of Theorem 6.8, nonzero differentials of (E^r, d^r) are induced by primary pivots. Theorem 6.4 states that each primary pivot produced by the SSSA is an invertible polynomial, hence each induced nonzero differential is an isomorphism. □

As a consequence of Corollary 6.2, whenever M is a smooth closed orientable 2-dimensional manifold, $f : M \rightarrow \mathbb{S}^1$ is a circle valued Morse function, $(\mathcal{N}_*(f), \Delta)$ is a Novikov chain complex with the finest filtration F and (E^r, d^r) is the associated spectral sequence, the modules $E_{p,q}^r$ are free of torsion for all p, q and $r \geq 0$.

Since the spectral (E^r, d^r) strongly converges to E^∞ then the modules $E_{p,q}^\infty$ are free for all p and q . In particular, by Theorem 5.1

$$E_{p,q}^\infty \cong GH_*(\mathcal{N})_{p,q} = \frac{F_p H_{p+q}(\mathcal{N})}{F_{p-1} H_{p+q}(\mathcal{N})}$$

and hence the associated graduated module $GH_*(\mathcal{N})_{p,q}$ is free for all p and q . Consequently,

$$E_{p,q}^\infty \cong GH_*(\mathcal{N})_{p,q} \cong H_*(\mathcal{N}_*(f), \partial).$$

i.e. the spectral sequence (E^r, d^r) converges to the homology of $(\mathcal{N}_*(f), \Delta)$.

We have proved the following theorem.

Theorem 6.9. *Let M be a smooth closed orientable 2-dimensional manifold, $f : M \rightarrow \mathbb{S}^1$ be a circle valued Morse function, $(\mathcal{N}_*(f), \Delta)$ be a Novikov chain complex with the finest filtration F and (E^r, d^r) be the associated spectral sequence. Then the modules $E_{p,q}^\infty$ of the spectral sequence are free for all p and q . Moreover, the spectral sequence (E^r, d^r) converges to the homology of $(\mathcal{N}_*(f), \Delta)$.*

We end this section with an example, where we calculate the spectral sequence for the filtered Novikov complex presented in Example 6.3 using the results proved herein.

Example 6.5. Let $(\mathcal{N}_*(f), \Delta)$ the Novikov complex presented in Example 6.3. Recall that the matrices produced by the SSSA are illustrated in Figures 6.6 to 6.11. Consider the finest filtration F on $(\mathcal{N}_*(f), \Delta)$ defined by

$$F_p \mathcal{N}_k = \bigoplus_{h_k^\ell, \ell \leq p+1} \mathbb{Z}((t)) \langle h_k^\ell \rangle.$$

$$\begin{array}{ccccccccc}
E^0: \mathbb{Z}((t))[h_0^1] & \mathbb{Z}((t))[h_0^2] & \mathbb{Z}((t))[h_1^3] & \mathbb{Z}((t))[h_1^4] & \mathbb{Z}((t))[h_1^5] & \mathbb{Z}((t))[h_1^6] & \mathbb{Z}((t))[h_2^7] & \mathbb{Z}((t))[h_2^8] \\
& \xleftarrow{d_2^1} & & & & \xleftarrow{d_6^1} & & \\
E^1: \mathbb{Z}((t))[h_0^1] & \mathbb{Z}((t))[h_0^2] & \mathbb{Z}((t))[h_1^3] & \mathbb{Z}((t))[h_1^4] & \mathbb{Z}((t))[h_1^5] & \mathbb{Z}((t))[h_1^6] & \mathbb{Z}((t))[h_2^7] & \mathbb{Z}((t))[h_2^8] \\
& & & & & & & \\
E^2: \mathbb{Z}((t))[h_0^1] & 0 & 0 & \mathbb{Z}((t))[h_1^4] & \mathbb{Z}((t))[h_1^5] & 0 & d_7^3 & 0 & \mathbb{Z}((t))[h_2^8] \\
& & & \xleftarrow{d_3^3} & & & & & \\
E^3: \mathbb{Z}((t))[h_0^1] & 0 & 0 & \mathbb{Z}((t))[h_1^4 + (t-1)^{-1}h_1^3] & \mathbb{Z}((t))[h_1^5] & 0 & 0 & 0 & \mathbb{Z}((t))[h_2^8 + t^{-1}h_2^7] \\
& & & \xleftarrow{\Delta_{2,3}} & & \xleftarrow{\Delta_{6,7}} & & & \\
E^4: & 0 & 0 & 0 & 0 & 0 & 0 & 0 & 0
\end{array}$$

Figure 6.17: A spectral sequence associated to the Novikov complex presented in Example 6.3.

Let (E^r, d^r) be the spectral sequence associated to this filtered Novikov complex. Recall that, since F is a finest filtration on $(\mathcal{N}_*(f), \Delta)$, then for each p there is at most one q such that $E_{p,q}^r$ can be nonzero. Hence, each diagram page of (E^r, d^r) can be collapsed and represented in one row, as in Figure 6.17.

It is easy to see that the Novikov homology of the complex $(\mathcal{N}_*(f), \Delta)$ is given by

$$H_0(\mathcal{N}_*(f), \partial) = 0, \quad H_1(\mathcal{N}_*(f), \partial) = 0, \quad H_2(\mathcal{N}_*(f), \partial) = 0.$$

Note that each nonzero $\mathbb{Z}((t))$ -module E_p^r is generated by a k -chain $\sigma_k^{p+1,r}$, produced in the r -th step of the SSSA. Moreover, the differentials d_2^1, d_6^1, d_3^3 and d_7^3 are induced by the multiplication by the invertible polynomials $\Delta_{2,3}^1, \Delta_{6,7}^1, \Delta_{1,4}^3$ and $\Delta_{5,8}^3$, respectively, and hence they are isomorphisms. Finally, the spectral sequence converges to the homology of $(\mathcal{N}_*(f), \Delta)$.

6.2.3 Ordered cancellation for circle valued Morse function

In this section, we present dynamical results obtained from the exploration of connections in a negative gradient flow associated to a circle valued Morse function using the algebraic techniques developed in Section 6.2.2. The main reference used herein is Lima, Manzoli Neto, de Rezende, and da Silveira (2017). Let M be a smooth closed orientable 2-dimensional manifold, $f : M \rightarrow \mathbb{S}^1$ be a circle valued Morse function, $(\mathcal{N}_*(f), \Delta)$ be a Novikov chain complex with the finest filtration \mathcal{F} and (E^r, d^r) be the associated spectral sequence. Let the Morse function $F : \overline{M} \rightarrow \mathbb{R}$ be the lift of f to the infinite cyclic covering space \overline{M} . Recall that, analogously to the classical Morse case, by Corollary 6.2, if $d^r : E_p^r \rightarrow E_{p-r}^r$ is a nonzero differential, then we have an algebraic cancellation, i.e. the modules E_p^{r+1} and E_{p-r}^{r+1} are both equal to zero. We prove the existence of a global dynamics corresponding to the algebraic unfolding of the spectral sequence, where the algebraic cancellations are associated to dynamical cancellations of singularities of the negative gradient flow of f on M .

Consider $\mathcal{F} = \{\mathcal{F}_p \mathcal{N}\}_{p \in P}$ on $(\mathcal{N}_*(f), \Delta)$ a finest filtration, where

$$F_p \mathcal{N} = \mathbb{Z}((t)) \left[h_{k_1}^1, h_{k_2}^2, \dots, h_{k_{p+1}}^{p+1} \right] \quad (6.3)$$

and $P = \{0, 1, \dots, m\}$ is an indexing set for the filtration \mathcal{F} , where $\# \text{Crit}(f) = m + 1$. The filtration \mathcal{F} induces an infinite filtration $\{\mathcal{F}_{\lambda, p}\}_{\lambda \in \mathbb{Z}, p \in P}$ in the covering space \overline{M}

$$\mathcal{F}_{\lambda, p} \mathcal{N} = \mathbb{Z} \left\langle t^\delta h_k^j \mid \begin{array}{l} \delta = \lambda \text{ and } j \leq p+1 \text{ or} \\ \delta > \lambda \text{ and } j \in \{1, \dots, m\} \end{array} \right\rangle$$

where $t^\lambda h_k^{p+1}$ is the lift of the singularity h_k^{p+1} at level λ , for $\lambda \in \mathbb{Z}$. For $p \in \{0, 1, \dots, m\}$ and $\lambda \in \mathbb{Z}$, we have

$$\mathcal{F}_{\lambda, p-1} \mathcal{N} \subset \mathcal{F}_{\lambda, p} \mathcal{N}, \quad \mathcal{F}_{\lambda, m} \mathcal{N} \subset \mathcal{F}_{\lambda-1, 0} \mathcal{N},$$

$$\mathcal{F}_{\lambda, p} \mathcal{N} \setminus \mathcal{F}_{\lambda, p-1} \mathcal{N} = t^\lambda h_k^{p+1} \text{ and } \mathcal{F}_{\lambda-1, 0} \mathcal{N} \setminus \mathcal{F}_{\lambda, m} \mathcal{N} = t^{\lambda-1} h_k^1.$$

Without loss of generality, we assume that f has only one critical point on each critical level set. For each critical point h_k^p of f , let c_p be a critical value of f such that $f(h_k^p) = c_p$. It follows that F also has only one critical point at each critical level set and $c_{\lambda, p} := c_p - \lambda$ is the critical value of F such that $F(t^\lambda h_k^p) = c_{\lambda, p}$, for all $\lambda \in \mathbb{Z}$.

Example 6.6. Let M be a torus and consider the negative gradient flow of a circle valued Morse function f on M as in Figure 6.18. We also present in Figure 6.18 the differential Δ of the Novikov complex $(\mathcal{N}_*(f), \Delta)$ associated to f and the associated infinite cyclic covering \overline{M} enriched with the induced filtration $\{\mathcal{F}_{\lambda, p}\}$, where $\mathcal{F} = \{\mathcal{F}_p \mathcal{N}\}_{p \in P}$ is the filtration on $(\mathcal{N}_*(f), \Delta)$ given by (6.3).

Recall that, by Theorem 6.8, the nonzero differentials of the spectral sequence are induced by the pivots in the SSSA. Moreover, it follows from Theorem 6.4 that the primary pivots are always invertible polynomials, hence the differentials $d_p^r : E_p^r \rightarrow E_{p-r}^r$ associated to primary pivots are isomorphisms and the ones associated to change-of-basis pivots always correspond to zero maps. Since the nonzero differentials are isomorphisms, at the next stage of the spectral sequence they produce algebraic cancellations, i.e. $E_p^{r+1} = E_{p-r}^{r+1} = 0$.

The next theorem is the main result in this section. It proves the existence of a sequence of dynamical cancellations of critical points of a circle valued Morse function $f : M \rightarrow \mathbb{S}^1$ which are in one-to-one correspondence with the algebraic cancellations performed by the spectral sequence associated to the filtered Novikov chain complex of f .

Theorem 6.10. (Ordered Cancellation Theorem via Spectral Sequences in the Novikov setting) Let $f : M \rightarrow \mathbb{S}^1$ be a circle valued Morse function on a smooth closed orientable 2-dimensional manifold M and $(\mathcal{N}_*(f), \Delta)$ be the Novikov chain complex associated to f . Let \mathcal{F} be a finest filtration in $(\mathcal{N}_*(f), \Delta)$ and let (E^r, d^r) be the associated spectral sequence. Then:

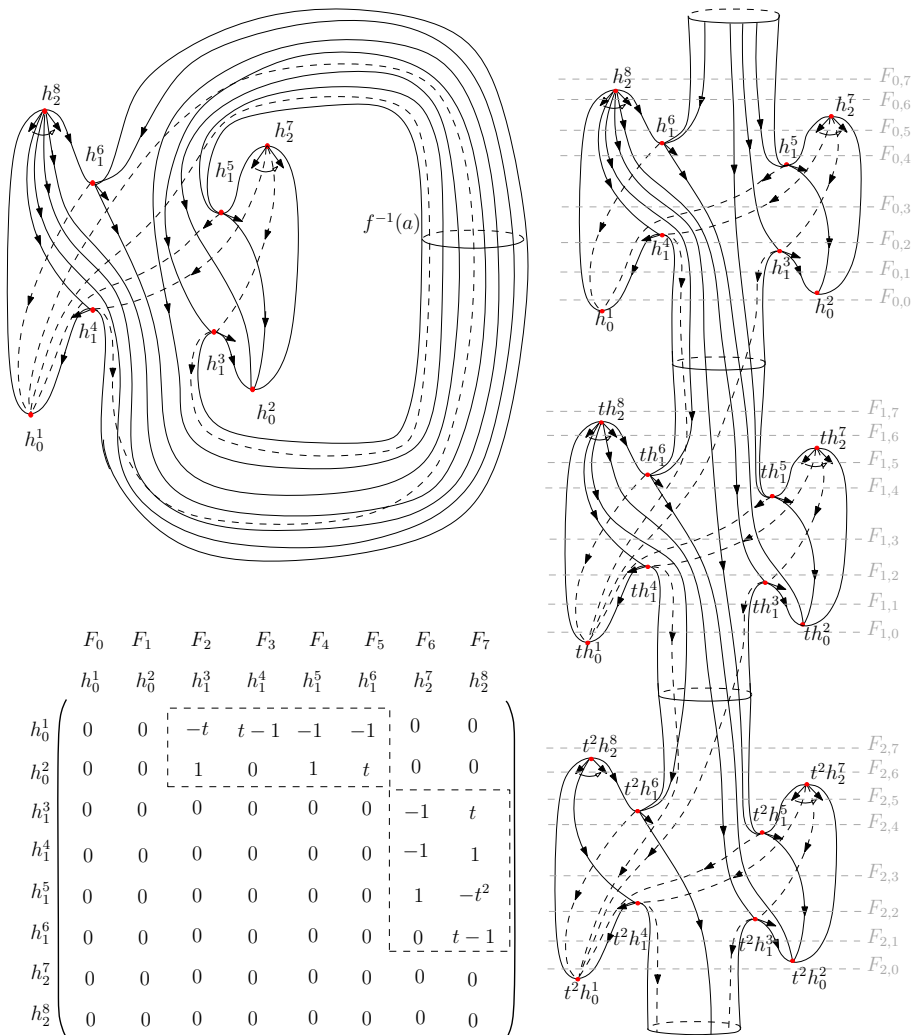


Figure 6.18: Circle valued Morse function on the torus, Novikov differential and infinite cyclic covering.

$$\begin{array}{ccccccccc} & \sigma_0^{1,1} & \sigma_0^{2,1} & \sigma_1^{3,1} & \sigma_1^{4,1} & \sigma_1^{5,1} & \sigma_1^{6,1} & \sigma_2^{7,1} & \sigma_2^{8,1} \\ \sigma_0^{1,1} = h_0^1 & 0 & 0 & -t & t-1 & -1 & -1 & 0 & 0 \\ \sigma_0^{2,1} = h_0^2 & 0 & 0 & 1 & 0 & 1 & t & 0 & 0 \\ \sigma_1^{3,1} = h_1^3 & 0 & 0 & 0 & 0 & 0 & 0 & -1 & t \\ \sigma_1^{4,1} = h_1^4 & 0 & 0 & 0 & 0 & 0 & 0 & -1 & 1 \\ \sigma_1^{5,1} = h_1^5 & 0 & 0 & 0 & 0 & 0 & 0 & 1 & -t^2 \\ \sigma_1^{6,1} = h_1^6 & 0 & 0 & 0 & 0 & 0 & 0 & 0 & t-1 \\ \sigma_2^{7,1} = h_2^7 & 0 & 0 & 0 & 0 & 0 & 0 & 0 & 0 \\ \sigma_2^{8,1} = h_2^8 & 0 & 0 & 0 & 0 & 0 & 0 & 0 & 0 \end{array}$$

(A 8x8 matrix with dashed lines separating blocks. A red circle highlights the value 1 at position (2,3).)

Figure 6.19: Δ^1 .

1. There exists a family of circle valued Morse functions $\{f^r\}_{r \geq 1}$, where $f = f^1$ and f^{r+1} is obtained from f^r by removing the pairs of critical points corresponding to the canceled modules of the r -th page of the spectral sequence. More specifically, the sequence of algebraic cancellations of the modules E_p^r, E_{p-r}^r are in one-to-one correspondence to the sequence of dynamical cancellations of critical points $h_k^{p+1}, h_{k-1}^{p-r+1}$ of f .
2. For each $r \geq 0$, the $(r+1)$ -th page of the spectral sequence completely determines all Novikov incidence coefficients between consecutive critical points of f^{r+1} .

Before we prove Theorem 6.10, we present an example that illustrates the algebraic-dynamical correspondence associating the algebraic unfolding of the spectral sequence to a family of circle valued Morse functions.

Example 6.7. Consider M, f and the associated filtered Novikov complex presented in Example 6.6. Applying the SSSA to the Novikov differential Δ , we obtain the sequence of Novikov matrices $\Delta^1, \dots, \Delta^6$ as in Figures 6.19 to 6.24

By Theorem 6.8, the primary pivots produced by the SSSA induce the differentials of the spectral sequence and, by Theorem 6.4, these pivots are all invertible polynomials. Hence each pivot determines an algebraic cancellation of the modules of the spectral sequence. Finally, it follows from Theorem 6.10, that each algebraic cancellation performed by the spectral sequence corresponds to a dynamical cancellation of critical points. Figures 6.25 to 6.28 show the corresponding dynamical cancellations of pairs of critical points. More specifically:

- Primary pivot $\Delta_{2,3}^1$ induces the differential $d_2^1 : E_2^1 \rightarrow E_1^1$, which causes the algebraic cancellation $E_2^2 = E_1^2 = 0$. Corresponding to this algebraic cancellation, we have the dynamical cancellation of the pair (h_0^2, h_1^3) . The resulting circle valued Morse function

$$\begin{array}{c}
 \sigma_0^{1,2} = h_0^1 & \sigma_0^{2,2} & \sigma_1^{3,2} & \sigma_1^{4,2} & \sigma_1^{5,2} & \sigma_1^{6,2} & \sigma_2^{7,2} & \sigma_2^{8,2} \\
 \sigma_0^{2,2} = h_0^2 & 0 & 0 & -t & t-1 & -1 & -1 & 0 & 0 \\
 \sigma_1^{3,2} = h_1^3 & 0 & 0 & 1 & 0 & 1 & t & 0 & 0 \\
 \sigma_1^{4,2} = h_1^4 & 0 & 0 & 0 & 0 & 0 & 0 & -1 & 1 \\
 \sigma_1^{5,2} = h_1^5 & 0 & 0 & 0 & 0 & 0 & 0 & 1 & -t^2 \\
 \sigma_1^{6,2} = h_1^6 & 0 & 0 & 0 & 0 & 0 & 0 & 0 & t-1 \\
 \sigma_2^{7,2} = h_2^7 & 0 & 0 & 0 & 0 & 0 & 0 & 0 & 0 \\
 \sigma_2^{8,2} = h_2^8 & 0 & 0 & 0 & 0 & 0 & 0 & 0 & 0
 \end{array}$$

Figure 6.20: Δ^2 .

$$\begin{array}{c}
 \sigma_0^{1,3} = h_0^1 & \sigma_0^{2,3} & \sigma_1^{3,3} & \sigma_1^{4,3} & \sigma_1^{5,3} & \sigma_1^{6,3} & \sigma_2^{7,3} & \sigma_2^{8,3} \\
 \sigma_0^{2,3} = h_0^2 & 0 & 0 & -t & t-1 & -1 & -1 & 0 & 0 \\
 \sigma_1^{3,3} = h_1^3 & 0 & 0 & 1 & 0 & 1 & t & 0 & 0 \\
 \sigma_1^{4,3} = h_1^4 & 0 & 0 & 0 & 0 & 0 & 0 & -1 & t \\
 \sigma_1^{5,3} = h_1^5 & 0 & 0 & 0 & 0 & 0 & 0 & 1 & -t^2 \\
 \sigma_1^{6,3} = h_1^6 & 0 & 0 & 0 & 0 & 0 & 0 & 0 & t-1 \\
 \sigma_2^{7,3} = h_2^7 & 0 & 0 & 0 & 0 & 0 & 0 & 0 & 0 \\
 \sigma_2^{8,3} = h_2^8 & 0 & 0 & 0 & 0 & 0 & 0 & 0 & 0
 \end{array}$$

Figure 6.21: Δ^3 .

$$\begin{array}{l}
 \sigma_0^{1,4} = h_0^1 \quad \sigma_0^{2,4} \quad \sigma_1^{3,4} \quad \sigma_1^{4,4} \quad \sigma_1^{5,4} \quad \sigma_1^{6,4} \quad \sigma_2^{7,4} \quad \sigma_2^{8,4} \\
 \sigma_0^{2,4} = h_0^2 \quad 0 \quad 0 \quad -t \quad t-1 \quad t-1 \quad -1 \quad 0 \quad 0 \\
 \sigma_1^{3,4} = h_1^3 \quad 0 \quad 0 \quad 1 \quad 0 \quad 0 \quad t \quad 0 \quad 0 \\
 \sigma_1^{4,4} = h_1^4 \quad 0 \quad 0 \quad 0 \quad 0 \quad 0 \quad 0 \quad -1 \quad 1 \\
 \sigma_1^{5,4} = h_1^5 - h_1^3 \quad 0 \quad 0 \quad 0 \quad 0 \quad 0 \quad 0 \quad 1 \quad -t^2 \\
 \sigma_1^{6,4} = h_1^6 \quad 0 \quad t-1 \\
 \sigma_2^{7,4} = h_2^7 \quad 0 \\
 \sigma_2^{8,4} = h_2^8 \quad 0 \quad 0
 \end{array}
 \left(\begin{array}{c} \sigma_0^{1,4} \\ \sigma_0^{2,4} \\ \sigma_1^{3,4} \\ \sigma_1^{4,4} \\ \sigma_1^{5,4} \\ \sigma_1^{6,4} \\ \sigma_2^{7,4} \\ \sigma_2^{8,4} \end{array} \right) = \left(\begin{array}{ccccccccc} 0 & 0 & -t & t-1 & t-1 & -1 & 0 & 0 \\ 0 & 0 & 1 & 0 & 0 & t & 0 & 0 \\ 0 & 0 & 0 & 0 & 0 & 0 & 0 & -t^2 \\ 0 & 0 & 0 & 0 & 0 & 0 & -1 & 1 \\ 0 & 0 & 0 & 0 & 0 & 0 & 1 & -t^2 \\ 0 & 0 & 0 & 0 & 0 & 0 & 0 & t-1 \\ 0 & 0 & 0 & 0 & 0 & 0 & 0 & 0 \\ 0 & 0 & 0 & 0 & 0 & 0 & 0 & 0 \end{array} \right)$$

Figure 6.22: Δ^4 .

$$\begin{array}{l}
 \sigma_0^{1,5} = h_0^1 \quad \sigma_0^{2,5} \quad \sigma_1^{3,5} \quad \sigma_1^{4,5} \quad \sigma_1^{5,5} \quad \sigma_1^{6,5} \quad \sigma_2^{7,5} \quad \sigma_2^{8,5} \\
 \sigma_0^{2,5} = h_0^2 \quad 0 \quad 0 \quad -t \quad t-1 \quad t^2-1 \quad 0 \quad 0 \quad 0 \\
 \sigma_1^{3,5} = h_1^3 \quad 0 \quad 0 \quad 1 \quad 0 \quad 0 \quad 0 \quad 0 \quad 0 \\
 \sigma_1^{4,5} = h_1^4 \quad 0 \quad 1-t^2 \\
 \sigma_1^{5,5} = h_1^5 - h_1^4 - h_1^3 \quad 0 \quad 0 \quad 0 \quad 0 \quad 0 \quad 0 \quad 1 \quad -t^2 \\
 \sigma_1^{6,5} = h_1^6 - th_1^3 \quad 0 \quad t-1 \\
 \sigma_2^{7,5} = h_2^7 \quad 0 \\
 \sigma_2^{8,5} = h_2^8 \quad 0 \quad 0
 \end{array}
 \left(\begin{array}{c} \sigma_0^{1,5} \\ \sigma_0^{2,5} \\ \sigma_1^{3,5} \\ \sigma_1^{4,5} \\ \sigma_1^{5,5} \\ \sigma_1^{6,5} \\ \sigma_2^{7,5} \\ \sigma_2^{8,5} \end{array} \right) = \left(\begin{array}{ccccccccc} 0 & 0 & -t & t-1 & t^2-1 & 0 & 0 & 0 \\ 0 & 0 & 1 & 0 & 0 & 0 & 0 & 0 \\ 0 & 0 & 0 & 0 & 0 & 0 & 0 & 0 \\ 0 & 0 & 0 & 0 & 0 & 0 & 0 & 1-t^2 \\ 0 & 0 & 0 & 0 & 0 & 0 & 1 & -t^2 \\ 0 & 0 & 0 & 0 & 0 & 0 & 0 & t-1 \\ 0 & 0 & 0 & 0 & 0 & 0 & 0 & 0 \\ 0 & 0 & 0 & 0 & 0 & 0 & 0 & 0 \end{array} \right)$$

Figure 6.23: Δ^5 .

$$\left(\begin{array}{ccccccccc}
 \sigma_0^{1,6} & \sigma_0^{2,6} & \sigma_1^{3,6} & \sigma_1^{4,6} & \sigma_1^{5,6} & \sigma_1^{6,6} & \sigma_2^{7,6} & \sigma_2^{8,6} \\
 \sigma_0^{1,6} = h_0^1 & 0 & 0 & -t & t-1 & 0 & 0 & 0 \\
 \sigma_0^{2,6} = h_0^2 & 0 & 0 & 1 & 0 & 0 & 0 & 0 \\
 \sigma_1^{3,6} = h_1^3 & 0 & 0 & 0 & 0 & 0 & 0 & 0 \\
 \sigma_1^{4,6} = h_1^4 & 0 & 0 & 0 & 0 & 0 & 0 & -t^2+t+2 \\
 \sigma_1^{5,6} = h_1^5 - h_1^4 - h_1^3 & 0 & 0 & 0 & 0 & 0 & 1 & -t^2 \\
 \sigma_1^{6,6} = h_1^6 + (-t-1)h_1^4 - th_1^3 & 0 & 0 & 0 & 0 & 0 & 0 & t-1 \\
 \sigma_2^{7,6} = h_2^7 & 0 & 0 & 0 & 0 & 0 & 0 & 0 \\
 \sigma_2^{8,6} = h_2^8 & 0 & 0 & 0 & 0 & 0 & 0 & 0
 \end{array} \right)$$

Figure 6.24: Δ^6 .

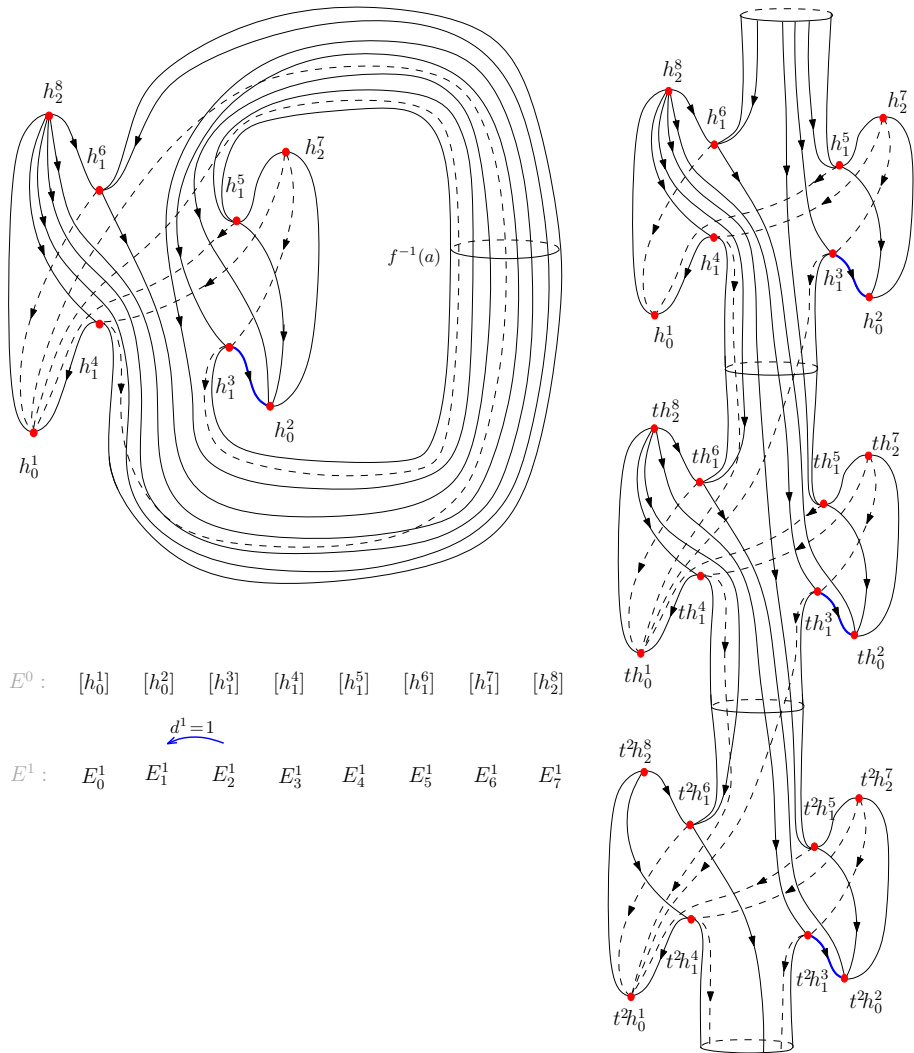
f^2 is equal to f outside a neighborhood of the critical points and the connection between them, see Figures 6.25 and 6.26. Note that in the negative gradient flow φ^2 occurs a birth of connecting orbits from h_1^5 to h_0^1 and from h_1^6 to h_0^1 , which are reflected in $\Delta_{1,5}^4$ and $\Delta_{1,6}^5$, respectively.

- Primary pivot $\Delta_{5,7}^2$ induces the differential $d_6^2 : E_6^2 \rightarrow E_4^2$, which causes the algebraic cancellation $E_6^3 = E_4^3 = 0$. Moreover, the primary pivot $\Delta_{6,8}^2$ induces the differential $d_7^2 : E_7^2 \rightarrow E_5^2$, which causes the algebraic cancellation $E_7^3 = E_5^3 = 0$. The corresponding dynamical cancellations of pairs of critical points are (h_1^5, h_2^7) and (h_1^6, h_2^8) , respectively. The resulting negative gradient flow φ^3 of the circle valued Morse function f^3 is presented in (6.27).

The cancellation of the pair (h_1^6, h_2^8) causes the birth of a repeller periodic orbit γ_R and two flow lines from γ_R to h_1^4 . The birth of γ_R is due to a primary pivot $\Delta_{6,8}^2$ which is a binomial and the period of γ_R is equal to the difference between the exponents of the binomial.

- Primary pivot $\Delta_{1,4}^3$ induces the differential $d_3^3 : E_3^3 \rightarrow E_0^3$, which causes the algebraic cancellation $E_3^4 = E_0^4 = 0$. The corresponding dynamical cancellation is the cancellation of the pair (h_0^1, h_1^4) and the resulting negative gradient flow φ^4 is illustrated in Figure 6.28. This cancellation, caused by the binomial primary pivot $\Delta_{1,4}^3 = t-1$, provokes the birth of an attractor periodic orbit γ_A .

Analogously to the proof of Theorem 5.10, for the proof of Theorem 6.10, we use an adaptation of the SSSA, the Smale's Cancellation Algorithm, presented in Section 5.5.2 which performs the same changes of basis, but in a different order and it is more conducive to dynamical interpretations. In fact, recall that when the pair of critical points h_k^{p+1} and

Figure 6.25: Algebraic-dynamical correspondence detected by Δ^1 .

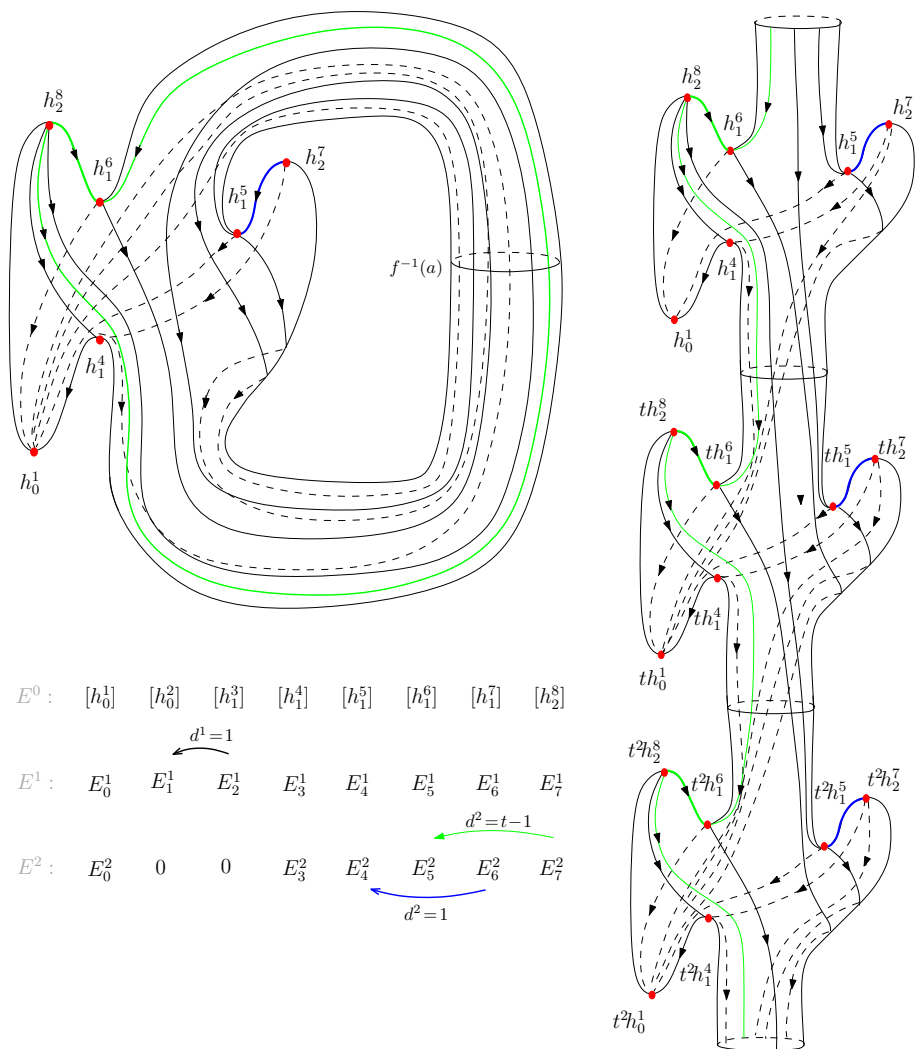


Figure 6.26: Algebraic-dynamical correspondence detected by Δ^2 - cancellation of the pair (h_0^2, h_1^3) .

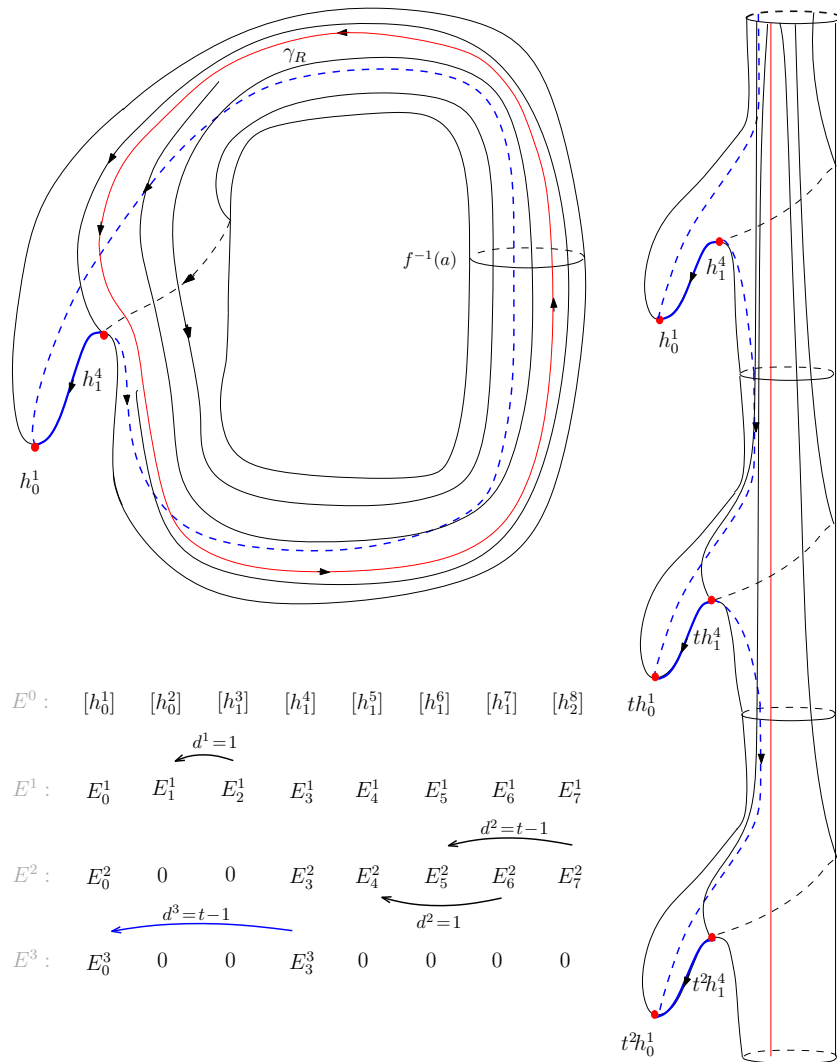
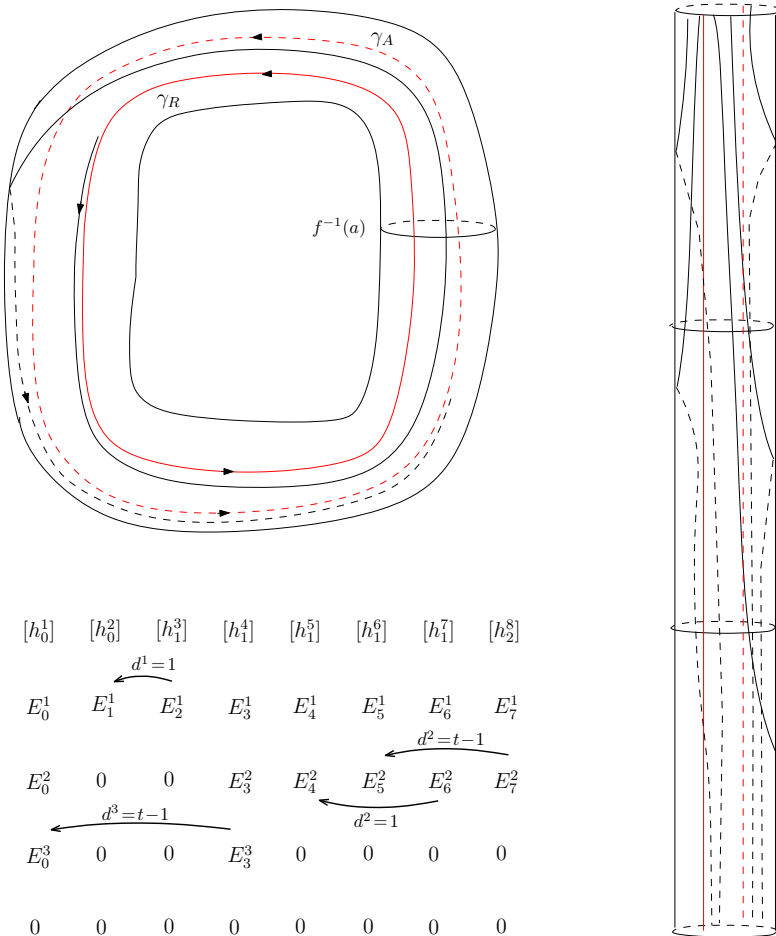


Figure 6.27: Algebraic-dynamical correspondence detected by Δ^3 - cancellation of the pairs (h_1^5, h_2^7) and (h_1^6, h_2^8) .

Figure 6.28: Cancellation of the pair (h_0^1, h_1^4) .

h_{k-1}^{p-r+1} is canceled, all the connecting orbits between index k critical points and h_{k-1}^{p-r+1} and also all the ones between h_k^{p+1} and index $k-1$ critical points are immediately removed and new orbits take their place. In order to reflect the death and birth of connecting orbits caused by the dynamical cancellations in terms of the changes in generators of the modules of the spectral sequence caused by the algebraic cancellations, all the changes of basis must be performed exactly when the algebraic cancellations occur. More specifically, if $\Delta_{p-r+1,p+1}^r$ is a primary pivot marked in step r of the SSSA, all changes of basis caused by $\Delta_{p-r+1,p+1}^r$ are performed in step $r+1$.

In Proposition 5.5 we have seen that for matrices with entries over \mathbb{Z} , the primary pivots on the r -th diagonal of $\tilde{\Delta}^r$ marked in the r -th step of the Smale's Cancellation Algorithm coincide in position and value with the ones on the r -th diagonal of Δ^r marked in the r -th step of the SSSA. The following proposition is the analogous result for Novikov matrices with coefficients over $\mathbb{Z}((t))$.

Proposition 6.3. (Primary Pivots Equality Property for Novikov Matrices) *Let $f : M \rightarrow \mathbb{S}^1$ be a circle valued Morse function on a smooth closed orientable 2-manifold M and $(\mathcal{N}_*(f), \Delta)$ be the Novikov chain complex associated to f . Let \mathcal{F} be a finest filtration in $(\mathcal{N}_*(f), \Delta)$ and let (E^r, d^r) be the associated spectral sequence. The primary pivots of the matrices $\tilde{\Delta}^r$ of the Smale's Cancellation Algorithm coincide in position and value with the ones of the matrices Δ^r of the SSSA.*

The proof of Proposition 6.3 is completely analogous to the one obtained for matrices with coefficients over \mathbb{Z} .

Proof. (of Theorem 6.10):

The proof is done by associating dynamical cancellations of critical points of f to the algebraic cancellations of the spectral sequence using Smale's First Cancellation Algorithm. We construct a family of negative gradient flows $\{\varphi^r\}$ of circle valued Morse functions f^r , $r = 1, \dots, \omega$, where $f^1 = f$ and f^{r+1} is obtained from f^r by canceling the pairs of critical points corresponding to the canceled modules of the r -th page of the spectral sequence, i.e. the pairs associated to the primary pivots on the r -th diagonal of Δ^r . Recall that the algebraic cancellation $E_p^{r+1} = E_{p-r}^{r+1} = 0$ is associated to the primary pivot $\Delta_{p-r+1,p+1}^r$ on the r -th diagonal of Δ^r in the SSSA, where the row $p-r+1$ is associated to $h_{k-1}^{p-r+1} \in \mathcal{F}_{p-r}C_{k-1} \setminus \mathcal{F}_{p-r-1}C_{k-1}$ and the column $p+1$ is associated to $h_k^{p+1} \in F_pC_k \setminus F_{p-1}C_k$. By Proposition 6.3, the primary pivot $\Delta_{p-r+1,p+1}^r$ of the SSSA is equal to the primary pivot $\tilde{\Delta}_{p-r+1,p+1}^r$ of Smale's Cancellation Algorithm. Hence, we must prove that whenever a primary pivot $\tilde{\Delta}_{p-r+1,p+1}^r$ on the r -th diagonal of $\tilde{\Delta}^r$ is marked, it is actually a Novikov incidence coefficient $N(h_k^{p+1}, h_{k-1}^{p-r+1}; f^r)$ between two singularities h_k^{p+1} and h_{k-1}^{p-r+1} of consecutive indices of φ^r .

Without loss of generality, we consider the orientations on the unstable manifolds of critical points of index 2 to be consistent. In this case, the Novikov differential Δ is characterized by Corollary 6.1.

The proof follows by induction in r . Since $d^0 = 0$, there are no algebraic cancellations on the first step, $f = f^1$, $\varphi^1 = \varphi$ and $\widetilde{\Delta}^1 = \Delta(\varphi^1) = \Delta(\varphi)$. Suppose that f^r and φ^r are defined and that the Novikov differential $\Delta(\varphi^r)$ is the submatrix of $\widetilde{\Delta}^r$ obtained when one removes all columns and rows corresponding to all primary pivots marked up to diagonal $r - 1$ of $\widetilde{\Delta}^r$, i.e., $N(h_k^j, h_{k-1}^i; f^r) = \widetilde{\Delta}_{ij}^r$ for all $h_k^j, h_{k-1}^i \in \text{Crit}(f^r)$. We must construct f^{r+1} and prove case $r + 1$. We assume that there is a unique primary pivot $\widetilde{\Delta}_{p-r+1, p+1}^r$ on the r -th diagonal of $\widetilde{\Delta}^r$. If we have more primary pivots $\{\widetilde{\Delta}_{p-r+1, p+1}^r\}$ on the r -th diagonal of $\widetilde{\Delta}^r$, we repeat the same construction for each pair of critical points $\{(h_k^{p+1}, h_{k-1}^{p-r+1})\}$ obtaining a family of flows $\{\varphi_\ell^r\}$ such that φ_ℓ^r has exactly two less singularities than $\varphi_{\ell-1}^r$. Finally, the flow φ^{r+1} is obtained from φ^r after the cancellation of all pairs of critical points corresponding to primary pivots on the r -th diagonal. We also assume that $k = 1$, i.e. $\widetilde{\Delta}_{p-r+1, p+1}^r$ is an entry in the first block and the pair of critical points (h_1^{p+1}, h_0^{p-r+1}) is composed by a saddle and a sink. The proof of case $k = 2$ is analogous.

Dynamical cancellation:

Let $\widetilde{\Delta}_{p-r+1, p+1}^r$ be a primary pivot on the r -th diagonal of $\widetilde{\Delta}^r$. It follows from Theorem 6.4 that $\widetilde{\Delta}_{p-r+1, p+1}^r = \pm t^\ell$ or $\widetilde{\Delta}_{p-r+1, p+1}^r = \mp t^{\tilde{\ell}} \pm t^\ell$, $\ell < \tilde{\ell} \in \mathbb{Z}$. By the induction hypothesis, $\widetilde{\Delta}_{p-r+1, p+1}^r$ is a Novikov incidence coefficient between two singularities h_1^{p+1} and h_0^{p-r+1} of the flow φ^r . For each $\lambda \in \mathbb{Z}$, consider the pair of critical points $t^\lambda h_1^{p+1}$ and $t^{\lambda+\ell} h_0^{p-r+1}$ of the lift F^r of f^r to the covering space \overline{M} . Clearly F^r can be perturbed if necessary so that there are no critical points in $(F^r)^{-1}[(c_{\lambda+\ell, p-r+1}, c_{\lambda, p+1})]$ (for a nice proof of this fact see Lemma 3.2 in Salamon (1990)). Now, by Smale's First Cancellation Theorem, one can equivariantly cancel the pairs of critical points $t^\lambda h_1^{p+1}$ and $t^{\lambda+\ell} h_0^{p-r+1}$, for all $\lambda \in \mathbb{Z}$, obtaining a new Morse–Smale function $F^{r+1} : \overline{M} \rightarrow \mathbb{R}$ such that $\text{Crit}(F^{r+1}) = \text{Crit}(F^r) \setminus \{t^\lambda h_k^{p+1}, t^{\lambda+\ell} h_{k-1}^{p-r+1} \mid \lambda \in \mathbb{Z}\}$. We have the following possibilities for F^r :

- 1.a The saddle $t^\lambda h_1^{p+1}$ connects with two different sinks $t^{\lambda+\ell} h_0^{p-r+1}$ and $t^{\lambda+\tilde{\ell}} h_0^{i_0}$. It follows from Corollary 5.1 that for every other saddle $t^\delta h_1^j$

$$n(t^\delta h_1^j, t^{\lambda+\tilde{\ell}} h_0^{i_0}; F^{r+1}) = n(t^\delta h_1^j, t^{\lambda+\ell} h_0^{p-r+1}; F^r) + n(t^\delta h_1^j, t^{\lambda+\tilde{\ell}} h_0^{i_0}; F^r), \quad (6.4)$$

and

$$n(t^\delta h_1^j, t^{\lambda+\tilde{\ell}} h_0^i; F^{r+1}) = n(t^\delta h_1^j, t^{\lambda+\tilde{\ell}} h_0^i; F^r), \quad i \neq i_0 \quad (6.5)$$

If $i_0 = p - r + 1$, since the cancellation is done equivariantly, a connecting orbit in φ^r from $t^\delta h_1^j$ to $t^{\lambda+\tilde{\ell}} h_0^{i_0}$ creates a flow line starting at $t^\delta h_1^j$ with empty ω -limit set.

- 1.b The saddle $t^\lambda h_1^{p+1}$ connects with exactly one sink $t^{\lambda+\ell} h_0^{p-r+1}$. In this case the intersection numbers between critical points of F^{r+1} remain the same.

Now define $f^{r+1} : M \rightarrow \mathbb{S}^1$ given by $f^{r+1}(x) = \text{Exp} \circ F^{r+1}(y)$, where $y \in E^{-1}(x)$ for all $x \in M$. Since the cancellation was done equivariantly then f^{r+1} is a circle valued Morse function which coincides with f^r outside a neighborhood of the canceled critical points and the orbits between them and $\text{Crit}(f^{r+1}) = \text{Crit}(f^r) \setminus \{h_1^{p+1}, h_0^{p-r+1}\}$.

Consequently we have the following possibilities for f^r :

2.a $\tilde{\Delta}_{p-r+1,p+1}^r = \pm t^\ell \mp t^{\tilde{\ell}}$, where $\ell < \tilde{\ell}$. In this case there is a double connection between h_1^{p+1} and h_0^{p-r+1} in the flow φ^r . This corresponds to case 1.a for $i_0 = p-r+1$. After the equivariant cancellation, there is no birth of connections between consecutive critical points of F^{r+1} , then

$$N(h_1^j, h_0^i; f^{r+1}) = N(h_1^j, h_0^i; f^r) \text{ for all } h_1^j, h_0^i \in \text{Crit}(f^{r+1}).$$

2.b $\tilde{\Delta}_{p-r+1,p+1}^r = \pm t^\ell$. Consider all critical points $h_0^i \in \text{Crit}(f^{r+1})$ such that $i < p-r+1$. Since the entry $\tilde{\Delta}_{i,p+1}^r$ belongs to the submatrix $\Delta(\varphi^r)$, by Corollary 6.1, we have two possible cases:

- $\tilde{\Delta}_{i,p+1}^r = 0$ for all $i < p-r+1$ such that $h_0^i \in \text{Crit}(f^{r+1})$, which corresponds to case 1.b. After the equivariant cancellation, the connections between consecutive critical points of F^{r+1} remain the same, hence

$$N(h_1^j, h_0^i; f^{r+1}) = N(h_1^j, h_0^i; f^r) \text{ for all } h_1^j \in \text{Crit}(f^{r+1}).$$

- There exists $i_0 < p-r+1$ such that $h_0^{i_0} \in \text{Crit}(f^{r+1})$, $\tilde{\Delta}_{i_0,p+1}^r = \mp t^{\tilde{\ell}}$ and $\tilde{\Delta}_{i,p+1}^r = 0$ for all $i < p-r+1$ with $i \neq i_0$ and $h_0^i \in \text{Crit}(f^{r+1})$. In this case, h_1^{p+1} connects two different sinks h_0^{p-r+1} and $h_0^{i_0}$ in the flow φ^r , which corresponds to case 1.a. It follows from (6.4) that for all $h_1^j \in \text{Crit}(f^{r+1})$

$$\begin{aligned} N(h_1^j, h_0^{i_0}; f^{r+1}) &= \sum_{\lambda \in \mathbb{Z}} n(h_1^j, t^\lambda h_0^{i_0}; F^{r+1}) t^\lambda \\ &= \sum_{\lambda \in \mathbb{Z}} n(t^{\tilde{\ell}} h_1^j, t^{\lambda+\tilde{\ell}} h_0^{i_0}; F^{r+1}) t^\lambda \\ &= \sum_{\lambda \in \mathbb{Z}} \left[n(t^{\tilde{\ell}} h_1^j, t^{\lambda+\ell} h_0^{p-r+1}; F^r) + n(t^{\tilde{\ell}} h_1^j, t^{\lambda+\tilde{\ell}} h_0^{i_0}; F^r) \right] t^\lambda \\ &= \sum_{\lambda \in \mathbb{Z}} n(h_1^j, t^{\lambda+\ell-\tilde{\ell}} h_0^{p-r+1}; F^r) t^\lambda + \sum_{\lambda \in \mathbb{Z}} n(h_1^j, t^\lambda h_0^{i_0}; F^r) t^\lambda \\ &= \sum_{\lambda-(\ell-\tilde{\ell}) \in \mathbb{Z}} n(h_1^j, t^\lambda h_0^{p-r+1}; F^r) t^{\lambda-(\ell-\tilde{\ell})} + N(h_1^j, h_0^{i_0}; f^r) \\ &= N(h_1^j, h_0^{p-r+1}; f^r) t^{\tilde{\ell}-\ell} + N(h_1^j, h_0^{i_0}; f^r). \end{aligned}$$

Moreover, $N(h_1^j, h_0^i; f^{r+1}) = N(h_1^j, h_0^i; f^r)$ for $i \neq i_0$.

Algebraic-Dynamical Correspondence

Let $\tilde{\Delta}_{p-r+1,p+1}^r$ be a primary pivot. We must analyze the entries $\tilde{\Delta}_{i,j}^{r+1}$ with $i < p - r + 1$ and $j > p + 1$. If there is a primary pivot in column/row i or column/row j , then the $\tilde{\Delta}_{i,j}^{r+1}$ is not in $\Delta(\varphi^{r+1})$. Otherwise,

$$\tilde{\Delta}_{i,j}^{r+1} = \tilde{\Delta}_{i,j}^r - \frac{\tilde{\Delta}_{p-r+1,j}^r}{\tilde{\Delta}_{p-r+1,p+1}^r} \tilde{\Delta}_{i,p+1}^r. \quad (6.6)$$

Consider the case where the entry $\tilde{\Delta}_{i,j}^r$ is such that $h_1^j, h_0^i \in \text{Crit}(f^{r+1})$. Hence, there are no primary pivots in column/row i nor in column/row j and $\tilde{\Delta}_{i,j}^r$ is an entry of $\Delta(\varphi^r)$ of f^r .

3.a If $\tilde{\Delta}_{p-r+1,p+1}^r = \pm t^\ell \mp t^{\tilde{\ell}}$, it follows from Corollary 6.1 that $\tilde{\Delta}_{i,p+1}^r = 0$ for $i < p - r + 1$ and $h_0^i \in \text{Crit}(f^{r+1})$. Thus, $\tilde{\Delta}_{i,j}^{r+1} = \tilde{\Delta}_{i,j}^r$. By the induction hypothesis and item 2.a $\tilde{\Delta}_{i,j}^{r+1} = N(h_1^j, h_0^i; f^{r+1})$, for all j such that $h_1^j \in \text{Crit}(f^{r+1})$.

3.b If $\tilde{\Delta}_{p-r+1,p+1}^r = \pm t^\ell$, we have two cases to consider.

- $\tilde{\Delta}_{i,p+1}^r = 0$ for all $i < p - r + 1$ such that $h_0^i \in \text{Crit}(f^{r+1})$. In this case, $\tilde{\Delta}_{i,j}^{r+1} = \tilde{\Delta}_{i,j}^r$ and, by the induction hypothesis and 2.b we have that $\tilde{\Delta}_{i,j}^{r+1} = N(h_1^j, h_0^i; f^{r+1})$.

- there exists $i_0 < p - r + 1$ with $h_0^{i_0} \in \text{Crit}(f^{r+1})$, $\tilde{\Delta}_{i_0,p+1}^r = \mp t^{\tilde{\ell}}$ and $\tilde{\Delta}_{i,p+1}^r = 0$ for all $i < p - r + 1$ with $i \neq i_0$ and $h_0^i \in \text{Crit}(f^{r+1})$. By (6.6), $\tilde{\Delta}_{i,j}^{r+1} = \tilde{\Delta}_{i,j}^r + \tilde{\Delta}_{p-r+1,j}^r t^{\tilde{\ell}-\ell}$. It follows from the induction hypothesis $\tilde{\Delta}_{i,j}^r = N(h_1^j, h_0^i; f^r)$ and $\tilde{\Delta}_{p-r+1,j}^r = N(h_1^j, h_0^p; f^r)$, hence, by 2.b we have that $\tilde{\Delta}_{i,j}^{r+1} = N(h_1^j, h_0^i; f^{r+1})$.

□

An important consequence of the proof of Theorem 6.10 is that the spectral sequence detects the birth of periodic orbits in the family f^r of circle valued Morse functions.

Theorem 6.11 (Detecting Periodic Orbits). *Suppose we are under the hypothesis of Theorem 6.10. Then there exists a family of circle valued Morse functions $\{f^r\}_{r \geq 1}$ as in Theorem 6.10(1) such that, for each algebraic cancellation corresponding to a binomial primary pivot $\Delta_{p-r+1,p+1}^r = \mp t^\ell \pm t^{\tilde{\ell}}$, the associated dynamical cancellation of critical points h_k^{p+1} and h_{k-1}^{p-r+1} causes the birth of a periodic orbit which crosses the regular value $f^{-1}(a) |\tilde{\ell} - \ell|$ times. This periodic orbit is an attractor if $k = 0$ and it is a repeller if $k = 1$.*

Proof. Suppose that $\Delta_{p-r+1,p+1}^r = \mp t^\ell \pm t^{\tilde{\ell}}$ is a binomial primary pivot. Then by the Smale's First Cancellation Theorem the pairs of critical points $t^\lambda h_k^{p+1}$ and $t^{\lambda+\ell} h_{k-1}^{p-r+1}$ of F^r in the covering space \overline{M} cancel equivariantly for all $\lambda \in \mathbb{Z}$. Moreover, the function F^{r+1} coincides with F^r outside a neighborhood U of the canceled critical points and the connecting orbit between them and a flow line γ from $t^{\lambda-\ell} h_k^{p+1}$ to $t^{\lambda+\tilde{\ell}} h_{k-1}^{p-r+1}$ arises in the negative gradient flow of F^{r+1} . Choosing the diffeomorphism given by Assertion 4 in Chapter 5 of Milnor (2015) such that γ coincides outside of U with the flow lines of the negative gradient flow of F^r going from $t^{\lambda-\ell} h_k^{p+1}$ to $t^{\lambda+\ell} h_{k-1}^{p-r+1}$ and from $t^\lambda h_k^{p+1}$ to $t^{\lambda+\tilde{\ell}} h_{k-1}^{p-r+1}$ when we cancel equivariantly in \overline{M} , we obtain a periodic orbit on the negative gradient flow of f^{r+1} on M . \square

Conclusion

In this book, we have presented state of the art tools in homotopy theory applied to dynamical systems by means of introducing Conley index theory and spectral sequence analysis for gradient-like flows. The far reaching spectrum of the techniques presented herein encompass different classes of smooth flows such as, Morse flows, Morse–Smale flows and Novikov flows.

We explored both the local homotopical invariants of the chain recurrent components, as well as the global invariants associated to the phase space. Many of these invariants are recorded in Lyapunov graphs which turn out to be useful global combinatorial objects that address questions of realization and Morsification of their associated flows.

Also, by defining adequate filtered Morse chain complexes in each of the classes above, the calculation via the dynamical spectral sequence of this complex has provided in depth knowledge into cancellation of critical points through the death and birth of connections.

As we have emphasized several times throughout this text, the power of Conley index theory in dealing with nonsmooth vector fields, in particular piecewise smooth vector fields is remarkable. This, in fact, has opened a new frontier of research that bridges Dynamical Systems and Singularity Theory.

We would like to close our final remarks by giving the reader a sneak preview of this new frontier conquered by using the techniques described in this book. We refer the reader to references Grulha Jr. et al. (2022, 2023), Lima, de Rezende, and Raminelli (2021), and Montúfar and de Rezende (2020), for the complete works.

In Gutierrez and Sotomayor (1982), it was proven that the conditions for structural stability of C^1 -vector fields, proven in the smooth case by Peixoto (1963), still hold in a non-smooth two-manifold M with singular locus composed by: cones \mathcal{C} , cross-caps \mathcal{W} , double \mathcal{D} and triple points \mathcal{T} . Hence, by considering the continuous flow associated to these piecewise smooth vector fields defined in Gutierrez and Sotomayor (1982), and henceforth called GS flows, one can apply the techniques in Chapter 1 to compute the Conley index of GS singularities. In Figure 6.29, we present a cross-cap singularity p of

repelling nature as well as its isolating block. The homotopy Conley index of p is

$$h(S) = \mathbb{S}^2 \vee \mathbb{S}^2,$$

hence the homology Conley index of p is given by:

$$CH_i(p) = \begin{cases} \mathbb{Z} \oplus \mathbb{Z}, & \text{if } i = 2 \\ 0, & \text{otherwise.} \end{cases}$$

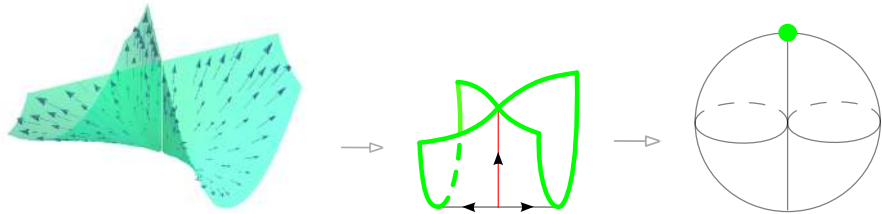


Figure 6.29: Cross-cap singularity and its homotopy Conley index.

By using the Poincaré–Hopf equalities in Chapters 2 and 4, a complete classification of Lyapunov semigraphs associated to isolating blocks of GS singularities is now made possible. Furthermore, global realization theorems for Lyapunov graphs associated to GS flows on singular 2-manifolds can be obtained. See Figures 6.30 and 6.31.

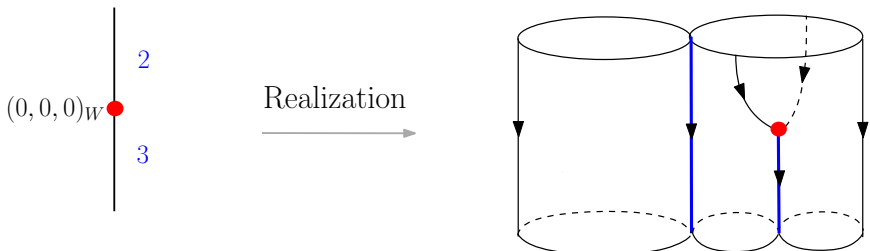


Figure 6.30: Realization of an abstract Lyapunov semigraph

By using the full power of the homotopical invariance of the Conley index, it is possible to speak of a homotopical deformation of the phase space while still retaining the homological index. By using the techniques in Chapter 5, a filtered GS chain complex can now be defined and its dynamical spectral sequence computed. See Figures 6.32 and 6.36.

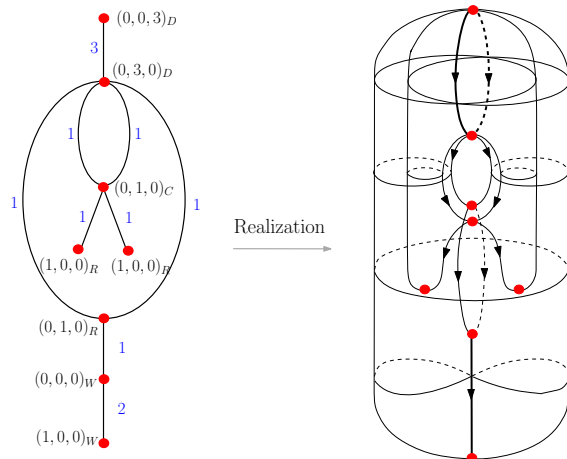
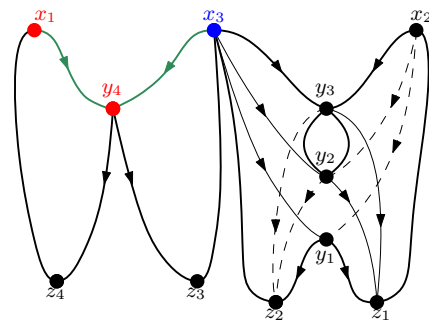
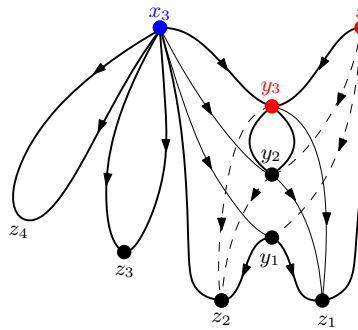


Figure 6.31: Realization of an abstract Lyapunov graph labelled with GS singularities as a GS flow on a singular 2-manifold



$$\begin{aligned}
 E^0 & \quad \mathbb{Z}[z_1] \quad \mathbb{Z}[z_2] \quad \mathbb{Z}[z_3] \quad \mathbb{Z}[z_4] \quad \mathbb{Z}[y_1] \quad \mathbb{Z}[y_2] \quad \mathbb{Z}[y_3] \quad \mathbb{Z}[y_4] \quad \mathbb{Z}[x_1] \quad \mathbb{Z}[x_2] \quad \mathbb{Z}[x_3] \\
 E^1 & \quad \mathbb{Z}[z_1] \quad \mathbb{Z}[z_2] \quad \mathbb{Z}[z_3] \quad \mathbb{Z}[z_4] \quad \mathbb{Z}[y_1] \quad \mathbb{Z}[y_2] \quad \mathbb{Z}[y_3] \quad \mathbb{Z}[y_4] \quad \mathbb{Z}[x_1] \quad \mathbb{Z}[x_2] \quad \mathbb{Z}[x_3]
 \end{aligned}$$

Figure 6.32: Algebraic-dynamical correspondence detected by Δ^1 .

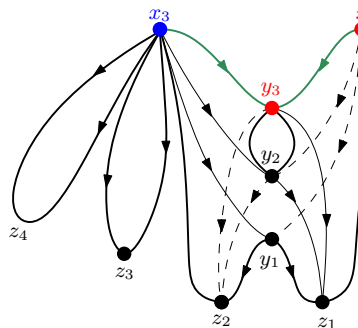


$$E^0 \quad \mathbb{Z}[z_1] \quad \mathbb{Z}[z_2] \quad \mathbb{Z}[z_3] \quad \mathbb{Z}[z_4] \quad \mathbb{Z}[y_1] \quad \mathbb{Z}[y_2] \quad \mathbb{Z}[y_3] \quad \mathbb{Z}[y_4] \quad \mathbb{Z}[x_1] \quad \mathbb{Z}[x_2] \quad \mathbb{Z}[x_3]$$

$$E^1 \quad \mathbb{Z}[z_1] \quad \mathbb{Z}[z_2] \quad \mathbb{Z}[z_3] \quad \mathbb{Z}[z_4] \quad \mathbb{Z}[y_1] \quad \mathbb{Z}[y_2] \quad \mathbb{Z}[y_3] \quad \mathbb{Z}[y_4] \quad \mathbb{Z}[x_1] \quad \mathbb{Z}[x_2] \quad \mathbb{Z}[x_3]$$

$$E^2 \quad \mathbb{Z}[z_1] \quad \mathbb{Z}[z_2] \quad \mathbb{Z}[z_3] \quad \mathbb{Z}[z_4] \quad \mathbb{Z}[y_1] \quad \mathbb{Z}[y_2] \quad \mathbb{Z}[y_3] \quad 0 \quad 0 \quad \mathbb{Z}[x_2] \quad \mathbb{Z}[x_3]$$

Figure 6.33: Algebraic-dynamical correspondence detected by Δ^2 .



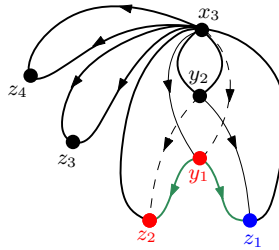
$$E^0 \quad \mathbb{Z}[z_1] \quad \mathbb{Z}[z_2] \quad \mathbb{Z}[z_3] \quad \mathbb{Z}[z_4] \quad \mathbb{Z}[y_1] \quad \mathbb{Z}[y_2] \quad \mathbb{Z}[y_3] \quad \mathbb{Z}[y_4] \quad \mathbb{Z}[x_1] \quad \mathbb{Z}[x_2] \quad \mathbb{Z}[x_3]$$

$$E^1 \quad \mathbb{Z}[z_1] \quad \mathbb{Z}[z_2] \quad \mathbb{Z}[z_3] \quad \mathbb{Z}[z_4] \quad \mathbb{Z}[y_1] \quad \mathbb{Z}[y_2] \quad \mathbb{Z}[y_3] \quad \mathbb{Z}[y_4] \quad \mathbb{Z}[x_1] \quad \mathbb{Z}[x_2] \quad \mathbb{Z}[x_3]$$

$$E^2 \quad \mathbb{Z}[z_1] \quad \mathbb{Z}[z_2] \quad \mathbb{Z}[z_3] \quad \mathbb{Z}[z_4] \quad \mathbb{Z}[y_1] \quad \mathbb{Z}[y_2] \quad \mathbb{Z}[y_3] \quad 0 \quad 0 \quad \mathbb{Z}[x_2] \quad \mathbb{Z}[x_3]$$

$$E^3 \quad \mathbb{Z}[z_1] \quad \mathbb{Z}[z_2] \quad \mathbb{Z}[z_3] \quad \mathbb{Z}[z_4] \quad \mathbb{Z}[y_1] \quad \mathbb{Z}[y_2] \quad \mathbb{Z}[y_3] \quad 0 \quad 0 \quad \mathbb{Z}[x_2] \quad \mathbb{Z}[x_3]$$

Figure 6.34: Algebraic-dynamical correspondence detected by Δ^3 .

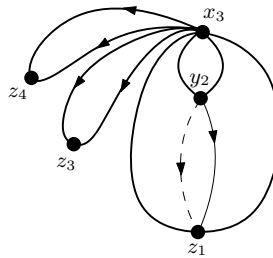


$$\begin{array}{ccccccccc}
 E^0 & \mathbb{Z}[z_1] & \mathbb{Z}[z_2] & \mathbb{Z}[z_3] & \mathbb{Z}[z_4] & \mathbb{Z}[y_1] & \mathbb{Z}[y_2] & \mathbb{Z}[y_3] & \mathbb{Z}[y_4] & \mathbb{Z}[x_1] & \mathbb{Z}[x_2] & \mathbb{Z}[x_3] \\
 E^1 & \mathbb{Z}[z_1] & \mathbb{Z}[z_2] & \mathbb{Z}[z_3] & \mathbb{Z}[z_4] & \mathbb{Z}[y_1] & \mathbb{Z}[y_2] & \mathbb{Z}[y_3] & \mathbb{Z}[y_4] & \mathbb{Z}[x_1] & \mathbb{Z}[x_2] & \mathbb{Z}[x_3] \\
 E^2 & \mathbb{Z}[z_1] & \mathbb{Z}[z_2] & \mathbb{Z}[z_3] & \mathbb{Z}[z_4] & \mathbb{Z}[y_1] & \mathbb{Z}[y_2] & \mathbb{Z}[y_3] & 0 & 0 & \mathbb{Z}[x_2] & \mathbb{Z}[x_3] \\
 E^3 & \mathbb{Z}[z_1] & \mathbb{Z}[z_2] & \mathbb{Z}[z_3] & \mathbb{Z}[z_4] & \mathbb{Z}[y_1] & \mathbb{Z}[y_2] & \mathbb{Z}[y_3] & 0 & 0 & \mathbb{Z}[x_2] & \mathbb{Z}[x_3]
 \end{array}$$

d_8^1

d_4^3

d_9^3

Figure 6.35: Algebraic-dynamical correspondence detected by Δ^3 .

$$\begin{array}{ccccccccc}
 E^0 & \mathbb{Z}[z_1] & \mathbb{Z}[z_2] & \mathbb{Z}[z_3] & \mathbb{Z}[z_4] & \mathbb{Z}[y_1] & \mathbb{Z}[y_2] & \mathbb{Z}[y_3] & \mathbb{Z}[y_4] & \mathbb{Z}[x_1] & \mathbb{Z}[x_2] & \mathbb{Z}[x_3] \\
 E^1 & \mathbb{Z}[z_1] & \mathbb{Z}[z_2] & \mathbb{Z}[z_3] & \mathbb{Z}[z_4] & \mathbb{Z}[y_1] & \mathbb{Z}[y_2] & \mathbb{Z}[y_3] & \mathbb{Z}[y_4] & \mathbb{Z}[x_1] & \mathbb{Z}[x_2] & \mathbb{Z}[x_3] \\
 E^2 & \mathbb{Z}[z_1] & \mathbb{Z}[z_2] & \mathbb{Z}[z_3] & \mathbb{Z}[z_4] & \mathbb{Z}[y_1] & \mathbb{Z}[y_2] & \mathbb{Z}[y_3] & 0 & 0 & \mathbb{Z}[x_2] & \mathbb{Z}[x_3] \\
 E^3 & \mathbb{Z}[z_1] & \mathbb{Z}[z_2] & \mathbb{Z}[z_3] & \mathbb{Z}[z_4] & \mathbb{Z}[y_1] & \mathbb{Z}[y_2] & \mathbb{Z}[y_3] & 0 & 0 & \mathbb{Z}[x_2] & \mathbb{Z}[x_3] \\
 E^4 & \mathbb{Z}[z_1] & 0 & \mathbb{Z}[z_3] & \mathbb{Z}[z_4] & 0 & \mathbb{Z}[y_2] & 0 & 0 & 0 & 0 & \mathbb{Z}[x_3]
 \end{array}$$

d_8^1

d_4^3

d_9^3

Figure 6.36: Algebraic-dynamical correspondence detected by Δ^4 .

Bibliography

- R. K. Ahuja, T. L. Magnanti, and J. B. Orlin (1993). *Network Flows: Theory, Applications and Algorithms*. Prentice-Hall, Englewood Cliffs, New Jersey, USA, pp. xvi+846. MR: 1205775. Zbl: 1201.90001 (cit. on p. 85).
- A. Banyaga and D. Hurtubise (2004). *Lectures on Morse homology*. Springer. MR: 2145196. Zbl: 1080.57001 (cit. on pp. 9, 205).
- M. A. Bertolim, D. V. S. Lima, M. P. Mello, K. A. de Rezende, and M. R. da Silveira (2016). “A global two-dimensional version of Smale’s Cancellation theorem via spectral sequences.” *Ergodic Theory and Dynamical Systems* 36.6, pp. 1795–1838. MR: 3530467. Zbl: 1378.37031 (cit. on pp. 196, 205, 209, 239, 250, 251, 256).
- (2017). “Algebraic and dynamical cancellations associated to spectral sequence.” *European Journal of Mathematics* 3, pp. 387–428. MR: 3695060. Zbl: 1374.37027 (cit. on pp. 196, 239, 250, 255, 256).
- M. A. Bertolim, M. P. Mello, and K. A. de Rezende (2003a). “Lyapunov graph continuation.” *Ergodic Theory and Dynamical Systems* 23.1, pp. 1–58. MR: 1971195. Zbl: 1140.37310 (cit. on pp. 51, 83, 100, 174).
- (2003b). “Lyapunov graph continuation.” *Ergodic Theory and Dynamical Systems* 23.1, pp. 1–58. MR: 1971195. Zbl: 1140.37310 (cit. on p. 68).
- (2005a). “Poincaré–Hopf and Morse inequalities for Lyapunov graphs.” *Ergodic Theory and Dynamical Systems* 25.1, pp. 1–39. MR: 2122910. Zbl: 1084.37013 (cit. on pp. 108, 110, 119, 120, 127, 174).
- (2005b). “Poincaré–Hopf inequalities.” *Transactions of the American Mathematical Society* 357.10, pp. 4091–4129. MR: 2159701. Zbl: 1134.37316 (cit. on pp. 108–110, 119, 120, 124).
- M. A. Bertolim, K. A. de Rezende, and O. Manzoli Neto (2007). “Isolating blocks for periodic orbits.” *Journal of dynamical and control systems* 13.1, pp. 121–134. MR: 2288945. Zbl: 1116.37010 (cit. on pp. 173, 174, 186, 187, 190).

- M. A. Bertolim, K. A. de Rezende, O. Manzoli Neto, and G. M. Vago (2006). “Isolating blocks for Morse flows.” *Geometriae Dedicata* 121, pp. 19–41. MR: 2276233. Zbl: 1105.37009 (cit. on pp. 173, 174, 177, 180, 182, 185, 190).
- M. A. Bertolim, K. A. de Rezende, and G. M. Vago (2006). “Minimal Morse flows on compact manifolds.” *Topology and its Applications* 153.18, pp. 3450–3466. MR: 2270598. Zbl: 1105.37019 (cit. on pp. 173, 179, 190).
- C. Conley (1978). *Isolated invariant sets and the Morse index*. 38. American Mathematical Soc. (cit. on pp. 15, 32, 64, 184).
- C. Conley and R. Easton (1971). “Isolated invariant sets and isolating blocks.” *Transactions of the American Mathematical Society* 158.1, pp. 35–61. MR: 0279830. Zbl: 0223.58011 (cit. on pp. 19, 21).
- O. Cornea (1989). “The genus and the fundamental group of high-dimensional manifolds.” *Stud. Cerc. Mat* 41.3, pp. 169–178. MR: 1010874. Zbl: 0694.57015 (cit. on p. 58).
- O. Cornea, K. A. de Rezende, and M. R. da Silveira (2010). “Spectral sequences in Conley’s theory.” *Ergodic Theory and Dynamical Systems* 30.4, pp. 1009–1054. MR: 2669409. Zbl: 1210.37009 (cit. on pp. 196, 212, 214, 219, 221, 229, 232, 234, 237, 270).
- R. N. Cruz, M. P. Mello, and K. A. de Rezende (2005). “Realizability of the Morse polytope.” *Qual. Theory Dyn. Syst.* 6.1, pp. 59–86. MR: MR2273490(2007i:37030) (cit. on pp. 84, 135).
- R. N. Cruz and K. A. de Rezende (1998). “Cycle Rank of Lyapunov Graphs and the Genera of Manifolds.” *Proceedings of the American Mathematical Society* 126.12, pp. 3715–3720. MR: 1618654. Zbl: 0926.57032 (cit. on p. 67).
- (1999). “Gradient-like flows on high-dimensional manifolds.” *Ergodic Theory and Dynamical Systems* 19.2, pp. 339–362. MR: 1685397. Zbl: 0942.37012 (cit. on pp. 56, 60, 61, 68, 173, 174, 185, 187, 190, 255).
- J. F. Davis and P. Kirk (2001). *Lecture notes in algebraic topology*. Vol. 35. American Mathematical Soc. Zbl: 1018.55001 (cit. on p. 197).
- J. Eells and N. H. Kuiper (1962). “Manifolds which are like projective planes.” *Publications Mathématiques de l’IHÉS* 14, pp. 5–46 (cit. on p. 179).
- L. R. Ford and D. R. Fulkerson (1962). *Flow in networks*. Princeton University Press, Princeton, NJ, pp. xiv+194. MR: 0159700 (cit. on p. 85).
- J. Franks (1982). *Homology and dynamical systems*. American Mathematical Soc. MR: 0669378. Zbl: 0497.58018 (cit. on pp. ix, 64, 67, 185, 191).
- (1985). “Nonsingular Smale flows on S^3 .” *Topology* 24.3, pp. 265–282. MR: 0815480. Zbl: 0609.58039 (cit. on p. 160).
- (1988). “A variation on the Poincaré–Birkhoff theorem.” *Contemp. Math* 81, pp. 111–117. MR: 0986260 (cit. on p. 15).
- R. Franzosa (1986). “Index filtrations and the homology index braid for partially ordered Morse decompositions.” *Transactions of the American Mathematical Society* 298.1, pp. 193–213. MR: 0857439. Zbl: 0626.58013 (cit. on pp. 39, 256).

- (1988). “The continuation theory for Morse decompositions and connection matrices.” *Transactions of the American Mathematical Society* 310.2, pp. 781–803. MR: 0973177. Zbl: 0708.58021 (cit. on p. 35).
- (1989). “The Connection Matrix Theory for Morse decompositions.” *Transactions of the American Mathematical Society* 311.2, pp. 561–592. MR: 0978368. Zbl: 0689 . 58030 (cit. on pp. 15, 191, 209, 256).
- R. Franzosa and K. Mischaikow (1998). “Algebraic transition matrices in the Conley index theory.” *Trans. Amer. Math. Soc.* 350.3, pp. 889–912. MR: 1360223. Zbl: 0896 . 58053 (cit. on p. 256).
- R. Franzosa and K. A. de Rezende (1993). “Lyapunov graphs and flows on surfaces.” *Trans. Amer. Math. Soc.* 340.2, pp. 767–784. MR: MR1127155(94b : 58086). Zbl: 0806 . 58042 (cit. on p. 58).
- R. Franzosa, K. A. de Rezende, and M. R. da Silveira (2014). “Continuation and bifurcation associated to the dynamical spectral sequence.” *Ergodic Theory and Dynamical Systems* 34.6, pp. 1849–1887. MR: 3272775. Zbl: 1314 . 37012 (cit. on pp. 196, 256).
- D. R. Fulkerson and O. Gross (1965). “Incidence matrices and interval graphs.” *Pacific journal of mathematics* 15.3, pp. 835–855. MR: 0186421. Zbl: 0132 . 21001 (cit. on p. 120).
- N. G. Grulha Jr., D. V. S. Lima, K. A. de Rezende, and M. A. J. Zigart (Aug. 2022). “Gutierrez–Sotomayor flows on singular surfaces.” *Topological Methods in Nonlinear Analysis* 60.1, pp. 221–265. MR: 4524867. Zbl: 07609701 (cit. on p. 302).
- (2023). “Conley Index Theory for Gutierrez–Sotomayor flows on singular 3-manifolds.” *Topological Methods in Nonlinear Analysis*. MR: 4524867 (cit. on p. 302).
- C. Gutierrez and J. Sotomayor (1982). “Stable vector fields on manifolds with simple singularities.” *Proceedings of the London Mathematical Society* 3.1, pp. 97–112. MR: 0662665. Zbl: 0504 . 58027 (cit. on p. 302).
- A. Hatcher (2002). *Algebraic topology*. 556. Cambridge University Press. MR: 1867354. Zbl: 1044 . 55001 (cit. on p. 30).
- A. J. Hoffman and J. B. Kruskal (1956). “Integral boundary points of convex polyhedra.” In: *Linear Inequalities and Related Systems. (AM-38)*. Vol. 38. Annals of Mathematics Studies. Princeton, NJ, USA: Princeton University Press, pp. 223–246. MR: 0085148. Zbl: 0072 . 37803 (cit. on p. 120).
- M. Hurley (1991). “Chain recurrence and attraction in non-compact spaces.” *Ergodic Theory and Dynamical Systems* 11.4, pp. 709–729. MR: 1145617. Zbl: 0785 . 58033 (cit. on p. 15).
- (1992). “Noncompact chain recurrence and attraction.” *Proceedings of the American Mathematical Society* 115.4, pp. 1139–1148. MR: 1098401. Zbl: 0759 . 58031 (cit. on p. 15).
- B. Korte and J. Vygen (2012). *Combinatorial optimization*. Vol. 21. Algorithms and Combinatorics book series (AC, volume 21). Springer. MR: 2850465. Zbl: 1237 . 90001 (cit. on p. 96).

- E. L. Lawler (2001). *Combinatorial Optimization: Networks and Matroids*. Dover Books on Mathematics Series. Dover Publications. MR: 1828330. Zbl: 1058.90057 (cit. on p. 85).
- G. G. E. Ledesma, O. Manzoli Neto, and K. A. de Rezende (2015). “Smale flows on $\mathbb{S}^2 \times \mathbb{S}^1$.” *Ergodic Theory and Dynamical Systems* 35.5, pp. 1546–1581. MR: 3365733. Zbl: 1352.37128 (cit. on pp. 163, 164).
- G. G. E. Ledesma, O. Manzoli Neto, K. A. de Rezende, and G. M. Vago (2018). “Lyapunov graphs for circle valued functions.” *Topology and its Applications* 245, pp. 62–91. MR: 3823990. Zbl: 1395.37011 (cit. on pp. 260, 262).
- D. V. S. Lima, O. Manzoli Neto, and K. A. de Rezende (2019). “On handle theory for Morse–Bott critical manifolds.” *Geometriae Dedicata* 202, pp. 265–309. MR: 4001817. Zbl: 1431.37010 (cit. on p. 68).
- D. V. S. Lima, O. Manzoli Neto, K. A. de Rezende, and M. R. da Silveira (Dec. 2017). “Cancellations for circle-valued Morse functions via spectral sequences.” 51, pp. 259–311. MR: 3784745. Zbl: 1393.37016 (cit. on pp. 196, 264, 266, 280, 282, 286).
- D. V. S. Lima and K. A. de Rezende (Apr. 2016). “Connection matrices for Morse–Bott flows.” *Topological Methods in Nonlinear Analysis* 44.2, pp. 471–495. Zbl: 1362 . 37040 (cit. on pp. 15, 35).
- D. V. S. Lima, K. A. de Rezende, and S. A. Raminelli (2021). “Homotopical Cancellation Theory for Gutierrez–Sotomayor Singular Flows.” *Journal of Singularities* 23, pp. 33–91. MR: 4243604. Zbl: 1469.58023 (cit. on p. 302).
- D. V. S. Lima, K. A. de Rezende, and M. R. da Silveira (2023). “Cancellations of Periodic Orbits for Nonsingular Morse–Smale Flows.” To appear in Ergodic Theory and Dynamical Systems (cit. on p. 256).
- J. Milnor (1963). *Morse theory, Based on lecture notes by M. Spivak and R. Wells*. 51. Princeton University Press. MR: 0163331. Zbl: 0108.10401 (cit. on pp. 9, 10, 61).
- (2015). *Lectures on the h-cobordism theorem*. Vol. 2258. Princeton University Press. MR: 0190942 (cit. on pp. 9, 48, 255, 301).
- H. Montúfar and K. A. de Rezende (2020). “Conley theory for Gutierrez–Sotomayor fields.” *Journal of Singularities* 22, pp. 241–277. MR: 4192702. Zbl: 1456 . 37024 (cit. on p. 302).
- M. Morse (1925). “Relations Between the Critical Points of a Real Function of n Independent Variables.” *Transactions of the American Mathematical Society* 27.3, pp. 345–396. MR: 1501318. Zbl: 51.0451.01 (cit. on p. 60).
- A. Pajitnov (2008). *Circle-valued Morse theory*. Vol. 32. Walter de Gruyter. MR: 2319639 (cit. on pp. 205, 264, 265).
- J. Palis and W. de Melo (2012). *Geometric theory of dynamical systems: an introduction*. Springer Science & Business Media (cit. on pp. 6, 7).
- M. M. Peixoto (1963). “Structural stability on two-dimensional manifolds: A further remark.” *Topology* 2.1-2, pp. 179–180. MR: 0149037. Zbl: 0116.06802 (cit. on p. 302).
- J. F. Reineck (1990). “The connection matrix in Morse–Smale flows.” *Transactions of the American Mathematical Society* 322.2, pp. 523–545. MR: 0972705. Zbl: 0714.58027 (cit. on pp. 15, 35, 209).

- (1995). “The connection matrix in Morse–Smale flows. II.” *Transactions of the American Mathematical Society* 347.6, pp. 2097–2110. MR: 1290731. Zbl: 0831 . 58031 (cit. on pp. 15, 35, 209).
- K. A. de Rezende (1987). “Smale flows on the three-sphere.” *Transactions of the American Mathematical Society* 303.1, pp. 283–310. MR: 0896023. Zbl: 0625 . 58019 (cit. on pp. 64, 158).
- (1993). “Gradient-like flows on 3-manifolds.” *Ergodic Theory and Dynamical Systems* 13.3, pp. 557–580. MR: 1245829. Zbl: 0822 . 57013 (cit. on p. 155).
- K. A. de Rezende and R. Franzosa (1993). “Lyapunov graphs and flows on surfaces.” *Transactions of the American Mathematical Society*, pp. 767–784. MR: 1127155. Zbl: 0806 . 58042 (cit. on pp. 150, 153).
- K. A. de Rezende, M. P. Mello, and M. R. da Silveira (2010). “Conley’s spectral sequence via the sweeping algorithm.” *Topology and its Applications* 157.13, pp. 2111–2130. MR: 2665234. Zbl: 1201 . 37019 (cit. on pp. 196, 219, 280).
- R. T. Rockafellar (1969). “The elementary vectors of a subspace of R^N .” In: *Combinatorial Mathematics and its Applications (Proc. Conf., Univ. North Carolina, Chapel Hill, N.C., 1967)*. Chapel Hill, N. C.: Univ. North Carolina Press, pp. 104–127. MR: MR0278972 (cit. on p. 88).
- D. Salamon (1985). “Connected simple systems and the Conley index of isolated invariant sets.” *Transactions of the American Mathematical Society* 291.1, pp. 1–41. MR: 0797044. Zbl: 0573 . 58020 (cit. on pp. 19, 21, 30, 36, 39).
- (1990). “Morse theory, the Conley index and Floer homology.” *Bull. London Math. Soc* 22.2, pp. 113–140. MR: 1045282. Zbl: 0709 . 58011 (cit. on pp. 191, 205, 208, 209, 256, 298).
- A. Schrijver (1986). *Theory of linear and integer programming*. Wiley-Interscience Series in Discrete Mathematics. A Wiley-Interscience Publication. Chichester: John Wiley & Sons Ltd., pp. xii+471. MR: 874114(88m : 90090) (cit. on p. 88).
- S. Smale (1961). “On gradient dynamical systems.” *Ann. Math.* 74.1, pp. 199–206. MR: 0133139. Zbl: 0136 . 43702 (cit. on p. 205).
- J. Smoller (2012). *Shock waves and reaction-diffusion equations*. Vol. 258. Springer Science & Business Media. MR: 0688146 (cit. on p. 32).
- E. Spanier (1989). *Algebraic topology*. Springer Science & Business Media. MR: 0210112 (cit. on pp. 197, 200).
- J. Weber (2006). “The Morse–Witten complex via dynamical systems.” *Expositiones Mathematicae* 24.2, pp. 127–159. MR: 2243274. Zbl: 1134 . 37324 (cit. on pp. 191, 205–207).

List of Symbols

- $\bar{0}$ homotopy type of the pointed one-point space, page 21
- $\bar{1}$ homotopy type of the pointed two-point space, page 21
- A^* dual repeller of A in S , page 36
- $C(A, A^*)$ set of connecting orbits of S with respect to the pair (A, A^*) , page 36
- $CH_*(S, \varphi)$ homology Conley index of S with respect to φ , page 29
- $CH(S)$ homology Conley index of S , page 29
- \mathcal{M}_{xy} connecting manifold of x and y , page 205
- $\mathcal{D}(S)$ \prec -ordered Morse decomposition of an isolated invariant set S , page 38
- $h(S)$ homotopy Conley Index of S , page 21
- $n(x, y)$ intersection number of the critical points x and y , page 207
- $\text{Inv}(N)$ maximal invariant set of N , page 5
- $\text{Inv}(N, \varphi)$ maximal invariant set of N with respect to φ , page 5
- $(C_*(f), \partial_*)$ Morse complex associated to f , page 209
- $C_k(f)$ Morse group, page 209
- M_I Morse sets, page 39
- \mathcal{M}_{xy} moduli space between x and y , page 205

- $(\mathcal{N}_*(f), \partial)$ Novikov complex, page 265
- $N(p, q; f)$ Novikov incidence coefficient between p and q , page 265
- N/L pointed space $(N/\sim, [L])$, page 20
- N^- exiting set of N , page 20
- N^+ entering set of N , page 20
- $\omega(Y)$ ω -limit set of Y , page 6
- $\mathcal{O}_\varphi(x)$ orbit of $x \in X$ with respect to the flow φ , page 2
- $\mathcal{R}(\varphi)$ set of chain recurrent points with respect to φ , page 11
- \mathcal{R} set of chain recurrent points, page 11
- Σ^n homotopy type of a pointed n -sphere, page 21
- $W^s(x), W^u(x)$ stable and the unstable manifolds of x , page 205
- \mathbb{S}^n n -dimensional sphere, page 8
- (E^r, d^r) Spectral Sequence, page 197
- $G(C)$ Graded module associated to the chain complex C , page 200
- $X \sqcup Y$ wedge sum of X and Y , page 25
- $X \wedge Y$ smash product of X and Y , page 26

Index

- α -limit set, 5
 ω -limit set, 5
 h_{κ}^{cd} -system, 83, 89
 $\mathcal{H}_{\kappa}^{cd}$ polytope, 100
 κ -connectivity inequality, 109
ntd-labelling, 135, 136
- A**
admissible Lyapunov graph
 of Morse type, 175
admissible ordering, 39
algebraic cancellation, 243
arc, 85
associated graded module, 200
attaching
 map, 61
 region, 61
 sphere, 61
attractor, 35
attractor-repeller
 decomposition, 36
 pair, 36
- B**
backward arc, 95
belt
 region, 61
- sphere, 61
Betti number vector, 59, 65
- C**
chain recurrent
 point, 11
 set, 11
characteristic sign, 207
circle valued Morse function, 258
circular Lyapunov digraph, 261
circulation, 87
 elementary, 87
complementarity condition, 112
conformal vectors, 88
Conley duality condition, 51
Conley index
 homology, 29
 homotopy, 21
Conley Polynomial, 40
Conley's Fundamental Theorem of
 Dynamical Systems, 13
connecting manifold, 205
connecting orbit, 36
cycle, 86
cycle number, 65, 172

D

directed graph, 85
 connected, 88
 directed network, 87
 directed semigraph, 64
 directed subgraph, 86

E

exit set, 18
 extreme point, 88

F

filtration
 bounded below, 200
 convergent, 200
 finest, 212
 finite, 200
 increasing, 199
 fixed point, 2
 flow, 87
 chain recurrent, 12
 continuous, 1
 generated by a vector field, 2
 gradient-like, 12
 negative gradient, 7
 strongly gradient-like, 12
 flow conservation equation, 87
 flow-ordering, 39
 function
 additive, 48
 subadditive, 48
 fundamental cobordism, 259

G

gap, 244
 generation sequence, 277
 gluing
 dual, 178
 invariant, 179
 null, 178
 trivial, 177
 gradient vector field, 7

H

handle

$(\ell - 1)$ -connecting, 61
 cocore, 61
 core, 61
 ℓ -disconnecting, 61
 ghost, 184
 index, 61
 β -invariant, 61
 round, 154
 homotopically equivalent, 20
 homotopy type, 21

I

incidence matrix, 86
 index filtration, 39, 49
 index pair, 18
 regular, 30
 intersection number, 207
 invariant set, 4
 isolated, 15
 positively, 18
 isolating neighborhood, 15

L

leading coefficient, 215
 lineage, 277
 Lyapunov function, 14
 circular, 260
 finite circular, 260
 Lyapunov graph, 64
 abstract, 65
 in dimension n , 64
 Lyapunov semigraph, 64
 in dimension n , 64
 Morsification, 68

M

maximal invariant set, 5
 moduli space, 205
 Morse
 boundary operator, 209
 complex, 209
 decomposition, 38
 function, 9
 generalized weak inequalities, 49

- index, 10
- Lemma, 10
- polytope, 110, 117
- reduced polytope, 119
- sets, 39
- Morse–Conley
 - inequalities, 45
 - polynomial inequalities, 41
 - weak inequalities, 49
- Morse–Smale
 - function, 10
 - transversality condition, 205
- N**
- node, 85
 - constant, 87
 - head, 85
 - tail, 85
- Novikov
 - complex, 265
 - differential, 265
 - incidence coefficient, 264
 - matrix, 269
- ntd*-labelling, 174
- O**
- orbit, 2
 - periodic, 2
 - regular, 2
 - singular, 2
- P**
- path, 85, 235
 - backward arc, 86
 - directed, 86
 - elementary, 235
 - forward arc, 86
- pivots
- change-of-basis, 215
- primary, 215
- Poincaré–Hopf
 - Equality, 56
 - Generalized Equality, 49
 - global inequalities , 59
 - inequalities, 84
 - inequalities for closed manifolds, 109
- pointed space, 20
- polyhedron, 88
- polytope, 97
- R**
- repeller, 35
 - dual, 36
- rest point, 2
- S**
- smash product, 26
- solution, 2
- spectral sequence, 197
 - convergent, 199
 - first-quadrant, 199
 - limit, 199
 - strongly convergent, 199
- Spectral Sequence Sweeping Algorithm, 213
- T**
- time t map, 2
- totally unimodular matrix, 88, 239
- trajectory, 2
- tree, 86, 88
- W**
- Ważewski property, 21, 30
- wedge sum, 25

Títulos Publicados — 34º Colóquio Brasileiro de Matemática

Uma introdução à convexidade em grafos – *Júlio Araújo, Mitre Dourado, Fábio Protti e Rudini Sampaio*

Uma introdução aos sistemas dinâmicos via exemplos – *Lucas Backes, Alexandre Tavares Baraviera e Flávia Malta Branco*

Introdução aos espaços de Banach – *Aldo Bazán, Alex Farah Pereira e Cecília de Souza Fernandez*

Contando retas em superfícies no espaço projetivo – *Jacqueline Rojas, Sally Andria e Wál Wallace Mangueira*

Paths and connectivity in temporal graphs – *Andrea Marino e Ana Silva*

Geometry of Painlevé equations – *Frank Loray*

Implementação computacional da tomografia por impedância elétrica – *Fábio Margotti, Eduardo Hafemann e Lucas Marcilio Santana*

Regularidade elíptica e problemas de fronteiras livres – *João Vitor da Silva e Gleydson Ricarte*

The ∞ -Laplacian: from AMLEs to Machine Learning – *Damião Araújo e José Miguel Urbano*

Homotopical dynamics for gradient-like flows – *Guido G. E. Ledesma, Dahisy V. S. Lima, Mariana Mello, Ketty A. de Rezende e Mariana R. da Silveira*



Instituto de
Matemática
Pura e Aplicada

Guido G. E. Ledesma

Graduated from the Universidad Nacional Mayor de San Marcos, Perú, and did his doctorate at the University of Campinas, both in Mathematics. His areas of interest are Dynamical Systems and Topology of 3-dimensional Manifolds.

Dahisy V. S. Lima

Pursued her undergraduate studies in Mathematics at the University of Brasília, followed by her doctoral degree at the University of Campinas. Throughout her academic journey, she has developed a strong research background in the fields of Algebraic Topology and Dynamical Systems.

Margarida P. Mello

After graduating in engineering, Margarida completed her PhD at Stanford University in Operations Research. While she has dabbled with nonlinear optimization, her true interests lie in the discrete realm, witnessing the beautiful results that stem from them in other areas. She enjoys tango dancing, and is currently fascinated with knitting.

Ketty A. de Rezende

Obtained her BA at the University of Brasília and her PhD at Northwestern University, in Mathematics. Her research in Qualitative Dynamical Systems is grounded on the interplay between Algebraic Topology and Dynamical Systems and more recently, Singularity Theory. After raising her 7 children, she is now captivated by two-up motorcycle riding with her husband.

Mariana R. da Silveira

Graduated from the University of São Paulo and obtained her doctorate at the University of Campinas, both in Mathematics. Her interests include Algebraic Topology and Topological Dynamical Systems. In addition to her dedication to Mathematics, she enjoys cooking and traveling.

Homotopical dynamics for gradient-like flows



Instituto de
Matemática
Pura e Aplicada

ISBN 978-85-244-0526-6



9 788524 405266